
The Geometry and Physics of Abelian Gauge Groups in F-Theory

Jan Keitel



München 2015

The Geometry and Physics of Abelian Gauge Groups in F-Theory

Jan Keitel

Dissertation
an der Fakultät für Physik
der Ludwig-Maximilians-Universität
München

vorgelegt von
Jan Keitel
aus Oberursel

München, 2015

Erstgutachter: Prof. Dr. Dieter Lüst

Zweitgutachter: PD Dr. Ralph Blumenhagen

Tag der mündlichen Prüfung: 14.07.2015

Zusammenfassung

Diese Arbeit befasst sich mit der Geometrie und den effektiven physikalischen Theorien Abelscher Eichgruppen in F-Theorie-Kompaktifizierungen.

Um passende Calabi-Yau Mannigfaltigkeiten mit Torus-Faserung zu konstruieren, nutzen wir Methoden der torischen Geometrie. Wir bestimmen Komponenten dieser Calabi-Yau-Mannigfaltigkeiten, die dazu geeignet sind, unabhängig voneinander untersucht zu werden. Dies erlaubt die Entwicklung von Methoden zur Konstruktion großer Zahlen von Mannigfaltigkeiten, die zu gegebenen Eichgruppen führen. In dem selben Rahmen erreichen wir eine teilweise Klassifizierung torischer Eichgruppen. Wir zeigen, dass der Feldinhalt der gewöhnlich betrachteten F-Theorie-Modelle starken Einschränkungen unterliegt. Um diese Begrenzungen zu umgehen, entwickeln wir einen Algorithmus mittels dessen wir Torus-Faserungen, die als “complete intersections” definiert sind, untersuchen können. Unter Benutzung dieses Algorithmus entdecken wir mehrere neuartige F-Theorie-Kompaktifizierungen. Zuletzt zeigen wir, wie Torus-Faserungen ohne Schnitt durch ein Netzwerk sukzessiver geometrischer Übergänge mit Faserungen mit mehreren Schnitten verbunden werden können.

Um die effektive Physik solcher Kompaktifizierungen bei niedrigen Energien zu untersuchen, nutzen wir die Dualität zwischen M-Theorie und F-Theorie. Nach der Bestimmung der effektiven Wirkung von F-Theorie mit Abelschen Eichgruppen in sechs Dimensionen vergleichen wir die quantenkorrigierten Chern-Simons-Kopplungen mit topologischen Größen der Kompaktifizierungsmannigfaltigkeit. Dies erlaubt es uns, den Materieinhalt der Theorien zu bestimmen. Unter bestimmten Bedingungen beweisen wir, dass gravitative und gemischte Anomalien in F-Theorie automatisch abwesend sind. Weiterhin berechnen wir die effektive Wirkung von F-Theorie-Kompaktifizierungen ohne Schnitt und schlagen vor, dass die Abwesenheit eines solchen Schnitts die Präsenz eines zusätzlichen massiven Eichfeldes zur Folge hat. Zuletzt zeigen wir durch Ausweitung unserer Analyse auf vier Dimensionen, dass Überbleibsel dieses massiven Eichfeldes sich in diskreten Symmetrien und entsprechenden Auswahlregeln für die Yukawa-Kopplungen der effektiven Theorie auswirken.

Abstract

In this thesis we study the geometry and the low-energy effective physics associated with Abelian gauge groups in F-theory compactifications.

To construct suitable torus-fibered Calabi-Yau manifolds, we employ the framework of toric geometry. By identifying appropriate building blocks of Calabi-Yau manifolds that can be studied independently, we devise a method to engineer large numbers of manifolds that give rise to a specified gauge group and achieve a partial classification of toric gauge groups. Extending our analysis from gauge groups to matter spectra, we prove that the matter content of the most commonly studied F-theory set-ups is rather constrained. To circumvent such limitations, we introduce an algorithm to analyze torus-fibrations defined as complete intersections and present several novel kinds of F-theory compactifications. Finally, we show how torus-fibrations without section are linked to fibrations with multiple sections through a network of successive geometric transitions.

In order to investigate the low-energy effective physics resulting from our compactifications, we apply M- to F-theory duality. After determining the effective action of F-theory with Abelian gauge groups in six dimensions, we compare the loop-corrected Chern-Simons terms to topological quantities of the compactification manifold to read off the massless matter content. Under certain assumptions, we show that all gravitational and mixed anomalies are automatically canceled in F-theory. Furthermore, we compute the low-energy effective action of F-theory compactifications without section and suggest that the absence of a section signals the presence of an additional massive Abelian gauge field. Adjusting our analysis to four dimensions, we show that remnants of this massive gauge field survive as discrete symmetries that impose selection rules on the Yukawa couplings of the effective theory.

Acknowledgments

First and foremost, I would like to express my deep gratitude to Thomas W. Grimm for taking me on as a member of his group and providing a level of supervision that I have rarely seen elsewhere. Not only did he immediately suggest research problems tailored towards my interests to me and constantly provided invaluable support with them, but he also initiated several collaborations from which I have hugely benefited and that I have thoroughly enjoyed. Thomas has made an enormous effort to equip me with the necessary skills to perform research on my own and has never faltered in his support, regardless of my own professional choices. I am very grateful to Dieter Lüst for providing such a productive and friendly environment to do research at this institute and for kindly offering to be my official supervisor and first referee at the Ludwig-Maximilians-Universität. Furthermore, I am deeply indebted to Ralph Blumenhagen for valuable discussions over the course of my PhD and for generously agreeing to serve as my second referee.

Most of what I know about toric geometry I have learned from Volker Braun and I would like to sincerely thank him for his expert advise and the many hours he patiently and cheerfully spent explaining mathematics and Sage to me. A special thanks goes to Iñaki García-Etxebarria as well as to Lara B. Anderson, Andreas Kapfer, Raffaele Savelli, and Matthias Weissenbacher for interesting and fruitful collaborations. Finally, I would like to thank Federico Bonetti, Tom G. Pugh, and Diego Regalado for the numerous discussions and the many enjoyable times that we have had in our group.

Last, but most certainly not least, I am tremendously grateful to my parents and my brother for the continuous and unwavering support that I have always received.

Contents

I	Introduction	7
1	Introduction	9
1.1	Effective Theories	11
1.2	From Points to Strings	13
1.3	The Web of String Theories	14
1.4	String Vacua and the Landscape	16
1.5	Outline of the Thesis	17
2	A Lightning Review of F-Theory	21
2.1	Type IIB Superstring Theory and its Low-Energy Limit	22
2.1.1	Branes in Type IIB	24
2.2	Type IIB and F-theory from M-Theory	27
2.2.1	Fiberwise Duality and F-Theory	29
2.3	Non-Abelian Gauge Theories	31
2.3.1	Matter and Yukawa Couplings	32
2.4	Abelian Gauge Theories	33
2.5	F-Theory Effective Actions	34
2.6	Model Building and GUTs	35
2.6.1	GUT Breaking Mechanisms	37
2.6.2	Further Issues and an F-Theory Wish List	38
2.7	Further Aspects of F-Theory	39

II	Geometry	41
3	Fiber Curves of Genus One	47
3.1	Weierstrass Models	49
3.1.1	The Group Law inside \mathbb{P}_{231}	51
3.2	Embedding Genus-One Curves	53
3.2.1	The Jacobian	55
3.3	Line Bundles on Curves Inside Toric Varieties	57
3.3.1	Sections of Line Bundles on Hypersurfaces	57
3.3.2	Sections of Line Bundles on Complete Intersections	58
3.4	Weierstrass Forms for Complete Intersections: The Algorithm	62
3.4.1	Kodaira Map	63
3.5	Weierstrass Forms for Complete Intersections: Results	63
3.5.1	Exceptions in Codimension Two	66
3.6	Non-Toric Non-Abelian Gauge Groups	67
3.7	Sections of Elliptic Fibrations	69
3.7.1	Toric Sections	69
3.7.2	Non-toric Sections	72
3.7.3	Overview	73
3.8	Classifying Toric Mordell-Weil Groups	73
3.8.1	Toric Mordell-Weil Groups for Hypersurfaces	76
3.8.2	Toric Mordell-Weil Groups for Complete Intersections of Codimension Two	76
3.9	Fibers without Section	82
3.9.1	Genus-One Fibrations with Two-Section	83
3.9.2	Genus-One Fibrations with Three-Section	84
3.9.3	Genus-One Fibrations with Four-Section	85
3.9.4	Mirror-Duality and Mordell-Weil Torsion	87
4	Non-Abelian Singularities from Tops	89
4.1	Toric Fibrations and Tops	90
4.1.1	$SU(5) \times U(1)^2$ with Toric Sections	91

4.2	Tops as Prisms	94
4.3	All $SU(5)$ -Tops for Hypersurfaces	95
4.4	Constraints on Matter Representations from Tops	98
4.4.1	$U(1)$ -Splits and Matter Representations	99
4.4.2	$U(1)$ -Splits and the Top	99
4.5	A No-Go-Theorem for Antisymmetric Representations	102
4.6	Tops for Complete Intersections	104
5	Fibered Calabi-Yau Manifolds	105
5.1	The Auxiliary Polytope of All Fibrations	105
5.2	Flatness of the Fibration	108
5.2.1	Codimension-Two Fibers	108
5.2.2	A General Flatness Criterion	109
5.2.3	Codimension-Three Fibers	110
5.2.4	Studying the Flatness of Some Examples	111
5.2.5	Flattening Base Change	112
5.3	Various Examples of Calabi-Yau Fibrations	113
5.3.1	$SU(5) \times U(1)$ with Non-Toric Section	114
5.3.2	$SU(5) \times U(1)^2$ with Different Antisymmetric Representations	121
5.3.3	$SU(5)$ and a Discrete Symmetry	125
5.3.4	Mordell-Weil Torsion \mathbb{Z}_4	128
III	Effective Actions	131
6	Five-Dimensional Supergravity Reductions	135
6.1	A Basis of Divisors for an Elliptically Fibered Calabi-Yau	136
6.2	M-Theory on a Calabi-Yau Threefold	140
6.3	Six-Dimensional $\mathcal{N} = (1, 0)$ -Supergravity on a Cycle	143
7	The Six-Dimensional Effective F-Theory Action	151
7.1	Classical Matchings	152
7.2	Loop corrections for Chern-Simons terms	153

7.3	Loop-corrected Matchings	155
7.3.1	Explicit Computation of k_{000} and k_0	156
7.3.2	Summary of all Loop-Corrected Chern-Simons Terms	158
7.3.3	Simplified Loop-Corrected Chern-Simons Terms	159
7.4	Six-Dimensional Anomalies and their Cancellation	161
7.4.1	Gravitational Anomalies	162
7.4.2	Mixed Anomalies	164
7.4.3	Pure Gauge Anomalies	166
8	F-Theory on Manifolds without Section	167
8.1	M-Theory on a Calabi-Yau Manifold without Section	169
8.2	Fluxed Circle Reduction	171
8.3	The Effective Action	173
9	Explicit Six-Dimensional F-Theory Models	177
9.1	Determining the Charged Spectrum from Chern-Simons Terms	178
9.2	F-Theory on Calabi-Yau Manifolds with Section	179
9.2.1	Example with Gauge Group $SU(2) \times U(1)$	179
9.2.2	Example with Gauge Group $SU(5) \times U(1)^2$	184
9.2.3	Example with Gauge Group $SU(5) \times U(1)^2$	185
9.3	F-Theory on Calabi-Yau Manifolds without Section	187
9.3.1	Constructing $(\mathbb{Y}, \mathcal{Y})$ Pairs with General Base Manifold	187
9.3.2	Physics of the Conifold Transition	192
9.3.3	Explicit Examples with Base \mathbb{P}^2	193
9.3.4	Chern-Simons Terms	197
10	Yukawas in the Presence of Massive $U(1)$s	205
10.1	The Stückelberg Axion in Four Dimensions	206
10.2	Yukawa Structures	208
10.3	String Interpretation of the Higgsing	209
10.4	A Class of Examples with Discrete Symmetries	212
10.4.1	Hypersurface Equation in \mathbb{P}_{112}	213

10.4.2	Non-Abelian Matter Curves and Yukawa Points	213
10.4.3	Curve Splitting and Conifold Transition	216
10.4.4	Discrete Charges and Forbidden Yukawa Couplings	217
10.4.5	An Explicit Example without Non-Minimal Singularities	218
IV	Closing Remarks	221
11	Conclusion	223
11.1	A Brief Summary	223
11.2	Future Areas of Research	226
V	Appendices	229
A	A Brief Introduction to Toric Geometry	231
A.1	Toric Varieties from Fans	231
A.1.1	Examples and Connection to GLSM Description	233
A.2	Compactness, Smoothness, and Orbit-Cone Correspondence	236
A.2.1	Orbit-Cone Correspondence	236
A.2.2	Smoothness	237
A.3	Intersection Theory	239
A.3.1	Divisors and Line Bundles	239
A.3.2	Homology and Intersection Theory	240
A.4	The Chern Class and the Calabi-Yau Condition	241
A.4.1	Chern Classes	242
A.4.2	Compactness and the Calabi-Yau Condition	243
A.5	Reflexive Polytopes and Calabi-Yau Hypersurfaces	244
A.6	Ricci-Flat Complete Intersections in Toric Varieties	246
A.6.1	Ids for Nef Partitions	247
A.7	The Kähler and the Mori Cone	247
A.7.1	The Kähler and the Mori Cone of Complete Intersections	248
A.8	Toric morphisms and Toric Fibrations	248

A.8.1	The Hirzebruch Surfaces	249
A.8.2	A Fibration with a Reducible Fiber	250
B	Non-toric Non-Abelian Gauge Groups	255
C	Details on the Calabi-Yau Geometries	261
C.1	Exact identities for the Second Chern Class	261
C.2	Signs of Matter Curves from the Mori Cone	262
C.3	Further Details on the No-Section Examples	264
C.3.1	Geometric Description of the Matter Multiplets in \mathbb{Y}	264
C.3.2	Non-Existence of a Section for \mathcal{Y}	268
C.4	Fans of various Ambient Spaces	269
C.4.1	Fan of the Threefold with Non-Toric Section	269
C.4.2	Fans of the Threefolds with Abelian Gauge Groups	270
D	Representation Theory	273
E	Circle Reduction of the Six-Dimensional Action	279
E.1	Supergravity Conventions	279
E.2	The Circle Reduction	280
E.3	Zeta Regularization for the Loop Calculations	284

Part I

Introduction

Chapter 1

Introduction

Throughout the history of science, physical theories have always been approximate descriptions of nature, valid only within a certain range of parameters and limited to a subset of physical interactions. Over time, progress in the field of physics has usually come either in the form of deepening the understanding of an existing theory by extracting and testing new theoretical predictions or by developing a new and more powerful physical theory. The latter kind of development has often been triggered by experiments probing regimes beyond the scope of the established theories. For such a novel physical theory to establish itself, it must correctly reproduce past experimental results and, as a necessary consequence, reduce to the theory it seeks to replace in some area of its parameter space, as for instance Einstein's general relativity contains Newton's classical mechanics.

Repeatedly, new theories have not only enlarged their predecessors' ranges of validity, but completely replaced the notion of the fundamental degrees of freedom governing our world. The advent of atomic physics brought with it for the first time a quantitative notion of atoms, the building blocks of matter. Subsequently, through the development of quantum mechanics these were shown to be comprised of more fundamental objects, namely nucleons and electrons. Finally, according to the theory of Quantum Chromodynamics, nucleons themselves possess a substructure, as they are described by bound states of quarks.

Another, and surprisingly often related form of progress in physics has been the *unification* of formerly distinct physical phenomena as manifestations of one and the same fundamental interaction under the tenets of a new theory. A prime example of such a unifying theory is Maxwell's electrodynamics, describing simultaneously magnetic and electric forces and showing that one can be converted into the other by a simple change of reference frame. Remarkably, these more general theories are typically "simpler" than the sum of their limiting cases, as their form is constrained by an underlying symmetry. One may thus entertain the hope that eventually a "theory of everything could be found — a theory unifying all fundamental interactions, reproducing all established physical theories in certain limits, and thus

describing at least in principle all physical phenomena. And in fact, owed perhaps to hubris stemming from the limits of both our intellectual and our current experimental capabilities, it seems that such a theory could possibly be in reach. After all, there are currently two fundamental theoretical frameworks left that appear to describe nature surprisingly well, albeit in different regimes: The Λ CDM model of standard cosmology and the Standard Model of particle physics supplemented by neutrino masses.

The former theory contains as its integral part Einstein’s theory of General Relativity, which describes the gravitational interactions between all matter. Perhaps unmatched in the simplicity of its guiding principles and in its formal aesthetic appeal, the theory of General Relativity describes gravity accurately at macroscopic distances and has led to a variety of theoretical predictions that have been confirmed experimentally, such as the gravitational redshift or gravitational lensing. The Standard Model, on the other side, provides a quantum theory of the electroweak force and the strong force, which — at the energy scales currently accessible to us — are the only relevant contributions to phenomena taking place at microscopic length scales. Over the past decades, the Standard Model has arguably been tested more thoroughly than any other past theory and continues to resist all attempts at falsification. Only recently, its last missing ingredient, the Higgs-boson, has likely been detected by experiments at the Large Hadron Collider [1]. While precision measurements of this new particle may require the development of new particle colliders such as the International Linear Collider whose construction could possibly soon be initiated in Japan, it currently seems unlikely that the Standard Model would have to be adjusted substantially.

Despite their tremendous successes, both the Λ CDM model and the Standard Model have clear deficiencies that one would wish to see addressed eventually. The most glaring shortcoming may possibly be our failure to understand the basic constituents of our universe: It is known from cosmological experiments that “dark matter” and “dark energy” respectively account for 27% and 68% of the energy content of the universe, while the particles that are so effectively described by the Standard Model, only contribute 5%. Even though many cosmological questions can be answered without a detailed knowledge of the microscopical properties of dark matter and dark energy, from a theoretical point of view it is clearly unsatisfactory not to know their origin. Of similar importance is that the contributions from dark matter and dark energy are not the only parameters that enter the Λ CDM model. In total, the Λ CDM model has six free parameters and the Standard Model contains another 20, all of which must be determined experimentally. Crucially, some of these parameters require a high degree of fine-tuning and are thus vulnerable to small changes. Despite the fact that certain anthropic arguments have been invoked to justify seemingly artificial tunings, there remains the hope that eventually a more powerful theoretical framework could both reduce the number of free parameters and make them less sensitive to small perturbations.

Finally, the most theoretical and yet arguably the most profound deficiency is the lack of a “quantum” description of gravity. While the Standard Model is formulated as a Quan-

tum Field Theory (QFT) and, after a hypothetical completion into a Grand Unified Theory (GUT)¹ can be extrapolated to arbitrarily high energies, attempting to treat General Relativity in the same fashion is doomed to fail: Its coupling constant has positive energy dimension, thereby rendering the theory of General Relativity non-renormalizable.

In view of these numerous challenges, it seems unreasonable to expect their complete resolution anytime soon. While it would certainly be desirable to solve these problems by simply extending the Quantum Field Theory corresponding to the Standard Model, the problems associated with a quantum theory of gravity make such a hope appear unreasonable. In the next section, we thus recall the concepts of renormalization and effective quantum field theories in order to suggest that the renormalizability of the theory of General Relativity can be understood as an indication that it is simply the low-energy limit of an ultra-violet complete theory. Next, we very briefly present in [section 1.2](#) the key idea underlying superstring theory, the theory proposed to unify General Relativity with Quantum Field Theory. In [section 1.3](#) we explain that there exist only five distinct such superstring theories and that all of them are believed to be limits of another, yet more general theory dubbed M-theory. We proceed in [section 1.4](#) with a short summary of the landscape problem of string theory and finally, give an outline of this thesis in [section 1.5](#).

1.1 Effective Theories

As stated above, progress in developing physical theories has frequently meant enlarging a theory’s range of validity, and has regularly proceeded by replacing (or explaining) the formerly fundamental degrees of freedom by a more microscopic version. In Quantum Field Theory, there exists a beautiful formalism implementing a general notion of “coarse-graining”, that is moving in the opposite direction, which is called Wilson’s Renormalization Group [[2](#), [3](#)]. In very rough terms, it can be understood as follows: Given a QFT \mathcal{T} valid up to an energy scale Λ , one can ask what the QFT \mathcal{T}' is that governs processes only up to an energy scale $\Lambda' < \Lambda$. The *effective theory* \mathcal{T}' is obtained from \mathcal{T} by decomposing the fields of \mathcal{T} in an energy basis and *integrating out* all degrees of freedom with energies E satisfying

$$\Lambda' < E < \Lambda. \tag{1.1.1}$$

In order for \mathcal{T}' to take into account the loop effects of the high-energy modes that are no longer part of its spectrum, this process of integrating out must correct the couplings of \mathcal{T} . Crucially, it will also lead to non-renormalizable corrections with coupling constant proportional to $\frac{1}{\Lambda'}$ that were previously absent. One thus notes that perturbation theory for \mathcal{T}' breaks down at energies $E \approx \Lambda'$ and, unsurprisingly, the QFT \mathcal{T}' has a cut-off at Λ' .

¹The Standard Model is a renormalizable gauge theory and can be applied at all energies that can be reached by current accelerators. Nevertheless, it is worth pointing out that the hypercharge part of the Standard Model gauge group has a positive β -function and is therefore afflicted with a Landau pole that may prevent it from being extrapolated to arbitrarily high energy scales. In practice, as discussed in the next section, this is entirely irrelevant — even if it exists, the relevant scale is larger than the Planck scale.

Turning this argument around, we are led to interpret non-renormalizable theories as effective theories with an inherent cut-off scale. Only for energies below the cut-off, we can expect the theory to make reasonable predictions. Renormalizable theories, on the other hand, may in principle be extrapolated to arbitrarily high energies. In practice, another complication must be taken into account. Unless the theory has a conformal symmetry, the coupling constant g is not independent of the energy scale — instead, it is renormalized according to

$$\frac{\partial g}{\partial \log \Lambda} = \beta(g), \quad (1.1.2)$$

with β called the β -function of the Quantum Field Theory. If $\beta(g) > 0$, as is the case for Quantum Electrodynamics (QED), then the coupling constant g becomes larger as the energy scale increases. In the absence of a non-trivial fixed point at high energies (i.e. in the UV), g will become infinite at an energy scale Λ_{Landau} and is said to have a *Landau pole*.² Theories with $\beta(g) < 0$, on the other hand, do not suffer from this particular problem: Here $g \rightarrow 0$ as one increases the energy scale and the theory is said to be *asymptotically free*. Interestingly, this is the case for the Yang-Mills theories of the Standard Model and their putative completions into a GUT.

One particularly well-known example of an effective theory is Fermi theory, suggested as a description for beta decay. Fermi theory contains parity violating four-fermion interactions, which are non-renormalizable in four dimensions. Nevertheless, it describes the weak interaction remarkably well up to energies of ≈ 100 GeV and in fact, together with QED, it can be considered as the low-energy effective theory of the electroweak interaction [4]. Weak interactions are mediated by W and Z bosons, which are made massive by the Higgs mechanism. After integrating out these massive gauge bosons, the renormalizable three-point interaction of the electroweak interaction is replaced by the effective four-point interaction. Naturally, one expects this effective description to break down at energies near the gauge boson masses.

More puzzling is the relation between the other constituent of the Standard Model, QCD, and the various candidates for its low-energy effective theories. QCD is a renormalizable and asymptotically free Yang-Mills theory with gauge group $SU(3)$. Its fundamental degrees of freedom are *gluons*, the analogues of the photon of QED or the W and Z bosons of the weak interaction. However, at low energies the QCD coupling constant becomes large and bound states of gluons, called baryons and mesons, form the relevant degrees of freedom. Since QCD is strongly coupled at low energies, our well-developed perturbative methods can no longer be relied on and as a result, we still lack a proper understanding of how the *confinement* of gluons works. Nevertheless, there is an important lesson to be learned: The fundamental degrees of freedom governing a low-energy effective theory can differ drastically from the

²It is important to point out that the β -function is normally calculated in perturbation theory and is therefore likely to receive important corrections for $g \geq 1$. Even if that is not the case, Λ_{Landau} may be far larger than the Planck scale and therefore irrelevant for all practical purposes.

degrees of freedom of its ultraviolet completion. Indeed, it is conceivable that the ultraviolet theory may no longer be a QFT.

Before we proceed by suggesting that this is precisely what happens in the case of General Relativity, let us pause for a moment and consider the scales that are involved. The fundamental scale of gravity is set by the Planck mass

$$m_{\text{Planck}} = \sqrt{\frac{\hbar c}{G}}, \quad (1.1.3)$$

leading to a Planck scale of $\Lambda_{\text{Planck}} \approx 10^{19}$ GeV. For all energy scales that are currently accessible to us, one can therefore safely use General Relativity. However, hope remains that cosmological experiments will eventually allow us to probe Planck scale physics.

1.2 From Points to Strings

The key concept of string theory is easily conveyed: Instead of assuming that the fundamental degrees of freedom are point-like objects in spacetime whose Lagrangian action is obtained by integrating the proper time over the particle's worldline, one postulates that the fundamental degrees of freedom are spatially extended objects, so-called *strings*. The concept of the worldline is then replaced by a two-dimensional *worldsheet* and the mass of the string is given by multiplying its length with the string tension

$$T = \frac{1}{2\pi\alpha'}. \quad (1.2.1)$$

The quantity α' is called the universal Regge-slope and its origin stems from early attempts to describe the strong interaction in terms of strings.

Considering how straightforward this proposal may seem, postulating that the fundamental objects of a theory are strings has astonishingly many implications. First however, note that the classical motion of a string can be decomposed into the motion of its center of mass and its oscillations around said center. Only if one probes lengths of the order of $\sqrt{\alpha'}$, the extended nature of the string becomes apparent — at lower scales, the string appears to be an ordinary point-like particle.

These oscillatory modes, called higher string modes, do nevertheless play a central role in the quantization of the string. When performing loop calculations in quantum field theory, it is customary to encounter UV-divergences, which can consistently be removed as long as the theory at hand is renormalizable. These divergences originate from integrating over arbitrarily high momenta running in a loop or, put differently, from probing arbitrarily small lengths with virtual particles. Remarkably, these divergences are absent in string theory. Heuristically, one can imagine the string “smoothing out” the formerly localized interaction

points and denying access to regimes smaller than the string scale.³ Surprisingly, quantizing string theory imposes constraints on the spacetime in which the strings propagate. In order to quantize string theory, one quantizes the two-dimensional worldsheet theory of the string, which can be shown to have a conformal symmetry. Demanding that this conformal symmetry be also a quantum symmetry and assuming a d -dimensional Minkowski spacetime, one finds that $d = 26$ for the bosonic string and $d = 10$ for the superstring.⁴

If one accepts the dimension of space-time as a necessary constraint that the consistency of the theory imposes, then one can compute the spectrum of a string in flat spacetime. Notably, a string can have two different sets of topologies, or, equivalently, satisfy two different kinds of boundary conditions. If the string is topologically a circle, then we call it a *closed string*. Strings that have the topology of an interval are *open strings*. While closed strings have no endpoints and propagate through all of spacetime, open strings must end on a subvariety of spacetime, a so-called *brane*. As it turns out, the bosonic string has tachyonic modes and therefore we disregard it. It is an essential property of string theory that one of the massless oscillation modes of the closed string has spin two and can thus be interpreted as a graviton, while the oscillation modes of the open string contain a spin-one field, i.e. a field with all the properties of the ordinary gauge fields in QFT.

It is in this sense that string theory unifies gravity with the type of QFT present in the Standard Model. As one would expect from any reasonable candidate for a unified theory, it reduces to a quantum field theory in its low-energy limit and, in particular, its gravitational interactions are described by General Relativity. Only at energies near the string scale the contributions of the higher string modes become relevant and seem to provide a consistent UV-completion of gravity. Whether string theory is in fact the “theory of everything”, is a completely different question, but its properties are enticing enough in order to merit a detailed study. In the next chapter, we tentatively discuss the low-energy theory governing the massless modes of the superstring in ten spacetime dimensions and find again that demanding the absence of anomalies provides stringent restrictions on the set of allowed superstring theories.

1.3 The Web of String Theories

For a superstring theory to be consistent, its low-energy effective theory must be as well. At energies much below the string scale, superstring theory is described by a *supergravity* theory, as can be shown by matching string scattering amplitudes with the amplitudes obtained in

³While there seems to be consensus that the extended nature of the string generally removes UV divergences, this has so far not been proven rigorously. We refer to [5, 6] for a proof of up to two loops and some general evidence for why UV-divergences should be absent in string theory.

⁴Bosonic string theory and superstring theory differ with respect to the fields of the worldsheet theory: The former consists solely of bosonic fields, while the latter includes also a pair of Majorana-Weyl spinors of opposite chirality for every bosonic field.

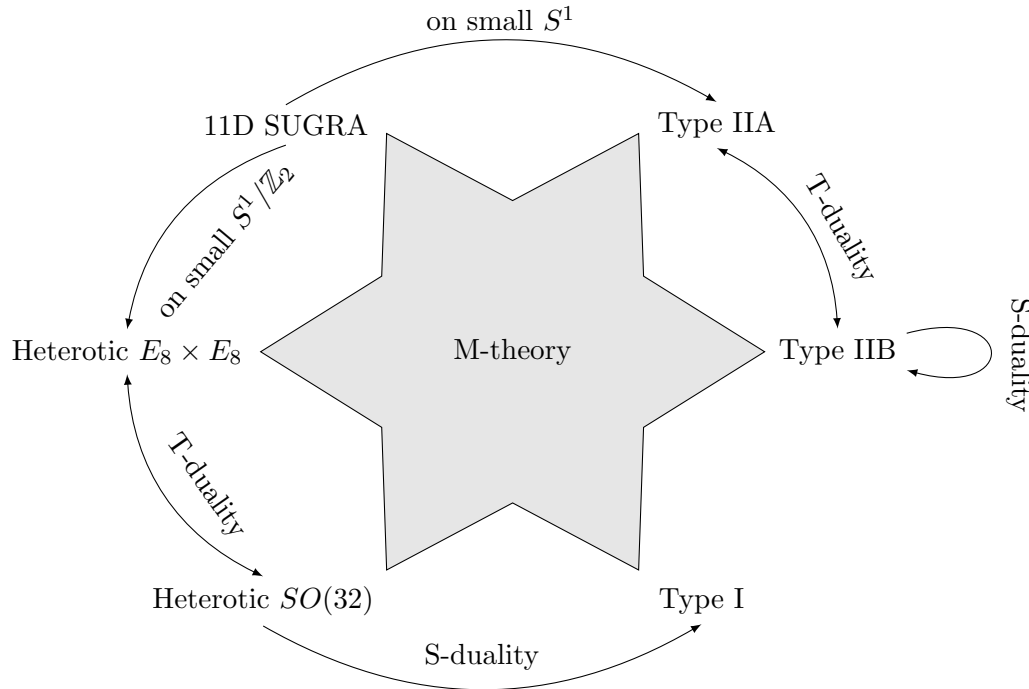


Figure 1.1: The so-called “M-theory star”, illustrating that each of the five superstring theories is the limit of another putative theory called M-theory in some area of its moduli space. The different superstring theories are connected to each other by duality transformations or certain limits.

supergravity. In the case at hand, we are hence concerned with the consistency conditions that a ten-dimensional supergravity theory must satisfy. One such necessary condition is the absence of both gauge and gravitational anomalies. As it turns out, the requirement of anomaly freedom places severe constraints on the set of allowed theories [7] and leaves only five superstring theories:

- Two theories with 32 supercharges, called Type IIA and Type IIB superstring theory.
- Three theories with 16 supercharges, namely Type I superstring theory and Heterotic superstring theory with gauge group $SO(32)$ or $E_8 \times E_8$.

While it is rather remarkable that self-consistency alone has so drastically reduced the set of all possible superstring theories, the big picture underlying these different theories remained a mystery for about a decade.

With the advent of the second string revolution, a more unified description began to emerge. As illustrated in [figure 1.1](#), the five different superstring theories can be connected to each other by certain duality transformations. More importantly, there is evidence for the

existence of a more general theory dubbed M-theory, whose fundamental degrees of freedom are two-dimensional branes called M2 branes. Type IIA string theory and Heterotic $E_8 \times E_8$ can be obtained from M-theory by compactifying on either a circle [8] or an interval [9]. These two theories can in turn be related to the remaining superstring theories, leading to the conjecture that the five superstring theories are simply the limits of a unique eleven-dimensional theory in different corners of the moduli space. Although there exists solid evidence for this conjecture, one has much less computational control over M-theory. While there is a microscopic description of string theory in terms of its worldsheet theory, no such picture of M-theory has been found. As a consequence, one can currently not compute M-theory corrections to eleven-dimensional supergravity directly, but must lift ten-dimensional string corrections to eleven dimensions.

1.4 String Vacua and the Landscape

In view of the dualities between the different five superstring theories and their conjectured connection to M-theory, one may prematurely be led to declare victory in the search for a theory of everything. After all, M-theory has only a single parameter — its fundamental length l_M . Unfortunately, one could not be further from the truth. The glaring problem that still needs to be addressed is the discrepancy between the ten and eleven spacetime dimensions in which superstring theories and M-theory are respectively defined, and the four (at least approximately) flat spacetime directions that we so clearly observe.

The most common solution to this problem is based on an idea outlined almost a century ago [10, 11] and proposes to endow the superfluous extradimensions with a compact topology and a size that is too small to be detectable by current experiments. The original paper describes a five-dimensional spacetime that is topologically a $\mathbb{R}^4 \times S^1$. Decomposing the five-dimensional metric yields a metric, a gauge field (the Kaluza-Klein vector field) and a scalar field in four dimensions. An additional Fourier expansion along the circle coordinate splits these fields into towers of fields with masses $n \cdot m_{KK}$, $n \in \mathbb{Z}$ that depend solely on the four spacetime dimensions. The Kaluza-Klein mass is proportional to the inverse circle radius such that small circle radii can lead to arbitrarily high masses for the massive Kaluza-Klein modes. Originally intended to unify gravity with the theory of electromagnetism, Kaluza-Klein theory was never an experimental success. However, despite its shortcomings, its key idea has lived on: One may try to interpret a complicated spectrum in four spacetime dimensions as an effective theory obtained from compactifying a higher-dimensional spacetime on a compact space of adequately small size.

To implement this approach for a superstring theory, one must compactify six dimensions. Unfortunately, however, no mechanism has been found that dynamically selects a geometry for these extradimensions — instead, their topology is currently treated as input into the theory. Whereas there is a very limited set of topologies for a single extradimension, namely either a circle or an interval, there are infinitely many different six-dimensional topologies.

In the absence of a vacuum selection mechanism or powerful self-consistency conditions, one must therefore constrain the compactification geometry further. One common but possibly unnecessary assumption is that the extradimensions should preserve minimal supersymmetry in four dimensions.⁵ In this case there appears to be evidence that this *landscape* of string vacua [14] may in fact be finite [15]. Compared to the situation one faces in Quantum Field Theory, this is tremendous progress: Instead of continuous parameters, one now has *discrete* parameters that can only take finitely many different values. In practice, however, this advantage is largely philosophical, as the number of vacua has been estimated to reach $\mathcal{O}(10^{500})$ [16, 17], eliminating any hope for a straightforward scan of all possibilities.

Nonetheless, not all is lost. Due to the more complicated nature of higher-dimensional compactification manifolds, computing the effective theory of a general compactification is a much more intricate problem than the circle reduction. First off, one can no longer perform a simple Fourier expansion, but must rather decompose the fields in terms of eigenfunctions of a suitable differential operator defined on the compact space. In first approximation, this is usually the Laplace operator, whose zero modes can elegantly be counted using index theorems and the cohomology of the compact space. For massive modes or in the presence of higher-order corrections, things quickly become far more complicated. Additional complications such as these prevent us from fully understanding the set of theories one obtains from string theory compactifications. In fact, it appears that certain effective theories may be very hard to obtain from string theory, potentially eliminating large areas of the landscape. Investigating such general string theory constraints is an active area of research, but two examples worth mentioning are the struggle to obtain deSitter vacua from string theory and to realize inflationary models with large tensor to scalar ratio [18, 19].

1.5 Outline of the Thesis

This thesis is concerned with the study of Abelian gauge theories in a certain class of Type IIB vacua and is split into clearly separated parts. The second chapter of [Part I](#) gives a technical introduction to these vacua via a formalism called F-theory and its definition via the duality with M-theory. It assumes familiarity with the basic concepts of string theory, supergravity and field theory. Meant to be a concise review of the concepts relevant to the latter parts of the thesis, it contains no original work.

In [Part II](#), we develop the geometrical methods to construct torus-fibered Calabi-Yau compactification manifolds that are essential to this thesis. This construction is split into three parts: The study of the torus fiber by itself, engineering and resolving singularities of

⁵Obviously, that does not imply that the resulting effective theory should be supersymmetric, since our observed universe clearly is not. Instead, it means that the supersymmetry of the superstring should not be entirely broken at energy scales near the Kaluza-Klein scale of the compactification, but a remnant of the original symmetry should survive up to lower energy scales, where it is then broken by a different mechanism. For an introduction to such supersymmetry breaking mechanisms we refer to [12, 13].

the fiber, and completions into globally well-defined torus fibrations. Since most information about the Abelian gauge theories that we are interested in is contained solely in the fiber geometry, [chapter 3](#) is the longest and contains several of the key technical insights of this work. With the intention of presenting in a unified manner the various advances made during the last three years, we describe how to construct tori, i.e. genus-one curves, as complete intersections in various types of ambient spaces. Next, we discuss the geometrical quantities of the fiber relevant to the study of F-theory vacua, namely the discriminant and the Mordell-Weil group. After presenting a novel algorithm to compute the discriminant for a general class of complete intersection manifolds, we employ it to classify the toric Mordell-Weil group of all elliptic curves (that is, genus-one curves with a marked rational point) embedded inside Gorenstein Fano varieties of dimensions two and three. Finally, we explain the construction of genus-one curves without marked rational points and elaborate on the transitions taking them to an elliptic curve. [Chapter 4](#) deals with engineering singularities of genus-one fibrations by embedding them into reducible ambient spaces. Such ambient spaces can be studied by toric methods, leading us to introduce the concept of tops and explain how to read off constraints on the Abelian matter charges of the resulting low-energy effective theory. Finally, we explore in [chapter 5](#) how to combine the fibers and their singularities with a given base manifold and present an algorithm to explicitly enumerate all possible fibrations. Globally defined fibrations must have constant fiber dimension in order to give rise to an appropriate effective field theory with only finitely many fields, which we rephrase into combinatorial conditions on the data of the ambient space geometry.

Equipped with this framework to construct and analyze wide ranges of torus-fibered Calabi-Yau manifolds, we proceed in [Part III](#) by studying the low-energy effective physics that these compactifications give rise to. The vast majority of our efforts is focused on six-dimensional string vacua. We thus derive in [chapter 6](#) and [chapter 7](#) the low-energy effective theory of a six-dimensional F-theory compactification with Abelian gauge factors and study the conditions for anomaly cancelation. In this context, we discover that for certain types of compactification geometries, namely those with non-holomorphic sections, Kaluza-Klein modes can become lighter than the zero modes and contribute non-trivially to ensure that anomalies are automatically canceled. These results are extended in [chapter 8](#) to cover genus-one fibrations without section, where we show that the absence of a section implies the presence of a massive Abelian gauge field in the low-energy effective theory. Several example compactifications are presented in [chapter 9](#), in which we also discuss the transition from an F-theory model without section to another model with multiple sections in terms of a conifold transition. [Chapter 10](#) forms the final part of this thesis and investigates further consequences of compactifications with massive Abelian gauge fields. We show that in these cases a discrete symmetry remains massless, which imposes selection rules on the Yukawa couplings in F-theory compactifications to four dimensions.

In addition to the concluding remarks made in [Part IV](#), this thesis is accompanied by a number of appendices, which are collected in [Part V](#). In particular, [Appendix A](#) deserves

to be mentioned, as it contains an introduction to toric geometry that is tailored towards the topics that are most relevant to this work. The remaining appendices provide proofs or detailed derivations of various statements made in the main text of this thesis.

This dissertation is based on the following publications:

- V. Braun, T. W. Grimm, and J. Keitel, *New Global F-theory GUTs with U(1) symmetries*, *JHEP* **1309** (2013) 154, [[arXiv:1302.1854](#)].
- V. Braun, T. W. Grimm, and J. Keitel, *Geometric Engineering in Toric F-Theory and GUTs with U(1) Gauge Factors*, *JHEP* **1312** (2013) 069, [[arXiv:1306.0577](#)].
- V. Braun, T. W. Grimm, and J. Keitel, *Complete Intersection Fibers in F-Theory*, *JHEP* **1503** (2015) 125, [[arXiv:1411.2615](#)].
- T. W. Grimm, A. Kapfer, and J. Keitel, *Effective action of 6D F-Theory with U(1) factors: Rational sections make Chern-Simons terms jump*, *JHEP* **1307** (2013) 115, [[arXiv:1305.1929](#)].
- L. B. Anderson, I. García-Etxebarria, T. W. Grimm, and J. Keitel, *Physics of F-theory compactifications without section*, *JHEP* **1412** (2014) 156, [[arXiv:1406.5180](#)].
- I. García-Etxebarria, T. W. Grimm, and J. Keitel, *Yukawas and discrete symmetries in F-theory compactifications without section*, *JHEP* **1411** (2014) 125, [[arXiv:1408.6448](#)].

Chapter 2

A Lightning Review of F-Theory

This second and final chapter of the introductory part of this thesis is concerned with reviewing some of the background material necessary for the understanding of what follows in the two core parts of this work.

Intended to be a concise introduction to F-theory, the chapter is structured as follows: We begin in [section 2.1](#) by recalling the massless field content of Type IIB string theory, the ten-dimensional supergravity theory obtained as its low-energy limit and the branes sourcing the various massless gauge fields and their generalizations. Particular emphasis is put on seven-branes, codimension-two objects in Type IIB string theory. Next, we summarize the field content and the action of eleven-dimensional supergravity, which is believed to constitute the low-energy limit of M-theory. After explaining how Type IIB string theory can be obtained by considering M-theory compactified on a torus of vanishing volume in [section 2.2](#), we define F-theory in various dimensions as M-theory compactified on a torus-fibered manifold after taking the limit of sending the torus volume to zero. Having introduced F-theory in this manner, we describe how it allows us to study rather involved Type IIB vacua, and in particular complicated seven-brane configurations, by analyzing the compactification geometry. Indeed, it is the dictionary between geometric quantities on the one side and physical observables on the other that is the underlying reason for much of the usefulness of F-theory. We illustrate in [section 2.3](#) how the non-Abelian gauge group of the low-energy limit of F-theory is encoded in singularities of the torus-fibration. Abelian gauge groups are a bit more subtle to detect, but since they form the central topic of this thesis, we explain their origin in [section 2.4](#). Having briefly discussed the geometric origin of the gauge theories in F-theory, we dedicate [section 2.5](#) to a more detailed description of how to actually perform the M-/F-theory limit to compute the low-energy effective action of F-theory. This is followed by [section 2.6](#), where we recall some of the key features of GUTs and comment on the properties that F-theory vacua would need to have in order to be suitable for GUT model building. Finally, we close in [section 2.7](#) with a summary of other areas of F-theory that are under intense investigation, but that we have not had time to discuss here.

Field	Degrees of Freedom	Name
$g_{\mu\nu}$	35	Graviton
ϕ	1	Dilaton
B_2	28	NS-NS two-form
C_0	1	R-R zero-form
C_2	28	R-R two-form
C_4	35	R-R four-form

Table 2.1: The world-volume fields corresponding to the bosonic massless modes of the Type IIB superstring. The first three fields are from the NS-NS sector, while the latter three are part of the Ramond-Ramond sector of the superstring.

Due to the constraints of time and space, we do not attempt to review the foundations of string theory. Fortunately, there exists a number of excellent books on string theory, such as [20–25], for example, and we refer the interested reader to these. Since F-theory is still very much under investigation, there is considerably less introductory material than on string theory in general, in particular with respect to anything beyond non-Abelian gauge groups in F-theory or any of the other more recent topics of research. Nevertheless, two good introductions to F-theory have been written [17, 26]. In particular, both these lecture notes and the further reviews [27, 28] contain considerably more detail with regard to model building in F-theory than we cover here. Last, but not least, let us also mention the dissertation [29], which has an outstanding introduction to the duality between M-theory and F-theory.

2.1 Type IIB Superstring Theory and its Low-Energy Limit

Let us now turn to Type IIB superstring theory and its low energy limit. The massless modes of the Type IIB superstring have 256 degrees of freedom. Due to supersymmetry, precisely half of these are bosonic and the other half is fermionic. In table 2.1 we summarize the ten-dimensional world-volume fields that they give rise to. The fermionic field content consists of two spin-1/2-fields of the same chirality called *dilatini* and two spin-3/2-fields, the *gravitini*, that also have the same chirality. As a consequence, Type IIB superstring theory is, unlike Type IIA, a *chiral* theory.

In the next step, we are interested in the low-energy limit of the Type IIB superstring, i.e. the theory governing the dynamics of these massless modes in a ten-dimensional spacetime. We limit ourselves to the action of the bosonic sector. After defining the field strengths

$$F_1 = dC_0, \quad F_3 = dC_2 - C_0 dB_2, \quad F_5 = dC_4 - \frac{1}{2}C_2 \wedge dB_2 + \frac{1}{2}B_2 \wedge dC_2, \quad (2.1.1)$$

we introduce the complex fields

$$\tau = C_0 + ie^{-\phi}, \quad G_3 = F_3 - ie^{-\phi}H_3 = dC_2 - \tau dB_2. \quad (2.1.2)$$

The low-energy limit of the Type IIB superstring is given by $\mathcal{N} = (2, 0)$ supergravity in ten dimensions. In terms of the fields that we have just defined and the ten-dimensional Ricci scalar R , the bosonic part of the supergravity action reads

$$S_{\text{IIB}} = \frac{2\pi}{l_s^8} \int_{M_{10}} \left[R * 1 - \frac{1}{2} \frac{d\tau \wedge *d\bar{\tau}}{(\text{Im } \tau)^2} - \frac{1}{2} \frac{G_3 \wedge *\bar{G}_3}{\text{Im } \tau} - \frac{1}{4} F_5 \wedge *F_5 - \frac{i}{4 \text{Im } \tau} C_4 \wedge G_3 \wedge \bar{G}_3 \right], \quad (2.1.3)$$

where M_{10} is the ten-dimensional spacetime manifold, l_s is the fundamental string length and we have chosen to work in the Einstein frame. To be precise, [Equation 2.1.3](#) defines only a *pseudo-action*. The equations of motion for the fields derived by varying the action must be supplemented by the self-duality condition for the five-form field strength given by

$$F_5 = *F_5. \quad (2.1.4)$$

A crucial feature of this action (and the reason for performing the field redefinitions of [Equation 2.1.2](#)) is that it exhibits an $SL(2, \mathbb{R})$ symmetry. Under the action

$$\tau \mapsto \frac{a\tau + b}{c\tau + d}, \quad \begin{pmatrix} C_2 \\ B_2 \end{pmatrix} \mapsto \begin{pmatrix} a & b \\ c & d \end{pmatrix} \begin{pmatrix} C_2 \\ B_2 \end{pmatrix}, \quad \text{where } ad - bc = 1, \quad (2.1.5)$$

and trivial transformations for the remaining fields, one easily checks that $\text{Im } \tau$ and G_3 transform according to

$$\text{Im } \tau \mapsto \frac{\text{Im } \tau}{|c\tau + d|^2}, \quad G_3 \mapsto \frac{1}{c\tau + d} G_3. \quad (2.1.6)$$

Using these transformations, one immediately sees that the Type IIB action of [Equation 2.1.3](#) has an $SL(2, \mathbb{R})$ symmetry. After quantizing the theory, not all of $SL(2, \mathbb{R})$ survives — in fact, only the subgroup $SL(2, \mathbb{Z})$ leaves the path-integral measure invariant. This subgroup, however, is believed to be a symmetry group of the full superstring and not only its low-energy limit. To grasp the importance of this symmetry, consider the element

$$S = \begin{pmatrix} 0 & 1 \\ -1 & 0 \end{pmatrix} \in SL(2, \mathbb{Z}). \quad (2.1.7)$$

Under this transformation the *axio-dilaton field* τ is mapped to $-\frac{1}{\tau}$. If we assume for simplicity that our background satisfies $C_0 = 0$ and recall that the vacuum expectation value of the dilaton field ϕ is related to the string coupling via $g_s = e^{\langle \phi \rangle}$, we find that the above transformation acts on g_s as

$$g_s \mapsto \frac{1}{g_s}. \quad (2.1.8)$$

The above symmetry therefore maps strong string coupling to weak string coupling and vice versa.

Field	Electric Source	Magnetic Source
B_2	Fundamental String	NS5 brane
C_0	D(-1) brane	D7 brane
C_2	D1 brane	D5 brane
C_4	D3 brane	D3 brane

Table 2.2: The form fields of Type IIB supergravity and their sources.

2.1.1 Branes in Type IIB

Next, we turn to studying the form fields B_2 and C_i , $i = 0, 2, 4$, which are generalizations of the usual gauge field (a one-form) that one is familiar with from field theory. Just as ordinary gauge fields have electric and magnetic sources, their generalizations do as well. To obtain an intuitive understanding of the nature of these sources, we recall Maxwell's equations generalized to d dimensions and to include magnetic charges:

$$d *_d F_2 = j_{\text{el}}^{(d-1)}, \quad d *_d F'_{d-2} = j_{\text{mag}}^{(3)}, \quad F'_{d-2} = *_d F_2 \quad (2.1.9)$$

For point charges, the currents take the form

$$j_{\text{el}}^{(d-1)} \sim \delta^{(d-1)}, \quad j_{\text{mag}}^{(3)} \sim \delta^{(3)}, \quad (2.1.10)$$

and we thus see that the electric charges of a one-form field are point-like particles regardless of the spacetime dimension. On the other hand, the dimension of the magnetic charges depends on the spacetime, as it is their *codimension* that is always three.

In the Abelian case, Equations (2.1.9) and (2.1.10) are easily generalized to form fields of degree p . Assuming again a d -dimensional spacetime, they read

$$d *_d F_{p+1} = j_{\text{el}}^{(d-p)}, \quad d *_d F'_{d-p-1} = j_{\text{mag}}^{(p+2)}, \quad F'_{d-p-1} = *_d F_{p+1}, \quad (2.1.11)$$

$$j_{\text{el}}^{(d-p)} \sim \delta^{(d-p)}, \quad j_{\text{mag}}^{(p+2)} \sim \delta^{(p+2)}. \quad (2.1.12)$$

From these equations we learn that the electric sources of a p -form field (which has a $(p+1)$ -form field strength) are $(p-1)$ -branes, while the magnetic sources are objects of codimension $p+2$, i.e. $(d-p-3)$ -branes. In summary, we find that form fields are sourced by objects whose dimension depends on the degree of the form and we list in [table 2.2](#) the electric and magnetic sources of the fields of Type IIB supergravity.

To get a better understanding of the properties of these different branes and their corresponding supergravity solutions, let us look at the equations of motion more closely. For simplicity, let us disregard the directions along which the branes are extended and focus on the $d-p-1$ dimensions transversal to a p -brane. In this transversal space, that we furthermore take to be flat, the field must fulfill the Laplace equation. Since the branes are point-particles

in the transversal dimensions, the solution is the Green's function of the Laplace operator acting solely on the transversal space. In $\mathbb{R}^{d>2}$, this Green's function is simply given by

$$G(r) \sim \frac{1}{r^{d-2}}, \quad (2.1.13)$$

where r is a radial coordinate, while in two dimensions it reads

$$G(r) \sim \log(r). \quad (2.1.14)$$

From the above equation, we see that codimension-two branes are special. For their lower-dimensional counterparts one can always find a region in spacetime where their contribution becomes negligible. In codimension two, that is for seven-branes in ten spacetime dimensions, this no longer holds: No matter how far one moves away from their location, their impact can still be felt and thus their backreaction on the geometry cannot be neglected.

Seven-Branes in Type IIB

Since seven-branes play such a special role in Type IIB, we are thus led to take a more careful look at them. Let us take the transversal space of a D7 brane to be \mathbb{C} , parametrized by a single complex coordinate z . In the vicinity of the brane, the solution for the axio-dilaton behaves as

$$\tau(z) = \frac{1}{2\pi i} \log\left(\frac{z}{\lambda}\right), \quad (2.1.15)$$

where λ is a complex parameter. Since $\tau(z)$ has a monodromy

$$\tau \mapsto \tau + 1 \quad (2.1.16)$$

represented by the $SL(2, \mathbb{Z})$ matrix

$$T = \begin{pmatrix} 1 & 1 \\ 0 & 1 \end{pmatrix} \quad (2.1.17)$$

as one circles the origin, we find that

$$\int_D d\tau = \oint_{\partial D} \tau = 1, \quad (2.1.18)$$

where D is a disk containing the origin and therefore there is indeed a D7 brane located at $z = 0$.

Globally, we do not expect $\tau(z)$ to be a good solution. Certainly, specifying $\tau(z)$ explicitly as we have just done is not necessarily the most convenient description — after all, $\tau(z)$ transforms under the $SL(2, \mathbb{Z})$ symmetry of Type IIB, whereas one would expect the right-hand side of [Equation 2.1.15](#) to remain invariant. To obtain an $SL(2, \mathbb{Z})$ -invariant equation determining τ , one needs to reformulate [Equation 2.1.15](#) in terms of a function of τ that is invariant under the transformation [\(2.1.5\)](#). Such a function is called a *modular function* of

weight zero and it turns out that every function of this kind can be written as a rational function of *Klein's j-invariant*. Klein's j -invariant has the asymptotic expansion

$$j(q) = \frac{1}{q} + 744 + \mathcal{O}(q) \quad (2.1.19)$$

in terms of $q \equiv e^{2\pi i\tau}$. Matching this expansion with [Equation 2.1.15](#), one arrives at

$$j(\tau(z)) = \frac{\lambda}{z}. \quad (2.1.20)$$

Crucially, the inverse map $j(\tau) \mapsto \tau$ has further monodromies apart from the one at $j(\tau = i\infty) = \infty$, namely

$$\tau \mapsto -\frac{1}{\tau} \quad \text{at } j(\tau = i) = 1728, \quad (2.1.21)$$

$$\tau \mapsto -\frac{1}{\tau} + 1 \quad \text{at } j(\tau = e^{\frac{i\pi}{3}}) = 0. \quad (2.1.22)$$

The first monodromy is just the strong-weak coupling transformation S introduced earlier, while the second transformation can be written as TS . Together, S and T generate all of $SL(2, \mathbb{Z})$. Since $i\infty$, i and $e^{\frac{i\pi}{3}}$ are the only fixed points of the fundamental domain of $SL(2, \mathbb{Z})$, these are all monodromies for this solution for τ .

Given such an explicit solution for τ , let us now examine the behavior of the imaginary part of τ , i.e. the dilaton, near the monodromies. At $z = 0$, the location of the D7 brane, we find that

$$\frac{1}{g_s} = e^{-\langle\phi\rangle} = \langle\text{Im } \tau\rangle \approx -\frac{1}{2\pi} \log\left(\frac{z}{\lambda}\right) \quad (2.1.23)$$

and $g_s \rightarrow 0$ as one approaches the D7 brane. For $|z| \ll |\lambda|$ one can hence expect string perturbation theory to be reliable. Crucially, this is no longer true near the other two fixed points of τ , where $g_s \sim \mathcal{O}(1)$. In fact, this should be rather unsurprising — after all, the monodromy around i maps weak coupling to strong coupling.

Indeed, even in this simple set-up, more than one brane is present. More importantly, while the brane at $z = 0$ is a D7 brane, the brane at $z = \infty$ is not: It is a $(0, 1)$ -brane. More generally, one can have (p, q) -branes, around which there is the $SL(2, \mathbb{Z})$ monodromy

$$\begin{pmatrix} 1 + pq & p^2 \\ -q^2 & 1 - pq \end{pmatrix}. \quad (2.1.24)$$

While one can always employ the global $SL(2, \mathbb{Z})$ symmetry of Type IIB to rotate a single (p, q) -brane into a D7 brane, this does not generally work for arrays of different types of seven-branes. In these cases, one can choose a certain brane to be a D7 brane (and thus the string coupling to be small in its vicinity), but there is no transformation to a frame in which *all* branes are of that type. Such set-ups are said to include *mutually non-local* strings and

Field	Degrees of Freedom	Name
$\hat{g}_{\mu\nu}$	44	Graviton
\hat{C}_3	84	M-theory three-form
ψ_μ	128	Gravitino

Table 2.3: The field content of eleven-dimensional supergravity.

while they provide for rich physics, they cannot reliably be treated using perturbative methods in Type IIB.

One could go into further detail and analyze such brane set-ups more closely in Type IIB or try to describe them using the language of string junctions [30–32], but we shall not attempt to do so here. Instead, the intention behind this section was to demonstrate that the inclusion of seven-branes in Type IIB superstring theory will generally lead to backgrounds with varying string coupling that can no longer be treated perturbatively, as it is impossible to neglect the backreaction of the branes. Further difficulties arise as soon as one considers compact transversal spaces, where all seven-brane charge must cancel, or if one analyses the deficit angle induced by the seven-brane geometry [33–35]. Many of these already subtle questions become largely inaccessible as soon as one studies compactifications to lower dimensions. At this point F-theory comes to the rescue by providing a convenient framework that translates these complicated issues into much more tractable geometrical problems.

2.2 Type IIB and F-theory from M-Theory

Unlike in the case of string theory, no microscopic description of the fundamental degrees of M-theory has been discovered so far. The closest attempt to achieving a microscopic formulation of M-theory has possibly been the BFSS matrix model, formulated in terms of D0 branes in the infinite momentum frame [36]. Nevertheless, if M-theory exists, then we know what its low-energy limit must be, since there is a unique supergravity theory in eleven dimensions.¹

In table 2.3 we display the field content of eleven-dimensional supergravity. Apart from the graviton and its superpartner, there is only a single additional field, the M-theory three-form. Its field strength $\hat{G}_4 = d\hat{C}_3$ has M2 branes as electric sources and M5 branes as their magnetic counterparts. The bosonic part of the eleven-dimensional action is given by

$$S_M = \frac{2\pi}{l_M^9} \int_{M_{11}} \left[\hat{R} * 1 - \frac{1}{2} \hat{G}_4 \wedge \hat{*} \hat{G}_4 - \frac{1}{6} \hat{C}_3 \wedge \hat{G}_4 \wedge \hat{G}_4 \right], \quad (2.2.1)$$

with l_M the fundamental M-theory length and, as in the Type IIB case, the fermionic part follows in principle from demanding that the action be supersymmetric.

¹In fact, if one requires only a single time direction and no fields with spin larger than two, then this theory is the *maximal-dimensional* supergravity.

To connect M-theory to Type IIB superstring theory, one must employ two duality transformations. First, one compactifies M-theory on a circle. In the limit of small circle radius, M-theory becomes Type IIA superstring theory, where the Type IIA spacetime is made up by the remaining ten M-theory dimensions. The second step consists of compactifying the Type IIA theory on yet another circle, which is T-dual to Type IIB on a circle of inverse radius. As the radius of the Type IIA circle is shrunk to zero, the circle direction of Type IIB decompactifies. Since the product of the two circles is topologically a two-torus $T^2 = S^1 \times S^1$, we thus arrive at the conclusion that M-theory on a torus becomes Type IIB string theory in the limit in which the torus volume approaches zero.

Let us now carry out the duality for the supergravity fields explicitly. We must therefore assume that our eleven-dimensional metric can be decomposed as $M_{11} = M_9 \times T^2$ and denote by x and y the two cycle coordinates of the T^2 . For the remainder of this section, we denote by sub- and superscripts whether we are dealing with M-theory quantities or Type IIB quantities whenever there might be ambiguities. Calling the complex structure of the torus τ^M and its volume v_M^0 measured in units of l_M , the eleven-dimensional line element splits up according to

$$d\hat{s}_{11}^2 = (ds_9^M)^2 + \frac{v_M^0 l_M^2}{\text{Im } \tau^M} |dx - \tau^M dy|^2 \quad (2.2.2)$$

and we can decompose the M-theory three-form as²

$$\hat{C}_3 = C_3^M + B_2^M \wedge l_M dx + C_2^M \wedge l_M dy + A_M^0 \wedge l_M dx \wedge l_M dy. \quad (2.2.3)$$

Similarly, we decompose the Type IIB spacetime as $M_{10} = M_9 \times S^1$ and denote the circle coordinate by u . The radius of the S^1 is denoted by r^{IIB} . Then the Type IIB fields decompose as

$$ds_{10}^2 = (ds_9^{\text{IIB}})^2 + (r^{\text{IIB}})^2 (du + l_s^{-1} A_{\text{IIB}}^0)^2, \quad B_2 = B_2^{\text{IIB}} + B_1^{\text{IIB}} \wedge l_s du, \quad (2.2.4)$$

$$C_2 = C_2^{\text{IIB}} + C_1^{\text{IIB}} \wedge l_s du, \quad C_4 = C_4^{\text{IIB}} + C_3^{\text{IIB}} \wedge l_s du. \quad (2.2.5)$$

Now one can identify the x -circle with the one reducing M-theory to Type IIA and use the Buscher rules (reviewed for instance in [37–39]) to map the Type IIA fields to their Type IIB counterparts. Performing the calculations, one finds the following expressions for the Type IIB field content in terms of M-theory data:

$$C_0 = \text{Re } \tau^M, \quad e^{-\phi} = \text{Im } \tau^M, \quad (2.2.6a)$$

$$l_s^{-2} B_2^{\text{IIB}} = l_M^{-2} B_2^M, \quad l_s^{-2} C_2^{\text{IIB}} = l_M^{-2} C_2^M, \quad (2.2.6b)$$

$$l_s^{-3} C_3^{\text{IIB}} = l_M^{-3} C_3^M, \quad l_s^{-1} A_{\text{IIB}}^0 = l_M^{-1} A_M^0, \quad (2.2.6c)$$

$$l_s^{-2} (ds_9^{\text{IIB}})^2 = \frac{\sqrt{v_M^0}}{l_M^2} (ds_9^M)^2, \quad l_s^{-1} r^{\text{IIB}} = (v_M^0)^{-\frac{3}{4}}. \quad (2.2.6d)$$

²Here we denote the one-form in the expansion by A_M^0 , since it is mapped to the Kaluza-Klein vector of the circle compactification of the Type IIB theory.

M-theory brane	Torus cycle wrapped	Type IIB brane
M2 brane	none	D3 brane
M2 brane	(p, q)	(p, q) -string
M5 brane	none	Kaluza-Klein monopole
M5 brane	(p, q)	(p, q) -five-brane
M5 brane	T^2	D3 brane
Kaluza-Klein monopole	(p, q)	(p, q) -seven-brane
Kaluza-Klein mode	$(0, 1)$	D(-1) brane

Table 2.4: The M-theoretic origin of the different seven-branes of Type IIB depending on whether they wrap no cycle, a (p, q) -cycle or all of the torus.

Finally, we are allowed to choose the dimensionless proportionality constant between the string length and the fundamental F-theory length. Setting

$$l_s = \frac{l_M}{\sqrt[4]{v_M^0}} \quad (2.2.7)$$

such that $(ds_9^{\text{IIB}})^2 = (ds_9^M)^2$ implies that the distances measured in M-theory and in our Type IIB frame are the same. From now on, we will omit lengths, knowing that they can always be restored by dimensional analysis. One key insight from this duality is that the complex structure modulus τ^M of the M-theory torus is mapped to the Type IIB axio-dilaton τ . Regarded from this point of view, the $SL(2, \mathbb{Z})$ symmetry of Type IIB is self-evident, as it nothing but the modular group acting on the M-theory two-torus.

Under this duality between M-theory and Type IIB superstring theory, the M2 brane and the M5 brane are mapped to different branes in Type IIB depending on the torus cycles that they wrap. A summary of how the different branes in Type IIB are obtained from M-theory objects is given in [table 2.4](#)

2.2.1 Fiberwise Duality and F-Theory

Until now, we have solely considered the duality between M-theory and Type IIB, which by itself is of little use to our aim of understanding D7 brane set-ups. However, it takes surprisingly little effort to generalize the duality such that it becomes *F-theory*. Instead of assuming that the eleven-dimensional spacetime is a direct product $M_{11} = M_9 \times T^2$, one can take it to be a non-trivial torus fibration

$$T_2 \rightarrow M_{11} \xrightarrow{\pi} M_9. \quad (2.2.8)$$

As long as the fibration is an *elliptic fibration*, i.e. it has a *global section*³, one can still split up the eleven-dimensional metric according to [Equation 2.2.2](#). The only modification is that

³That is, there exists a map $s : M_9 \rightarrow M_{11}$ such that $\pi \circ s$ is the identity on M_9

the complex structure τ will now depend on the base M_9 . In fact, even in the absence of such a global section, one can make sense of the duality between M-theory and Type IIB, as we discuss in detail in [chapter 8](#).

Typically, one considers eleven-dimensional spacetimes of the form $\mathbb{R}^{1,10-2n} \times Y_n$, where Y_n is a torus fibration (or *genus-one* fibration in more formal terms). Requiring that Y_n is Kähler and has a vanishing first Chern-class $c_1(Y_n) = 0$ guarantees the existence of a Ricci-flat metric, such that compactifying on Y_n and applying the duality between M-theory and Type IIB superstring theory leads to a $(12 - 2n)$ -dimensional Type IIB background with minimal supersymmetry. The principal benefit of this construction is that for a non-trivial fibration, the complex structure τ of the fiber and thus the axio-dilaton of the resulting string theory vacuum varies over the base manifold. In particular, a non-trivial fibration will have a codimension-one locus in the base manifold over which τ diverges, signaling the presence of seven-branes. Geometrically, the location of these branes has a clear interpretation as the base locus over which a torus-cycle degenerates. If a (p, q) -cycle of the fiber shrinks to zero volume along a base cycle Σ , then there exists a (p, q) -brane wrapping Σ and extending along the non-compact dimensions of the resulting Type IIB vacuum.

To detect singularities of the elliptic fiber, one can compute the *discriminant* Δ of the genus-one fiber curve. The condition that Y_n is a Calabi-Yau manifold implies that Δ must be a section of a certain line bundle on the base, namely

$$\Delta \in \Gamma(B, K_B^{-12}), \quad (2.2.9)$$

where K_B is the canonical bundle of the complex base manifold B . Given Δ , one can simply find all loci along which at least one of the torus cycles shrinks by solving

$$\Delta = 0. \quad (2.2.10)$$

Remarkably, by starting with a genus-one fibered Calabi-Yau manifold we have thus obtained a description of a Type IIB vacuum with seven-branes and varying string coupling. In particular, as we will suggest in the following section, one can apply this framework to construct vacua with mutually non-local seven-branes that give rise to exceptional gauge symmetries. This approach to constructing Type IIB vacua is called F-theory. In the original paper [40] it was speculated that the torus that we used to compactify M-theory on was to be understood as a torus on which a twelve-dimensional theory, F-theory, had been compactified on. Although there is some evidence in favor of this hypothesis, there also exist convincing arguments against it, such as the absence of the Kähler modulus determining the fiber volume or the fact that there exists no supergravity theory with only a single timelike direction in twelve dimensions. As a consequence, we define F-theory as M-theory on a torus-fibered Calabi-Yau manifold in the limit of taking the fiber volume to zero and disregard the notion of a twelve-dimensional origin. From now on, when we talk about F-theory, we refer to studying strongly-coupled Type IIB vacua via the M-/F-theory limit.

Last, but not least, let us point out that taking the M-/F-theory limit can be vastly more subtle than one might at first think. As we will see in the next section, the fiber geometry becomes more complicated if non-Abelian gauge groups are present in the low-energy effective theory and there are in fact competing limits to be performed. For a more detailed discussion of such matters, we refer to [41].

2.3 Non-Abelian Gauge Theories

As hinted at above, one of the motivations to study F-theory is the elegance with which it allows the construction of exceptional gauge groups in Type IIB. Unlike weakly-coupled Type IIB brane set-ups, which permit only the construction of the classical A , B , C and D gauge algebras, F-theory vacua feature mutually non-local seven-branes, thus allowing exceptional gauge algebras as well. In this section, we give a brief summary of how non-Abelian gauge symmetries can be detected in the M-theory geometry.

In the previous section, we mentioned that seven-branes wrap cycles in the base manifold defined by the vanishing locus of the discriminant, i.e. $\Delta = 0$. To differentiate between a single seven-brane and the stacks of seven-branes that give rise to a non-Abelian gauge theory on the brane world-volume, we expand Δ along a normal coordinate w to the vanishing locus:

$$\Delta = \sum_{i=0} \Delta^{(i)} w^i \tag{2.3.1}$$

A necessary criterion for a non-Abelian gauge theory to exist is that $\Delta^{(0)} = \Delta^{(1)} = 0$, that is, Δ must vanish at least quadratically with respect to w . Compared to the case where Δ vanishes only linearly, there is an important difference. In the case that $\Delta = \mathcal{O}(w)$ near a singularity, the fiber of Y_n degenerates, but the total space of the fibration remains smooth. However, if Δ vanishes at least quadratically and induces a non-Abelian gauge theory, then Y_n itself becomes singular.

In this case, it is helpful to *resolve*⁴ the singularity. Performing the resolution leads to a set of exceptional divisors consisting of a two-sphere fibered over the base locus of the former singularity. In this fashion, the torus fiber is replaced by a set of two-spheres intersecting each other in a certain pattern. It is a beautiful property of F-theory that these two-spheres intersect as the nodes of the affine Dynkin diagram of the gauge algebra they give rise to. Fortunately for physicists, singularities of elliptic surfaces were classified by Kodaira

⁴Alternatively, one can *deform* the singularity [42, 43]. Physically, the difference between a resolution and a deformation is that the former corresponds to moving to the Coulomb branch of the resulting low-energy effective theory, while the latter corresponds to Higgsing the gauge group. Note that here we are talking about the odd-dimensional supergravity theory *before* applying T-duality and sending the radius of the T-duality circle to zero.

A different approach to singular spaces was taken in [44, 45], where the authors attempt to understand the singular geometry directly.

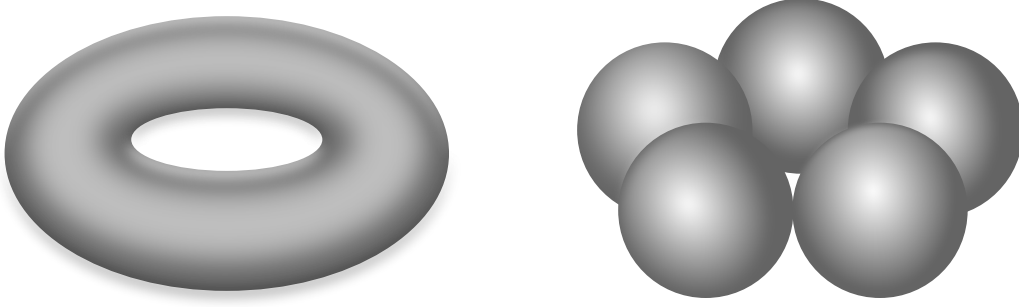


Figure 2.1: A schematic representation of the generic fiber and the reducible fiber after resolving an $A_4 \simeq \mathfrak{su}(5)$ singularity. If the fibration has a global section, then one section must be chosen as the zero section determining the “origin” on the elliptic fiber. One can take the node intersected by the zero section as the affine node of the Dynkin diagram.

[46] and one can use his classification to precisely identify the type of singularity that the compactification manifold has. We will recall the full classification in [chapter 3](#) and explain in detail how to read off the singularity type.

Importantly, it takes precisely $\text{rank } \mathfrak{g}$ exceptional divisors to resolve a singularity whose low-energy effective gauge algebra is \mathfrak{g} . As we will see in detail in [Part III](#) of this thesis, the two-forms dual to these exceptional divisors are those whose expansion coefficients become the generators of the Cartan subalgebra, i.e. those gauge fields that commute with all generators of the gauge algebra. For this reason, we will occasionally refer to the exceptional divisors as *Cartan divisors* and to singularities that give rise to non-Abelian gauge symmetries as *non-Abelian singularities*.

2.3.1 Matter and Yukawa Couplings

Just as one can relate the (non-Abelian) gauge fields of the resulting low-energy effective theory to singularities of the compactification manifold that occur at codimension one in the base, it is also possible to find a geometric description for matter fields and their Yukawa couplings.

From intersecting brane scenarios, reviewed for instance in [47, 48], we expect matter fields to be located at the intersection of two branes and similarly, the Yukawa couplings at a triple brane intersection. In the compactification geometry, such brane intersections manifest themselves in *singularity enhancements*. At certain codimension-two loci in the base, the rank of the non-Abelian singularity will generically increase by one. Such enhancements will generically lead to matter states and their representations can be obtained from the branching rule of the adjoint representation of the enhanced gauge algebra $\mathfrak{g}_{\text{enh}}$ to \mathfrak{g} . Two examples that we will repeatedly encounter in this thesis are two rank-one enhancements of $\mathfrak{su}(5)$, namely

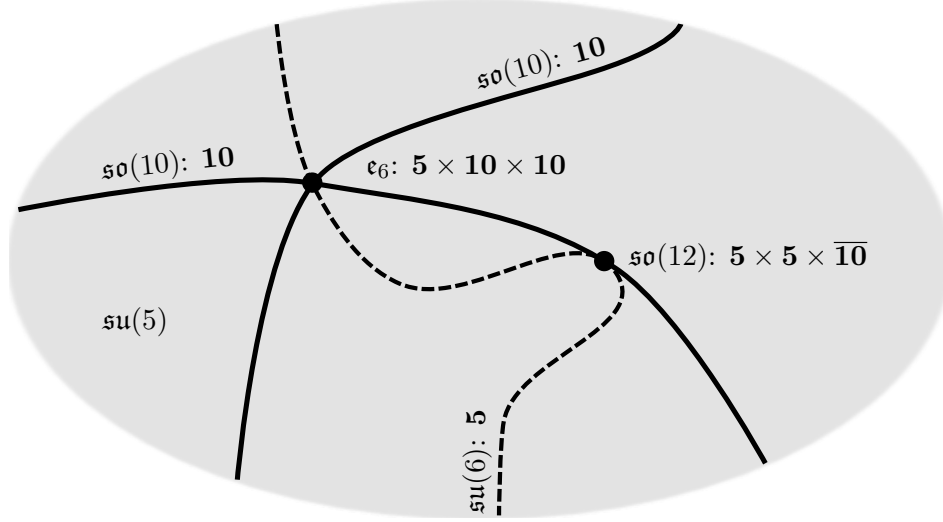


Figure 2.2: A pictorial description of how matter fields and Yukawa couplings arise at the intersection of multiple branes that occur in higher codimensions in the base manifold. The big gray blob symbolizes an $SU(5)$ GUT divisor.

those to $\mathfrak{so}(10)$ and $\mathfrak{su}(6)$. One finds that

$$\begin{aligned} \mathfrak{su}(6) : \quad & \mathbf{35} \rightarrow \mathbf{24} + \mathbf{5} + \bar{\mathbf{5}} + \mathbf{1} \\ \mathfrak{so}(10) : \quad & \mathbf{45} \rightarrow \mathbf{24} + \mathbf{10} + \bar{\mathbf{10}} + \mathbf{1}, \end{aligned} \tag{2.3.2}$$

and thus the fundamental and the antisymmetric representations of $\mathfrak{su}(5)$ can be associated with singularity enhancements to $\mathfrak{su}(6)$ and $\mathfrak{so}(10)$.

Similarly, one can create a dictionary between the enhanced gauge algebra and the resulting Yukawa coupling. In the case of $SU(5)$ one finds the following map:

$$\mathfrak{su}(7) : \mathbf{5} \times \bar{\mathbf{5}} \times \mathbf{1} \quad \mathfrak{so}(12) : \mathbf{5} \times \mathbf{5} \times \bar{\mathbf{10}} \quad \mathfrak{e}_6 : \mathbf{10} \times \mathbf{10} \times \mathbf{5} \tag{2.3.3}$$

For GUT model building, it is essential to point out that the last coupling is associated with an enhancement to an exceptional gauge algebra that cannot occur in weakly-coupled models. In F-theory, on the other hand, areas of strong coupling with mutually non-local seven-branes can lead to exceptional symmetries.

2.4 Abelian Gauge Theories

Compared to non-Abelian gauge symmetries, Abelian gauge groups are encoded in a slightly more subtle geometric quantity: The Mordell-Weil group of the elliptic fibration. In [chapter 3](#) we explain this group in far more detail, but roughly speaking, it is generated by the homology classes of global sections of the fibration modulo the homology in the base manifold.

Regardless of the details, it is easy to compute the Abelian rank of an F-theory model of an elliptically fibered Calabi-Yau manifold Y :

$$\text{rank}_{U(1)} = h^{1,1}(Y) - h^{1,1}(B) - 1 - \sum_i \text{rank } \mathfrak{g}_i \quad (2.4.1)$$

Here B is the base manifold of B and \mathfrak{g}_i are the gauge algebras of the non-Abelian singularities. As we will see in detail, the Abelian gauge fields are obtained by expanding the M-theory three-form in these $(1, 1)$ -forms.

It is remarkable that even though the Mordell-Weil group was related to the Abelian gauge symmetry already in the early papers [49, 50], it took fifteen years until a systematic study of Abelian gauge symmetries was begun [51, 52]. Since their systematic study and construction is the main topic of this dissertation, we postpone a more detailed treatment of their geometry to [Part II](#) and their physics to [Part III](#) of this thesis.

2.5 F-Theory Effective Actions

While F-theory allows one to read off many of the properties of the resulting low-energy theory directly from the M-theory geometry, studying the supergravity theories involved in the M-/F-theory limit and performing the duality carefully is essential. In this section we therefore give a concise summary of how to obtain an *effective* action for F-theory by elaborating on the discussion of [section 2.2](#). Let us also note that such computations were first performed in [53, 54] and that they form an essential part of [Part III](#) of this thesis.

The first part of determining the effective action of F-theory on a possibly singular Calabi-Yau n -fold Y_{sing} is to resolve the singularities, yielding a smooth Calabi-Yau manifold Y . Next, one compactifies M-theory on Y to obtain a supergravity theory in $11 - 2n$ dimensions. Instead of trying to perform the limit of sending the fiber volume to zero explicitly, one now approaches the duality from the Type IIB side. After reading off the gauge group from the geometry of Y , one takes a general $(12 - 2n)$ -dimensional supergravity theory with arbitrary matter and reduces it on a circle. In the third and final step, the two $(11 - 2n)$ -dimensional theories that one has thus obtained have to be matched. While this is immediately possible for a subsector of the $(11 - 2n)$ -dimensional supergravity theory (called the *classical* sector), it cannot be done in general. Key to understanding the underlying reason for this apparent mismatch is to recognize that the M-theory reduction is a theory of only the massless nodes — all contributions from massive fields have “automatically” been integrated out in the reduction. In particular, this includes the W-bosons of the gauge theory and all particles with non-zero charge under any of the gauge fields, as resolving the non-Abelian singularities implies giving a non-zero vacuum expectation value to the scalars in the vector multiplets of the theory. Only after also integrating out the massive modes of the circle reduced theory, one can therefore expect the two theories to be the same. This approach is summarized and illustrated in [figure 2.3](#).

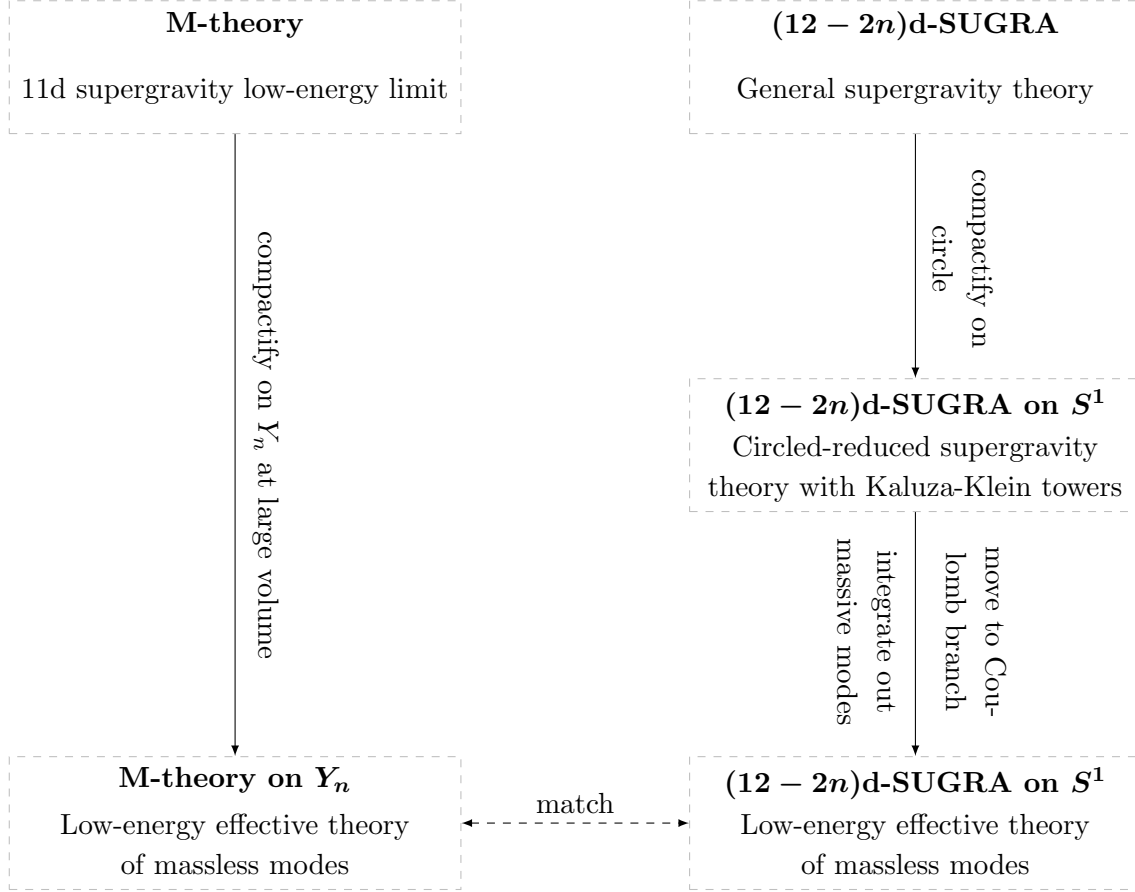


Figure 2.3: Summary of how to compute the low-energy effective action of F-theory in a given dimension.

2.6 Model Building and GUTs

Since its conception [40] almost twenty years ago, F-theory has attracted considerable attention. However, work on F-theory can largely be divided into two phases: After a burst of activity in the first years after its formulation, interest abated until the field was revived by the two independent but strongly related works of [55] and [56, 57] which suggested using F-theory for GUT model building. Here we give a short overview of the properties of F-theory that make it attractive for studying GUT models. For more details we refer the reader to [28, 48].

As mentioned already in the first chapter, there are arguments favoring a unification of the electroweak force with the strong force and the running of gauge couplings indicates that this may occur at $\Lambda_{\text{GUT}} \approx 10^{16}$ GeV. The simple gauge group of lowest rank that contains the Standard Model gauge group $SU(3) \times SU(2) \times U(1)$ is $SU(5)$, leading to the proposal of Georgi and Glashow [58] of an $SU(5)$ GUT model. There the hypercharge generator of the

Standard Model $U(1)$ is identified with the Cartan element

$$T = \begin{pmatrix} 2 & & & & \\ & 2 & & & \\ & & 2 & & \\ & & & -3 & \\ & & & & -3 \end{pmatrix} \quad (2.6.1)$$

of $SU(5)$. Furthermore, the Standard Model matter representations can be nicely packaged into representations of $SU(5)$ according to

$$\mathbf{10} = (Q_L, u_R^C, e_R^C), \quad \mathbf{1} = (\nu_R^C) \quad (2.6.2)$$

$$\bar{\mathbf{5}}_{\mathbf{M}} = (d_R^C, L), \quad \mathbf{5}_{\mathbf{H}} = (T_u, H_u), \quad \bar{\mathbf{5}}_{\mathbf{H}} = (T_d, H_d), \quad (2.6.3)$$

where the superscript C denotes charge conjugation and there is a set of $\mathbf{10}$, $\bar{\mathbf{5}}_{\mathbf{M}}$ and $\mathbf{1}$ representations for every family of the Standard Model. The only additional fields not present in the Standard Model are the Higgs triplets T_u and T_d and the twelve extra gauge boson degrees of freedom from the breaking $SU(5) \rightarrow SU(3) \times SU(2) \times U(1)$. Furthermore, the Yukawa couplings can be rewritten into Yukawa couplings of the $SU(5)$ gauge theory as in

$$\mathbf{10} \times \mathbf{10} \times \mathbf{5}_{\mathbf{H}} : Q_L u_R^C H_u \quad (2.6.4)$$

$$\mathbf{10} \times \bar{\mathbf{5}}_{\mathbf{M}} \times \bar{\mathbf{5}}_{\mathbf{H}} : L e_R^C H_d + Q_L d_R^C H_d. \quad (2.6.5)$$

The fact that the Standard Model representations can so easily be accommodated into $SU(5)$ representations was initially considered as theoretical evidence for the existence of such an $SU(5)$ GUT.

However, subsequent experiments showed that at least the most naive version of such an $SU(5)$ GUT is not a correct description of nature. Arguably the most pressing problem of simple $SU(5)$ GUTs is the prediction of proton decay. Couplings of the type

$$\mathbf{10} \times \bar{\mathbf{5}}_{\mathbf{M}} \times \bar{\mathbf{5}}_{\mathbf{M}} : Q_L d_R^C L + u_R^C d_R^C d_R^C + L L e_R^C \quad (2.6.6)$$

and similarly for $\mathbf{10} \times \bar{\mathbf{5}}_{\mathbf{H}} \times \bar{\mathbf{5}}_{\mathbf{H}}$ lead to proton decay, a tightly constrained experimental quantity, and in the absence of a further symmetry that could impose additional selection rules, there is no good reason for why they should be absent.

If one were to realize GUT scenarios in string theory, one option would thus be to study $SU(5)$ GUT theories with additional symmetries, either in the form of Abelian gauge groups or discrete symmetry groups. To construct such an $SU(5)$ GUT, one may be tempted to use a weakly-coupled brane set-up in Type II superstring theory.⁵ Unfortunately, there is one

⁵There is a vast number of factors one must pay attention to when trying to construct halfway realistic string compactifications, which we largely neglect here. We refer to [47] for a comprehensive review of model buildings with branes and fluxes.

major problem with that: In such intersecting brane scenarios Yukawa couplings originate from local enhancements of the gauge group and can be read off by branching the adjoint representation of the enhanced gauge group down to $SU(5)$. One finds that

$$\mathbf{48} \xrightarrow{\mathfrak{su}(7) \rightarrow \mathfrak{su}(5)} \mathbf{24} + (\mathbf{5} + \bar{\mathbf{5}} + \mathbf{1} + \text{c.c.}) + 2 \times \mathbf{1} \quad (2.6.7a)$$

$$\mathbf{66} \xrightarrow{\mathfrak{so}(12) \rightarrow \mathfrak{su}(5)} \mathbf{24} + (\mathbf{10} + \bar{\mathbf{5}} + \bar{\mathbf{5}} + \text{c.c.}) + 2 \times \mathbf{1} \quad (2.6.7b)$$

$$\mathbf{78} \xrightarrow{\mathfrak{e}_6 \rightarrow \mathfrak{su}(5)} \mathbf{24} + (\mathbf{10} + \mathbf{10} + \mathbf{5} + \text{c.c.}) + 4 \times \mathbf{1}, \quad (2.6.7c)$$

which connects the $\mathbf{10} \times \mathbf{10} \times \mathbf{5}$ Yukawa coupling to a local enhancement to E_6 , as we already stated in [Equation 2.3.3](#). Exceptional gauge groups, however, can not be obtained using weakly coupled methods. Nevertheless, this Yukawa coupling is responsible for the top mass as can be seen from [Equation 2.6.4](#) and generating it purely from non-perturbative instanton corrections requires a large amount of fine-tuning.

2.6.1 GUT Breaking Mechanisms

In order to solve this problem, it is necessary to consider string theory vacua with exceptional gauge groups. The most obvious candidate is the Heterotic String with gauge group $E_8 \times E_8$, but as discussed previously, they can also be obtained from F-theory. Regardless of their origin, any GUT group must eventually be broken to the gauge group of the Standard Model and there exist various mechanisms to do this.

Possibly the most straightforward mechanism to achieve GUT breaking is to include a Higgs field in the adjoint representation of the GUT group. Geometrically, such a Higgs field would correspond to a deformation modulus of the brane on which the GUT is defined and would be counted by the sections of the canonical bundle of the GUT divisor S , that is they are elements of $H^0(S, K_S)$.

Furthermore, there are two more stringy GUT breaking mechanisms, that one would not ordinarily consider in field theory. The first such mechanism uses Wilson lines to break the GUT group. These also correspond to fields transforming in the adjoint representation of the GUT group and are obtained from elements of $H^1(S)$. Wilson lines are usually used to break the gauge group of the Heterotic String. The second stringy mechanism uses hypercharge flux, i.e. flux in the direction of the Cartan generator T defined in [Equation 2.6.1](#), depends on no strong-coupling effects and can equally well be used in perturbative set-ups.

Recently, hypercharge has been investigated in the context of the Heterotic String. However, under a certain set of assumptions, the authors of [\[59\]](#) proof a no-go theorem, showing one can not obtain Standard Model physics from Heterotic String Theory using hypercharge flux. In F-theory, on the other hand, no such constraint is believed to exist and realizing viable models with hypercharge breaking remains an active area of research [\[60–63\]](#).

2.6.2 Further Issues and an F-Theory Wish List

The combination of exceptional gauge symmetries, hypercharge flux and the connection to well-controlled IIB mechanisms make F-theory an attractive candidate for GUT building. For this reason, let us now identify a few key F-theory model configurations that could potentially be of interest for serious GUT phenomenology. The most obvious quantity one needs to control is the non-Abelian gauge group, which is most often assumed to be either $SU(5)$ or $SO(10)$. As mentioned above, it is important to ensure that the gauge symmetry is enhanced to E_6 at certain points in the base.

Next, to address proton decay, one would like to construct F-theory models with distinguishable $\mathbf{5}$ -representations to accommodate $\mathbf{5}_H$ and $\mathbf{5}_M$. For two representations to be distinguishable, i.e. to obey different rules in field theory, they must carry different charges under an additional symmetry. This symmetry can either be continuous (in the simplest case a $U(1)$) or discrete. Geometrically, such a symmetry would force the $\mathbf{5}$ -curve to split into different irreducible components. Naively, one might think that the presence of two $\mathbf{5}$ -curves and a $\mathbf{10}$ -curve will be enough in order to forbid couplings to the type given in Equation 2.6.6, but this is not true. If one also attempts to generate the correct number of generations, use hypercharge flux to break the GUT group and satisfy four-dimensional anomaly cancellation, one needs either two additional $\mathbf{5}$ -curves or further $\mathbf{10}$ -curves, as was elegantly shown in [64]. In summary, the most straightforward models one could hope for have an $SU(5) \times U(1)^k \times \mathbb{Z}_n$ gauge groups, where either $k > 0$ or $n > 0$. Furthermore, they should have a total of at least five different $\mathbf{5}$ and $\mathbf{10}$ representations, and enhance to E_6 at the intersection of some of the $\mathbf{5}$ and $\mathbf{10}$ curves.

Clearly, these are not the only conditions that a contender for at least a semi-realistic F-theory GUT model would need to satisfy. In fact, there exists a host of issues that we have not addressed here. To begin with, for the hypercharge $U(1)$ not to become massive by the flux needed to break the GUT group, the GUT divisor must have a suitable topology: It must possess $(1, 1)$ -forms that become trivial if lifted to the entire base manifold [62]. In addition, there are many other “constraints” from the Standard Model, such as the correct form of the CKM matrix [65–70], an appropriate hierarchy between the strength of the gravitational interaction and the gauge couplings [71–73], neutrino physics or possible constraints from inflation [74, 75]. Another significant topic that we have fully omitted here is moduli stabilization. Generically, F-theory compactifications have a number of additional neutral fields that correspond to deformations and rescalings of the compactification geometry. The general hope is that Type IIB moduli stabilization mechanisms are applicable to more general F-theory models as well, but actually stabilizing all moduli for a given model is highly challenging.

It is for these reasons that we strongly emphasize that even though the constructions carried out in this thesis may partially be motivated by their potential application to GUT building and an improved understanding of the string landscape, we do not in the least suggest

to provide realistic F-theory models. Instead, we undertake a general study of Abelian gauge groups in F-theory and discover that they are closely related to discrete symmetries.

2.7 Further Aspects of F-Theory

In this final section of the introductory part of this dissertation, we would like to point out several areas of research in F-theory that we have not been able to mention, but that are interesting in their own right.

From the beginning on, F-theory has been recognized to be dual to the heterotic string [40, 49, 50]. One of the central pieces of the duality is the spectral cover construction developed in [76], which was later adapted to compute spectra in local F-theory models [66, 77] and extended to include Abelian factors in semi-local models to study and classify possible local $SU(5) \times U(1)^r$ GUT model spectra [60, 78–81]. Despite the early efforts, the duality with the heterotic string continues to be studied [82–84] and further work may be needed in order to fully understand the heterotic duals of F-theory models with Abelian gauge groups [85].

A topic that we completely omitted in our short introduction to F-theory are weak-coupling limits of F-theory. The essential idea behind such limits is to deform the complex structure of the fibration such that τ approaches $i\infty$ over all of the base. The first person to systematically study this problem was Sen [86, 87]. Despite this early and important work, taking the weak-coupling limit of a general F-theory model is far from understood — in fact, one would not expect to even be able to find an area in the complex moduli space in which a theory with exceptional gauge groups becomes weakly coupled. Recently, new orientifold limits have been explored [88–90] and in [91, 92] a new stable version of the limit was developed. Based on this stable Sen limit, the authors of [93] managed to study (a limited set of) massless and massive $U(1)$ s and confirmed the proposal to use an expansion in non-Kähler forms made in [62] for the latter.

Another area of F-theory is concerned with using F-theory to study gauge theories in various dimensions. Already in [94] it was recognized that the gauge theories obtained by compactifying M-theory on Calabi-Yau threefolds related to each other by flop transitions are connected to each other by different choices of Weyl chambers. This idea was later extended to four dimensions in [95] and has recently been described systematically in [96–100]. It turns out that there is a nice relation to the singularity enhancements of elliptic fibrations in higher codimensions as studied in [101–104]. Equally interesting are the efforts to use F-theory in order to construct and classify SCFTs in six dimensions [105–111] or to study their anomaly polynomials [112]. Automatic anomaly cancelation for F-theory vacua was studied in [113–115].

In a somewhat similar spirit to the classification of six-dimensional SCFTs, there has been a program to partially classify F-theory models by concentrating on so-called non-Higgsable clusters [116–121]. There are various further efforts to explore the F-theory landscape by

finding suitable building blocks and by deriving constraints valid on the range of allowed supergravity models. In addition to those developed in this thesis, there have for instance been the works of [84, 122–127].

Finally, let us mention that α' -corrections to F-theory effective actions have recently started to receive attention [128–131] and it will be interesting to study their potential impact on model building scenarios. There are various other recent developments in F-theory, ranging over topics as diverse as period computations [132], to matrix factorizations [44, 45], orbifolds in F-theory [133] and hypercharge flux [63]. Many of these topics overlap and it is exciting to contemplate their further development in the coming years.

Part II

Geometry

Much of the appeal of F-theory and certainly a considerable part of its computational power stems from the fact that F-theory encodes the configuration of fully backreacted Type IIB seven-brane systems geometrically. Using F-theory, intricate physical questions can be translated into their geometrical counterparts, which may turn out to be far more accessible due to the advances of Modern Mathematics. Having as much control as possible over the manifolds on which we compactify F-theory is therefore absolutely essential. It is the objective of this chapter to provide the necessary mathematical background and an appropriate framework for constructing and analyzing suitable Calabi-Yau manifolds.

We begin by presenting a “wish list” of sorts and specify the properties that we require our compactification manifolds to have. In order to study the F-theory scenarios of interest to us, we require a complex Calabi-Yau manifold Y subject to the following demands:

- Y is smooth.
- Y has a fibration with projection map $\pi : Y \rightarrow B$, such that the fiber $\pi^{-1}(p)$ is a curve of genus one over generic points p in the complex base manifold B .
- The fibration Y has a specified number of independent global sections.
- There exists a blow-down map taking Y to Y_{sing} , where Y_{sing} is a singular manifold with singularities of a specific kind over a given set of base loci.

Ideally, one would like to find an algorithm that takes as input the number of independent sections, the set of pairs of base loci and singularities and possibly the base manifold itself, and produces from that a list of all such Calabi-Yau manifolds. By further refining the physical input of this algorithm, the ultimate hope would then be to be able to exhaustively survey the landscape of string vacua. Needless to say, this goal remains far in the distance. However, if one accepts not to be given a list of *all* such manifolds, but instead only of *some* manifolds satisfying the given criteria, then much progress has been made in the past years. In the following, we outline our approach to this problem, explain how to break it down to a set of three sub-tasks and focus on answering them separately in the different chapters of this part of the thesis.

The first step (and possibly a simplification) is to restrict to Calabi-Yau manifolds Y_n of complex dimension n that can be constructed as complete intersections of codimension c inside toric varieties X_{n+c} . By ensuring that X_{n+c} are sufficiently smooth spaces, one can achieve that Y_n itself is smooth, too. Next, one translates the other physical requirements on Y_n into requirements on X_{n+c} and demands that there is a blow-down map taking X_{n+c} to $X_{n+c, \text{sing}}$. Under this map Y_n is mapped from a *generic* and smooth complete intersection inside X_{n+c} to a *non-generic* and singular complete intersection $Y_{n, \text{sing}}$ inside $X_{n+c, \text{sing}}$, where our notion of genericity is with respect to the position inside the complex structure moduli space of Y_n . We illustrate this approach in [figure 2.4](#).

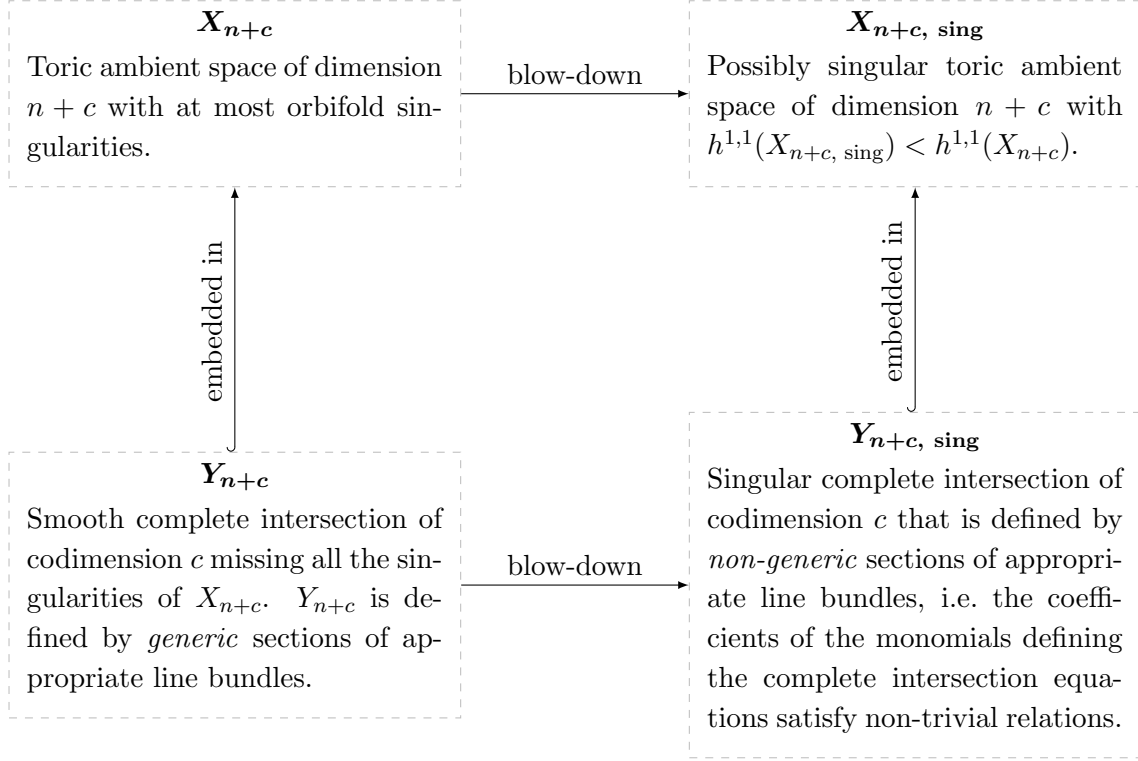


Figure 2.4: Under the blow-down map, the ambient space X_{n+c} is mapped to a different ambient space $X_{n+c, \text{sing}}$ with $h^{1,1}(X_{n+c, \text{sing}}) < h^{1,1}(X_{n+c})$. Under this map the set of all complete intersections Y_n inside X_{n+c} is mapped to a set of Calabi-Yau manifolds inside $X_{n+c, \text{sing}}$ whose complex structure coefficients lie on a locus of positive codimension within the complex structure moduli space of complete intersections of the same homology class.

The second step is to split up the construction of X_{n+c} into appropriate sub-tasks in order to determine the relevant quantities that can be treated independently. We suggest the following separation of tasks:

1. By studying the global sections of the fibration that are generated by a subset of divisors of X_{n+c} , one can examine a subgroup of the Abelian gauge group called the toric Mordell-Weil group MW_T solely by studying the ambient space of the *generic* fiber of the fibration.
2. Focusing on the singularities of $Y_{n, \text{sing}}$ that lead to non-Abelian gauge groups in the compactified effective theory which originate from the fibration of X_{n+c} , one can harness the full power of toric geometry and translate the singularities into combinatorial objects called *tops*. These can then be studied (and in some cases even classified) on their own.
3. Finally, one can enumerate all fibrations with a given set of generic fibers and tops and

study the remaining properties that depend on the *whole* fibration.

In [figure 2.5](#) we depict this procedure.

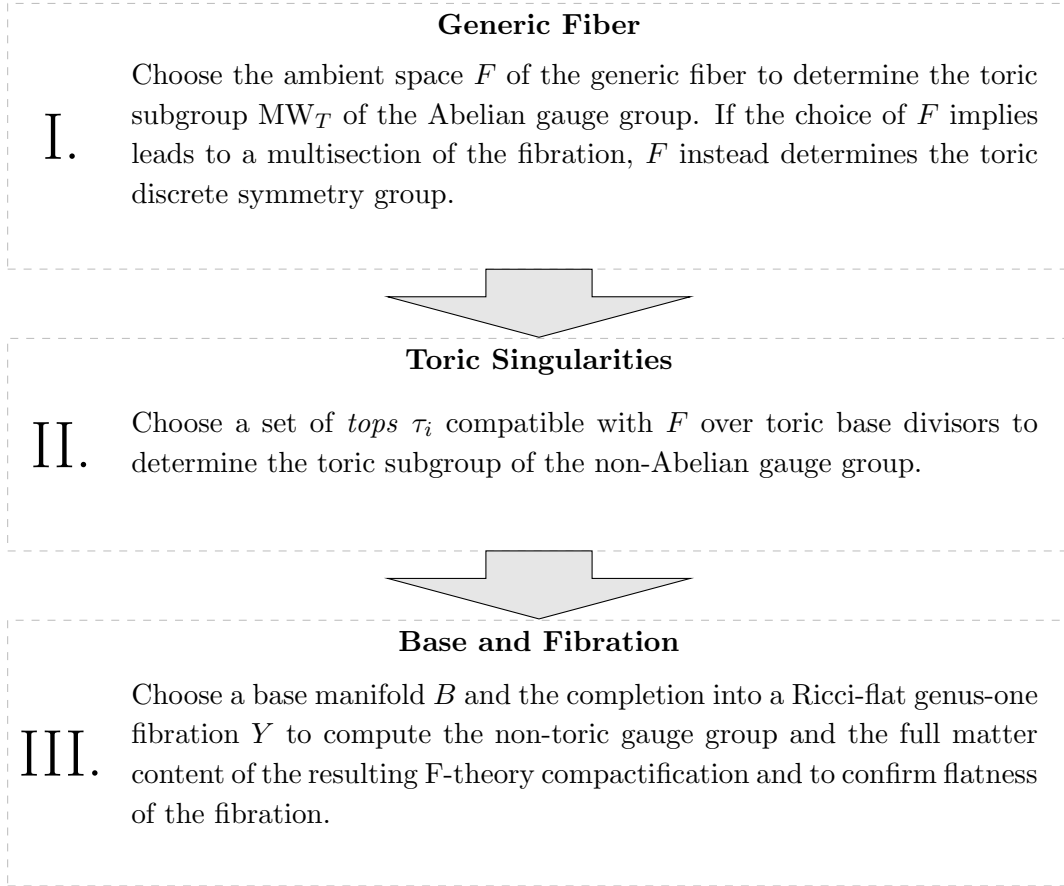


Figure 2.5: Engineering a genus-one fibered Calabi-Yau manifold Y_n can be split into three sub-tasks: Choosing an ambient space for the embedding of the generic fiber, selecting tops that determine the fibration of the ambient space X_{n+c} , and finally completing the ingredients with a base manifold into the full fibration.

The contents of this part of the thesis strictly follow this subdivision of tasks. In [chapter 3](#) we provide a framework to study genus-one curves inside arbitrary toric ambient spaces. [Chapter 4](#) is devoted to the engineering of singularities of the fibration and contains an in-depth explanation of what *tops* are. Finally, [chapter 5](#) provides an algorithm for combining these building blocks into full-fledged genus-one fibered Calabi-Yau manifolds.

Chapter 3

Fiber Curves of Genus One

Given a fibration whose generic fiber is a curve C of genus one and possibly a set of global sections defining points on the curve, the two main quantities one is interested in are:

- The discriminant Δ — it vanishes if and only if the genus-one curve is singular and contains information about the type of singularity.
- The discrete group MW_T generated by the global sections with respect to the group law on the curve.

Providing the means to compute these quantities for a large class of genus-one curves is the goal of this chapter and we approach the problem as illustrated in [figure 3.1](#): If the curve is defined as a hypersurface inside the weighted projective space \mathbb{P}_{231} then it has long been known how to determine Δ and MW_T . Furthermore, every genus-one curve with at least one special point (i.e. an elliptic curve) can be embedded in \mathbb{P}_{231} . If the genus-one curve has no special point (that is, the fibration has no global section), then there exists an intermediate map taking C to its Jacobian $\text{Jac}(C)$, which is an elliptic curve. The discriminant of the Jacobian is the same as the discriminant of C and it therefore suffices to embed $\text{Jac}(C)$ inside \mathbb{P}_{231} . Given the distinguished role that \mathbb{P}_{231} plays, it is natural to wonder why one should ever want to consider other ambient spaces. The underlying reason is that it is much simpler to treat smooth spaces. If the elliptic curve (or more generally, the Calabi-Yau manifold) is not a smooth complete intersection inside the toric ambient space, then it is much harder to deduct properties of the complete intersection geometry from the toric ambient space geometry that we have under firm control. However, the embedding into \mathbb{P}_{231} does not necessarily have to map the curve onto a smooth curve and therefore it simplifies many calculations to start with the curve embedded into a different space in which the singularities are resolved.

These concepts will be explained in more detail later on, but put in a nutshell, the problem of computing Δ and MW_T of an arbitrary genus-one fibration can be reduced to finding an embedding of the fiber into \mathbb{P}_{231} . In [section 3.1](#) we therefore review the geometry

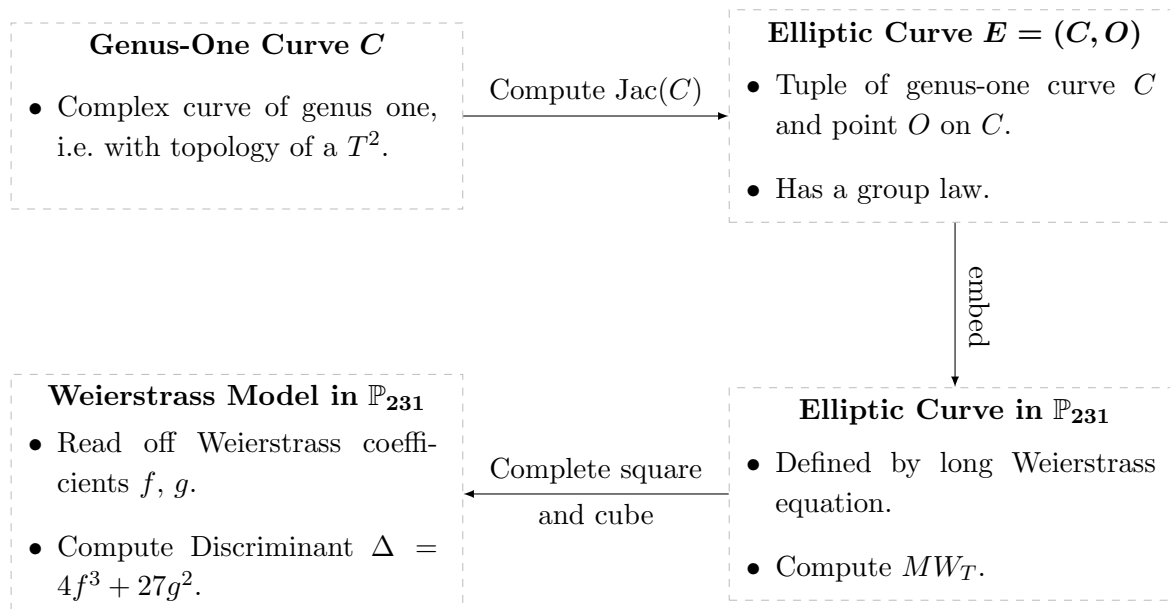


Figure 3.1: For every elliptic curve, there is guaranteed to exist an embedding into \mathbb{P}_{231} and we can compute Δ and MW_T for the embedded curve. If the genus-one fibration has no section, then MW_T is trivial, anyway. To compute Δ of a genus-one curve C , one can equally well compute the discriminant of the Jacobian of C , $\text{Jac}(C)$, which *is* an elliptic curve.

of elliptic curves inside \mathbb{P}_{231} and explain how to compute their discriminant, read off the singularity types, and compute MW_T . To substantiate the claim that every elliptic curve can be embedded into \mathbb{P}_{231} , we recall the embeddings of general genus-one curves in [section 3.2](#) using the line bundles on the curves. This leads us straight to [section 3.3](#), where we review line bundles on genus-one curves embedded inside toric varieties. [Section 3.4](#) contains the explicit algorithm that the previous sections have worked towards and [section 3.5](#) showcases its usefulness by applying it to all the 3134 genus-one curves that can be obtained as complete intersections of codimension two inside a toric variety. Given this set of discriminants, we perform in [section 3.6](#) a quick survey of the singularities that the genus-one curves in different ambient spaces generically develop in the blow-down limit.

The next sections deal with computing MW_T . In [section 3.7](#) we study global sections of genus-one fibrations and, among other things, define what is meant precisely by the *toric* sections that generate MW_T . This is followed by a classification of the toric Mordell-Weil groups for elliptic curves up to codimension two in [section 3.8](#). Last but not least, we comment on a few properties of genus-one fibrations *without* section and their relation to fibers with multiple sections in [section 3.9](#).

3.1 Weierstrass Models

The most general genus-one curve inside the weighted projective space \mathbb{P}_{231} is defined by the *long Weierstrass equation*

$$C : y^2 + a_1xyz + a_3yz^3 = x^3 + a_2x^2z^2 + a_4xz^4 + a_6z^6, \quad (3.1.1)$$

where the a_i determine the complex structure of C . We first explain how to compute the discriminant Δ of C , before proceeding with an explanation of the group law on the curve. To find Δ , one must complete the square with respect to y and the cube with respect to x .¹ One obtains the *short Weierstrass equation*

$$E : y^2 = x^3 + fxz^4 + gz^6 \quad (3.1.2)$$

with *Weierstrass coefficients*

$$\begin{aligned} f &= \left(\frac{1}{48}\right) \cdot (-a_1^4 - 8a_1^2a_2 - 16a_2^2 + 24a_1a_3 + 48a_4) \\ g &= \left(\frac{1}{864}\right) \cdot (a_1^6 + 12a_1^4a_2 + 48a_1^2a_2^2 - 36a_1^3a_3 + 64a_2^3 - 144a_1a_2a_3 \\ &\quad - 72a_1^2a_4 + 216a_3^2 - 288a_2a_4 + 864a_6). \end{aligned} \quad (3.1.3)$$

Note that the point $O : [1 : 1 : 0]$ is always a solution to the above equations, making the pair $E \equiv (C, O)$ an elliptic curve. Somewhat imprecisely, we often say that C is an elliptic curve, but we always mean the pair (C, O) . Since the two equations (3.1.1) and (3.1.2) are called *Weierstrass equations*, one often calls F-theory models with such elliptic fibers *Weierstrass models*.

Next, consider Equation 3.1.1 in the affine patch $U_{x,y}$ defined by $z = 1$. Only O is not contained in this patch. Restricted to $U_{x,y}$, C is the double cover of the complex plane together with two branch cuts: One branch cut connects two of the roots of the cubic polynomial in x given by the right-hand side of Equation 3.1.2 and the second branch cut reaches from the remaining root to O , the point at infinity. C becomes singular if and only if (at least) one of its cycles shrinks. From figure 3.2 it is obvious that this happens when at least two of the roots of the cubic polynomial in x collide, i.e. if and only if the discriminant

$$\Delta = 4f^3 + 27g^2 \quad (3.1.4)$$

of said polynomial vanishes. Given an elliptic curve in short Weierstrass form, we can thus always compute its discriminant. As a side remark, we note that f , g , and Δ are not invariant under rescalings of the homogeneous coordinates according to $[x : y : z] \cong [\lambda^2x : \lambda^3y : \lambda z]$ with $\lambda \in \mathbb{C}^*$. Applying such a rescaling to Equation 3.1.1 and dividing by λ^6 , one has that

$$f \mapsto \lambda^{-4}f, \quad g \mapsto \lambda^{-6}g, \quad \Delta \mapsto \lambda^{-12}\Delta. \quad (3.1.5)$$

¹For this to be possible, the characteristic of the field the a_i belong to must neither be two nor three.

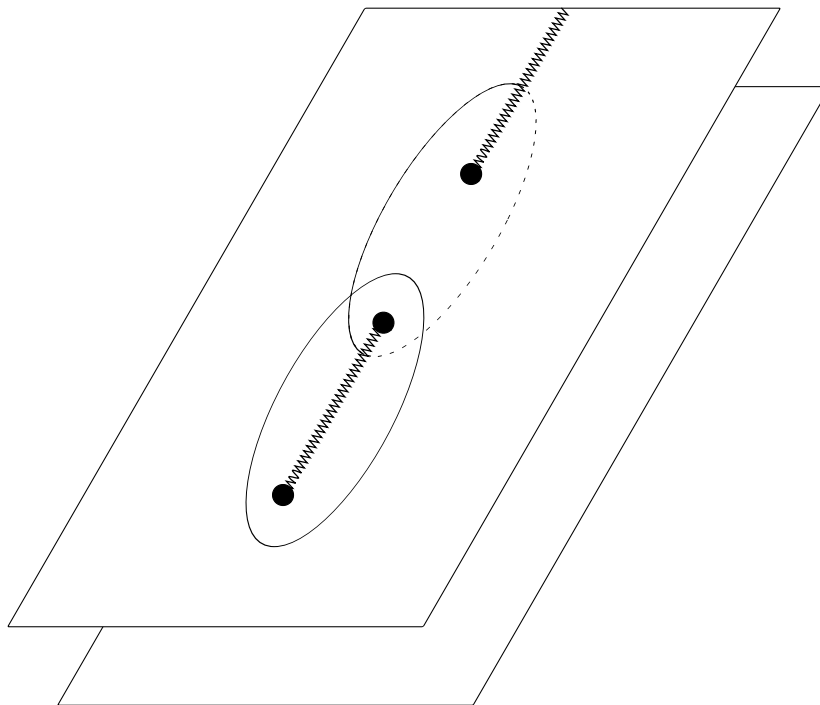


Figure 3.2: A visualization of Equation 3.1.2 restricted to the affine patch $U_{x,y}$ parametrized by x and y . Since Equation 3.1.2 is quadratic in y and cubic in x , y undergoes a monodromy $y \mapsto -y$ along small circles around the zeroes in x and along a circle around ∞ . Demanding that y be single-valued, E is thus described by a double cover of \mathbb{C} with one branch cut connecting two of the zeroes in x and a second cut connecting the third zero and infinity. Here we have drawn the branch cuts in zigzag lines and illustrated a valid choice of one-cycles generating the homology group $H_1(E, \mathbb{Z})$.

However, the j -invariant

$$j(\tau) = 1728 \frac{4f^3}{4f^3 + 27g^2} \quad (3.1.6)$$

does remain unmodified.

In general, one can consider elliptic curves over more exotic fields, such as function fields. Of special relevance to us are Calabi-Yau manifolds that have an elliptic fibration. Then the elliptic curve is defined by an equation of the form of Equation 3.1.1 in which the coefficients a_i are rational functions in the complex variables parametrizing the base manifold B and the elliptic curve is defined over the function field consisting of such rational functions. In this case, Δ is a rational function and its vanishing locus defines a divisor in the base manifold. Over this divisor the elliptic fiber is singular. In fact, the triple (f, g, Δ) contains more information than only the *location* of the singularities: It also encodes the *type* of singularity.

Denote by u_0 a normal coordinate to an irreducible component Σ of the divisor $\Delta = 0$. Then the vanishing orders of f , g and Δ with respect to u_0 determine the singularity type along Σ . For example, consider a base locus along which f and g remain non-zero, but Δ vanishes quadratically:

$$f = \mathcal{O}(1), \quad g = \mathcal{O}(1), \quad \Delta = \mathcal{O}(u_0^2). \quad (3.1.7)$$

Along this locus the whole fibration becomes singular and in the resulting low-energy effective theory there is a D7 brane with an $SU(2)$ gauge group. In the seminal work of [46],

	$\text{ord}_\Sigma(f)$	$\text{ord}_\Sigma(g)$	$\text{ord}_\Sigma(\Delta)$	eqn. of monodromy cover	$\mathfrak{g}(\Sigma)$
I_0	≥ 0	≥ 0	0	–	–
I_1	0	0	1	–	–
I_2	0	0	2	–	$\mathfrak{su}(2)$
$I_m, m \geq 3$	0	0	m	$\psi^2 + (9g/2f) _{z=0}$	$\mathfrak{sp}(\lfloor \frac{m}{2} \rfloor)$ or $\mathfrak{su}(m)$
II	≥ 1	1	2	–	–
III	1	≥ 2	3	–	$\mathfrak{su}(2)$
IV	≥ 2	2	4	$\psi^2 - (g/z^2) _{z=0}$	$\mathfrak{sp}(1)$ or $\mathfrak{su}(3)$
I_0^*	≥ 2	≥ 3	6	$\psi^3 + (f/z^2) _{z=0} \cdot \psi + (g/z^3) _{z=0}$	\mathfrak{g}_2 or $\mathfrak{so}(7)$ or $\mathfrak{so}(8)$
$I_{2n-5}^*, n \geq 3$	2	3	$2n+1$	$\psi^2 + \frac{1}{4}(\Delta/z^{2n+1})(2zf/9g)^3 _{z=0}$	$\mathfrak{so}(4n-3)$ or $\mathfrak{so}(4n-2)$
$I_{2n-4}^*, n \geq 3$	2	3	$2n+2$	$\psi^2 + (\Delta/z^{2n+2})(2zf/9g)^2 _{z=0}$	$\mathfrak{so}(4n-1)$ or $\mathfrak{so}(4n)$
IV^*	≥ 3	4	8	$\psi^2 - (g/z^4) _{z=0}$	\mathfrak{f}_4 or \mathfrak{e}_6
III^*	3	≥ 5	9	–	\mathfrak{e}_7
II^*	≥ 4	5	10	–	\mathfrak{e}_8
non-min.	≥ 4	≥ 6	≥ 12	–	–

Table 3.1: Kodaira–Tate classification of singular fibers, monodromy covers, and gauge algebras, taken from [134]. The column with the gauge algebras is to be understood as follows: Assume that the defining equation of the monodromy cover splits into n irreducible pieces. Then the resulting gauge algebra is the n^{th} algebra listed in the last column.

Kodaira analyzed and classified all possible singularities of elliptic fibrations. His findings are summarized in table 3.1. Let us point out that strictly speaking, Kodaira’s classification only holds for elliptically fibered K3 manifolds. However, it is believed to also apply to higher-dimensional elliptic fibrations as long as one considers base loci of codimension one. In higher codimensions, more exotic singularities may occur [89, 102].

3.1.1 The Group Law inside \mathbb{P}_{231}

Let us begin with a general discussion of the group law on elliptic curves and assume that C is a genus-one curve inside \mathbb{P}_{231} as in Equation 3.1.1 and O is the point at infinity. O will be the neutral element of the group action that we are about to define. We call the pair (C, O)

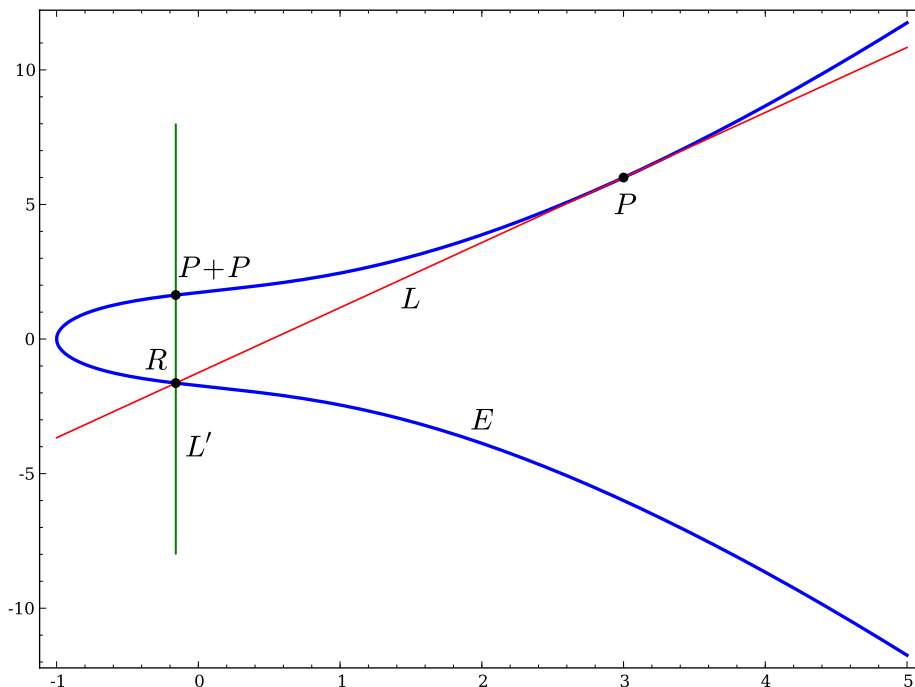


Figure 3.3: Example of the group law on the cubic $y^2 = x^3 + 2x + 3$ with the point at infinity as the neutral element. The point $P = (3 : 6 : 1)$ is, up to a sign, the single generator of the Mordell-Weil group $E(\mathbb{Q}) \simeq \mathbb{Z}$. The graphics shows how to compute $P + P$.

E. Furthermore, we restrict the a_i in the long Weierstrass equation to be elements of a field K , which we keep general for the time being.

Next, assume that P and Q are solutions to the equation defining C with coefficients in K . Then one can define an Abelian group action $+$: $E(K) \times E(K) \rightarrow E(K)$ as follows: If $P \neq Q$, let L be the line connecting P and Q , otherwise take it to be the line tangent to $P = Q$. According to Bézout's theorem, L intersects C precisely once more, at a point we call $R = P \diamond Q$. Next, we repeat the same procedure for R and the neutral element O and define

$$P + Q \equiv O \diamond R = O \diamond (P \diamond Q). \quad (3.1.8)$$

It is straightforward to check that this $+$ -map obeys all group axioms, even though the \diamond -map does not. In particular, $P + Q$ is an element of $E(K)$. [Figure 3.3](#) depicts the group law for an example curve. Let us remark that given a curve in Weierstrass form and a set of points P_i , one can equally well choose another point than O as the neutral element by adjusting the definition of [Equation 3.1.8](#) accordingly.

To apply this to the case relevant to us, let K again be the field of homogeneous rational functions in the complex variables parametrizing the base manifold B . Instead of points, one

now has global sections that cut out points over generic points in the base. Since the group of global sections is finitely generated, so is the group (called the *Mordell-Weil group*) that it generates in the generic fiber, which thus takes the form

$$\text{MW} = \mathbb{Z}^r \oplus \text{MW}_{\text{torsion}}, \quad (3.1.9)$$

where the torsion part $\text{MW}_{\text{torsion}}$ is a finite Abelian group.

As long as the a_i in Equation 3.1.1 are completely generic, the resulting elliptic fibration will have only a single section defined by the divisor $z = 0$ that cuts out the point $O : [1 : 1 : 0]$ and therefore its Mordell-Weil group will be trivial. More interesting are *non-generic* and in particular *singular* curves inside \mathbb{P}_{231} that one obtains by embedding curves inside other toric varieties into \mathbb{P}_{231} , as they may have more sections. Such cases will be studied in much greater detail in section 3.7 and section 3.8.

3.2 Embedding Genus-One Curves

In the introduction of this section, we stated without proof that every genus-one curve together with a choice of point on it can be embedded into \mathbb{P}_{231} . In this section we study more general embeddings of genus-one curves with line bundles of differing degree using an old argument by Deligne [135]. The embedding into \mathbb{P}_{231} then follows as a special case.

Let us begin by stating the Riemann-Roch theorem specialized to a curve C of genus one. Given a line bundle \mathcal{L} on C , the following holds:

$$h^0(C, \mathcal{L}) = \deg \mathcal{L} - g + 1 \quad (3.2.1)$$

In particular, the number of sections of \mathcal{L} is equal to its degree if C is a genus-one curve.

Next, let C be a genus-one curve and \mathcal{L} a line bundle of degree one. Denote the single section of \mathcal{L} by z . \mathcal{L}^2 has degree two and must thus have two sections. We know that one of them is z^2 and denote the other one by x . \mathcal{L}^3 is a degree-three line bundle, but we can only build two sections from the ones we know so far, namely xz and z^3 , so there must be a third one that we call y . Continuing this game, we find that \mathcal{L}^4 has four sections, but since we can construct all of them from the ones we already know (x^2, xz^2, yz, z^4), there is no need to introduce a new variable. Similarly, the five sections of \mathcal{L}^5 must be xy, x^2z, xz^3, yz^2 , and z^5 . Things change with \mathcal{L}^6 . As a degree-six line bundle, we know that it must have six independent sections, but we can construct seven:

$$x^3, xyz, x^2z^2, xz^4, y^2, yz^3, z^6 \quad (3.2.2)$$

Consequently, these seven sections must satisfy a linear relation among them. Redefining x , y , and z such as to absorb coefficients in front of x^3 and y^2 , one finds that such a relation is precisely the long Weierstrass form of Equation 3.1.1 and that the sections x , y , and z parametrize a \mathbb{P}_{231} .

The same procedure can be repeated starting with a line bundle of degree $d > 1$. As long as $d \leq 4$, one finds an embedding as a complete intersection into a (weighted) projective space and we list the four cases in [table 3.2](#). For $d > 4$, the embedding is no longer a complete intersection, which can lead to technical complications.

Degree of line bundle \mathcal{L}	Line bundle \mathcal{L}^k used for equation	Embedding space
1	\mathcal{L}^6	\mathbb{P}_{231}
2	\mathcal{L}^4	\mathbb{P}_{112}
3	\mathcal{L}^3	\mathbb{P}^2
4	\mathcal{L}^2	\mathbb{P}^3

Table 3.2: Given a genus-one curve C and a degree- d line bundle \mathcal{L} on it, one can use the sections of \mathcal{L} and its tensor powers as coordinates parametrizing an embedding space. For some k one will find that not all sections of \mathcal{L}^k built from sections of \mathcal{L}^m with $m < k$ are independent anymore and we give the smallest such k here. Then the relations between these sections define a hypersurface (or in the case of \mathbb{P}^3 a complete intersection) inside the embedding space.

To make a connection between line bundles and points on genus-one curves, note that a point P on a curve is a divisor and there exists a dual line bundle $\mathcal{O}(P)$ of degree one. Given a genus-one curve and a point on it, one can thus always use the line bundle $\mathcal{O}(P)$ to find an embedding into \mathbb{P}_{231} . Put differently, every elliptic curve can be written in the Weierstrass form of [\(3.1.1\)](#).

For a genus-one curve and $n > 1$ points P_1, \dots, P_n , there exist multiple embeddings obtained by using any of the line bundles $\mathcal{O}(P_1)$, $\mathcal{O}(P_1 + P_2)$, \dots , $\mathcal{O}(\sum_i P_i)$. Note however, that in a certain sense, embeddings using line bundles of degree $d > 1$ are different from embeddings into \mathbb{P}_{231} . As we saw above, every fibration with fiber in \mathbb{P}_{231} has a global section defined by $z = 0$. In the case of higher-degree embeddings, there is no such coordinate that would define a section. Since the homogeneous coordinates of the spaces \mathbb{P}_{112} , \mathbb{P}^2 , and \mathbb{P}^3 correspond to sections of line bundles of degree $d = 2, 3, 4$, setting them to zero cuts out d points in the generic fiber. In general, these points will undergo monodromies as one moves along the base manifold and it is therefore impossible to split the divisor intersecting the fiber in d points into d divisors cutting out only single points (i.e. sections). Only for special choices of the complex structure does the divisor split into reducible parts. In particular, the genus-one curves are singular at these loci in complex structure moduli space.

In summary, the degree- d with $d > 1$ embeddings of fibrations with at least d global sections map the fibers to singular curves inside \mathbb{P}_{112} , \mathbb{P}^2 , and \mathbb{P}^3 . Only after resolving $d - 1$ times do the curves become smooth. Put differently, a generic fibration with fiber inside \mathbb{P}_{112} , \mathbb{P}^2 , or \mathbb{P}^3 does not have a section, but instead their homogeneous coordinates define two-sections, three-sections and four-sections, respectively. The relations between curves inside

these different spaces are illustrated in [figure 3.4](#). In [section 3.9](#) we discuss genus-one curves inside \mathbb{P}_{112} , \mathbb{P}^2 , and \mathbb{P}^3 in detail. There we also show explicitly the conditions on the complex structure moduli for a curve to have multiple sections and explain how to resolve the resulting singularities.

3.2.1 The Jacobian

Having understood how to embed elliptic curves into \mathbb{P}_{231} , what remains to be seen is how to treat a general genus-one curves without the additional choice of a point on them. As fibrations with these fibers do not possess global sections, there is no point in computing their Mordell-Weil groups, but one would still like to find their discriminants. To this end, we introduce the concept of the *Jacobian variety* $\text{Jac}(C)$ of a genus-one curve C . $\text{Jac}(C)$ is isomorphic to C , has the same discriminant and has an Abelian group structure. If C has a distinguished point O and is thus an elliptic curve, then the group structure of $\text{Jac}(C)$ is the same as the group structure of (C, O) .

Consider an elliptic curve (C, O) . The group of degree-zero divisors modulo principal divisors on C is called $\text{Pic}^0(C)$. One can show that the map

$$C \rightarrow \text{Pic}^0(C), \quad P \mapsto [P - O] \tag{3.2.3}$$

is both a group homomorphism (with respect to the elliptic curve group law on C and the addition in $\text{Pic}^0(C)$) and a bijection. In particular, $\text{Pic}^0(C)$ is defined for any genus-one curve C and is therefore the more general concept. The Jacobian variety $\text{Jac}(C)$ is a one-dimensional variety that has the group structure of $\text{Pic}^0(C)$.

To gain a bit more intuition, we now assume that C is defined over the complex numbers so that we can define coordinates on $\text{Jac}(C)$. Let A and B be two one-cycles generating $H_1(C, \mathbb{Z})$ and let λ be the unique holomorphic one-form on C . Then the two periods of λ , $\int_A \lambda$ and $\int_B \lambda$ generate a lattice $\Lambda \cong \mathbb{Z}^2$. Since C is defined over the complex numbers, there exist solutions and we can pick a base point $p_0 \in C$. The Abel-Jacobi map defined via

$$C \rightarrow \text{Jac}(C) \cong \mathbb{C}/\Lambda, \quad p \mapsto \left(\int_{p_0}^p \lambda \right) \pmod{\Lambda} \tag{3.2.4}$$

is a map from the genus-one curve to its Jacobian variety. Note that one can naturally extend the map to degree-zero divisors of C and that there exist theorems (by Abel and Jacobi) showing that the extended map is a bijection between $\text{Pic}^0(C)$ and $\text{Jac}(C)$.

Crucially, the Jacobian variety of a genus-one curve is an *elliptic curve*, as becomes clear from the representation as a quotient \mathbb{C}/Λ : Here, the group law is just the addition of complex numbers modulo Λ and the neutral element (and thus the distinguished point) is zero. As a consequence, one can embed $\text{Jac}(C)$ in \mathbb{P}_{231} . Evidently, $\text{Jac}(C)$ is singular whenever Λ does not generate a lattice, which in turn is precisely when one of the cycles of C shrink. Hence, C and $\text{Jac}(C)$ share the same discriminant.

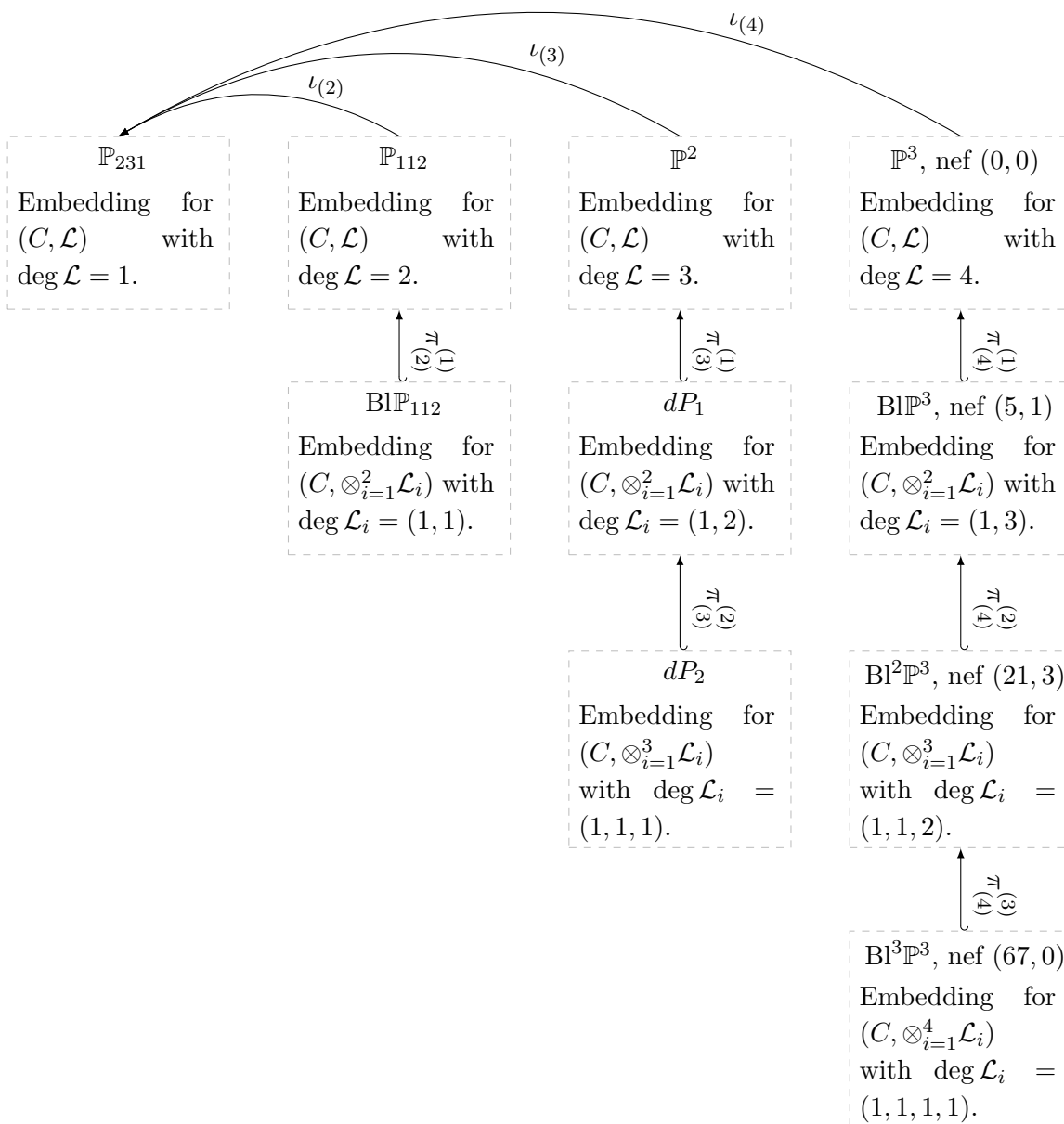


Figure 3.4: The spaces that a genus-one curve with line bundle of degree up to four can be embedded into using the (generalized) argument of Deligne. If the line bundle is the tensor product of smaller-degree line bundles, then the natural embeddings are not into \mathbb{P}_{231} , \mathbb{P}_{112} , \mathbb{P}^2 , and \mathbb{P}^3 , but into spaces obtained from these by blowing up. The i^{th} blow-down map of the space into which a genus-one curve with j marked points can be embedded is $\pi_{(j)}^{(i)}$. The maps $\iota_{(j)}$ are $j^2 : 1$ and (up to isogeny) map the genus-one curve to its Jacobian inside \mathbb{P}_{231} .

Finally, we remark that there exist methods in the literature that compute the short Weierstrass form of the Jacobian of general genus-one curves inside \mathbb{P}_{112} , \mathbb{P}^2 , and \mathbb{P}^3 [136, 137]. These methods are based on classical invariant theory [138] and have been implemented in Sage [139]. As we will see later, it is important to point out that these maps are generally not injective, but rather $4 : 1$, $9 : 1$, and $16 : 1$. That is, the map from the Jacobian of the embedding of a genus-one curve with degree- d line bundle to Weierstrass form inside \mathbb{P}_{231} is $d^2 : 1$.

3.3 Line Bundles on Curves Inside Toric Varieties

Computing a genus-one curve's embedding into Weierstrass form depends crucially on determining and controlling the sections of line bundles on the curve, as we learned in [section 3.2](#). So far, our discussion has been independent of the embedding of these genus-one curves, since all the relevant quantities were intrinsic to the curves themselves. Now, however, it is time to consider the specific set-ups we are interested in, namely genus-one curves embedded as complete intersections inside Gorenstein Fano toric varieties. As often in such constructions, we hope to obtain the relevant line bundles on the genus-one curves from restrictions of line bundles of the ambient space. If that is the case, then we can exploit theorems from toric geometry in order to study the line bundles on the complete intersection curve. It is the intention of this section to discuss the relations between line bundles (and their sections) on a complete intersection and the line bundles on the toric ambient space.

3.3.1 Sections of Line Bundles on Hypersurfaces

Line bundles on toric hypersurfaces are considerably easier to treat than complete intersections. In order to compute the line bundle cohomology on the anticanonical hypersurface inside a toric variety X , one can simply use the short exact sequence of sheaves

$$0 \longrightarrow \mathcal{O}_X(K_X) \longrightarrow \mathcal{O}_X \longrightarrow \mathcal{O}_Y \longrightarrow 0, \quad (3.3.1)$$

where $-K_X$ is the anticanonical divisor of X and Y is the genus-one curve that it cuts out. The short exact sequence induces a long exact sequence

$$0 \longrightarrow H^0(X, \mathcal{O}_X(K_X)) \longrightarrow H^0(X, \mathcal{O}_X) \longrightarrow H^0(Y, \mathcal{O}_Y) \longrightarrow H^1(X, \mathcal{O}_X(K_X)) \longrightarrow \dots \quad (3.3.2)$$

in cohomology. By tensoring [Equation 3.3.1](#) with a line bundle \mathcal{L} , one can compute the line bundle cohomology of $\mathcal{L}|_Y$ on Y

$$0 \longrightarrow H^0(X, \mathcal{L} \otimes \mathcal{O}_X(K_X)) \longrightarrow H^0(X, \mathcal{L}) \longrightarrow H^0(Y, \mathcal{L}|_Y) \longrightarrow H^1(X, \mathcal{L} \otimes \mathcal{O}_X(K_X)) \longrightarrow \dots \quad (3.3.3)$$

and one finds that there are two sources of sections of $\mathcal{L}|_Y$:

$$H^1(X, \mathcal{L} \otimes \mathcal{O}(K_X)) \oplus H^0(X, \mathcal{L}) \quad (3.3.4)$$

This is in fact a general problem when studying algebraic varieties as embedded subvarieties. The sections of a line bundle $\mathcal{L}|_Y$ may or may not extend to sections of \mathcal{L} over the whole ambient space $X \supset Y$. If they do not, then the choice of ambient space was an inconvenient one. One should either look for a different ambient space to embed into, or for a different line bundle on the ambient space whose sections behave more favorably.

3.3.2 Sections of Line Bundles on Complete Intersections

The generalization of the previous subsection to complete intersections of codimension greater than one requires additional mathematical formalism, which we briefly review next.

Koszul and Residues

The one indispensable tool for studying complete intersections is the Koszul complex and the associated hypercohomology spectral sequence. In the interest of a self-contained presentation let us quickly review these and refer to [140] for more details.

The simplest way to think of line bundle valued cohomology groups $H^k(\mathbb{P}^d, \mathcal{O}(n))$ is as holomorphic degree- k differential forms that transform like degree- n homogeneous polynomials under rescalings of the homogeneous coordinates. More generally, we can consider multiple homogeneous rescalings which just amounts to a toric variety X and line bundle \mathcal{L} . Then $H^k(X, \mathcal{L})$ are holomorphic degree- k differential forms, transforming like homogeneous polynomials whose degree of homogeneity is determined by the line bundle \mathcal{L} . Ultimately, we are interested in a Calabi-Yau submanifold $Y \subset X$ cut out by two² transverse polynomials $p_1 = p_2 = 0$. There are three ways to obtain a degree- k differential form on Y :

1. Restriction of a degree- k form on X ,
2. Residue integration of a degree- $(k+1)$ form around a small circle around either $p_1 = 0$ or $p_2 = 0$, and
3. Two-fold residue integration around $p_1 = p_2 = 0$ of a degree- $(k+2)$ form.

It is convenient to define the residue operators $\text{Res}_j(\omega) = \frac{1}{2\pi i} \oint \frac{(p_j \omega)}{p_j}$ and split the potential contributions $E_1^{p,q}$ to $H^{p+q}(Y, \mathcal{L}|_Y)$ into $(-p)$ -fold residues of q -forms. Note the minus sign in the definition of p , as the residue operator has differential degree -1 . We also have to be careful with the degree under homogeneous rescalings, as the residue operator Res_j

²The whole discussion of this section generalizes to arbitrary codimension, but for simplicity we restrict ourselves to codimension two.

has us multiply by the homogeneous polynomial p_j . The polynomial p_j defines a divisor $D_j = V(p_j) = \{p_j = 0\}$, and the cohomology groups of the line bundle $\mathcal{O}(D_j)$ precisely involve differential forms of the same degree of homogeneity as p_j . Hence, the residue operator actually maps

$$\text{Res}_j : H^{k+1}(X, \mathcal{L} \otimes \mathcal{O}(-D_j)) \longrightarrow H^k(Y, \mathcal{L}|_Y). \quad (3.3.5)$$

Putting everything together, the potential contributions to the cohomology for a three-dimensional toric variety X fill out the tableau

$$E_1^{p,q}(\mathcal{L}) =$$

$q=3$	$H^3(X, \mathcal{L} \otimes \mathcal{O}(-D_1 - D_2))$	$H^3(X, \mathcal{L} \otimes \mathcal{O}(-D_1)) \oplus H^3(X, \mathcal{L} \otimes \mathcal{O}(-D_2))$	$H^3(X, \mathcal{L})$
$q=2$	$H^2(X, \mathcal{L} \otimes \mathcal{O}(-D_1 - D_2))$	$H^2(X, \mathcal{L} \otimes \mathcal{O}(-D_1)) \oplus H^2(X, \mathcal{L} \otimes \mathcal{O}(-D_2))$	$H^2(X, \mathcal{L})$
$q=1$	$H^1(X, \mathcal{L} \otimes \mathcal{O}(-D_1 - D_2))$	$H^1(X, \mathcal{L} \otimes \mathcal{O}(-D_1)) \oplus H^1(X, \mathcal{L} \otimes \mathcal{O}(-D_2))$	$H^1(X, \mathcal{L})$
$q=0$	$H^0(X, \mathcal{L} \otimes \mathcal{O}(-D_1 - D_2))$	$H^0(X, \mathcal{L} \otimes \mathcal{O}(-D_1)) \oplus H^0(X, \mathcal{L} \otimes \mathcal{O}(-D_2))$	$H^0(X, \mathcal{L})$
	$p=-2$	$p=-1$	$p=0$

$$\Rightarrow H^{p+q}(Y, \mathcal{L}|_Y). \quad (3.3.6)$$

with the map to H^{p+q} being either $\text{Res}_1 \text{Res}_2$, $\text{Res}_1 \oplus \text{Res}_2$, or restriction for the three respective columns. That way, the entries along the diagonal can contribute to $H^{p+q}(Y, \mathcal{L}|_Y)$, but we have no reason to believe that these are all independent.

In particular, the restrictions of two different k -forms α_1, α_2 may very well be cohomologous on Y , even if they are not on X . Clearly, this is the case when $\alpha_1 - \alpha_2 = d \text{Res}(\omega)$ for some k -form ω . Similarly, two forms on Y that came from different residues might be related by a double residue. This is implemented by a nilpotent³ differential $d_1 : E_1^{p,q} \rightarrow E_1^{p+1,q}$. Only the cohomology with respect to d_1 has a chance of contributing to $H^{p+q}(Y, \mathcal{L}|_Y)$. We arrange the d_1 -cohomology groups in the E_2 -tableau

$$E_2^{p,q} = \frac{\ker(d_1 : E_1^{p,q} \rightarrow E_1^{p+1,q})}{\text{img}(d_1 : E_1^{p-1,q} \rightarrow E_1^{p,q})}. \quad (3.3.7)$$

Unfortunately, this is not the end of it and even a d_1 -cohomology class need not survive to a non-zero element of $H^{p+q}(Y, \mathcal{L}|_Y)$. This is the case when two different k -forms α_1, α_2 on X are related via a double residue of a $(k+1)$ -form, $\alpha_1 - \alpha_2 = d \text{Res}_1 \text{Res}_2(\omega)$. This is implemented by yet another nilpotent differential $d_2 : E_2^{p,q} \rightarrow E_2^{p+2,q-1}$. Its cohomology forms the entries of the E_3 -tableau.

In general, a spectral sequence is an infinite sequence of tableaux $E_i^{p,q}$ and differentials $d_i : E_i^{p,q} \rightarrow E_i^{p+i,q+1-i}$. In the case of a two-fold complete intersection, this process stabilizes at $E_3 = E_\infty$ because all higher differentials are starting or ending outside of the 3×4 region

³That $d_1^2 = 0$ requires a suitable sign choice; schematically $d_1^{p=-2} = (p_1, p_2)$ and $d_1^{p=-1} = \begin{pmatrix} -p_2 \\ p_1 \end{pmatrix}$.

with the non-zero entries. The diagonals of the E_∞ tableau are a filtration of the cohomology groups $H^{p+q}(Y, \mathcal{L}|_Y)$. In particular, this implies that

$$\dim H^k(Y, \mathcal{L}|_Y) = \sum_{p+q=k} \dim E_\infty^{p,q} \quad (3.3.8)$$

and therefore one can reconstruct the dimension of the line bundle cohomology groups on the complete intersection from the knowledge of the dimensions of the E_∞ tableau entries.

Sections of Line Bundles on Complete Intersections

For a complete intersection $Y \subset X$ of two equations, that is, sections of $\mathcal{O}(D_1)$ and $\mathcal{O}(D_2)$, the analogous Koszul resolution of the structure sheaf to the hypersurface case of [Equation 3.3.1](#) is

$$0 \longrightarrow \underbrace{\mathcal{O}_X(-D_1 - D_2)}_{\mathcal{R}^{-2}} \longrightarrow \underbrace{\mathcal{O}_X(-D_1) \oplus \mathcal{O}_X(-D_2)}_{\mathcal{R}^{-1}} \longrightarrow \underbrace{\mathcal{O}_X}_{\mathcal{R}^0} \longrightarrow \mathcal{O}_Y \longrightarrow 0. \quad (3.3.9)$$

A long exact sequence is just a spectral sequence whose E_1 tableau has only two non-zero adjacent columns. Now, we have *three* columns $q = -2, -1, 0$ in the spectral sequence

$$E_1^{p,q} = H^q(X, \mathcal{L} \otimes \mathcal{R}^p) \quad \Rightarrow \quad H^{p+q}(X, \mathcal{L} \otimes \mathcal{O}_Y) = H^{p+q}(Y, \mathcal{L}|_Y). \quad (3.3.10)$$

The first differential d_1 is just the induced map of [Equation 3.3.9](#) on the sheaf cohomology groups as familiar from the hypersurface case. However, we now have two new effects to consider:

- There are *three* sources for sections of the line bundle \mathcal{L}_Y restricted to the complete intersection, namely

$$\bigoplus_p E_1^{p,-p} = H^2(X, \mathcal{L} \otimes \mathcal{R}^{-2}) \oplus H^1(X, \mathcal{L} \otimes \mathcal{R}^{-1}) \oplus H^0(X, \mathcal{L}). \quad (3.3.11)$$

- There is a higher differential $d_2 : H^1(X, \mathcal{L} \otimes \mathcal{R}^{-2}) \rightarrow H^0(X, \mathcal{L})$ that will identify sections of \mathcal{L} beyond the obvious identifications (coming from d_1).

The first point point is the same one that we encountered for hypersurfaces and again, it may well be that a section of $\mathcal{L}|_Y$ cannot be obtained by restricting sections of \mathcal{L} . More interesting is the second point, which we will now discuss in detail.

The Second Differential

Consider a nef partition $-K = D_1 + D_2$ of the anticanonical divisor of the three-dimensional ambient toric variety into two numerically effective divisors D_1 and D_2 . The complete intersection elliptic curve Y is defined by two polynomials p_1, p_2 as

$$Y = V(p_1) \cap V(p_2), \quad p_1 \in H^0(X, \mathcal{O}_X(D_1)), \quad p_2 \in H^0(X, \mathcal{O}_X(D_2)), \quad (3.3.12)$$

Homogeneous coordinate z	x_0	x_1	y_0	y_1	y_2
Point $n_z \in \nabla$	$\begin{pmatrix} 1 \\ 0 \\ 0 \end{pmatrix}$	$\begin{pmatrix} -1 \\ 0 \\ 0 \end{pmatrix}$	$\begin{pmatrix} 0 \\ 1 \\ 0 \end{pmatrix}$	$\begin{pmatrix} 0 \\ 0 \\ 1 \end{pmatrix}$	$\begin{pmatrix} 0 \\ -1 \\ -1 \end{pmatrix}$

Table 3.3: The toric variety $\mathbb{P}^1 \times \mathbb{P}^2$.

where $V(p)$ denotes the divisor defined by $p = 0$. A section s of a line bundle \mathcal{L} always defines a section s_Y of $\mathcal{L}|_Y$ by restriction, but different sections on X might yield the same section on Y . Clearly, we can add any section vanishing on Y to s without changing the restriction. The obvious candidates of sections of \mathcal{L} vanishing on Y are the image

$$d_1 : H^0(X, \mathcal{L} \otimes \mathcal{O}(-D_1)) + H^0(X, \mathcal{L} \otimes \mathcal{O}(-D_2)) \xrightarrow{\begin{pmatrix} p_1 \\ p_2 \end{pmatrix}} H^0(X, \mathcal{L}) \quad (3.3.13)$$

Hence, the easy identifications just boil down to working with the quotient by the image of d_1 .

What this section is concerned about is another identification that we have to perform on the sections on the ambient space, coming from the d_2 differential. To clarify this, we will look at an explicit example. In fact, the example is very simple. Consider $\mathbb{P}^1 \times \mathbb{P}^2$ with the non-product nef partition $D_1 = \mathcal{O}(1, 1)$, $D_2 = \mathcal{O}(1, 2)$. We let x_0, x_1 be the two homogeneous coordinates on \mathbb{P}^1 and y_0, y_1, y_2 be the three homogeneous coordinates on \mathbb{P}^2 . The toric data is also summarized in [table 3.3](#). A particularly simple choice of equations that nevertheless defines a smooth complete intersection is

$$\begin{aligned} p_1 = x_0(y_0 + y_1) + x_1y_2 &\in H^0(\mathbb{P}^1 \times \mathbb{P}^2, \mathcal{O}_{\mathbb{P}^1 \times \mathbb{P}^2}(D_1)) \\ p_2 = x_0y_2^2 + x_1y_0y_1 &\in H^0(\mathbb{P}^1 \times \mathbb{P}^2, \mathcal{O}_{\mathbb{P}^1 \times \mathbb{P}^2}(D_2)). \end{aligned} \quad (3.3.14)$$

We now need to pick a line bundle \mathcal{L} on the ambient $\mathbb{P}^1 \times \mathbb{P}^2$. The lowest degree choice would be $\mathcal{O}(1, 0)$, which has degree two and would provide an embedding into \mathbb{P}_{112} . However, it has not enough sections on the ambient space. For example, we would need all four sections of $\mathcal{O}(1, 0)^2|_Y = \mathcal{O}(2, 0)|_Y$ to define the homogeneous coordinate of \mathbb{P}_{112} with weight two, but $\dim H^0(\mathbb{P}^1 \times \mathbb{P}^2, \mathcal{O}(1, 0)) = 3$. Hence, we are led to look at the next-smallest degree line bundle

$$\mathcal{L} = \mathcal{O}(0, 1), \quad H^0(\mathbb{P}^1 \times \mathbb{P}^2, \mathcal{L}) = \text{span}\{y_0, y_1, y_2\} \quad (3.3.15)$$

It is easy to see that the three sections of \mathcal{L} restrict to a basis of three independent sections of $H^0(Y, \mathcal{L}|_Y)$ on the complete intersection. We also remind the reader that the embedding in the degree-three case arises as the one relation between the ten cubic monomials $\text{Sym}^3 H^0(Y, \mathcal{L}|_Y)$ inside the nine-dimensional $H^0(Y, \mathcal{L}^3|_Y)$ and thus embeds the genus-one curve inside \mathbb{P}^2 . The

first tableau of the spectral sequence of [Equation 3.3.10](#) is

$$E_1^{p,q}(\mathcal{L}^3) = H^q(X, \mathcal{L}^3 \otimes \mathcal{R}^p) = \begin{array}{c|ccc} & & & \\ \hline q=3 & 0 & 0 & 0 \\ \hline q=2 & 0 & 0 & 0 \\ \hline q=1 & \mathbb{C} & 0 & 0 \\ \hline q=0 & 0 & 0 & \mathbb{C}^{10} \\ \hline & p=-2 & p=-1 & p=0 \\ \hline \end{array} \Rightarrow H^{p+q}(Y, \mathcal{L}^3|_Y). \quad (3.3.16)$$

Clearly, the relation among the ten sections of $H^3(\mathbb{P}^1 \times \mathbb{P}^2, \mathcal{L}^3)$ is not coming from d_1 because the domain vanishes, see [Equation 3.3.13](#). Instead, we have to quotient by the image of d_2 , which is clearly equivalent to knowing the embedding in \mathbb{P}^2 . But of course we do not know the embedding yet! Hence we have to go back to the geometry and use a different approach to find the relations between the sections.

3.4 Weierstrass Forms for Complete Intersections: The Algorithm

In order to find the relations between the sections that are imposed by the second differential, we propose to directly compute the relations between the sections on the ambient space by restricting to all affine coordinate patches. Clearly, two sections are equal if they are equal in every affine patch. In any given patch we can use a local trivialization to write the sections as polynomials, and polynomials are equal if and only if their difference is in the ideal generated by the inhomogenized defining equations. For example, consider the patch $x_1 = y_2 = 1$ in the example of [section 3.3.2](#). As it turns out, we only have to consider this single patch in this particular example. The inhomogenized defining equations define the ideal

$$I = \langle \hat{x}_0(\hat{y}_0 + \hat{y}_1) + 1, \hat{x}_0 + \hat{y}_0\hat{y}_1 \rangle = \langle \hat{x}_0\hat{y}_1^2 - \hat{x}_0^2 + \hat{y}_1, \hat{x}_0\hat{y}_0 + \hat{x}_0\hat{y}_1 + 1, \hat{y}_0\hat{y}_1 + \hat{x}_0 \rangle, \quad (3.4.1)$$

where the second set of generators forms a degrevlex⁴ Gröbner basis and we have denoted the inhomogeneous coordinates by hats. The ten cubics generating $\text{Sym}^3 H^0(Y, \mathcal{L}|_Y)$ are, in inhomogeneous coordinates,

$$\{\hat{y}_0^3, \hat{y}_0^2\hat{y}_1, \hat{y}_0\hat{y}_1^2, \hat{y}_1^3, \hat{y}_0^2, \hat{y}_0\hat{y}_1, \hat{y}_1^2, \hat{y}_0, \hat{y}_1, 1\}, \quad (3.4.2)$$

and their normal form modulo I is

$$\{\hat{y}_0^3, \hat{x}_0\hat{y}_1 + 1, -\hat{x}_0\hat{y}_1, \hat{y}_1^3, \hat{y}_0^2, -\hat{x}_0, \hat{y}_1^2, \hat{y}_0, \hat{y}_1, 1\}. \quad (3.4.3)$$

Hence, the single relation between the ten sections, after restricting them to the complete intersection and restoring the homogeneous coordinates, is

$$y_0^2 y_1 + y_0 y_1^2 - y_2^3 = 0. \quad (3.4.4)$$

⁴That is, a degree reverse lexicographic Gröbner basis.

This is now the well-known case of a cubic in three homogeneous variables parametrizing a \mathbb{P}^2 . Its short Weierstrass form is

$$Y^2 = X^3 + \frac{1}{4}, \quad (3.4.5)$$

which has discriminant $\Delta = \frac{27}{16}$ and j -invariant 0.

3.4.1 Kodaira Map

Given a complete intersection inside a Gorenstein Fano toric ambient space X , one will generally still have considerable freedom in choosing the line bundle \mathcal{L} which realizes the embedding as the relation between (powers of) restrictions of its sections to the genus-one curve. This is nothing but the Kodaira map. For example, in the degree-three case the three sections of \mathcal{L} just realize the Kodaira embedding of the elliptic curve Y in \mathbb{P}^2 . For the purpose of finding the embedding, we want the degree to be as small as possible, and in particular ≤ 4 . However, as we essentially study the elliptic curve through its Kodaira map, we can only consider line bundles of positive degree. Otherwise the Kodaira map would shrink Y to a point, which obviously would not retain any information. Therefore, a good starting point for looking for line bundles \mathcal{L} on the ambient toric variety is the cone in $H^2(X, \mathbb{Z})$ of line bundles with at least one section. This cone is generated by the first Chern classes of divisors $V(z_i)$ cut out by a single homogeneous coordinate. The degree on Y is a linear form

$$\deg(\mathcal{L}|_Y) = \int_X \omega_{D_1} \wedge \omega_{D_2} \wedge c_1(\mathcal{L}), \quad (3.4.6)$$

and so finding all candidates for appropriate line bundles is just a question of enumerating weighted integer vectors to up to a certain degree bound.

3.5 Weierstrass Forms for Complete Intersections: Results

Having formulated the algorithm as concretely as possible, we now wish to apply it to a sample set of toric elliptic curves. The Weierstrass forms of genus-one curves realized as toric hypersurfaces were already studied in [137], albeit using a somewhat different approach. Here we treat the considerably richer set of genus-one curves defined as complete intersections inside three-dimensional Gorenstein Fano toric varieties.

As reviewed in [section A.6](#), such a complete intersection elliptic curve is defined by a nef partition of a three-dimensional reflexive polytope. In three dimensions, there exist 4319 reflexive polytopes and these have 3134 distinct nef partitions. In [figure 3.5](#) and [figure 3.6](#) we provide a statistical overview of the distribution of nef partitions among the different reflexive polytopes. One important observation is that 16 of the 3134 nef partitions are direct

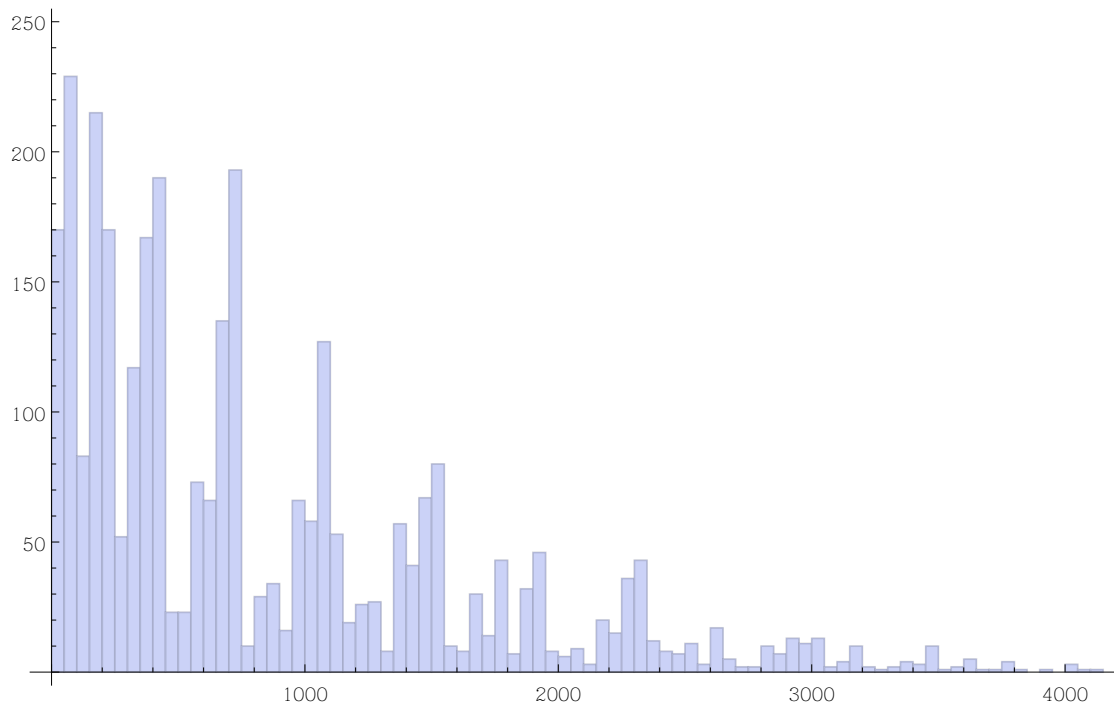


Figure 3.5: Histogram of the number of nef partitions of the 4319 reflexive polytopes in three dimensions.

products. Up to lattice isomorphisms, they are obtained as

$$\nabla_1 = \left\langle \begin{pmatrix} 1 \\ 0 \\ 0 \end{pmatrix}, \begin{pmatrix} -1 \\ 0 \\ 0 \end{pmatrix} \right\rangle_{\text{conv}}, \quad \nabla_2 = \left\langle \begin{pmatrix} 0 \\ v_i \end{pmatrix} \text{ where } v_i \in F_j \right\rangle_{\text{conv}}, \quad (3.5.1)$$

where F_j is one of the 16 reflexive polygons. Their PALP ids are contained in [table 3.4](#). The total ambient space corresponding to the face fan of Δ° is $\mathbb{P}^1 \times F_j$ and the complete intersection factors into a quadratic equation inside \mathbb{P}^1 and the anticanonical hypersurface in F_j . Therefore these nef partitions consist of two disjoint elliptic curves, each of which is described by a hypersurface inside a two-dimensional toric variety. Both of them have the same complex structure. Clearly, set-ups of this kind do not occur for genus-one curves defined as hypersurfaces.

We applied the algorithm to all of the 3118 remaining nef partitions and were able to compute the Weierstrass form for all but the two examples treated in [subsection 3.5.1](#). Whenever there were multiple line bundles that could be used to find an embedding of the genus-one curves, we determined all embeddings and confirmed that the j -invariant was indeed the same. Since the full list of results is too long to be included in the text of this thesis, we

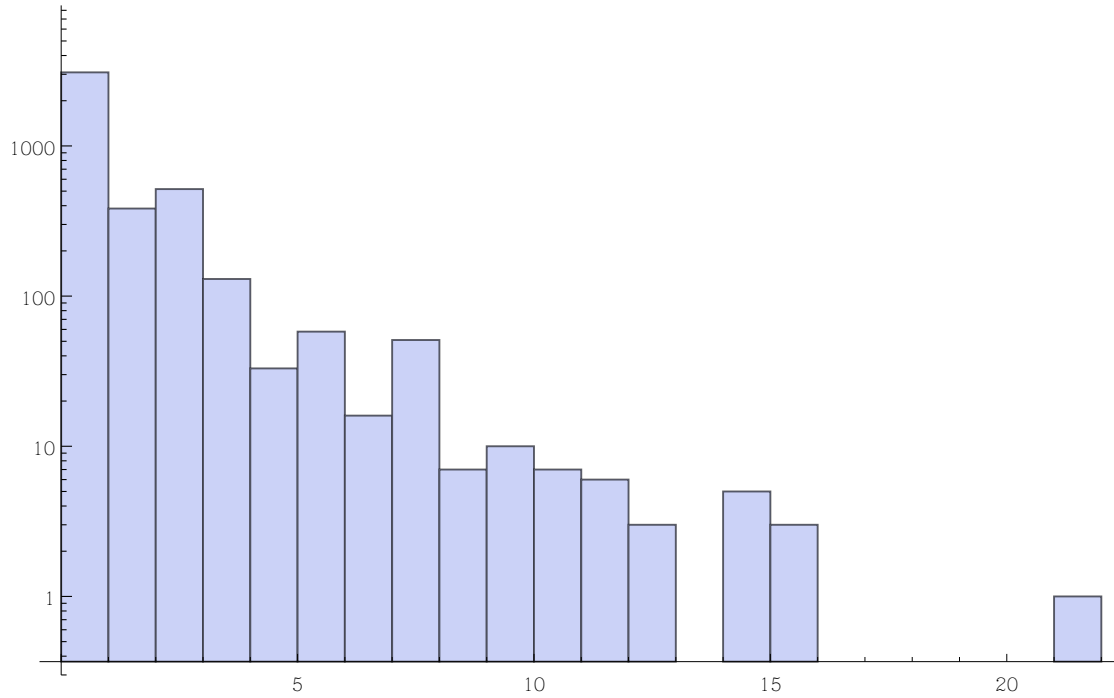


Figure 3.6: Histogram of the number of polytopes that have a given number of nef partitions. There are 3090 reflexive three-dimensional polytopes that do not admit a nef partition. The reflexive polytope with PALP id 214 has the most nef partitions, namely 21.

$\mathbb{P}^1 \times$	F_1	F_2	F_3	F_4	F_5	F_6	F_7	F_8
PALP id	(4, 2)	(30, 1)	(29, 3)	(17, 1)	(84, 8)	(61, 2)	(218, 0)	(149, 3)

$\mathbb{P}^1 \times$	F_9	F_{10}	F_{11}	F_{12}	F_{13}	F_{14}	F_{15}	F_{16}
PALP id	(194, 5)	(113, 0)	(283, 0)	(356, 3)	(453, 0)	(505, 0)	(509, 0)	(768, 1)

Table 3.4: The PALP ids for the 16 nef partitions that are direct products inside the spaces $\mathbb{P}^1 \times F_i$, where the F_i are the reflexive polygons defined in figure 3.7.

have created a website at

$$\text{http://wwth.mpp.mpg.de/members/jkeitel/Weierstrass/} \tag{3.5.2}$$

containing a database of Weierstrass forms. In subsection 3.8.2 we explain in detail how to extract the Weierstrass forms and other relevant information from the database.

3.5.1 Exceptions in Codimension Two

It turns out that there are only two three-dimensional nef partitions (out of 3134) for which the algorithm of section 3.4 fails, that is, there is no line bundle on the ambient toric variety such that

- The degree $\deg(\mathcal{L}|_Y) \leq 4$, and
- All required⁵ sections for finding the Weierstrass form are restrictions of sections from the ambient space.

The first exception is just $\mathbb{P}^1 \times \mathbb{P}^2$ with the nef partition $D_1 = \mathcal{O}(2, 1)$ and $D_2 = \mathcal{O}(0, 2)$. Again using $[x_0 : x_1] \in \mathbb{P}^1$ and $[y_0 : y_1 : y_2] \in \mathbb{P}^2$ as homogeneous coordinates, the two defining polynomials are

$$\begin{aligned} p_1 &= \sum_{i=0}^2 (a_{00i}x_0^2 + a_{01i}x_0x_1 + a_{11i}x_1^2)y_i, \\ p_2 &= \sum_{i,j=0}^2 b_{ij}y_iy_j = \begin{pmatrix} y_0 & y_1 & y_2 \end{pmatrix} \begin{pmatrix} b_{00} & b_{10} & b_{20} \\ b_{01} & b_{11} & b_{21} \\ b_{02} & b_{12} & b_{22} \end{pmatrix} \begin{pmatrix} y_0 \\ y_1 \\ y_2 \end{pmatrix}. \end{aligned} \quad (3.5.3)$$

Projection onto the \mathbb{P}^1 factor defines a map $Y = V(\langle p_1, p_2 \rangle) \rightarrow \mathbb{P}^1$. Its pre-image consists of two points: For fixed $[x_0 : x_1] \in \mathbb{P}^1$, the first equation p_1 is a line and the second equation p_2 is a conic in \mathbb{P}^2 , which necessarily intersect in two points. These two points can degenerate to a single point with multiplicity two, and they must do so at precisely four pre-images because a torus is the double cover of \mathbb{P}^1 branched at four branch points. In other words, the discriminant $\delta_{\mathbb{P}^1}$ of the double cover $Y \rightarrow \mathbb{P}^1$ is a quartic in the variables x_0, x_1 with coefficients involving a 's and b 's but no y 's.

The form of the discriminant is constrained by symmetry; $SL(2, \mathbb{C}) \times SL(3, \mathbb{C})$ acts naturally on the ambient space. The complete intersection Y is not invariant under this symmetry, but its Weierstrass form must be. More formally, we can combine the action on the homogeneous coordinates with an action on the coefficients such that the combined action does not change the equations p_1, p_2 . For example, the $M_3 \in SL(3, \mathbb{C})$ -part of the action is

$$\begin{pmatrix} y_0 \\ y_1 \\ y_2 \end{pmatrix} \mapsto M_3 \begin{pmatrix} y_0 \\ y_1 \\ y_2 \end{pmatrix}, \quad \begin{pmatrix} a_{ij0} \\ a_{ij1} \\ a_{ij2} \end{pmatrix} \mapsto M_3^{-1} \begin{pmatrix} a_{ij0} \\ a_{ij1} \\ a_{ij2} \end{pmatrix}, \quad (b_{ij}) \mapsto (M_3^{-1})^T (b_{ij}) M_3^{-1}. \quad (3.5.4)$$

A *covariant* is a polynomial that does not transform under the combined group action, obvious examples are p_1 and p_2 . An *invariant* is a covariant that, furthermore, does not depend on

⁵For degree-one, we require the sections of $\mathcal{L}, \mathcal{L}^2, \mathcal{L}^3$, and \mathcal{L}^6 . For degree-two, we require $\mathcal{L}, \mathcal{L}^2$, and \mathcal{L}^4 . For degree-three, we require \mathcal{L} and \mathcal{L}^3 . For degree-four, we require \mathcal{L} and \mathcal{L}^2 .

the homogeneous coordinates, for example $\det(b_{ij})$. The discriminant δ_1 that we are looking for must be a covariant of bi-degree $(4, 0)$ in $[x_0 : x_1]$ and $[y_0 : y_1 : y_2]$.

The tersest way to characterize δ_1 completely is as the Θ' -invariant [138, 141] of the system of two conics (p_1^2, p_2) . That is, ignore the action on the \mathbb{P}^1 factor for the moment and consider p_1^2 and p_2 as two quadratics in $[y_0 : y_1 : y_2]$. The determinant Δ of the coefficient matrix of a quadratic is clearly an invariant of the action on \mathbb{P}^2 , hence so is every ϵ -coefficient in the formal expansion⁶

$$\Delta(p_1^2 + \epsilon p_2) = \Delta(p_1^2) + \epsilon \Theta(p_1^2, p_2) + \epsilon^2 \Theta'(p_1^2, p_2) + \epsilon^3 \Delta(p_2) \quad (3.5.5)$$

We note that $\delta_1(x_0, x_1) = \Theta'(p_1^2, p_2)$ is quartic in x_0 and x_1 , quadratic in the coefficients a_{ijk} and quadratic in the coefficients b_{ij} . Finally, the equation of a double cover branched at the zeroes of δ_1 is

$$Y^2 = \delta_1(x_0, x_1), \quad (3.5.6)$$

for which we already know how to write the Weierstrass form [139, 142], as it is simply a genus-one curve inside \mathbb{P}_{112} .

It remains to consider the second exceptional case. Geometrically, it is the product $\mathbb{P}^1 \times dP_1$, that is, a simple blowup⁷ of the first case along a curve $\mathbb{P}^1 \times \{\text{pt.}\}$. Moreover, the two divisors defining the nef partition are just the pull-backs of the two divisors of the first case. In terms of toric geometry, this means that the dual polytope ∇ contains the dual polytope of $\mathbb{P}^1 \times \mathbb{P}^2$. Dually, the polytope Δ is contained in the polytope of $\mathbb{P}^1 \times \mathbb{P}^2$. Hence the formula for bringing the complete intersection into Weierstrass form is simply a specialization of the formula from the first case where some coefficients are set to zero.

3.6 Non-Toric Non-Abelian Gauge Groups

While studying the embedding genus-one curves with two points in section 3.2, we noted that these are mapped to singular curves in \mathbb{P}_{112} . The singularity could be resolved by blowing up \mathbb{P}_{112} and the exceptional divisor introduced in the blow-up provided one of the homology classes of the sections.

In our approach, we generally take the reverse route: Starting with a smooth genus-one curve embedded inside a toric ambient space X with a given $h^{1,1}(X)$, we map the curve into its Weierstrass form inside \mathbb{P}_{231} . The ambient spaces we use tend to have a richer homology than \mathbb{P}_{231} and this process is generally a blow-down eliminating $h^{1,1}(X) - 1$ variables and producing a singular Weierstrass model. Generally, the blow-up divisors are of two different types on the resolved side:

⁶The invariants $\Delta(p_1^2)$ and $\Theta(p_1^2, p_2)$ vanish because p_1^2 is a degenerate conic.

⁷We use the notation where $\mathbb{P}^2 = dP_0$.

- They can resolve singularities occurring at the collision of two or more sections and provide the homology class of a multisection.
- They can resolve non-Abelian singularities, i.e. those along which the discriminant vanishes at least quadratically. We call these *non-toric* non-Abelian singularities.

This section is dedicated to the study of the latter type and we proceed by examining the example given in [Equation 3.5.3](#) further.

In order to study the non-Abelian singularities of a Weierstrass model defined by the triple (f, g, Δ) , one must attempt to factor f , g , and Δ . If they contain non-trivial factors along which Δ vanishes at least to second order, then the fibration has a non-Abelian singularity along the base divisor defined by the vanishing of this factor. In the case of [Equation 3.5.3](#), f , g and Δ are unfortunately too long to be displayed here and we refer to the database for the full expressions. While f and g do not have any non-trivial factors, the discriminant Δ can be decomposed into $\Delta = \sigma \cdot \Delta'$, where

$$\sigma = (b_{(12)}b_{(02)}b_{(01)} - b_{00}b_{(12)}^2 - b_{11}b_{(02)}^2 - b_{22}b_{(01)}^2 + 4b_{22}b_{11}b_{00})^2 \quad (3.6.1)$$

$b_{(ij)} \equiv b_{ij} + b_{ji}$, and Δ' the remaining linear factor. Correspondingly, there is an $\mathfrak{su}(2)$ singularity along the locus $\Sigma : \sigma = 0$. Note furthermore that $h^{1,1}(\mathbb{P}^1 \times \mathbb{P}^2) = 2$ and therefore there exists one more independent divisor on the resolved side than in the blown-down Weierstrass model. This additional divisor serves as the Cartan divisor of $SU(2)$ and is a \mathbb{P}^1 fibration over the base locus Σ . In the set-ups relevant to us, the b_{ij} are sections of line bundles on the base manifold. Depending on the details of the full fibration, it is possible that $\sigma = 0$ does not have any solutions, as would for instance be the case when the polynomial σ is just a constant. Obviously, if that happens, then the singularity is not realized. Furthermore, in these cases the additional divisor class provided by the blow-up divisor will become trivial upon restriction to the complete intersection defining the genus-one curve inside X . Toricly, the ray corresponding to the blow-up divisor will then lie inside a facet of the reflexive polytope specifying the ambient space of the Calabi-Yau manifold. Whether or not this happens depends of course on the full reflexive polytope and not only the reflexive subpolytope corresponding to the ambient fiber space.

In order to find all possible singularities that a completely generic⁸ fibration with fiber inside a given ambient space has, we fully resolve the fan of the toric ambient space. That is, we use every non-zero interior point of the reflexive polytope as a ray. The irreducible factors of Δ occurring at least quadratically then constitute the set of generic non-toric non-Abelian singularities. We call these singularities non-toric, because they cause the genus-one fiber to split into multiple \mathbb{P}^1 s while the toric ambient fiber space remains irreducible. This is in

⁸Here our notion of genericity equivalent to demanding that all factors of Δ define divisors that are realized in the base manifold. The analogous requirement on the reflexive polytope defining the full Calabi-Yau manifold is that none of its non-zero integral points are interior points of a facet.

contrast to the non-Abelian singularities that one usually tries to engineer and that we study in [chapter 4](#).

For hypersurface fiber curves, the existence of such non-toric non-Abelian singularities was noted in [\[143\]](#) and investigated in detail in [\[144\]](#). In [Appendix B](#) we provide the full list of non-toric non-Abelian singularities for the genus-one fibers embedded in three-dimensional Gorenstein Fano toric varieties.

We remark that since the maximum number of integral points of a reflexive polytope of given dimension is bounded from above, the maximum number of exceptional divisors obtained from the ambient space of the fiber and therefore the total rank of the non-toric gauge group is, too. To illustrate this, consider the 16 reflexive polygons. The reflexive polygon with the most integral points is the one corresponding to the toric variety $\mathbb{P}^2/\mathbb{Z}_3$. Its nine non-zero points give rise to seven independent homology classes. One of them corresponds to the neutral element of the elliptic curve, so the maximum allowed gauge rank is six. In fact, one can show that the maximal non-toric gauge group is $SU(3)^3/\mathbb{Z}_3$ [\[144\]](#). Since three-dimensional reflexive polytopes can contain more integral points than their two-dimensional analogues (the largest one has 39 integral points), the non-toric gauge group content is considerably more diverse. Not only can one find non-toric GUT candidates, but there are also fibers that generically exhibit E_6 , E_7 , and E_8 singularities.

3.7 Sections of Elliptic Fibrations

In the previous sections points on genus-one curves and the associated global sections obtained by fibering these curves over a base manifold have played a central role: They are the key objects distinguishing an elliptic fibration from a general genus-one fibration and the line bundles dual to the divisors they define can be used to embed an elliptic fiber into \mathbb{P}_{231} . Besides their mathematical relevance, they are also important physical observables, since the rank of the Mordell-Weil group that they generate is the rank of the Abelian sector of the resulting low-energy effective theory. In this section we examine them more closely and introduce the notion of *holomorphic* (versus *non-holomorphic*) and *toric* (versus *non-toric*) sections. Every global section is either holomorphic or non-holomorphic and either toric or non-toric. As we will see, assigning one of the four possible combinations of these attributes to a section is a convenient way of characterizing some of the key properties of the section and we include in [subsection 3.7.3](#) two tables summarizing the most relevant properties.

3.7.1 Toric Sections

We call a section of a genus-one fibration a *toric section* if it is defined by the vanishing of a single homogeneous coordinate of the toric ambient space. In this sense a toric section is a section that descends from a *torus-invariant* divisor of the ambient space. One can easily check whether a torus-invariant divisor $V(z_i)$ of the ambient space gives rise to a action by

integrating the $(1, 1)$ -form dual to $V(z_i)$:

$$d \equiv \int_C \omega_{V(z_i)} = C \cap V(z_i) \quad (3.7.1)$$

If $d = 1$, then $V(z_i)$ cuts out a single point in the generic fiber C and thus $z_i = 0$ defines a section of the fibration. Importantly, the calculation of Equation 3.7.1 is independent of the full fibration — it depends only on the ambient space of the fiber.⁹ Consequently, the set of *toric* sections is independent of the choice of fibration. Given a toric section, it is easy to find its expression in homogeneous coordinates. Using the Stanley-Reisner ideal, one can set most coordinates to one until one is left with a linear equation that can be solved.

We can furthermore make another distinction between two different kinds of sections, both of which will feature prominently in this thesis. The first and simpler case is that of a holomorphic section, meaning that there is a holomorphic embedding $s : B \hookrightarrow Y$ of the base in the elliptic fibration such that the composition $\pi \circ s = \text{id}_B$ with the projection map $\pi : Y \rightarrow B$ is the identity map on B . The second and more complicated case is that of a rational section, that is, we require only a birational morphism $s' : B \dashrightarrow B' \subset Y$ such that $\pi \circ s' = \text{id}_B$. This means that $s' : B \rightarrow B'$ is generically one-to-one, but not defined over some points. In particular, the topologies of B and B' may differ. The points where s' cannot be defined is where the divisor $B' \subset Y$ wraps a whole fiber component. Clearly, a holomorphic section is a special case of a rational section, but we stress that rational sections are perfectly fine for F-theory compactifications. For physics applications, the rational sections give us important additional freedom: A holomorphic section must intersect any fiber in a single point, that is, it intersects a single irreducible fiber component with intersection number one. Rational sections, on the other hand, can wrap components of codimension-two fibers and therefore have more freedom in the intersection numbers. This translates into less constraints for the $U(1)$ matter charges, as we will see in later parts of this thesis. For clarity, we refer

⁹For hypersurfaces, the condition $d = 1$ can be translated into a condition on the ray corresponding to the divisor $V(z_i)$. We can always assume that the ambient fiber space is smooth and that homogeneous coordinates are ordered with respect to the angle between their corresponding ray and a coordinate axis. Put differently, z_i and $z_{i\pm 1}$ have rays that share a 2-face. Then we have $[V(z_i)] \cap [V(z_j)] = \delta_{i,j-1} + \delta_{i,j+1}$ for $i \neq j$ and, therefore the requirement that $d = 1$ implies that a toric section $V(z_i)$ must satisfy

$$[V(z_i)] \cap [V(z_i)] = -1. \quad (3.7.2)$$

To translate this into the geometry of the fan, let us denote the ray corresponding to the toric coordinate z_i by v_i . Then (3.7.2) is satisfied if the lattice spanned by the edges connecting v_i with its neighboring rays,

$$N_i = \text{span}(v_i - v_{i-1}, v_i - v_{i+1}) \quad (3.7.3)$$

is the same as the fan lattice N , i.e.

$$V(z_i) \text{ is a section} \iff N_i = N. \quad (3.7.4)$$

In particular, only vertices of a fiber polygon can give rise to toric sections. Given this simple geometric prescription, one can easily read off the toric sections of a given fiber polygon.

to rational sections that are not holomorphic as non-holomorphic sections and refrain from using the name rational section.

One example that we have already encountered is the section of an elliptic fibration with fiber inside \mathbb{P}_{231} . One has that $C \cap V(z) = 1$ and hence $z = 0$ defines a toric section. In [section 3.1](#) we found that its coordinate expression is $[1 : 1 : 0]$. Note that the section is equally well-defined over every point of the base of the fibration, since the homogeneous fiber coordinates do not depend on the base coordinates. It is thus a *holomorphic* section.

Homogeneous coordinate z	z_0	z_1	z_2	f_0
Point $n_z \in \nabla$	$\begin{pmatrix} 1 \\ 0 \end{pmatrix}$	$\begin{pmatrix} 0 \\ 1 \end{pmatrix}$	$\begin{pmatrix} -1 \\ -1 \end{pmatrix}$	$\begin{pmatrix} 1 \\ 1 \end{pmatrix}$

Table 3.5: The toric variety dP_1 obtained by blowing up \mathbb{P}^2 at $[0 : 0 : 1]$.

A slightly more interesting example is given by the fiber embedded inside dP_1 , whose toric data we list in [table 3.5](#). One can confirm that the divisor $V(f_0)$ gives rise to a global section and that the Stanley-Reisner ideal of dP_1 is generated by

$$\langle z_0 z_1, z_2 f_0 \rangle. \tag{3.7.5}$$

The most general anticanonical hypersurface inside dP_1 is given by

$$p = a_0 z_0^3 f_0^2 + a_1 z_0^2 z_1 f_0^2 + a_2 z_0 z_1^2 f_0^2 + a_3 z_1^3 f_0^2 + a_4 z_0^2 z_2 f_0 + a_5 z_0 z_1 z_2 f_0 + a_6 z_1^2 z_2 f_0 + a_7 z_0 z_2^2 + a_8 z_1 z_2^2 = 0 \tag{3.7.6}$$

and we can find the coordinate expression of the section by plugging f_0 into [Equation 3.7.6](#). Since $z_2 f_0$ is contained in the Stanley-Reisner ideal, one can scale z_2 to one and is left with

$$a_7 z_0 + a_8 z_1 = 0. \tag{3.7.7}$$

We thus find

$$V(f_0) \cap C : \begin{cases} [z_0 : z_1 : 1 : 0] \cong \mathbb{P}^1 & \text{if } a_7 = a_8 = 0 \\ [-a_8 : a_7 : 1 : 0] & \text{otherwise,} \end{cases} \tag{3.7.8}$$

where we have denoted the fiber by C . The crucial difference between this section and the one of the previous example is that over the codimension-two base locus defined by $a_7 = a_8 = 0$ the section does not cut out a single point in the fiber, but a whole \mathbb{P}^1 instead! Therefore $V(f_0)$ defines a *non-holomorphic* section.

3.7.2 Non-toric Sections

Conversely, a section is called *non-toric* if it is not defined by the vanishing of a homogeneous coordinate. As a result, it is generally much harder and often impossible to find an explicit coordinate expression.¹⁰

Fortunately, most of the relevant computations depend only on the homology class of the section and in many cases, this can be guessed. Here we present a set of conditions a putative homology class $[s]$ of a section must satisfy:

- $[s]$ must intersect the generic fiber C once, i.e.

$$\int_C \omega_s = C \cap [s] = 1. \quad (3.7.9)$$

- The line bundle dual to $[s]$ must have a section, i.e. we require that $h^0(Y, \mathcal{O}_Y(s)) > 0$. In order to compute the number of sections, we can use the same techniques as in [section 3.3](#). If Y is a hypersurface in X , then one can tensor [Equation 3.3.1](#) with the line bundle dual to s and obtains the following long exact sequence

$$\begin{aligned} \cdots \longrightarrow H^0(X, \mathcal{O}_X(s)) \longrightarrow H^0(Y, \mathcal{O}_Y(s)) \longrightarrow \\ \longrightarrow H^1(X, \mathcal{O}_X(s + K_X)) \longrightarrow H^1(X, \mathcal{O}_X(s)) \longrightarrow \cdots \end{aligned} \quad (3.7.10)$$

in cohomology. Alternatively, if Y is a complete intersection of the two¹¹ divisors D_1 and D_2 , one can either use the machinery of spectral sequences or one can also split up the long exact sequence of the Koszul resolution

$$0 \longrightarrow \underbrace{\mathcal{O}_X(-D_1 - D_2)}_{\mathcal{R}^{-2}} \longrightarrow \underbrace{\mathcal{O}_X(-D_1) \oplus \mathcal{O}_X(-D_2)}_{\mathcal{R}^{-1}} \longrightarrow \underbrace{\mathcal{O}_X}_{\mathcal{R}^0} \longrightarrow \mathcal{O}_Y \longrightarrow 0. \quad (3.7.11)$$

into two short exact sequences. After twisting them with the line bundle of the putative section they read

$$\begin{aligned} 0 \longrightarrow \mathcal{R}^{-2} \otimes \mathcal{O}_X(s) \longrightarrow \mathcal{R}^{-1} \otimes \mathcal{O}_X(s) \longrightarrow \mathcal{N} \longrightarrow 0 \\ 0 \longrightarrow \mathcal{N} \longrightarrow \mathcal{R}^0 \otimes \mathcal{O}_X(s) \longrightarrow \mathcal{O}_Y \otimes \mathcal{O}_Y(s) \longrightarrow 0. \end{aligned} \quad (3.7.12)$$

Each of them induces a long exact sequence in cohomology, i.e.

$$\begin{aligned} 0 \longrightarrow H^0(X, \mathcal{O}_X(-D_1 - D_2 + s)) \longrightarrow H^0(X, \mathcal{O}_X(-D_1 + s) \oplus \mathcal{O}_X(-D_2 + s)) \longrightarrow \\ \longrightarrow H^0(X, \mathcal{N}) \longrightarrow H^1(X, \mathcal{O}_X(-D_1 - D_2 + s)) \longrightarrow \cdots \end{aligned} \quad (3.7.13)$$

¹⁰One notable example in the literature is the case of dP_1 . In [\[145\]](#) the homology class of the non-toric section was found and in [\[144\]](#) the authors managed to write down an explicit coordinate expression.

¹¹As before, this straightforwardly generalized to higher complete intersections of higher codimension.

and

$$\begin{aligned} 0 \longrightarrow H^0(X, \mathcal{N}) \longrightarrow H^0(X, \mathcal{O}_X(s)) \longrightarrow \\ \longrightarrow H^0(Y, \mathcal{O}_Y(s)) \longrightarrow H^1(X, \mathcal{N}) \longrightarrow \dots \end{aligned} \quad (3.7.14)$$

In both cases, the line bundle cohomology on the ambient space X can be calculated using toric methods implemented in Sage [139] and from these one infers the cohomology dimensions of the line bundles on Y . For more details on line bundle cohomology computations, we refer to [146].

- The homology class of the section should not contain exceptional divisors of the ambient space. If it does, then the exceptional divisors need to be subtracted from $[s]$.

Non-toric sections can be both holomorphic and non-holomorphic. However, in the absence of a coordinate description, it may be more challenging to find the base loci over which they wrap entire fiber components.

As a final disclaimer, we remark that while these conditions are necessary for the homology class $[s]$ to represent a section of the genus-one fibration, they may not be sufficient and one should treat non-toric sections with care. In subsection 5.3.1 we will study an example in which a non-toric section is present and will show that it appears to be physically consistent.

3.7.3 Overview

As a recapitulation of the contents of this section, we display in table 3.6 and table 3.7 the most important properties of the four types of sections that we distinguish.

3.8 Classifying Toric Mordell-Weil Groups

Having laid out the groundwork in the previous section, we are finally in a position to define the *toric Mordell-Weil group* MW_T . MW_T is the second main quantity determined solely by the fiber that we are interested in computing, as we stated already in the introduction of this chapter.

Given an elliptically fibered Calabi-Yau manifold Y , we denote by s_i , $i = 0, \dots, n$ the *toric sections*. Choosing without loss of generality s_0 as the *zero section*, i.e. the neutral element with respect to the group law of a generic fiber of Y , we define

$$\sigma_i \equiv s_{i+1} - s_0, \quad i = 0, \dots, n-1. \quad (3.8.1)$$

The group generated by the σ_i is the *toric Mordell-Weil group* of Y . Of course, a general Y may also have non-toric sections and in this case the toric Mordell-Weil group is only a subgroup of the full Mordell-Weil group:

$$MW_T(Y) \subseteq MW(Y) \quad (3.8.2)$$

Toric Sections	Non-Toric Sections
<ul style="list-style-type: none"> • Specified by the vanishing of a single toric coordinate. • Easily determined by imposing Equation 3.7.1 with $d = 1$. • Existence and properties with respect to the Mordell-Weil group law depend only on the ambient space of the <i>fiber</i>, not on the entire fibration. • Coordinate expression can always be found by solving the equations defining the genus-one fiber. 	<ul style="list-style-type: none"> • Not specified by the vanishing of a single toric coordinate. • While coordinate expressions can be determined in special cases, finding them is technically involved. Nevertheless, their homology classes can often be guessed. • Existence may depend on details of the entire genus-one fibration.

Table 3.6: Summary of the differences between holomorphic and non-holomorphic sections of an elliptic fibration.

The reason for nevertheless studying $MW_T(Y)$ is that unlike $MW(Y)$, the toric Mordell-Weil group depends only on the ambient space of the generic fiber of the fibration Y . We can hence write

$$MW_T(Y) = MW_T(F), \quad (3.8.3)$$

where F is the Gorenstein Fano toric variety in which the generic fiber of Y is embedded. While details of the fibration of Y may induce additional non-toric sections, the set of toric sections depends only on the properties of F . In terms of toric geometry, this is easy to understand. As noted in [subsection 3.7.1](#), toric sections always correspond to vertices of the reflexive polytope defining the toric ambient space. As such, they must always be included in the fan of the toric variety. On the other hand, a non-toric section may consist of linear combinations of divisors involving integral points of the polytope that are not vertices. Since they depend on details of the polytope of the full fibration X , it is thus possible that their restriction to the Calabi-Yau manifold Y is trivial and that hence the non-toric section is not realized.

By computing the toric Mordell-Weil groups of elliptic curves inside Gorenstein Fano toric varieties of different dimensions, one can thus *classify* the toric Mordell-Weil groups and in the remainder of this section, this is precisely what we will strive to do. [Subsection 3.8.1](#) contains

Holomorphic Sections	Non-holomorphic Sections
<ul style="list-style-type: none"> • Defines a single point in the fiber over every point in the base and thus intersects fiber components only with intersection number zero or one. • Embeds the base holomorphically into the space of the entire fibration and thus the divisor it defines has the same topology as the base. • If the section is also toric, then all intersection theoretical properties are independent of the base manifold. 	<ul style="list-style-type: none"> • Defines a single point in the fiber over dense subsets in the base, but may cut out entire fiber components over codimension-two loci in the base manifold. Consequently, the section may have negative intersection numbers with a fiber component or intersect multiple fiber components. • Embeds only dense subsets of the base holomorphically into the space of the entire fibration. The divisor it defines is birational to the base manifold and thus does not necessarily have the same topology.

Table 3.7: Summary of the differences between toric and non-toric sections of an elliptic fibration.

the explicit results for the 16 two-dimensional Gorenstein Fano varieties. In codimension two, there exist already 3134 different nef partitions and therefore we do not list them here explicitly. However, [subsection 3.8.2](#) contains a summary of the results and explains how to access a database containing the full information about all 3134 group laws. Here we can already give a concise summary of the different toric Mordell-Weil groups that elliptic curves up to codimension two can have, which is given in [table 3.8](#).

Codimension	\mathbb{Z}_2	\mathbb{Z}_3	\mathbb{Z}_4	\mathbb{Z}	$\mathbb{Z} \oplus \mathbb{Z}_2$	\mathbb{Z}^2	$\mathbb{Z}^2 \oplus \mathbb{Z}_2$	\mathbb{Z}^3	$\mathbb{Z}^3 \oplus \mathbb{Z}_2$	\mathbb{Z}^4
1	✓	✓	×	✓	✓	✓	×	✓	×	×
2	✓	✓	✓	✓	✓	✓	✓	✓	✓	✓

Table 3.8: The full list of toric Mordell-Weil groups of elliptic curves embedded in Gorenstein Fano toric varieties in codimensions one and two.

Before proceeding with the classification results, let us remark on how to compute the

Mordell-Weil group laws for a given fiber ambient space in practice. While we computed the Weierstrass forms of the genus-one curves (or their Jacobians if they do not have an elliptic curve structure) by keeping the coefficients in the complete intersection equations general, this approach makes little sense for determining the Mordell-Weil group laws. Instead, we generated a considerable number¹² of curves with random complex structure coefficients in \mathbb{Z} . We then computed the explicit coefficients of the points cut out by toric sections, mapped these to the elliptic curve in Weierstrass form and determined the relations between them. Special care has to be taken when mapping the points from the original elliptic curve to the curve in Weierstrass form. As discussed in [section 3.3](#) our map works through an intermediate embedding inside \mathbb{P}_{231} , \mathbb{P}_{112} , \mathbb{P}^2 , or \mathbb{P}^3 , and the maps from the last three spaces to Weierstrass form are not injective: They in fact map the elliptic curves $4 : 1$, $9 : 1$ and $16 : 1$, respectively. As a consequence, distinct points on the original curve may be mapped to the same point of the curve in Weierstrass form and therefore torsion factors of the Mordell-Weil group may get lost. To make sure that we find the correct torsion groups, it is therefore crucial to use different embeddings of the same curve in case that the points on the curve in Weierstrass satisfy non-trivial relations with respect to the Mordell-Weil group law. While the map from \mathbb{P}^2 to Weierstrass form may eliminate a \mathbb{Z}_3 torsion factor, the map from \mathbb{P}_{112} will not, and one can therefore determine the correct toric Mordell-Weil groups even in the presence of torsion.

The computations were performed using PALP [\[147\]](#), Sage [\[139\]](#) and in particular the Sage modules for polytopes [\[148\]](#) and toric geometry [\[149\]](#). Furthermore, we made heavy use of the Sage interface to Singular [\[150\]](#).

3.8.1 Toric Mordell-Weil Groups for Hypersurfaces

As there only exist 16 different reflexive polytopes, we take the liberty to recall their form in [figure 3.7](#). Among these are of course also the examples studied in [section 3.2](#) and [section 3.7](#) and we have taken care to color the vertices giving rise to toric sections red. Let us point out that three of the reflexive polytopes do not have any toric sections, namely $F_1 = \mathbb{P}^2$, $F_2 = \mathbb{P}^1 \times \mathbb{P}^1$, and $F_4 = \mathbb{P}_{112}$. In the first case, all toric divisors have degree three, while the divisors of lowest degree of the latter two cases are of degree two.

For the remaining ambient spaces, we have computed the toric Mordell-Weil group that a generic curve inside them has. Depending on the ambient space, the σ_i of [Equation 3.8.1](#) may satisfy non-trivial relations among each other and we summarize our results for all the toric Mordell-Weil groups of hypersurface fibers in [table 3.9](#).

3.8.2 Toric Mordell-Weil Groups for Complete Intersections of Codimension Two

Since the total number of reflexive polytopes of a certain dimension grows very fast, it would be futile to list the toric data of all three-dimensional nef partitions. Instead, we again refer

¹²By considerable, we mean $\mathcal{O}(100)$ in order to make sure that we indeed obtain a generic example.

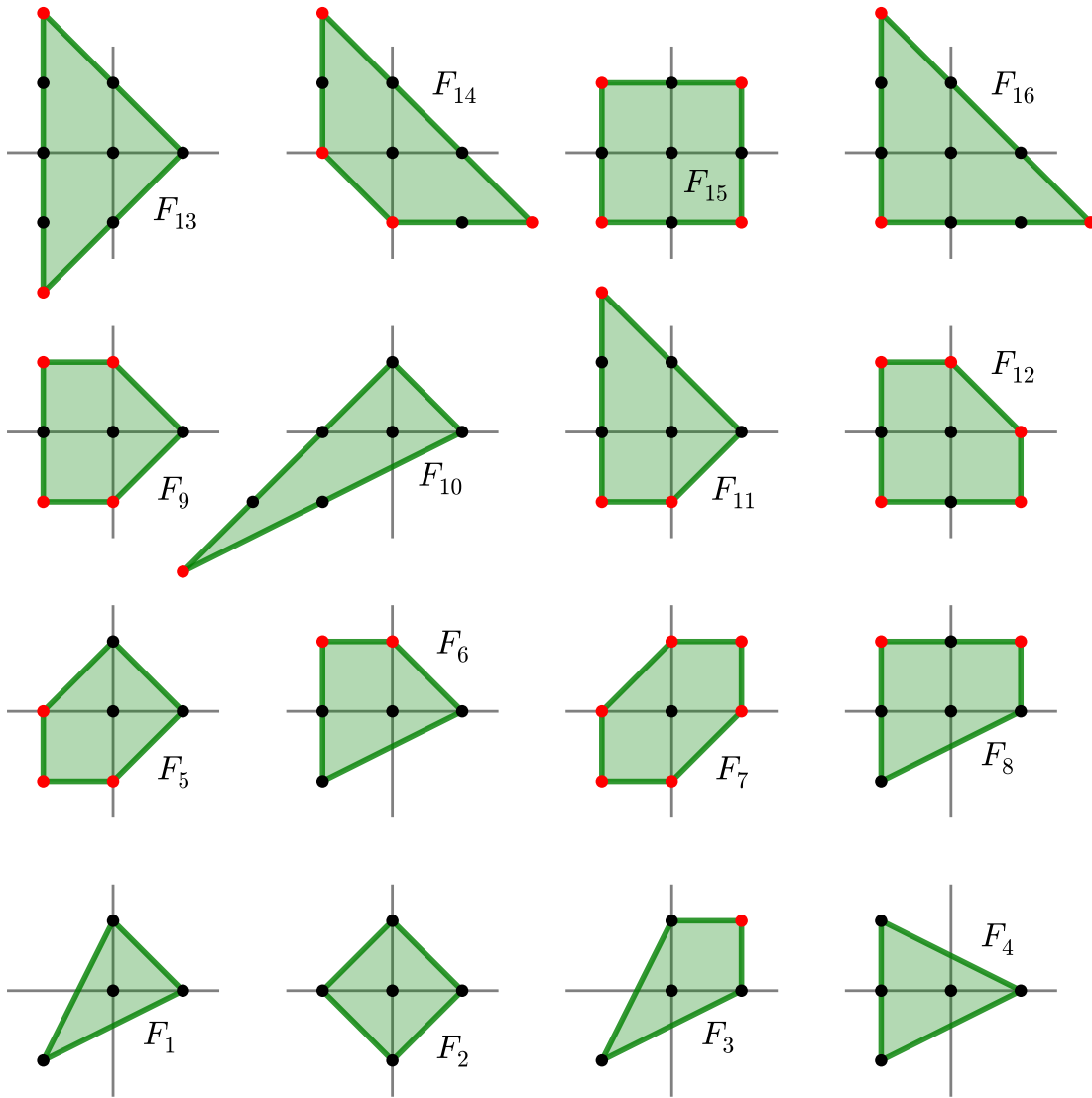


Figure 3.7: The 16 reflexive polygons. F_i and F_{17-i} are dual for $i = 0, \dots, 6$, and self-dual for $i = 7, \dots, 10$. The corresponding toric surfaces are also known as $F_1 = \mathbb{P}^2$, $F_2 = \mathbb{P}^1 \times \mathbb{P}^1$, $F_3 = dP_1$, $F_4 = \mathbb{P}^2[1, 1, 2]$, $F_5 = dP_2$, $F_7 = dP_3$, $F_{10} = \mathbb{P}^2[1, 2, 3]$, where dP_n are the del Pezzo surfaces obtained by blowing up \mathbb{P}^2 at n points. Vertices defining toric sections are colored red. This was first derived in Figure 1 of [151].

Fiber polygon	Toric sections	Relations	MW_T
F_3	$(1, 1) \simeq s_0$		0
F_5	$(0, -1) \simeq s_0$ $(-1, -1) \simeq s_1$ $(-1, 0) \simeq s_2$		$\mathbb{Z} \oplus \mathbb{Z}$
F_6	$(0, 1) \simeq s_0$ $(-1, 1) \simeq s_1$		\mathbb{Z}
F_7	$(-1, -1) \simeq s_0$ $(0, -1) \simeq s_1$ $(1, 0) \simeq s_2$ $(1, 1) \simeq s_3$ $(0, 1) \simeq s_4$ $(-1, 0) \simeq s_5$	$\sigma_0 = \sigma_2 + \sigma_3$ $\sigma_4 = \sigma_1 + \sigma_2$	$\mathbb{Z} \oplus \mathbb{Z} \oplus \mathbb{Z}$
F_8	$(-1, 1) \simeq s_0$ $(1, 1) \simeq s_1$		\mathbb{Z}
F_9	$(-1, -1) \simeq s_0$ $(0, -1) \simeq s_1$ $(0, 1) \simeq s_2$ $(-1, 1) \simeq s_3$	$\sigma_0 = \sigma_1 + \sigma_2$	$\mathbb{Z} \oplus \mathbb{Z}$
F_{10}	$(-3, -2) \simeq s_0$		0
F_{11}	$(-1, -1) \simeq s_0$ $(0, -1) \simeq s_1$ $(-1, 2) \simeq s_2$	$\sigma_0 = 2\sigma_1$	\mathbb{Z}
F_{12}	$(-1, -1) \simeq s_0$ $(1, -1) \simeq s_1$ $(1, 0) \simeq s_2$ $(0, 1) \simeq s_3$ $(-1, 1) \simeq s_4$	$\sigma_0 = \sigma_2 + \sigma_3$ $\sigma_3 = \sigma_0 + \sigma_1$	$\mathbb{Z} \oplus \mathbb{Z}$
F_{13}	$(-1, -2) \simeq s_0$ $(-1, 2) \simeq s_1$	$2\sigma_0 = 0$	\mathbb{Z}_2
F_{14}	$(-1, 0) \simeq s_0$ $(-1, 2) \simeq s_1$ $(2, -1) \simeq s_2$ $(0, -1) \simeq s_3$	$\sigma_0 = 2\sigma_1$ $\sigma_2 = \sigma_0 + \sigma_1$	\mathbb{Z}
F_{15}	$(-1, -1) \simeq s_0$ $(1, -1) \simeq s_1$ $(1, 1) \simeq s_2$ $(-1, 1) \simeq s_3$	$2\sigma_1 = 0$ $\sigma_2 = \sigma_0 + \sigma_1$	$\mathbb{Z} \oplus \mathbb{Z}_2$
F_{16}	$(-1, -1) \simeq s_0$ $(2, -1) \simeq s_1$ $(-1, 2) \simeq s_2$	$3\sigma_1 = 0$ $\sigma_2 = 2\sigma_1$	\mathbb{Z}_3

Table 3.9: The toric sections corresponding to the reflexive polygons, the relations they are subject to and MW_T , the toric subgroup of the Mordell-Weil group generated by them.

to the website

<http://wwwth.mpp.mpg.de/members/jkeitel/Weierstrass/> (3.8.4)

containing a database of the 3134 nef partitions of three-dimensional reflexive polyhedra. For each such nef partition, there exists a file of the form `RP_NEF.txt` and in the following, we explain what we computed and how it is encoded in the database records.

For every nef partition of a three-dimensional reflexive polytope, we computed the following data:

- The two defining equations of the complete intersection with general coefficients a_i .
- The Weierstrass coefficients f and g of equation (3.1.2) in terms of a_i .
- The integral points v_i of Δ° that are promoted to toric sections $s_i = V(z_i)$ after fibering the elliptic curve over a base manifold.
- The relations between the Mordell-Weil group elements $\sigma_i = s_{i+1} - s_0$ that we have already used in the hypersurface case.
- The resulting toric Mordell-Weil group, including its torsion part.
- The Kodaira types of the non-toric singularities that occur if all a_i are generic.

Let us illustrate the file format of the data base using the nef partition (2355, 0):

Summary for nef partition with id (2355, 0).

Defining data of the nef partition:

```
rays = [z0: (1, 0, 0), z1: (0, 1, 0), z2: (0, 0, 1), z3: (-1, 1, 1),
z4: (2, -1, -1), z5: (1, 0, -1), z6: (1, -1, 0), z7: (-1, 1, 0),
z8: (-1, 0, 1), z9: (-2, 1, 1), z10: (1, -1, -1), z11: (0, 0, -1),
z12: (0, -1, 0), z13: (-1, 0, 0)]
nabla_1 = (0, 1, 2, 3, 4, 5, 6)
nabla_2 = (7, 8, 9, 10, 11, 12, 13)
```

Toric Mordell-Weil group:

```
zero = (0, 1, 0)
generators = [s0: (0, 0, 1), s1: (2, -1, -1), s2: (-2, 1, 1),
s3: (0, 0, -1), s4: (0, -1, 0)]
relations = [s0-s3 = (1), s1-s2 = (1), s4 = (1)]
group = Z^2 x Z_2
```

Complete intersection equations:

$$\begin{aligned} p1 &= a3*z0*z1*z2*z3*z4*z5*z6 + a2*z1*z3*z5*z7*z9*z11*z13 \\ &+ a1*z2*z3*z6*z8*z9*z12*z13 + a0*z4*z5*z6*z10*z11*z12*z13 \\ p2 &= a7*z0*z1*z2*z3*z7*z8*z9 + a6*z0*z1*z4*z5*z7*z10*z11 \\ &+ a5*z0*z2*z4*z6*z8*z10*z12 + a4*z7*z8*z9*z10*z11*z12*z13 \end{aligned}$$

Weierstrass coefficients:

$$\begin{aligned} f &= [...] \\ g &= [...] \end{aligned}$$

Generic non-Abelian singularities:

$$\begin{aligned} a7: & (0, 0, 2), I_2 \\ a6: & (0, 0, 2), I_2 \\ a5: & (0, 0, 2), I_2 \\ a4: & (0, 0, 2), I_2 \\ a3: & (0, 0, 2), I_2 \\ a2: & (0, 0, 2), I_2 \\ a1: & (0, 0, 2), I_2 \\ a0: & (0, 0, 2), I_2 \end{aligned}$$

The first block summarizes the toric data defining the nef partition. The first line defines the variable names z_i assigned to the homogeneous variables associated with each ray of the ambient fan and the second line specifies the nef partition by listing the indices of the rays spanning ∇_1 and ∇_2 . In this example

$$\nabla_1 = \langle v_0 v_1 v_2 v_3 v_4 v_5 v_6 \rangle_{\text{conv}}, \quad \nabla_2 = \langle v_7 v_8 v_9 v_{10} v_{11} v_{12} v_{13} \rangle_{\text{conv}}. \quad (3.8.5)$$

The second paragraph contains information about the toric Mordell-Weil group. This particular example has six divisors that become (not necessarily independent) sections after fibering the elliptic curve over a base manifold and the toric Mordell-Weil group generated by these divisors is $\mathbb{Z}^2 \oplus \mathbb{Z}_2$. Note that there is a slight clash in notation between the database and conventions of this thesis: Here s_i denotes the section s_{i+1} . Choosing the divisor corresponding to the ray $(0, 1, 0)^T$ as the divisor s_0 that cuts out the neutral element on the curve, the remaining five divisors $\sigma_i = s_{i+1} - s_0$, $i = 0, \dots, 4$ satisfy three relations. To specify these relations we denote by (i) the generator of the torsion part times i . Here, this means that the section σ_4 generates the \mathbb{Z}_2 factor and, up to this torsion part, the pairs of sections σ_0 and σ_3 , and σ_1 and σ_2 , are identified under the Mordell-Weil group law. Next, the record contains the two complete intersection equations in order to define the coefficients a_i determining the complex structure of the elliptic curve. The Weierstrass coefficients (omitted here due to their length) are then given in terms of the a_i . Finally, we list the non-Abelian singularities that a such an elliptic curve with generically chosen a_i will have. In this case, there is an additional $SU(2)^8$ gauge group with branes located along the eight base loci $a_i = 0$ for $i = 0, \dots, 7$.

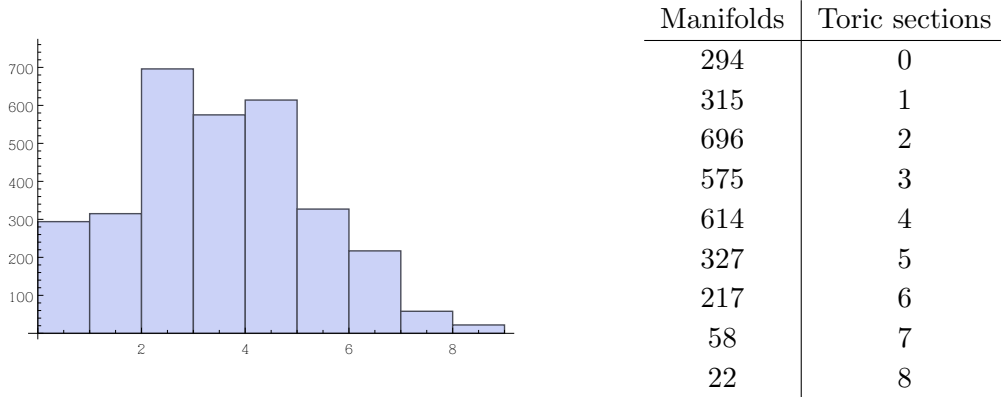


Figure 3.8: Histogram of the number of toric sections for the 3118 nef partitions of three-dimensional reflexive polytopes that are not direct products.

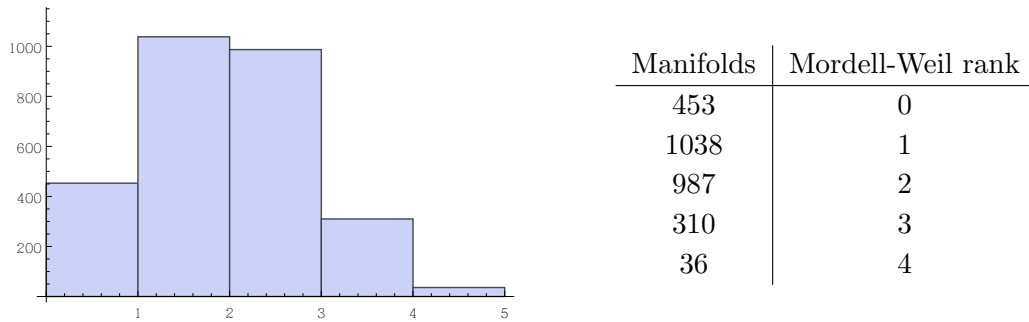


Figure 3.9: Histogram of the toric Mordell-Weil rank for the nef partitions of three-dimensional reflexive polytopes. The 326 complete intersections that are either a direct product or do not have a toric section are excluded.

Finally, let us give an overview of the results in codimension two. We list in [figure 3.8](#) the distribution of the number of toric divisors corresponding to sections among the complete intersection curves. Note that not all of these divisors will be independent in homology. In [figure 3.9](#) we give the distribution of the toric Mordell-Weil ranks. The highest *toric* rank that we find is four. Naturally, not all groups of the same rank are equal, as some have additional

Trivial group	\mathbb{Z}_2	\mathbb{Z}_3	\mathbb{Z}_4	\mathbb{Z}	$\mathbb{Z} \oplus \mathbb{Z}_2$	\mathbb{Z}^2	$\mathbb{Z}^2 \oplus \mathbb{Z}_2$	\mathbb{Z}^3	$\mathbb{Z}^3 \oplus \mathbb{Z}_2$	\mathbb{Z}^4
315	113	24	1	931	107	985	2	309	1	36

Table 3.10: The full toric Mordell-Weil groups for the elliptic fibers of codimension two. Note that we have omitted direct products and the genus-one curves that do not have a single toric point.

torsion factors. In [table 3.10](#) we give a complete survey of the toric Mordell-Weil groups for the models that possess at least one toric section. As was shown already in [table 3.8](#), there

are also additional toric Mordell-Weil groups when compared with the elliptic curves that are embedded in toric surfaces.

3.9 Fibers without Section

Throughout this chapter, we have repeatedly stressed that not every genus-one fibration is an elliptic fibration — only the existence of a global section endows the generic fiber with the structure of an elliptic curve. Until recently, the F-theory literature had focused solely on elliptic fibrations. By now, genus-one fibrations without section are understood to provide perfectly well-defined F-theory backgrounds. In fact, they have recently even been shown [144, 152–155] to generate discrete symmetries in the low-energy effective theory. For this reason, we dedicate this section to studying the geometry of genus-one fibrations without section.

We begin by recalling the classification results of section 3.8. There we found that there exist three genus-one hypersurfaces without section and from figure 3.8 we see that there are a further 294 three-dimensional nef partitions without a toric section. Nevertheless, these toric fiber ambient spaces of course have $h^{1,1} > 0$. Some of these divisors will wrap entire fiber components over codimension-one loci in the base. These are the \mathbb{P}^1 -fibrations corresponding to exceptional divisors resolving a non-Abelian singularity. However, not all fiber divisors are of this type: Instead, there are also divisors that intersect the generic fiber d times and wrap fiber components only over base loci that are at least codimension-two in the base manifold, namely those divisors satisfying Equation 3.7.1. We call such divisors d -sections of the genus-one fibration. It is worthwhile to remark that genus-one fibrations with, for instance, only two-sections and three-sections may still have a section as long as that section is non-toric and given by the difference of two such divisors. To show that a given fiber does indeed not have a section, one must therefore show that none of the possible linear combinations of fiber divisors is a section.

In the remainder of this section, we give examples of the three different kinds of multi-sections that are realized in genus-one curves embedded either as hypersurfaces or complete intersection of codimension two. To study multisections of degree two, three and four, we can recall our findings of section 3.2, where we showed that *every* genus-one curve with a degree-two (or degree-three and degree-four) line-bundle can be embedded into \mathbb{P}_{112} (or \mathbb{P}^2 and \mathbb{P}^3 , respectively). If one further assumes that the line bundle can be written as a tensor product of smaller-degree line bundles, then the proper embedding is into a blow-up of one of these spaces. In the following, we will put particular focus on understanding the blow-down maps (or, equivalently, the corresponding blow-ups) $\pi_{(j)}^{(i)}$ in figure 3.4.

We remark that much of the material of the following subsections was first studied in [52], [156, 157], and [158], respectively.

3.9.1 Genus-One Fibrations with Two-Section

We begin with a detailed study of genus-one curves inside \mathbb{P}_{112} , the space that we identified as the embedding space for genus-one curves with degree-two line bundles. The most general anticanonical hypersurface inside \mathbb{P}_{112} is given by

$$C : w^2 + b_0u^2w + b_1uvw + b_2v^2w = c_0u^4 + c_1u^3v + c_2u^2v^2 + c_3uv^3 + c_4v^4, \quad (3.9.1)$$

where we have chosen $[u : v : w]$ to be the homogeneous coordinates of \mathbb{P}_{112} . Since u corresponds to a section of a degree-two line bundle, the equation $u = 0$ is quadratic:

$$w^2 + b_2v^2w = c_4v^4 \quad (3.9.2)$$

Going to the affine patch defined by $v = 1$, we see that the divisor $u = 0$ does indeed intersect the generic fiber twice and thus defines a two-section. Similarly, one can confirm that the divisor $v = 0$ is another two-section and $w = 0$ defines a four-section. Of course, this can also be confirmed by computing intersection numbers of the form $C \cap \{u = 0\} = 2$. Therefore, a genus-one fibration with fiber embedded in \mathbb{P}_{112} does clearly not have a toric section. Furthermore, one cannot build a non-toric section from linear combinations of torus-invariant divisors with *integral* coefficients.

In later chapters, we will study the low-energy physics of such F-theory compactifications, but here we restrict to studying further geometric properties to the two-section $u = 0$. Locally, the divisor $\{u = 0\}$ cuts out two separate points in the fiber and one might be tempted to try and split $\{u = 0\}$ into two components, each given by a section. However, this cannot be achieved globally, since the points are interchanged under monodromies as one moves along the base manifold. Only after setting $c_4 = 0$ does [Equation 3.9.2](#) factor into two irreducible components that give rise to the two sections

$$s_0 : [0 : 1 : 0], \quad s_1 : [0 : 1 : -b_2]. \quad (3.9.3)$$

There is still no divisor corresponding to a single section. However, due to tuning $c_4 \rightarrow 0$, C has become singular. This singularity can be resolved by a blow-up at $[0 : 1 : 0]$, which introduces a new coordinate e via the substitutions

$$u \mapsto u \cdot e, \quad w \mapsto w \cdot e \quad (3.9.4)$$

and the proper transform of the equation defining the elliptic curve is

$$ew^2 + b_0e^2u^2w + b_1euvw + b_2v^2w = c_0e^3u^4 + c_1e^2u^3v + c_2eu^2v^2 + c_3uv^3. \quad (3.9.5)$$

[Equation 3.9.5](#) defines a smooth curve inside $\text{Bl}_{[0:1:0]}\mathbb{P}_{112}$ with homogeneous coordinates $[u : v : w : e]$ and now the two points of [Equation 3.9.3](#) can be obtained by setting one of the homogeneous coordinates to zero

$$u = 0 : [0 : 1 : 1 : -b_2] = s_0$$

$$e_1 = 0 : \begin{cases} [u : 1 : w : 0] \cong \mathbb{P}^1 & \text{if } b_2 = c_3 = 0 \\ [b_2 : 1 : c_3 : 0] = s_1 & \text{otherwise.} \end{cases} \quad (3.9.6)$$

This means in particular that an elliptic fibration with fiber embedded in $\text{Bl}_{[0:1:0]}\mathbb{P}_{112}$ has (at least) two global sections given by the divisors $u = 0$ and $e = 0$. Let us note that instead of setting c_4 to zero, one could similarly have tuned $c_0 \rightarrow 0$ and thus split the two-section corresponding to $\{v = 0\}$ into two parts. However, the outcome would have been the same, since u and v are exchanged under the \mathbb{Z}_2 lattice automorphism of the \mathbb{P}_{112} polygon (F_4 in [figure 3.7](#)).

3.9.2 Genus-One Fibrations with Three-Section

Next, consider the most general cubic in \mathbb{P}^2 defined by

$$a_0u^3 + a_1u^2v + a_2u^2w + a_3uv^2 + a_4uvw + a_5uw^2 + a_6v^3 + a_7v^2w + a_8vw^2 + a_9w^3 = 0. \quad (3.9.7)$$

\mathbb{P}^2 has only a single divisor class, called the hyperplane class H , and all three divisors $\{u = 0\}$, $\{v = 0\}$, and $\{w = 0\}$ lie in this class. Of course, this is also imposed by the S_3 lattice automorphism group under which the \mathbb{P}^2 polygon ($= F_1$) is invariant and which permutes the three vertices corresponding to the homogeneous coordinates of \mathbb{P}^2 . Since $C \cap H = 3$, the three torus-invariant divisors all define three-sections and again one cannot find linear combinations with integral coefficients that would give a non-toric section.

Mimicking what we did in the two-section case, we look for transitions to fiber spaces in which a three-section splits into different irreducible components. Without loss of generality we can try make the divisor $u = 0$ reducible. Inserting $u = 0$ into [Equation 3.9.7](#) leads to

$$a_6v^3 + a_7v^2w + a_8vw^2 + a_9w^3 = 0 \quad (3.9.8)$$

and we can set $a_9 = 0$. Then [Equation 3.9.8](#) splits into a section

$$s_0 : [0 : 0 : 1] \quad (3.9.9)$$

and a two-section defined by

$$a_6v^2 + a_7vw + a_8w^2 = 0. \quad (3.9.10)$$

To resolve the singularities induced by the tuning, one blows up the point $[0 : 0 : 1]$ by introducing the new coordinate e_1 and the substitutions

$$u \mapsto u \cdot e_1, \quad v \mapsto v \cdot e_1 \quad (3.9.11)$$

leading to the proper transform

$$a_0e_1^2u^3 + a_1e_1^2u^2v + a_2e_1u^2w + a_3e_1^2uv^2 + a_4e_1uvw + a_5uw^2 + a_6e_1^2v^3 + a_7e_1v^2w + a_8vw^2 = 0. \quad (3.9.12)$$

The resulting space is dP_1 and $\{e_1 = 0\}$ corresponds to the section s_0 , while the divisor $\{u = 0\}$ has become the two-section that is mapped to [Equation 3.9.10](#).¹³

$$\begin{aligned} e_1 = 0 : & \begin{cases} [z_0 : z_1 : 1 : 0] \cong \mathbb{P}^1 & \text{if } a_5 = a_8 = 0 \\ [a_8 : -a_5 : 1 : 0] = s_0 & \text{otherwise} \end{cases} \\ u = 0 : & a_6 e_1^2 + a_7 e_1 w + a_8 w^2 = 0 \end{aligned} \quad (3.9.13)$$

Unlike in the two-section case, one can perform another transition by tuning coefficients such that the two-section defined by $u = 0$ splits into two sections. Setting $a_6 = 0$ splits the two-section into $e_1 = 0$ and $w = 0$ and the resulting singularity is resolved by another blow-up introducing the coordinate e_2 and the substitutions

$$u \mapsto u \cdot e_2, \quad w \mapsto w \cdot e_2 \quad (3.9.14)$$

leading to the proper transform

$$a_0 e_1^2 e_2^2 u^3 + a_1 e_1^2 e_2 u^2 v + a_2 e_1 e_2^2 u^2 w + a_3 e_1^2 u v^2 + a_4 e_1 e_2 u v w + a_5 e_2^2 u w^2 + a_7 e_1 v^2 w + a_8 e_2 v w^2 = 0 \quad (3.9.15)$$

inside dP_2 . Now all three sections are defined by torus-invariant divisors

$$\begin{aligned} e_1 = 0 : & \begin{cases} [u : v : 1 : 0 : 1] \cong \mathbb{P}^1 & \text{if } a_5 = a_8 = 0 \\ [a_8 : -a_5 : 1 : 0 : 1] = s_0 & \text{otherwise} \end{cases} \\ e_2 = 0 : & \begin{cases} [u : 1 : w : 0 : 1] \cong \mathbb{P}^1 & \text{if } a_3 = a_7 = 0 \\ [a_7 : 1 : -a_3 : 0 : 1] = s_1 & \text{otherwise} \end{cases} \\ u = 0 : & \begin{cases} [0 : 1 : 1 : e_1 : e_2] \cong \mathbb{P}^1 & \text{if } a_7 = a_8 = 0 \\ [0 : 1 : 1 : a_8 : -a_7] = s_2 & \text{otherwise} \end{cases} \end{aligned} \quad (3.9.16)$$

and in the blow-down limit $e_1 = e_2 = 1$ they map to

$$s_0 = [0 : 0 : 1] \quad s_1 = [0 : 1 : 0] \quad s_2 = [0 : a_8 : -a_7] \quad (3.9.17)$$

inside \mathbb{P}_2 . Plugging these into [Equation 3.9.7](#) one can confirm that they are the three solutions to $u = 0$ if one sets a_6 and a_9 to zero.

3.9.3 Genus-One Fibrations with Four-Section

Finally, let us treat the last case, namely the complete intersection of two quadrics in \mathbb{P}^3 . Denoting by z_i , $i = 1, \dots, 4$ the homogeneous coordinates of \mathbb{P}^3 , the most general such

¹³In [\[145\]](#) it was first noted that such an ambient fiber space can give rise to a non-toric section as defined in [subsection 3.7.2](#) whose homology class is given by $[u] - [e_1] + \dots$. Roughly speaking, one can subtract the section from the two-section and obtain another proper section. Recently, the explicit coordinate expression of this non-toric section was found in [\[144\]](#).

Homogeneous coordinate z	z_0	z_1	z_2	z_3
Vertex $n_z \in \Delta^\circ$	$\begin{pmatrix} 1 \\ 0 \\ 0 \end{pmatrix}$	$\begin{pmatrix} 0 \\ 1 \\ 0 \end{pmatrix}$	$\begin{pmatrix} 0 \\ 0 \\ 1 \end{pmatrix}$	$\begin{pmatrix} -1 \\ -1 \\ -1 \end{pmatrix}$

Table 3.11: The toric variety \mathbb{P}^3 .

Homogeneous coordinate z	z_0	z_1	z_2	z_3	e_1	e_2	e_3
Vertex $n_z \in \Delta^\circ$	$\begin{pmatrix} 1 \\ 0 \\ 0 \end{pmatrix}$	$\begin{pmatrix} 0 \\ 1 \\ 0 \end{pmatrix}$	$\begin{pmatrix} 0 \\ 0 \\ 1 \end{pmatrix}$	$\begin{pmatrix} -1 \\ -1 \\ -1 \end{pmatrix}$	$\begin{pmatrix} 1 \\ 1 \\ 1 \end{pmatrix}$	$\begin{pmatrix} 0 \\ 0 \\ -1 \end{pmatrix}$	$\begin{pmatrix} 0 \\ -1 \\ 0 \end{pmatrix}$

Table 3.12: The toric variety $\text{Bl}^3\mathbb{P}^3$.

complete intersection can be written as

$$\begin{aligned}
p_1 &= a_9 z_0^2 + a_8 z_0 z_1 + a_7 z_0 z_2 + a_6 z_0 z_3 + a_5 z_1^2 + a_4 z_1 z_2 + a_3 z_1 z_3 + a_2 z_2^2 \\
&\quad + a_1 z_2 z_3 + a_0 z_3^2 \\
p_2 &= a_{19} z_0^2 + a_{18} z_0 z_1 + a_{17} z_0 z_2 + a_{16} z_0 z_3 + a_{15} z_1^2 + a_{14} z_1 z_2 + a_{13} z_1 z_3 + a_{12} z_2^2 \\
&\quad + a_{11} z_2 z_3 + a_{10} z_3^2.
\end{aligned} \tag{3.9.18}$$

Torically, this is the nef partition

$$\nabla_1 = \langle v_0 v_1 \rangle_{\text{conv.}}, \quad \nabla_2 = \langle v_2 v_3 \rangle_{\text{conv.}}, \tag{3.9.19}$$

of the reflexive polytope of [table 3.11](#) and it has the PALP id $(0, 0)$. Just as \mathbb{P}^2 , \mathbb{P}^3 has a single divisor class H , and any linear polynomial in the z_i defines a divisor of this class. H intersects the genus-one curve defined by [Equation 3.9.18](#) four times and therefore the four torus-invariant divisors $z_i = 0$ all define four-sections.

As for the other two spaces, one can split up the four-section into four independent sections by restricting the complex structure coefficients a_i and resolving the resulting singularities. To completely split up the four-section of \mathbb{P}^3 , it takes three blow-ups. Since they proceed in completely the same fashion as for \mathbb{P}^2 and \mathbb{P}_{112} we do not follow them step by step, but only present the final result.

The toric data of the ambient space obtained from blowing up \mathbb{P}^3 three times is displayed in [table 3.12](#) and the nef partition is given by

$$\begin{aligned}
D_1 &= V(z_0) + V(z_1) + V(e_1) + V(e_2) \\
D_2 &= V(z_2) + V(z_3) + V(e_3).
\end{aligned} \tag{3.9.20}$$

Its PALP id is $(67, 0)$ ¹⁴ and it is related to \mathbb{P}^3 via the coordinate maps

$$z_0 \mapsto e_1 e_2 e_3 z_0, \quad z_1 \mapsto e_1 e_2 z_1, \quad z_2 \mapsto e_1 e_3 z_2, \quad z_3 \mapsto e_2 e_3 z_3. \quad (3.9.21)$$

The complete intersection equations are given by

$$\begin{aligned} p_1 &= a_9 e_1 e_2 e_3 z_0^2 + a_8 e_1 e_2 z_0 z_1 + a_7 e_1 e_3 z_0 z_2 + a_6 e_2 e_3 z_0 z_3 \\ &\quad + a_4 e_1 z_1 z_2 + a_3 e_2 z_1 z_3 + a_1 e_3 z_2 z_3 \\ p_2 &= a_{19} e_1 e_2 e_3 z_0^2 + a_{18} e_1 e_2 z_0 z_1 + a_{17} e_1 e_3 z_0 z_2 + a_{16} e_2 e_3 z_0 z_3 \\ &\quad + a_{14} e_1 z_1 z_2 + a_{13} e_2 z_1 z_3 + a_{11} e_3 z_2 z_3 \end{aligned} \quad (3.9.22)$$

and one sees that the blow-down limit $e_1 = e_2 = e_3 = 1$ maps a generic curve inside $\text{Bl}^3 \mathbb{P}^3$ to a non-generic curve inside \mathbb{P}^3 , since its complex structure coefficients always obey

$$a_0 = a_2 = a_5 = a_{10} = a_{12} = a_{15} = 0. \quad (3.9.23)$$

The torus-invariant divisors of the ambient space $\text{Bl}^3 \mathbb{P}^3$ supply four sections, namely

$$\begin{aligned} e_1 = 0 &: [a_1 a_{13} - a_{11} a_3 : a_6 a_{11} - a_{16} a_1 : a_3 a_{16} - a_{13} a_6 : 1 : 0 : 1 : 1] = s_0 \\ e_2 = 0 &: [a_1 a_{14} - a_{11} a_4 : a_7 a_{11} - a_{17} a_1 : 1 : a_4 a_{17} - a_{14} a_7 : 1 : 0 : 1] = s_1 \\ e_3 = 0 &: [a_3 a_{14} - a_{13} a_4 : 1 : a_8 a_{13} - a_{18} a_3 : a_4 a_{18} - a_{14} a_8 : 1 : 1 : 0] = s_2 \\ z_0 = 0 &: [0 : 1 : 1 : 1 : a_3 a_{11} - a_{13} a_1 : a_1 a_{14} - a_{11} a_4 : a_4 a_{13} - a_{14} a_3] = s_3, \end{aligned} \quad (3.9.24)$$

where we have only written down the expressions for generic values of the non-zero a_i s — over codimension two and codimension three loci in the base, the sections wrap entire fiber components.

3.9.4 Mirror-Duality and Mordell-Weil Torsion

Before concluding this section we would like to draw the reader's attention to a remarkable observation first made in [144] for \mathbb{P}_{112} and \mathbb{P}^2 and noted again for \mathbb{P}^3 in [159]. To this end, consider the mirror duals of the generic genus-one curves inside these three ambient spaces: The mirror dual of a genus-one curve inside \mathbb{P}_{112} is an elliptic curve inside the toric variety defined by the reflexive polygon F_{12} of figure 3.7 and the mirror dual of a cubic inside \mathbb{P}^2 is a curve inside $\mathbb{P}^2/\mathbb{Z}_3$. Lastly, the mirror dual of the curve defined by the nef partition $(0, 0)$ is given by the nef partition with PALP id $(3415, 0)$.

The results of section 3.8 show that the torsion part of the toric Mordell-Weil groups of these three spaces are \mathbb{Z}_2 , \mathbb{Z}_3 , and \mathbb{Z}_4 . We hence note that the mirror dual of a genus-one curve with an n -section appears to be an elliptic curve whose Mordell-Weil group has a \mathbb{Z}_n

¹⁴We note that the PALP ids of the ambient space after one and two blow-ups are $(5, 1)$ and $(21, 3)$, respectively. Note that these are the unique ways in which one can blow-up \mathbb{P}^3 torically, as one can relate blow-ups along other loci to these spaces via an $SL(3, \mathbb{Z})$ rotation.

torsion part. This strange “coincidence” becomes even more intriguing once one considers the implications for the low-energy effective theory. As will be shown in [Part III](#), the low-energy effective theory associated with an n -sections appears to have a \mathbb{Z}_n discrete symmetry. On the other hand, the Mordell-Weil torsion \mathbb{Z}_n acts in a very different manner: It quotients out (a subgroup of) the center of a non-toric non-Abelian gauge group $SU(n \cdot k)$ [160]. That mirror duality (performed solely on the elliptic fiber) should exchange these two quantities is a non-trivial conjecture and it would be fascinating to find a physical process explaining this behavior.

Chapter 4

Non-Abelian Singularities from Tops

The presence of non-Abelian gauge symmetries in the low-energy effective physics of an F-theory compactification is invariably connected to singularities of the compactification manifold and their resolution. After resolving, the formerly singular genus-one fiber is replaced by a set of two-spheres intersecting each other in patterns that determine the associated gauge theory algebra. We are thus led to construct genus-one fibrations whose fiber becomes reducible over a specified set of base loci. Generally, there are two ways in which the genus-one fiber can be forced to split into different irreducible components. To understand their difference, we recall in [figure 4.1](#) how our Calabi-Yau manifolds Y are constructed. The key point in the construction of genus-one fibrations is that one considers ambient spaces $X \supset Y$ that possess a fibration themselves. In such a setup, the two scenarios in which the fiber of Y can become reducible are:

- E , the fiber of Y , becomes reducible, but the fiber of the ambient space fibration, F , does not.
- F becomes reducible and forces the genus-one fiber E to become reducible as well.

The first scenario corresponds to the non-toric gauge groups that we examined in [section 3.6](#). However, the second option is the much more appealing one and its study will be the focus of this chapter. Since it is the *toric* fibration of the ambient space that becomes reducible over certain base loci in this scenario, its behavior is determined by the combinatorial data contained in the fan of the ambient space X . Instead of dealing with complicated algebro-geometric objects, one can instead manipulate discrete data. Exploiting computational control inherited from the ambient space was one of the dominant themes of the previous chapter and it remains our guiding principle here as well.

$$\begin{array}{ccccc}
 F & \longrightarrow & X_{n+c} & \xrightarrow{\pi} & B_{n-1} \\
 \uparrow & & \uparrow & \nearrow \pi' & \\
 E & \longrightarrow & Y_n & &
 \end{array}$$

Figure 4.1: In order to construct Calabi-Yau manifolds Y_n with a genus-one fibration π' and fiber E , we construct toric ambient spaces X_{n+c} that are fibered themselves. Here F is the ambient space of the fiber and π is the projection of the ambient space fibration from which π' is obtained by restriction.

We begin in [section 4.1](#) by introducing the concept of a certain polytope called a *top*, the combinatorial object encoding the degeneration of the toric fibration over a certain base divisor. In [section 4.2](#) we explain that tops can be understood both as a polytope and as a prism. While the former description may be more intuitive, the latter turns out to be more convenient for the classification of [\[161\]](#), whose application to $SU(5)$ gauge groups we work out explicitly in [section 4.3](#). Next, we explain in [section 4.4](#) how tops also impose constraints on the charges of the non-Abelian matter representations under additional toric $U(1)$ gauge groups. It is of phenomenological importance that the matter fields in the antisymmetric $SU(5)$ representation of elliptic fibrations with fibers embedded as hypersurfaces all share the same Abelian charges, a statement proved in [section 4.5](#). To circumvent this restriction on the matter content while still considering generic Calabi-Yau manifolds inside toric ambient spaces necessarily leads to the study of complete intersection fibers. [Section 4.6](#) comments briefly on how to generalize tops to fibers of higher codimension.

Finally, we would wish to point out again that [Appendix A](#) contains a concise introduction to the concepts of toric geometry needed in this thesis. Of particular importance to the understanding of this chapter is [section A.8](#), in which the concepts of toric fibrations are recalled.

4.1 Toric Fibrations and Tops

As we have just mentioned, we intend to engineer genus-one fibered Calabi-Yau manifolds whose fibers split into sets of \mathbb{P}^1 s as dictated by discrete toric data. To achieve this, we embed them into toric ambient spaces that are fibrations whose fibers become reducible themselves. Keeping our original goal in mind, we first recall some of the key properties of toric morphisms mentioned in [section A.8](#):

- A fan morphism $\varphi : \Sigma' \rightarrow \Sigma$ induces a toric morphism $\tilde{\varphi} : X_{\Sigma'} \rightarrow X_{\Sigma}$.
- The fiber of $\tilde{\varphi}$ over a point $p \in X_{\Sigma}$ depends only on the torus orbit that p is an element of.
- Every fiber of $\tilde{\varphi}$ is a (possibly reducible) toric variety and the generic fiber is irreducible.

A toric morphism is called a fibration if the dimension of all its fibers is the same and a bundle if all the fibers are isomorphic. We are hence interested in toric fibrations that are not bundles and in particular, we wish to read off how the fan morphism φ determines the properties of $\tilde{\varphi}$. Referring to [section A.8](#) for the general theory behind this, we define here only the quantity most relevant to us: The *top*, which was first introduced by Candelas et al. in [\[162\]](#).

Let Σ be a fan with a fan morphism $\varphi : \Sigma \rightarrow \Sigma_B$ that gives rise to a fibration with two-dimensional fibers. Given a base ray $b \in \Sigma_B$, we call the polytope

$$\tau(b) = \langle \cup_{z \in \mathbb{Z}_{\geq 0}} \varphi^{-1}(z \cdot b) \rangle_{\text{conv}}. \quad (4.1.1)$$

the *top* over b . Note that $\tau(b)$ is three-dimensional and its elements are graded by z . The elements corresponding to $z = 0$ are just the kernel of φ and therefore they are the rays spanning the fan of the generic fiber. We call the convex hull of the integral points of $\tau(b)$ that are not in the kernel of φ the *cap* of τ . If the cap consists of just a single point, then τ is said to be *trivial*. The key observation of Candelas was that the geometry of the cap already determines the intersection properties of the blow-up divisors and allows to read off the low-energy effective gauge theory group of an F-theory compactification.

For simplicity, let us restrict to two-dimensional caps made up only of elements with $z = 1$, i.e. polygons with k boundary points. The graph consisting of the boundary points and the edges between them is a circle and it corresponds to the affine Dynkin diagram of the gauge algebra it induces, namely the affine Dynkin diagram of A_{k-1} . In order to see how this works in practice, we study an explicit example with an $SU(5)$ top placed over one of the base divisors.

4.1.1 $SU(5) \times U(1)^2$ with Toric Sections

While we will eventually wish to study full-fledged Calabi-Yau manifolds, we focus here only on the fiber and the top over a single base divisor and postpone discussing the entire fibration to [chapter 5](#). Consider a genus-one curve embedded as a hypersurface inside the toric variety corresponding to the reflexive polygon F_{12} of [figure 3.7](#). From [subsection 3.8.1](#) we know that this choice of ambient space implies that there are five toric sections — every single fiber ambient space divisor descends to a toric section of the fibration. However, not all of the generators are independent with respect to the Mordell-Weil group law and therefore the toric Mordell-Weil group is only \mathbb{Z}^2 . As a consequence, we expect there to be a toric $U(1)^2$ gauge group factor in the low-energy effective theory.

To engineer an $SU(5)$ singularity along a base divisor we consider a toric variety with the toric data given in [table 4.1](#). For our purposes, we can keep the base manifold and the choice of fibration general and parametrize them by the u_i vectors and their corresponding homogeneous variables. The only requirement that we put is that the u_i vectors with $i > 0$ only appear once on the right hand side, which is the same as demanding that the tops $\tau(u_i)$

Homogeneous coordinate z	Point $n_z \in \nabla$
f_0	-1 -1 0
f_1	1 -1 0
f_2	1 0 0
f_3	0 1 0
f_4	-1 1 0
e_0	-2 0 u_0
e_1	-1 0 u_0
e_2	0 0 u_0
e_3	-1 1 u_0
e_4	-2 1 u_0
$u_i, i > 0$	n_1^i n_2^i u_i

Table 4.1: The toric data of the fiber F_{12} and its corresponding $SU(5)$ top placed over a base ray u_0 . In order to specify the full fibration, the remaining base rays u_i and the line bundles on the base that the fiber coordinates are sections of must be chosen. This is symbolized by the entry with u_i in the table. Note that the u_i are $\dim_{\mathbb{C}} B$ -dimensional vectors.

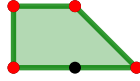


Figure 4.2: The unique $SU(5)$ top for the F_{12} fiber. The exceptional divisors intersected by one of the five toric sections are colored red. For more information on the intersection patterns we refer to [section 4.4](#) and [figure 4.3](#).

with $i > 0$ are trivial. On the other hand, the top over u_0 is non-trivial and its cap is the polygon with four vertices and five boundary points shown in [figure 4.2](#). From the discussion above we expect an $SU(5)$ gauge theory to be located on the base divisor defined by the base ray u_0 . To see that this is indeed the case, we write down the hypersurface inside the fiber ambient space that is defined by this class of F-theory models. It reads

$$p = a_0 e_3 e_4 f_2 f_3^2 f_4^2 + a_1 e_1 e_2^2 e_3 f_1^2 f_2^2 f_3 + a_2 f_0 f_1 f_2 f_3 f_4 + a_3 e_0^2 e_1 e_3 e_4^2 f_0^2 f_3 f_4^2 \quad (4.1.2)$$

$$+ a_4 e_0 e_1 e_2 f_0^2 f_1^2 f_2 + a_5 e_0^2 e_1 e_4 f_0^3 f_1 f_4,$$

where the a_j are sections of line bundles over the base manifold, i.e. homogeneous polynomials in u_i . Using the methods of [chapter 3](#), we find that the corresponding Weierstrass model (see [Equation 3.1.2](#)) has the Weierstrass coefficients

$$f = \left(-\frac{1}{48}\right) \cdot \left(a_2^4 - 8a_0 a_2^2 a_4 \cdot u_0 + (-8a_1 a_2^2 a_3 + 16a_0^2 a_4^2 + 24a_0 a_1 a_2 a_5) \cdot u_0^2 \quad (4.1.3)\right.$$

$$\left. - 16a_0 a_1 a_3 a_4 u_0^3 + 16a_1^2 a_3^2 \cdot u_0^4\right)$$

Base Locus	Vanishing degrees of f, g and Δ			Gauge Algebra
$a_0 = 0$	0	0	2	$\mathfrak{su}(2)$
$a_1 = 0$	0	0	2	$\mathfrak{su}(2)$
$u_0 = 0$	0	0	5	$\mathfrak{su}(5)$

Table 4.2: The three singular loci of the Calabi-Yau manifold of [table 4.1](#) in codimension one in the base.

Base Locus	Vanishing degrees of f, g and Δ			Gauge Algebra	$SU(5)$ representation
$a_4 = 0$	0	0	6	$\mathfrak{su}(6)$	5
$a_5 = 0$	0	0	6	$\mathfrak{su}(6)$	5
$a_0 a_5 = -a_2 a_3$	0	0	6	$\mathfrak{su}(6)$	5
$a_2 = 0$	2	3	7	$\mathfrak{so}(10)$	10

Table 4.3: The four enhanced singularity loci of the Calabi-Yau manifold of [table 4.1](#) in codimension two in the base and the associated matter representations of $SU(5)$.

and

$$\begin{aligned}
g = \left(-\frac{1}{864} \right) \cdot \left(-a_2^6 + 12a_0 a_2^4 a_4 \cdot u_0 + (12a_1 a_2^4 a_3 - 48a_0^2 a_2^2 a_4^2 - 36a_0 a_1 a_2^3 a_5) \cdot u_0^2 \right. \\
+ (-24a_0 a_1 a_2^2 a_3 a_4 + 64a_0^3 a_4^3 + 144a_0^2 a_1 a_2 a_4 a_5) \cdot u_0^3 \\
+ (-48a_1^2 a_2^2 a_3^2 - 96a_0^2 a_1 a_3 a_4^2 + 144a_0 a_1^2 a_2 a_3 a_5 - 216a_0^2 a_1^2 a_5^2) \cdot u_0^4 \\
\left. - 96a_0 a_1^2 a_3^2 a_4 \cdot u_0^5 + 64a_1^3 a_3^3 u_0^6 \right), \quad (4.1.4)
\end{aligned}$$

implying that the discriminant has the expansion

$$\begin{aligned}
\Delta = \left(-\frac{1}{16} \right) \cdot a_0^2 \cdot a_1^2 \cdot u_0^5 \cdot \left(a_4 \cdot a_5 \cdot (-a_2 a_3 + a_0 a_5) \cdot a_2^4 \right. \\
\left. - a_2^2 \cdot (-a_2^2 a_3^2 a_4^2 - 8a_0 a_2 a_3 a_4^2 a_5 - a_1 a_2^2 a_3 a_5^2 + 8a_0^2 a_4^2 a_5^2 + a_0 a_1 a_2 a_5^3) \cdot u_0 \right) + \mathcal{O}(u_0^7) \quad (4.1.5)
\end{aligned}$$

with respect to $u_0 \equiv e_0 e_1 e_2 e_3 e_4$, which serves as a normal coordinate to the base divisor over which the fibration has the singularity enforced by the top.

From these explicit expressions one can read off the vanishing degrees of f , g , and Δ along different base loci of codimension one. [Table 4.2](#) contains the three loci and we note that there is in fact an $SU(5)$ gauge symmetry along the base divisor over which we placed a non-trivial top. Since we expanded f , g and Δ in the direction normal to the $SU(5)$ singularity, we can even read off its enhancement loci, which are not directly visible from the toric data. [Table 4.3](#) shows that we expect to find up to three curves which all contain matter in the fundamental representation of $SU(5)$, but are distinguished by the additional Abelian symmetries. We cannot directly read off their charges from the ambient space geometry, but we will infer constraints in [section 4.4](#) before explicitly calculating the charges later on.

Furthermore, there are two non-toric non-Abelian $SU(2)$ factors and we note that if they are realized in the full-fledged fibration (i.e. the polynomials a_0 and a_1 are non-constant), then one must include the additional rays $(-1 \ 0 \ 0)$ and $(0 \ -1 \ 0)$ in the toric data of [table 4.1](#) to resolve the singularities. Since the $SU(2)$ loci are not defined by the vanishing of a single homogeneous coordinate, finding their matter states is slightly more involved and we refer to [[144](#), [163](#)] for an introduction to the necessary techniques.

In summary, we see that the chosen top does indeed induce an $SU(5)$ gauge group in the low-energy effective theory obtained by considering F-theory on this Calabi-Yau manifold. More examples and an explicit relation between the top geometry and the ensuing singularity can be found in the original papers [[161](#), [162](#)].

4.2 Tops as Prisms

In addition to the description of the top given in the previous section, there exists another equivalent one introduced in [[161](#)] which can sometimes be more useful. Before formulating it, we need to make a general remark regarding the uniqueness of a top. As mentioned above, the fiber of a top τ is a reflexive polygon and it is given by the facet of τ at $z = 0$. First, note that we can always rescale z such that there are points in τ with $z = 1$. Second, the $GL(3, \mathbb{Z})$ -subgroup generated by $(x, y, z) \mapsto (x + \alpha z, y + \beta z, z)$ still acts on the top after fixing the fiber polygon and therefore the x, y coordinates of the points with $z = 1$ can be shifted arbitrarily.

Assuming without loss of generality that τ has this form, we can consider its dual (see [Equation A.5.3](#) for a definition). Since τ is not reflexive¹, its dual polyhedron τ° is not a lattice polytope. Instead, it is an infinite polyhedron. This can be understood better by taking a closer look at the inequalities defining τ° . The vertices $(x_i, y_i, 0)$ corresponding to vertices of the fiber F of τ lead to inequalities of the type

$$x^* x_i + y^* y_i \geq -1, \quad (4.2.1)$$

where (x^*, y^*, z^*) are the coordinates of the dual polyhedron and the remaining vertices give inequalities

$$z^* z_i \geq -1 - x^* x_i - y^* y_i \quad (4.2.2)$$

with $z_i > 0$. Hence τ° is a prism over the dual of F . Since F is a reflexive polygon, so is F° and thus every vertex of τ° is of the form $(x^*, y^*, z^*(x, y))$ with $(x^*, y^*) \in F^\circ$. Furthermore, the vertex dual to the facet of τ at $z = 1$ is the point $(0, 0, -1)$ of τ° . Therefore the data defining τ° (and hence of course τ) consists of F° and the function $z^*(x^*, y^*)$ evaluated at the

¹As one can see from its definition, τ is only a part of a reflexive polytope. In fact, its name stems from the original constructions of [[162](#)], where $K3$ surfaces over a \mathbb{P}^1 base were considered. Since the polytope of a $K3$ is three-dimensional and the base polytope consists only of two points, the top is half of a $K3$ polytope - the other part is the “bottom.”

Fiber	F_1	F_2	F_3	F_4	F_5	F_7	F_9	F_{12}	F_{13}	F_{14}	F_{15}	F_{16}
$ \text{Aut}_{\text{lattice}} $	6	8	2	2	2	12	2	2	2	2	8	6

Table 4.4: The twelve reflexive polygons with non-trivial lattice automorphism groups and their respective orders. Observe that the lattice automorphism groups of a polygon and its dual are the same.

non-zero integral points (i.e. the boundary points) of F° . Again, there is a residual $GL(3, \mathbb{Z})$ symmetry action on the coordinate choices, since two functions z^* that differ only by a linear function define the same top. Shifting by a linear function, one can always bring z^* in a form where $z^*(p) \geq -1$ for all boundary points.

Bouchard and Skarke used this dual presentation of the top in [161] to classify all possible tops that have the 16 reflexive polygons as fibers and in the appendix of their paper one finds a list of all allowed z^* values together with the singularity types they result in. In the case that we are most interested in, namely that of A -type singularities, one must still identify tops that are related by automorphisms of the fiber polygon. Computing these automorphism groups and applying the results to $SU(5)$ tops is the goal of the next section.

4.3 All $SU(5)$ -Tops for Hypersurfaces

In order to extract all possible $SU(5)$ tops with reflexive fiber polygons from [161], one must first compute the lattice automorphism groups of the 16 reflexive polygons. The lattice automorphism group $\text{Aut}_{\text{lattice}}(P)$ of a d -dimensional polytope P is the integral subgroup of the automorphism group

$$\text{Aut}(P) \subset E(d) = GL(d, \mathbb{R}) \ltimes \mathbb{R}^d \quad (4.3.1)$$

which in turn is defined as the subgroup of the Euclidean group preserving P . In table 4.4 we list the twelve polygons with non-trivial lattice automorphism groups. Evidently, these lattice automorphisms act as permutations on the tuple obtained by evaluating z^* on the boundary points of the dual fiber polytope F^* . One must therefore identify those tops in [161] whose z^* tuples are related by such permutations. After accounting for these identifications, one is left with the 37 distinct $SU(5)$ tops that we list in figure 4.3. In this figure, we draw the $SU(5)$ tops without reference to a the origin of a coordinate system, since they can be shifted arbitrarily. The tuple of integers next to each top gives the dual description in terms of z^* .

Finally, we remark that there exist three fiber polygons that do not possess $SU(5)$ tops, namely F_{13} , F_{15} , and F_{16} . A comparison with table 3.9 shows that these are precisely the fibers whose toric Mordell-Weil group has \mathbb{Z}_2 and \mathbb{Z}_3 torsion factors. Mordell-Weil torsion \mathbb{Z}_n has the effect of quotienting out (a subgroup of) the center of the non-Abelian gauge group [160] and it can therefore only act on gauge groups whose center contains \mathbb{Z}_n . This restricts $SU(N)$ groups to $SU(n \cdot k)$ with $k \in \mathbb{N}$ and, in this case, forbids $SU(5)$.

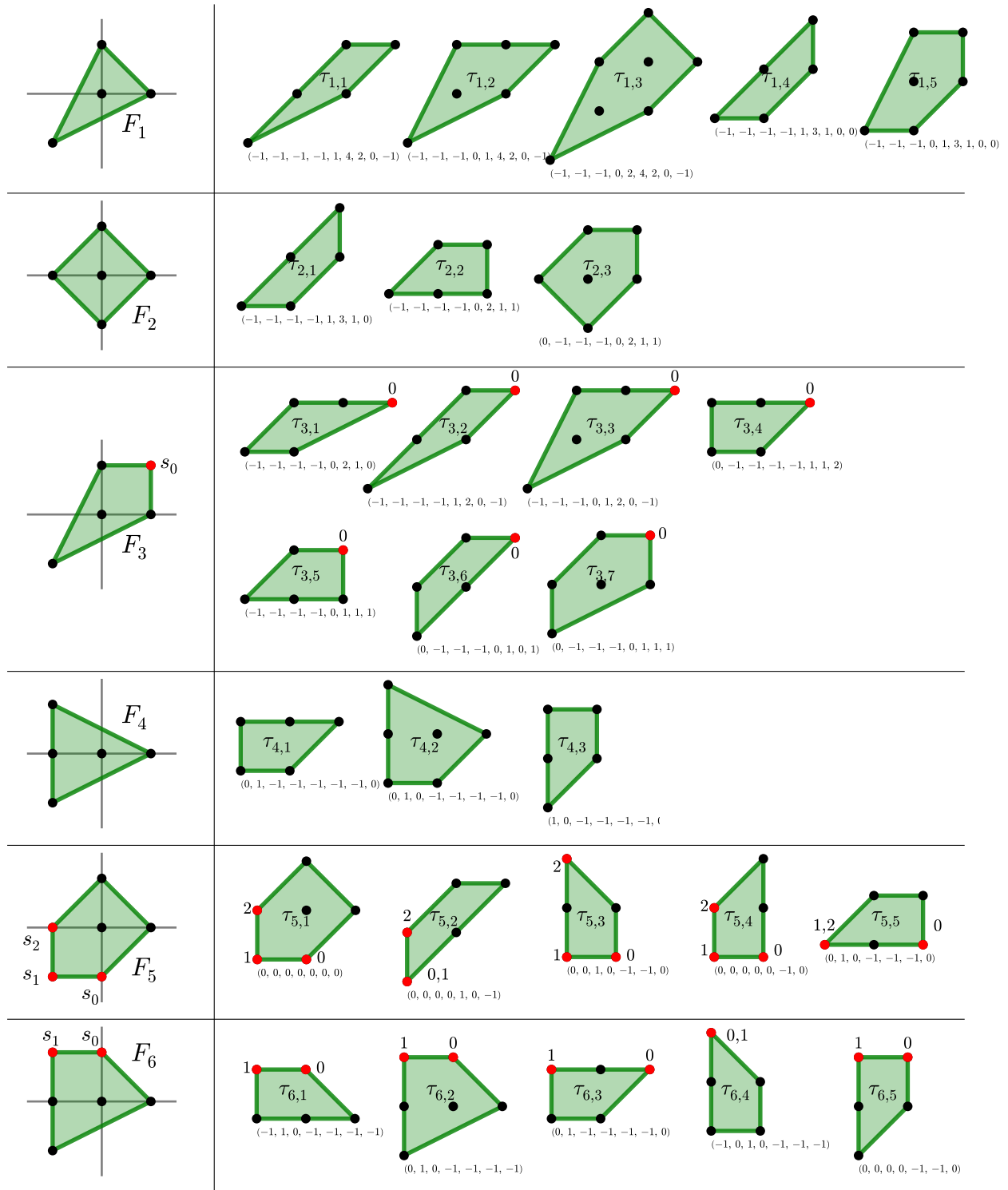


Figure 4.3: The $SU(5)$ tops based on the 16 reflexive polygons. Numbers next to boundary points of the facet in the $z = 1$ plane indicate which toric sections intersect the associated exceptional divisor.

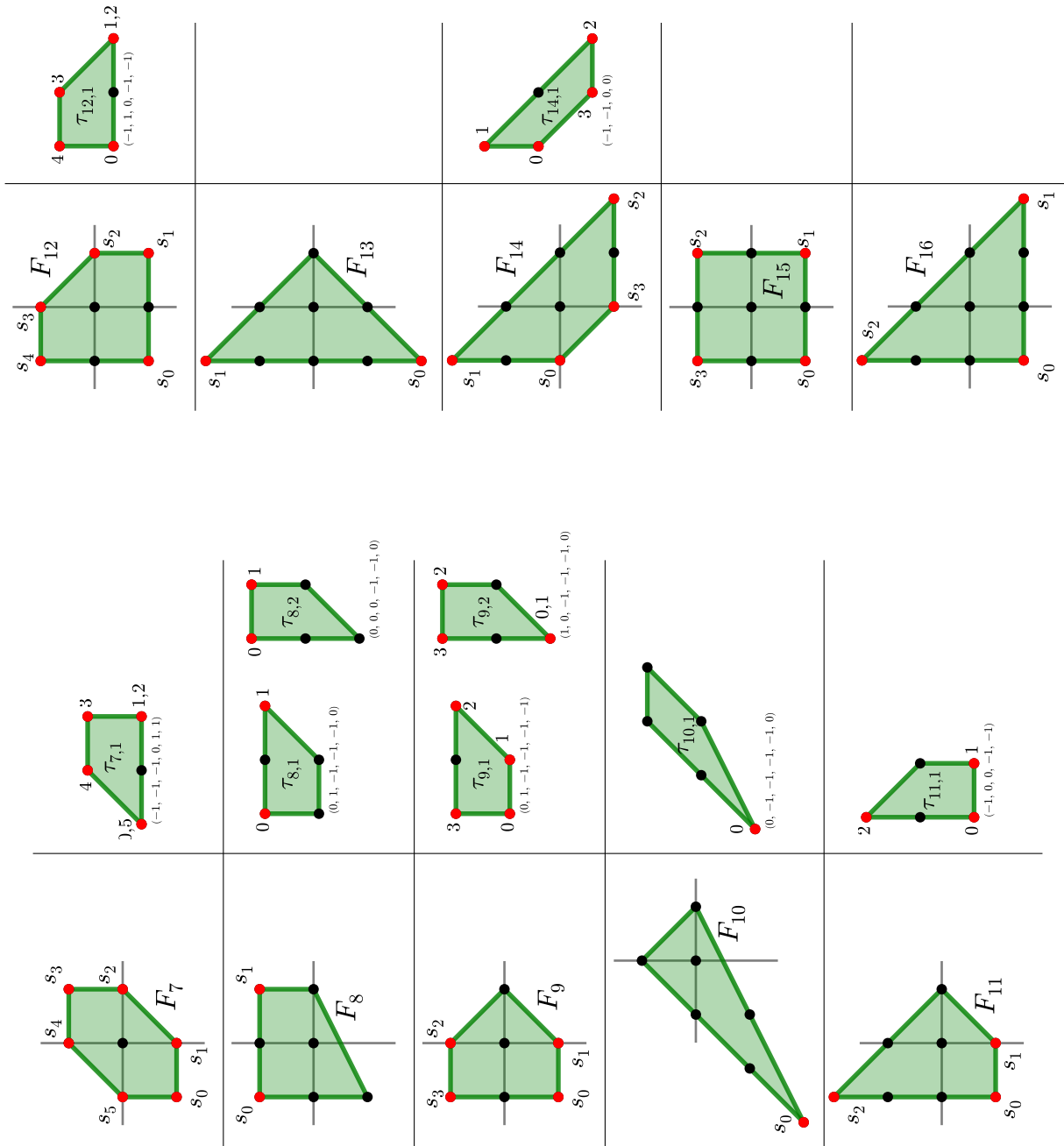


Figure 4.3: (continued) The $SU(5)$ tops $\tau_{i,j}$ based on the 16 reflexive polygons. For each reflexive polygon (the fiber polygon at $z = 0$), the admissible facets at $z = 1$ are listed. Below each the values of z^* on the vertices of the dual polygon (in clockwise order, starting at the “y”-axis) are given, which provide an equivalent way of specifying the top. See discussion at the beginning of [section 4.2](#).

4.4 Constraints on Matter Representations from Tops

After developing the formalism to compute the toric Mordell-Weil group purely from the toric data of the ambient fiber space in [chapter 3](#) and devising a method to engineer tops inducing non-Abelian gauge symmetries in the preceding sections, it is natural to ask whether the toric ambient space also determines the matter representations present in the F-theory compactification.

Since matter arises in codimension two in the base manifold, the influence of the toric ambient space geometry is weaker and it is not possible to read off the full set of matter fields. The best one can achieve is to find the *maximum set* of matter representations — whether these are actually present in a given compactification then depends on the choice of base manifold and fibration, similarly to the non-toric non-Abelian gauge groups of [section 3.6](#). In fact, this is what we did in for the example of [subsection 4.1.1](#), where we found three distinct **5** curves and a **10** curve. Similarly, one can also determine the singlet curves or matter belonging to non-toric non-Abelian gauge groups by looking for the most general singularity enhancements in codimension two as for example in [[144](#), [156–158](#), [163](#), [164](#)]. By analyzing the intersection patterns between the \mathbb{P}^1 s of the degenerated fiber and the sections, one can then also compute the $U(1)$ charges of the matter.

Here we take a complimentary route and focus on the constraints of the matter charges that are directly visible in the toric data of a top, namely the $U(1)$ *split*. To explain what we mean by that, we have to illustrate schematically to which divisors the $U(1)$ fields of the low-energy effective theory correspond. Let s_0 be the *zero section*, i.e. the section generating the neutral element of the elliptic fiber and let $\sigma = s - s_0$ generate a factor \mathbb{Z} of the toric Mordell-Weil group. If we assume that there is only a single non-Abelian singularity, then the associated $U(1)$ divisor is (up to an overall rescaling to ensure integral charges) obtained by applying the Shioda map [[165](#), [166](#)] and reads

$$D_{U(1)} = \sigma - \pi^*(D_b) - \underbrace{(\sigma \cap \mathcal{C}_{\alpha_I})(\mathcal{C}^{-1})^{IJ} D_J}_{\text{determines split}}. \quad (4.4.1)$$

Here $\pi^*(D_b)$ is the pullback of a base divisor specified later, the \mathcal{C}_{α_I} are the \mathbb{P}^1 fiber curves over the non-Abelian singularity that do generically not intersect s_0 and the D_I are the \mathcal{C}_{α_I} fibered over the base locus of the singularity. Finally, \mathcal{C}_{IJ} is simply a constant matrix related to the Cartan matrix of the non-Abelian Lie algebra. The important point is that the third term depends on the intersection number $\sigma \cap \mathcal{C}_{\alpha_I}$ which is computed purely in the fiber. It is this term that is determined already by the top and we will now study its impact on the $U(1)$ charges.

For simplicity, we restrict to $SU(5)$ groups, but the same arguments can be applied to other gauge groups, since the Shioda map of [Equation 4.4.1](#) depends on the type of gauge algebra only through the constant matrix \mathcal{C}_{IJ} . $(\mathcal{C}^{-1})^{IJ}$ has fractional entries and in the case

of $SU(5)$ we multiply $D_{U(1)}$ by five to ensure that all contributions in Equation 4.4.1 have integral coefficients.

4.4.1 $U(1)$ -Splits and Matter Representations

F-theory compactifications with gauge groups $SU(5)$ usually have three different $SU(5)$ representations: The fundamental representation $\mathbf{5}$ and the antisymmetric representation $\mathbf{10}$ obtained from local singularity enhancements to $SU(6)$ and $SO(10)$, respectively, and the singlet representation originating from loci away from the non-Abelian singularity.

Due to the rescaling, the $U(1)$ charges of the matter fields in the singlet representation of $SU(5)$ are divisible by five,

$$Q_{U(1)}(\mathbf{1}) \in 5\mathbb{Z}, \quad (4.4.2)$$

since the third term of Equation 4.4.1 (the only one whose coefficients are not multiples of five) does not contribute. This is because the singlets are located away from the non-Abelian singularity along which the divisors D_I are localized.

Non-trivial $SU(5)$ representations come from loci along the non-Abelian singularity and now the third term of Equation 4.4.1 does contribute. However, its contribution depends only on the intersection numbers $D_I \cap \mathcal{C}'_{\alpha_j}$, where the \mathcal{C}'_{α_j} are the fiber components *after* the additional singularity enhancement. Since this intersection pattern is determined by group theory (i.e. whether the enhancement is to $SU(6)$ or to $SO(10)$), the contribution of the third term is the same for two matter fields if they are in the same representation under $SU(5)$, independently of whether they are charged differently under additional $U(1)$ symmetries. In a nutshell, one has that

$$\begin{aligned} Q_{U(1)}(\mathbf{5}) &\in 5\mathbb{Z} + k \\ Q_{U(1)}(\mathbf{10}) &\in 5\mathbb{Z} + k', \end{aligned} \quad (4.4.3)$$

where $k \in \{0, 1, 2, 3, 4\}$ and since $\mathbf{10}$ is the antisymmetric representation one furthermore finds that $k' = 2k$. Again, n is determined by the first two terms and will generally take different² values for a given non-Abelian representation. k , on the other hand, will not and is called the *split* of a given $U(1)$ with respect to this $SU(5)$ gauge factor.

4.4.2 $U(1)$ -Splits and the Top

Next, we relate the integer k determining the split to the geometry of the top. To do so, recall the discussion of section 2.3 and remember that the choice of fiber curves \mathcal{C}_{α_I} as they were introduced earlier in this section depends on which section one chooses as the zero

²Of course, n only takes finitely many different values. In fact, since it is an intersection number, there are strong constraints on the allowed values, since the intersection number between a rational section and a fiber component can only take very special values [52].

section s_0 : The generic fiber over an $SU(5)$ singularity has five fiber components with a circular intersection pattern. Generically³, s_0 intersects only one of them. This component is identified as the affine node of the affine Dynkin diagram of $\mathfrak{su}(5)$ and the remaining \mathbb{P}^1 become the fiber curves \mathcal{C}_{α_I} and correspond to the simple roots of $\mathfrak{su}(5)$.

Since one expects the low-energy effective theory of an F-theory background to be independent of the choice of zero section⁴, it is clear that k can only depend on the relative position between the intersection of s and s_0 with the fiber. In figure 4.4 we show the only five options, corresponding to $k = 0, 1, 2, 3, 4$, respectively. Note that identifying the \mathbb{P}^1 com-

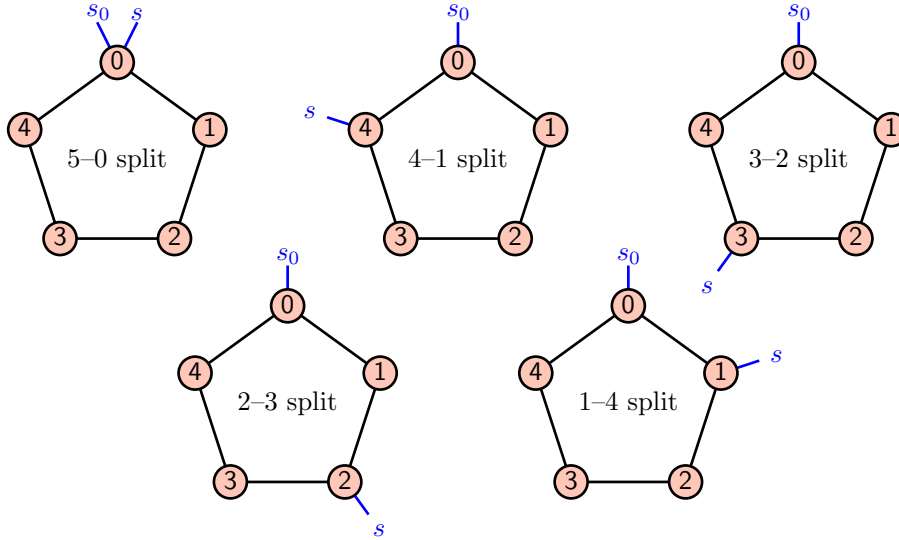


Figure 4.4: The different splits for the case in which s_0 denotes the zero section and $\sigma = s - s_0$ is one of possibly more independent Mordell-Weil generators. In the case of a single $U(1)$, the $i-(5-i)$ -split and the $(5-i)-i$ -split are equivalent under to the \mathbb{Z}_2 outer automorphism of $\mathfrak{su}(5)$.

ponents with simple roots of $\mathfrak{su}(5)$ is unique only up to a \mathbb{Z}_2 ambiguity corresponding to the outer automorphism $\mathcal{C}_{\alpha_I} \leftrightarrow \mathcal{C}_{\alpha_{5-I}}$. After eliminating said ambiguity, one is left with only three possible intersections patterns in the case of a single $U(1)$ generator, namely the first three of figure 4.4. If there are multiple $U(1)$ generators σ_m , then there exists a split k_m with respect to each of them and the \mathbb{Z}_2 automorphism of $\mathfrak{su}(5)$ acts on all of them simultaneously.

As argued above, the intersection structure between toric sections and the irreducible fiber components is already fixed by the top alone. In fact, one can easily read off the intersection numbers from the geometry of the top. $SU(N)$ tops have a two-dimensional cap

³If s_0 is a non-holomorphic section, then there can be loci of codimension two in the base manifold over which it intersects two components.

⁴Further implications of the independence of the F-theory compactification of the choice of a zero section was recently explored in [115].

whose boundary points correspond to the \mathbb{P}^1 fiber components. If we let v be a vertex of the fiber polygon corresponding to a toric section s and denote the lattice points corresponding to the i -th fiber component by w_i , then s intersects the i -th fiber component if and only if v and w_i share an edge. Using this prescription, we have determined the intersection numbers for all $SU(5)$ tops in [figure 4.3](#) by listing the sections intersecting a certain exceptional divisor next to the corresponding lattice point of the $z = 1$ facet of the top.

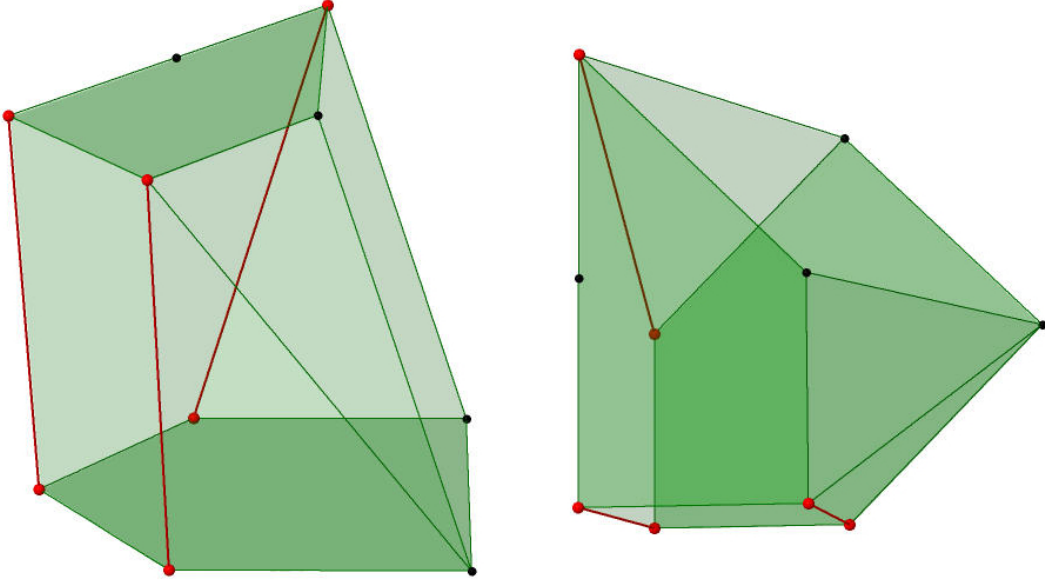


Figure 4.5: Two different three-dimensional visualizations of the entire top $\tau_{5,3}$. Fiber vertices corresponding to sections and lattice points associated to exceptional divisors intersecting them are colored red, as are the edges connecting them.

To give an example, consider the top $\tau_{5,3}$. From [table 3.9](#), we see that the toric sections generate a subgroup $MW_T \cong \mathbb{Z} \oplus \mathbb{Z}$ of the entire Mordell-Weil group. Now, pick s_0 as the zero section and assign simple roots α_i in clockwise order to the boundary points of $\tau_{5,3}$. Taking $\sigma_0 = s_1 - s_0$ and $\sigma_1 = s_2 - s_0$ as generators of $U(1)_1$ and $U(1)_2$, we find that the charges of the **5** representations must satisfy

$$Q_{U(1)_1}(\mathbf{5}) \equiv 1 \pmod{5} \quad \text{and} \quad Q_{U(1)_2}(\mathbf{5}) \equiv 3 \pmod{5}. \quad (4.4.4)$$

In [figure 4.5](#) we present a three-dimensional visualization of the intersection structure for $\tau_{5,3}$.

Finally, let us point out that the above notion of splits agrees with the cases that have been analyzed with the split spectral cover constructions [[60](#), [78–80](#)] only in the case of a single $U(1)$. As soon as there are multiple Abelian gauge symmetries, our notation describes the “split” between the section generating the particular $U(1)$ symmetry and the zero section, whereas the split spectral cover constructions denote by split the factorization pattern of the

spectral cover. Hence, when there are multiple $U(1)$ s we determine a split with respect to each one of them.

4.5 A No-Go-Theorem for Antisymmetric Representations

We now turn to the **10** matter fields of the $SU(5)$ gauge theory. Somewhat surprisingly, their geometric origin is different from the **5** matter fields. The **5** matter fields come from an individual \mathbb{P}^1 in the I_5 Kodaira fiber degenerating into two irreducible components, but this kind of degeneration will never yield a codimension-two I_1^* Kodaira fiber where the **10** matter field is localized: Splitting nodes of the I_5 Kodaira fiber will never eliminate the fundamental group $\pi_1(I_5) = \mathbb{Z}$ of the Kodaira fiber, but $\pi_1(I_1^*) = 0$. The only way to obtain a simply connected fiber is to have the hypersurface equation vanish identically on a toric curve of the top. That is, along the intersection of the irreducible components of the toric surfaces in the fiber of the ambient toric variety. Note that the irreducible components of the two-dimensional ambient space fiber correspond to the vertices of the top that are not interior to a facet and not part of the fiber polygon. They intersect in a toric curve $\simeq \mathbb{P}^1$ whenever the triangulation induced by the fan joins two vertices.

As we will see in [chapter 5](#), if an $SU(5)$ -top contains a point interior to a facet then the fibration is not flat, i.e. there are base loci over which the fiber dimension jumps. Non-flat fibrations leads to low-energy theories that are not ordinary gauge theories and therefore we only have to focus on tops without facet interior points. For an $SU(5)$ top this means that the facet at height $z = 1$ is a degenerate lattice pentagon with one of the lattice points at a midpoint of an edge. Up to isomorphism, there is only a single such lattice pentagon, see [figure 4.3](#). There are two fine triangulations T_1 and T_2 of this boundary facet and they are shown on the left hand side of [figure 4.6](#). Regardless of the triangulation, the degenerate toric ambient space fiber consists of five irreducible surfaces $V(e_0), \dots, V(e_4)$. These always intersect cyclically in toric curves, that is, $V(e_i) \cap V(e_{i+1}) \simeq \mathbb{P}^1$. Depending on the triangulation, they additionally intersect as the internal one-simplices in the triangulation, that is,

- Triangulation T_1 : $V(e_0) \cap V(e_3) \simeq \mathbb{P}^1$ and $V(e_0) \cap V(e_2) \simeq \mathbb{P}^1$,
- Triangulation T_2 : $V(e_0) \cap V(e_3) \simeq \mathbb{P}^1$ and $V(e_1) \cap V(e_3) \simeq \mathbb{P}^1$.

The Calabi-Yau hypersurface generically intersects the toric \mathbb{P}^1 s corresponding to the boundary one-simplices in a point, and is a non-zero constant on the toric \mathbb{P}^1 corresponding to the internal one-simplices. As argued in the beginning of this section, the **10** matter is localized when the whole toric \mathbb{P}^1 is contained in the hypersurface, that is, where the above constant happens to be zero.⁵ Since the internal one-simplices are internal to the same facet of the top, the hypersurface always vanishes simultaneously on both toric curves. These two toric

⁵This is at a codimension-one curve of the discriminant, that is, it is of codimension two in the base.

\mathbb{P}^1 s intersect in a toric point, the containing two-simplex. Hence they form two nodes joined by an edge in the dual fiber diagram, which will turn out to be the middle two nodes of the \tilde{D}_5 extended Dynkin diagram.

Intersecting the hypersurface Y with the ambient space irreducible surface components of a fiber yields additional curve components for the degenerate elliptic fiber. These necessarily contain the toric curves of the adjacent internal one-simplices as irreducible components. For example, in triangulation T_1 the intersection $Y \cap V(e_0)$ contains both toric surfaces $V(e_0) \cap V(e_3)$ and $V(e_0) \cap V(e_2)$ as irreducible components. Likewise, $Y \cap V(e_4)$ contains none of the toric \mathbb{P}^1 since the vertex e_4 is not adjacent to an interior one-simplex. This fixes the degeneration of the I_5 Kodaira fiber, that is the five curves $Y \cap V(e_i)$ away from the matter curve, to be the one shown on the right hand side of figure 4.6.

This is the key observation: The triangulation of the top fixes the degeneration of the codimension-one Kodaira fiber at the codimension-two **10** matter curves of a toric hypersurface. Since the triangulation is fixed for a given manifold, the degeneration is the same for all **10**. Importantly, this behavior is different from that of the **5** matter curves, where different degenerations occur over different codimension-two fibers. As a corollary, the $U(1)$ charges of all **10** matter representations are equal. In other words, if one wants to construct F-theory GUTs such that the **10** fields carry different $U(1)$ charges then one needs to consider complete intersections such that the fiber is at least codimension-two in the ambient space fiber [89, 158, 159].

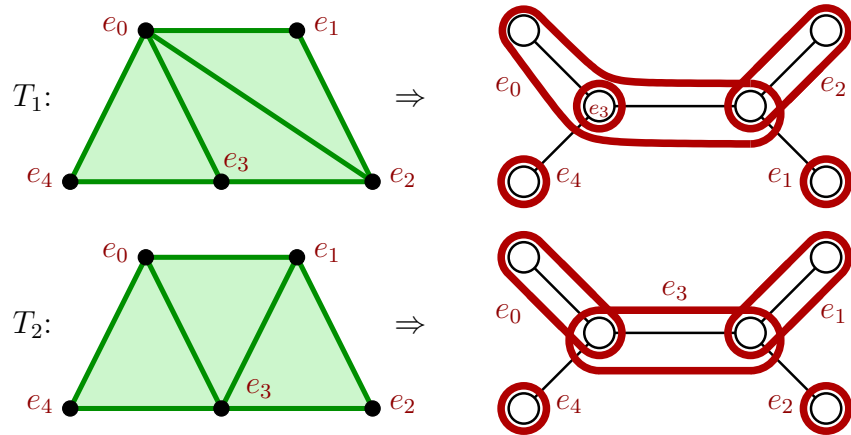


Figure 4.6: Left: The two possible fine triangulations of the lattice polygon at height $z = 1$ in the $SU(5)$ -top. Right: The corresponding degeneration of the $I_5 \rightarrow I_1^*$ Kodaira fiber.

4.6 Tops for Complete Intersections

As a direct conclusion from the preceding section we are led to complete intersection elliptic curves. In fact, constructing F-theory models with multiple antisymmetric $SU(5)$ representations was part of the motivation to provide the framework of [section 3.4](#) and to classify the toric Mordell-Weil groups for three-dimensional Gorenstein Fano varieties.

In principle the toric machinery applies equally to Calabi-Yau manifolds with fibers embedded in higher-dimensional ambient spaces and one can extend the definition of a top to higher dimensions: A genus-one fibration with codimension- d fibers has $(d + 1)$ -dimensional tops, which can then be combined to form a reflexive polytope. Unfortunately, however, there does not yet exist an analogous classification to that of [\[161\]](#) and therefore the exhaustive list of $SU(5)$ tops is not yet known for higher-dimensional tops. Nevertheless, it is possible to construct *some* $SU(5)$ tops simply by making an ansatz and confirming that it leads to an $SU(5)$ singularity in the blow-down limit, as we will show in [subsection 5.3.2](#).

Chapter 5

Fibered Calabi-Yau Manifolds

With the building blocks studied in the previous chapter at hand, the last remaining step and the goal of this chapter is to combine them with a base manifold into a full-fledged Calabi-Yau manifold. Once that is achieved, one can then attempt to answer so far unresolved questions that depend not only on details of the fiber geometry, but also on properties of the full fibration.

As elaborated on in the introduction to [Part II](#), the ultimate goal in studying string compactifications is not only to construct a single manifold satisfying a set of criteria, but rather to identify all such spaces. Achieving the latter objective remains far out of reach, but at least some progress can be noted: Given a top and a toric base, we explain in [section 5.1](#) how to obtain all varieties corresponding to the reflexive polytopes made up of these building blocks. In possession of an algorithm to construct explicit fibrations, we proceed with the study of global properties of the compactification. As we will show, Calabi-Yau manifolds constructed inside toric ambient spaces may have fibrations that are *non-flat*, i.e. their fiber dimension increases over certain base loci. Crucially, this happens generically already for Calabi-Yau fourfolds with a resolved $SU(5)$ -singularity. Since flat fibrations appear to be essential for phenomenologically viable F-theory models, [section 5.2](#) is dedicated to studying the conditions under which fibrations are flat. Using different examples, we show that for certain combinations of top and base one cannot construct flat fibrations. Finally, we construct a range of different example manifolds in [section 5.3](#) to illustrate as concretely as possible how to handle non-toric $U(1)$ s and manipulate complete intersection fibers giving rise to $SU(5)$ models with multiple antisymmetric representations and additional discrete symmetries.

5.1 The Auxiliary Polytope of All Fibrations

By definition, the top describes the degeneration of the ambient space fibration and thus that of the genus-one fibration over a toric divisor in the base. This base divisor is defined by one of the rays in the base fan. The obvious question is how this data can be completed into

that of a compact Calabi-Yau manifold, that is, how to combine the top and the choice of base fan to a reflexive polytope. In fact, this has a nice answer: The remaining choices for a lattice polytope after fixing the tops and the base again are parametrized by the integral points of a further auxiliary polytope.¹ This just follows from convexity, and one needs to verify reflexivity and flatness of the fibration by hand.

In particular, we will be interested in the case of a single top together with trivial tops over the remaining rays of the base fan. For the purposes of this section, we will only consider the case where the base fan equals \mathbb{P}^n , whose rays are generated by the unit vectors e_1, \dots, e_n together with $-\sum e_i$. Then

- The fixed top can be chosen to project to $[0, e_1]$.
- The single point generating the trivial top over each of e_2, \dots, e_n can be chosen to have fiber coordinates $(0, 0)$ by a $GL(n, \mathbb{Z})$ rotation fixing all previous tops.
- The final point, generating the trivial top over $-\sum e_i$, has coordinates $(p_1, p_2) \in \mathbb{Z}^2$ with no remaining freedom of coordinate redefinition.

This parametrizes the choices of completion to a polytope by a pair of integers (p_1, p_2) . These are constrained by convexity: Having fixed the height-one points of the other tops, there is only a finite range of (p_1, p_2) such that the fiber (preimage of the origin in the base) of the convex hull does not exceed the chosen fiber polygon. These are linear constraints, turning the allowed region for (p_1, p_2) into a polygon (with not necessarily integral vertices). Note that the p_k correspond to choosing the line bundles that the homogeneous coordinates (and therefore their coefficients) are sections of. In fact, one can derive the same linear constraints by demanding that all the line bundle that the complex structure coefficients are sections of do indeed admit a section [167].

It turns out that all lattice polytopes for a single $SU(5)$ top over \mathbb{P}^n that one constructs just by demanding convexity, as above, are automatically reflexive. Their total number for small values of n is listed in table 5.1. We included also the cases \mathbb{P}^4 and \mathbb{P}^5 that, when used as base of an F-theory compactification, would not lead to a gauge theory in four or six dimensions. However, the construction can be supplemented by additional polynomials specifying the actual base as hypersurface in \mathbb{P}^4 or complete intersection in \mathbb{P}^5 . For example, the Fano threefold obtained by a quartic constraint in \mathbb{P}^4 is a viable choice for the base. Note that realizing the base itself as hypersurface or complete intersection can be also phenomenologically motivated. Such realizations allow for more exhaustive choices of fluxes on the GUT brane as demonstrated in the models of [168, 169]. This applies in particular to hypercharge flux [57, 64, 170] that is non-trivial on the GUT brane but trivial on the entire base manifold. Our construction thus extends straightforwardly to these more involved Calabi-Yau fourfold examples.

¹This polytope is not necessarily integral, that is, its vertices are in general rational.

Fiber	Top	$N_{\mathbb{P}^1}^{SU(5)}$	$N_{\mathbb{P}^2}^{SU(5)}$	$N_{\mathbb{P}^3}^{SU(5)}$	$N_{\mathbb{P}^4}^{SU(5)}$	$N_{\mathbb{P}^5}^{SU(5)}$
F_1	$\tau_{1,1}$	1	5	12	22	35
F_1	$\tau_{1,2}$	1	5	12	22	35
F_1	$\tau_{1,3}$	1	4	8	14	21
F_1	$\tau_{1,4}$	1	5	12	22	35
F_1	$\tau_{1,5}$	1	5	11	18	27
F_2	$\tau_{2,1}$	2	9	20	30	42
F_2	$\tau_{2,2}$	3	10	21	36	55
F_2	$\tau_{2,3}$	3	8	15	24	35
F_3	$\tau_{3,1}$	2	9	20	35	54
F_3	$\tau_{3,2}$	3	10	21	36	55
F_3	$\tau_{3,3}$	3	10	21	36	55
F_3	$\tau_{3,4}$	3	10	21	36	55
F_3	$\tau_{3,5}$	3	10	21	36	55
F_3	$\tau_{3,6}$	3	10	21	36	55
F_3	$\tau_{3,7}$	3	10	21	36	55
F_4	$\tau_{4,1}$	3	10	21	36	55
F_4	$\tau_{4,2}$	3	10	21	36	55
F_4	$\tau_{4,3}$	3	10	21	36	55
F_5	$\tau_{5,1}$	6	12	20	31	44
F_5	$\tau_{5,2}$	5	15	30	50	75
F_5	$\tau_{5,3}$	5	15	30	50	75
F_5	$\tau_{5,4}$	6	16	31	51	76
F_5	$\tau_{5,5}$	5	15	30	50	75
F_6	$\tau_{6,1}$	6	16	31	51	76
F_6	$\tau_{6,2}$	6	16	31	51	76
F_6	$\tau_{6,3}$	5	15	30	50	75
F_6	$\tau_{6,4}$	5	15	30	50	75
F_6	$\tau_{6,5}$	6	16	31	51	76
F_7	$\tau_{7,1}$	8	18	30	45	63
F_8	$\tau_{8,1}$	8	21	40	65	96
F_8	$\tau_{8,2}$	8	21	40	65	96
F_9	$\tau_{9,1}$	8	21	40	65	96
F_9	$\tau_{9,2}$	8	21	40	65	96
F_{10}	$\tau_{10,1}$	8	21	40	65	96
F_{11}	$\tau_{11,1}$	11	27	50	80	117
F_{12}	$\tau_{12,1}$	11	27	50	80	117
F_{14}	$\tau_{14,1}$	14	23	38	57	80

Table 5.1: Number $N_{\mathbb{P}^n}^{SU(5)}$ of reflexive polytopes fibered over \mathbb{P}^n with one $SU(5)$ -top and n trivial tops, modulo fiber-preserving automorphisms.

The above algorithm can directly be generalized to more complicated base manifolds than \mathbb{P}^n or to higher-dimensional tops in a straightforward manner. For every homology class of the toric basis there is a tuple of integers (p_1^k, \dots, p_d^k) , where k now runs over the homology classes and d is the dimension of the fiber ambient space defined by the top.

5.2 Flatness of the Fibration

Not all compactifications of F-theory give rise to ordinary gauge theories, as they may contain tensionless strings yielding an infinite tower of massless fields in the low-energy effective action. While there is nothing wrong with that, these theories have to be excluded when one looks for phenomenologically viable theories. Alternatively, one could try to lift all but finitely many of these massless fields through fluxes. The geometric origin of these massless strings [49, 50, 171, 172] are three-branes wrapping a curve inside a surface of vanishing volume in the F-theory limit. Such a surface must necessarily sit over a point in the discriminant locus, that is, in a fiber of the elliptic fibration that is at least two-dimensional. Clearly, this cannot happen if all degenerate fibers are of Kodaira type. Hence, any $K3$ hypersurface in a toric variety constructed by gluing two tops along the fiber polygon has all fibers one-dimensional. As already mentioned in the introduction of this chapter, a fibration with the property that all fibers are of the same dimension is called *flat*.²

For the case of hypersurfaces in toric varieties, there are two possible sources for non-flat fibers:

- The ambient toric fiber can jump in dimension. That is, the toric fibration of the ambient space can already fail to be flat [137]. This happens in particular if one places two non-Abelian tops on neighboring base rays such that the intersection is not a Miranda model [173].
- Even if the ambient toric fibration is flat, the hypersurface equation can vanish identically in the fiber direction for certain fibers. Then the fiber of the elliptic fibration becomes two-dimensional.

The flatness of the ambient toric fibration can easily be checked [137, 149, 174] using toric methods. In particular, this is always the case when only a single non-trivial top is used. Hence, we will focus in the remainder of this paper on the second source for non-flat fibers. In this case, the non-flat fibers do not generally lie over toric fixed points.

5.2.1 Codimension-Two Fibers

While elliptic $K3$ s are always flat fibrations, a toric Calabi-Yau threefold hypersurface can be non-flat even if the ambient toric fibration is. These codimension-two (over the base,

²Flat in the sense of homological algebra, that is, the functions in a neighborhood of each fiber are a flat module over the function ring of the base.

codimension-one inside the discriminant) non-flat fibers come from lattice points interior to the $z = 1$ facets. This is because a point interior to a facet corresponds to a toric divisor such that the hypersurface equation restricts to a (generically non-zero) constant. However, a point interior to a facet of the top is usually not interior to a facet of the entire four-dimensional polytope. This means that the hypersurface equation is *not* constant on the corresponding divisor in the ambient space, but only in the fiber direction. In fact, this fiber-wise constant is a section of a nef line bundle over the (toric) discriminant component, and therefore has a zero somewhere. This is the location of the non-flat fiber.

There is one loophole in the argument: If the base ray over which the non-trivial top is placed, is itself a point interior to a facet of the base polytope, then a point interior to a facet of the top is also interior to a facet of the four-dimensional polytope. Geometrically, this means that the discriminant component is a curve of self-intersection -2 and the hypersurface again avoids the corresponding toric divisor entirely. However, this is not a physically desirable situation: The hypersurface equation restricted to this discriminant component is now independent of the point along the discriminant. Therefore, there are no codimension-two degenerations at all, and in particular no matter curves. Hence we will not consider this case in the following, and only allow tops with no points interior to facets.

For example, consider the del Pezzo surface of degree two, that is F_5 in [figure 4.3](#), as the fiber polygon. Then one of the tops, namely $\tau_{5,1}$, will have non-flat fibers and the remaining four tops $\tau_{5,2}, \dots, \tau_{5,5}$ yield flat fibrations in codimension two.

5.2.2 A General Flatness Criterion

Having described the flatness criterion for codimension-two fibers, we now proceed to generalize it to arbitrary codimension. As an example, we then apply it to the physically relevant case of codimension-three fibers in elliptically fibered fourfolds.

By an analogous argument as in the previous section, a Calabi-Yau hypersurface in an ambient flat fibration will be flat itself if the hypersurface equation never vanishes identically in the fiber direction. For simplicity, consider the case where there is only a single non-trivial top. To understand the hypersurface equation we collect the monomials of the hypersurface equation $p = 0$ by their dependence on the top homogeneous coordinates $z_\tau = \{z_{\tau,1}, \dots, z_{\tau,k}\}$ as

$$p(z_\tau, z) = \sum_{\vec{i}=(i_1, \dots, i_k) \in I} z_\tau^{\vec{i}} p_{\vec{i}}(z) = \sum_{\vec{i} \in I} z_\tau^{\vec{i}} \left(\sum_{\vec{j} \in J_{\vec{i}}} a_{\vec{i}\vec{j}} z^{\vec{j}} \right), \quad a_{\vec{i}\vec{j}} \in \mathbb{C}. \quad (5.2.1)$$

The irreducible components of the degenerate fiber induced by the top are the toric divisors $z_{\tau,\ell} = 0$ corresponding to the integral points of the top that are not in the fiber polygon. One needs to check for every irreducible component that the fibration is flat. The irreducible fiber component $z_{\tau,\ell} = 0$ projects to one discriminant component D_τ , and the local coordinates on D_τ are the rays in the star of $\pi(\tau)$ in the base. Each of the polynomials $p_{\vec{i}}(z)$ only depends on the base coordinates and therefore defines a divisor $V_\tau(p_{\vec{i}}) \subset D_\tau$ on the discriminant. Then

a generic hypersurface is a flat fibration over D_τ if these divisors do not meet, that is,

$$D_\tau \ni \bigcap_{\substack{\vec{i} \in I \\ z_\tau^\ell \nmid z_\tau^{\vec{i}}}} V_\tau(p_{\vec{i}}) = \bigcap_{\substack{\vec{i} = (i_1, \dots, i_k) \in I \\ i_\ell = 0}} V_\tau(p_{\vec{i}}) = \emptyset. \quad (5.2.2)$$

The summation range I is over all fiber monomials, that is, integral points of the dual of the top polytope intersected with the projection of the dual polytope of the ambient toric variety. The summation range $J_{\vec{i}}$ is the fiber of the projection of the dual polytope, that is, over all integral points of the dual polytope whose monomial is divisible by $z_\tau^{\vec{i}}$.

Phrasing [subsection 5.2.1](#) in this language, if $z_{\tau, \ell}$ corresponds to the ray generated by an integral point interior to a facet of the top, then $I = \{\vec{i}\}$ consists of only a single element. The corresponding divisor $V_\tau(p_{\vec{i}}) \subset D_\tau$ will generically be non-empty and, therefore, the fibration non-flat. The only loophole is if the divisor is empty, that is, $J_{\vec{i}} = \{\vec{j}\}$ consists of a single point which then must be a vertex of the dual polytope. But this means that the point was not just interior to a facet of the top, but interior to a facet (dual to \vec{j}) of the ambient toric variety.

5.2.3 Codimension-Three Fibers

We now apply the flatness criterion to Calabi-Yau fourfold hypersurfaces. As we will see, flatness is a non-generic property in the sense that it imposes additional equations on the polytope of compactifications defined in [section 5.1](#). Hence, the flat fourfold fibrations are identified with integral points in a strictly smaller-dimensional polytope than the set of all convex lattice polytopes with the specified top and base.

The new source for non-flat fibers are irreducible fiber components such that there are only two distinct fiber monomials. These correspond to integral points of the top such that their dual face in the dual top contains exactly two points, that is, such that the dual face is an interval. In other words, the corresponding integral point of the top is along an edge of the top such that it is contained in only two two-faces. Note that this is the case for *every* $SU(5)$ -top that is not already non-flat in codimension two due to an integral point interior to a facet. This is because the polygon at height $z = 1$ of the $SU(5)$ -top, see [figure 4.3](#), is a lattice polygon with circumference five in lattice units. But such a lattice polygon has either an interior point or is degenerate, see also [figure 4.3](#). Therefore, each $SU(5)$ top that is flat in codimension-two yields a non-trivial flatness condition in codimension-three associated to the integral point on the edge.

For simplicity, let us assume that the discriminant component D_τ of the $SU(5)$ -top is a toric surface where any two effective divisors intersect. This will always be the case in the examples below, where we will be using $D_\tau = \mathbb{P}^2$. Consider now the toric divisor $z_{\tau, \ell} = 0$ corresponding to the integral point interior to an edge. The index set $I = \{\vec{i}^{(0)}, \vec{i}^{(1)}\}$ consists of two elements, corresponding to the two facets $F_{\tau, 2}^{(0)}, F_{\tau, 2}^{(1)}$ of the top adjacent to the edge. The fibration is then flat if and only if one of the divisors is trivial, say, $V_\tau(p_{\vec{i}^{(1)}}) \subset D_\tau$.

$\nabla_{10,1}(p_1, p_2)$	fiber		base		
	1	0	0	0	0
fiber	0	1	0	0	0
	-3	-2	0	0	0
	0	0	1	0	0
$\tau_{10,1}$	-1	0	1	0	0
	-2	-1	1	0	0
	-3	-2	1	0	0
	-1	-1	1	0	0
trivial top	0	0	0	1	0
trivial top	0	0	0	0	1
trivial top	p_1	p_2	-1	-1	-1

$\nabla_{3,6}(p_1, p_2)$	fiber		base		
	1	0	0	0	0
fiber	0	1	0	0	0
	-1	0	0	0	0
	-1	-1	0	0	0
	-2	-1	1	0	0
$\tau_{3,6}$	-1	-1	1	0	0
	-1	0	1	0	0
	0	-1	1	0	0
	0	0	1	0	0
trivial top	0	0	0	1	0
trivial top	0	0	0	0	1
trivial top	p_1	p_2	-1	-1	-1

Table 5.2: Parametrization $(p_1, p_2) \in \mathbb{Z}^2$ of all polytopes with base \mathbb{P}^3 and top $\tau_{10,1}$ (left) and $\tau_{3,6}$ (right), respectively. The fibration is the projection on the last three coordinates.

This is the case if $J_{\bar{\tau}(1)}$ contains a single element, which then must be a vertex of the dual ambient space polytope. Hence, the facet $F_{\bar{\tau},2}^{\bar{\tau}(1)}$ of the top is contained in only a single facet of the ambient space polytope. Note that one of the facets $F_{\bar{\tau},2}^{(0)}, F_{\bar{\tau},2}^{(1)}$ of the $SU(5)$ -top will be parallel to the fiber polygon and the other will contain at least one point of the fiber polygon. The former will always be contained in at least two facets of the ambient space unless the base ray $\pi(\tau)$ is an interior point of a facet of the base polytope. As discussed in [subsection 5.2.1](#), this is not a particularly interesting case and we will ignore it in the following. Therefore, the facet $F_{\bar{\tau},2}^{\bar{\tau}(1)}$ of interest is the one that contains at least one point of the fiber polygon.

5.2.4 Studying the Flatness of Some Examples

The constraints from flatness of the fibration can rule out a fixed combination of top and base polytope. To see this explicitly, we will look at two examples in this section, namely the top $\tau_{10,1}$ and $\tau_{3,6}$, respectively, to construct an elliptic fibration over \mathbb{P}^3 . Note that $\tau_{10,1}$ is the unique $SU(5)$ -top in Weierstrass form, that is, with ambient space fiber $\mathbb{P}^2[1, 2, 3]$. The $\tau_{3,6}$ used here has different coordinates than in [figure 4.3](#), but it is $GL(2, \mathbb{Z})$ -equivalent to it. As described in [section 5.1](#), we can choose coordinates such that everything except the fiber coordinates of a single point are fixed. These are shown in [table 5.2](#).

Imposing convexity of the five-dimensional polytopes amounts to the inequalities

$$\begin{aligned}
 \nabla_{10,1}(p_1, p_2) : \quad & p_1 + p_2 \leq 4, \quad -p_1 + p_2 \leq 3, \quad p_1 - 2p_2 \leq 3 \\
 \nabla_{3,6}(p_1, p_2) : \quad & p_1 + p_2 \leq 4, \quad -p_1 \leq 2, \quad p_1 - 2p_2 \leq 2, \quad -p_1 + p_2 \leq 3.
 \end{aligned}
 \tag{5.2.3}$$

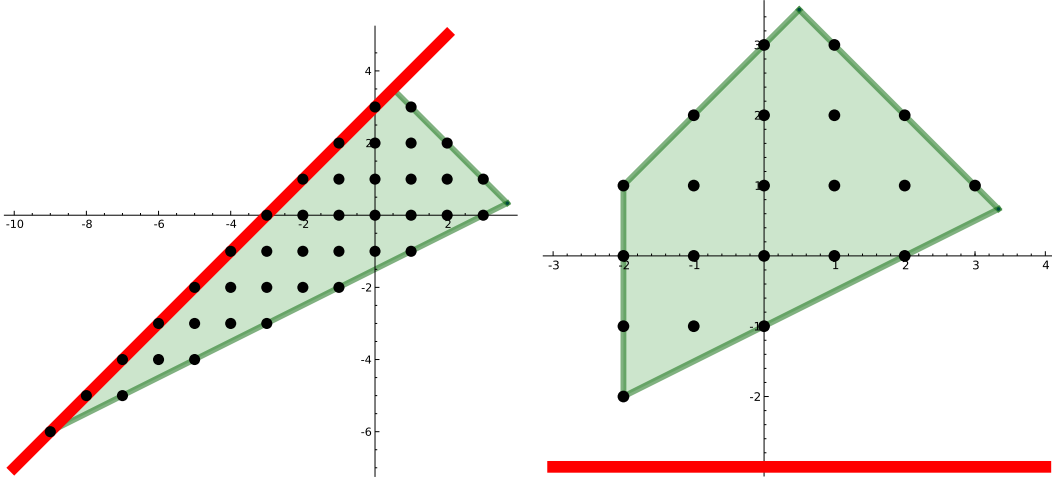


Figure 5.1: The black points are the solution set (p_1, p_2) for $SU(5)$ models with top $\tau_{10,1}$ (left) and $\tau_{3,6}$ (right) fibered over \mathbb{P}^3 . The green polygon is the convexity constraint from Equation 5.2.3. The red line is the condition of flatness of the fibration, see Equation 5.2.6.

The interior point of an edge in the $\tau_{10,1}$ -top is $(-2, -1, 1, 0, 0)$. The relevant two-face of the top for the flatness criterion is

$$F_{\tau_{10,1,2}}^{(1)} = \langle (-3, -2, 1, 0, 0), (-1, 0, 1, 0, 0), (-3, -2, 0, 0, 0), (0, 1, 0, 0, 0) \rangle \quad (5.2.4)$$

This facet is contained in the (p_1, p_2) -independent supporting hyperplane of the total polytope $\nabla_{10,1}(p_1, p_2)$ defined by

$$(1, -1, 0, -1, -1) \cdot \vec{x} + 1 = 0. \quad (5.2.5)$$

It is contained in further facets of $\nabla_{10,1}$ unless the final point $(p_1, p_2, -1, -1, -1)$ is also on this hyperplane, and therefore cannot span an independent facet. This is a linear equation for (p_1, p_2) . Together with the result for the second example, this equation is

$$\begin{aligned} \nabla_{10,1}(p_1, p_2) : \quad p_1 - p_2 &= -3 \\ \nabla_{3,6}(p_1, p_2) : \quad p_2 &= 3 \end{aligned} \quad (5.2.6)$$

The constraints coming from convexity and flatness are shown in figure 5.1. We observe that there are many flat elliptic fibrations using the $\tau_{10,1}$ top, but none with the $\tau_{3,6}$ top.

5.2.5 Flattening Base Change

It is perhaps unexpected that for \mathbb{P}^3 , the simplest choice of base for a Calabi-Yau fourfold, the top $\tau_{3,6}$ cannot be used to construct a flat elliptic fibration. However, this does not rule out every fibration with this top — combined with base manifolds other than \mathbb{P}^3 , one can

$\nabla_{3,6}^{\mathbb{P}^1 \times \mathbb{P}^2}(p_1, p_2; p_3, p_4)$	fiber		base		
fiber	1	0	0	0	0
	0	1	0	0	0
	-1	0	0	0	0
	-1	-1	0	0	0
$\tau_{3,6}$	-2	-1	1	0	0
	-1	-1	1	0	0
	-1	0	1	0	0
	0	-1	1	0	0
	0	0	1	0	0
trivial top	p_1	p_2	-1	0	0
trivial top	0	0	0	1	0
trivial top	0	0	0	0	1
trivial top	p_3	p_4	-1	-1	-1

Table 5.3: Parametrization $(p_1, p_2; p_3, p_4) \in \mathbb{Z}^4$ of all polytopes with base $\mathbb{P}^1 \times \mathbb{P}^2$ and single $SU(5)$ -top $\tau_{3,6}$ over $\{\text{pt.}\} \times \mathbb{P}^2$. The fibration is the projection on the last three coordinates.

achieve flatness in codimension three. Here we show that there exist flat fibrations with $\tau_{3,6}$ as top over the base $\mathbb{P}^1 \times \mathbb{P}^2$. Since it is instructional to consider a different base than just \mathbb{P}^n , we will give some of the details of the possible reflexive polytopes for this base manifold.

First of all, not all divisors of the base are equivalent any more. For definiteness, we put the divisor of the $SU(5)$ singularity at $D_\tau = \{\text{pt.}\} \times \mathbb{P}^2 \subset \mathbb{P}^1 \times \mathbb{P}^2$. Up to coordinate changes, there are now four integers parametrizing the possible embeddings in a five-dimensional polytope, see [table 5.3](#). The polytope of compactifications is now four-dimensional, and contains 75 integral points. These are the 75 solutions to the convexity constraints. Again, it turns out that for this choice of base all polytopes that are allowed by convexity are actually reflexive. All have $h^{1,1} = 8$, corresponding to a single $U(1)$. Out of these, three polytopes yield a flat fibration. These are

$$(p_1, p_2; p_3, p_4) \in \{(0, 0; -3, -3), (0, 1; -3, -3), (1, 1; -3, -3)\}. \quad (5.2.7)$$

5.3 Various Examples of Calabi-Yau Fibrations

As a conclusion of [Part II](#) of this thesis, we now present a selection of full-fledged genus-one fibered Calabi-Yau manifolds that can serve as F-theory backgrounds. We begin in [subsection 5.3.1](#) with a six-dimensional Calabi-Yau manifold constructed from the top $\tau_{3,6}$ and show that it possesses both a toric and a non-toric section leading to an $SU(5) \times U(1)$ gauge group. In order to analyze the matter states of the resulting F-theory compactification, we

Homogeneous coordinate z	Divisor $V(z)$	Point $n_z \in \nabla \cap N$			
u_1	H_1	-1	-1	-1	-1
u_2	H_2	0	0	0	1
e_0	D_0	-2	-1	1	0
e_1	D_1	-1	0	1	0
e_2	D_2	0	0	1	0
e_3	D_3	0	-1	1	0
e_4	D_4	-1	-1	1	0
f_0	F_0	-1	0	0	0
f_1	F_1	0	1	0	0
f_2	F_2	1	0	0	0
f_3	F_3	-1	-1	0	0

Table 5.4: The toric data for the smooth Calabi-Yau threefold Y inside the toric ambient space X . Together with the origin, these are the only integral points in the lattice polytope ∇ and we will be using the notation on the right for the corresponding toric divisors. The Hodge numbers are $h^{11}(Y) = 7$ and $h^{21}(Y) = 63$. Together with the fact that there is a I_5 discriminant component, the Shioda-Tate-Wazir formula [175] tells us that $\text{rank } MW(Y) = 1$. The fan is given in (C.4.1).

explain how to use toric methods to explicitly compute their charges. Next, we continue with Calabi-Yau manifolds whose elliptic fiber is given by a complete intersection instead of just a hypersurface. As we demonstrate in subsection 5.3.2, the additional freedom of a complete intersection allows to realize $SU(5)$ models with different antisymmetric representations. Furthermore, we construct F-theory models with a discrete \mathbb{Z}_4 symmetry as well as Calabi-Yau manifolds with a \mathbb{Z}_4 Mordell-Weil torsion factor in subsection 5.3.3 and subsection 5.3.4, respectively.

Let us emphasize that these examples are not the only F-theory geometries analyzed in this work — in fact, in Part III we study several additional elliptically fibered Calabi-Yau manifolds. However, while we will still be relying on the methods developed in this part of the thesis, Part III will focus on the physical implications of rational sections and multisections, while here we concentrate largely on the geometric properties of these spaces.

5.3.1 $SU(5) \times U(1)$ with Non-Toric Section

As promised above, let us now construct a Calabi-Yau manifold with the top $\tau_{3,6}$. From subsection 3.8.1 we know that such a fibration has a single toric section. However, the interesting aspect of our construction is the presence of an additional *non-toric* section. Since this section is present already in a Calabi-Yau threefold, we choose a two-dimensional base (for simplicity, a \mathbb{P}^2) for the top. We note that this construction can of course be extended to higher dimensions. However, as discussed thoroughly in section 5.2, it then becomes necessary

to pay attention to possible non-minimal singularities in codimension three in the base, which make the fibration non-flat. In fact, as shown in [subsection 5.2.4](#) and [subsection 5.2.5](#), it becomes necessary to use other base manifolds than \mathbb{P}^3 (such as $\mathbb{P}^1 \times \mathbb{P}^2$) to allow for flat fibrations with this top.

To be completely explicit, we will be considering the Calabi-Yau hypersurface [151] in the ambient toric variety specified by [table 5.4](#). The elliptic fibration is a toric morphism, that is, it is induced by a map of the fan Σ of the toric ambient space, given explicitly in [Equation C.4.1](#), to the fan of \mathbb{P}^2 by projecting on the last two coordinates of $N \simeq \mathbb{Z}^4$. In terms of homogeneous coordinates, the projection map $\pi : X \rightarrow \mathbb{P}^2$ is given by

$$\pi : [u_1 : u_2 : e_0 : \dots : e_4 : f_0 : \dots : f_3] \mapsto [e_0 e_1 e_2 e_3 e_4 : u_1 : u_2] \quad (5.3.1)$$

and we thus introduce $u_0 \equiv e_0 e_1 e_2 e_3 e_4$, the combination mapping to the third homogeneous coordinate of the base manifold \mathbb{P}^2 . We see that the homogeneous coordinates f_0, \dots, f_3 corresponding to the rays in the kernel of the projection parametrize the fiber in the ambient space. The I_5 discriminant component is the curve $[0 : u_1 : u_2] \in \mathbb{P}^2$ and the five divisors D_0, \dots, D_4 map to it. In a generic fiber of the discriminant (codimension-one over the base), the Calabi-Yau hypersurface cuts out a \mathbb{P}^1 in each of the five components, yielding the I_5 Kodaira fiber.

Since the generic fiber is a dP_1 ³, there is precisely one toric section defined by $f_0 = 0$. To compute the coordinate expression of the section, we simply solve the hypersurface equation. Homogeneous coordinates whose points are not in the star of the cone $\langle n_{f_0} \rangle$ cannot vanish simultaneously with f_0 and can be scaled to one.⁴ Setting $f_0 = 0$, $f_2 = d_i = 1, i > 0$ the hypersurface equation takes the form

$$p : \alpha_0 f_1 + (\alpha_1 u_1^2 + \alpha_2 u_1 u_2 + \alpha_3 u_2^2 + \alpha_4 u_1 e_0 + \alpha_5 u_2 e_0 + \alpha_6 e_0^2) f_3 = 0. \quad (5.3.2)$$

This equation can be solved trivially for the homogeneous fiber coordinates $[f_1 : f_3]$ along the F_0 divisor. In fact, $f_1 \neq 0 = f_3$ is forbidden if all coefficients α_m are sufficiently generic, so we may scale $f_3 = 1$ as well. Thus, the section is

$$\begin{aligned} s_0 : [u_0 : u_1 : u_2] &\mapsto [u_1 : u_2 : u_0 : 1 : 1 : 1 : 1 : 0 : f_1(u_0, u_1, u_2) : 1 : 1], \\ f_1(u_0, u_1, u_2) &= -\frac{1}{\alpha_0} (\alpha_1 u_1^2 + \alpha_2 u_1 u_2 + \alpha_3 u_2^2 + \alpha_4 u_1 u_0 + \alpha_5 u_2 u_0 + \alpha_6 u_0^2). \end{aligned} \quad (5.3.3)$$

We see that $s_0 = \{p = f_0 = 0\}$ is not only a section, which could have been learned from intersection theory alone, but also that it is a holomorphic section.

It remains to find a second section, namely the generator of the Mordell-Weil group. This is made more interesting by the fact that none of the remaining toric fiber divisors $F_1|_Y$, $F_2|_Y$, $F_3|_Y$ defines a section for us. In fact, $F_1|_Y$ and $F_3|_Y$ define two-sections and $F_2|_Y$

³The corresponding reflexive polygon of [table 3.9](#) is F_3 and it is related to the toric data of the fiber in [table 5.4](#) by a simple change of basis.

⁴These coordinates lie in the Stanley-Reisner ideal when multiplied with f_0

a three-section. Hence we will approach this section differently, and, instead of explicitly finding its equation, we will determine its homology class by following the steps outlined in [subsection 3.7.2](#). From here on we drop the subscript Y and implicitly assume that we are talking about restrictions of F_i to the hypersurface when we are talking about multisections. A first guess at finding the non-toric section, which is wrong but instructive, is to take $[F_1 - F_0]$. It is a two-section minus a section and therefore, numerically, a section. In more elaborate terms,⁵ the generic fiber has the homology class $H_1 \cap H_2 = \pi^{-1}([1 : 0 : 0])$. By a simple intersection computation, its intersection with the tentative section is therefore

$$[F_1 - F_0] \cap H_1 \cap H_2 \cap Y = 1. \quad (5.3.4)$$

However, other intersection numbers show that the class $[F_1 - F_0]|_Y$ does not contain a section. By intersecting the fibral⁶ divisors with H_1, H_2 we obtain the irreducible component curves $\mathcal{C}_{\alpha_I} \simeq \mathbb{P}^1$ of the I_5 Kodaira fibers as $\mathcal{C}_{\alpha_I} = C_I \cap Y$ with

$$C_I = D_I \cap H_1 = D_I \cap H_2. \quad (5.3.5)$$

Computing the intersection numbers with the tentative section, we obtain

$$[F_1 - F_0] \cap \mathcal{C}_{\alpha_I} = \begin{cases} -1 & I = 0, \\ 1 & I = 1, 2, \\ 0 & I = 3, 4. \end{cases} \quad (5.3.6)$$

The fact that the intersection number is negative means that the I_5 component curve \mathcal{C}_0 is contained in $[F_1 - F_0]$ as we slide it along over the discriminant. That is, the whole fibral divisor D_0 is contained in $[F_1 - F_0]$. But since a rational section may only contain components of codimension-two fibers and not complete fibral divisors (which are codimension-one over the base), $[F_1 - F_0]$ is not a rational section after all. However, it is clear that this can be fixed by subtracting the fibral divisor D_0 .

Therefore our new best guess for the class of the section generating the Mordell-Weil group is $[F_1 - F_0 - D_0]$. Computing intersection numbers, one finds that it still does not work and one needs to subtract further vertical divisors. After repeating the same steps several times, the end result is the homology class

$$[s_1] = [F_1 - F_0 - D_0 - D_3 - D_4 + H_1]. \quad (5.3.7)$$

To show that this homology class actually contains a section, we apply the techniques of [subsection 3.3.1](#) and compute the line bundle cohomology of $\mathcal{O}_Y(s_1)$, where Y is the Calabi-Yau hypersurface inside X . The toric cohomology groups can easily be computed to be

$$\dim H^i(X, \mathcal{O}_X(s + K_X)) = \begin{cases} 1 & i = 1, \\ 0 & \text{else,} \end{cases} \quad \dim H^i(X, \mathcal{O}_X(s_1)) = 0. \quad (5.3.8)$$

⁵Note that the divisors $H_1 = \pi^{-1}([* : 0 : *])$ and $H_2 = \pi^{-1}([* : * : 0])$ are elliptic fibrations over the coordinate \mathbb{P}^1 in the base that intersect the discriminant transversely.

⁶The *fibral* divisors D_i are the divisors swept out by irreducible components of the I_5 Kodaira fiber as we move the curves along over the discriminant.

Therefore, the long exact sequence

$$\begin{aligned} \cdots \longrightarrow H^0(X, \mathcal{O}_X(s_1)) &\longrightarrow H^0(Y, \mathcal{O}_Y(s_1)) \longrightarrow \\ &\longrightarrow H^1(X, \mathcal{O}_X(s_1 + K_X)) \longrightarrow H^1(X, \mathcal{O}_X(s_1)) \longrightarrow \cdots \end{aligned} \quad (5.3.9)$$

tells us that the homology class $[s_1] = [F_1 - F_0 - D_0 - D_3 - D_4 + H_0]$ contains a unique variety s_1 representing it.

This is the section generating the Mordell-Weil group and, as we will see in the following, it is only a rational section. Computing the intersection number $s_1 \cap \mathcal{C}_{\alpha_1}$ and noticing that s_0 intersects only \mathcal{C}_0 from Equation 5.3.3, we note that this elliptic fibration is of the 4–1 split type. Finally, we note from the sheaf cohomology computation that the section s_1 exists only on the Calabi-Yau hypersurface and does not extend to a section on the whole ambient toric variety. This is why its construction has been so tedious.

Intersection Theory

By computing the discriminant of the elliptic fibration as a degree-36 polynomial over the base \mathbb{P}^2 explicitly [137], one can always enumerate the codimension-two fibers where the I_5 Kodaira fiber degenerates further. We now pick a sufficiently generic hypersurface using random coefficients, find the location of the codimension-two fibers numerically, and analyze the hypersurface in these special fibers. Roughly, the hypersurface will factorize in one of the irreducible components of the toric ambient fiber, and this defines the charge of the localized matter field.

Naively, we face an impasse: the combinatorial description of the geometry of the ambient toric variety knows nothing about whether a hypersurface equation factorizes or not. Hence no toric intersection computation on the toric variety X can possibly capture the irreducible curves that are stuck on the codimension-two fiber; but the zero modes on those curves are precisely the matter fields that we are after. However, this argument is a bit too simple minded and, while we cannot use simply intersection theory on X , toric methods still apply. The trick is to construct the irreducible components of the fibers of the ambient space, which are two-dimensional toric varieties. The hypersurface restricted to the ambient toric fiber will factorize into multiple irreducible components, each of which has its own divisor class on the surface. Then all that remains is to pull back the sections to this fiber component and apply the usual toric intersection theory there.

To clarify this procedure, let us look at an example and consider the irreducible fiber component $\mathcal{C}_0 \equiv \mathcal{C}_{\alpha_0} = D_0 \cap H_1$ of the I_5 Kodaira fiber that intersects the zero-section s_0 . The star of the corresponding ray $\langle n_{e_0} \rangle$ contains the homogeneous coordinates $u_1, u_2, e_1, e_2, e_4, f_0, f_1,$ and f_3 . We set e_0 to zero and all remaining variables to one. According to the fibration map of Equation 5.3.1, the point on the I_5 discriminant locus $[0 : u_1 : u_2] \in \mathbb{P}^2$ is parametrized by the ratio of u_1 and u_2 , which we treat in the following as numerical constants

that have been fixed to restrict us to a particular codimension-two fiber. Plugging this into the hypersurface equation, we obtain four non-zero terms

$$p(u_1, u_2, 0, e_1, e_2, 1, e_4, f_0, f_1, 1, f_3) = \beta_0 e_1 e_2^2 e_4 f_1 + \beta_1 e_1 e_2 f_0 f_1^2 + \beta_2 e_2 e_4 f_3 + \beta_3 f_0 f_1 f_3, \quad (5.3.10)$$

where β_0, \dots, β_3 are constants depending on the fixed u_1, u_2 .

For certain values of the u_1, u_2 the coefficients β_i become special and the hypersurface equation factorizes. This is how the I_5 Kodaira fiber degenerates further at codimension-two fibers. A computation shows that [176]

- at two distinct codimension-two fibers the coefficient β_2 vanishes and the polynomial factorizes as

$$p(u_1, u_2, 0, e_1, e_2, 1, e_4, f_0, f_1, 1, f_3) = f_1 \times (\beta_0 e_1 e_2^2 e_4 + \beta_1 e_1 e_2 f_0 f_1 + \beta_3 f_0 f_3), \quad (5.3.11)$$

- at three distinct codimension-two fibers the hypersurface equation factors as

$$p(u_1, u_2, 0, e_1, e_2, 1, e_4, f_0, f_1, 1, f_3) = (\beta'_0 e_1 e_2 f_1 + \beta'_1 f_3) \times (\beta'_2 e_2 e_4 + \beta'_3 f_0 f_1), \quad (5.3.12)$$

- and at 14 further codimension-two degenerate fibers the hypersurface equation on the fiber component C_0 does not factorize. Instead, other irreducible components of the I_5 fiber, that is, $\mathcal{C}_{\alpha_I} = D_I \cap H_1$ for $I \neq 0$, become reducible.
- Finally, there are three remaining codimension-two fibers where multiple I_5 components factor simultaneously. This is where the **10** matter fields are localized.

To understand the intersection theory on the fiber, we have to construct the ambient fiber component $C_0 = D_0 \cap H_1$ as a toric variety. That is, the remaining homogeneous coordinates $e_1, e_2, e_4, f_0, f_1, f_3$ on the right hand side of Equation 5.3.10 are the homogeneous coordinates of a two-dimensional toric variety. The toric surface can be reconstructed from knowing how the homogeneous coordinate rescalings act. First, one has to identify the subset of homogeneous rescalings on the four-dimensional toric variety X that do not change the values of u_1 and u_2 . Then, ignore the action on e_0 , since it is being set to zero. The result is that the toric surface on which Equation 5.3.10 is defined is the one shown in figure 5.2. In more elaborate terms, this is the relative star construction of [174]. This toric surface is embedded into the fiber of the toric variety X over $[0 : u_1 : u_2]$ via

$$i_0 : [e_1 : e_2 : e_4 : f_0 : f_1 : f_3] \mapsto [u_1 : u_2 : 0 : e_1 : e_2 : 1 : e_4 : f_0 : f_1 : 1 : f_3] \quad (5.3.13)$$

We now take advantage of the toric surface description of the fiber component. First, we can formulate the factorization of the hypersurface equation as follows:

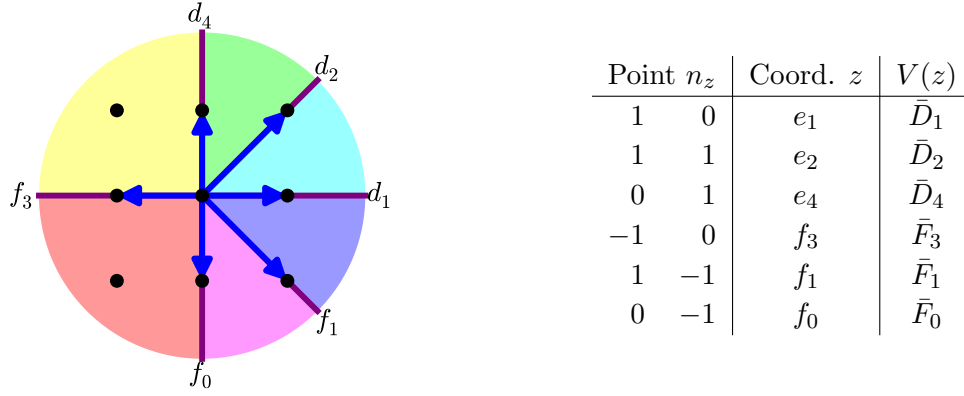


Figure 5.2: The toric ambient space fiber C_0 , that is, one of the five irreducible components of $\pi^{-1}([0 : u_1 : u_2])$.

- At two distinct codimension-two fibers, where the hypersurface factors as in Equation 5.3.11, the I_5 fiber component splits into two irreducible components with homology classes

$$V(p) = (\bar{F}_1) + (\bar{F}_0 + \bar{F}_3), \quad (5.3.14)$$

- and at three distinct codimension-two fibers, where the hypersurface equation factors as Equation 5.3.12, the I_5 fiber component splits into two irreducible components with homology classes

$$V(p) = (\bar{F}_0 + \bar{F}_1) + (\bar{F}_3). \quad (5.3.15)$$

Furthermore, the sections s_0, s_1 , as divisors on X , can be pulled back by the embedding map i_0 , see Equation 5.3.13. The details of the toric algorithm for the pullback by the fiber embedding can be found in [174]. The result is that

$$\begin{aligned} i_0^*(s_0) &= \bar{F}_0, \\ i_0^*(s_1) &= \bar{F}_3 - \bar{F}_0. \end{aligned} \quad (5.3.16)$$

To summarize, the I_5 Kodaira fiber degenerates at $2 + 3$ codimension-two fibers by splitting the irreducible component intersecting the zero-section in two, yielding a fiber of Kodaira type I_6 . However, in the first two fibers it splits into two curves that are distinct from the split in the last three fibers. The fiber components and their intersection number with the sections is given in table 5.5.

Fundamental Matter

The two different degenerations of the I_5 Kodaira fiber into codimension-two I_6 -type fibers result in localized $2 \times \mathbf{5}$ and $3 \times \mathbf{5}$ matter of $SU(5)$. They will turn out to be distinguished by their $U(1)$ charge, as we are about to see. The $U(1)$ charge is given by the intersection of

I_6 component	$\bar{\mathcal{C}}_0$	$\bar{\mathcal{C}}_{\alpha_1}$	$\bar{\mathcal{C}}_{\alpha_2}$	$\bar{\mathcal{C}}_{\alpha_3}$	$\bar{\mathcal{C}}_{\alpha_4}$	$\bar{\mathcal{C}}_{\alpha_5}$
Realization	$\bar{F}_0 + \bar{F}_1$	\bar{F}_3	\mathcal{C}_{α_1}	\mathcal{C}_{α_2}	\mathcal{C}_{α_3}	\mathcal{C}_{α_4}
$\cap s_0$	0	1	0	0	0	0
$\cap s_1$	1	-1	0	0	1	0

I_6 component	$\bar{\mathcal{C}}_0$	$\bar{\mathcal{C}}_{\alpha_1}$	$\bar{\mathcal{C}}_{\alpha_2}$	$\bar{\mathcal{C}}_{\alpha_3}$	$\bar{\mathcal{C}}_{\alpha_4}$	$\bar{\mathcal{C}}_{\alpha_5}$
Realization	\bar{F}_3	$\bar{F}_0 + \bar{F}_1$	\mathcal{C}_{α_1}	\mathcal{C}_{α_2}	\mathcal{C}_{α_3}	\mathcal{C}_{α_4}
$\cap s_0$	1	0	0	0	0	0
$\cap s_1$	-1	1	0	0	1	0

Table 5.5: Intersection numbers of the two different I_6 -type codimension-two fibers where the codimension-one I_5 fiber splits the fiber component intersecting the zero section. The curves $\bar{\mathcal{C}}_{\alpha_I}$ are the I_6 fiber components in cyclic order. The curves \mathcal{C}_{α_I} are the I_5 fiber components $\mathcal{C}_{\alpha_I} = D_I \cap H_1 \cap Y$.

the curves stuck at codimension-two fiber, that is, the irreducible components of the factored I_5 component, with the image of the section under the Shioda map [52] $S : MW(X) \rightarrow H_4(X, \mathbb{Q})$. For a single I_5 Kodaira fiber, this boils down to

$$\begin{aligned}
 U(1)\text{-charge}(\bar{\mathcal{C}}_{\alpha_I}) &= \bar{\mathcal{C}}_{\alpha_I} \cap S(s_1) \\
 &= \bar{\mathcal{C}}_{\alpha_I} \cap s_1 - \bar{\mathcal{C}}_{\alpha_I} \cap s_0 + \sum_{1 \leq a, b \leq 4} (\bar{\mathcal{C}}_{\alpha_I} \cap D_a) \begin{pmatrix} 4 & 3 & 2 & 1 \\ 5 & 5 & 5 & 5 \\ 3 & 6 & 4 & 2 \\ 3 & 5 & 5 & 5 \\ 2 & 4 & 6 & 3 \\ 5 & 5 & 5 & 5 \\ 1 & 2 & 3 & 4 \\ 5 & 5 & 5 & 5 \end{pmatrix}_{ab} (s_1 \cap \mathcal{C}_b) \quad (5.3.17)
 \end{aligned}$$

For example, consider $\bar{\mathcal{C}}_0 = \bar{F}_0 + \bar{F}_1$, a curve contributing to the $2 \times \mathbf{5}$. Its intersections with s_0, s_1 are listed in the upper half of [table 5.5](#).

$$U(1) - \text{charge}(2 \times \mathbf{5}) = 1 - 0 + (0 \ 0 \ 0 \ 1) \begin{pmatrix} 4 & 3 & 2 & 1 \\ 5 & 5 & 5 & 5 \\ 3 & 6 & 4 & 2 \\ 3 & 5 & 5 & 5 \\ 2 & 4 & 6 & 3 \\ 5 & 5 & 5 & 5 \\ 1 & 2 & 3 & 4 \\ 5 & 5 & 5 & 5 \end{pmatrix} \begin{pmatrix} 0 \\ 0 \\ 1 \\ 0 \end{pmatrix} = \frac{8}{5} \quad (5.3.18)$$

Similarly, the $U(1)$ charge of the other $3 \times \mathbf{5}$ ends up being $\frac{7}{5}$. As noted above, there are 14 further codimension-two fibers giving rise to $\mathbf{5}$ and 3 more yielding $\mathbf{10}$ matter. Their $U(1)$ charge can be computed by straightforward application of the same methods and we will leave the details as an exercise to the reader. The result is that, after clearing denominators to make the $U(1)$ charges integral, the $SU(5)$ -charged spectrum is

$$2 \times \mathbf{5}_8 + 3 \times \mathbf{5}_7 + 6 \times \mathbf{5}_3 + 8 \times \mathbf{5}_2 + 3 \times \mathbf{10}_1. \quad (5.3.19)$$

A Calabi-Yau fourfold obtained by replacing the two-dimensional base manifold by a threefold will generically have the same types of representations arising, since they are determined by the behavior at a generic point on a matter curve. In other words, after intersecting the matter curve with a divisor crossing it, the same analysis for the $SU(5) \times U(1)$ representation content

v_0	v_1	v_2	v_3	v_4	v_5
$\begin{pmatrix} 1 \\ 0 \\ 0 \end{pmatrix}$	$\begin{pmatrix} 0 \\ 1 \\ 0 \end{pmatrix}$	$\begin{pmatrix} 0 \\ 0 \\ 1 \end{pmatrix}$	$\begin{pmatrix} -1 \\ 0 \\ -1 \end{pmatrix}$	$\begin{pmatrix} -1 \\ -1 \\ 0 \end{pmatrix}$	$\begin{pmatrix} 1 \\ 1 \\ 1 \end{pmatrix}$

Table 5.6: Vertices of the three-dimensional reflexive polytope with PALP id 22.

applies. Of course, the six-dimensional quaternionic representations will be split up into conjugate pairs of four-dimensional representations, and the multiplicity of the representations will be different. In fact, the multiplicities do depend on the four-form flux which is a phenomenon for fourfolds that has no threefold analogue.

5.3.2 $SU(5) \times U(1)^2$ with Different Antisymmetric Representations

Let us now proceed with Calabi-Yau manifolds whose fibers are complete intersections. As shown in [section 4.5](#), genus-one fibrations with fibers embedded as hypersurfaces can never have more than a single type of antisymmetric $SU(5)$ representations. Evading this constraint is one of the key reasons to study complete intersection fibers and therefore we show precisely such an example.

In order to confirm the existence of multiple **10** representations, we are led to consider a nef partition with non-trivial toric Mordell-Weil group. To be concrete, let us pick the following nef partition of the polytope given in [table 5.6](#):

$$\nabla_1 = \langle v_1 v_2 v_3 v_4 v_5 \rangle_{\text{conv}}, \quad \nabla_2 = \langle v_0 \rangle_{\text{conv}}. \quad (5.3.20)$$

Since ∇_2 is one-dimensional, this nef partition is a *projection*. In particular, this means that we can directly solve the second equation, plug the result into the first equation and obtain the Weierstrass form of a hypersurface equation. According to the conventions of [subsection A.6.1](#), this nef partition has the unique id $(22, 0)$. Looking it up in our classification results, we find that it has three sections, namely the divisors corresponding to the rays v_1 , v_2 , and v_5 . Let us pick the divisor $s_0 = V(z_5)$ as the neutral element of our elliptic curve. Then $\sigma_0 = V(z_0) - V(z_5)$ and $\sigma_1 = V(z_2) - V(z_5)$ generate a $\mathbb{Z} \oplus \mathbb{Z}$ group.

Next, we write down the equations that define the complete intersection inside the three-dimensional toric variety corresponding to the reflexive polytope of [table 5.6](#). Keeping the coefficients general, the equations of the complete intersection defined by the nef partition of [Equation 5.3.20](#) are

$$p_1 = \tilde{a}_0 z_1^2 z_2^2 z_5^3 + \tilde{a}_1 z_1^2 z_2 z_3 z_5^2 + \tilde{a}_2 z_1 z_2^2 z_4 z_5^2 + \tilde{a}_3 z_1^2 z_3^2 z_5 + \tilde{a}_4 z_1 z_2 z_3 z_4 z_5 + \tilde{a}_5 z_2^2 z_4^2 z_5 \quad (5.3.21)$$

$$p_2 = \tilde{b}_0 z_1 z_2 z_5 + \tilde{b}_1 z_1 z_3 + \tilde{b}_2 z_2 z_4 + \tilde{b}_3 z_0. \quad (5.3.22)$$

e_0	e_1	e_2	e_3	e_4
$\begin{pmatrix} 0 \\ 0 \\ 0 \\ u_0 \end{pmatrix}$	$\begin{pmatrix} -1 \\ -1 \\ -1 \\ u_0 \end{pmatrix}$	$\begin{pmatrix} -1 \\ -1 \\ 0 \\ u_0 \end{pmatrix}$	$\begin{pmatrix} 0 \\ -1 \\ -1 \\ u_0 \end{pmatrix}$	$\begin{pmatrix} 1 \\ 0 \\ 0 \\ u_0 \end{pmatrix}$

Table 5.7: Torically, the blowup of [Equation 5.3.23](#) corresponds to introducing the top defined here, where u_0 is a ray of the fan of the base. The GUT brane will then be located on the divisor corresponding to u_0 . Note that here we and in [Equation 5.3.23](#) we are denoting the rays and the corresponding homogeneous variables by the same letters.

Here one can see that this nef partition is indeed a projection: By solving $p_2 = 0$ for z_0 and inserting the solution in p_1 the complete intersection is reduced to a hypersurface inside the toric variety corresponding to the polytope obtained by projecting along v_0 . However, this suffices for our purposes. Since it is the limited number of triangulations of the $SU(5)$ tops for a codimension-one hypersurface that constrains the **10** charges, we are still circumventing this constraint here by considering triangulations of the higher-dimensional variety in which the elliptic curve has codimension two.

Next, we tune the \tilde{a}_i and \tilde{b}_i such as to enforce an $SU(5)$ singularity along the divisor $e_0 = 0$ in the base manifold. Then we resolve this singularity by introducing exceptional divisors e_i , $i = 1, \dots, 4$ and find that the coefficients \tilde{a}_i and \tilde{b}_i take the form

$$\begin{aligned}
\tilde{a}_0 &= a_0 \cdot e_0^3 e_1 e_2^2 e_4^2 & \tilde{a}_1 &= a_1 \cdot e_0^2 e_1 e_2 e_4 & \tilde{a}_2 &= a_2 \cdot e_0^2 e_1 e_2^2 e_4 \\
\tilde{a}_3 &= a_3 \cdot e_0 e_1 & \tilde{a}_4 &= a_4 \cdot e_0 e_1 e_2 & \tilde{a}_5 &= a_5 \cdot e_0 e_1 e_2^2 \\
\tilde{a}_6 &= a_6 \cdot e_0 e_4 & \tilde{a}_7 &= a_7 \cdot e_0 e_1^2 e_2 e_3 & \tilde{a}_8 &= a_8 \cdot e_0 e_1^2 e_2^2 e_3 \\
\tilde{a}_9 &= a_9 \cdot e_0 e_1 e_3 e_4 & \tilde{a}_{10} &= a_{10} & \tilde{a}_{11} &= a_{11} \cdot e_1 e_3 \\
& & \tilde{a}_{12} &= a_{12} \cdot e_0 e_1 e_3^2 e_4^2 & &
\end{aligned} \tag{5.3.23}$$

and

$$\tilde{b}_0 = b_0 \cdot e_0 e_2 e_4 \quad \tilde{b}_1 = b_1 \quad \tilde{b}_2 = b_2 \cdot e_2 \quad \tilde{b}_3 = b_3 \cdot e_3 e_4. \tag{5.3.24}$$

Here a_i and b_i are polynomials in the base variables that depend on e_i only through the combination $u_0 \equiv e_0 e_1 e_2 e_3 e_4$. The toric data corresponding to this blowup are given in [table 5.7](#).

As a power series in u_0 , the Weierstrass coefficients read

$$f = -\frac{1}{48} \left(a_{10}^4 \cdot b_1^4 + 4 \cdot a_{10}^2 \cdot b_1^2 \cdot c_1 \cdot u_0 + c_2 \cdot u_0^2 \right) + \mathcal{O}(u_0^3) \tag{5.3.25}$$

$$g = \frac{1}{864} \left(a_{10}^6 \cdot b_1^6 + 6 \cdot a_{10}^4 \cdot b_1^4 \cdot c_1 \cdot u_0 + 3b_1^2 \cdot a_{10}^2 \cdot c_3 \cdot u_0^2 + c_4 \cdot u_0^3 \right) + \mathcal{O}(u_0^4), \tag{5.3.26}$$

Name	Equation	Singularity type	$SU(5)$ representation
T_1	$a_{10} \cap u_0$	$SO(10)$	10
T_2	$b_1 \cap u_0$	$SO(10)$	10
F_1	$a_{11} \cap u_0$	$SU(7)$	5
F_2	$b_2 \cap u_0$	$SU(7)$	5
F_3	$c_5 \cap u_0$	$SU(7)$	5
F_4	$c_6 \cap u_0$	$SU(7)$	5
F_5	$c_7 \cap u_0$	$SU(7)$	5
F_6	$b_3 \cap u_0$	$SU(7)$	5

Table 5.8: The matter curves for the top of [table 5.7](#).

where the c_i are irreducible polynomials in a_i and b_i . This implies that the discriminant $\Delta = 4f^3 + 27g^2$ takes the form

$$\Delta = \frac{1}{16} \left(a_{10}^4 \cdot b_1^4 \cdot a_{11} \cdot b_2 \cdot b_3 \cdot c_5 \cdot c_6 \cdot c_7 \cdot u_0^5 + a_{10}^2 \cdot b_1^2 \cdot c_8 \cdot u_0^6 + c_9 \cdot u_0^7 \right) + \mathcal{O}(u_0^8) \quad (5.3.27)$$

with

$$c_5 = a_{10}a_{12}b_1^2 - a_9a_{10}b_1b_3 + a_6a_{11}b_1b_3 + a_3a_{10}b_3^2 \quad (5.3.28)$$

$$c_6 = -a_8a_{10}b_1^2 + a_5a_{11}b_1^2 + a_7a_{10}b_1b_2 - a_4a_{11}b_1b_2 + a_3a_{11}b_2^2 \quad (5.3.29)$$

$$c_7 = a_3a_{10}^2b_0^2 + a_4a_6a_{10}b_0b_1 - a_1a_{10}^2b_0b_1 + a_5a_6^2b_1^2 - a_2a_6a_{10}b_1^2 + a_0a_{10}^2b_1^2 \\ - 2a_3a_6a_{10}b_0b_2 - a_4a_6^2b_1b_2 + a_1a_6a_{10}b_1b_2 + a_3a_6^2b_2^2. \quad (5.3.30)$$

From the vanishing orders of the f , g and Δ we observe that there are eight distinct matter curves and list them in [table 5.8](#).

While the appearance of two different **10** curves and six distinct **5** curves is promising, it is crucial to check which of these curves are actually realized in a generic fibration of this top over a base manifold. Next, we therefore fiber this space over a \mathbb{P}^3 . Doing so can be achieved by embedding the rays of [table 5.6](#) into \mathbb{Z}^6 according to

$$v_i \mapsto w_i \equiv (v_i, 0, 0, 0), \quad i = 1, \dots, 5, \quad (5.3.31)$$

adding the blowup rays from [table 5.7](#) with $u_0 = (1, 0, 0)$ and adding the remaining three base rays:

$$w_7 = (0, 0, 0, -1, -1, -1), \quad w_8 = (n_1, n_2, n_3, 0, 1, 0), \quad w_9 = (0, 0, 0, 0, 0, 1). \quad (5.3.32)$$

Here the n_i are integers encoding the fibration of the fiber over the base. More specifically, the n_i determine which line bundles the fiber coordinates are sections of. For our purposes, we choose $(n_1, n_2, n_3) = (-1, 0, 0)$. After using PALP to compute all nef partitions of the resulting polytope, we pick the one with

$$\nabla_1 = \langle w_1, w_2, w_3, w_4, w_5, w_6, w_7, w_8, e_0, e_1, e_2 \rangle_{\text{conv}}, \quad \nabla_2 = \langle w_0, e_3, e_4 \rangle_{\text{conv}}. \quad (5.3.33)$$

Singularity type	Coupling	Multiplicity
$SU(7)$	$\mathfrak{5}_{(4,3)} \times \overline{\mathfrak{5}}_{(1,2)}$	54
$SU(7)$	$\mathfrak{5}_{(-1,3)} \times \overline{\mathfrak{5}}_{(1,2)}$	39
$SU(7)$	$\mathfrak{5}_{(-1,3)} \times \overline{\mathfrak{5}}_{(-4,-3)}$	36
$SU(7)$	$\mathfrak{5}_{(-6,-7)} \times \overline{\mathfrak{5}}_{(1,2)}$	27
$SU(7)$	$\mathfrak{5}_{(-6,-7)} \times \overline{\mathfrak{5}}_{(-4,-3)}$	12
$SU(7)$	$\mathfrak{5}_{(-6,-7)} \times \overline{\mathfrak{5}}_{(1,-3)}$	9
$SU(7)$	$\mathfrak{5}_{(-6,-2)} \times \overline{\mathfrak{5}}_{(1,2)}$	9
$SU(7)$	$\mathfrak{5}_{(-6,-2)} \times \overline{\mathfrak{5}}_{(-4,-3)}$	6
$SU(7)$	$F\mathfrak{5}_{(-6,-2)} \times \overline{\mathfrak{5}}_{(1,-3)}$	6
$SU(7)$	$\mathfrak{5}_{(-6,-7)} \times \overline{\mathfrak{5}}_{(6,2)}$	3
$SO(12)$	$\overline{\mathbf{10}}_{(-3,-1)} \times \mathfrak{5}_{(4,3)} \times \mathfrak{5}_{(-1,-2)}$	15
$SO(12)$	$\overline{\mathbf{10}}_{(2,4)} \times \mathfrak{5}_{(-1,-2)} \times \mathfrak{5}_{(-1,-2)}$	3
$SO(12)$	$\overline{\mathbf{10}}_{(2,4)} \times \mathfrak{5}_{(-6,-2)} \times \mathfrak{5}_{(4,3)}$	3
E_6	$\mathbf{10}_{(3,1)} \times \mathbf{10}_{(3,1)} \times \mathfrak{5}_{(-6,-2)}$	3
E_6	$\mathbf{10}_{(3,1)} \times \mathbf{10}_{(-2,-4)} \times \mathfrak{5}_{(-1,3)}$	3

Table 5.9: All couplings involving multiple non-Abelian matter representations in the example of Equation 5.3.32. Note that there are additional non-minimal singularities that we do not list here.

It has Hodge numbers $h^{1,1} = 8$, $h^{2,1} = 0$, and $h^{3,1} = 141$. For this specific choice of fibration, both b_0 and b_3 are constants. Consequently, the curve F_6 is not realized. However, all other curves exist and in particular, there are two different antisymmetric representations. Using the Chern-Simons matching as in [95, 113, 114] and explained in detail in section 9.1, we find that the realized curves have the following charges under the two $U(1)$ s:

$$T_1 : \mathbf{10}_{(3,1)}, \quad T_2 : \mathbf{10}_{(-2,-4)} \quad (5.3.34)$$

$$F_1 : \mathfrak{5}_{(-6,-7)}, \quad F_2 : \mathfrak{5}_{(-6,-2)}, \quad F_3 : \mathfrak{5}_{(-1,3)}, \quad F_4 : \mathfrak{5}_{(4,3)}, \quad F_5 : \mathfrak{5}_{(-1,-2)} \quad (5.3.35)$$

We also find the following singlet states:

$$\mathbf{1}_{(5,0)}, \quad \mathbf{1}_{(0,5)}, \quad \mathbf{1}_{(5,5)}, \quad \mathbf{1}_{(5,10)}, \quad \mathbf{1}_{(10,5)}, \quad \mathbf{1}_{(10,10)}. \quad (5.3.36)$$

Finally, we compute the Yukawa couplings for the given example and find the ones listed in table 5.9.

In summary, we have managed to construct a fully explicit F-theory model with gauge group $SU(5) \times U(1)^2$, in which the *torically realized* $SU(5)$ singularity gives rise to a gauge theory with two different $\mathbf{10}$ representations. Clearly the example studied here is not intended to be used as a full-fledged GUT model. In more realistic models several issues would need

to be addressed, such as the fact that there exist non-minimal singularities at points in the base manifold whose resolution leads to a non-flat fibration. Furthermore, the topology of the GUT divisor is too simple in order to allow hypercharge flux with the desired properties. In principle, both these points can be addressed by choosing the fibration more carefully than we did following [Equation 5.3.32](#).

5.3.3 $SU(5)$ and a Discrete Symmetry

The third example we consider is a nef partition of the three-dimensional polytope with the least integral points, that is the one corresponding to \mathbb{P}^3 . All toric divisors $V(z_i)$ inside \mathbb{P}^3 lie in the same homology class and therefore it can only have two nef partitions: The one corresponding to a partition of 3+1 vertices and the nef partition corresponding to a partition of 2+2 vertices. The first is again a projection and to have some variety, we therefore focus on the latter. That is, we take our nef partition to be

$$\nabla_1 = \langle v_0, v_3 \rangle_{\text{conv}}, \quad \nabla_2 = \langle v_1, v_2 \rangle_{\text{conv}}. \quad (5.3.37)$$

This implies automatically that all toric divisors intersect a generic complete intersection of this type in four points:

$$V(z_i) \cap E = \int_E [V(z_i)] = \int_{\mathbb{P}^3} [2H] \cdot [2H] \cdot [H] = 4. \quad (5.3.38)$$

A generic fibration with this fiber will therefore not have a section. F-theory models without section have recently received quite some attention, see [[144](#), [152–155](#), [177](#), [178](#)]. However, in these models the Calabi-Yau manifolds always had two- or three-sections leading to \mathbb{Z}_2 or \mathbb{Z}_3 discrete gauge symmetries, respectively. As the biquadric in \mathbb{P}^3 has a four-section, we expect to find a discrete \mathbb{Z}_4 gauge group. In the following we will try to collect some further evidence for this.

To do so, let us take the same approach as with the previous example and write down the defining equations of the complete intersection. They read

$$\begin{aligned} p_1 &= \tilde{a}_0 z_0^2 + \tilde{a}_1 z_0 z_1 + \tilde{a}_2 z_1^2 + \tilde{a}_3 z_0 z_2 + \tilde{a}_4 z_1 z_2 + \tilde{a}_5 z_2^2 + \tilde{a}_6 z_0 z_3 + \tilde{a}_7 z_1 z_3 + \tilde{a}_8 z_2 z_3 + \tilde{a}_9 z_3^2 \\ p_2 &= \tilde{b}_0 z_0^2 + \tilde{b}_1 z_0 z_1 + \tilde{b}_2 z_1^2 + \tilde{b}_3 z_0 z_2 + \tilde{b}_4 z_1 z_2 + \tilde{b}_5 z_2^2 + \tilde{b}_6 z_0 z_3 + \tilde{b}_7 z_1 z_3 + \tilde{b}_8 z_2 z_3 + \tilde{b}_9 z_3^2. \end{aligned} \quad (5.3.39)$$

Note that such biquadrics have been studied before in [[89](#)] and, with the restriction to the triple blowup of \mathbb{P}^3 , in [[158](#)]. Since this nef partition is not a projection, one cannot bring this complete intersection into Weierstrass form by solving one of the equations for one variable and substituting the result into the other equation.

Next, we tune the \tilde{a}_i and \tilde{b}_i such as to enforce an $SU(5)$ singularity along the divisor $e_0 = 0$ in the base manifold. Then we resolve this singularity by introducing exceptional

e_0	e_1	e_2	e_3	e_4
$\begin{pmatrix} 0 \\ 0 \\ 0 \\ u_0 \end{pmatrix}$	$\begin{pmatrix} -1 \\ -1 \\ -1 \\ u_0 \end{pmatrix}$	$\begin{pmatrix} -1 \\ -1 \\ 0 \\ u_0 \end{pmatrix}$	$\begin{pmatrix} 0 \\ -1 \\ 0 \\ u_0 \end{pmatrix}$	$\begin{pmatrix} 0 \\ -1 \\ -1 \\ u_0 \end{pmatrix}$

Table 5.10: As before, the blowup of equations (5.3.40) and (5.3.41) corresponds to introducing the top defined here, where u_0 is a ray of the fan of the base. The GUT brane will then be located on the divisor corresponding to u_0 . We again denote rays and corresponding homogeneous variables by the same letters.

divisors e_i , $i = 1, \dots, 4$ as specified torically in terms of the top of table 5.10. We find that the coefficients \tilde{a}_i and \tilde{b}_i take the form

$$\begin{aligned}
\tilde{a}_0 &= a_0 \cdot e_1^2 e_2^2 e_3 e_4 & \tilde{a}_1 &= a_1 \cdot e_1 e_2^2 e_3 & \tilde{a}_2 &= a_2 \cdot e_0 e_1 e_2^3 e_3^2 \\
\tilde{a}_3 &= a_3 \cdot e_1 e_2 & \tilde{a}_4 &= a_4 \cdot e_0 e_1 e_2^2 e_3 & \tilde{a}_5 &= a_5 \cdot e_0 e_1 e_2 \\
\tilde{a}_6 &= a_6 \cdot e_1 e_2 e_3 e_4 & \tilde{a}_7 &= a_7 \cdot e_2 e_3 & \tilde{a}_8 &= a_8 \\
&& \tilde{a}_9 &= a_9 \cdot e_3 e_4 & &
\end{aligned} \tag{5.3.40}$$

and

$$\begin{aligned}
\tilde{b}_0 &= b_0 \cdot e_1 e_4 & \tilde{b}_1 &= b_1 & \tilde{b}_2 &= b_2 \cdot e_0 e_2 e_3 \\
\tilde{b}_3 &= b_3 \cdot e_0 e_1 e_4 & \tilde{b}_4 &= b_4 \cdot e_0 & \tilde{b}_5 &= b_5 \cdot e_0^2 e_1 e_4 \\
\tilde{b}_6 &= b_6 \cdot e_0 e_1 e_3 e_4^2 & \tilde{b}_7 &= b_7 \cdot e_0 e_3 e_4 & \tilde{b}_8 &= b_8 \cdot e_0^2 e_1 e_3 e_4^2 \\
&& \tilde{b}_9 &= b_9 \cdot e_0^2 e_1 e_3^2 e_4^3 & &
\end{aligned} \tag{5.3.41}$$

Here a_i and b_i are polynomials in the base variables that depend on e_i only through the combination $u_0 \equiv e_0 e_1 e_2 e_3 e_4$. As a power series in u_0 , the Weierstrass coefficients read

$$f = -\frac{1}{768} \left(a_8^4 \cdot b_1^4 + 2 \cdot a_8^2 \cdot b_1^2 \cdot c_1 \cdot u_0 + c_2 \cdot u_0^2 \right) + \mathcal{O}(u_0^3) \tag{5.3.42}$$

$$g = \frac{1}{55296} \left(a_8^6 \cdot b_1^6 - 3 \cdot a_8^4 \cdot b_1^4 \cdot c_1 \cdot u_0 + a_8^2 \cdot b_1^2 \cdot c_3 \cdot u_0^2 + c_4 \cdot u_0^3 \right) + \mathcal{O}(u_0^4), \tag{5.3.43}$$

where the c_i are irreducible polynomials in a_i and b_i . Then the discriminant is

$$\Delta = \frac{1}{2^{16}} \left(a_8^4 \cdot b_1^4 \cdot c_5 \cdot c_6 \cdot c_7 \cdot c_8 \cdot u_0^5 + a_8^2 \cdot b_1^2 \cdot c_9 \cdot v_0^6 + c_{10} \cdot u_0^7 \right) + \mathcal{O}(u_0^8) \tag{5.3.44}$$

with

$$c_5 = -b_1 b_3 b_4 + b_0 b_4^2 + b_1^2 b_5 \tag{5.3.45}$$

$$c_6 = a_3 a_7 a_8 b_0 - a_1 a_8^2 b_0 - a_3 a_6 a_8 b_1 + a_0 a_8^2 b_1 + a_3^2 a_9 b_1 \tag{5.3.46}$$

$$c_7 = -a_5 a_7^2 b_1 + a_4 a_7 a_8 b_1 - a_2 a_8^2 b_1 - a_3 a_7 a_8 b_2 + a_1 a_8^2 b_2 + a_3 a_7^2 b_4 - a_1 a_7 a_8 b_4 \tag{5.3.47}$$

$$\begin{aligned}
c_8 &= -a_3^2 b_1 b_3 b_4 + a_9^2 b_0 b_4^2 + a_9^2 b_1^2 b_5 + a_8 a_9 b_1 b_4 b_6 + a_8 a_9 b_1 b_3 b_7 - 2 a_8 a_9 b_0 b_4 b_7 \\
&\quad - a_8^2 b_1 b_6 b_7 + a_8^2 b_0 b_7^2 - a_8 a_9 b_1^2 b_8 + a_8^2 b_1^2 b_9.
\end{aligned} \tag{5.3.48}$$

Name	Equation	Singularity type	$SU(5)$ representation
T_1	$a_8 \cap u_0$	$SO(10)$	10
T_2	$b_1 \cap u_0$	$SO(10)$	10
F_1	$c_5 \cap u_0$	$SU(7)$	5
F_2	$c_6 \cap u_0$	$SU(7)$	5
F_3	$c_7 \cap u_0$	$SU(7)$	5
F_4	$c_8 \cap u_0$	$SU(7)$	5

Table 5.11: The matter curves in the example with the elliptic fiber embedded as a biquadric in \mathbb{P}^3 .

Singularity type	Coupling	Multiplicity
$SU(7)$	$F_1 \times F_2$	30
$SU(7)$	$F_1 \times F_3$	42
$SU(7)$	$F_1 \times F_4$	36
$SU(7)$	$F_2 \times F_3$	33
$SU(7)$	$F_2 \times F_4$	40
$SU(7)$	$F_3 \times F_4$	56
$SO(12)$	$T_1 \times F_1 \times F_4$	6
$SO(12)$	$T_1 \times F_2 \times F_2$	1
$SO(12)$	$T_1 \times F_3 \times F_3$	2
$SO(12)$	$T_2 \times F_1 \times F_1$	6
$SO(12)$	$T_2 \times F_2 \times F_3$	9
$SO(12)$	$T_2 \times F_4 \times F_4$	9
E_6	$T_1 \times T_1 \times F_3$	3
E_6	$T_1 \times T_2 \times F_2$	3
E_6	$T_2 \times T_2 \times F_3$	12

Table 5.12: All couplings involving multiple non-Abelian matter representations in the example with the elliptic fiber embedded in \mathbb{P}^3 . Note that there are additional non-minimal singularities that do not list here.

We observe that there are six distinct matter curves and list them in [table 5.11](#). This by itself is another piece of evidence that there exists in fact an order four discrete symmetry. Arguing along the lines of [\[152, 154\]](#), it is this symmetry that helps to distinguish the four **5** representations that would otherwise have identical quantum numbers in the low-energy effective action.

As before, we can make this more concrete by constructing an explicit example. To do so, we use the same embedding into \mathbb{Z}^6 as in equation [\(5.3.32\)](#), but this time we set $(n_1, n_2, n_3) = (0, 0, 1)$ and denote the rays obtained by embedding the base divisors by w_5 ,

w_6 , and w_7 . The resulting six-dimensional lattice polytope has 33 nef partitions. Of these, let us pick the nef partition

$$\nabla_1 = \langle w_0, w_3, w_5, e_1, e_2, e_3, e_4 \rangle_{\text{conv}}, \quad \nabla_2 = \langle w_1, w_2, e_0, w_6, w_7 \rangle_{\text{conv}}, \quad (5.3.49)$$

which has the Hodge numbers $h^{1,1} = 6$, $h^{2,1} = 0$, and $h^{3,1} = 110$. For this explicit example, we find that all the curves listed in [table 5.11](#) are in fact realized geometrically. In [table 5.12](#) we furthermore list the Yukawa points involving multiple non-Abelian representations. Since Yukawa couplings must be invariant under gauge symmetries, the couplings that do not involve singlets allow us to determine the \mathbb{Z}_4 charges of the six matter curves. Let us denote the neutral element of \mathbb{Z}_4 by 0 and call the generator e . Then we have that the two couplings involving only T_1 and F_3 imply

$$2 \cdot Q_{\mathbb{Z}_4}(T_1) + Q_{\mathbb{Z}_4}(F_3) = 0, \quad 2 \cdot Q_{\mathbb{Z}_4}(F_3) = T_1 \quad (5.3.50)$$

which immediately leads to

$$Q_{\mathbb{Z}_4}(T_1) = Q_{\mathbb{Z}_4}(F_3) = 0. \quad (5.3.51)$$

The remaining couplings then imply that

$$Q_{\mathbb{Z}_4}(F_2) = Q_{\mathbb{Z}_4}(T_2) = 2e. \quad (5.3.52)$$

Last but not least, we have $Q_{\mathbb{Z}_4}(F_{1/4}) \in \{e, 3e\}$. However, e and $3e$ are the only order-four elements of \mathbb{Z}_4 and we could just as well take $e' = 3e$ as the generator of \mathbb{Z}_4 . As a consequence, one can simply choose that

$$Q_{\mathbb{Z}_4}(F_1) = e, \quad Q_{\mathbb{Z}_4}(F_4) = 3e. \quad (5.3.53)$$

With these charge assignments one finds that singlets with all allowed \mathbb{Z}_4 charges must be present in order to make all the couplings of [table 5.12](#) invariant.

Put in a nutshell, we find that one can easily realize F-theory models with a non-Abelian gauge group accompanied solely by an additional discrete symmetry of order four. A convenient way of doing so proceeds by embedding the elliptic fiber as a biquadric inside \mathbb{P}^3 . There are numerous ways of extending the treatment here, such as connecting this model to others in terms of Higgsings and conifold transitions in the circle-compactified theories.

5.3.4 Mordell-Weil Torsion \mathbb{Z}_4

As a final example, let us take a quick look at a model with Mordell-Weil torsion \mathbb{Z}_4 . This torsion group does not exist generically for codimension-one elliptic fibers [[143](#), [144](#), [160](#)] and even in codimension two there is only a single example as can be seen from [table 3.10](#).

Mordell-Weil torsion was studied extensively in [[160](#)] and it was found that it impacts the global structure of the non-Abelian gauge group. Given a singularity of type A_{n-1} ,

v_0	v_1	v_2	v_3	v_4	v_5	v_6	v_7
$\begin{pmatrix} 1 \\ 0 \\ 0 \end{pmatrix}$	$\begin{pmatrix} 0 \\ 1 \\ 0 \end{pmatrix}$	$\begin{pmatrix} 1 \\ -1 \\ 0 \end{pmatrix}$	$\begin{pmatrix} -1 \\ 0 \\ 0 \end{pmatrix}$	$\begin{pmatrix} 0 \\ 1 \\ 2 \end{pmatrix}$	$\begin{pmatrix} -1 \\ 0 \\ -2 \end{pmatrix}$	$\begin{pmatrix} -1 \\ -2 \\ -2 \end{pmatrix}$	$\begin{pmatrix} 2 \\ 1 \\ 2 \end{pmatrix}$

Table 5.13: Vertices of the three-dimensional reflexive polytope with PALP id 3415.

v_8	v_9	v_{10}	v_{11}	v_{12}	v_{13}
$\begin{pmatrix} 0 \\ -1 \\ -1 \end{pmatrix}$	$\begin{pmatrix} 1 \\ 0 \\ 1 \end{pmatrix}$	$\begin{pmatrix} -1 \\ -1 \\ -1 \end{pmatrix}$	$\begin{pmatrix} 0 \\ 0 \\ 1 \end{pmatrix}$	$\begin{pmatrix} -1 \\ -1 \\ -2 \end{pmatrix}$	$\begin{pmatrix} 0 \\ 0 \\ 0 \end{pmatrix}$
v_{14}	v_{15}	v_{16}	v_{17}	v_{18}	
$\begin{pmatrix} 1 \\ 1 \\ 2 \end{pmatrix}$	$\begin{pmatrix} 0 \\ 0 \\ -1 \end{pmatrix}$	$\begin{pmatrix} 1 \\ 1 \\ 1 \end{pmatrix}$	$\begin{pmatrix} -1 \\ 0 \\ -1 \end{pmatrix}$	$\begin{pmatrix} 0 \\ 1 \\ 1 \end{pmatrix}$	

Table 5.14: Integral points of the reflexive polytope with PALP id 3415 that are neither vertices nor the origin. In order to fully resolve every fibration of the nef partition (5.3.55) one must use all of these points as rays of the toric fan.

the universal covering group is $SU(n)$, which, without Mordell-Weil torsion, constitutes the gauge group of the F-theory model. In the presence of a non-trivial Mordell-Weil torsion group \mathbb{Z}_k this changes: The non-Abelian gauge group becomes $SU(n)/\mathbb{Z}_k$. By construction the universal covering group has a trivial first fundamental group, and therefore the effect of non-trivial Mordell-Weil torsion is that the non-Abelian gauge group of the low-energy effective theory is no longer simply connected:

$$\pi_1(SU(n)/\mathbb{Z}_k) = \mathbb{Z}_k. \quad (5.3.54)$$

In the examples studied in [160] Mordell-Weil torsion groups \mathbb{Z}_2 and \mathbb{Z}_3 always came accompanied by gauge groups of type $SU(2n)$ and $SU(3n)$, respectively. Since $SU(n)$ has a \mathbb{Z}_n center generated by the identity matrix times $e^{\frac{2\pi i}{n}}$, one can mod out \mathbb{Z}_k by eliminating the center (or a subgroup thereof) of $SU(k \cdot n)$.

The corresponding reflexive polytope has PALP id 3415 and we list its defining data in table 5.13. It has a single nef partition, namely

$$\nabla_1 = \langle v_0, v_3, v_5, v_6 \rangle_{\text{conv}}, \quad \nabla_2 = \langle v_1, v_2, v_4, v_7 \rangle_{\text{conv}}. \quad (5.3.55)$$

In order to write down the most general complete intersection corresponding to this nef partition, we must use every integral point of the polytope defined in table 5.13 apart from the origin. The additional eleven points are listed in table 5.14.

After resolution, the complete intersection defined by (5.3.55) is defined by the following two polynomials:

$$\begin{aligned} p_1 &= a_0 z_0 z_3 z_5 z_6 z_8 z_{10} z_{12} z_{15} z_{17} + a_1 z_0^2 z_7^2 z_8 z_9 z_{14} z_{15} z_{16} + a_2 z_3^2 z_4^2 z_{10} z_{11} z_{14} z_{17} z_{18} \\ p_2 &= b_0 z_1^2 z_5^2 z_{12} z_{15} z_{16} z_{17} z_{18} + b_1 z_2^2 z_6^2 z_8 z_9 z_{10} z_{11} z_{12} + b_2 z_1 z_2 z_4 z_7 z_9 z_{11} z_{14} z_{16} z_{18}. \end{aligned} \quad (5.3.56)$$

This time we are not interested in engineering additional singularities, but rather in confirming that models with this fiber contain the $SU(4)$ gauge factors that we expect to exist. To this end we compute the discriminant of the elliptic curve and find

$$f = -\frac{1}{48} \cdot (16a_1^2 a_2^2 b_0^2 b_1^2 - 16a_0^2 a_1 a_2 b_0 b_1 b_2^2 + a_0^4 b_2^4) \quad (5.3.57)$$

$$g = \frac{1}{864} \cdot (8a_1 a_2 b_0 b_1 - a_0^2 b_2^2) \cdot (8a_1^2 a_2^2 b_0^2 b_1^2 + 16a_0^2 a_1 a_2 b_0 b_1 b_2^2 - a_0^4 b_2^4) \quad (5.3.58)$$

$$\Delta = -\frac{1}{16} \cdot a_0^2 \cdot b_2^2 \cdot a_1^4 \cdot a_2^4 \cdot b_0^4 \cdot b_1^4 \cdot (-16a_1 a_2 b_0 b_1 + a_0^2 b_2^2). \quad (5.3.59)$$

From the vanishing orders we see that there are two I_2 and four I_4 singularities. Since

$$\frac{9g}{2f} \Big|_{a_1=0} = \frac{9g}{2f} \Big|_{a_2=0} = \frac{9g}{2f} \Big|_{b_1=0} = \frac{9g}{2f} \Big|_{b_2=0} = -\frac{1}{4} a_0^2 b_3^2 \quad (5.3.60)$$

the I_4 singularities are of split type (see [134] or Appendix B) and we therefore see that there is indeed a non-toric $SU(2)^2 \times SU(4)^4 / \mathbb{Z}_4$ gauge group. One can mod out the \mathbb{Z}_4 torsion by identifying it with the diagonal subgroup of the center $\mathbb{Z}_4^{\oplus 4}$ of the $SU(4)$ gauge group part.

It is interesting to see that up to a lattice isomorphism the reflexive polytope ∇° associated to the nef partition (5.3.55) is precisely the polytope with PALP id 0. Under the same lattice isomorphism, the Δ_i of (5.3.55) are mapped to the ∇_i of (5.3.37) and we therefore see that the fiber considered in this subsection is mirror-dual to the fiber of subsection 5.3.3. In particular, it appears that under this duality the discrete gauge group part is mapped to the torsion part of the Mordell-Weil group and vice versa. The same behavior was observed in [144] for hypersurface fibers and, as noted in subsection 3.9.4, it is intriguing to speculate about a possible physical reason underlying this observation.

Finally, let us note that it would be interesting to study explicit realizations of such fibrations. While this is possible in principle, the large number of involved points might make it technically challenging to find a triangulation that gives rise to an appropriate toric fan of the ambient variety. In the recent work [179] it was used that the relevant triangulations are star triangulations with respect to the origin in order to speed up the calculation. It would be exciting to incorporate such an algorithm in the Sage software package and apply it to these spaces.

Part III

Effective Actions

One of the central objects of field theory, both classical and quantum, is the Lagrangian action. While there are field theories for which no such Lagrangian can be defined [180–184], its study is of crucial importance whenever it does exist. In our specific context, we are not interested in the action at energies near the string scale, but at energies small compared to both the string scale and the scale of the compactification manifold. Such a *low-energy effective action* will usually contain only finitely many fields (as opposed to the infinitely many massive string excitations) and its computation provides the link between string theory and the quantum field theories we use to describe our observed universe.

In the third and final part of this dissertation, we therefore study the field theories that arise as the low-energy limits of F-theory compactifications on the geometries introduced in the previous chapters. Ideally, one would wish to be able to do two things:

- Given any genus-one fibered Calabi-Yau manifold, one would want to compute the quantum field theory it gives rise to as precisely as possible.
- Given a set of physical observables, one would like to determine as many geometrical properties as possible that the compactification manifold must have.

Stated in such generality, these are clearly two very difficult problems and solving them is currently (and will possibly always be) simply too hard. To nevertheless make progress in this direction, it has proven very fruitful to isolate particular physical quantities and attempt to study them on their own. One such example is the local study of GUTs in F-theory [55–57, 185], in the course of which it was realized that much of the essential information governing the non-Abelian gauge dynamics is captured already by the geometry of the neighborhood of the branes the gauge theories are located at.

To study gauge theories with Abelian gauge groups we take a different approach. Since Abelian gauge symmetries in F-theory are inextricably linked to global properties of the compactification manifold, it does not seem justifiable to take a local limit. However, matter charged under Abelian gauge groups in F-theory is essentially a *six-dimensional* quantity in F-theory, as it is localized along loci of complex codimension two in the base of the compactification manifold. While F-theory compactifications to four dimensions are considerably richer due to the additional presence of G -flux and Yukawa couplings, it suffices to study their six-dimensional siblings to understand most of their features. In fact, as we have seen in [Part II](#), much of the information specifying the gauge theory is contained already in the fiber geometry (i.e. the *top*) and does not depend on whether one completes the top to a Calabi-Yau threefold or a Calabi-Yau fourfold.

Consequently, most of our effort is concentrated on studying F-theory in six dimensions. As outlined in the introduction of this thesis, we use M-/F-theory duality in order to obtain the F-theory effective action. We begin in [chapter 6](#) by recalling on the one side the effective actions of M-theory compactified on a Calabi-Yau threefold with section and reduce on the other side the general six-dimensional supergravity action with $\mathcal{N} = (1, 0)$ supersymmetry

on a circle. After matching both sides in [chapter 7](#), we obtain the effective F-theory action in six dimensions for elliptically fibered Calabi-Yau manifolds. This analysis is extended to compactifications without section in [chapter 8](#), where we encounter massive Abelian gauge fields. In [chapter 9](#) we illustrate the general concepts obtained thus far by computing the low-energy effective matter spectrum of various genus-one fibered Calabi-Yau threefolds, including manifolds with multiple sections and those without section. Finally, we extend our study of F-theory on genus-one fibrations without section to four-dimensional models by examining the impact of discrete symmetries on the Yukawa couplings of the effective theory in [chapter 10](#).

Chapter 6

Five-Dimensional Supergravity Reductions

As discussed in [Part I](#), effective actions of F-theory compactifications can be obtained by using the chain of S- and T-dualities that connect M-theory on a Calabi-Yau manifold with torus fibration to Type IIB superstring theory on the base of the fibration times a circle. To employ the duality to obtain the six-dimensional F-theory effective action for theories with Abelian gauge symmetries, it is necessary to compute the effective action of M-theory on a Calabi-Yau threefold as well as to reduce a general $\mathcal{N} = (1, 0)$ supergravity theory on a circle. We illustrated this procedure in [figure 2.3](#).

Since the five- and six-dimensional supergravity theories discussed in this chapter may not be overly familiar, we summarize the relevant matter multiplets in tables [6.1](#) and [6.2](#) before proceeding with the reductions. Note that in six dimensions there is an additional

Multiplet	Field Content
Gravity	1 graviton, 1 self-dual two-form, 1 left-handed Weyl gravitino
Vector	1 vector, 1 left-handed Weyl gaugino
Tensor	1 anti-self-dual two-form, 1 real scalar, 1 right-handed Weyl tensorino
Hyper	4 real scalars , 1 right-handed Weyl hyperino

Table 6.1: The massless spectrum of six-dimensional $\mathcal{N} = (1, 0)$ supergravity. Note that one can substitute each Weyl spinor by two symplectic Majorana-Weyl spinors. The gravity multiplet has 24 real degrees of freedom, while the other three multiplets all have eight degrees of freedom.

Multiplet	Field Content
Gravity	1 graviton, 1 vector, 1 Dirac gravitino
Vector	1 vector, 1 real scalar, 1 Dirac gaugino
Hyper	4 real scalars, 1 Dirac hyperino

Table 6.2: The massless spectrum of five-dimensional $\mathcal{N} = 2$ supergravity. The gravity multiplet has 16 real degrees of freedom, while the other two multiplets both have eight degrees of freedom.

massless multiplet, the tensor multiplet, that contains as part of its bosonic field content an anti-self-dual two-form. The existence of such a two-form can be understood via group theory. The massless fields in six dimensions are classified via the representations of $SO(4)$ and, in particular, there exists a completely antisymmetric tensor ϵ_{ijkl} invariant under $SO(4)$ which can be used to impose an (anti-)self-duality condition on the antisymmetric representation with two indices. Notably, this does not work anymore for massless five-dimensional fields, since their representations are those of $SO(3)$. Here the invariant tensor is ϵ_{ijk} and it can be used to dualize the antisymmetric representation into a vector. Upon reduction to five dimensions, a massless two-form field can therefore be dualized into a massless vector field and therefore the tensor multiplet reduces to a vector multiplet in five dimensions. We emphasize, however, that this is true only for *massless* fields. The representations of massive fields in six and five dimensions are those of $SO(5)$ and $SO(4)$, respectively and thus there do exist massive tensor multiplets in five dimensions. For a more detailed discussion of such massive tensor fields and the reduction of tensor multiplets we refer to [186, 187].

Before proceeding with the reductions of M-theory on a Calabi-Yau threefold in section 6.2 and $\mathcal{N} = (1, 0)$ -supergravity on a circle in section 6.3, we first introduce in section 6.1 the basis of divisors and their respective dual $(1, 1)$ -forms that we will perform the reduction on. Note that in the following most of our fields will be five-dimensional. To emphasize when that is not the case, we use hatted fields for fields living in eleven or six dimensions. For the remainder of this chapter, we assume that our compactification manifold is elliptically fibered, that is we assume the existence of a (not necessarily holomorphic) section of the torus fibration.

6.1 A Basis of Divisors for an Elliptically Fibered Calabi-Yau

Let us now fix our notation and choose a convenient divisor basis of the elliptically fibered Calabi-Yau manifold. Our conventions are essentially the same as in [54, 95, 113, 157]. As before, we assume $Y \rightarrow Y_{\text{sing}}$ to be the smooth blow-up of Y_{sing} along all singular loci. We then choose the following basis of divisors D_Λ and their respective dual two-forms $\omega_\Lambda \in H^{1,1}(Y, \mathbb{Z})$:

- The divisor D_0 dual to the two-form along which the M-theory three-form is expanded to give the Kaluza-Klein vector field A^0 . D_0 is obtained by shifting the zero section s_0 according to (6.1.4). We denote the (1,1)-form dual to s_0 by $\omega_{\hat{0}}$.
- Vertical divisors $D_\alpha = \pi^*(D_\alpha^b)$, $\alpha = 1, \dots, h^{1,1}(B)$ obtained as pullbacks of a basis of divisors D_α^b on the base manifold B of the fibration, where π is the projection from Y to the base manifold B .
- Exceptional divisors D_I obtained by resolving singularities of the elliptic fibration Y_{sing} along the divisor S^b in the base manifold, where S^b is the base divisor along which the fibration has non-Abelian singularities. The D_I are fibrations of an irreducible fiber component (isomorphic to a \mathbb{P}^1) over S^b and are also called *Cartan divisors*.
- $U(1)$ divisors D_m obtained by applying the Shioda map given in (6.1.7) to each of the independent generators σ_m , $m = 0, \dots, \text{rank MW}(Y) - 1$ of the Mordell-Weil group of the fibration.

In order to define the shifts mentioned above, it is convenient to introduce the intersection product on the base manifold as

$$D_\alpha^b \cdot D_\beta^b = (D_\alpha \cdot D_\beta)_B = D_\alpha \cdot D_\beta \cdot s_0 \equiv \eta_{\alpha\beta}, \quad (6.1.1)$$

so that we can lower and raise Greek indices using $\eta_{\alpha\beta}$ and its inverse, $\eta^{\alpha\beta}$. Furthermore, we can project a two-cycle $\mathcal{C} \subset Y$ to the base via

$$\pi(\mathcal{C}) = (\mathcal{C} \cdot D^\alpha) D_\alpha^b. \quad (6.1.2)$$

As was noted in [41, 113, 188], D_0 is obtained by requiring that

$$D_0 \cdot D_0 \cdot D_\alpha = 0, \quad (6.1.3)$$

which can be achieved by choosing

$$D_0 = s_0 - \frac{1}{2}(s_0 \cdot s_0 \cdot D^\alpha) D_\alpha. \quad (6.1.4)$$

In a similar fashion, the Shioda map shifts the Mordell-Weil generators σ_m such that specific intersection numbers of D_m with D_0 , D_I and D_α vanish, as we will see in (6.1.11c). This orthogonalization procedure turns out to be crucial for the matching of M-theory and F-theory later. First, however, we must recall the intersection properties of the exceptional divisors obtained by blowing up the singularity of the elliptic fibration. Given a base divisor S^b over which the elliptic fiber of Y_{sing} develops non-Abelian singularities, the blow-up divisors of Y intersect as

$$D_I \cdot D_J \cdot D_\alpha = -\mathcal{C}_{IJ} \left(S^b \cdot D_\alpha^b \right), \quad (6.1.5)$$

where \mathcal{C}_{IJ} denotes the coroot intersection matrix, which we define in the group theory conventions of [Appendix D](#).

Having associated the exceptional blow-up divisors D_I with the Cartan generators of \mathfrak{g} , one can go a step further and define a rational curve localized over a single point in the base manifold for each root of \mathfrak{g} . For the simple roots α_I of \mathfrak{g} , one chooses a base divisor D^b intersecting S^b exactly once and takes the intersection product between $D = \pi^*(D^b)$ and D_I :

$$\mathcal{C}_{\alpha_I} = -D_I \cdot D \quad \text{for} \quad D^b \cdot S^b = 1 \quad (6.1.6)$$

From [Equation 6.1.5](#), one can see that the intersection $D_I \cdot \mathcal{C}_{\alpha_J}$ reproduces the I th component of the simple root α_J in the Dynkin basis of the root system of \mathfrak{g} . Note that these are the same conventions as used in the example of [subsection 5.3.1](#). With these definitions, we are ready to give an explicit formula for the Shioda map relating Mordell-Weil generators $\sigma_m = s_{m+1} - s_0$ to their associated $U(1)$ -divisors:

$$\begin{aligned} D_m &= \sigma_m - (\sigma_m \cdot s_0 \cdot D^\alpha) D_\alpha - (\sigma_m \cdot \mathcal{C}_{\alpha_I}) (\mathcal{C}^{-1})^{IJ} D_J \\ &= s_{m+1} - s_0 - ((s_{m+1} - s_0) \cdot s_0 \cdot D^\alpha) D_\alpha - (s_{m+1} \cdot \mathcal{C}_{\alpha_I}) (\mathcal{C}^{-1})^{IJ} D_J \end{aligned} \quad (6.1.7)$$

Let us now discuss the intersection numbers in this basis and emphasize clearly the difference between a holomorphic and a non-holomorphic zero section s_0 . We begin by examining the geometry of the blow-up divisors D_I . A *holomorphic* zero section marks a single point in each fiber. In particular, when this point lies over S^b , it is on the original fiber component¹ and not on the resolution \mathbb{P}^1 s of the rational curves \mathcal{C}_{α_I} . Therefore the following equation holds as an identity in the Chow ring of Y :²

$$s_0 \cdot D_I = 0, \quad \text{if } s_0 \text{ is holomorphic.} \quad (6.1.8)$$

On the other hand, a non-holomorphic zero section may wrap the entire fiber component over lower-dimensional loci of the base. Since this fiber component intersects the resolution divisors as the affine node in the extended Dynkin diagram of \mathfrak{g} , its intersection with a Cartan divisor *can* be non-zero. However, since the locus over which a non-holomorphic zero section can wrap the entire fiber component has at least codimension two in the base, so has $s_0 \cdot D_I$. The intersection with a vertical divisor therefore vanishes and we find that

$$D_\alpha \cdot s_0 \cdot D_I = 0 \quad (6.1.9)$$

even for a non-holomorphic zero section.

¹Assuming that the resolution locus in the base is S^b , one can associate the divisor $\pi^*(S^b) - \sum_I D_I$ with the affine node of the Dynkin diagram of \mathfrak{g} . Intersecting this divisor with $\pi^*(D^b)$ such that $D^b \cdot S^b = 1$ gives the rational curve associated with the original fiber component.

²The Chow ring of an algebraic variety X is formed by equivalence classes of the subvarieties of X , where the equivalence relation is given by rational equivalence. The multiplicative structure is defined by taking the intersection of two subvarieties.

The other peculiarity of having a non-holomorphic zero section is that one can no longer evaluate expressions involving s_0 by using adjunction to the base manifold. Recall that

$$s_0 \cdot s_0 = s_0|_B = K_B, \quad \text{if } s_0 \text{ is holomorphic.} \quad (6.1.10)$$

However, for a non-holomorphic zero section this needs no longer be the case, since the divisors s_0 and B are only birationally equivalent, but *not isomorphic*.

To put it in a nutshell, a non-holomorphic zero section may intersect blow-up divisors over points in the base and the divisor corresponding to that section is no longer isomorphic to the base manifold. With this in mind, we can now list the intersection numbers both for a non-holomorphic zero section and for its holomorphic counterpart. We begin by stating intersections that hold *both for a non-holomorphic and for a holomorphic* zero section:

$$D_\alpha \cdot D_\beta \cdot D_\gamma = 0, \quad D_0 \cdot D_\alpha \cdot D_\beta = \eta_{\alpha\beta}, \quad D_0 \cdot D_0 \cdot D_\alpha = 0, \quad (6.1.11a)$$

$$D_\alpha \cdot D_\beta \cdot D_I = 0, \quad D_\alpha \cdot D_0 \cdot D_I = 0, \quad D_\alpha \cdot D_I \cdot D_J = -\mathcal{C}_{IJ}(S^b \cdot D_\alpha^b), \quad (6.1.11b)$$

$$D_\alpha \cdot D_\beta \cdot D_m = 0, \quad D_\alpha \cdot D_I \cdot D_m = 0, \quad D_0 \cdot D_\alpha \cdot D_m = 0, \quad (6.1.11c)$$

$$D_\alpha \cdot D_m \cdot D_n = \pi(D_m \cdot D_n)_\alpha. \quad (6.1.11d)$$

All three equations in (6.1.11a) describe intersections on the base manifold. The first one is a triple intersection product between codimension-one objects in the base and therefore vanishes. Using this fact, the second equation simply reduces to the definition in Equation 6.1.1 and the third equation can be verified directly by inserting Equation 6.1.4. Next of all, the three equations in (6.1.11b) are a direct consequence of the blow-up geometry and were discussed above. Equation 6.1.11d is just a formal rewriting of the intersection number using Equation 6.1.2 and we stress that unlike in [113], we do not require D_m and D_n be orthogonal to each other. Lastly, the remaining three equations (6.1.11c) follow from the orthogonalization properties of the Shioda map. They can be verified by inserting the expression in Equation 6.1.7 and exploiting that all sections intersect the generic fiber component precisely once, that is

$$s_m \cdot E = s_0 \cdot E = D_0 \cdot E = 1, \quad (6.1.12)$$

where the class of the generic fiber E is given as

$$D_\alpha \cdot D_\beta = E\eta_{\alpha\beta}. \quad (6.1.13)$$

In a second step, we now assume to have a *holomorphic* zero section s_0 . Using the definition of the Shioda map we evaluate

$$s_0 \cdot D_m = 0, \quad \text{if } s_0 \text{ is holomorphic.} \quad (6.1.14)$$

Exploiting (6.1.8), (6.1.14) and (6.1.10) one can then show that

$$D_0 \cdot D_m \cdot D_n = -\frac{1}{2}\pi(D_m \cdot D_n)_\alpha K^\alpha, \quad D_0 \cdot D_I \cdot D_J = -\frac{1}{2}K^\alpha(D_\alpha \cdot D_I \cdot D_J), \quad (6.1.15a)$$

$$D_0 \cdot D_0 \cdot D_I = 0, \quad D_0 \cdot D_0 \cdot D_m = 0, \quad D_0 \cdot D_I \cdot D_m = 0, \quad (6.1.15b)$$

$$D_0 \cdot D_0 \cdot D_0 = \frac{1}{4}K^\alpha K_\alpha, \quad (6.1.15c)$$

where K^α are the expansion coefficients of the canonical class of B in $K_B = K^\alpha D_\alpha^b$. All equations in (6.1.15b) are a direct consequence of Equation 6.1.8 and Equation 6.1.14. Equation 6.1.15c follows from applying the adjunction formula. Finally, the two equations in (6.1.15a) both follow from applying Equation 6.1.8, Equation 6.1.14 and the adjunction formula. We stress that the relations of (6.1.15) are not valid for a non-holomorphic zero section.

6.2 M-Theory on a Calabi-Yau Threefold

With the preliminary discussion finished, let us now begin in earnest and present the first of two effective supergravity theories in five dimensions, namely the one obtained by reducing M-theory on a smooth genus-one fibered Calabi-Yau threefold Y . In terms of figure 2.3, we proceed with the first column, displayed again in figure 6.1. To perform the dimensional reduction one expands the M-theory three-form \hat{C}_3 along the harmonic forms of Y . Recall that the non-vanishing Hodge numbers are

$$\begin{aligned} h^{0,0}(Y) = h^{3,3}(Y) = 1, & \quad h^{3,0}(Y) = h^{0,3}(Y) = 1, \\ h^{1,1}(Y) = h^{2,2}(Y), & \quad h^{2,1}(Y) = h^{1,2}(Y). \end{aligned} \quad (6.2.1)$$

The cohomology group $H^{1,1}(Y)$ consists of the cohomology classes Poincaré-dual to the divisors of the Calabi-Yau threefold introduced in the previous section 6.1. For $H^3(Y)$ we introduce a real symplectic basis (α_K, β^K) , $K = 1 \dots h^{2,1} + 1$. The reduction then reads

$$\hat{C}_3 = \xi^K \alpha_K - \tilde{\xi}_K \beta^K + A^0 \wedge \omega_0 + A^\alpha \wedge \omega_\alpha + A^I \wedge \omega_I + A^m \wedge \omega_m + C_3, \quad (6.2.2)$$

where we have introduced the vectors

$$(A^\Lambda) = (A^0, A^\alpha, A^I, A^m), \quad (6.2.3)$$

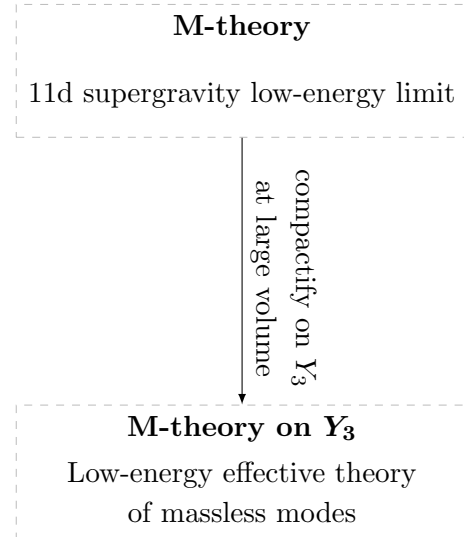


Figure 6.1: Reducing M-theory on Y_3 .

a five-dimensional three-form C_3 and real scalars $(\xi^K, \tilde{\xi}_K)$. Similarly, one can expand the Kähler form of Y as

$$\hat{J} = v^0 \omega_0 + v^\alpha \omega_\alpha + v^I \omega_I + v^m \omega_m \quad (6.2.4)$$

to obtain the five-dimensional scalars v^Λ . One of the vectors from the \hat{C}_3 -reduction belongs to the gravity multiplet and comprises the graviphoton, while the remaining vectors form $V = h^{1,1}(Y) - 1$ vector multiplets. The corresponding scalars are the v^Λ . Note that these $h^{1,1}(Y)$ scalars are distributed among vector multiplets and the universal hypermultiplet. The vector multiplets contain normalized scalars

$$L^\Lambda = \mathcal{V}^{-1/3} v^\Lambda, \quad (L^\Lambda) \equiv (R, L^\alpha, \xi^I, \xi^m), \quad (6.2.5)$$

while the total volume, given by

$$\mathcal{V} = \frac{1}{3!} \mathcal{V}_{\Lambda\Sigma\Theta} v^\Lambda v^\Sigma v^\Theta, \quad (6.2.6)$$

is part of the universal hypermultiplet. The five-dimensional three-form C_3 is dualized into a real scalar Φ and also sits in the universal hypermultiplet. Concerning the scalars $(\xi^K, \tilde{\xi}_K)$, we note that $2h^{1,2}(Y)$ degrees of freedom together with the complex structure moduli form $h^{1,2}(Y)$ hypermultiplets. The remaining two degrees of freedom from these scalars enter the universal hypermultiplet.

Having obtained the above data of the massless modes, we can easily derive the gravity and vector sector in the canonical form of five-dimensional $\mathcal{N} = 2$ supergravity. The prepotential is given by

$$\mathcal{N} = \frac{1}{3!} \mathcal{V}_{\Lambda\Sigma\Theta} L^\Lambda L^\Sigma L^\Theta, \quad (6.2.7)$$

where we have defined the intersection numbers

$$\mathcal{V}_{\Lambda\Sigma\Theta} = D_\Lambda \cdot D_\Sigma \cdot D_\Theta. \quad (6.2.8)$$

Recall that these intersections were discussed in [section 6.1](#) and that they take the special form [\(6.1.11\)](#) in the case of an elliptic fibration. If the manifold admits a holomorphic zero section, then the additional relations [\(6.1.15\)](#) hold. We are now in a position to write down the prepotential. As discussed in more detail in [\[54, 94, 187, 189\]](#), the prepotential of the resolved threefold contains both classical and one-loop terms when interpreted in the dual F-theory setup. To distinguish these contributions in M-theory, let us define an ϵ -scaling for the five-dimensional M-theory fields. The limit $\epsilon \rightarrow 0$ corresponds to the F-theory limit and enforces that both the volume of the elliptic fiber and the blow-up divisors shrink to zero. For the scalar fields v^Λ we set³

$$v^0 \mapsto \epsilon v^0, \quad v^\alpha \mapsto \epsilon^{-1/2} v^\alpha, \quad v^I \mapsto \epsilon^{1/4} v^I, \quad v^m \mapsto \epsilon^{1/4} v^m. \quad (6.2.9)$$

³For consistency checks on these scaling relations we refer to [\[54\]](#).

On the level of the redefined fields this reads

$$R \mapsto \epsilon R, \quad L^\alpha \mapsto \epsilon^{-1/2} L^\alpha, \quad \xi^I \mapsto \epsilon^{1/4} \xi^I, \quad \xi^m \mapsto \epsilon^{1/4} \xi^m. \quad (6.2.10)$$

In this limit only classical terms are non-zero. Hence, we can divide the prepotential into a part surviving as $\epsilon \rightarrow 0$ and a part that vanishes in the limit. Accordingly, the classical part of the prepotential is given by

$$\begin{aligned} \mathcal{N}_{class}^M &= \frac{1}{2} \eta_{\alpha\beta} R L^\alpha L^\beta - \frac{1}{2} \mathcal{C}_{IJ} \eta_{\alpha\beta} S^{b,\alpha} L^\beta \xi^I \xi^J \\ &\quad + \frac{1}{2} \pi (D_m \cdot D_n)^\alpha \eta_{\alpha\beta} L^\beta \xi^m \xi^n. \end{aligned} \quad (6.2.11)$$

The one-loop part of the prepotential cannot be given in such an explicit form. It reads

$$\begin{aligned} \mathcal{N}_{loop}^M &= \frac{1}{6} \mathcal{V}_{000} RRR + \frac{1}{2} \mathcal{V}_{00m} RR\xi^m + \frac{1}{2} \mathcal{V}_{00I} RR\xi^I + \frac{1}{2} \mathcal{V}_{0IJ} R\xi^I \xi^J \\ &\quad + \frac{1}{2} \mathcal{V}_{0mn} R\xi^m \xi^n + \mathcal{V}_{0mI} R\xi^m \xi^I + \frac{1}{6} \mathcal{V}_{IJK} \xi^I \xi^J \xi^K \\ &\quad + \frac{1}{6} \mathcal{V}_{mnk} \xi^m \xi^n \xi^k + \frac{1}{2} \mathcal{V}_{mIJ} \xi^m \xi^I \xi^J + \frac{1}{2} \mathcal{V}_{Imn} \xi^I \xi^m \xi^n. \end{aligned} \quad (6.2.12)$$

In case there is a holomorphic zero section, one can use (6.1.15) to simplify the above expression to

$$\begin{aligned} \mathcal{N}_{loop}^M &= \frac{1}{24} K^\alpha K^\beta \eta_{\alpha\beta} RRR + \frac{1}{4} \mathcal{C}_{IJ} K^\alpha S^{b,\beta} \eta_{\alpha\beta} R\xi^I \xi^J \\ &\quad - \frac{1}{4} \pi (D_m \cdot D_n)^\alpha K^\beta \eta_{\alpha\beta} R\xi^m \xi^n \\ &\quad + \frac{1}{6} \mathcal{V}_{IJK} \xi^I \xi^J \xi^K + \frac{1}{6} \mathcal{V}_{mnk} \xi^m \xi^n \xi^k \\ &\quad + \frac{1}{2} \mathcal{V}_{mIJ} \xi^m \xi^I \xi^J + \frac{1}{2} \mathcal{V}_{Imn} \xi^I \xi^m \xi^n. \end{aligned} \quad (6.2.13)$$

In fact, by inserting the ϵ -rescaled fields one can check that \mathcal{N}_{loop}^M vanishes in the limit $\epsilon \rightarrow 0$, while \mathcal{N}_{class}^M stays finite.

The above analysis leads to an effective action in which massive modes appearing in the M-theory reduction have been integrated out already. Let us remark on how these massive states arise in the five-dimensional M-theory reduction. On the Coulomb branch of the dual circle reduced six-dimensional $\mathcal{N} = (1, 0)$ theory, non-Cartan vector multiplets, charged hypermultiplets and KK-modes become massive. By taking the decompactification limit $r \rightarrow \infty$ and by moving to the origin of the Coulomb branch all these modes therefore become massless again. In the dual M-theory setting they arise from M2 branes wrapping rational curves in the fiber that shrink to zero volume in the F-theory limit. These modes, which are massive on the Coulomb branch, wrap the \mathbb{P}^1 s resolving the singularities in the fibration. In fact, as we move towards the origin of the Coulomb branch, the \mathbb{P}^1 s shrink in size and the M2 brane states become light. Similarly, the KK-modes arise from M2 branes with volume

contribution depending on the volume of the generic elliptic fiber. The KK-mass also becomes zero as $r \rightarrow \infty$ in the decompactification limit and all such modes become massless.

Before we conclude this section, let us discuss the dimensional reduction of known higher curvature corrections in M-theory. Their lift to F-theory proceeds along the lines of [54, 128, 129], but we focus here on the term quartic in the curvature two-form and linear in \hat{C}_3 . Concretely, this term in the eleven-dimensional action is given by

$$\hat{S}_{C\mathcal{R}^4}^{(11)} = -\frac{1}{96} \int_{M_{11}} \hat{C}_3 \wedge [\text{tr } \hat{\mathcal{R}}^4 - \frac{1}{4}(\text{tr } \hat{\mathcal{R}}^2)^2]. \quad (6.2.14)$$

Upon dimensional reduction on a general Calabi-Yau threefold, one finds, among other terms, the five-dimensional Chern-Simons terms [190]

$$S_{AR\mathcal{R}}^{(5)M} = \frac{1}{48} c_\Lambda \int_{M_5} A^\Lambda \wedge \text{tr } \mathcal{R} \wedge \mathcal{R}, \quad (6.2.15)$$

where

$$c_\Lambda = \int_Y \omega_\Lambda \wedge c_2(Y). \quad (6.2.16)$$

The comparison with F-theory will show that the c_α -term is a classical Chern-Simons term, while the other terms involving c_0 , c_I , c_m are induced at one-loop. We discuss this matter in more detail in [chapter 7](#).

On the M-theory side, one can use the geometry of Y to evaluate the various components $(c_\Lambda) = (c_\alpha, c_0, c_I, c_m)$. In the case of c_α , it is possible to perform this calculation without knowledge of the specific manifold. One finds that

$$c_\alpha = -12K_\alpha, \quad (6.2.17)$$

where $K_\alpha = \eta_{\alpha\beta} K^\beta$ and K^β are the expansion coefficients of the canonical class in terms of vertical divisors. Notably, the result is independent of whether the zero section of Y is holomorphic or not. For details on the calculation, we refer to [section C.1](#).

If, on the other hand, we do have a holomorphic zero section, then we can explicitly evaluate another coefficient to find that

$$c_0 = 52 - 4h^{1,1}(B) \quad \text{if } s_0 \text{ is holomorphic.} \quad (6.2.18)$$

Again, we defer details to [section C.1](#).

6.3 Six-Dimensional $\mathcal{N} = (1, 0)$ -Supergravity on a Cycle

The effective action of F-theory compactified on a singular Calabi-Yau threefold is a six-dimensional $\mathcal{N} = (1, 0)$ -supergravity theory and we proceed with the second step by following the procedure outlined in [figure 6.2](#). Let us denote the six-dimensional space-time manifold by M_6 . In the following, we denote the number of vector multiplets by V , the number of tensor multiplets by T , and the number of hypermultiplets by H .

We allow for a non-Abelian gauge group G , which splits into a simple non-Abelian part G_{nA} and $n_{U(1)}$ $U(1)$ -factors as

$$G = G_{\text{nA}} \times U(1)^{n_{U(1)}}. \quad (6.3.1)$$

Our goal is to find the F-theory effective action of a $\mathcal{N} = (1, 0)$ theory with gauge group G . Since the tensors in the spectrum obey (anti-)self-duality constraints, we can only give a pseudo-action for this theory for which the additional constraints have to be imposed manually at the level of the equations of motion. For the sake of simplicity we only display the bosonic part of this pseudo-action. The fermionic couplings can then be inferred by using the general supergravity actions found in [191–194]. Our conventions are summarized in section E.1 and follow largely the ones used in [54].

Let us collectively denote the anti-self-dual tensors from the tensor multiplets and the self-dual tensor from the gravity multiplet by \hat{B}^α , $\alpha = 1 \dots T + 1$. The real scalars in the tensor multiplets parametrize the manifold

$$SO(1, T)/SO(T). \quad (6.3.2)$$

For a convenient description of this coset space we introduce $T + 1$ scalars j^α and a constant metric $\Omega_{\alpha\beta}$ with signature $(+, -, \dots, -)$. Due to the constraint

$$\Omega_{\alpha\beta} j^\alpha j^\beta \stackrel{!}{=} 1 \quad (6.3.3)$$

one scalar degree of freedom is redundant. Furthermore, it is useful to define another non-constant positive metric

$$g_{\alpha\beta} = 2j_\alpha j_\beta - \Omega_{\alpha\beta}. \quad (6.3.4)$$

Here and in the following indices are raised and lowered using $\Omega_{\alpha\beta}$.

The gauge connection for the simple non-Abelian group is denoted by \hat{A} and the Abelian ones are denoted by \hat{A}^m , where $m = 1 \dots n_{U(1)}$. The field strength two-forms read

$$\hat{F} = d\hat{A} + \hat{A} \wedge \hat{A}, \quad \hat{F}^m = d\hat{A}^m \quad (6.3.5)$$

and the Chern-Simons forms are defined as

$$\hat{\omega}^{CS} = \text{tr}(\hat{A} \wedge d\hat{A} + \frac{2}{3}\hat{A} \wedge \hat{A} \wedge \hat{A}), \quad \hat{\omega}^{CS, mn} = \hat{A}^m \wedge d\hat{A}^n. \quad (6.3.6)$$

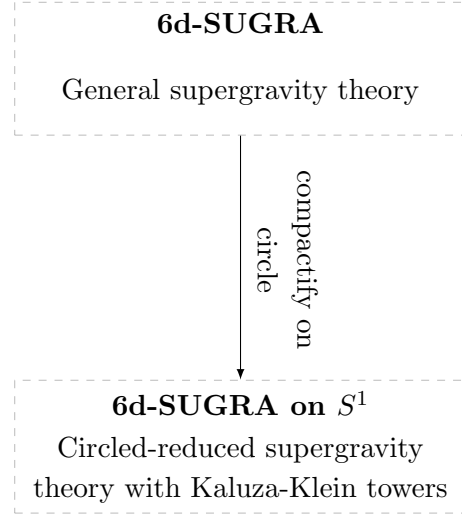


Figure 6.2: Circle reduction of the six-dimensional supergravity theory.

Let us now turn to the gravity sector, which is described by the spin connection $\hat{\omega}$ on M_6 , the curvature two-form

$$\hat{\mathcal{R}} = d\hat{\omega} + \hat{\omega} \wedge \hat{\omega} \quad (6.3.7)$$

and the Ricci-Scalar \hat{R} . The gravitational Chern-Simons form is defined as

$$\hat{\omega}_{grav}^{CS} = \text{tr}(\hat{\omega} \wedge d\hat{\omega} + \frac{2}{3}\hat{\omega} \wedge \hat{\omega} \wedge \hat{\omega}). \quad (6.3.8)$$

Moreover, there are four real scalars in each hypermultiplet, which we collectively denote by q^U , $U = 1 \dots 4H$. These parametrize a quaternionic manifold with metric h_{UV} . Since the hypermultiplets may transform in some representation \mathbf{R} of the simple non-Abelian gauge group and may also carry $U(1)$ -charges, we introduce the covariant derivative

$$\hat{D}q^U = dq^U + \hat{A}^{\mathbf{R}}q^U - iq_m \hat{A}^m q^U, \quad (6.3.9)$$

where $\hat{A}^{\mathbf{R}}$ denotes the Lie-algebra valued gauge connection of G_{nA} in the representation \mathbf{R} .

Since the six-dimensional $\mathcal{N} = (1, 0)$ spectrum is chiral, the theory is potentially anomalous. For some spectra, one can employ the Green-Schwarz mechanism [7, 195, 196] to cancel these anomalies. We therefore include the Green-Schwarz counterterm in the action, which reads

$$\hat{S}^{GS} = -\frac{1}{2} \int_{M_6} \Omega_{\alpha\beta} \hat{B}^\alpha \wedge \hat{X}_4^\beta, \quad (6.3.10)$$

where

$$\hat{X}_4^\alpha = \frac{1}{2} a^\alpha \text{tr} \hat{\mathcal{R}} \wedge \hat{\mathcal{R}} + 2 \frac{b^\alpha}{\lambda(\mathfrak{g})} \text{tr} \hat{F} \wedge \hat{F} + 2b_{mn}^\alpha \hat{F}^m \wedge \hat{F}^n. \quad (6.3.11)$$

The constants a^α , b^α , b_{mn}^α will later be given in terms of geometrical data of the internal Calabi-Yau space. We have furthermore inserted a group theoretical factor $\lambda(\mathfrak{g})$ defined in Equation D.0.2 for later convenience. The Green-Schwarz term can be used to cancel those anomalies whose anomaly polynomial factorizes as

$$\hat{I}_8 = -\frac{1}{2} \Omega_{\alpha\beta} \hat{X}_4^\alpha \wedge \hat{X}_4^\beta, \quad (6.3.12)$$

provided that we assign an appropriate transformation to the tensors under gauge and local Lorentz transformations, which turns out to be

$$\delta \hat{B}^\alpha = d\hat{\Lambda}^\alpha - \frac{1}{2} a^\alpha \text{tr} \hat{l} d\hat{\omega} - 2b^\alpha \text{tr} \hat{\lambda} d\hat{A} - 2b_{mn}^\alpha \hat{\lambda}^m d\hat{A}^n, \quad (6.3.13)$$

where \hat{l} , $\hat{\lambda}$, $\hat{\lambda}^m$ are the respective parameters of local Lorentz and gauge transformations

$$\delta \hat{\omega} = d\hat{l} + [\hat{\omega}, \hat{l}], \quad \delta \hat{A} = d\hat{\lambda} + [\hat{A}, \hat{\lambda}], \quad \delta \hat{A}^m = d\hat{\lambda}^m \quad (6.3.14)$$

and the one-forms $\hat{\Lambda}^\alpha$ encode the standard gauge transformations of two-forms. The precise conditions the matter spectrum has to satisfy in order for the factorization (6.3.12) to take place will be reviewed in section 7.4. The gauge invariant field strength for the tensors then takes the form

$$\hat{G}^\alpha = d\hat{B}^\alpha + \frac{1}{2}a^\alpha \hat{\omega}_{grav}^{CS} + 2\frac{b^\alpha}{\lambda(\mathfrak{g})} \hat{\omega}^{CS} + 2b_{mn}^\alpha \hat{\omega}^{CS,mn}. \quad (6.3.15)$$

Note that the \hat{G}^α are subject to a duality constraint

$$g_{\alpha\beta} \hat{*} \hat{G}^\beta = \Omega_{\alpha\beta} \hat{G}^\beta, \quad (6.3.16)$$

which has to be enforced in addition to the equations of motion derived from the pseudo-action. The bosonic part of the pseudo-action for six-dimensional $\mathcal{N} = (1, 0)$ supergravity with gauge group G reads

$$\begin{aligned} \hat{S}^{(6)} = & \int_{M_6} + \frac{1}{2} \hat{R} \hat{*} 1 - \frac{1}{4} g_{\alpha\beta} \hat{G}^\alpha \wedge \hat{*} \hat{G}^\beta - \frac{1}{2} g_{\alpha\beta} dj^\alpha \wedge \hat{*} dj^\beta - h_{UV} \hat{D}q^U \wedge \hat{*} \hat{D}q^V \\ & - 2\Omega_{\alpha\beta} j^\alpha \frac{b^\beta}{\lambda(\mathfrak{g})} \text{tr } \hat{F} \wedge \hat{*} \hat{F} - 2\Omega_{\alpha\beta} j^\alpha b_{mn}^\beta \hat{F}^m \wedge \hat{*} \hat{F}^n \\ & - \Omega_{\alpha\beta} \frac{b^\alpha}{\lambda(\mathfrak{g})} \hat{B}^\beta \wedge \text{tr } \hat{F} \wedge \hat{F} - \Omega_{\alpha\beta} b_{mn}^\alpha \hat{B}^\beta \wedge \hat{F}^m \wedge \hat{F}^n \\ & - \frac{1}{4} \Omega_{\alpha\beta} a^\alpha \hat{B}^\beta \wedge \text{tr } \hat{\mathcal{R}} \wedge \hat{\mathcal{R}} - \hat{V} \hat{*} 1, \end{aligned} \quad (6.3.17)$$

where \hat{V} is the scalar potential. In the following we do not need the precise form of \hat{V} and refer for example to [191, 192, 197–199] for more details.

In a next step we compactify this theory on a circle of radius r and thus choose the six-dimensional space-time to be of the form $M_6 = S^1 \times M_5$. Let us briefly summarize the results of this reduction here and defer technical details and conventions to Appendix E. The coordinate along the circle is denoted by y . We write A^0 for the Kaluza-Klein vector and call the corresponding field-strength $F^0 = dA^0$. Let us also define $Dy = dy - A^0$. Recall that expressions without hats are of five-dimensional origin and are hence independent of y . It is important to stress here that we only approach a two-derivative reduction for the moment. We therefore also neglect higher curvature contributions. This implies that we can omit the gravitational contribution in the Green-Schwarz terms of Equation 6.3.10 and all other gravitational contributions from the tensors proportional to a^α . Later on, we revisit these terms and discuss them in more detail.

Hypermultiplets in six dimensions reduce trivially to five-dimensional hypermultiplets. The six-dimensional vectors \hat{A} , \hat{A}^m reduce to five-dimensional vectors A , A^m and scalars ζ , ζ^m . Tensors \hat{B}^α in the six-dimensional theory reduce to five-dimensional tensors B^α with field-strength G^α and vectors A^α with field-strength $F^\alpha = dA^\alpha$. These reductions can be inserted into the six-dimensional pseudo-action. One then has to integrate over the circle direction to

obtain a five-dimensional pseudo-action. Reducing the (anti-)self-duality constraint (6.3.16) yields a relation between the tensor field-strength G^α and the vector field-strength \mathcal{F}^α given by

$$\mathcal{F}^\alpha = F^\alpha - 4 \frac{b^\alpha}{\lambda(\mathfrak{g})} \text{tr}(\zeta F) + 2 \frac{b^\alpha}{\lambda(\mathfrak{g})} \text{tr}(\zeta \zeta) F^0 - 4b_{mn}^\alpha \zeta^m F^n + 2b_{mn}^\alpha \zeta^m \zeta^n F^0. \quad (6.3.18)$$

This condition can be used to obtain a proper five-dimensional supergravity action depending only on \mathcal{F}^α by eliminating the dependence of the five-dimensional pseudo-action on the tensors B^α in favor of the vectors A^α . While this is always possible at the massless Kaluza-Klein level for the compactified tensors, doing so will no longer work at the massive level. Furthermore, we also perform a Weyl rescaling to arrive at the canonical form of the Einstein-Hilbert term.

The last step is to push the theory onto the five-dimensional Coulomb branch by switching on vacuum expectation values for the scalars in the vector multiplets. This results in giving mass terms to the W-bosons (and by supersymmetry also to their fermionic partners) and the charged hypermultiplets. The massive W-bosons break the simple non-Abelian gauge group to its maximal torus $U(1)^{\text{rank}(G_{\text{nA}})}$. Below the mass scale characteristic of the gauge group breaking, all massive states have to be integrated out from the five-dimensional effective action. We discuss the induced corrections in section 7.3. On the massless level we are only left with the Cartan generators and the generators of the Abelian gauge symmetry, which generically stay massless. We thus find the residual gauge symmetry

$$U(1)^{\text{rank}(G_{\text{nA}})} \times U(1)^{n_{U(1)}}. \quad (6.3.19)$$

In the following, the $U(1)$ s originating from the non-Abelian Cartan generators are labeled by $I = 1, \dots, \text{rank}(G_{\text{nA}})$.

Let us summarize the massless bosonic fields of the Coulomb branch effective theory and their completion into five-dimensional $\mathcal{N} = 2$ multiplets. We distinguish three types of five-dimensional multiplets:

- The gravity multiplet consists of the five-dimensional metric (graviton) and in general a linear combination of A^0 and A^α (graviphoton).
- We find $\text{rank}(G_{\text{nA}}) + n_{U(1)} + T + 1$ vector multiplets. The vectors are A^I , A^m and $T + 1$ linear combinations of A^0 and A^α . The corresponding scalar degrees of freedom are provided by ζ^I , ζ^m , r and j^α supplemented by the constraint $\Omega_{\alpha\beta} j^\alpha j^\beta \stackrel{!}{=} 1$ from the six-dimensional theory. Recall that $\alpha = 1, \dots, T + 1$, $m = 1, \dots, n_{U(1)}$, and $I = 1, \dots, \text{rank}(G_{\text{nA}})$.
- The only massless five-dimensional hypermultiplets arise from H^{neutral} six-dimensional hypermultiplets that transform trivially under G .

To specify the Coulomb branch action, we first need to introduce some additional notation. The Cartan generators \mathcal{T}_I are chosen to be in the coroot basis, i.e. we have the following

relation to the Cartan generators T^M in the usual basis given around [Equation D.0.3](#):

$$\mathcal{T}_I = \alpha_I^\vee \cdot T. \quad (6.3.20)$$

According to the convention [\(D.0.3\)](#), the trace normalization for the Cartan generators in the coroot basis reads

$$\text{tr}(\mathcal{T}_I \mathcal{T}_J) = \lambda(\mathfrak{g}) \mathcal{C}_{IJ}, \quad (6.3.21)$$

where the coroot inner product matrix \mathcal{C}_{IJ} is defined in [\(D.0.1\)](#).⁴

To simplify our expressions, we introduce indices $\hat{I} = (I, m)$, $\hat{J} = (J, n)$, etc. running over all $U(1)$ s in the Coulomb branch group [\(6.3.19\)](#). In particular, we define

$$b_{\hat{I}\hat{J}}^\alpha = \begin{pmatrix} b^\alpha \mathcal{C}_{IJ} & 0 \\ 0 & b_{mn}^\alpha \end{pmatrix}, \quad (6.3.22)$$

where $\hat{I}, \hat{J} = 1, \dots, \text{rank}(G) + n_{U(1)}$.

The five-dimensional action on the Coulomb branch then reads

$$\begin{aligned} S^{(5)F} = \int_{M_5} & + \frac{1}{2} R * 1 - \frac{2}{3} r^{-2} dr \wedge * dr - \frac{1}{2} g_{\alpha\beta} dj^\alpha \wedge * dj^\beta - h_{uv} dq^u \wedge * dq^v \\ & - 2r^{-2} \Omega_{\alpha\beta j}{}^\alpha b_{\hat{I}\hat{J}}^\beta d\zeta^{\hat{I}} \wedge * d\zeta^{\hat{J}} - \frac{1}{4} r^{8/3} F^0 \wedge * F^0 - \frac{1}{2} r^{-4/3} g_{\alpha\beta} \mathcal{F}^\alpha \wedge * \mathcal{F}^\beta \\ & - 2r^{2/3} \Omega_{\alpha\beta j}{}^\alpha b_{\hat{I}\hat{J}}^\beta (F^{\hat{I}} - \zeta^{\hat{I}} F^0) \wedge *(F^{\hat{J}} - \zeta^{\hat{J}} F^0) + \mathcal{L}_{\text{CS}}^{\text{p}} + \mathcal{L}_{\text{CS}}^{\text{np}}, \end{aligned} \quad (6.3.23)$$

where gauge-invariant Chern-Simons terms are given by

$$\mathcal{L}_{\text{CS}}^{\text{p}} = -\frac{1}{2} \Omega_{\alpha\beta} A^0 \wedge F^\alpha \wedge F^\beta + 2\Omega_{\alpha\beta} b_{\hat{I}\hat{J}}^\alpha A^\beta \wedge F^{\hat{I}} \wedge F^{\hat{J}}, \quad (6.3.24)$$

and non-gauge-invariant Chern-Simons terms read

$$\begin{aligned} \mathcal{L}_{\text{CS}}^{\text{np}} = & -2\Omega_{\alpha\beta} b_{\hat{I}\hat{J}}^\alpha b_{\hat{K}\hat{L}}^\beta \zeta^{\hat{K}} \zeta^{\hat{L}} \zeta^{\hat{I}} A^{\hat{J}} \wedge F^0 \wedge F^0 \\ & + 2\Omega_{\alpha\beta} (b_{\hat{I}\hat{J}}^\alpha b_{\hat{K}\hat{L}}^\beta + 2b_{\hat{I}\hat{K}}^\alpha b_{\hat{J}\hat{L}}^\beta) \zeta^{\hat{K}} \zeta^{\hat{L}} A^{\hat{I}} \wedge F^{\hat{J}} \wedge F^0 \\ & - 2\Omega_{\alpha\beta} (2b_{\hat{I}\hat{J}}^\alpha b_{\hat{K}\hat{L}}^\beta + b_{\hat{I}\hat{L}}^\alpha b_{\hat{J}\hat{K}}^\beta) \zeta^{\hat{L}} A^{\hat{I}} \wedge F^{\hat{J}} \wedge F^{\hat{K}}. \end{aligned} \quad (6.3.25)$$

Note that the five-dimensional expression $\mathcal{L}_{\text{CS}}^{\text{np}}$ arises from the reduction of the six-dimensional non-gauge-invariant Green-Schwarz term [\(6.3.10\)](#). In contrast to six dimensions, $\mathcal{L}_{\text{CS}}^{\text{np}}$ can be canceled by adding a one-loop counter-term in five-dimensions that renders the action gauge invariant [\[54, 200\]](#). In the vector field sector, we have only kept Cartan and Abelian gauge fields (and their respective scalar partners) and, similarly, in the hyper sector also only the massless, i.e. uncharged scalars, denoted by q^u , $u = 1 \dots 4H^{\text{neutral}}$.

⁴Note that all roots and weights appearing in this work are still associated to the Cartan generators T^M and not to \mathcal{T}_I .

The information about the gravity and vector sector of five-dimensional $\mathcal{N} = 2$ supergravity is contained entirely in the real prepotential \mathcal{N} . In the canonical form of the supergravity, \mathcal{N} is a cubic polynomial in the scalar fields M^Λ . The M^Λ are so-called very special coordinates and encode the scalar degrees of freedom in the five-dimensional $\mathcal{N} = 2$ vector multiplets subjected to one normalization constraint

$$\mathcal{N} \stackrel{!}{=} 1, \quad (6.3.26)$$

which reduces the degrees of freedom by one. Generally, the prepotential can be written as

$$\mathcal{N} = \frac{1}{3!} k_{\Lambda\Sigma\Theta} M^\Lambda M^\Sigma M^\Theta, \quad (6.3.27)$$

where $k_{\Lambda\Sigma\Theta}$ is constant and symmetric in all indices. The canonical form of the action then reads

$$\begin{aligned} S^{(5)} = \int_{M_5} & + \frac{1}{2} R * 1 - \frac{1}{2} G_{\Lambda\Sigma} dM^\Lambda \wedge *dM^\Sigma - h_{uv} dq^u \wedge *dq^v \\ & - \frac{1}{2} G_{\Lambda\Sigma} F^\Lambda \wedge *F^\Sigma - \frac{1}{12} k_{\Lambda\Sigma\Theta} A^\Lambda \wedge F^\Sigma \wedge F^\Theta. \end{aligned} \quad (6.3.28)$$

Note that the fields A^Λ comprise the graviphoton and the vectors from the vector multiplet. Here, we have also defined the metric

$$G_{\Lambda\Sigma} = -\frac{1}{2} \partial_{M^\Lambda} \partial_{M^\Sigma} \log \mathcal{N} |_{\mathcal{N}=1}. \quad (6.3.29)$$

The effective action (6.3.23) of the circle reduced six-dimensional $\mathcal{N} = (1, 0)$ supergravity is not yet in the canonical form (6.3.28) of five-dimensional $\mathcal{N} = 2$ supergravity and we therefore have to perform a field redefinition. It turns out that the fields

$$\begin{aligned} M^0 &= r^{-4/3} \\ M^\alpha &= r^{2/3} (j^\alpha + 2r^{-2} b_{\hat{I}j}^\alpha \zeta^{\hat{I}} \zeta^j) \\ M^{\hat{I}} &= r^{-4/3} \zeta^{\hat{I}} \end{aligned} \quad (6.3.30)$$

yield the right structure, which is analogous to the redefinition found in [54]. Let us further define

$$\mathcal{N}_p^F = \Omega_{\alpha\beta} M^0 M^\alpha M^\beta - 4\Omega_{\alpha\beta} b_{\hat{I}j}^\alpha M^\beta M^{\hat{I}} M^j, \quad (6.3.31)$$

which is the polynomial part of the prepotential for our setting. As was already pointed out in [54], this has to be supplemented by a non-polynomial part \mathcal{N}_{np}^F , which is found by imposing the special geometry constraint

$$\mathcal{N}_p^F + \mathcal{N}_{np}^F \stackrel{!}{=} \Omega_{\alpha\beta} j^\alpha j^\beta = 1 \quad (6.3.32)$$

to be

$$\mathcal{N}_{\text{np}}^F = 4\Omega_{\alpha\beta} b_{\hat{I}\hat{J}}^\alpha b_{\hat{K}\hat{L}}^\beta \frac{M^{\hat{I}} M^{\hat{J}} M^{\hat{K}} M^{\hat{L}}}{M^0}. \quad (6.3.33)$$

Hence, the prepotential is not a cubic polynomial, but still a homogeneous function of degree three. The reason for deviating from the canonical case lies in the non-trivial transformation behavior of the six-dimensional tensors under gauge transformations. This required introducing the redefined field strength (6.3.15), which, when reduced to five dimensions, yields the modified vector field strength (6.3.18). In this way, all non-gauge-invariance of the classical six-dimensional action is contained in the Green-Schwarz terms, while all non-gauge-invariance of the five-dimensional action is encoded in the Chern-Simons terms (6.3.25). Apart from the Chern-Simons terms (6.3.25), the action is therefore obtained in exactly the same way as the canonical supergravity action (6.3.28). The metric $G_{\Lambda\Sigma}$ again has to be calculated using Equation 6.3.29, this time taking into account both the polynomial and non-polynomial parts, i.e. the sum $\mathcal{N}_{\text{p}}^F + \mathcal{N}_{\text{np}}^F$. More subtleties arise in the analysis of the Chern-Simons terms. It turns out that the two contributions (6.3.24) and (6.3.25) can be brought into the form

$$S_{CS}^{(5)F} = -\frac{1}{12} \int_{M_5} (\mathcal{N}_{\text{p}}^F)_{\Lambda\Sigma\Theta} A^\Lambda \wedge F^\Sigma \wedge F^\Theta - \frac{1}{16} \int_{M_5} (\mathcal{N}_{\text{np}}^F)_{\hat{I}\Sigma\Theta} A^{\hat{I}} \wedge F^\Sigma \wedge F^\Theta, \quad (6.3.34)$$

where the indices on \mathcal{N}^F indicate that derivatives are taken with respect to the corresponding scalar fields. Note that the second part is not symmetric in the indices, since one cannot integrate by parts.

Finally, let us make a short remark on higher curvature terms. Their reduction proceeds along the same lines as in [54]. By including gravitational contributions in the Green-Schwarz terms and in the tensor transformations, one induces a five-dimensional Chern-Simons term

$$S_{A\mathcal{R}\mathcal{R}}^{(5)F} = \frac{1}{2} \int_{M_5} \Omega_{\alpha\beta} a^\alpha A^\beta \wedge \text{tr } \mathcal{R} \wedge \mathcal{R}. \quad (6.3.35)$$

We note that there are additional higher curvature corrections to the circle reduced action when including higher curvature terms in six dimensions. However, the new Chern-Simons term (6.3.35) turns out to be sufficient to extract the geometrical interpretation of a^α in F-theory when the matching with M-theory is performed.

Chapter 7

The Six-Dimensional Effective F-Theory Action

In the previous chapter we found the prepotentials for the five-dimensional reduction of M-theory on an elliptically fibered Calabi-Yau threefold and the circle reduction of a general $\mathcal{N} = (1, 0)$ -supergravity in six dimensions that we took as an ansatz for the effective F-theory action we set out to compute. The crucial missing step in the derivation of the F-theory effective action is to match these two theories. However, as we have explained previously, this is not as straightforward as one might have expected it to be. While the M-theory action as specified by the prepotential of [Equation 6.2.7](#) and [Equation 6.2.12](#) must be understood as the effective action with all massive fields integrated out, this is not true for the circle reduction: Here infinitely many additional massive states such as the W-bosons, the charged matter hypermultiplets, and also all the Kaluza-Klein towers are still present. Only after integrating out these additional fields does one expect the two effective theories of [chapter 6](#) (and hence also their prepotentials) to be the same.

The main task of this chapter is therefore to determine the loop corrections to the prepotential of [Equation 6.3.31](#) and thus to follow the last step of [figure 2.3](#) that is displayed again in [figure 7.1](#). Equivalently, we can also compute the corrections to the Chern-Simons terms. First however, we identify in [section 7.1](#) the part of the prepotential that is unaffected by such loop correction and that can hence already be matched. We then recall in [section 7.2](#) the impact that integrating out fields has on the Chern-Simons terms and use the

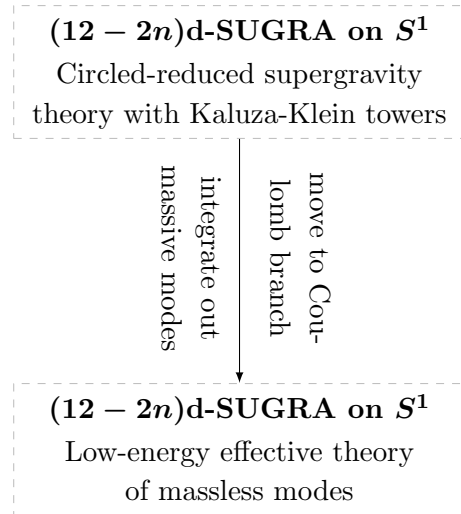


Figure 7.1: Integrating out massive modes of the circle reduced theory.

results summarized there to determine the loop-corrections in [section 7.3](#). Importantly, the loop-corrected Chern-Simons terms depend explicitly on the matter spectrum of the F-theory model. In the M-theory reduction, however, these Chern-Simons terms are given by intersection numbers of the elliptically fibered Calabi-Yau manifold and one can use the matching conditions to determine the matter spectrum of the resulting low-energy effective F-theory action. Finally, we recall in [section 7.4](#) the role of anomalies in six dimensions and show that one can at least partially prove that F-theory backgrounds automatically lead to anomaly-free supergravity theories in six dimensions.

7.1 Classical Matchings

As we have just noted, we are not yet in a position to perform a complete match of the two prepotentials obtained in [chapter 6](#). However, we can already identify a subset of terms that are not affected by loop corrections, namely those surviving in the limit $\epsilon \rightarrow 0$ of [Equation 6.2.7](#) and the gravitational Chern-Simons term proportional to c_α . Matching the expressions on both sides one obtains relations among the fields given by

$$\begin{aligned} M^0 &= 2R & M^\alpha &= \frac{1}{2}L^\alpha \\ M^I &= \frac{1}{2}\xi^I & M^m &= \frac{1}{2}\xi^m. \end{aligned} \tag{7.1.1}$$

In addition, the constant couplings specifying the six-dimensional $\mathcal{N} = (1, 0)$ action are identified as

$$\begin{aligned} b^\alpha &= S^{b,\alpha} & b_{mn}^\alpha &= -\pi(D_m \cdot D_n)^\alpha \\ \Omega_{\alpha\beta} &= \eta_{\alpha\beta}. \end{aligned} \tag{7.1.2}$$

Furthermore, matching the classical higher curvature terms [\(6.3.35\)](#) and [\(6.2.15\)](#) gives

$$a^\alpha = K^\alpha, \tag{7.1.3}$$

after identifying $c_\alpha = -12\eta_{\alpha\beta}K^\beta$ as in [Equation 6.2.17](#). The identifications [\(7.1.1\)](#), [\(7.1.2\)](#), [\(7.1.3\)](#) and the discussion of the proceeding subsections imply that the Hodge numbers of the resolved Calabi-Yau threefold Y and its base B are related to the spectrum as

$$h^{1,1}(Y) = 1 + h^{1,1}(B) + \text{rank } \mathfrak{g} + n_{U(1)} \tag{7.1.4}$$

$$h^{1,1}(B) = T + 1, \tag{7.1.5}$$

$$h^{2,1}(Y) = H^{\text{neutral}} - 1. \tag{7.1.6}$$

In particular, inverting [Equation 7.1.4](#) provides an easy way of calculating the rank $n_{U(1)}$ of the Mordell-Weil group of a given Calabi-Yau manifold. These identifications of geometrical quantities with the characteristic data of the effective action are in accordance with the matchings found in [\[49, 50, 54, 122, 125, 196, 201\]](#).

	spin-1/2 fermion	self-dual tensor $B_{\mu\nu}$	spin-3/2 fermion ψ_μ
c_{AFF}	$\frac{1}{2}$	-2	$\frac{5}{2}$
c_{ARR}	-1	-8	19

Table 7.1: The different constant multipliers for the shifts of the Chern-Simons terms.

7.2 Loop corrections for Chern-Simons terms

In this section we summarize the general formulae required to evaluate one-loop Chern-Simons coefficients in a five-dimensional effective theory obtained by circle compactification.

As was found in [94, 187, 189], one can generate new Chern-Simons terms in a five-dimensional theory by integrating out massive spin-1/2 fermions, spin-3/2 fermions and massive tensors. In particular, as shown in [186, 187], the five-dimensional tensors contributing in this loop computation have to be self-dual in the sense of [202], i.e. the tensors must be given by complex two-forms $B_{\mu\nu}$ with kinetic terms $\bar{B} \wedge dB$ and mass terms $m\bar{B} \wedge *B$. Integrating out a massive state causes the Chern-Simons coefficients to shift according to [187]

$$k_{\Lambda\Sigma\Theta} \mapsto k_{\Lambda\Sigma\Theta} + c_s c_{AFF} q_\Lambda q_\Sigma q_\Theta \text{sign}(m) \quad (7.2.1)$$

$$k_\Lambda \mapsto k_\Lambda + c_s c_{ARR} q_\Lambda \text{sign}(m), \quad (7.2.2)$$

where $\Lambda, \Sigma, \Theta \neq \alpha$ and the constant coefficients c_{AFF} and c_{ARR} are given in table 7.1. c_s is an additional multiplier taking the values ± 1 depending on the chirality of the original six-dimensional state.

The external legs of the loops one must evaluate to arrive at these expressions are the gauge bosons A^Λ , A^Σ , A^Θ for the term in Equation 7.2.1 and two gravitons and a gauge boson A^Λ for the Chern-Simons coefficient of Equation 7.2.2. It is necessary to integrate out all massive spin-1/2 fermions, spin-3/2 fermions and self-dual tensors. The charge of the mode under A^Λ is written as q_Λ , where the conventions are such that the covariant derivative reads $\partial_\mu - iqA_\mu$. We denoted the mass by m appearing in the equations of motion as

$$(\not{\partial} - m_{1/2})\psi = 0, \quad (\gamma^{\rho\mu\nu}\partial_\mu - m_{3/2}\gamma^{\rho\nu})\psi_\nu = 0, \quad (*d - im_B)B = 0 \quad (7.2.3)$$

for a spin-1/2 fermion ψ , a spin-3/2 fermion ψ_μ and a self-dual tensor B .

In our setting we reduce six-dimensional symplectic Majorana-Weyl spinors on a circle. The symplectic Majorana condition for two fermions ψ^1 and ψ^2 in six dimensions reads

$$\psi^i = \varepsilon^{ij}\psi^{jc}, \quad (7.2.4)$$

where ψ^{ic} denotes the charge conjugated spinor and ε^{ij} is the usual antisymmetric epsilon tensor in two dimensions. One can now expand the spinors in Fourier modes along the circle direction

$$\psi^i(x, y) = \sum_{n=-\infty}^{+\infty} \psi_{(n)}^i(x) e^{iny/r}. \quad (7.2.5)$$

The $\psi_{(n)}^i$ are the Kaluza-Klein modes of the fermions. To determine the fermionic degrees of freedom in the circle reduced theory, we apply the symplectic Majorana condition (7.2.4) to the expansion (7.2.5)

$$\sum_{n=-\infty}^{+\infty} \psi_{(n)}^i(x) e^{iny/r} = \varepsilon^{ij} \sum_{n=-\infty}^{+\infty} \psi_{(n)}^{jc}(x) e^{-iny/r}. \quad (7.2.6)$$

Comparing coefficients, we obtain the constraint

$$\psi_{(n)}^i = \varepsilon^{ij} \psi_{(-n)}^{jc}, \quad (7.2.7)$$

which simply states that in five dimensions, the degrees of freedom of two former six-dimensional symplectic Majorana-Weyl fermions are entirely comprised of the Kaluza-Klein tower of one of the fermions, e.g. ψ^1 . This means that one only needs to include one fermion per multiplet when integrating out massive fermionic modes.

Put together, we have to integrate out hyperini, which gain masses on the Coulomb-branch, KK-modes of hyperini, massive non-Cartan gaugini, KK-modes of gaugini and tensorini, KK-modes of gravitini, and KK-modes of former six-dimensional (anti-)self-dual tensors¹. In general, there can be two separate contributions to their masses. First of all, the charged hyperini and non-Cartan gaugini have Coulomb branch masses. Secondly, there is a contribution from the KK-level for all KK-modes. According to [187], the mass terms then take the form

$$m_{1/2} = c_{1/2} \left(m_{CB} + n m_{KK} \right), \quad m_{CB} = (q_{1/2})_{\hat{I}} \zeta^{\hat{I}}, \quad (7.2.8)$$

where n is the Kaluza-Klein level and m_{CB} is the Coulomb branch mass of the fermion under consideration. The term $(q_{1/2})_{\hat{I}} \zeta^{\hat{I}}$ denotes the contraction of the charges $(q_{1/2})_{\hat{I}}$ under the Cartan generators $\mathcal{T}_{\hat{I}}$ in the coroot basis and the $U(1)$ s appearing in Equation 6.3.19 with the $\zeta^{\hat{I}}$ carrying indices \hat{I} introduced around Equation 6.3.22. The $\zeta^{\hat{I}}$ are the VEVs of the scalars corresponding to the $U(1)$ s in Equation 6.3.19. In the reductions of the six-dimensional theories considered above, the spin-3/2 fermions and the tensors are neutral under the six-dimensional gauge group. They only can admit a Kaluza-Klein mass at level n of the form

$$m_{3/2} = -c_{3/2} \cdot n \cdot m_{KK}, \quad m_B = c_B \cdot n \cdot m_{KK}. \quad (7.2.9)$$

The factors $c_{1/2}$, $c_{3/2}$, c_B are related to the respective representations of $SO(4)$, the massive little group in five dimensions. In the subsequent calculations, it is important that $c_{1/2}$, $c_{3/2}$ are equal to +1 for modes coming from six-dimensional left-handed fermions and -1 for those coming from right-handed ones. Similarly, c_B is +1 for former six-dimensional self-dual tensors and -1 for anti-self-dual tensors in six dimensions. In table 7.2 we list the cumulative contribution of integrating out an entire supersymmetry multiplet.

¹KK-modes are charged under the Kaluza-Klein vector A^0 . The covariant derivative reads $\partial_\mu + inA_\mu^0$.

Multiplet	Hyper	Vector	Tensor	Gravity
c_{AFF}	$-\frac{1}{2}$	$\frac{1}{2}$	$\frac{1}{2}$	$\frac{3}{2}$
c_{ARR}	1	-1	5	15

Table 7.2: The different constant multipliers for the shifts of the Chern-Simons terms depending on the type of six-dimensional $\mathcal{N} = (1, 0)$ -multiplet whose five-dimensional analogue is integrated out. Note that this is the contribution of a single five-dimensional multiplet and not the entire Kaluza-Klein tower. We remark that in order to obtain the right contribution of a tensor multiplet, one must take into account that an (anti-)self-dual tensor in six dimensions reduces to a real five-dimensional tensor and therefore contributes only half the factor of [table 7.1](#).

7.3 Loop-corrected Matchings

Given the explicit expressions of [Equation 7.2.1](#) and [Equation 7.2.2](#), we can compute the loop corrections to the prepotential terms that we have so far not been able to match. First, however, we introduce a bit of notation.

- We write \mathcal{R} for a representation of the whole gauge group G , while representations of G_{nA} are referred to as \mathbf{R} .
- For a representation \mathcal{R} we denote the weights of the whole representation (including $U(1)$ -factors) by w . Weights of only G_{nA} are called \mathbf{w} . By the roots α of G (and analogously by the coroots of G) we mean explicitly only the roots of G_{nA} , possibly embedded into the root lattice of G . The set of roots of G is called $\Phi(G)$.
- Expanding the non-Abelian vector fields in the coroot basis of G_{nA} , the charge of a weight \mathbf{w} of a representation \mathbf{R} under the Cartan vector field A^I is

$$q_I^{\mathbf{w}} \equiv \langle \alpha_I^\vee, \mathbf{w} \rangle, \quad (7.3.1)$$

where α_I^\vee is the respective coroot. Similarly, we denote the charge of a root α under A^I by q_I^α . Together with the charges q_m of the representation \mathcal{R} under the Abelian vector fields A^m they can be combined into a vector

$$q_I^w = (q_I^{\mathbf{w}}, q_m) \quad (7.3.2)$$

and similarly for the roots.

- $H(\mathcal{R})$ is the number of hypermultiplets transforming in a representation \mathcal{R} . The complete number of involved hypermultiplets is then $\dim(\mathcal{R}) \cdot H(\mathcal{R})$, where $\dim(\mathcal{R})$ is the dimension of the representation \mathcal{R} . One similarly defines $H(\mathbf{R})$. Let $H(q_m, q_n)$ denote

the total number of hypermultiplets with $U(1)$ -charges (q_m, q_n) and proceed likewise for $H(q_m, q_n, q_k, q_l)$. Furthermore, we write $H(\mathbf{R}, q_m)$ for the number of hypermultiplets transforming in the representation \mathbf{R} and carrying $U(1)$ -charge q_m . An analogous statement holds for $H(\mathbf{R}, q_m, q_n)$. Note that when a hypermultiplet transforms in some representation \mathcal{R} in our notation, this actually means that one complex scalar and one symplectic Majorana-Weyl fermion in the multiplet transform in \mathcal{R} , while the other complex scalar and fermion transform in the conjugate representation \mathcal{R}^* .

- Traces with respect to the representation \mathbf{R} are denoted by $\text{tr}_{\mathbf{R}}$ and tr refers to the trace in the fundamental representation.
- We denote the (floored) ratio between the Coulomb branch mass and the Kaluza-Klein mass of a particle corresponding to a weight w by

$$l_w \equiv \left\lfloor \frac{|m_{CB}^w|}{|m_{KK}|} \right\rfloor = \lfloor r|w \cdot \zeta| \rfloor . \quad (7.3.3)$$

and similarly for W-bosons labeled by roots α . Here we have introduced the contraction

$$w \cdot \zeta \equiv \langle \alpha_I^\vee, \mathbf{w} \rangle \zeta^I + q_m \zeta^m = q_I^w \zeta^{\hat{I}} \quad (7.3.4)$$

of the weight w of a representation \mathcal{R} of the total gauge group G with the vacuum expectation value of the scalars $\zeta^{\hat{I}}$ in the vector multiplets. As before, the scalars ζ^I are the expansion coefficients in the coroot basis of G .

- Finally, we write

$$\text{sign}(w) \equiv \text{sign}(w \cdot \zeta) \quad (7.3.5)$$

and similarly for the roots α .

To compute the actual loop corrections to the Chern-Simons coefficient $k_{\Lambda\Sigma\Theta}$, one must integrate out the (possibly infinite) set of massive fields that are charged with respect to all three vector fields A^Λ , A^Σ , and A^Θ . At the end of the previous section we listed all massive fields in the circle-reduced theory that can theoretically contribute. In the following, our task is to identify the correct subset of fields for the Chern-Simons coefficient in question, restrict the sums of [Equation 7.2.1](#) (or [Equation 7.2.2](#)) correspondingly and evaluate the resulting expressions using the formulas derived in [section E.3](#). In the following, we will carry out these steps in full detail for the Chern-Simons coefficients k_{000} and k_I , before we then summarize the results for all the other coefficients in [subsection 7.3.2](#).

7.3.1 Explicit Computation of k_{000} and k_0

The coefficients k_{000} and k_I are generated entirely by the one-loop corrections to the Chern-Simons coefficients obtained by integrating out the massive states that are still present in the

circle reduction of [section 6.3](#). To see how this type of computation is performed, we carry it out in detail for these two coefficients. As all the other formulae of [subsection 7.3.2](#) are obtained analogously, the reader should be able to reproduce them on his own.

To compute the loop corrections to k_{000} , one must integrate out all matter states charged under the vector field A^0 , i.e. every field with non-zero Kaluza-Klein charge. We therefore have to integrate out all the fields mentioned in [section 7.2](#): the hyperinos, the gauginos, the antisymmetric two-tensors, the tensorinos, the gravitino and the two-tensor originating in the six-dimensional gravity multiplet. Using [table 7.2](#), we find

$$k_{000} = \sum_{n=-\infty}^{\infty} (-n)^3 \left[\frac{3}{2} + \frac{T}{2} + \frac{1}{2} \sum_{\text{vectors}} \text{sign}(m) - \frac{1}{2} \sum_{\mathcal{R}} H(\mathcal{R}) \sum_{w \in \mathcal{R}} \text{sign}(m) \right]. \quad (7.3.6)$$

Here the first contribution is the Kaluza-Klein tower of the gravity multiplet, and the second term corresponds to the six-dimensional tensors. The spinors of the third and the fourth term require additional information in order to perform the sums, as their mass terms include a contribution from the Coulomb branch:

$$m = m_{CB} + n \cdot m_{KK} = q_I \zeta^{\hat{I}} + \frac{n}{r}. \quad (7.3.7)$$

If the states are neutral (as is the case for the neutral hypermultiplets and the vector fields whose zero mode remains massless), then m obviously does not depend on the $\zeta^{\hat{I}}$ anymore and the sum can be performed. We point out that in our notation, the n^{th} state in the Kaluza-Klein tower has charge $-n$. Using [Equation E.3.8](#) to regularize the infinite sum, we find

$$\begin{aligned} k_{000} &= \frac{-1}{60} \left(\frac{3}{2} + \frac{T}{2} + \frac{V}{2} - \frac{H}{2} \right) + \frac{1}{4} \left[\sum_{\alpha \in \Phi(G)} l_{\alpha}^2 (l_{\alpha} + 1)^2 - \sum_{\mathcal{R}} H(\mathcal{R}) \sum_{w \in \mathcal{R}} l_w^2 (l_w + 1)^2 \right] \\ &= \frac{1}{120} (H - V - T - 3) + \frac{1}{4} \left[\sum_{\alpha \in \Phi(G)} l_{\alpha}^2 (l_{\alpha} + 1)^2 - \sum_{\mathcal{R}} H(\mathcal{R}) \sum_{w \in \mathcal{R}} l_w^2 (l_w + 1)^2 \right]. \end{aligned} \quad (7.3.8)$$

Computing k_I is very similar, but we nevertheless go through the steps to illustrate how to compute the corrections for states charged not under A^0 , but a different vector field. Since only states charged with respect to A^I contribute, we only need to consider hyperinos from charged hypers and gauginos from the W-bosons of G_{nA} . We thus have that

$$\begin{aligned} k_I &= \sum_{n=-\infty}^{\infty} \left[\sum_{\mathcal{R}} H(\mathcal{R}) \sum_{w \in \mathcal{R}} q_I^{\mathbf{w}} \text{sign}(m) - \sum_{\alpha \in \Phi(G)} q_I^{\alpha} \text{sign}(m) \right] \\ &= \sum_{\mathcal{R}} H(\mathcal{R}) \sum_{w \in \mathcal{R}} (2l_w + 1) q_I^{\mathbf{w}} \text{sign}(w) - \sum_{\alpha \in \Phi(G)} (2l_{\alpha} + 1) q_I^{\alpha} \text{sign}(\alpha), \end{aligned} \quad (7.3.9)$$

where we have again inserted the explicit expressions for the mass of the hyperinos and gauginos and used [Equation E.3.4](#) to evaluate the infinite sum.

7.3.2 Summary of all Loop-Corrected Chern-Simons Terms

Having illustrated explicitly how to compute the loop corrections, we spare the reader the detailed computations for the remaining Chern-Simons coefficients and instead give a comprehensive summary of all coefficients. We find that the loop-corrected Chern-Simons coefficients for the $A \wedge F \wedge F$ term are

$$k_{000} = \frac{1}{120}(H - V - T - 3) + \frac{1}{4} \left[\sum_{\alpha \in \Phi(G)} l_\alpha^2 (l_\alpha + 1)^2 - \sum_{\mathcal{R}} H(\mathcal{R}) \sum_{w \in \mathcal{R}} l_w^2 (l_w + 1)^2 \right] \quad (7.3.10a)$$

$$k_{00I} = \frac{1}{6} \left[\sum_{\alpha \in \Phi(G)} l_\alpha (l_\alpha + 1) (2l_\alpha + 1) q_I^\alpha \text{sign}(\alpha) - \sum_{\mathcal{R}} H(\mathcal{R}) \sum_{w \in \mathcal{R}} l_w (l_w + 1) (2l_w + 1) q_I^{\mathbf{w}} \text{sign}(w) \right] \quad (7.3.10b)$$

$$k_{00m} = -\frac{1}{6} \sum_{\mathcal{R}} H(\mathcal{R}) \sum_{w \in \mathcal{R}} l_w (l_w + 1) (2l_w + 1) q_m \text{sign}(w) \quad (7.3.10c)$$

$$k_{0IJ} = \frac{1}{12} \left[\sum_{\alpha \in \Phi(G)} (1 + 6l_\alpha (l_\alpha + 1)) q_I^\alpha q_J^\alpha - \sum_{\mathcal{R}} H(\mathcal{R}) \sum_{w \in \mathcal{R}} (1 + 6l_w (l_w + 1)) q_I^{\mathbf{w}} q_J^{\mathbf{w}} \right] \quad (7.3.10d)$$

$$k_{0Im} = -\frac{1}{12} \sum_{\mathcal{R}} H(\mathcal{R}) \sum_{w \in \mathcal{R}} (1 + 6l_w (l_w + 1)) q_I^{\mathbf{w}} q_m \quad (7.3.10e)$$

$$= -\frac{1}{2} \sum_{\mathcal{R}} H(\mathcal{R}) \sum_{w \in \mathcal{R}} l_w (l_w + 1) q_I^{\mathbf{w}} q_m$$

$$k_{0mn} = -\frac{1}{12} \sum_{\mathcal{R}} H(\mathcal{R}) \sum_{w \in \mathcal{R}} (1 + 6l_w (l_w + 1)) q_m q_n \quad (7.3.10f)$$

$$k_{IJK} = \frac{1}{2} \left[\sum_{\alpha \in \Phi(G)} (2l_\alpha + 1) q_I^\alpha q_J^\alpha q_K^\alpha \text{sign}(\alpha) - \sum_{\mathcal{R}} H(\mathcal{R}) \sum_{w \in \mathcal{R}} (2l_w + 1) q_I^{\mathbf{w}} q_J^{\mathbf{w}} q_K^{\mathbf{w}} \text{sign}(w) \right] \quad (7.3.10g)$$

$$k_{IJm} = -\frac{1}{2} \sum_{\mathcal{R}} H(\mathcal{R}) \sum_{w \in \mathcal{R}} (2l_w + 1) q_I^{\mathbf{w}} q_J^{\mathbf{w}} q_m \text{sign}(w) \quad (7.3.10h)$$

$$k_{Imn} = -\frac{1}{2} \sum_{\mathcal{R}} H(\mathcal{R}) \sum_{w \in \mathcal{R}} (2l_w + 1) q_I^{\mathbf{w}} q_m q_n \text{sign}(w) \quad (7.3.10i)$$

$$k_{mnk} = -\frac{1}{2} \sum_{\mathcal{R}} H(\mathcal{R}) \sum_{w \in \mathcal{R}} (2l_w + 1) q_m q_n q_k \text{sign}(w). \quad (7.3.10j)$$

To arrive at the second line of [Equation 7.3.10e](#) we used that the weights of any given representation all sum up to zero, as we show in [Appendix D](#).

For the higher curvature terms, we determine the loop corrected expressions for k_Λ to be

$$k_0 = \frac{1}{6}(H - V + 5T + 15) - \left[\sum_{\alpha \in \Phi(G)} (l_\alpha + 1)l_\alpha - \sum_{\mathcal{R}} H(\mathcal{R}) \sum_{w \in \mathcal{R}} (l_w + 1)l_w \right] \quad (7.3.11a)$$

$$k_I = \sum_{\mathcal{R}} H(\mathcal{R}) \sum_{w \in \mathcal{R}} (2l_w + 1)q_I^w \text{sign}(w) - \sum_{\alpha \in \Phi(G)} (2l_\alpha + 1)q_I^\alpha \text{sign}(\alpha) \quad (7.3.11b)$$

$$k_m = \sum_{\mathcal{R}} H(\mathcal{R}) \sum_{w \in \mathcal{R}} (2l_w + 1)q_m \text{sign}(w). \quad (7.3.11c)$$

7.3.3 Simplified Loop-Corrected Chern-Simons Terms

As is obvious from looking at these results, there is a case for which most of the above expressions simplify considerably, namely when

$$l_\alpha = l_w = 0 \quad \forall \alpha, w. \quad (7.3.12)$$

From the definition in [Equation 7.3.3](#), one sees that this happens if and only if

$$m_{CB} < m_{KK}, \quad (7.3.13)$$

that is, if there is a hierarchy between the Kaluza-Klein mass and the Coulomb branch mass for all fields. Put differently, there are additional contributions from states whose lightest Kaluza-Klein mode is not the zero mode. In this case, the contributions of the Kaluza-Klein levels n and $-n$ do not cancel (nor can they be resummed neatly without incurring a shift) and there are additional contributions. In all the examples we have encountered so far, the presence of a holomorphic zero section was a sufficient condition to guarantee that [Equation 7.3.12](#) is satisfied. However, as we learned in [Part II](#), it is completely natural to consider non-holomorphic zero sections and we will see in [chapter 9](#) that in such models the full expressions of [Equation 7.3.10](#) and [Equation 7.3.11](#) must be used in order to be able to match the circle-reduced theory to the M-theory reduction. Let us emphasize that models with non-holomorphic zero section illustrate that in the F-theory limit the exceptional blow-up divisors cannot be shrunk independently from the elliptic fiber. Instead, they must be taken to zero volume simultaneously, for their volumes satisfy inequalities among each other.

For completeness, we list again the loop-corrected Chern-Simons terms, but this time assuming that the mass hierarchy of [Equation 7.3.13](#) between Coulomb branch mass and Kaluza-Klein scale is obeyed. Leaving out the Chern-Simons coefficients that are not cor-

rected, one finds

$$k_{000} = \frac{1}{120}(H - V - T - 3) \quad (7.3.14a)$$

$$k_{0IJ} = \frac{1}{12} \left[\sum_{\alpha \in \Phi(G)} q_I^\alpha q_J^\alpha - \sum_{\mathcal{R}} H(\mathcal{R}) \sum_{w \in \mathcal{R}} q_I^{\mathbf{w}} q_J^{\mathbf{w}} \right] \quad (7.3.14b)$$

$$= \frac{C_{IJ}}{12} \lambda(\mathfrak{g}) \left(A_{\text{adj}} - \sum_{\mathbf{R}} H(\mathbf{R}) A_{\mathbf{R}} \right)$$

$$k_{0mn} = -\frac{1}{12} \sum_{\mathcal{R}} H(\mathcal{R}) \sum_{w \in \mathcal{R}} q_m q_n \quad (7.3.14c)$$

$$k_{IJK} = \frac{1}{2} \left[\sum_{\alpha \in \Phi(G)} q_I^\alpha q_J^\alpha q_K^\alpha \text{sign}(\alpha) - \sum_{\mathcal{R}} H(\mathcal{R}) \sum_{w \in \mathcal{R}} q_I^{\mathbf{w}} q_J^{\mathbf{w}} q_K^{\mathbf{w}} \text{sign}(w) \right] \quad (7.3.14d)$$

$$k_{IJm} = -\frac{1}{2} \sum_{\mathcal{R}} H(\mathcal{R}) \sum_{w \in \mathcal{R}} q_m q_I^{\mathbf{w}} q_J^{\mathbf{w}} \text{sign}(w) \quad (7.3.14e)$$

$$k_{Imn} = -\frac{1}{2} \sum_{\mathcal{R}} H(\mathcal{R}) \sum_{w \in \mathcal{R}} q_I^{\mathbf{w}} q_m q_n \text{sign}(w) \quad (7.3.14f)$$

$$k_{mnk} = -\frac{1}{2} \sum_{\mathcal{R}} H(\mathcal{R}) \sum_{w \in \mathcal{R}} q_m q_n q_k \text{sign}(w), \quad (7.3.14g)$$

where we used in [Equation 7.3.14b](#) a set of group theory identities that we prove in [Appendix D](#).

Obtained in exactly the same fashion, the Chern-Simons coefficients for the $A \wedge \mathcal{R} \wedge \mathcal{R}$ term read

$$k_0 = \frac{1}{6}(H - V + 5T + 15) \quad (7.3.15a)$$

$$k_I = \sum_{\mathcal{R}} H(\mathcal{R}) \sum_{w \in \mathcal{R}} q_I^{\mathbf{w}} \text{sign}(w) - \sum_{\alpha \in \Phi(G)} q_I^\alpha \text{sign}(\alpha) \quad (7.3.15b)$$

$$k_m = \sum_{\mathcal{R}} H(\mathcal{R}) \sum_{w \in \mathcal{R}} q_m \text{sign}(w). \quad (7.3.15c)$$

To conclude this section, we again stress that the loop-corrected Chern-Simons terms depend explicitly on the matter content of the low-energy effective F-theory action. However, on the M-theory side the Chern-Simons coefficients are specified in terms of the topology of the elliptically fibered Calabi-Yau variety, as can be seen from [Equation 6.2.7](#). If one were able to solve the equations in [\(7.2.1\)](#) and [\(7.2.2\)](#) explicitly for the multiplicities $H(\mathcal{R})$, one could find closed expressions for the F-theory spectrum in terms of the intersection data of the compactification manifold. Unfortunately, the $\text{sign}(m)$ functions (whose values depend on the choice of triangulation of the fan of the ambient space variety), prevent us from doing that. Nevertheless, it is possible to compute the spectra using the matching conditions for all concrete examples studied so far. In [section 9.1](#) we will discuss in detail how to determine these spectra explicitly.

7.4 Six-Dimensional Anomalies and their Cancelation

Anomalies in quantum field theory describe the breakdown of a classical symmetry of the Lagrangian under quantization. Even if the classical action is invariant under some symmetry, the path integral measure need not be. In those cases where it is not, the quantum effective action does not exhibit the classical symmetry anymore. For gauge symmetries, this spells a disaster, because certain current conservation laws are violated at the quantum level. For $2n$ -dimensional theories a useful method of capturing anomalies in a gauge invariant way proceeds via the anomaly polynomial, a formal polynomial of degree $n + 1$ in the curvature two-forms, where two auxiliary dimensions are introduced. These polynomials were worked out in [203].

In our conventions, the six-dimensional $\mathcal{N} = (1, 0)$ anomaly polynomial is given by [203]

$$\begin{aligned}
\hat{I}_8 = & -\frac{1}{360}(H - V + 29T - 273)[\text{tr } \hat{\mathcal{R}}^4 + \frac{5}{4}(\text{tr } \hat{\mathcal{R}}^2)^2] - \frac{1}{8}(9 - T)(\text{tr } \hat{\mathcal{R}}^2)^2 \\
& - \frac{1}{6} \text{tr } \hat{\mathcal{R}}^2 [\text{tr}_{\text{adj}} \hat{F}^2 - \sum_{\mathbf{R}} H(\mathbf{R}) \text{tr}_{\mathbf{R}} \hat{F}^2 - \sum_{m,n,q_m,q_n} H(q_m, q_n) q_m q_n \hat{F}^m \hat{F}^n] \\
& + \frac{2}{3} [\text{tr}_{\text{adj}} \hat{F}^4 - \sum_{\mathbf{R}} H(\mathbf{R}) \text{tr}_{\mathbf{R}} \hat{F}^4] - \frac{8}{3} \sum_{\mathbf{R}, m, q_m} H(\mathbf{R}, q_m) q_m (\text{tr}_{\mathbf{R}} \hat{F}^3) \hat{F}^m \\
& - 4 \sum_{\mathbf{R}, m, n, q_m, q_n} H(\mathbf{R}, q_m, q_n) q_m q_n (\text{tr}_{\mathbf{R}} \hat{F}^2) \hat{F}^m \hat{F}^n \\
& - \frac{2}{3} \sum_{m,n,k,l,q_m,q_n,q_k,q_l} H(q_m, q_n, q_k, q_l) q_m q_n q_k q_l \hat{F}^m \hat{F}^n \hat{F}^k \hat{F}^l .
\end{aligned} \tag{7.4.1}$$

As already mentioned in [chapter 6](#), under suitable conditions these anomalies may be canceled by a generalized Green-Schwarz mechanism induced by non-trivial transformations of the tensors. In fact, this is possible if the anomaly polynomial factorizes as

$$\hat{I}_8 = -\frac{1}{2} \Omega_{\alpha\beta} X_4^\alpha X_4^\beta , \tag{7.4.2}$$

as can be seen by applying the descent equations to [Equation 6.3.10](#). This factorization condition gives the anomaly constraints [7, 195].

In this section, we study the remarkable connection² between anomaly cancelation in the six-dimensional theory and the coefficients of the Chern-Simons terms in the five-dimensional theory obtained by reducing the former theory on a circle. Using the loop-corrected Chern-Simons terms of [section 7.3](#) and comparing them to the expressions of the M-theory reduction, we deduce a set of *matching equations*. If every F-theory background gave rise to an anomaly-free theory in six dimensions, then the anomaly conditions in six dimensions would have to be implied by the matching equations in one dimension lower. Here we prove that under the

²See also the recent paper [112] for a beautiful application of this link.

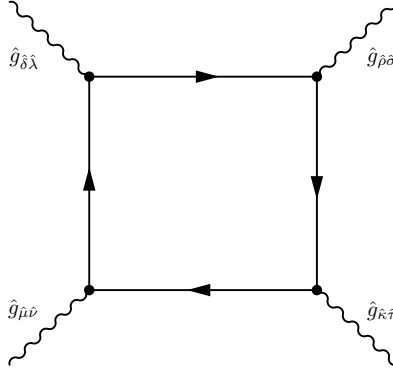


Figure 7.2: The box diagram encoding the purely gravitational anomaly.

assumption of a holomorphic zero section and the condition that all matter states satisfy

$$m_{CB} < m_{KK} \quad (7.4.3)$$

the *gravitational* and the *mixed* anomalies are automatically canceled.

While we cannot show in full generality that every F-theory background is anomaly-free, we have not found any counter-examples, and in fact, we believe that it should always be true. Indeed, we show in [chapter 9](#) that for explicit examples with non-holomorphic zero sections all anomalies are canceled as well. A more exhaustive proof of automatic anomaly cancellation in F-theory is given in the recent work of [115] and a previous study of four-dimensional anomalies was carried out in [113]. We further note that six-dimensional anomalies in F-theory were also studied in [54, 186, 188].

The structure of this section is as follows: We study gravitational anomalies in [subsection 7.4.1](#), mixed anomalies in [subsection 7.4.2](#) and pure gauge anomalies in [subsection 7.4.3](#). Each of these three subsections is structured in a similar fashion. First we present the relevant six-dimensional anomaly conditions, then we relate the respective box-diagram capturing the anomaly to a triangle diagram in five dimensions and recall the corresponding Chern-Simons coefficient. Finally, we attempt to deduce the anomaly conditions from the matching equations of that particular Chern-Simons term.

7.4.1 Gravitational Anomalies

The purely gravitational anomaly conditions are given by

$$4(12 - T) = \frac{1}{6}(H - V + 5T + 15) \quad (7.4.4a)$$

$$\frac{1}{4}a^\alpha a^\beta \Omega_{\alpha\beta} = \frac{1}{120}(H - V - T - 3) \quad (7.4.4b)$$

and they are captured by the one-loop box diagram whose vertices are all gravitons. To con-

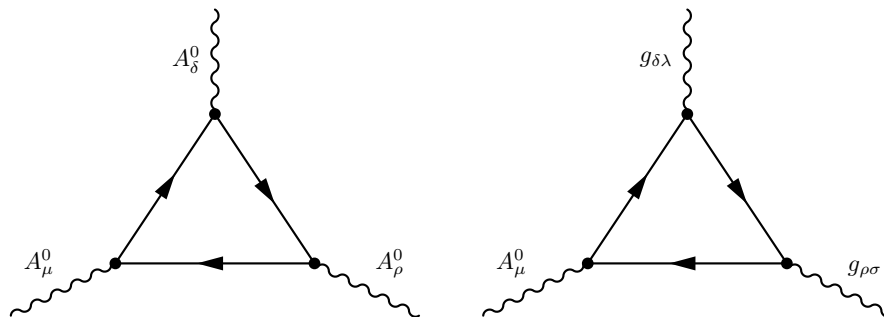


Figure 7.3: The two triangle diagrams inducing k_{000} and k_0 , respectively.

nect the gravitational anomalies to Chern-Simons terms in five dimensions, one can perform a heuristic dimensional reduction of the box diagram as described in [186]. In order to compactify the box graph on a circle, we replace one of the external six-dimensional gravitons by the S^1 -component of the metric $\langle r^2 \rangle$ and treat it as a background field. After reducing the other six-dimensional gravitons to Kaluza-Klein vectors A^0 , one obtains the first triangle diagram of figure 7.3. If one instead reduces two of the six-dimensional gravitons to five-dimensional gravitons, one ends up with the second triangle diagram displayed in the figure.

Crucially, these two diagrams are just the ones whose evaluation yields the loop corrections to the Chern-Simons coefficients k_{000} and k_0 . Keeping our intention to show automatic anomaly cancellation in F-theory in mind, we thus recall the expressions worked out in section 7.3. Under the assumption that Equation 7.4.3 is satisfied, they read

$$k_{000} = \frac{1}{120}(H - V - T - 3) \quad (7.4.5a)$$

$$k_0 = \frac{1}{6}(H - V + 5T + 15). \quad (7.4.5b)$$

The matching equations for the Chern-Simons terms are obtained by demanding that these Chern-Simons coefficients equal the topological quantities

$$k_{000} = D_0 \cdot D_0 \cdot D_0, \quad k_0 = \int_{D_0} c_2(Y). \quad (7.4.6)$$

If D_0 is obtained by shifting a *holomorphic* zero section, then we can explicitly evaluate the intersection numbers to find

$$\frac{1}{4}K^\alpha K^\beta \eta_{\alpha\beta} = \frac{1}{120}(H - V - T - 3) \quad (7.4.7a)$$

$$4(13 - h^{1,1}(B)) = \frac{1}{6}(H - V + 5T + 15), \quad (7.4.7b)$$

where we used Equation 6.1.15c and Equation 6.2.18. After using that $T = h^{1,1}(B) - 1$ as noted in Equation 7.1.5, Equation 7.4.7b reduces to the anomaly condition (7.4.4a). Similarly,

after inserting [Equation 7.1.2](#) and [Equation 7.1.3](#), we find that [Equation 7.4.7a](#) implies that the anomaly condition [\(7.4.4b\)](#) is always canceled.

To actually show that the gravitational anomaly is canceled for a given geometry, one has to express V , H and T in terms of geometric data of the underlying elliptic fibration. While we already know how to do this for T , we have not yet discussed H and V . The number of neutral hypermultiplets can be inferred from the reduction of the M-theory three-form. In [section 7.1](#) we found it to be

$$H^{\text{neutral}} = h^{2,1}(Y) + 1. \quad (7.4.8)$$

Computing the number of charged hypermultiplets is more involved, since they arise on the M-theory side by wrapping M2 branes on rational curves in the fiber. These may be determined from the topology and intersection numbers of the seven-branes specified by the discriminant of the elliptic fibration. While we are able to determine them for each explicit example of [chapter 9](#), a general formula has yet to be found. In contrast, the number of vectors, at least for the ADE groups, is given generally in terms of the dual Coxeter number $c_{G_{\text{nA}}}$ and the rank of G_{nA} supplemented by the number of Abelian gauge factors as

$$V = \dim(G) = (c_{G_{\text{nA}}} + 1) \text{rank}(G_{\text{nA}}) + n_{U(1)}. \quad (7.4.9)$$

Using the topological identity $K^\alpha K^\beta \eta_{\alpha\beta} = 10 - h^{1,1}(B)$ one finds that the gravitational anomaly [\(7.4.4b\)](#) is canceled automatically in F-theory provided that can also find a relation of the type $H - V = 302 - 29h^{1,1}(B)$. Relating H and V to topological data, one might use index theorems and an explicit expression for the Euler number of Y to prove such an identity (see e.g. [\[126\]](#)).

7.4.2 Mixed Anomalies

The mixed anomalies can be summarized as

$$\frac{1}{2} \mathcal{C}_{IJ} a^\alpha b^\beta \Omega_{\alpha\beta} = \frac{1}{12} \mathcal{C}_{IJ} \lambda(\mathfrak{g}) \left(A_{\text{adj}} - \sum_{\mathbf{R}} H(\mathbf{R}) A_{\mathbf{R}} \right) \quad (7.4.10a)$$

$$\frac{1}{2} a^\alpha b_{mn}^\beta \Omega_{\alpha\beta} = -\frac{1}{12} \sum_{q_m, q_n} H(q_m, q_n) q_m q_n. \quad (7.4.10b)$$

As before, we have arranged the anomaly conditions in a form that we will reproduce using the matching equations of the M-/F-theory duality. The two box graphs encoding the gravitational-non-Abelian anomaly and the gravitational-Abelian anomaly, respectively, are displayed in [figure 7.4](#).

Performing the same heuristic “dimensional reduction” of the two box diagrams, one obtains different kinds of triangle diagrams. In [figure 7.5](#) we show the two diagrams that are obtained by replacing one of the gravitons with the background field value $\langle r^2 \rangle$, reducing the

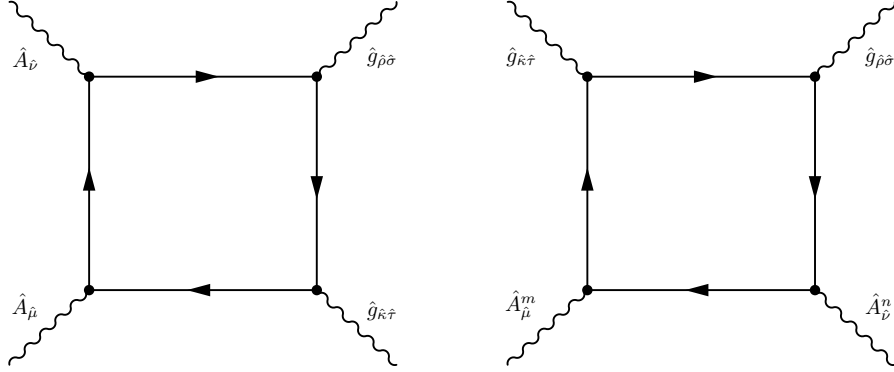


Figure 7.4: The box diagram encoding the gravitational-non-Abelian and the gravitational-Abelian anomaly.

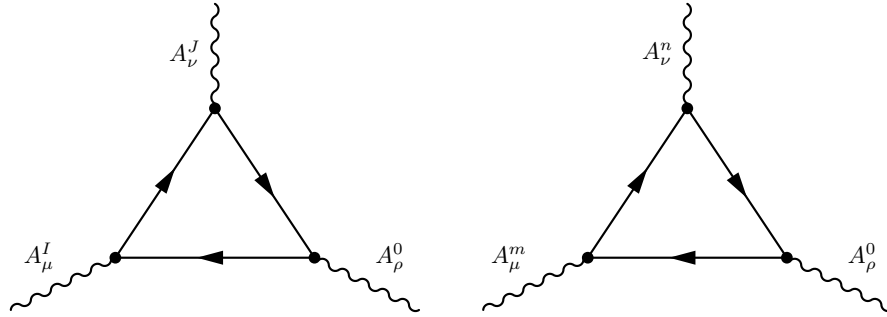


Figure 7.5: The two triangle diagrams inducing k_{0IJ} and k_{0mn} , respectively.

other graviton to the graviphoton and the six-dimensional vectors to their five-dimensional counterparts. They are the diagrams involved in computing the two Chern-Simons coefficients

$$k_{0IJ} = \frac{1}{12} \mathcal{C}_{IJ} \lambda(\mathfrak{g}) \left(A_{adj} - \sum_{\mathbf{R}} H(\mathbf{R}) A_{\mathbf{R}} \right) \quad (7.4.11a)$$

$$k_{0mn} = -\frac{1}{12} \sum_{q_m, q_n} H(q_m, q_n) q_m q_n, \quad (7.4.11b)$$

where we again assumed that $m_{CB} < m_{KK}$ for all states and recalled [Equation 7.3.14](#). As before, the matching equations read $D_0 \cdot D_I \cdot D_J = k_{0IJ}$ and in the presence of a holomorphic zero section, we can use [Equation 6.1.15a](#) and [Equation 6.1.11b](#) to find

$$\frac{1}{2} \mathcal{C}_{IJ} K^\alpha (S^b \cdot D_\alpha^b)_B = \frac{1}{12} \mathcal{C}_{IJ} \lambda(\mathfrak{g}) \left(A_{adj} - \sum_{\mathbf{R}} H(\mathbf{R}) A_{\mathbf{R}} \right) \quad (7.4.12a)$$

$$-\frac{1}{2} \pi (D_m \cdot D_n)_\alpha K^\alpha = -\frac{1}{12} \sum_{q_m, q_n} H(q_m, q_n) q_m q_n. \quad (7.4.12b)$$

Using the classical matchings $a^\alpha = K^\alpha$, $b^\alpha = S^{b,\alpha}$, $b_{mn}^\alpha = -\pi(D_m \cdot D_n)^\alpha$, and $\Omega_{\alpha\beta} = \eta_{\alpha\beta}$, these are precisely the mixed anomaly conditions.

The two box diagrams of [figure 7.4](#) give rise to two more diagrams if one instead replaces one of the vector fields $A_\mu^{\hat{I}}$ by a background field $\langle \zeta^{\hat{I}} \rangle$. These diagrams are the ones that are used to compute the Chern-Simons coefficients k_I and k_m , but their matching does not appear to be necessary to show anomaly cancellation.

7.4.3 Pure Gauge Anomalies

At last, the cancellation conditions for pure gauge anomalies read

$$0 = B_{\text{adj}} - \sum_{\mathbf{R}} H(\mathbf{R}) B_{\mathbf{R}} \quad (7.4.13a)$$

$$\frac{b^\alpha}{\lambda(\mathfrak{g})} \frac{b^\beta}{\lambda(\mathfrak{g})} \Omega_{\alpha\beta} = \frac{1}{3} \left(\sum_{\mathbf{R}} H(\mathbf{R}) C_{\mathbf{R}} - C_{\text{adj}} \right) \quad (7.4.13b)$$

$$0 = \sum_{\mathbf{R}, q_m} H(\mathbf{R}) q_m E_{\mathbf{R}} \quad (7.4.13c)$$

$$\frac{b^\alpha}{\lambda(\mathfrak{g})} b_{mn}^\beta \Omega_{\alpha\beta} = \sum_{\mathbf{R}, q_m, q_n} H(\mathbf{R}, q_m, q_n) q_m q_n A_{\mathbf{R}} \quad (7.4.13d)$$

$$\left(b_{mn}^\alpha b_{kl}^\beta + b_{mk}^\alpha b_{nl}^\beta + b_{ml}^\alpha b_{nk}^\beta \right) \Omega_{\alpha\beta} = \sum_{q_m, q_n, q_k, q_l} H(q_m, q_n, q_k, q_l) q_m q_n q_k q_l. \quad (7.4.13e)$$

The constants $A_{\mathbf{R}}$, $B_{\mathbf{R}}$, $C_{\mathbf{R}}$, and $E_{\mathbf{R}}$ are defined as proportionality factors between traces in different representations as in

$$\begin{aligned} \text{tr}_{\mathbf{R}} \hat{F}^2 &= A_{\mathbf{R}} \text{tr} \hat{F}^2 \\ \text{tr}_{\mathbf{R}} \hat{F}^3 &= E_{\mathbf{R}} \text{tr} \hat{F}^3 \\ \text{tr}_{\mathbf{R}} \hat{F}^4 &= B_{\mathbf{R}} \text{tr} \hat{F}^4 + C_{\mathbf{R}} (\text{tr} \hat{F}^2)^2. \end{aligned} \quad (7.4.14)$$

Note that the anomaly cancellation conditions (7.4.13), too, are mapped to non-trivial identities among five-dimensional Chern-Simons terms by dimensional reduction of box diagrams whose four legs are given by six-dimensional vector fields. However, unlike for the gravitational and the mixed gravitational-gauge anomaly cancellation conditions, we are not able to show in full generality that these are automatically satisfied for a given compactification geometry and we thus refrain from showing the Feynman diagrams. Nevertheless, we can determine the six-dimensional spectrum using the five-dimensional Chern-Simons terms for various examples in [chapter 9](#), and check that anomaly cancellation is satisfied on a case by case basis.

Chapter 8

F-Theory on Manifolds without Section

Historically, the F-theory literature has almost exclusively focused on studying F-theory compactifications on manifolds whose torus fibration has a section. While such a restriction may simplify computations, there exists no physical reason to disregard genus-one fibrations without section and recently there has been a flurry of papers [144, 152–155, 159, 177, 178, 204] exploring these new scenarios. In this chapter, we present the *low-energy effective* description of F-theory on a Calabi-Yau manifold without section essentially as it was first understood in [153].

The starting point of such an analysis is an observation made by Witten in [205]: In the absence of a section, the metric on the Calabi-Yau manifold cannot be made block-diagonal with respect to the base and the fiber. Nevertheless reducing M-theory on the manifold leads to the presence of at least one shift-gauged axion in the reduced theory, as we recall again in [section 8.1](#).

Applying T-duality to this set-up, the off-diagonal metric components are mapped to three-form fluxes along the T-dual cycle. These fluxes can in turn be reinterpreted as circle fluxes for an axion. In [section 8.2](#) we thus extend the discussion of [section 6.3](#) to a *fluxed* circle reduction. Of equal importance is the inclusion of an additional Abelian vector field in the ansatz for the six-dimensional F-theory effective action. The presence of such an additional $U(1)$ can be motivated by studying the geometry of the manifold without section. Restricting for simplicity to a fibration with a two-section, there should be a geometrical limit in which the two-section “disentangles” and splits into two proper sections, as we saw in [section 3.9](#). Physically, this limit should correspond to tuning the mass parameter of a vector field to zero. We implement the mass of the vector field by giving a charge to the axion that has a flux background in the circle reduction. Then the Abelian vector field obtains a Stückelberg mass after absorbing the axion. In this manner, we thus link the flux background in the circle

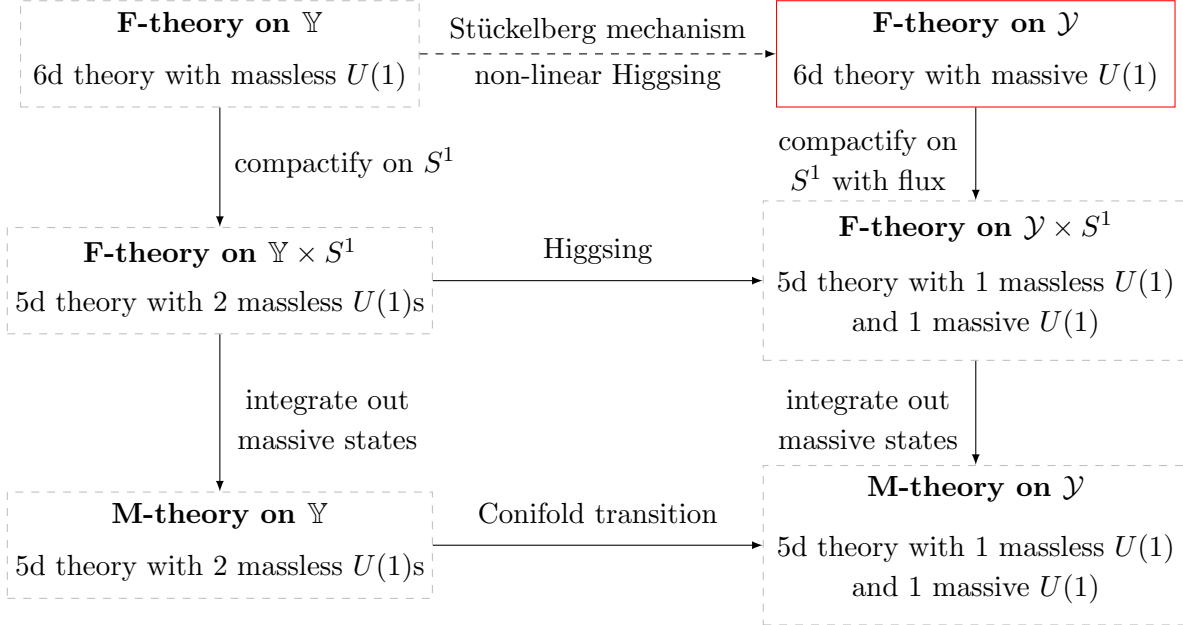


Figure 8.1: Overview of our discussion. The object of interest is in the top-right corner, corresponding to the six-dimensional theories coming from F-theory on a space without section \mathcal{Y} . In the examples we will discuss explicitly these compactifications are closely related (by making some fields massive) to F-theory on spaces with section \mathbb{Y} , giving the six-dimensional theories in the top-left corner. Compactification of these theories on S^1 gives two five-dimensional theories, in the middle row, which can also be obtained by M-theory on the corresponding Calabi-Yau threefolds (shown in the bottom row). The five-dimensional theories are related by Higgsing, or equivalently, by conifold transitions in M-theory.

reduction to the vector field mass and expect the former to disappear if the latter does, too. Finally, in [section 8.3](#) we summarize in detail the resulting effective F-theory action.

In [figure 8.1](#) we give an overview of the different theories involved in this discussion. Let us point out that whenever we discuss F-theory compactifications on genus-one fibered Calabi-Yau manifolds without section, we from now on do not denote the manifolds by Y anymore. In order to distinguish between the space without section and the space obtained by taking the limit of disentangling the multisection, we denote the former by \mathcal{Y} and the latter by \mathbb{Y} . Both are perfectly smooth spaces, but as we will see in [section 9.3](#), they can be related by a conifold transition passing through a singular point in moduli space. We also restrict all of the following discussion to models with a two-section in order to be as explicit as possible. Nevertheless, we expect the essential points of our discussion to carry over to multisections of higher degree and remind the reader that we have already studied their geometries in [section 3.9](#) and in the example in [subsection 5.3.3](#).

8.1 M-Theory on a Calabi-Yau Manifold without Section

To begin the M-theory reduction, we must consider the differences in the Calabi-Yau metric depending on whether the genus-one fibered space has, or does not have, a section. Let us denote by u^i the local (complex) coordinates on the base B of \mathcal{Y} and by (x, y) local coordinates on the torus fiber. In the case that the fibration admits a section, it is possible to describe the base B as a complex (algebraic) hypersurface within \mathcal{Y} given locally by a defining equation, $f(x, y, u) = 0$. This realization of B as a hypersurface (in fact sub-manifold) of \mathcal{Y} makes it possible to use geodesics to define coordinates normal to B within \mathcal{Y} consistently for each coordinate patch in B , and as a result the three-fold metric takes a complex, Kähler version of Gaussian normal form [206, 207]. That is, the metric can be made block-diagonal with respect to the fiber/base with $g_{I5} = g_{I6} = 0$ for $I = 1, \dots, 4$ denoting base directions and 5, 6 fiber directions.

By contrast, it was noted in [205] that in the case that \mathcal{Y} has multisections only, the base is no longer a submanifold of \mathcal{Y} and no such hypersurface description exists. As a result, there must exist *some* coordinate patch in B for which the diagonalization described above fails and g_{I5} and/or $g_{I6} \neq 0$. Let us consider such a patch and over it, take a semi-flat approximation to the Calabi-Yau metric [33, 208, 209]. Away from any singular fibers the metric takes the local form

$$ds^2(\mathcal{Y}) = g_{i\bar{j}} du^i d\bar{u}^{\bar{j}} + \frac{v^0}{\text{Im}\tau} |X - \tau Y|^2, \quad (8.1.1)$$

where at each point of B one parametrizes the complex structure of the torus fiber by $\tau(u)$ and v^0 is the overall area of the T^2 fiber, which is constant over the base. The presence of off-diagonal (fiber/base) metric components is parametrized here by vectors (\tilde{X}, \tilde{Y}) on B in

$$X = dx + \tilde{X}, \quad Y = dy + \tilde{Y}, \quad K = \tilde{X} - \tau \tilde{Y}, \quad (8.1.2)$$

where we have introduced a complex vector K on B in order to re-write the metric in complex coordinates. Defining $z = x - \tau y$, Equation 8.1.1 takes the form

$$ds^2(\mathcal{Y}) = g_{i\bar{j}} du^i d\bar{u}^{\bar{j}} + \frac{v^0}{\text{Im}\tau} \left| dz - \frac{\text{Im}z d\tau}{\text{Im}\tau} + K \right|^2 \quad (8.1.3)$$

and we locally define on \mathcal{Y} the two-form

$$\omega_0 = \frac{1}{\text{Im}\tau} \left(dz - \frac{\text{Im}z d\tau}{\text{Im}\tau} + K \right) \wedge \left(d\bar{z} - \frac{\text{Im}z d\bar{\tau}}{\text{Im}\tau} + \bar{K} \right) = 2Y \wedge X. \quad (8.1.4)$$

In terms of ω_0 the globally defined two-form on \mathcal{Y} is given by $J = J_{\text{base}} + v^0 \omega_0$. If K is a (1,0)-form then J is of type (1,1) and we find compatibility of Equation 8.1.1 with the complex structure [210]. Using that τ is holomorphic in the base coordinates it follows that $d(K/\text{Im}\tau)$ and $d(\bar{K}/\text{Im}\tau)$ are both (1,1)-forms. Together with the fact that

$$\frac{i(K - \bar{K})}{2\text{Im}\tau} = \tilde{Y}, \quad \frac{i(\bar{\tau}K - \tau\bar{K})}{2\text{Im}\tau} = \tilde{X}, \quad (8.1.5)$$

we obtain finally that $\langle d\tilde{X} \rangle$ and $\langle d\tilde{Y} \rangle$ are (1,1)-forms. In the following we will consider the case that

$$\langle d\tilde{X} \rangle = -n\tilde{\omega}, \quad \langle d\tilde{Y} \rangle = 0, \quad (8.1.6)$$

where $\tilde{\omega}$ is an appropriately normalized (1,1)-form on B . The ansatz (8.1.6) implies the presence of exactly one gauged axion c and has to be generalized accordingly for more involved situations. In this simplest setup, however, $\langle d\tilde{Y} \rangle$ has to vanish for the consistency of the effective theory.

Let us now consider M-theory on the space (8.1.1) and perform the M-theory to F-theory limit. The eleven-dimensional metric and M-theory three-form are expanded as

$$ds_{11}^2 = ds_5^2 + ds^2(\mathcal{Y}), \quad C_3^M = B_2^M \wedge X + C_2^M \wedge Y + \frac{1}{2}A^0 \wedge \omega_0 + \dots, \quad (8.1.7)$$

where the dots indicate the expansion into further harmonic (1,1)-forms of \mathcal{Y} irrelevant to the present discussion. We also expand $B_2^M = b\tilde{\omega}$ and $C_2 = c\tilde{\omega}$ and compute

$$dC_3^M = db \wedge X \wedge \tilde{\omega} - nb\tilde{\omega}^2 + (dc + nA^0) \wedge Y \wedge \tilde{\omega} + \frac{1}{2}F^0 \wedge \omega_0 + \dots, \quad (8.1.8)$$

where we have used $d\omega_0 = 2nY \wedge \tilde{\omega}$. We note that the non-trivial background $\langle d\tilde{X} \rangle$ implies that the axion c is gauged by the vector A^0 . Following the M-theory to F-theory duality, which we discuss next, one finds that with the expansion (8.1.7) the vector A^0 maps precisely to the Kaluza-Klein vector of the reduction from six to five dimensions.

Due to the presence of non-trivial \tilde{X}, \tilde{Y} in Equation 8.1.1 the standard M-theory to F-theory limit is modified (see [17] for a review). To fix an $SL(2, \mathbb{Z})$ frame, let us pick an A-cycle and a B-cycle of the genus-one fiber with local coordinates x and y , respectively. In order to perform the duality we first go from M-theory to Type IIA by splitting the metric with respect to the A-cycle according to

$$ds_{11}^2 = e^{4\phi_{\text{IIA}}/3}(dx + C_1^{\text{IIA}})^2 + e^{-2\phi_{\text{IIA}}/3}ds_{\text{IIA}}^2. \quad (8.1.9)$$

Comparing with Equation 8.1.1 one finds the Type IIA R-R one-form C_1^{IIA} and metric ds_{IIA}^2 to be

$$C_1^{\text{IIA}} = \text{Re } \tau dy + \text{Re } K \quad (8.1.10)$$

$$ds_{\text{IIA}}^2 = \sqrt{\frac{v^0}{\text{Im } \tau}} \left(\frac{v^0}{\text{Im } \tau} (\text{Im } \tau dy + \text{Im } K)^2 + g_{i\bar{j}} du^i d\bar{u}^{\bar{j}} \right) \quad (8.1.11)$$

with $e^{4\phi_{\text{IIA}}/3} = \frac{v}{\text{Im } \tau}$. Using the T-duality rules along the B-cycle one encounters non-trivial NS-NS and R-R two-forms

$$C_2^{\text{IIB}} = C_2^M + \tilde{X} \wedge dy, \quad B_2^{\text{IIB}} = B_2^M + \tilde{Y} \wedge dy. \quad (8.1.12)$$

In order to make contact with the M-theory reduction on an *elliptically* fibered manifold, we only need to set $\tilde{X} = \tilde{Y} = 0$ and replace ω_0 by twice the ω_0 defined as the Poincaré-dual of Equation 6.1.4. Apart from the presence of the flux and the axion c , the remaining M-theory reduction proceeds as in section 6.2.

8.2 Fluxed Circle Reduction

Having performed the M-theory reduction in the previous section, we can now modify the ansatz for the six-dimensional theory that we made in [section 6.3](#). The presence of non-trivial C_2^{IIB} and B_2^{IIB} in [Equation 8.1.12](#) implies that the F-theory reduction should include three-form fluxes

$$F_3 = \langle dC_2^{\text{IIB}} \rangle = -n \tilde{\omega} \wedge dy. \quad (8.2.1)$$

Notably, this flux has one leg around the circle used to compactify six to five dimensions and therefore it can be reinterpreted as a flux background for the axion c whose presence we motivated in the previous section. That is, we compactify the six-dimensional theory on a *fluxed* circle by requiring that

$$\int_{S^1} \langle dc \rangle = n. \quad (8.2.2)$$

Furthermore, as reasoned in the introduction of this chapter, there should be an additional six-dimensional *massive* vector field \hat{A}^1 under which the axion c must be charged. Let us denote this charge by m . Using the standard ansatz of [Equation E.2.1](#) for the background metric this implies that the kinetic term of the axion c reduces as

$$\mathcal{L}_c = G_{cc} |\hat{\mathcal{D}}c|^2 = G_{cc} |\mathcal{D}c|^2, \quad (8.2.3)$$

where G_{cc} is the metric for the field c . In other words, the six-dimensional invariant derivative of the axion c is replaced by

$$\mathcal{D}c = dc + mA^1 + nA^0, \quad (8.2.4)$$

where A^0 is the Kaluza-Klein vector of the circle reduction and A^1 is the vector field obtained by reducing \hat{A}^1 . We stress that this modification only appears in the five-dimensional effective theory and mixes the reduced $U(1)$ vector A^1 with the Kaluza-Klein vector A^0 . After absorbing the axion c via a Stückelberg mechanism, the mass term in the five-dimensional theory reads

$$\mathcal{L}_{\text{mass}} = G_{cc} |mA^1 + nA^0|^2, \quad (8.2.5)$$

To evaluate the effective theory for the massless degrees of freedom only, we therefore first have to choose an appropriate basis of one massless vector field \tilde{A}^0 and one massive vector field \tilde{A}^1 . Starting with the two gauge fields A^0 and A^1 , the most general transformation to a new basis of gauge fields \tilde{A}^0 and \tilde{A}^1 can be expressed as

$$\tilde{A}^i = \frac{1}{a^2 + b^2} N^i_j A^j, \quad N^i_j = \begin{pmatrix} b & -a \\ a & b \end{pmatrix}. \quad (8.2.6)$$

Note that the orthogonality of the columns of N^i_j guarantees that the kinetic terms of \tilde{A}^i remain diagonal under the transformation if they are already diagonal before. In the following

we would like to identify \tilde{A}^1 with the massive $U(1)$ with mass term (8.2.5). This implies that a and b in Equation 8.2.6 are identified to be

$$a = n, \quad b = m. \quad (8.2.7)$$

We also need to transform the charges $q_j^{\mathbf{w}}$ under the A^i of a state \mathbf{w} . The transformation (8.2.6) introduces new charges \tilde{q}_i as

$$\tilde{q}_i = q_j (N^T)^j{}_i. \quad (8.2.8)$$

To compare the fluxed circle reduction to the M-theory reduction on \mathcal{Y} , we thus rotate into the new basis \tilde{A}^i and then drop the couplings of the massive gauge field \tilde{A}^1 . As in section 7.3 we have to consistently integrate out all massive modes before we are able to perform the matching. In order to check that the reduction of the proposed six-dimensional F-theory action indeed matches the M-theory reduction, we will compare the five-dimensional Chern-Simons terms in the following section. First, however, we conclude this section by noting that the constant couplings k_{mnk} and k_m transform under the basis change (8.2.6) as

$$\begin{aligned} \tilde{k}_{mnk} &= k_{abc} (N^T)^a{}_m (N^T)^b{}_n (N^T)^c{}_k, & \tilde{k}_{mn\alpha} &= k_{ab\alpha} (N^T)^a{}_m (N^T)^b{}_n, \\ \tilde{k}_{m\alpha\beta} &= k_{a\alpha\beta} (N^T)^a{}_m, & \tilde{k}_m &= k_a (N^T)^a{}_m \end{aligned} \quad (8.2.9)$$

with $\tilde{k}_{\alpha\beta\gamma} = k_{\alpha\beta\gamma} = 0$ and $\tilde{k}_\alpha = k_\alpha$ as above and similarly if one replaces α by a non-Abelian index I .¹

Using these expressions together with Equation 8.2.6 and Equation 8.2.7, we find the non-vanishing classical Chern-Simons terms for the massless five-dimensional gauge fields (\tilde{A}^0, A^α) to be

$$\tilde{k}_{00\alpha} = -n^2 \Omega_{\alpha\beta} b_{11}^\beta, \quad \tilde{k}_{0\alpha\beta} = m \Omega_{\alpha\beta}, \quad (8.2.10)$$

$$\tilde{k}_\alpha = \Omega_{\alpha\beta} a^\beta. \quad (8.2.11)$$

Let us stress that $\tilde{k}_{00\alpha}$ is non-zero for models without section and depends on the classical coupling of the extra $U(1)$. Crucially, this is not the case for any of the models with sections considered in the literature so far. In chapter 9 we show explicitly that for genus-one fibered Calabi-Yau manifolds without section, the intersection number $D_0 \cdot D_0 \cdot D_\alpha$ that this Chern-Simons coefficient is mapped to is indeed non-zero.

The Chern-Simons terms induced by integrating out the massive states at one loop level are obtained from (8.2.9) using Equation 7.3.10. For the triple coupling one finds for the

¹Regrettably, we continue to denote here by m, n and k indices of Abelian gauge fields according to the convention introduced in section 6.1. They are not to be confused with the charges m and n of the axion c under the five-dimensional vector fields A^1 and A^0 .

massless gauge field \tilde{A}^0 that

$$\tilde{k}_{000} = k_{000}m^3 - 3k_{001}nm^2 + 3k_{011}n^2m - k_{111}n^3 \quad (8.2.12)$$

$$\begin{aligned} &= \frac{m^3}{120} (H - V - T - 3) \\ &+ \frac{1}{4} \sum_{\mathcal{R}} H(\mathcal{R}) \sum_{w \in \mathcal{R}} \left(-m^3 l_{\mathbf{w}}^2 (l_{\mathbf{w}} + 1)^2 \right. \\ &\quad \left. + 2nm^2 q_1^{\mathbf{w}} l_{\mathbf{w}} (l_{\mathbf{w}} + 1) (2l_{\mathbf{w}} + 1) \text{sign}(w) \right. \\ &\quad \left. - n^2 m (q_1^{\mathbf{w}})^2 (1 + 6l_{\mathbf{w}} (l_{\mathbf{w}} + 1)) \right. \\ &\quad \left. + 2n^3 (q_1^{\mathbf{w}})^3 (2l_{\mathbf{w}} + 1) \text{sign}(w) \right). \end{aligned} \quad (8.2.13)$$

Furthermore, one finds the one-loop contribution to \tilde{k}_0 to be

$$\begin{aligned} \tilde{k}_0 &= k_0 m - k_1 n \\ &= \frac{m}{6} (H - V + 5T + 15) \\ &+ \sum_{\mathcal{R}} H(\mathcal{R}) \sum_{w \in \mathcal{R}} \left(ml_{\mathbf{w}} (l_{\mathbf{w}} + 1) - n q_1^{\mathbf{w}} (2l_{\mathbf{w}} + 1) \text{sign}(w) \right). \end{aligned} \quad (8.2.14)$$

8.3 The Effective Action

Having performed the M-theory reduction on a genus-one fibration without section and matched it to a fluxed circle reduction of a six-dimensional supergravity theory with an additional axion and an Abelian vector field \hat{A}^1 , we are finally in a position to summarize the low-energy effective F-theory action of this class of models.

Much of the data is the same as in [section 7.1](#), including the condition that $k_{\Lambda\Theta\Sigma}$ must equal the intersection number $D_{\Lambda} \cdot D_{\Theta} \cdot D_{\Sigma}$ and the number of neutral hypermultiplets and tensors. The crucial addition is the presence of the massive vector field \hat{A}^1 that we describe (using the Stückelberg mechanism) in terms of a massless Abelian vector field and an axion c that is non-linearly charged under it.

As for the models with section, we do not have a closed formula to determine the number of charged hypermultiplets. Instead, they must be determined by making an ansatz for a spectrum such that the matching equations for the Chern-Simons terms are satisfied. There is, however, a relation between the charged matter spectra of the theory with a massive $U(1)$ and the theory in which the $U(1)$ is massless. For simplicity, let us concentrate on the case without a non-Abelian gauge group and denote by $H_{U(1)}$ the number of hypermultiplets charged under the massless $U(1)$ vector field. In the transition to the multisection model, i.e. the one in which \hat{A}^1 is massive, one of the hypermultiplets disappears and instead there is now an axion c that is charged non-linearly under \hat{A}^1 . To see how this works explicitly, let us denote the scalars in the $H_{U(1)} - 1$ linearly charged matter hypermultiplets by h^s . In

summary one then has²

$$\hat{D}c = dc + m\hat{A}^1, \quad \hat{D}h^s = dh^s + q^s \hat{A}^1 h^s, \quad (8.3.1)$$

where q^s is the charge of the state h^s .

After gauge fixing the $U(1)$ gauge symmetry, the kinetic term $|\hat{D}c|^2$ of the axion c becomes a mass term for \hat{A}^1 , which is proportional to m^2 . Hence, the $U(1)$ can become massive by “eating” the axion c . In F-theory the shift gauging (8.3.1) can arise from a geometric Stückelberg mechanism [62]. More precisely, if the seven-brane action induces a six-dimensional coupling

$$S_{\text{St}} = \int_{M^{5,1}} m c_4 \wedge \hat{F}^1, \quad (8.3.2)$$

then the four-form c_4 can be dualized into the axion c to obtain the gauging (8.3.1).

For D7-branes at weak coupling the effective coupling (8.3.2) arises indeed from a non-trivial Chern-Simons coupling $\int_{\mathcal{M}_8} C_6 \wedge F$, where C_6 is the R-R six-form of Type IIB string theory, and $\mathcal{M}_8 = M^{5,1} \times \mathcal{C}^{D7}$ is the eight-dimensional subspace wrapped by the D7-brane and its orientifold image [211]. Comparing Equation 8.3.2 with these Chern-Simons terms one finds $m c_4 = \int_{\mathcal{C}^{D7}} C_6$, which determines m as an intersection number at weak string coupling. Since the axion c is the dual of c_4 in six dimensions, it arises in the expansion of the R-R two-form C_2 as

$$C_2 = c \tilde{\omega}, \quad (8.3.3)$$

where $\tilde{\omega}$ is a $(1, 1)$ -form on the Type IIB covering space that is negative under the orientifold involution and should be identified with the form in Equation 8.1.6. Since there is no flux involved in this mechanism, it was termed geometric Stückelberg mechanism in [62].

In fact, we can determine m from a purely geometric argument. Let us consider the fiber geometry of a two-section for a moment. By definition, a two-section cuts out two different points over a generic point in the base manifold. Let us call these points P and Q . *Locally*, the two-section is therefore indistinguishable from the sum of two separate sections cutting out P and Q , respectively. In a given patch, one could try to define divisors $V(P)$ and $V(Q)$ and follow the usual procedure of applying the Shioda map [165, 166] to obtain a suitable set of massless gauge fields. Choosing $V(P)$ as the zero section, one would thus obtain the two “local divisors”

$$D_0 = V(P), \quad D_1 = \lambda (V(Q) - V(P)) \quad (8.3.4)$$

up to some irrelevant vertical parts, where λ is an arbitrary normalization constant. However, since we have a two-section, *globally* the two points P and Q undergo monodromies and the

²Since the scalars c and h^s remain scalars without redefinition when compactifying the theory to five dimensions, we have slightly abused notation and not put a hat on them to distinguish them from their five-dimensional counterparts.

only well-defined quantity is the divisor $V(P) + V(Q)$. Consequently, as the massless $U(1)$ gauge field corresponds to the two-section, its associated divisor must satisfy

$$\tilde{D}_0 \sim 2\lambda D_0 + D_1, \quad (8.3.5)$$

where the proportionality constant is just another normalization factor that we can choose arbitrarily. Comparing [Equation 8.3.5](#) to the expression for \tilde{A}^0 in [Equation 8.2.6](#), one hence finds

$$m = 2\lambda, \quad n = -1. \quad (8.3.6)$$

This geometric argument therefore implies that both the flux present in the circle reduction and the charge m of the axion under \hat{A}^1 are in fact fixed uniquely up to physically irrelevant rescalings of the massless $U(1)$ gauge field.

For completeness, let us consider the effective theory at an energy scale below the mass of the $U(1)$. In order to obtain this theory we have to integrate out the massive vector multiplet containing \hat{A}^1 , which was obtained by a massless vector multiplet “eating” a massless hypermultiplet. In other words one finds

$$V \rightarrow V - 1, \quad H \rightarrow H - 1, \quad (8.3.7)$$

consistent with the cancelation of the gravitational anomaly. Furthermore, all hypermultiplets charged under the massive $U(1)$ are neutral in the effective theory and one has

$$H_{\text{charged}} \rightarrow 0, \quad H_{\text{neutral}} \rightarrow H_{\text{neutral}} + H_{U(1)} - 1. \quad (8.3.8)$$

While this theory is a valid effective theory at the massless level, it cannot be used in order to perform the F-theory to M-theory duality.

In [figure 8.2](#) we give a comprehensive summary of all the theories involved, including those in five dimensions, and give their matter spectra. While most of the discussion in this chapter has been abstract and focused on the six-dimensional theories, we will use the examples in [section 9.3](#) to discuss the actual transitions from a massless $U(1)$ to a massive one in more detail.

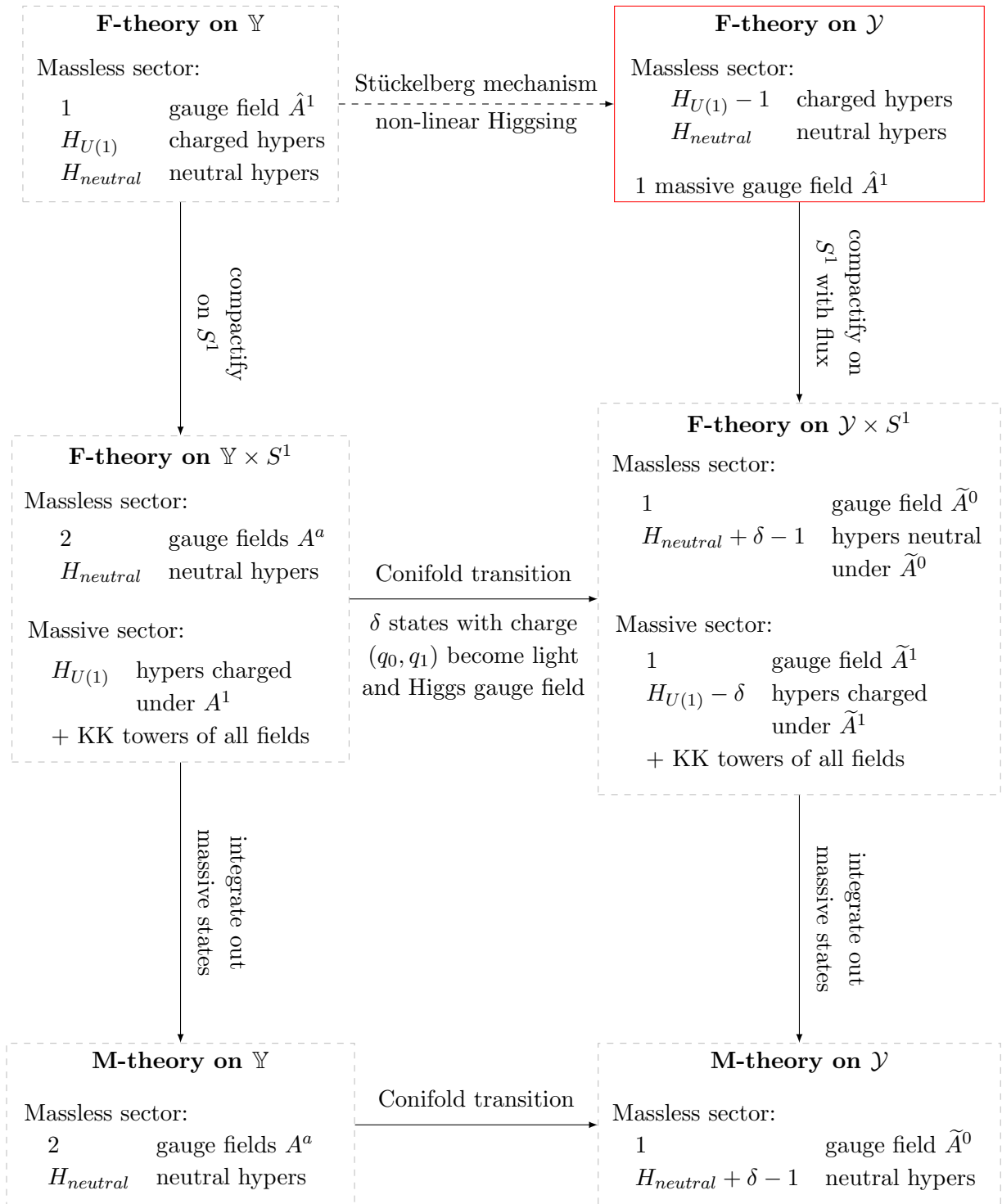


Figure 8.2: A comprehensive summary of relations between the different theories and their spectra.

Chapter 9

Explicit Six-Dimensional F-Theory Models

Having derived the low-energy effective actions of six-dimensional F-theory models both with and without section in the preceding chapters, one might be tempted to argue that the discussion is complete — after all, the couplings and matter fields that we have been able to match are now determined in terms of general topological quantities of the compactification manifold. In practice, however, much is learned by nevertheless evaluating the general expressions for examples that one can explicit construct. Not only do these examples serve as a valuable additional check of the abstract calculations, but they also provide inspiration to reconsider and possibly weaken the assumptions that we make when deriving the effective actions. In the context of F-theory reductions, this led to studying models with non-holomorphic sections or genus-one fibrations without section, both of which had originally been neglected.

Constructing non-trivial F-theory backgrounds with the features one desires is another challenge in itself. While the low-energy effective action by itself a priori seems to impose few restrictions on the spectrum apart from anomaly freedom, there may well exist much stronger constraints from the geometry. One prominent such example is the rank of the Abelian gauge group. While one would hardly expect there to be stringent bounds from a purely field-theoretic argument, obtaining F-theory models with high Abelian rank is of considerable difficulty. No general bound has so far been proven, but it seems conceivable that one may exist, as the highest Abelian rank that has so far been explicitly constructed is only four.

In this chapter, we employ the toolkit developed in [Part II](#) of this thesis to construct genus-one fibered Calabi-Yau manifolds and use them as a test ground for the effective actions obtained in [chapter 7](#) and [chapter 8](#). We begin in [section 9.1](#) with a general discussion about how to compute the matter spectrum using the loop-induced Chern-Simons terms derived in [section 7.3](#). Next, we study three different F-theory compactifications with multiple sections

in [section 9.2](#) before we finally provide a whole class of genus-one fibrations without section in [section 9.3](#) and study both the geometry and the physics of their transitions to elliptic Calabi-Yau manifolds with multiple sections.

9.1 Determining the Charged Spectrum from Chern-Simons Terms

One of the crucial observations of [chapter 7](#) was that the Chern-Simons terms in the circle-reduced theory contain much information about both the charged and the non-charged spectrum of the theory, while they are given by intersection numbers determined purely in terms of the topology of the Calabi-Yau compactification manifold on the M-theory side. This insight was what allowed us to prove that under certain assumptions the gravitational and the mixed anomaly conditions are automatically fulfilled for any F-theory model. We however also noted that it was not possible to explicitly solve the matching equations obtained in the M-/F-theory duality for the F-theory spectrum — partially because of the sign-functions appearing in equations [\(7.3.10\)](#) and [\(7.3.11\)](#) that depend on the Mori cone of the compactification manifold.

Despite the lack of a closed expression for the F-theory matter spectrum, one can still compute the matter multiplicities for given examples. To do so, one proceeds as follows:

- From the toric data of the compactification manifold Y one extracts the gauge group and the *matter split* using the methods discussed in [section 4.4](#). Restricting the intersection numbers of the sections with the irreducible fiber components to a reasonable range of integers then allows one to make an ansatz for representations present in the matter spectrum. If the manifold is not toric, then one must determine this ansatz differently, for example by analyzing all possible degenerations of the fiber geometry independently of the base, such as in [subsection 4.1.1](#).
- Keeping the multiplicities of the representations general, one next computes the induced Chern-Simons terms. The additional geometric input needed for this calculations is the sign-function for the weights of the matter representation as defined in [Equation 7.3.5](#). We explain in [section C.2](#) how it can be obtained for a toric Calabi-Yau manifold.
- Finally, one derives equations for the matter multiplicities by demanding that the Chern-Simons terms of the circle-reduced theory equal the intersection numbers of the Calabi-Yau geometry.

If one obtains multiple solutions or no solution at all, then the ansatz has been incorrectly chosen. However, this has not happened for any of the examples we have studied so far. Otherwise, we have obtained the matter spectrum of our F-theory model.

9.2 F-Theory on Calabi-Yau Manifolds with Section

In this section we present three explicit examples of six-dimensional F-theory models obtained from elliptically fibered Calabi-Yau manifolds with multiple sections.

We begin in [subsection 9.2.1](#) with what might be considered the most involved example: An F-theory model with gauge group $SU(2) \times U(1)^2$ for which one of the sections is non-toric and, depending on the triangulation of the ambient space, the zero section may further be non-holomorphic. The remaining two F-theory models both have an $SU(5) \times U(1)^2$ group. While the first one has a holomorphic zero section, the ambient space of the second one admits triangulations leading to a non-holomorphic zero section.

9.2.1 Example with Gauge Group $SU(2) \times U(1)$

The example that we discuss here has both a phase with a holomorphic zero section and a phase in which the zero section is non-holomorphic. Specifically, we take our Calabi-Yau threefold to be embedded in the toric ambient space whose rays are listed in [table 9.1](#). Since

Homogeneous coordinate z	Divisor $V(z)$	Point $n_z \in \nabla \cap N$			
u_1	H	-1	-1	-1	-1
u_2		0	0	0	1
e_0		-2	-1	1	0
e_1	D_1	-1	0	1	0
f_0	F_0	-1	0	0	0
f_1	F_1	0	1	0	0
f_2		1	0	0	0
f_3		-1	-1	0	0

Table 9.1: The toric data of the ambient space X_I of the smooth Calabi-Yau threefold Y_I with Hodge numbers are $h^{1,1}(Y_I) = 4$ and $h^{2,1}(Y_I) = 84$. We give names to only the divisors that we use as a homology basis.

the projection onto the last two lattice coordinates is a well-defined fan morphism, it induces a toric morphism $\pi' : X_I \rightarrow \mathbb{P}^2$ from the toric ambient space X_I to the base manifold $B = \mathbb{P}^2$. The kernel of the fan morphism is a two-dimensional reflexive polytope and therefore an anticanonical hypersurface will in fact cut out an elliptic curve inside the generic fiber of π' . Hence, the anticanonical hypersurface inside X_I indeed defines an elliptically fibered Calabi-Yau threefold with its projection map given by $\pi = \pi'|_{Y_I}$.

Next of all, one can confirm that there exists a total of four fine star triangulations. To see that these descend to only two inequivalent triangulations of the hypersurface, we examine their Stanley-Reisner ideals. All four of them share the common elements

$$e_1 f_3, f_1 f_3, f_0 f_2, u_1 u_2 e_1, e_0 f_1 f_2, u_1 u_2 e_0 f_2, u_1 u_2 e_0 f_1. \tag{9.2.1}$$

The additional elements depend on the choice of triangulation and the four possible combinations are

$$\begin{Bmatrix} e_1 f_0 \\ e_0 f_1 \end{Bmatrix} \times \begin{Bmatrix} u_1 u_2 e_0 \\ f_0 f_3 \end{Bmatrix}. \quad (9.2.2)$$

However, by writing down the equation $p = 0$ for a generic anticanonical hypersurface inside this toric ambient space, one can confirm that

$$p|_{f_0=f_3=0} \sim f_1 e_1 f_2^2 \quad \text{and} \quad p|_{u_1=u_2=e_0=0} \sim f_1 e_1 f_2^2. \quad (9.2.3)$$

In both cases the common elements of the Stanley-Reisner ideals make it impossible to find solutions to $p = 0$ and hence there are no points on the Calabi-Yau threefold for which $f_0 = f_3 = 0$ or $u_1 = u_2 = e_0 = 0$. We therefore find that the second factor of Equation 9.2.2 is irrelevant and there are only two inequivalent triangulations of the Calabi-Yau threefold — one corresponding to including $e_1 f_0$ in the Stanley-Reisner ideal and the other corresponding to choosing $e_0 f_1$ instead. Their respective fans are given in Equation C.4.2 and Equation C.4.3.

To proceed further, we define a basis of divisors. Since $h^{1,1}(B) = 1$, there is precisely one independent vertical divisor, namely

$$H = \pi^{-1}([1 : 1 : 0]). \quad (9.2.4)$$

There is only a single exceptional divisor D_1 and therefore the gauge group of the resulting low-energy effective theory is $SU(2)$.

In this example, the most interesting feature are the sections. From the Hodge numbers of Y_I and the fact that the gauge group is $SU(2)$, we see that the Mordell-Weil group must have rank one. First, however, we concentrate on the zero section s_0 , which is realized as the toric divisor F_0 . In order to understand the impact of the two different triangulations, we try to find an explicit form for the section by using the equation defining Y_I inside the toric ambient space X_I . Since $f_0 f_2$ is contained in both Stanley-Reisner ideals, we set $f_0 = 0$ and $f_2 = 1$ to find

$$p(f_0 = 0, f_2 = 1) = f_3 (\alpha_1 d_0^2 d_1^2 + \alpha_2 h_0 d_0 d_1 + \alpha_3 h_1 d_0 d_1 + \alpha_4 h_0^2 + \alpha_5 h_0 h_1 + \alpha_6 h_1^2) - \beta d_1 f_1, \quad (9.2.5)$$

where α_i and β are generic constants. We can now see the crucial difference between the two inequivalent triangulations:

1. Let us first assume that $e_1 f_0$ is an element of the Stanley-Reisner ideal. In this case we can safely scale e_1 to one. Furthermore, for generic β , $f_3 = 0$ would imply that $f_1 = 0$, too, which is excluded by Equation 9.2.1. Hence we can assume that $f_3 \neq 0$ and scale it to one as well. One thus obtains the explicit form for the section

$$s_0 : [u_1 : u_2 : e_0] \mapsto [u_1 : u_2 : e_0 : 1 : 0 : f_1(u_1, u_2, e_0) : 1 : 1], \quad (9.2.6)$$

where

$$f_1(u_1, u_2, e_0) = \frac{1}{\beta} (\alpha_1 d_0^2 d_1^2 + \alpha_2 h_0 d_0 d_1 + \alpha_3 h_1 d_0 d_1 + \alpha_4 h_0^2 + \alpha_5 h_0 h_1 + \alpha_6 h_1^2) . \quad (9.2.7)$$

In particular, one sees that the zero section is *holomorphic* and we call the corresponding Calabi-Yau threefold $Y_{I, \text{hol}}$.

2. Alternatively, we can take $e_0 f_1$ to be contained in the Stanley-Reisner ideal. In this case there is nothing that prevents e_1 from becoming zero and therefore we cannot simply scale it to one anymore. As a consequence, we cannot find a *holomorphic* expression for f_1 in terms of the base coordinates. With this triangulation, s_0 defines a *non-holomorphic* zero section and we denote the corresponding threefold by $Y_{I, \text{non-hol}}$.

Furthermore, note that after setting $f_0 = e_1 = 0$, we can scale f_2 and f_3 to one and find

$$p(e_1 = 0, f_0 = 0, f_2 = 1, f_3 = 1) = \alpha_4 h_0^2 + \alpha_5 h_0 h_1 + \alpha_6 h_1^2 \quad (9.2.8)$$

with f_1 left unconstrained. Since u_1 and u_2 cannot both be zero at the same time and the above equation implies that $u_1 = 0 \leftrightarrow u_2 = 0$ for generic α_i , we can set $u_2 = 1$. This leaves us with the quadratic constraint

$$0 = \alpha_4 u_1^2 + \alpha_5 u_1 + \alpha_6 \quad (9.2.9)$$

on u_1 and two unconstrained coordinates e_0 and f_1 . So far we have used three out of four scaling relations and therefore the intersection between s_0 and D_1 has complex dimension one and, in particular,

$$s_0 \cdot D_1 \neq 0 \quad (9.2.10)$$

in the Chow ring of the Calabi-Yau threefold. This is exactly what we expect from [Equation 6.1.8](#) for a *non-holomorphic* zero section.

Let us therefore quickly summarize the content of the Stanley-Reisner ideal and its relation to the properties of the zero section:

$$e_1 f_3, f_1 f_3, f_0 f_2, f_0 f_3, u_1 u_2 e_0, u_1 u_2 e_1, e_0 f_1 f_2, \times \begin{cases} e_1 f_0 : s_0 \text{ holomorphic} \\ e_0 f_1 : s_0 \text{ non-holomorphic} \end{cases} \quad (9.2.11)$$

Unfortunately, we cannot repeat the same discussion for the second section, the generator of the Mordell-Weil group, since only one section is realized torically. Nevertheless, one can still determine its homology class, namely

$$[s_1] = [F_1] - [F_0], \quad (9.2.12)$$

which can be shown to have the correct intersection numbers with the remaining divisors and contains a unique global section over the Calabi-Yau threefold, as can be checked using the

techniques of [subsection 3.7.2](#). Lastly, plugging in the defining equations, the shifted base divisor D_0 and the $U(1)$ -divisor $D_{U(1)}$ are

$$D_0 = s_0 + \frac{3}{2}H \quad (9.2.13)$$

$$D_{U(1)} = 2s_1 - 2s_0 - 16H + 2D_1, \quad (9.2.14)$$

where we have taken the freedom to re-scale the $U(1)$ -divisor by a factor of two in order to obtain integer charges.

Going through the algorithm outlined at the beginning of this section, one can determine the cones \widehat{M} for both triangulations of the reflexive polytope and finds

$$\widehat{M}(Y_{I, \text{hol.}}) = \langle e_2 + 4e_{U(1)} + e_{KK}, -6e_{U(1)} - e_{KK}, e_1 \rangle \quad (9.2.15a)$$

$$\widehat{M}(Y_{I, \text{non-hol.}}) = \langle -e_2 - 4e_{U(1)} - e_{KK}, 4e_{U(1)} + e_{KK}, -e_1 - 2e_{U(1)} \rangle. \quad (9.2.15b)$$

Here we have picked e_i , $i = 1, 2$ to be the generators of the $\mathfrak{su}(2)$ weight lattice and imposed the equivalence relation $\sum_i e_i \sim 0$. Clearly, the curve corresponding to the weight $\tilde{m} = e_2 + 4e_{U(1)} + e_{KK}$ is flopped in the transition from one triangulation to another. In the Calabi-Yau threefold with holomorphic zero section $\text{sign}(\tilde{m}) = 1$, while convexity of the Mori cone implies that $\text{sign}(\tilde{m}) = -1$ for the threefold with non-holomorphic zero section.

Next of all, we wish to determine the matter spectrum. As mentioned above, one can either try to extract this data from $\widehat{M}(Y_I)$, or examine the singularity enhancements by studying the explicit hypersurface equation. In this particular case, the charged matter spectrum can be found to consist of the representations

$$\mathbf{2}_0, \mathbf{2}_2, \mathbf{2}_4, \mathbf{1}_2, \mathbf{1}_4, \quad (9.2.16)$$

where the subscript indicates the $U(1)$ -charge of the state. Note that even though there is matter transforming under the antisymmetric representation $\Lambda^2(\mathbf{2}) = \mathbf{1}$ of $SU(2)$, it carries no charge under any of the Cartan generators and can therefore be neglected in the following analysis. Given this set of representations, we now wish to determine whether or not there exist multiplicities $H(\mathcal{R})$ such that all Chern-Simons coefficients can be matched. Before doing so, we remark on the crucial difference between the two triangulations. In the case of the *holomorphic* zero section, one can use [Equation 9.2.15a](#) to confirm that

$$\text{sign}(w, n_{KK}) = 1 \text{ for } n_{KK} \geq 1 \quad (9.2.17)$$

and

$$\text{sign}(w, n_{KK}) = -1 \text{ for } n_{KK} \leq -1 \quad (9.2.18)$$

for all weights w of the representations \mathcal{R} in [\(9.2.16\)](#). As a consequence, all contributions from Kaluza-Klein modes running in the loops either cancel among each other perfectly or add up in a simply summable way discussed in [section 7.3](#). For the *non-holomorphic* zero

section this is no longer true. As noted above, there is a single curve which undergoes a flop transition from one triangulation to another and therefore

$$e_2 + 4e_{U(1)} + e_{KK} \quad (9.2.19)$$

is no longer contained in $\widehat{M}(Y_{I, \text{non-hol.}})$. No curve with negative Kaluza-Klein charge lies in $\widehat{M}(Y_{I, \text{non-hol.}})$. As a consequence, there are two Kaluza-Klein modes whose contributions to the Chern-Simons terms have to be treated differently in the calculation. This corresponds to violating the hierarchy in [Equation 7.3.13](#) and was discussed at length in [section 7.3](#).

Taking this into account, one can calculate the induced Chern-Simons terms on the field theoretic side for generic matter multiplicities $H(\mathcal{R})$. Matching them with the intersection numbers on the M-theory side gives a system of linear equations whose unique solution is

$$\begin{aligned} H(\mathbf{2}_0) &= 12, & H(\mathbf{2}_2) &= 8, & H(\mathbf{2}_4) &= 2, \\ H(\mathbf{1}_2) &= 112, & H(\mathbf{1}_4) &= 36. \end{aligned} \quad (9.2.20)$$

To check anomaly cancellation for this spectrum one also needs to read off the anomaly coefficients. For the base $B = \mathbb{P}^2$ one has

$$\Omega_{11} = H \cdot H = 1, \quad a^1 = -3, \quad (9.2.21)$$

where the basis element generating $H^{1,1}(B)$ is H . In this example the location of the seven-branes are specified by

$$b_{SU(2)}^1 = 1, \quad b_{U(1)}^1 = 64. \quad (9.2.22)$$

Given these explicit expressions and the spectrum [\(9.2.20\)](#), it is straightforward to check that all six-dimensional anomalies are canceled.

An Intriguing Observation

Before finishing with this example, we would like to make one further observation. First of all, let us make contact with the analysis of phase transitions in [\[189\]](#). As we have just noted, there are exactly two points in the base manifold B over which matter in the $\mathbf{1}_4$ representation is located. To each of these matter points belong two isolated fibral curves, represented by the weights $e_1 + 4e_{U(1)}$ and $e_2 + 4e_{U(1)}$, plus the whole tower of Kaluza-Klein states for each weight. Flopping $\mathcal{C} \equiv e_2 + 4e_{U(1)} + e_{KK}$ in the transition from one triangulation to another, one therefore flops *two* curves in the manifold, one associated to each matter point. According to Witten's analysis, we therefore expect all intersection numbers

$$D_\Lambda \cdot D_\Sigma \cdot D_\Theta \quad (9.2.23)$$

to jump by

$$2(D_\Lambda \cdot \mathcal{C})(D_\Sigma \cdot \mathcal{C})(D_\Theta \cdot \mathcal{C}), \quad (9.2.24)$$

which is precisely what we find.

In the triangulation with a non-holomorphic zero section, there is one more intriguing fact. In the previous analysis, we observed that there are precisely two points in the base manifold over which the zero section wraps an entire fiber component instead of marking a single point, namely those for which Equation 9.2.9 was fulfilled. Notably, these are precisely the points over which matter in the $\mathbf{1}_4$ representation is located.

9.2.2 Example with Gauge Group $SU(5) \times U(1)^2$

Next, we consider a Calabi-Yau threefold that gives rise to a $U(1)^2$ Abelian gauge factor. Its defining reflexive polytope is given in table 9.2. As before, we choose the base manifold to be $B = \mathbb{P}^2$. The 216 different fine star triangulations of the toric ambient space result

Homogeneous coordinate z	Divisor $V(z)$	Point $n_z \in \nabla \cap N$			
u_1	H	3	2	1	1
u_2		3	2	0	-1
e_0		3	2	-1	0
e_1	D_1	2	1	-1	0
e_2	D_2	1	0	-1	0
e_3	D_3	0	0	-1	0
e_4	D_4	1	1	-1	0
f_0	F_0	3	2	0	0
f_1	F_1	-1	-1	0	0
f_2	F_2	-1	0	0	0
f_3		1	0	0	0
f_4		-2	-1	0	0

Table 9.2: The toric data of the ambient space X_{II} of the smooth Calabi-Yau threefold Y_{II} with Hodge numbers are $h^{1,1}(Y_{II}) = 8$ and $h^{2,1}(Y_{II}) = 75$.

in twelve inequivalent triangulations of the embedded hypersurface Y_{II} . Since all of these triangulations have a holomorphic zero section, we limit ourselves to studying the particular triangulation whose fan is given by Equation C.4.4. Compared to the previous example, the main difference lies in the sections. There are now two independent Mordell-Weil group generators and, conveniently, they are both realized as toric divisors $f_1 = 0$ and $f_2 = 0$, respectively. Furthermore, the sections $s_1 = F_1$ and $s_2 = F_2$ do not intersect the zero section $s_0 = F_0$, i.e. $s_0 \cdot s_i = 0$, $i = 1, 2$.

Since the base manifold is again a \mathbb{P}^2 , the shifted base divisor reads $D_0 = s_0 + \frac{3}{2}H$ as

before. Applying the Shioda map and rescaling by a factor of five yields the $U(1)$ -generators

$$D_5 = 5\sigma_1 - 5s_0 - 15H + 3D_1 + 6D_2 + 4D_3 + 2D_4 \quad (9.2.25a)$$

$$D_6 = 5\sigma_2 - 5s_0 - 15H + 1D_1 + 2D_2 + 3D_3 + 4D_4. \quad (9.2.25b)$$

By the same logic as before, one calculates that

$$\begin{aligned} \widehat{M}(Y_{II}) = \langle & -e_4 - 3e_{U(1)_1} - e_{U(1)_2}, e_4 - 2e_{U(1)_1} - 4e_{U(1)_2}, e_3 + 33e_{U(1)_1} + e_{U(1)_2}, \\ & e_1 + e_5 + e_{U(1)_1} - 3e_{U(1)_2}, e_2 + e_4 + e_{U(1)_1} + 2e_{U(1)_2}, \\ & e_1 - e_2, -e_1 + e_5 + e_{KK}, -5e_{U(1)_1} + 5e_{U(1)_2} + e_{KK} \rangle. \end{aligned} \quad (9.2.26)$$

The matter spectrum turns out to be

$$\mathbf{5}_{-2,-4}, \mathbf{5}_{-2,1}, \mathbf{5}_{3,1}, \mathbf{10}_{1,2}, \mathbf{1}_{5,0}, \mathbf{1}_{0,5}, \mathbf{1}_{5,5}. \quad (9.2.27)$$

As before, the non-Abelian sector can be determined directly from demanding that the sign function on the weight space is well-defined. Having determined the set of all possible representations, we search for a solution for the match of the five-dimensional Chern-Simons coefficients in order to determine the number of representations the low-energy effective theory contains. Again, a unique solution exists and it reads

$$\begin{aligned} H(\mathbf{5}_{-2,-4}) = 5, \quad H(\mathbf{5}_{-2,1}) = 7, \quad H(\mathbf{5}_{3,1}) = 7, \\ H(\mathbf{10}_{1,2}) = 3, \quad H(\mathbf{1}_{5,0}) = 28, \quad H(\mathbf{1}_{0,5}) = 35, \quad H(\mathbf{1}_{5,5}) = 35. \end{aligned} \quad (9.2.28)$$

To conclude, we check that all six-dimensional anomalies are canceled for this example. Since the base is again \mathbb{P}^2 we use [Equation 9.2.21](#) and the brane locations specified by

$$b_{SU(5)}^1 = 1, \quad b_{U(1)_{11}}^1 = 120, \quad b_{U(1)_{12}}^1 = 65, \quad b_{U(1)_{22}}^1 = 130 \quad (9.2.29)$$

to show anomaly cancelation for the spectrum [\(9.2.28\)](#).

9.2.3 Example with Gauge Group $SU(5) \times U(1)^2$

Lastly, we present an example with gauge group $SU(5) \times U(1)^2$, which, unlike the previous one, has triangulations in which the zero section is non-holomorphic. Of the 324 different triangulations admitted by the toric ambient space, only 18 descend to inequivalent triangulations of the anticanonical hypersurface. Half of these possess a holomorphic zero section. Apart from the holomorphy of the zero section, the only other difference between the different phases is the sub-wedge of the Weyl chamber that the vacuum expectation value of the adjoint scalar lies in [\[94–96\]](#). We therefore concentrate on one triangulation with a holomorphic zero section and another one in which the zero section is non-holomorphic. Their respective fans are given by [Equation C.4.5](#) and [Equation C.4.6](#).

Choosing an appropriate basis of divisors is fairly straightforward, since both Mordell-Weil group generators are realized torically and we again have $s_i = F_i$ for $i = 0, 1, 2$. After

Homogeneous coordinate z	Divisor $V(z)$	Point $n_z \in \nabla \cap N$			
u_1	H	3	1	-1	-1
u_2		0	-3	0	1
e_0		-1	-1	1	0
e_1	D_1	-1	0	1	0
e_2	D_2	0	1	1	0
e_3	D_3	0	0	1	0
e_4	D_4	0	-1	1	0
f_0	F_0	-1	-1	0	0
f_1	F_1	1	2	0	0
f_2	F_2	-1	0	0	0
f_3		0	1	0	0
f_4		1	-1	0	0

Table 9.3: The toric data of the ambient space X_{III} of the smooth Calabi-Yau threefold Y_{III} with Hodge numbers are $h^{1,1}(Y_{III}) = 8$ and $h^{2,1}(Y_{III}) = 75$.

rescaling by a factor of five in order to avoid fractional charges, we therefore find that the shifted divisors are

$$D_0 = s_0 + \frac{3}{2}H \quad (9.2.30a)$$

$$D_{U(1)_1} = 5s_1 - 5s_0 - 15H + 3D_1 + 6D_2 + 4D_3 + 2D_4 \quad (9.2.30b)$$

$$D_{U(1)_2} = 5s_2 - 5s_0 - 40H + 4D_1 + 3D_2 + 2D_3 + D_4. \quad (9.2.30c)$$

Next of all, one calculates that the cones are given by

$$\begin{aligned} \widehat{M}(Y_{III, \text{hol.}}) = \langle & e_5 - 2e_{U(1)_1} - 6e_{U(1)_2}, e_2 + 3e_{U(1)_1} + 4e_{U(1)_2}, \\ & -e_1 + 2e_{U(1)_1} + 6e_{U(1)_2} + e_{KK}, -5e_{U(1)_1} - 15e_{U(1)_2} - e_{KK}, \\ & 5e_{U(1)_1}, -5e_{U(1)_1} - 5e_{U(1)_2}, e_3 - e_4, \\ & -e_1 - e_5 - e_{U(1)_1} - 3e_{U(1)_2}, e_1 + e_4 + e_{U(1)_1} + 3e_{U(1)_2} \rangle \end{aligned} \quad (9.2.31)$$

and

$$\begin{aligned} \widehat{M}(Y_{III, \text{non-hol.}}) = \langle & e_2 + 3e_{U(1)_1} + 4e_{U(1)_2}, e_1 - 2e_{U(1)_1} - 6e_{U(1)_2} - e_{KK}, \\ & -e_1 + e_5 + e_{KK}, 5e_{U(1)_1}, -5e_{U(1)_1} - 5e_{U(1)_2}, e_3 - e_4, \\ & -e_1 - e_5 - e_{U(1)_1} - 3e_{U(1)_2}, e_1 + e_4 + e_{U(1)_1} + 3e_{U(1)_2} \rangle. \end{aligned} \quad (9.2.32)$$

Comparing these two cones, one finds a number of differences corresponding to changing the sub-wedge of the Weyl chamber [96]. However, there is one additional flop

$$-e_1 + 2e_{U(1)_1} + 6e_{U(1)_2} + e_{KK} \leftrightarrow e_1 - 2e_{U(1)_1} - 6e_{U(1)_2} - e_{KK} \quad (9.2.33)$$

which has the effect that the two weights $e_1 - 2e_{U(1)_1} - 6e_{U(1)_2} \pm e_{KK}$ do not have opposite signs anymore. Therefore the contributions of the corresponding Kaluza-Klein modes do not cancel and must be taken into account when matching their Chern-Simons terms.

The matter spectrum can be determined to be

$$\mathbf{5}_{-2,-6}, \mathbf{5}_{-2,-1}, \mathbf{5}_{3,4}, \mathbf{10}_{1,3}, \mathbf{1}_{0,5}, \mathbf{1}_{5,5}, \mathbf{1}_{5,10}. \quad (9.2.34)$$

Taking the Kaluza-Klein modes into account, one can match the Chern-Simons coefficients obtained from integrating out matter on the field theory with those given by intersection numbers of the M-theory geometry. Once again, there is a unique solution and the multiplicities one obtains are

$$\begin{aligned} H(\mathbf{1}_{0,5}) &= 35, & H(\mathbf{1}_{5,5}) &= 28, & H(\mathbf{1}_{5,10}) &= 35 \\ H(\mathbf{5}_{-2,-6}) &= 5, & H(\mathbf{5}_{-2,-1}) &= 7, & H(\mathbf{5}_{3,4}) &= 7 \\ H(\mathbf{10}_{1,3}) &= 3. \end{aligned} \quad (9.2.35)$$

One can easily check that all six-dimensional anomalies are canceled for this example. To do so, we use [Equation 9.2.21](#) and the brane locations specified by

$$b_{SU(5)}^1 = 1, \quad b_{U(1)_{11}}^1 = 120, \quad b_{U(1)_{12}}^1 = 185, \quad b_{U(1)_{22}}^1 = 380. \quad (9.2.36)$$

9.3 F-Theory on Calabi-Yau Manifolds without Section

Having studied examples with multiple section, we now turn to the no-section case whose effective physics were discussed in [chapter 8](#). We illustrate how the physics, and in particular the transition between a phase with a massive Abelian vector field to a phase with a massless $U(1)$, work in an especially transparent set of examples. These examples are given by pairs of Calabi-Yau threefolds $(\mathbb{Y}, \mathcal{Y})$ related by a conifold transition, where \mathbb{Y} has two independent sections and \mathcal{Y} has no section, but rather a multisection. Our discussion begins in [subsection 9.3.1](#) by keeping the treatment of the $(\mathbb{Y}, \mathcal{Y})$ pairs independent of the base manifolds. In [subsection 9.3.2](#) we review some well-known facts about the physics of conifold transition, before we proceed in [subsection 9.3.3](#) by constructing explicit Calabi-Yau manifolds with base manifold \mathbb{P}^2 . Finally, we evaluate the Chern-Simons terms of some of the specific examples in [subsection 9.3.4](#) and give a general argument explaining why they have to match. In [figure 9.1](#) we give a pictorial description of the essential physical process studied in the following subsections.

9.3.1 Constructing $(\mathbb{Y}, \mathcal{Y})$ Pairs with General Base Manifold

The basic observation allowing us to construct large numbers of such pairs is that there is a natural conifold transition implicit in most recent constructions of spaces with two sections.

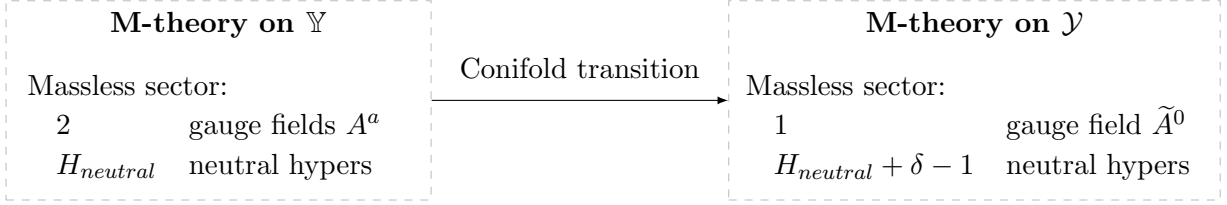


Figure 9.1: The two theories obtained by compactifying M-theory on \mathbb{Y} and \mathcal{Y} , respectively, are connected by a conifold transition in which δ hypermultiplets become light.

As described in [52], for example, the generic model with two sections is obtained by taking a Calabi-Yau hypersurface in $\widehat{\mathbb{P}}_{112}$. Let us parametrize $\widehat{\mathbb{P}}_{112}$ by the coordinates

$$\begin{array}{c|cccc} & y_1 & y_2 & w & t \\ \mathbb{C}_1^* & 1 & 1 & 2 & 0 \\ \mathbb{C}_2^* & 0 & 0 & 1 & 1 \end{array}, \quad (9.3.1)$$

where here we choose a GLSM representation of the toric variety. For a dictionary between the GLSM picture and the representation of a toric variety using fans, we refer to subsection A.1.1. We blow-up the \mathbb{Z}_2 singularity in the fiber to have a nicer ambient space, and to be able to realize torically the Cartan divisor in some of the examples below. The Stanley-Reisner ideal (*SRI* in what follows) is generated by $\langle y_1 y_2, wt \rangle$. The generic Calabi-Yau hypersurface is a degree (4, 2) hypersurface in these coordinates, which we parametrize as

$$gw^2 + wtP(y_1, y_2) + t^2Q(y_1, y_2) = 0, \quad (9.3.2)$$

with $P(y_1, y_2)$ a quadratic function in y_i

$$P(y_1, y_2) = \alpha y_1^2 + \beta y_1 y_2 + f y_2^2 \quad (9.3.3)$$

and $Q(y_1, y_2)$ a quartic

$$Q = y_1(by_1^3 + cy_1^2 y_2 + dy_1 y_2^2 + ey_2^3) + ay_2^4 \equiv y_1 Q'(y_1, y_2) + ay_2^4. \quad (9.3.4)$$

Since the elliptic fiber will be fibered over a base, g and the coefficients of P, Q will be sections of appropriate degree in the coordinates of the base (we will study some explicit examples below).¹ In order to have two sections, we set $a = 0$, so Q takes the form

$$Q = y_1(by_1^3 + cy_1^2 y_2 + dy_1 y_2^2 + ey_2^3) = y_1 Q'(y_1, y_2). \quad (9.3.5)$$

The restricted Calabi-Yau equation becomes

$$\phi \equiv gw^2 + wtP(y_1, y_2) + t^2 y_1 Q'(y_1, y_2) = 0. \quad (9.3.6)$$

¹The models constructed in [52] correspond to taking $g = 1$, which imposes some restrictions on the allowed fibrations. We do not impose such restriction.

When the coefficients are chosen in this way, there are two sections of (9.3.6) that can easily be found. Take $y_1 = 0$. Since $y_1 y_2$ belongs to the SRI of $\widehat{\mathbb{P}}_{112}$, we can set $y_2 = 1$. We end up with

$$w(gw + tf) = 0. \quad (9.3.7)$$

We thus find a first section at $w = 0$ (we can then set $t = 1$ using \mathbb{C}_2^*), and a second section at $gw = -tf$. For generic choices of g, f and at generic points of the base, this equation has a unique solution, giving a second section, but at the zeroes of g, f it will behave in interesting ways.

Singularities. The hypersurface (9.3.6) will be singular when $\phi = d\phi = 0$. It is easy to check that solutions of this set of equations exist for $w = y_1 = e = f = 0$. For two-dimensional bases of the fibration, $e = f = 0$ generically has a set of solutions given by points. Close to one such zero, for generic values of the coefficients, Equation 9.3.6 becomes

$$\lambda_1 w^2 + \lambda_2 w f + \lambda_3 w y_1 + \lambda_4 y_1^2 + \lambda_4 y_1 e = 0 \quad (9.3.8)$$

where λ_i are constants,² and one should see w, y_1, f, e as local variables for a \mathbb{C}^4 neighborhood of the singularity in the ambient space. Generically this is a non-degenerate quadratic form on the ambient space variables, defining locally a conifold singularity. For later reference, note that the number of such singularities is given by the number of points in $e = f = 0$, or slightly more formally by the intersection of the homology classes of the divisors $[e] \cdot [f]$ on the base. Associated with these singularities there will be massless hypermultiplets coming from wrapped M2 branes, which will be the essential states in our discussion.

Deformation. Since the singularities are conifolds, we expect that there are two ways of smoothing out the singularities. The first is by deformation, i.e. changing the Calabi-Yau Equation 9.3.6. Our only option is to consider deformations away from $a = 0$. This indeed modifies the analysis above in that a singularity would require $a = f = e = 0$, but for non-vanishing a and a two-dimensional base there is generically no solution to this system (by simple dimension counting), so there is no singularity anymore. An important observation for our purposes below is that under this deformation the two sections no longer exist independently, but they rather recombine into a unique global object. Setting $y_1 = 0$ in Equation 9.3.2 gives

$$gw^2 + wtf + at^2 = 0, \quad (9.3.9)$$

which no longer factorizes globally. The two sections above still exist locally and can be found by solving for w , but there is a \mathbb{Z}_2 monodromy coming from going around zeros of the discriminant $t^2(f^2 - 4ag)$, which exchanges the two roots. This is thus a case with a

²These constants can be easily read from Equation 9.3.6, but we only need that they are non-vanishing constants.

bi-section, but no section. In the examples below the non-existence of a section can also be easily verified using Oguiso's criteria [49, 212] and we collect some of the relevant details in subsection C.3.2. All in all, this gives the first element of our pair, the deformed Calabi-Yau threefold \mathcal{Y} .

Resolution. On the other hand, one can do a blow-up of the conifold in order to desingularize the geometry. A simple toric way of achieving this is by blowing up the $y_1 = w = 0$ point, which is the point of intersection of the conifolds with the fiber, as done in [52]. More concretely, we replace the fiber by the following GLSM:

$$\begin{array}{c|ccccc} & y_1 & y_2 & w & t & s \\ \hline \mathbb{C}_1^* & 1 & 1 & 2 & 0 & 0 \\ \mathbb{C}_2^* & 0 & 0 & 1 & 1 & 0 \\ \mathbb{C}_3^* & 1 & 0 & 1 & 0 & -1 \end{array} \quad (9.3.10)$$

The new Stanley-Reisner ideal is given by $\langle wy_1, wt, st, sy_2, y_1y_2 \rangle$. Notice in particular that $w = y_1 = 0$ does not belong to the ambient space anymore. The Calabi-Yau hypersurface in this space is of degree $(4, 2, 1)$ and can be parametrized, matching with the proper transform of (9.3.6), by

$$\tilde{\phi} \equiv gw^2s + wtP(sy_1, y_2) + t^2y_1Q'(sy_1, y_2) = 0. \quad (9.3.11)$$

The sections transform naturally under the blow-up. In particular, the $w = y_1 = 0$ section transforms to $s = 0$. Setting $s = 0$ in Equation 9.3.11, and setting $t = y_2 = 1$ since they cannot vanish when $s = 0$, one gets

$$wf + y_1e = 0 \quad (9.3.12)$$

so this section maps to $(y_1, y_2, w, t, s) = (-f, 1, e, 1, 0)$. Let us denote this section by σ_0 . We will take it to be our zero section, parametrizing the F-theory limit.

The other section is given by $y_1 = 0$. Plugging this into Equation 9.3.11, and setting $w = y_2 = 1$, one gets

$$gs + tf = 0. \quad (9.3.13)$$

We thus find a second section at $(y_1, y_2, w, t, s) = (0, 1, 1, -g, f)$, which we denote by σ . We think of this section as generating a $U(1)$ symmetry in the six-dimensional theory obtained by putting F-theory on \mathbb{Y} , choosing σ_0 as the zero section.

So, as expected, deformation does not recombine the sections, but rather we stay with two independent sections of the fibration. It is also not hard to see that the resulting space is generically non-singular, as one may have expected from the fact that we are considering the most general equation over the blown-up fiber. We denote the resulting space by \mathbb{Y} .

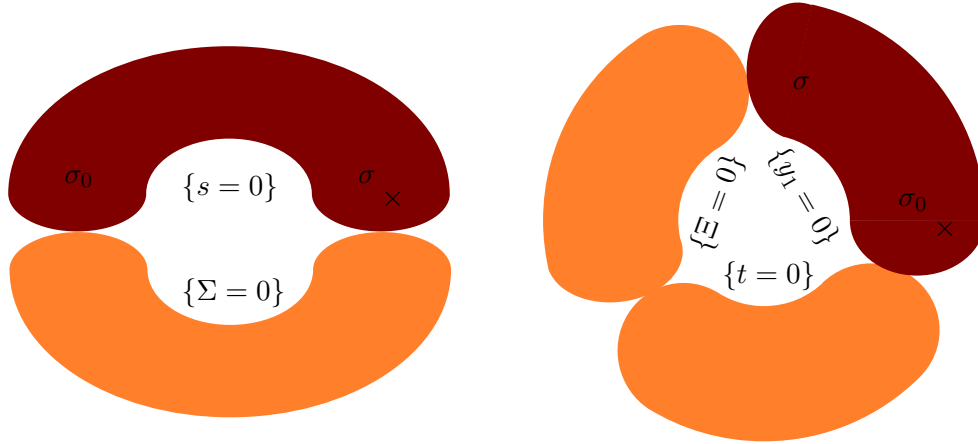


Figure 9.2: Schematic behavior of the fiber geometry over the two non-holomorphic loci. On the left, the locus $\{e = f = 0\}$ is depicted. σ_0 wraps the entire fiber component, while σ cuts out a single point. On the right, the locus $\{f = g = 0\}$ is shown, where σ becomes non-holomorphic and σ_0 cuts out a point in the same fiber component. Fiber components wrapped by a section are colored dark red.

Holomorphy of the sections. Looking at the sections we just found, we see that they are ill-defined over some points in the base. In particular, σ_0 is ill-defined over $f = e = 0$, since over these points σ_0 would be $(0, 1, 0, 1, 0)$, but $y_1 w$ is in the Stanley-Reisner ideal. Similarly, σ becomes ill-defined over $g = f = 0$, since st is in the Stanley-Reisner ideal. This is a hallmark of rationality of the sections (as opposed to holomorphy): the sections are not given by a single point in the fiber everywhere, but over some subspaces (where σ_0 and σ becomes ill-defined in our examples) they wrap components of the fiber.

It is not hard to be more explicit about the behavior of these sections at the problematic points. Setting $f = e = 0$, and $s = 0$, the Calabi-Yau equation (9.3.11) becomes identically satisfied, so the section at this point jumps in dimension. Similarly for σ , since at $y_1 = f = g = 0$ Equation 9.3.11 is identically satisfied, so σ again jumps in dimension at these points.

Let us study the behavior of the elliptic fiber at these points more carefully. For $f = e = 0$, the Calabi-Yau equation becomes

$$s(gw^2 + wty_1P'(sy_1, y_2) + t^2y_1^2Q''(sy_1, y_2)) \equiv s\Sigma = 0 \tag{9.3.14}$$

where $P' = P/(sy_1)$, and $Q'' = Q'/(sy_1)$, which are homogeneous polynomials when f and e vanish, of degrees 1 and 2 respectively in the y_i . We see that at this locus the elliptic fiber degenerates into two components, given by $s = 0$ and $\Sigma = 0$. When $s = 0$ we can gauge fix \mathbb{C}_1^* and \mathbb{C}_2^* in Equation 9.3.10 by setting $t = y_2 = 0$, so we end up with the y_1, w coordinates, with relative SRI $\langle wy_1 \rangle$, and identified by the \mathbb{C}^* action $(y_1, w) = (\lambda y_1, \lambda w)$. This is the usual description of \mathbb{P}^1 , as one could have expected from the fact that $s = 0$ was the blow-up divisor. The curve Σ defines a degree $(4, 2, 2)$ divisor on the ambient space, and a simple

adjunction computation gives then that Σ has genus 0, i.e. it is also a \mathbb{P}^1 . More explicitly

$$\begin{aligned}\chi(\Sigma) &= \int_{\Sigma} c_1(T\Sigma) = \int_A (c_1(TA) - \Sigma)\Sigma \\ &= - \int_A [0, 0, 1] \wedge [4, 2, 2] = 2 \int_A [w] \wedge [s] \\ &= 2,\end{aligned}\tag{9.3.15}$$

where A denotes the ambient toric space (9.3.10), and on the second line we have denoted the divisor classes by their toric weights.

These two spheres intersect over a point. Setting $s = 0$ (and thus $y_2 = t = 1$) in the equation for Σ we get:

$$gw^2 + wy_1P'(0, y_2) + y_1^2Q''(0, y_2) = 0.\tag{9.3.16}$$

This is a quadratic on the exceptional \mathbb{P}^1 , which has exactly two solutions. So we recover the usual picture of the T^2 fiber degenerating into two spheres, touching at two points. The rational section σ_0 wraps one of the two sphere components, namely $s = 0$.

A similar analysis holds for σ . Setting $g = f = 0$ in Equation 9.3.11, the Calabi-Yau equation factorizes as

$$y_1t(wsP'(sy_1, y_2) + tQ'(sy_1, y_2)) \equiv y_1t\Xi = 0.\tag{9.3.17}$$

We find that there are three components in the fiber. By the same kind of analysis as above we find that they are \mathbb{P}^1 s: for $y_1 = 0$ and $t = 0$ this is immediately obvious by looking at Equation 9.3.10. One also has that $\Xi = 0$ is an equation of degree $(3, 1, 0)$, and an adjunction computation gives that it has genus zero.

The intersections between the three spheres can be computed easily, with the result that any two of the three spheres intersect at exactly one point. Our section σ wraps the $y_1 = 0$ component. A summary of the fiber geometry is contained in figure 9.2.

9.3.2 Physics of the Conifold Transition

The low energy description of the conifold transition is well understood, starting with the seminal paper by Strominger [213] (see also [214, 215], and [216] for a treatment specialized to M-theory on Calabi-Yau threefolds), so we will be brief here.

The basic physics mechanism in effective field theory language is simply a Coulomb/Higgs branch transition: at the conifold point there are a number of massless hypermultiplets, coming from M2 branes wrapped on the collapsed S^2 cycles. We can smooth the conifold points in two ways: deformation or resolution. On the resolved side the two-spheres take finite size, and this corresponds to making the M2 states massive. In field theoretic terms, this mass terms are associated with the introduction of (geometry dependent) mass terms

for the hypermultiplets. More in detail, in M-theory compactified on a smooth Calabi-Yau threefold \mathbb{Y} , there are $n_H = h^{2,1}(\mathbb{Y}) + 1$ hypermultiplets, and $h^{1,1}(\mathbb{Y})$ $U(1)$ gauge fields. A particular combination of these belongs to the gravity multiplet, and the other $n_V = h^{1,1}(\mathbb{Y}) - 1$ $U(1)$ fields belong to vector multiplets. These vector multiplets have a real bosonic scalar component. The size of the resolved two-spheres (keeping the overall size of the Calabi-Yau threefold fixed) is precisely encoded in the values of these scalars, so resolving the conifold singularities corresponds to going into a Coulomb branch of the field theory.

On the other hand, there is a Higgs branch obtained by giving vacuum expectation values to the massless hypermultiplets. This corresponds to smoothing out the conifold singularities by complex deformations. Since the massless hypermultiplets are naturally charged under the $U(1)$ symmetries (M2 branes couple electrically to C_3), giving a vacuum expectation value will make some of the $U(1)$ vector multiplets massive.

There is a simple relation between the counting of massless fields in the five-dimensional theory and the Hodge numbers of the spaces related by the conifold transition. Assume that there are P two-spheres degenerating at P conifold points. Typically not all of these two-spheres are linearly independent, but there are R homology relations between them (so $P - R$ independent classes vanish). Writing down the low energy effective field theory for the hypermultiplets at the conifold point, one can easily see [214, 215] that there are precisely R flat directions of the hypermultiplets, along which one can Higgs them. A generic such Higgsing will then give mass to $P - R$ vectors. All in all, M-theory on the resolved Calabi-Yau threefold \mathbb{Y} gives rise to a massless spectrum with $(n_H(\mathbb{Y}), n_V(\mathbb{Y})) = (h^{2,1}(\mathbb{Y}) + 1, h^{1,1}(\mathbb{Y}) - 1)$. At the conifold point, P extra hypers become massless: $(n_H^0, n_V^0) = (h^{2,1}(\mathbb{Y}) + 1 + P, h^{1,1}(\mathbb{Y}) - 1)$. Higgsing then removes $P - R$ hyper-vector pairs: $(n_H(\mathcal{Y}), n_V(\mathcal{Y})) = (h^{2,1}(\mathbb{Y}) + 1 + R, h^{1,1}(\mathbb{Y}) - 1 - P + R)$. On the other hand, these numbers are just $h^{2,1}(\mathcal{Y}) + 1$ and $h^{1,1}(\mathcal{Y}) - 1$, respectively, so we learn that the conifold transition acts on the Hodge numbers as

$$(h^{2,1}(\mathcal{Y}), h^{1,1}(\mathcal{Y})) = (h^{2,1}(\mathbb{Y}) + R, h^{1,1}(\mathbb{Y}) - P + R). \quad (9.3.18)$$

This formula will provide a nice consistency check that we are identifying the geometry properly in our forthcoming examples (in our examples, $P - R = 1$, so $h^{1,1}(\mathbb{Y}) - h^{1,1}(\mathcal{Y}) = 1$). A simple quantity to check, in particular, is the difference in Euler numbers

$$\begin{aligned} \chi(\mathbb{Y}) - \chi(\mathcal{Y}) &= 2(h^{2,1}(\mathcal{Y}) - h^{2,1}(\mathbb{Y})) - 2(h^{1,1}(\mathcal{Y}) - h^{1,1}(\mathbb{Y})) \\ &= 2P \end{aligned} \quad (9.3.19)$$

giving the number of conifold points involved in the transition.

9.3.3 Explicit Examples with Base \mathbb{P}^2

Having described the general setup for our main class of examples, we are now ready to construct a number of examples of conifold transitions removing the section. For simplicity, we will stay with a \mathbb{P}^2 base.

Let us start on the deformed side \mathcal{Y} . The set of Calabi-Yau threefolds T^2 -fibered over \mathbb{P}^2 can be described as hypersurfaces on the toric ambient space described by the GLSM

$$\begin{array}{c|cccccc} & x_1 & x_2 & x_3 & y_1 & y_2 & w & t \\ \hline \mathbb{C}_1^* & 1 & 1 & 1 & 0 & a & b & 0 \\ \mathbb{C}_2^* & 0 & 0 & 0 & 1 & 1 & 2 & 0 \\ \mathbb{C}_3^* & 0 & 0 & 0 & 0 & 0 & 1 & 1 \end{array} \quad (9.3.20)$$

The last four coordinates parametrize the fiber $\widehat{\mathbb{P}}_{112}$, while the first three coordinates parametrize the base \mathbb{P}^2 . The fibration map $\pi: X \rightarrow \mathbb{P}^2$ simply “forgets” about the last four coordinates of any point in X . In principle the last four entries in the first row (the charges of y_1, y_2, w, t under \mathbb{C}_1^*) can be arbitrary integers, but it is easy to convince oneself that by redefining (if necessary) the y_i and the \mathbb{C}_i^* , any such fibration can be brought to the canonical form (9.3.20), with $a \geq 0$.

The generic equation in these variables is given by Equation 9.3.2. In order to have a Calabi-Yau threefold, Equation 9.3.2 must be a homogeneous polynomial of degree $(3 + a + b, 4, 2)$. Tracing the definitions above, this implies that the interesting coefficients of Equation 9.3.2 are homogeneous functions on the x_i of degrees

$$\deg(a) = 3 - 3a + b \quad (9.3.21)$$

$$\deg(e) = 3 - 2a + b \quad (9.3.22)$$

$$\deg(f) = 3 - a \quad (9.3.23)$$

$$\deg(g) = 3 + a - b. \quad (9.3.24)$$

There are a finite number of allowed values for (a, b) , obtained by imposing that all the coefficients of (9.3.2) be holomorphic functions on the x_i (in particular, there should be no poles). These conditions define a polygon in the (a, b) plane, as pointed out in chapter 5, and the different cases, given in table 9.4, correspond to integral points of this auxiliary polygon.

There are some interesting features in this table. Notice that the first three entries have $\deg(g) = 0$. Taking g a generic non-zero constant, we find that Q becomes a holomorphic section, since the $f = g = 0$ locus does not exist anymore. Similarly, for the $(0, -3)$ example the σ_0 section is holomorphic, and for the $(3, 6)$ example both sections are holomorphic. In the rest of the cases both sections are rational.

The resolved side \mathbb{Y} is given by hypersurfaces on toric ambient spaces described by GLSMs of the following form:

$$\begin{array}{c|ccccccc} & x_1 & x_2 & x_3 & y_1 & y_2 & w & t & s \\ \hline \mathbb{C}_1^* & 1 & 1 & 1 & 0 & a & b & 0 & 0 \\ \mathbb{C}_2^* & 0 & 0 & 0 & 1 & 1 & 2 & 0 & 0 \\ \mathbb{C}_3^* & 0 & 0 & 0 & 0 & 0 & 1 & 1 & 0 \\ \mathbb{C}_4^* & 0 & 0 & 0 & 1 & 0 & 1 & 0 & -1 \end{array} \quad (9.3.25)$$

(a, b)	$h^{1,1}(\mathcal{Y})$	$h^{2,1}(\mathcal{Y})$	$\deg(a)$	$\deg(e)$	$\deg(f)$	$\deg(g)$
(0, 3)	2	128	6	6	3	0
(1, 4)	2	132	4	5	2	0
(2, 5)	2	144	2	4	1	0
(0, -2)	3	59	1	1	3	5
(0, -1)	3	65	2	2	3	4
(0, 0)	3	75	3	3	3	3
(0, 1)	3	89	4	4	3	2
(0, 2)	3	107	5	5	3	1
(1, 0)	3	69	0	1	2	4
(1, 1)	3	79	1	2	2	3
(1, 2)	3	93	2	3	2	2
(1, 3)	3	111	3	4	2	1
(2, 3)	3	105	0	2	1	2
(2, 4)	3	123	1	3	1	1
(3, 6)	3	165	0	3	0	0
(0, -3)	6	60	0	0	3	6

Table 9.4: Hodge numbers and polynomials degrees for various fibrations over \mathbb{P}^2

As before, we could in principle have given a charge to s under \mathbb{C}_1^* , but there is always a way of redefining the fields and \mathbb{C}^* symmetries in order to set this charge to 0. Imposing that the coefficients of Equation 9.3.11 are sections of line bundles of non-negative degree on the \mathbb{P}^2 base, one finds 31 different possible values for (a, b) . All those in table 9.4 are included, and in addition there are a few models which are only possible on the resolved side, since the blow-up fixes the coefficient of the y_2^4 term in Q to vanish, so there is one less constraint. We will only be interested in the ones coming from conifold transitions on \mathcal{Y} .

Identifying the models in the canonical way, we can immediately compute the Hodge numbers of the resolved spaces using PALP, for instance, and the results are given in table 9.5. Computing from here the expected number of conifold points, with the results shown in the last column of table 9.5, one sees easily by comparing with the values in table 9.4 that in all cases the expected number of conifold points precisely agrees with the expectation from the discussion given above:

$$\frac{1}{2}(\chi(\mathbb{Y}) - \chi(\mathcal{Y})) = \deg(e) \cdot \deg(f). \tag{9.3.26}$$

In table 9.5 we summarize information about the models obtained by resolving the manifolds from table 9.4, including the chiral spectrum in six dimensions, obtained via the techniques described in [95, 114]. Here $H(\mathcal{R})$ denotes the net amount of chiral matter (six-

(a, b)	$h^{1,1}(\mathbb{Y})$	$h^{2,1}(\mathbb{Y})$	P	$H(\mathbf{1}_2)$	$H(\mathbf{1}_4)$	$H(\mathbf{2}_1)$	$H(\mathbf{2}_3)$	$H(\mathbf{3}_0)$
(0, 3)	3	111	18	144	18	0	0	0
(1, 4)	3	123	10	140	10	0	0	0
(2, 5)	3	141	4	128	4	0	0	0
(0, -2)	4	57	3	64	3	55	15	6
(0, -1)	4	60	6	76	6	52	12	3
(0, 0)	4	67	9	90	9	45	9	1
(0, 1)	4	78	12	106	12	34	6	0
(0, 2)	4	93	15	124	15	19	3	0
(1, 0)	4	68	2	72	2	56	8	3
(1, 1)	4	76	4	86	4	48	6	1
(1, 2)	4	88	6	102	6	36	4	0
(1, 3)	4	104	8	120	8	20	2	0
(2, 3)	4	104	2	90	2	38	2	0
(2, 4)	4	121	3	108	3	21	1	0
(3, 6)	3	165	0	108	0	0	0	0
(0, -3)	6	60	0	—	—	—	—	—

Table 9.5: Hodge numbers and chiral spectra for the resolved versions of the manifolds in [table 9.4](#). All $U(1)$ charges have been rescaled by 2. P denotes the expected number of conifold points, obtained from [Equation 9.3.19](#). The last entry in the table corresponds to a space with many non-torically realized divisors, so we will not analyze it here.

dimensional hypers) in the representation \mathcal{R} . We denote the representation by \mathbf{N}_m , where \mathbf{N} is the representation under the gauge group $SU(2)$ (to be explained below), and m the $U(1)$ -charge. We define the divisor class generating the $U(1)$ -charge as [\[114\]](#)

$$D_{U(1)} = 2\sigma - 2\sigma_0 - 4\pi^*c_1(TB) + E. \quad (9.3.27)$$

We have denoted by $\pi: \mathbb{Y} \rightarrow \mathbb{P}^2$ the fibration map, π^* its pullback to cohomology on X , σ, σ_0 denote the extra section and the zero section described above, and E is the divisor associated with the Cartan of $SU(2)$. The single manifold with $h^{1,1}(\mathbb{Y}) = 6$ has three divisors that do not descend from the ambient space and it is unclear what the full gauge group and matter spectrum are, so we will not analyze it here. Lastly, let us remark that we find that

$$H(\mathbf{1}_4) = \frac{1}{2}(\chi(\mathbb{Y}) - \chi(\mathcal{Y})) = [e] \cdot [f] \quad (9.3.28)$$

which strongly suggests that it is precisely the $\mathbf{1}_4$ multiplets that are involved in the conifold transition.

The existence of an $SU(2)$ symmetry in the cases with $h^{1,1}(\mathbb{Y}) > 3$ can be argued for as follows. Consider the $g = 0$ locus on the base (this is only possible if $\deg(g) > 0$). Over this divisor, the Calabi-Yau equation becomes

$$\tilde{\phi}|_{g=0} = t(wP + ty_1Q') \equiv t\Lambda = 0. \quad (9.3.29)$$

We see that over this divisor on the base the T^2 factorizes. The $t = 0$ piece defines a \mathbb{P}^1 , and it is not hard to prove that $\Lambda = 0$ is also a \mathbb{P}^1 , intersecting $t = 0$ at two points. This is the familiar affine $SU(2)$ structure over a zero of the discriminant, so we expect a $SU(2)$ enhancement over $g = 0$. A short computation shows, in addition, that the section σ_0 intersects Λ at a point, and σ intersects $t = 0$ at a point. Since we chose σ_0 as our zero section, we interpret the component not intersecting it, namely $t = 0$, as the one associated with the W bosons enhancing the gauge symmetry to $SU(2)$. All in all, we learn that E in [Equation 9.3.27](#) is just $\{t = 0\} \cap \{\tilde{\phi} = 0\}$, or $[t]$ in brief (abusing notation slightly).

In fact, we are now in a position to compute the charges of some of the multiplets in [table 9.5](#) from first principles. We start by discussing the $\mathbf{1}_4$ multiplets, which are the main actors in the conifold transition. The other representations can be obtained analogously, with some extra effort. Since these representations are less directly relevant for the conifold transition, we demote their discussion to [subsection C.3.1](#).

We claim that the $\mathbf{1}_4$ multiplets comes from $f = e = 0$. We have explained above that when $f = e = 0$ the fiber becomes split into two components, given by $\{s = 0\} \cup \{\Sigma = 0\}$. Since st belongs in the Stanley-Reisner ideal, the hyper wrapping $s = 0$ has no charge under the $SU(2)$ symmetry. Its charge under the $U(1)$ is given by

$$Q_{U(1)} = \mathcal{C}_s \cdot (2\sigma - 2\sigma_0 - 12[x_1] + [t]). \quad (9.3.30)$$

We have denoted by \mathcal{C}_s the component of the fiber over $f = e = 0$ given by $s = 0$, and we used the fact that $[x_1]$ is the pullback of the hyperplane on \mathbb{P}^2 . Since $x_1 = 0$ will generically not intersect $f = e = 0$, we have $\mathcal{C}_s \cdot [x_1] = 0$. Similarly, since st is in the Stanley-Reisner ideal, $\mathcal{C}_s \cdot [t] = 0$. We have already determined above that σ intersects \mathcal{C}_s at a point, so $\mathcal{C}_s \cdot \sigma = 1$. On the other hand, σ_0 becomes rational at $f = e = 0$, so the calculation is less straightforward. Consider the total class of the (factorized) T^2 fiber, given by $\mathcal{C}_s + \mathcal{C}_\Sigma$, with the last component being the $\Sigma = 0$ locus. Since the total fiber can move as a holomorphic divisor into a smooth T^2 , which intersects σ_0 at a point, it must be the case that $(\mathcal{C}_s + \mathcal{C}_\Sigma) \cdot \sigma_0 = 1$. On the other hand, on the factorized locus it is clear that $\mathcal{C}_\Sigma \cdot \sigma_0 = 2$ (the two points where the \mathbb{P}^1 components touch). So we conclude $\mathcal{C}_s \cdot \sigma_0 = -1$. Substituting all this into [Equation 9.3.30](#) we obtain $Q_{U(1)} = 4$, as claimed.

9.3.4 Chern-Simons Terms

In this final subsection, we confirm geometrically that the Chern-Simons terms of the theory obtained by compactifying M-theory on \mathcal{Y} are in fact related to the Chern-Simons terms of

M-theory on \mathbb{Y} as described in [Equation 8.2.9](#). Instead of delving into concrete examples right away and showing explicitly that this prescription is correct on a case by case basis, let us make a general geometric argument first. As the Chern-Simons terms of the five-dimensional models are given in terms of intersection numbers, we need to understand how the intersection form on \mathcal{Y} is obtained from the intersection form of \mathbb{Y} . Fortunately for us, this was studied long ago, see for example [\[216\]](#). Denoting by \mathcal{K}_i , $i = 1, \dots, h^{1,1}(\mathbb{Y})$ a basis of the Kähler cone on \mathbb{Y} and by $\tilde{\mathcal{K}}_i$, $i = 1, \dots, h^{1,1}(\mathcal{Y})$ the corresponding Kähler cone basis on \mathcal{Y} , we choose the \mathcal{K}_i such that under the conifold transition they are mapped to divisors on \mathcal{Y} according to

$$\mathcal{K}_i \mapsto \begin{cases} \tilde{\mathcal{K}}_i & \text{if } i \leq h^{1,1}(\mathcal{Y}) \\ 0 & \text{otherwise.} \end{cases} \quad (9.3.31)$$

Then the intersection numbers of the $\tilde{\mathcal{K}}_i$ on \mathcal{Y} are the same as of the \mathcal{K}_i on \mathbb{Y} , i.e.

$$\tilde{\mathcal{K}}_i \cdot \tilde{\mathcal{K}}_j \cdot \tilde{\mathcal{K}}_k = \mathcal{K}_i \cdot \mathcal{K}_j \cdot \mathcal{K}_k. \quad (9.3.32)$$

Put differently, the intersection form on \mathcal{Y} is obtained by restricting the intersection form on \mathbb{Y} . That is, given expressions for the volumes \mathcal{V} and $\tilde{\mathcal{V}}$ of \mathbb{Y} and \mathcal{Y} in terms of the Kähler parameters v^i and \tilde{v}^i , one has that

$$\tilde{\mathcal{V}} = \mathcal{V}(v^1 = \tilde{v}^1, \dots, v^{h^{1,1}(\mathcal{Y})} = \tilde{v}^{h^{1,1}(\mathcal{Y})}, 0, \dots). \quad (9.3.33)$$

Presented with this simple relation between triple intersections on \mathbb{Y} and \mathcal{Y} , let us now return to the discussion of the Chern-Simons terms of M-theory on \mathcal{Y} . Given two independent sections on \mathbb{Y} we know that only a certain linear combination $D_{U(1)}$ is left untouched by the conifold transition – the other $U(1)$ -divisor is eliminated as the corresponding gauge field gains a mass term. Identifying the surviving $U(1)$ amounts to making the same clever choice of basis as for the \mathcal{K}_i above. Then, [Equation 9.3.32](#) tells us that the intersection numbers of the surviving $U(1)$ -divisor are *precisely the same* as on the resolved side. Therefore, we are left with two questions to examine in our specific examples, namely:

1. Which divisor $D_{U(1)}$ survives the conifold transition?
2. Why is $D_{U(1)} \cdot c_2(\mathbb{Y}) = \tilde{D}_{U(1)} \cdot c_2(\mathcal{Y})$?

Around [Equation 8.3.5](#) we gave a general argument for how to identify $D_{U(1)}$ and, in fact, we will show explicitly that this prescription does in fact select the correct divisor for the examples below. The second point is more difficult to answer generally, but we can confirm it on a case by case basis.

Put in a nutshell, we have explained generally that after a clever change of basis the Chern-Simons terms of the theories corresponding to \mathbb{Y} and \mathcal{Y} are simply obtained by "dropping" the massive $U(1)$. Of course, one can also confirm this statement explicitly through the calculation of intersection numbers and in the remainder of this section we will perform an example calculation.

A Close Look at the Model with $(a, b) = (0, 3)$

For concreteness, let us study the manifold with $(a, b) = (0, 3)$ by beginning on the resolved side. We find that the Mori cone is generated by the three curves

$$\begin{array}{c} \mathcal{C}_1 \\ \mathcal{C}_2 \\ \mathcal{C}_3 \end{array} \left\| \begin{array}{cccccc} x_1 & x_2 & x_3 & y_1 & y_2 & w & s \\ \hline 1 & 1 & 1 & -3 & 0 & 0 & 3 \\ 0 & 0 & 0 & -1 & 1 & 0 & 2 \\ 0 & 0 & 0 & 1 & 0 & 1 & -1 \end{array} \right. \quad (9.3.34)$$

and we can hence choose

$$\mathcal{K}_1 = x_1, \quad \mathcal{K}_2 = y_2, \quad \mathcal{K}_3 = w \quad (9.3.35)$$

as a basis of the Kähler cone satisfying $\mathcal{K}_i \cdot \mathcal{C}^j = \delta_i^j$. Expressing the Kähler form $J = \sum_{i=1}^3 v^i [\mathcal{K}_i]$ in terms of two-forms dual to these divisors, one finds that the overall volume of the Calabi-Yau can be written as

$$\mathcal{V} = (v^1)^2 v^2 + \frac{3}{2} (v^1)^2 v^3 + 6v^1 v^2 v^3 + \frac{15}{2} v^1 (v^3)^2 + 9v^2 (v^3)^2 + \frac{21}{2} (v^3)^3. \quad (9.3.36)$$

Let us turn to the two divisors generating the $U(1)$ symmetries in five dimensions. One is obtained by appropriately shifting the zero section [52, 114], while the other can be computed by applying the Shioda map to the other section. Naturally, a different choice of zero section will lead to interchanged results for the divisor expansions. Since the resulting physics remain unaffected, we choose the divisor $s = 0$, or σ_0 in the notation of subsection 9.3.1, as the zero section during the rest of this discussion. Note that in this particular basis the divisors generating the two $U(1)$ s have the expansion

$$D_0 = \frac{9}{2} \mathcal{K}_1 + 2\mathcal{K}_2 - \mathcal{K}_3, \quad D_1 = -24\mathcal{K}_1 - 6\mathcal{K}_2 + 4\mathcal{K}_3. \quad (9.3.37)$$

Now we discuss the deformed manifold \mathcal{Y} . Its Mori cone is spanned by

$$\begin{array}{c} \tilde{\mathcal{C}}_1 \\ \tilde{\mathcal{C}}_2 \end{array} \left\| \begin{array}{cccccc} x_1 & x_2 & x_3 & y_1 & y_2 & w \\ \hline 1 & 1 & 1 & 0 & 0 & 3 \\ 0 & 0 & 0 & 1 & 1 & 2 \end{array} \right. \quad (9.3.38)$$

and a good choice of Kähler basis is for example given by

$$\tilde{\mathcal{K}}_1 = x_1, \quad \tilde{\mathcal{K}}_2 = y_2. \quad (9.3.39)$$

Then the volume of the deformed manifold is

$$\tilde{\mathcal{V}} = (\tilde{v}^1)^2 \tilde{v}^2. \quad (9.3.40)$$

Obviously, the intersection rings of \mathbb{Y} and \mathcal{Y} are related as in Equation 9.3.33, with \mathcal{K}_3 the divisor eliminated during the conifold transition. Up to an overall rescaling, there is hence a

unique combination of D_0 and D_1 that is left invariant under the conifold map, namely the one not containing \mathcal{K}_3 . It is³

$$D_{U(1)} \sim 4D_0 + D_1. \quad (9.3.41)$$

Since we rescaled the six-dimensional $U(1)$ divisor on \mathbb{Y} by $\lambda = 2$, this is precisely the expression that we expect from [Equation 8.3.5](#). Lastly, we can check by explicit computation that $D_{U(1)} \cdot c_2(\mathbb{Y}) = \tilde{D}_{U(1)} \cdot c_2(\mathcal{Y})$.

A Close Look at the Model with $(a, b) = (0, -2)$

As a second example, we repeat the analysis for one of the models that contain an additional $SU(2)$ factor to show that the above discussion is independent of the existence of additional gauge group factors. Again, we begin with the resolved manifold \mathbb{Y} , whose Mori cone is this time spanned by the curves

$$\begin{array}{c|cccccccc} & x_1 & x_2 & x_3 & y_1 & y_2 & w & s & t \\ \hline \mathcal{C}_1 & 1 & 1 & 1 & 0 & 0 & -2 & 0 & 0 \\ \mathcal{C}_2 & 0 & 0 & 0 & 1 & 1 & 0 & 0 & -2 \\ \mathcal{C}_3 & 0 & 0 & 0 & 1 & 0 & 1 & -1 & 0 \\ \mathcal{C}_4 & 0 & 0 & 0 & -1 & 0 & 0 & 1 & 1 \end{array} \quad (9.3.42)$$

and we pick

$$\mathcal{K}_1 = x_1, \quad \mathcal{K}_2 = y_2, \quad \mathcal{K}_3 = t + 2y_2, \quad \mathcal{K}_4 = w + 2x_1 \quad (9.3.43)$$

as the basis of the Kähler cone. The volume of the resolved manifold is then

$$\begin{aligned} \mathcal{V} &= (v^1)^2 v^2 + 2(v^1)^2 v^3 + 5v^1 v^2 v^3 + 5v^1 (v^3)^2 + 5v^2 (v^3)^2 + \frac{10}{3}(v^3)^3 + \frac{3}{2}(v^1)^2 v^4 \\ &\quad + 5v^1 v^2 v^4 + 10v^1 v^3 v^4 + 10v^2 v^3 v^4 + 10(v^3)^2 v^4 + \frac{7}{2}v^1 (v^4)^2 \\ &\quad + 5v^2 (v^4)^2 + 10v^3 (v^4)^2 + \frac{7}{3}(v^4)^3. \end{aligned} \quad (9.3.44)$$

Choosing $\sigma_0 = \{s = 0\}$ as zero section and expanding the $U(1)$ divisors of the five-dimensional theory in a basis of \mathcal{K}_i one finds

$$D_0 = \frac{3}{2}\mathcal{K}_1 + \mathcal{K}_3 - \mathcal{K}_4, \quad D_1 = -12\mathcal{K}_1 - 3\mathcal{K}_3 + 4\mathcal{K}_4. \quad (9.3.45)$$

Additionally, there is a third $U(1)$ which is enhanced to the non-Abelian $SU(2)$ factor in the F-theory limit. We denote it by E and its expansion reads

$$E = -2\mathcal{K}_1 + \mathcal{K}_2. \quad (9.3.46)$$

³Note that in [chapter 8](#) we denoted the $U(1)$ -divisor remaining massless by \tilde{D}_0 . Here we call it $D_{U(1)}$ to emphasize that it not necessarily a divisor on \mathcal{Y} .

Changing to the deformed manifold \mathcal{Y} corresponding to F-theory with a massive $U(1)$, we find that its Mori cone is generated by

$$\begin{array}{c|cccccc} & x_1 & x_2 & x_3 & y_1 & y_2 & w & t \\ \hline \tilde{\mathcal{C}}_1 & 1 & 1 & 1 & 0 & 0 & -2 & 0 \\ \tilde{\mathcal{C}}_2 & 0 & 0 & 0 & 1 & 1 & 0 & -2 \\ \tilde{\mathcal{C}}_3 & 0 & 0 & 0 & 0 & 0 & 1 & 1 \end{array} \quad (9.3.47)$$

and we parametrize the Kähler form in terms of two-forms Poincaré-dual to

$$\tilde{\mathcal{K}}_1 = x_1, \quad \tilde{\mathcal{K}}_2 = y_2, \quad \tilde{\mathcal{K}}_3 = t + 2y_2. \quad (9.3.48)$$

The volume of \mathcal{Y} is given by

$$\tilde{\mathcal{V}} = (\tilde{v}^1)^2 \tilde{v}^2 + 2(\tilde{v}^1)^2 \tilde{v}^3 + 5\tilde{v}^1 \tilde{v}^2 \tilde{v}^3 + 5\tilde{v}^1 (\tilde{v}^3)^2 + 5\tilde{v}^2 (\tilde{v}^3)^2 + \frac{10}{3} (\tilde{v}^3)^3 \quad (9.3.49)$$

and one can see that it is obtained by restricting the volume of the resolved phase according to

$$\tilde{\mathcal{V}} = \mathcal{V}|_{v^4=0, v^i=\tilde{v}^i}. \quad (9.3.50)$$

Consequently, we see that the above choice of \mathcal{K}_i is again a good one in the sense of equations (9.3.31) and (9.3.33) and one transitions from \mathbb{Y} to \mathcal{Y} by dropping \mathcal{K}_4 . Since Equation 9.3.46 does not contain \mathcal{K}_4 , we observe that it is left untouched by the conifold transition and does not take part in the mixing involving the remaining two $U(1)$ s. Requiring again that the surviving $U(1)$ must not contain \mathcal{K}_4 , one finds that, up to an overall rescaling, it is given by

$$D_{U(1)} = 4D_0 + D_1, \quad (9.3.51)$$

which, as before, matches the prescription of Equation 8.3.5 with $\lambda = 2$. In summary, we find that the discussion of the case with additional $SU(2)$ gauge symmetry is almost identical to the one of the simpler models with only Abelian gauge groups. As before, we identify a curve shrinking to zero volume in the conifold limit. The intersection form of the deformed model is then obtained by dropping the divisor dual to that curve from the intersection form of the resolved phase. As the $SU(2)$ Cartan divisor does not contain the divisor that is eliminated in the conifold transition, it does not mix with any of the other $U(1)$ s during the conifold transition. Finally, one can again confirm that $D_{U(1)} \cdot c_2(\mathbb{Y}) = \tilde{D}_{U(1)} \cdot c_2(\mathcal{Y})$, thereby showing that the Chern-Simons terms corresponding to the higher curvature terms are matched as well.

Explicit Formulas for the Chern-Simons Terms

Technically, the previous discussion already ensures the matching of the Chern-Simons terms as discussed in section 8.2. Nevertheless, it may be illuminating to consider the discussion from

a different angle. Let us therefore evaluate formulas (8.2.13) and (8.2.14) for the examples at hand and show that they predict the correct intersection numbers. Turning the discussion around, one can also use these relations to *compute the spectrum of \mathcal{Y}* without making use to the resolved manifold \mathbb{Y} .

(a, b)	V	$H_{neutral}$	$H(\mathbf{1}_2)$	$H(\mathbf{1}_4)$	\tilde{k}_0	\tilde{k}_{000}
$(0, 3)$	1	112	144	18	-168	432
$(1, 4)$	1	124	140	10	-128	304
$(2, 5)$	1	142	128	4	-80	208
$(3, 6)$	1	166	108	0	-24	144

Table 9.6: Spectra and Chern-Simons coefficients of \tilde{A}^0 for the models with two sections and $h^{1,1} = 3$. Here, the Chern-Simons terms are obtained from the geometry and can be shown to match the field theory computation. All $U(1)$ charges have been rescaled by two.

This time, we restrict ourselves to models with purely Abelian gauge group, where we know the spectrum to consist of $\mathbf{1}_2$ and $\mathbf{1}_4$ states. Assuming furthermore that

$$l_{\mathbf{1}_2} = 0, \quad l_{\mathbf{1}_4} = 1 \quad (9.3.52)$$

as is the case when \mathbb{Y} has a non-holomorphic zero section (corresponding to σ_0 as above), the formulas for \tilde{k}_{000} and \tilde{k}_0 simplify to

$$\begin{aligned} \tilde{k}_{000} &= \frac{m^3}{120} (H - V - T - 3) \\ &+ \frac{1}{4} H(\mathbf{1}_2) (-4n^2 m + 16n^3 \text{sign}(\mathbf{1}_2)) \\ &+ \frac{1}{4} H(\mathbf{1}_4) (-4m^3 - 208n^2 m + (384n^3 + 48nm^2) \text{sign}(\mathbf{1}_4)) . \end{aligned} \quad (9.3.53)$$

and

$$\begin{aligned} \tilde{k}_0 &= \frac{m}{6} (H - V + 5T + 15) \\ &+ H(\mathbf{1}_2) (-2n \text{sign}(\mathbf{1}_2)) + H(\mathbf{1}_4) (2m - 12n \text{sign}(\mathbf{1}_4)) . \end{aligned} \quad (9.3.54)$$

To be as concrete as possible, we plug in $n = -1$ and $m = 4$ as we found above and use that for these manifolds $\text{sign}(\mathbf{1}_2) = \text{sign}(\mathbf{1}_4) = -1$ and $T = 0$ to find

$$\tilde{k}_{000} = \frac{8}{15} (H - V - 3) + 16H(\mathbf{1}_4) \quad (9.3.55)$$

$$\tilde{k}_0 = \frac{2}{3} (H - V + 15) - 2H(\mathbf{1}_2) - 4H(\mathbf{1}_4) . \quad (9.3.56)$$

Evaluating the formulas, one easily confirms that they indeed match the intersection numbers given in [table 9.6](#). Note that [table 9.6](#) contains the spectra of the F-theory models on the resolved manifolds \mathbb{Y} . However, they can easily be translated to the case of a massive $U(1)$ corresponding to F-theory on \mathcal{Y} . F-theory on \mathcal{Y} has $H_{neutral} - 1$ neutral hypermultiplets and $V = 0$ massless vectors as shown in [figure 8.2](#). In six dimensions, the charged spectrum is the same on \mathbb{Y} and \mathcal{Y} with the difference that the $U(1)$ field in F-theory on \mathcal{Y} is massive. However, upon doing the fluxed circle reduction to five dimensions, the $\mathbf{1}_4$ states with KK-level $\hat{n} = -1$ are neutral under the mixed massless $U(1)$ gauge field \tilde{A}^0 and must therefore be counted as additional neutral states not counted by $h^{2,1}(\mathcal{Y})$.

We remark that these are the same results as one would get by starting with the conjectured six-dimensional F-theory set-up with a massive $U(1)$. In fact, by computing the Mori cones of \mathbb{Y} and \tilde{X} one can show that the sign functions for the states $\mathbf{1}_2$ and $\mathbf{1}_4$ agree in the deformed and the resolved phases.

Finally, let us comment on directly computing spectra of F-theory models \mathcal{Y} without section. In the examples studied, we gained a computational advantage by finding models \mathbb{Y} with section that are related to \mathcal{Y} by conifold transitions. Ideally, however, one would like to compute the spectra of F-theory on \mathcal{Y} without making this detour. In general, this is going to be more difficult due to the fact that there are less divisors on \mathcal{Y} and therefore less intersection numbers to extract information from even though the spectra are equally complicated. As it turns out, for cases with a single $U(1)$ there are generally more unknown variables than equations obtained from matching the Chern-Simons terms. However, if one also requires all anomalies to be canceled, it *is possible* to compute the spectra directly from \mathcal{Y} for the cases presented here. Incorporating these methods into a general approach by extending the variety of models studied here seems to be a promising direction of study.

Chapter 10

Yukawas in the Presence of Massive $U(1)$ s

Compared to F-theory compactifications to six dimensions, four-dimensional F-theory models are considerably richer. Two of the key features present are G -flux, the flux of the M-theory three-form, and Yukawa couplings in the effective theory that are controlled by geometric quantities located at codimension three in the base manifold.

G -flux induces chirality in the four-dimensional matter spectrum [95, 217] and integrals over the flux are thus the quantities that the three-dimensional equivalents of the loop-corrected Chern-Simons terms in Equation 7.3.10 and Equation 7.3.11 have to be matched to [95]. In order to compute not only chiral indices, but the actual number of representations present in the four-dimensional effective F-theory action, one needs more precise information about the flux data, namely that specified in terms of the Deligne cohomology of the flux [218].

Compared to fluxes, Yukawa couplings in global compactifications have been much less studied so far, both those that involve singlets and those that do not. While their assumed geometrical counterparts, intersections of different matter curves in codimension three in the base manifold, have received attention [144, 156, 157, 163, 164, 167, 219, 220], it appears crucial to point out that the relation to T-branes [83, 221], and in particular the low energy effective theory and local models [66, 70, 222–225] remain to be explored. Since the strength of a Yukawa coupling is not an integer, one does not expect it to be given by a topological quantity and its precise value is therefore expected to be much harder to calculate. In this chapter, we therefore limit ourselves to checking whether a codimension-three intersection exists in order to determine whether a Yukawa coupling is expected to be realized.

Following this reasoning, we show in this chapter that certain Yukawa couplings allowed by the continuous gauge symmetry of the four-dimensional effective F-theory action are not present in F-theory models without section. We argue that this is due to discrete symmetries

surviving as remnants of the massive $U(1)$ vector field that exists in such models as we learned [chapter 8](#). A similar analysis was performed in [152] and later extended in [204].

Before beginning in earnest, let us emphasize that unlike in the six-dimensional case that most of this part of the dissertation has dealt with, we do not derive the four-dimensional effective F-theory action. Instead, we use the results of [53] and focus entirely on extending the study of F-theory compactifications without section in [chapter 8](#) to four dimensions. In order to distinguish the four-dimensional case from the six-dimensional one, we use subscripts to denote the complex dimensions of the Calabi-Yau manifolds.

10.1 The Stückelberg Axion in Four Dimensions

In a four-dimensional theory with $\mathcal{N} = 1$ supersymmetry the axion c must arise from a complex field. We take it to be the real part of a complex field G , $\text{Re } G = c$. The field G is obtained when expanding the M-theory three-form as [53, 226]

$$C_3 = iG\bar{\Psi} - i\bar{G}\Psi, \quad (10.1.1)$$

where Ψ is a $(2, 1)$ -form on the Calabi-Yau fourfold \mathcal{Y}_4 . Using this definition of G , one can derive the four-dimensional effective theory. The relevant $U(1)$ gauging appears in the kinetic term of G given by

$$\mathcal{L}_4 = K_{G\bar{G}}\hat{D}_\mu G\hat{D}^\mu\bar{G}, \quad \hat{D}G = dG + m\hat{A}^1. \quad (10.1.2)$$

Upon ‘eating’ the axion $\text{Re } G$, the kinetic term (10.1.2) becomes a mass term for \hat{A}^1 , and the mass is simply given by $K_{G\bar{G}}$. Furthermore, it was shown in [53, 226] that for a massless G $K_{G\bar{G}}$ takes the form

$$K_{G\bar{G}} = \frac{i}{2\mathcal{V}} \int_{\mathcal{Y}_4} J \wedge \bar{\Psi} \wedge \Psi. \quad (10.1.3)$$

Note that since Ψ is a $(2, 1)$ -form on \mathcal{Y}_4 , it depends on the complex structure moduli z^k of \mathcal{Y}_4 . Remarkably, the moduli dependence of Ψ can be specified by a *holomorphic* function $h(z)$. In the simplest situation one finds that [53, 74]

$$K_{G\bar{G}} \propto (\text{Im } h)^{-1}. \quad (10.1.4)$$

Moving along the complex structure moduli space, the coupling $K_{G\bar{G}}$ setting the mass of the $U(1)$ can become zero.

Let us comment on the points at which the $U(1)$ becomes massless. In order to do that, we extrapolate the behavior of $K_{G\bar{G}}$ using the results from a Calabi-Yau threefold. Indeed, the analogous coupling in a Calabi-Yau threefold compactification depends crucially on the complex structure moduli and can be specified by a holomorphic pre-potential $\mathcal{F}(z)$. In this

case, the function h can be thought of as a second derivative of the pre-potential $\mathcal{F}(z)$. One then expects that at special points $z^i \approx 0$, $i = 1, \dots, n_{\text{con}}$ in complex structure moduli space one has

$$h(z) = \sum_i a_i \log z^i + \dots, \quad (10.1.5)$$

where a_i are constants and the dots indicate terms that are polynomial in the complex structure parameter z^i . Geometrically, as we discuss in more detail below, this indicates that the points $z^i = 0$ are conifold points and a geometric transition takes place. In fact, as discussed already in the previous chapter, the Calabi-Yau threefold with a bi-section \mathcal{Y}_3 can transition to a Calabi-Yau threefold with two sections \mathbb{Y}_3 by means of a conifold transition. In the Calabi-Yau fourfold case a similar transition from \mathcal{Y}_4 to \mathbb{Y}_4 can take place. In this case, however, one finds a whole curve of conifold points:

$$\mathcal{Y}_3 \xrightarrow{\text{tune } z^i} \mathcal{Y}_3^{\text{sing}} \text{ with conifold points} \xrightarrow{\text{resolve}} \mathbb{Y}_3 \quad (10.1.6)$$

$$\mathcal{Y}_4 \xrightarrow{\text{tune } z^i} \mathcal{Y}_4^{\text{sing}} \text{ with conifold curve} \xrightarrow{\text{resolve}} \mathbb{Y}_4 \quad (10.1.7)$$

We stress that the resolved branch \mathbb{Y} can only be accessed in the lower-dimensional theory, i.e. in M-theory on \mathbb{Y} . Nevertheless, the existence of the branch \mathbb{Y} naturally leads us to another interpretation of the setup with a $U(1)$ made massive by a linear Higgs mechanism.

To introduce the linear Higgs mechanism picture, let us approach the singular geometry from the side of \mathbb{Y}_4 . At the singular point one also finds that there are new matter states in the four-dimensional effective theory that are charged under the $U(1)$. In other words, these admit the couplings

$$\hat{\mathcal{D}}\phi = d\phi + i\hat{q}\hat{A}^1\phi, \quad (10.1.8)$$

where \hat{q} is the $U(1)$ -charge of the complex field ϕ . This implies that one can also think of giving a mass to the $U(1)$ by turning on a vacuum expectation value for the field ϕ . In the F-theory compactifications under consideration the field ϕ will be a matter field arising from the open string sector on intersecting seven-branes. It will further be a singlet under any additional non-Abelian group and therefore be denoted by $\mathbf{1}_{\hat{q}}$, where the subscript indicates the $U(1)$ -charge. Working with the open string matter field ϕ should be considered as the dual picture to working with the closed string field G . In order to match the charges one expects an identification

$$\mathbf{1}_{\hat{q}} \text{ (open string)} \leftrightarrow A(z)e^{2\pi i r G} \text{ (closed string)}, \quad (10.1.9)$$

where $mr = -\hat{q}$, and $A(z)$ is a coefficient that generally depends on the complex structure moduli of \mathcal{Y}_4 . Working with either $\mathbf{1}_{\hat{q}}$ or G degrees of freedom should give a dual description of the same physical effective theory.

Let us close this section by noting that the fact that the $U(1)$ is massive implies that it will be absent in the effective theory at energy scales below its mass. In this effective theory the selection rules originally imposed by the $U(1)$ gauge symmetry will remain as discrete symmetries.

10.2 Yukawa Structures

In the following we discuss the Yukawa structures of $SU(5)$ GUTs engineered in an F-theory compactification without section. Therefore, let us consider a $SU(5)$ GUT with $\mathbf{10}$ representations and $\mathbf{5}$ representations. Furthermore, we include a number of GUT singlets $\mathbf{1}$. In order to make contact with the discussion of [section 10.1](#) we distinguish representations by an additional $U(1)_1$ charge, corresponding to the Abelian gauge field \hat{A}^1 introduced above. We indicate the $U(1)_1$ charges of the $\mathbf{10}$, $\mathbf{5}$ and $\mathbf{1}$ states will by a subscript q as in

$$\mathbf{10}_q, \mathbf{5}_q, \mathbf{1}_q : \quad \mathbf{R}_q \rightarrow e^{2\pi i q \Lambda} \mathbf{R}_q, \quad (10.2.1)$$

where a gauge transformation of \hat{A}^1 acts as $\hat{A}^1 \rightarrow \hat{A}^1 + d\Lambda$.

Since we are interested in Yukawa couplings, the relevant terms in the $U(1)$ -invariant perturbative superpotential are

$$W_{\text{pert}} : \quad \sum_{q_1+q_2+q_3=0} \mathbf{10}_{q_1} \mathbf{10}_{q_2} \mathbf{5}_{q_3}, \quad \sum_{q_1+q_2+q_3=0} \mathbf{10}_{q_1} \bar{\mathbf{5}}_{q_2} \bar{\mathbf{5}}_{q_3}. \quad (10.2.2)$$

This generically implies that various couplings are absent. As an example, which we will realize in F-theory below, let us assume that we have a 4-split, i.e. $k = 4$ in [Equation 4.4.3](#), with the representations

$$\mathbf{5}_{-6}, \mathbf{5}_{-1}, \mathbf{5}_4, \mathbf{10}_3, \mathbf{1}_5, \mathbf{1}_{10}. \quad (10.2.3)$$

The perturbatively permitted cubic Yukawas are then

$$\mathbf{10}_3 \times \mathbf{10}_3 \times \mathbf{5}_{-6}, \quad \mathbf{10}_3 \times \bar{\mathbf{5}}_1 \times \bar{\mathbf{5}}_{-4}, \quad (10.2.4)$$

plus additional couplings involving the singlet states.

Let us now contrast this to the case in which the $U(1)$ vector field has gained a mass term. As discussed above, this implies that the low-energy gauge symmetry is reduced to $\mathbb{Z}_2 \times SU(5)$. For our specific set-up we find that the \mathbb{Z}_2 charges are as follows:

$$\begin{aligned} Q_{\mathbb{Z}_2}(\mathbf{5}_4) &= 0, & Q_{\mathbb{Z}_2}(\mathbf{5}_{-1}) &= 1, & Q_{\mathbb{Z}_2}(\mathbf{5}_{-6}) &= 0, \\ Q_{\mathbb{Z}_2}(\mathbf{10}_3) &= 1, & Q_{\mathbb{Z}_2}(\mathbf{1}_5) &= 1, & Q_{\mathbb{Z}_2}(\mathbf{1}_{10}) &= 0 \end{aligned} \quad (10.2.5)$$

In particular, this means that at masses below the Stückelberg mass of our $U(1)$ gauge field, the two curves $\mathbf{5}_4$ and $\mathbf{5}_{-6}$ should be indistinguishable. Furthermore, the singlets $\mathbf{1}_{10}$ are not charged under any massless gauge field anymore.

Under the remaining gauge symmetry, we expect to find the Yukawa couplings

$$\mathbf{10}_3 \times \mathbf{10}_3 \times \mathbf{5}_{-6}, \quad \mathbf{10}_3 \times \mathbf{10}_3 \times \mathbf{5}_4, \quad \mathbf{10}_3 \times \bar{\mathbf{5}}_1 \times \bar{\mathbf{5}}_{-4}, \quad \mathbf{10}_3 \times \bar{\mathbf{5}}_1 \times \bar{\mathbf{5}}_6 \quad (10.2.6)$$

plus additional couplings involving the singlet states. It is crucial to point out, however, that the coupling $\mathbf{10}_3 \times \mathbf{10}_3 \times \mathbf{5}_{-1}$ is still ruled out by the \mathbb{Z}_2 symmetry and we do not expect it to be realized in our example geometries.

It is particularly interesting to stress the role of the singlets in the setup. In the example of [section 10.4](#), we show that the singlet states $\mathbf{1}_{10}$ are involved in the Higgsing described in [section 10.1](#). In fact, the spectrum (10.2.3) arises in the open string interpretation of the F-theory setting. The closed string axion appears as the phase of the $\mathbf{1}_{10}$ using the identification (10.1.9). Furthermore, we will find in our concrete example that there are couplings of the form

$$\mathbf{1}_{10} \times \mathbf{5}_{-6} \times \bar{\mathbf{5}}_{-4}. \quad (10.2.7)$$

Given such a coupling in the open string picture, one may thus wonder whether from the closed string point of view a non-perturbative superpotential appears that involves the complex field G . Concretely, inspired by the identification (10.1.9) we have in mind terms of the form

$$W_{\text{non-pert}} = \dots + \sum_{q_1+q_2-rm=0} A(z)e^{2\pi irG} \mathbf{5}_{q_1} \bar{\mathbf{5}}_{q_2}. \quad (10.2.8)$$

As we will explain in [section 10.3](#), some of these couplings are indeed present, and can be reinterpreted in terms of the classical couplings (10.2.7).

Let us close this subsection with some comments on the non-perturbative couplings (10.2.8). Superpotential couplings of a similar type induced by stringy instantons have been studied intensively in orientifold compactifications as reviewed in detail in [227]. Remarkably, the couplings (10.2.8) appear to be of somewhat different nature. They do not depend on the Kähler moduli and therefore are not suppressed at large volume. However, this is not a contradiction to a de-compactification argument, since these couplings are localized near the intersection of seven-branes. The instantons give a mass for certain $\mathbf{5}$ -states that will therefore be absent in the effective theory for the massless modes only. We will see in our concrete examples that this picture is indeed consistent. It would be very interesting to perform a more thorough study of the instantons inducing the couplings (10.2.8). Interestingly, this can already be done in the weak coupling limit.

10.3 String Interpretation of the Higgsing

Let us now try to understand better the link between geometric quantities on the one hand and field theory quantities on the other. We emphasize that the fact that a new branch of moduli space opens up in the M-theory compactification, connecting via a geometric transition our

Calabi-Yau background to a large network of spaces, is not essential for our discussion. An alternative, more self-contained, viewpoint is that we are studying the physics of the Higgsed (i.e. deformed) branch close to a particular point in moduli space where extra degrees of freedom appear. Nevertheless, we will keep using the M-theory viewpoint for convenience, since discussions about geometry and M2 brane states can be easily understood there.

Let us start with the case of the five-dimensional transition, i.e. a conifold transition for a Calabi-Yau threefold in M-theory. This case is well understood by now and we briefly recall the discussion of the transition given in [213, 214]. Take a Calabi-Yau threefold \mathcal{Y} . As we tune some of the complex structure moduli, there are codimension R subspaces in complex structure moduli space where \mathcal{Y} develops conifold singularities. Geometrically, this implies the simultaneous vanishing of a number of periods

$$z^i = \int_{\Pi_i} \Omega, \quad i = 1, \dots, P \quad (10.3.1)$$

with Π_i a set of elements of $H^3(\mathcal{Y}, \mathbb{Z})$, and Ω the holomorphic three-form of \mathcal{Y} . More pictorially, we have P three-spheres contracting to zero size. Not all of these three-spheres are homologically independent, only R of them are. Our examples all have $P - R = 1$, and henceforth we restrict the discussion to this case for concreteness.

Consider the defining equation of the Calabi-Yau fourfold without a section that we will study later. As in section 9.3, we choose to embed the fiber inside \mathbb{P}_{112} and we saw already in section 3.9 that this gives rise to a two-section. We call our variables¹

$$\begin{aligned} p_{112} &= \tilde{a}_0 w^2 + \tilde{a}_1 y_1^2 w + \tilde{a}_2 y_1 y_2 w + \tilde{a}_3 y_2^2 w + \tilde{a}_4 y_1^4 \\ &\quad + \tilde{a}_5 y_1^3 y_2 + \tilde{a}_6 y_1^2 y_2^2 + \tilde{a}_7 y_1 y_2^3 + \tilde{a}_8 y_2^4 \\ &= 0, \end{aligned} \quad (10.3.2)$$

with the \tilde{a}_i being sections of line bundles of appropriate degree in the base. The conifold locus in moduli space is obtained by tuning R coefficients in this equation, which allow us to set $\tilde{a}_8 = 0$, modulo local coordinate redefinitions. The same argument as in the previous chapter then shows that there are conifold singularities at the P points in the base given by the solutions of $\tilde{a}_3 = \tilde{a}_7 = 0$.

In the five-dimensional effective field theory, as we approach the conifold locus, a massive $U(1)$ vector multiplet becomes light. When we hit the conifold locus in moduli space the massive vector multiplet becomes massless, and it splits into a massless vector multiplet and a massless charged hyper. The physics is thus that of an unHiggsing process. Going in the reverse direction, i.e. taking $\tilde{a}_8 \neq 0$, corresponds to giving a vacuum expectation value to the charged hyper, and thus an ordinary five-dimensional Higgsing process.

For our purposes it will be useful to understand the geometric manifestation of this Higgsing in more detail. (The basic picture was given in [228].) Consider the theory at the

¹We changed notation with respect to section 9.3, the most relevant part of the dictionary for comparison to that section is $\{\tilde{a}_8, \tilde{a}_3, \tilde{a}_7\} \rightarrow \{a, f, e\}$.

conifold locus. We have a massless $U(1)$ vector multiplet², which in M-theory comes from a supergravity reduction of the form $C_3 = A \wedge \omega$, with A the five-dimensional vector boson and ω a harmonic two-form in the threefold \mathcal{Y} . By Poincaré duality, we can also think of ω as defining a four-cycle D in \mathcal{Y} .

As we start making $\tilde{a}_8 \neq 0$, the $U(1)$ should acquire a mass. The geometric manifestation of this fact is that ω is no longer a harmonic form, but rather becomes a low-lying eigenform of the Laplacian of \mathcal{Y} , or dually, the four-cycle D becomes a four-chain with boundary. In fact, the four-chain is easy to describe: as we deform away from the conifold locus, the P conifold singularities are replaced by P three-spheres S_i . There is a relation in homology between these spheres, i.e. there is a four-chain in homology with boundary on these spheres. This four-cycle is D .

Coming back to the $\tilde{a}_8 = 0$ conifold locus, we have that there are also P hypermultiplets charged under the $U(1)$. They come from M2 branes wrapping the vanishing size holomorphic S^2 at the conifold singularity. As we deform away from the conifold locus, $R = P - 1$ hypermultiplets stay massless, and get reinterpreted in the geometry as complex structure moduli of the R growing classes in homology, plus the integrals of C_3 and C_6 over the same homology classes. The massive vector boson comes from reducing C_3 over the (non-zero) eigenform of the Laplacian connected to the four-cycle becoming a four-chain in the conifold transition. From this discussion, it follows that one should identify the closed string axion entering the Stückelberg mechanism in the geometric description of the massive $U(1)$ given above with the phase of the charged hypermultiplet getting a vacuum expectation value and entering the non-linear realization of the $U(1)$ gauge symmetry becoming massive.

One take-home message from this discussion is that there is a deep interrelation between the field theory and the geometry, and a duality dictionary of sorts: what we see in the field theory as a Higgsing of a field appears in the geometry as a particular four-cycle getting boundaries and becoming a four-chain. There is also a nice interplay between field theory and string theory when it comes to the corrections to the theory: as explained in [228], and further substantiated in [229], in order to reproduce the right hypermultiplet moduli space metric one expects from field theory, one should sum an infinite set of non-perturbative corrections coming from M2 brane instantons in M-theory.

A similar picture will hold in the case of compactifications on a Calabi-Yau fourfold. We now have an M-theory compactification down to three dimensions, and there is a $U(1)$ symmetry that becomes Higgsed as we resolve the conifold singularities. The $U(1)$ vector boson comes from the reduction of $C_3 = A \wedge \omega$. Poincaré duality now tells us that we should be looking for a *six*-cycle in the geometry that opens up in the resolution process and has boundaries on five-cycles. These five-cycles have a simple interpretation: instead of having conifold points in the total space, we now have conifold *curves*. As we deform the

²Typically there will be other $U(1)$ vector multiplets in the low energy theory, but one can choose a basis in which they decouple from the physics of the transition.

defining equation, we obtain a set of five-cycles given by fibrations of the deformation S^3 over the matter curve being Higgsed.³ The massive $U(1)$ is associated with the open chain with boundaries on these five-cycles. The conifold periods analog to Equation 10.3.1 can be studied using the recent results of [132, 231]. However, the relevant couplings, as discussed in section 10.1, should rather be encoded by $J \wedge \Psi$ integrated over the five-cycles involved in the transition.

We now obtain a possible reinterpretation of the perturbative field theory discussion in terms of geometry: the cubic terms that give rise upon Higgsing to mass couplings between the two $\mathbf{5}$ curves that recombine can be understood geometrically as being given by M2 instanton corrections wrapping the contracting three-cycle, as we approach the conifold point at $\tilde{a}_g = 0$. Notice that the discussion is reminiscent of the $\mathcal{N} = 2$ discussion in [228, 229]. It would be quite interesting here, for the same reasons, to elucidate the microscopics of the instanton viewpoint.

10.4 A Class of Examples with Discrete Symmetries

In this section, we present a class of Calabi-Yau manifolds that realize the effects discussed in the preceding discussion. To do so, we start in subsection 10.4.1 by constructing a class of elliptically fibered manifolds without section, with fiber a generic quartic in \mathbb{P}_{112} . Next, we enforce an $SU(5)$ singularity along a divisor of the base manifold and study the low-energy effective action of F-theory on the Calabi-Yau manifold. In subsection 10.4.2 we find that despite the absence of massless $U(1)$ gauge factors in the effective action, there are different matter curves distinguished by a discrete gauge symmetry that is a remnant of a massive $U(1)$ vector field. Furthermore, we encounter that not all the Yukawa couplings that would naively be allowed by the $SU(5)$ gauge symmetry are realized geometrically. In fact, we show that those couplings that do exist correspond precisely to those invariant under the additional discrete symmetry.

Moving to the conifold locus in complex structure moduli space we note in subsection 10.4.3 that one of the matter curves becomes reducible and splits into two parts. We note that this is a manifestation of the $U(1)$ becoming massless at the singular point and the restoration of the full Abelian gauge symmetry. Resolving the conifold singularities allows us to confirm that the map between the full $U(1)$ -charges and the charge under the discrete remnant group left over after the Higgsing process is as expected.

³Note that this kind of setup has been studied before in [230].

10.4.1 Hypersurface Equation in \mathbb{P}_{112}

Following the discussion of [chapter 8](#), we embed a genus-one curve inside \mathbb{P}_{112} . The most general such genus-one curve is given by [Equation 10.3.2](#), which we reproduce here

$$\begin{aligned} p_{112} &= \tilde{a}_0 w^2 + \tilde{a}_1 y_1^2 w + \tilde{a}_2 y_1 y_2 w + \tilde{a}_3 y_2^2 w + \tilde{a}_4 y_1^4 + \tilde{a}_5 y_1^3 y_2 + \tilde{a}_6 y_1^2 y_2^2 + \tilde{a}_7 y_1 y_2^3 + \tilde{a}_8 y_2^4 \\ &= 0, \end{aligned} \tag{10.4.1}$$

where the \tilde{a}_i determine the complex structure of the genus-one curve. After fibering the curve over a suitable base, the \tilde{a}_i become sections of line bundles over the base manifold. As discussed before, an elliptic fibration with such a generic fiber does not have a section, but rather a two-section defined by $y_1 = 0$. However, after tuning $\tilde{a}_8 \rightarrow 0$ the genus-one curve becomes singular and the two-section splits into two independent sections. These can then be most conveniently described after resolving the singularity obtained by the tuning. Note further that \mathbb{P}_{112} exhibits an orbifold singularity at the origin and, in general, this singularity should be resolved. Here, however, we restrain from doing so and instead impose a condition on \tilde{a}_0 later on that makes sure that our hypersurface does not hit the orbifold singularity.

Next, let us tune the complex structure coefficients in such a manner that the elliptic fibration obtains an $SU(5)$ singularity and then resolve this singularity using the methods of [chapter 4](#). As we saw there, the ambient fiber space \mathbb{P}_{112} has three inequivalent $SU(5)$ tops. Let us pick the first one, called $\tau_{4,1}$ in [figure 4.3](#), and denote the four blow-up variables and the variable corresponding to the affine node by e_i , $i = 0, \dots, 4$. Then this choice of $SU(5)$ top implies that the coefficients a_i must factor according to

$$\begin{aligned} \tilde{a}_0 &= e_0^2 e_1 e_4 \cdot a_0 & \tilde{a}_1 &= e_1 e_2 \cdot a_1 & \tilde{a}_3 &= e_0 e_3 e_4 \cdot a_3 & \tilde{a}_4 &= e_1^3 e_2^4 e_3^2 e_4 \cdot a_4 \\ \tilde{a}_5 &= e_1^2 e_2^3 e_3^2 e_4 \cdot a_5 & \tilde{a}_6 &= e_1 e_2^2 e_3^2 e_4 \cdot a_6 & \tilde{a}_7 &= e_2 e_3^2 e_4 \cdot a_7 & \tilde{a}_8 &= e_0 e_2 e_3^3 e_4^2 \cdot a_8, \end{aligned} \tag{10.4.2}$$

where the a_i are irreducible polynomials and $\tilde{a}_2 = a_2$. Unlike the \tilde{a}_i , it is crucial that the a_i depend on e_i only through the combination $e_0 e_1 e_2 e_3 e_4$.

10.4.2 Non-Abelian Matter Curves and Yukawa Points

Having tuned the complex structure coefficients in the above manner, the next step is to verify that this does produce an $SU(5)$ singularity and to examine what sort of matter representations arise at codimension two in the base manifold.

To do this, let us now compute the Weierstrass form [\(3.1.2\)](#) of the Jacobian of the above genus-one curve. One finds that the Weierstrass coefficients f and g also depend on the e_i only through the combination $e_0 e_1 e_2 e_3 e_4$ and we can therefore go to a patch in which

$e_1 = e_2 = e_3 = e_4 = 1$ without losing any information. In that case f and g read

$$\begin{aligned} f = & -\frac{1}{48} \cdot \left(a_2^4 - 8e_0 \cdot a_1 \cdot a_2^2 \cdot a_3 + 8e_0^2 \cdot (2a_1^2 a_3^2 - a_0 a_2^2 a_6 + 3a_0 a_1 a_2 a_7) \right. \\ & + 8e_0^3 \cdot a_0 \cdot (3a_2 a_3 a_5 - 2a_1 a_3 a_6 - 6a_1^2 a_8) \\ & \left. + 16e_0^4 \cdot a_0 \cdot (-3a_3^2 a_4 + a_0 a_6^2 - 3a_0 a_5 a_7) + 192e_0^5 \cdot a_0^2 a_4 a_8 \right) \end{aligned} \quad (10.4.3)$$

and

$$\begin{aligned} g = & \frac{1}{864} \cdot \left(a_2^6 - 12e_0 \cdot a_1 \cdot a_2^4 \cdot a_3 + 12e_0^2 \cdot a_2^2 \cdot (4a_1^2 a_3^2 - a_0 a_2^2 a_6 + 3a_0 a_1 a_2 a_7) \right. \\ & + 4e_0^3 \cdot (-16a_1^3 a_3^3 + 9a_0 a_2^3 a_3 a_5 + 6a_0 a_1 a_2^2 a_3 a_6 - 36a_0 a_1^2 a_2 a_3 a_7 - 18a_0 a_1^2 a_2^2 a_8) \\ & + 12e_0^4 \cdot a_0 \cdot (-6a_2^2 a_3^2 a_4 - 12a_1 a_2 a_3^2 a_5 + 8a_1^2 a_3^2 a_6 + 4a_0 a_2^2 a_6^2 \\ & \quad - 6a_0^2 a_2^2 a_5 a_7 - 12a_0^2 a_1 a_2 a_6 a_7 + 18a_0^2 a_1^2 a_7^2 + 24a_0 a_1^3 a_3 a_8) \\ & + 48e_0^5 \cdot a_0 \cdot (6a_1 a_3^3 a_4 - 3a_0 a_2 a_3 a_5 a_6 + 2a_0 a_1 a_3 a_6^2 + 18a_0 a_2 a_3 a_4 a_7 \\ & \quad - 3a_0 a_1 a_3 a_5 a_7 - 12a_0 a_2^2 a_4 a_8 + 18a_0 a_1 a_2 a_5 a_8 - 12a_0 a_1^2 a_6 a_8) \\ & + 8e_0^6 \cdot a_0^2 \cdot (27a_3^2 a_5^2 - 72a_3^2 a_4 a_6 - 8a_0 a_6^3 + 36a_0 a_5 a_6 a_7 - 108a_0 a_4 a_7^2 - 144a_1 a_3 a_4 a_8) \\ & \left. + 288e_0^7 \cdot a_0^3 \cdot (-3a_5^2 a_8 + 8a_4 a_6 a_8) \right). \end{aligned} \quad (10.4.4)$$

From that it follows directly that the discriminant, defined by $\Delta = 4f^3 + 27g^2$, obeys

$$\begin{aligned} \Delta = & \frac{a_0^2}{16} \cdot \left(e_0^5 \cdot a_2^4 \cdot (-a_3 a_7 + a_2 a_8) \cdot (-a_2^3 a_4 + a_1 a_2^2 a_5 - a_1^2 a_2 a_6 + a_1^3 a_7) \right. \\ & - e_0^6 \cdot a_2^2 \cdot (a_2^4 a_3^2 a_4 a_6 - a_1 a_2^3 a_3^2 a_5 a_6 + a_1^2 a_2^2 a_3^2 a_6^2 + 11a_1 a_2^3 a_3^2 a_4 a_7 \\ & \quad - 10a_1^2 a_2^2 a_3^2 a_5 a_7 + 8a_1^3 a_2 a_3^2 a_6 a_7 - 8a_1^4 a_3^2 a_7^2 + a_0 a_2^4 a_4 a_7^2 \\ & \quad - a_0 a_1 a_2^3 a_5 a_7^2 + a_0 a_1^2 a_2^2 a_6 a_7^2 - a_0 a_1^3 a_2 a_7^3 - 12a_1 a_2^4 a_3 a_4 a_8 \\ & \quad \left. + 11a_1^2 a_2^3 a_3 a_5 a_8 - 10a_1^3 a_2^2 a_3 a_6 a_8 + 8a_1^4 a_2 a_3 a_7 a_8 + a_1^4 a_2^2 a_8^2) \right. \\ & + e_0^7 \cdot (a_2^5 a_3^3 a_4 a_5 - a_1 a_2^4 a_3^3 a_5^2 + 10a_1 a_2^4 a_3^3 a_4 a_6 - 8a_1^2 a_2^3 a_3^3 a_5 a_6 + 8a_1^3 a_2^2 a_3^3 a_6^2 \\ & \quad + 40a_1^2 a_2^3 a_3^3 a_4 a_7 - 32a_1^3 a_2^2 a_3^3 a_5 a_7 + a_0 a_2^5 a_3 a_5^2 a_7 + 16a_1^4 a_2 a_3^3 a_6 a_7 \\ & \quad - 12a_0 a_2^5 a_3 a_4 a_6 a_7 + 8a_0 a_1 a_2^4 a_3 a_5 a_6 a_7 - 8a_0 a_1^2 a_2^3 a_3 a_6^2 a_7 - 16a_1^5 a_3^3 a_7^2 \\ & \quad + 48a_0 a_1 a_2^4 a_3 a_4 a_7^2 - 41a_0 a_1^2 a_2^3 a_3 a_5 a_7^2 + 46a_0 a_1^3 a_2^2 a_3 a_6 a_7^2 \\ & \quad - 36a_0 a_1^4 a_2 a_3 a_7^3 - 50a_1^2 a_2^4 a_3^2 a_4 a_8 + 40a_1^3 a_2^3 a_3^2 a_5 a_8 - a_0 a_2^6 a_5^2 a_8 \\ & \quad - 32a_1^4 a_2^2 a_3^2 a_6 a_8 + 16a_0 a_2^6 a_4 a_6 a_8 - 12a_0 a_1 a_2^5 a_5 a_6 a_8 + 12a_0 a_1^2 a_2^4 a_6^2 a_8 \\ & \quad + 16a_1^5 a_2 a_3^2 a_7 a_8 - 40a_0 a_1 a_2^5 a_4 a_7 a_8 + 34a_0 a_1^2 a_2^4 a_5 a_7 a_8 \\ & \quad \left. - 44a_0 a_1^3 a_2^3 a_6 a_7 a_8 + 30a_0 a_1^4 a_2^2 a_7^2 a_8 + 8a_1^5 a_2^2 a_3 a_8^2) + \mathcal{O}(e_0^8) \right). \end{aligned} \quad (10.4.5)$$

Obviously, there is an $SU(5)$ singularity along the GUT divisor defined by $e_0 = 0$. Additionally, if a_0 has zeros, there will be a further $SU(2)$ singularity whose Cartan divisor is

precisely the divisor obtained from blowing up the \mathbb{Z}_2 orbifold singularity of \mathbb{P}_{112} . Here we ignore this additional part by making sure later on that a_0 is in fact a constant, which implies that the Calabi-Yau hypersurface avoids the orbifold singularity. Furthermore, there are three different curves on the GUT divisor over which the $SU(5)$ singularity is enhanced, namely

$$T \equiv a_2 = 0 \quad (10.4.6)$$

$$F_1 \equiv -a_2^3 a_4 + a_1 a_2^2 a_5 - a_1^2 a_2 a_6 + a_1^3 a_7 = 0 \quad (10.4.7)$$

$$F_2 \equiv -a_3 a_7 + a_2 a_8 = 0. \quad (10.4.8)$$

Since we have that

$$f|_{T=0} = \mathcal{O}(e_0^2), \quad g|_{T=0} = \mathcal{O}(e_0^3), \quad \Delta|_{T=0} = \mathcal{O}(e_0^7) \quad (10.4.9)$$

$$f|_{F_1=0} = \mathcal{O}(e_0^0), \quad g|_{F_1=0} = \mathcal{O}(e_0^0), \quad \Delta|_{F_1=0} = \mathcal{O}(e_0^6) \quad (10.4.10)$$

$$f|_{F_2=0} = \mathcal{O}(e_0^0), \quad g|_{F_2=0} = \mathcal{O}(e_0^0), \quad \Delta|_{F_2=0} = \mathcal{O}(e_0^6) \quad (10.4.11)$$

we find that there are $SU(6)$ singularities along the curves $F_i = 0$ and that there is an $SO(10)$ singularity at $T = 0$. Consequently, the $F_i = 0$ curves host fundamental matter representations, while the $T = 0$ curve is the location of the antisymmetric $\mathbf{10}$ representation of $SU(5)$. We denote the representation located at $F_1 = 0$ and F_2 by $\mathbf{5}'$ and $\mathbf{5}''$, respectively.

Before proceeding any further, let us remark here already that without further gauge symmetries than $SU(5)$, one would not expect to find different $\mathbf{5}$ -curves as we just have. We therefore expect there to be an additional gauge symmetry that can differentiate the two curves. However, from the absence of sections we know that it cannot be an Abelian gauge group. It will, in fact, turn out to be a discrete symmetry that distinguishes the $\mathbf{5}$ -curves.

Next, let us consider the Yukawa points on the GUT divisor, i.e. those points at which several of the curves meet and the singularity is enhanced even further. We first consider points that involve the $\mathbf{10}$ representation. Since we have that

$$f|_{T=0} = -\frac{1}{3} \cdot \left(e_0^2 \cdot a_1^2 \cdot a_3^2 - e_0^3 \cdot a_0 \cdot a_1 \cdot (a_3 a_6 + 3a_1 a_8) \right. \\ \left. + e_0^4 \cdot a_0 \cdot (-3a_3^2 a_4 + a_0 a_6^2 - 3a_0 a_5 a_7) + 12e_0^5 \cdot a_0^2 a_4 a_8 \right) \quad (10.4.12)$$

$$g|_{T=0} = \frac{1}{864} \cdot \left(-64e_0^3 \cdot a_1^3 \cdot a_3^3 + 24e_0^4 \cdot a_0 \cdot a_1^2 \cdot (4a_3^2 a_6 + 9a_0^2 a_7^2 + 12a_0 a_1 a_3 a_8) \right. \\ \left. + 48e_0^5 \cdot a_0 \cdot a_1 \cdot (6a_3^3 a_4 + 2a_0 a_3 a_6^2 - 3a_0 a_3 a_5 a_7 - 12a_0 a_1 a_6 a_8) + \mathcal{O}(e_0^6) \right) \quad (10.4.13)$$

we find the enhancements listed in [table 10.1](#).

Additionally, there are couplings between the two $\mathbf{5}$ -curves and singlets under the non-Abelian gauge group. We do not give the explicit equation of the singlet curve here, but note that we find the couplings list in [table 10.2](#).

Equation	Involved curves	Singularity	Coupling	Multiplicity
$\{a_1 = 0\} \cap \{a_2 = 0\}$	T, F_1	non-minimal	-	0
$\{a_2 = 0\} \cap \{a_3 = 0\}$	T, F_2	E_6	$\mathbf{10} \times \mathbf{10} \times \mathbf{5}''$	27
$\{a_2 = 0\} \cap \{a_7 = 0\}$	T, F_1, F_2	$SO(12)$	$\mathbf{10} \times \bar{\mathbf{5}}' \times \bar{\mathbf{5}}''$	18

Table 10.1: Yukawa couplings involving only non-Abelian representations. Note that all the couplings are located on the GUT divisor defined by $e_0 = 0$. The multiplicities were evaluated explicitly for the example manifold given in [subsection 10.4.5](#).

Involved curves	Singularity	Coupling	Multiplicity
F_1, F_2	$SU(7)$	$\mathbf{1} \times \mathbf{5}' \times \mathbf{5}''$	108

Table 10.2: Yukawa couplings involving both non-Abelian and Abelian representations. Note that all the couplings are located on the GUT divisor defined by $e_0 = 0$. The multiplicities were evaluated explicitly for the example manifold given in [subsection 10.4.5](#).

10.4.3 Curve Splitting and Conifold Transition

Before going into the details of the particular base we used in order to compute the precise number of Yukawa points given in the above tables, let us first, in the spirit of [chapter 9](#), go to the conifold locus in moduli space, where we obtain a model with two sections, or equivalently an extra massless $U(1)$. This gives a curve of conifold singularities located at $a_3 = a_7 = 0$. As noted above, this corresponds to tuning $a_8 \rightarrow 0$. Interestingly, this transition has an effect on the $\mathbf{5}$ -curves in the geometry, since F_2 becomes reducible:

$$F_2|_{a_8=0} = - \underbrace{a_3}_{F_{2,1}} \cdot \underbrace{a_7}_{F_{2,2}} \quad (10.4.14)$$

If we denote the fundamentals at $F_{2,1} = 0$ by $\mathbf{5}''$ and those at $F_{2,2} = 0$ by $\mathbf{5}'''$ then we find the Yukawa couplings listed in [table 10.3](#).

In [table 10.4](#) we summarize the couplings that do not involve the antisymmetric representation. We do not give explicit expressions for the singlet curve involved in the first two couplings, as they are not complete intersections and contain a large number of terms.

At the conifold locus in complex structure moduli space, we can also compute the $U(1)$ -charges of the matter states using the techniques from [section 9.1](#). After rescaling the $U(1)$ factor to avoid fractional charges, we find the following charge assignments:

$$\mathbf{10} = \mathbf{10}_3, \quad \mathbf{5}' = \mathbf{5}_{-1}, \quad \mathbf{5}'' = \mathbf{5}_{-6}, \quad \mathbf{5}''' = \mathbf{5}_4 \quad (10.4.15)$$

Furthermore, we find that the singlet involved in the $\mathbf{1} \times \mathbf{5}'' \times \bar{\mathbf{5}}'''$ coupling has $U(1)$ -charge 10, while the singlets in the other two $\mathbf{5} \times \bar{\mathbf{5}}$ couplings have $U(1)$ -charge 5.

Equation	Involved curves	Singularity	Coupling	Multiplicity
$\{a_1 = 0\} \cap \{a_2 = 0\}$	T, F_1	non-minimal	-	0
$\{a_2 = 0\} \cap \{a_3 = 0\}$	$T, F_{2,1}$	E_6	$\mathbf{10} \times \mathbf{10} \times \mathbf{5}''$	27
$\{a_2 = 0\} \cap \{a_7 = 0\}$	$T, F_1, F_{2,2}$	$SO(12)$	$\mathbf{10} \times \bar{\mathbf{5}}' \times \bar{\mathbf{5}}'''$	18

Table 10.3: Yukawa couplings involving only non-Abelian representations. Note that all the couplings are located on the GUT divisor defined by $e_0 = 0$. The multiplicities were evaluated explicitly for the example manifold given in [subsection 10.4.5](#) after transitioning to the conifold point and resolving the singularities appearing there.

Equation	Involved curves	Singularity	Coupling	Multiplicity
-	$F_1, F_{2,1}$	$SU(7)$	$\mathbf{1} \times \mathbf{5}' \times \bar{\mathbf{5}}''$	54
-	$F_1, F_{2,2}$	$SU(7)$	$\mathbf{1} \times \mathbf{5}' \times \bar{\mathbf{5}}'''$	54
$\{a_3 = 0\} \cap \{a_7 = 0\}$	$F_{2,1}, F_{2,2}$	$SU(7)$	$\mathbf{1} \times \mathbf{5}'' \times \bar{\mathbf{5}}'''$	54

Table 10.4: Yukawa couplings involving both non-Abelian and Abelian representations. Note that all the couplings are located on the GUT divisor defined by $e_0 = 0$. The multiplicities were evaluated explicitly for the example manifold given in [subsection 10.4.5](#) after transitioning to the conifold point and resolving the singularities appearing there.

10.4.4 Discrete Charges and Forbidden Yukawa Couplings

Finally, let us move away from the conifold locus again by deforming $\tilde{a}_8 \neq 0$. Looking at the multiplicities of the Yukawa couplings given in tables [10.1](#), [10.2](#), [10.3](#), and [10.4](#), the following picture about the physics of the deformation process suggests itself rather naturally. The action takes place on the $\mathbf{5}'' = \mathbf{5}_{-6}$ and $\mathbf{5}''' = \mathbf{5}_4$ curves, since they have the same \mathbb{Z}_2 charge according to [\(10.2.5\)](#). We observe that precisely where these two curves intersect, they have a Yukawa coupling with the $\mathbf{1}_{10}$ singlet parameterizing the deformation. As this singlet gets a vacuum expectation value, the two curves recombine into a single object that we called $\mathbf{5}''$ in [subsection 10.4.2](#). Since this is a local operation close to the intersection of the two curves, we expect the rest of the Yukawa couplings involving the $\mathbf{1}_5$ singlets to simply come along for the ride. And indeed, the multiplicities of the Yukawa points are conserved, if one compares with the results in the previous section.

To finish this subsection, let us quickly summarize the \mathbb{Z}_2 charges of the matter curves

away from the conifold locus. There one finds that⁴

$$Q_{\mathbb{Z}_2}(\mathbf{5}') = 1, \quad Q_{\mathbb{Z}_2}(\mathbf{5}'') = 0, \quad Q_{\mathbb{Z}_2}(\mathbf{10}) = 1, \quad (10.4.16)$$

which is compatible with the couplings we found in [table 10.1](#). Note that this is precisely what we expect based on the discussion of [section 10.2](#). In particular, we find that the coupling

$$\mathbf{10} \times \mathbf{10} \times \mathbf{5}' \quad (10.4.17)$$

is not invariant under the \mathbb{Z}_2 action and is *not realized geometrically*, although it would be allowed by all massless continuous symmetries.

10.4.5 An Explicit Example without Non-Minimal Singularities

After keeping much of the previous discussion independent of the actual choice of base manifold, let us now present the toric data of an explicit example here. In doing this, it is important to recall that as soon as one considers three-dimensional base manifolds, there will generally be non-minimal singularities corresponding to non-flat points of the fibration. We took this into account in the above discussion, making [tables 10.1](#) and [10.3](#) both contain an entry corresponding to such a non-minimal singularity. The relevant conditions will generically have non-trivial solutions at codimension three in the base manifold. The fact that there generically are such non-flat points does not imply that examples without them are impossible, or particularly convoluted. The condition one needs to satisfy is

$$\{a_1 = 0\} \cap \{a_2 = 0\} = \emptyset \quad (10.4.18)$$

and as we will now show some simple geometries admit solutions to this equation.

Our explicit model is as follows. Take a toric ambient space defined by a fine star triangulation of the rays given in [table 10.5](#). As can be seen from the defining data, the generic ambient fiber space is \mathbb{P}_{112} .

The base manifold is $\mathbb{P}^1 \times \mathbb{P}^2$ and the resolved $SU(5)$ singularity discussed in [subsection 10.4.1](#) lies on the base divisor $\{\text{pt}\} \times \mathbb{P}^2 \subset \mathbb{P}^1 \times \mathbb{P}^2$. Note that making the geometric transition by going to the conifold locus and resolving the conifold singularities corresponds torically to introducing another ray with entries $(0, 1, 0, 0, 0)$ as in [section 9.3](#), which automatically imposes $a_8 = 0$.

Given the explicit data of the ambient space in which our Calabi-Yau manifold is embedded, there is an easy way of confirming the absence of non-flat points. As discussed in [chapter 5](#), at the non-flat points one of the irreducible fiber components grows an extra dimension. In the notation of [table 10.5](#), the irreducible fiber components are the horizontal parts of the exceptional divisors $e_i = 0$. The irreducible fiber component which generically

⁴Note that since we are not at the conifold locus anymore, $\mathbf{5}''$ corresponds to the matter curve $F_2 = 0$.

Homogeneous coordinate z	Point $n_z \in \nabla \cap N$				
v_0	-3	-3	0	1	0
v_1	0	0	0	0	1
v_2	0	0	0	-1	-1
u_1	0	-1	-1	0	0
e_0	0	0	1	0	0
e_1	-1	1	1	0	0
e_2	-2	1	1	0	0
e_3	-2	0	1	0	0
e_4	-1	0	1	0	0
y_2	-1	-1	0	0	0
y_1	-1	1	0	0	0
w	1	0	0	0	0

Table 10.5: Homogeneous coordinates of the ambient toric space and the corresponding rays of the toric fan.

jumps in dimension is the one whose ray does not correspond to a vertex of the top, i.e. $e_4 = 0$.

Let us therefore examine this component with care. On the divisor $e_4 = 0$ the hypersurface equation (10.4.1) reduces to

$$p_{112}|_{e_4=0} = \tilde{a}_1 \cdot y_1^2 w + \tilde{a}_2 \cdot y_2^2 w. \tag{10.4.19}$$

However, for the above choice of space, one finds that

$$\tilde{a}_1 = e_1 e_2 \cdot \underbrace{(\alpha_1 e_0 + \alpha_2 v_1)}_{a_1}, \tag{10.4.20}$$

with α_i two generically non-zero constants. In the base, e_0 and v_1 are just the homogeneous coordinates of a \mathbb{P}_1 and in particular $e_0 = v_1 = 0$ is forbidden. As a consequence, there are no solutions to $e_0 = a_1 = 0$.

Part IV

Closing Remarks

Chapter 11

Conclusion

In this final chapter we conclude by briefly summarizing the contents of this thesis and pointing out several open research questions that could potentially be relevant to future investigations.

11.1 A Brief Summary

The work presented in this work can largely be categorized into two subjects, as is reflected in the structure of this thesis: First, we established a framework in order to systematically construct and analyze genus-one fibered Calabi-Yau manifolds of different dimensions. Second, we used these manifolds in order to compute the low-energy effective theories that F-theory compactifications on them give rise to. Given how clearly separated the two topics are in this thesis, it is important to keep in mind that there is no advantage in pursuing them individually when carrying out actual research. Instead, many of the advances come through the interplay of geometric and physical problems. Oftentimes physical questions provide the motivation to study the “relevant” geometric quantities or give an intuition for what the answer should be. Naturally, this exchange works in the opposite direction as well: As we have emphasized repeatedly, much of the computational control that we have over F-theory vacua comes from the advanced geometrical tools that complex algebraic geometry provides. Nevertheless, let us adhere to the structure of this thesis and begin by recapitulating the contents of [Part II](#).

The first step in a systematic construction of genus-one fibered Calabi-Yau manifolds is to identify the building blocks that can be studied separately. Our analysis led to a three-step procedure: Begin by constructing the genus-one fiber by embedding it into an appropriate ambient space, use reducible ambient spaces in order to engineer reducible fibers that become singular in some blow-down limit, and complete the *top* that one has thus obtained into a fibered ambient space. Apart from a few exceptions, all of our computational control over the Calabi-Yau manifolds is inherited from the power that we have over the ambient spaces in which these are embedded and which can be controlled using toric geometry.

To understand the geometry of the genus-one fibers, one must essentially control two quantities: The discriminant and the Mordell-Weil group. While discriminants can always be computed from a Weierstrass model and every genus-one curve has an associated Weierstrass model that shares the same discriminant, finding the map to this Weierstrass model is in general an unsolved problem. In fact, it is the key technical obstacle that we needed to overcome. To solve this problem for a large range of genus-one curves defined as complete intersections, we presented an algorithm that uses an old idea of Deligne to embed the genus-one curve into one of four toric ambient spaces for which the maps to Weierstrass form have been worked out. Notably, the details of the algorithm are independent of toric methods. Given the map from a genus-one curve inside a certain ambient space to its Weierstrass form, one can immediately compute the Mordell-Weil group of the curve. After fibering the curve over a base manifold, additional generators may appear, but the generators of the generic genus-one curve in this ambient space will still form a subgroup, that we call the *toric* Mordell-Weil group. To assess the effectiveness of our algorithm, we successfully applied it to the 3134 genus-one curves obtained as complete intersections of codimension two. We used the Weierstrass forms that we thus obtained in order to classify the toric Mordell-Weil groups of all hypersurface and codimension-two complete intersections fibers and furthermore also determined all possible non-toric non-Abelian gauge groups. For the first time, we identified torsional Mordell-Weil groups, extended the Mordell-Weil ranks that one can construct and explained in detail the properties of non-holomorphic sections.

In the next step, we carefully studied the formalism of toric fibrations and their degenerations that are captured by tops. We computed all possible $SU(5)$ tops for hypersurface fibers and explained how constraints on the Abelian matter charges can be directly read off from the combinatorial data of the top. Furthermore, we provided a rigorous proof that hypersurface fibers will never lead to multiple antisymmetric $SU(5)$ representations in the low-energy effective theory and that motivates the study of the more complicated class of complete intersection fibers.

Finally, we suggested the first algorithm to systematically and quickly enumerate all possible ways in which a given top can be fibered over a base manifold. We explained that full-fledged fibrations must satisfy at least one additional consistency condition, namely the flatness of the fibration. To check for flatness, we formulated a combinatorial condition on the data of the toric ambient space and showed that flatness is non-generic with respect to an auxiliary polytope encoding the full set of fibrations. As an illustration of our methods, we constructed a number of example fibrations, showed how to use toric methods in order to compute matter charges, constructed $SU(5)$ models with multiple antisymmetric representations and explained how to obtain the discrete symmetry group \mathbb{Z}_4 .

Having developed a framework to generate large classes of appropriately fibered Calabi-Yau manifolds, we turned to computing the low-energy effective actions that result from considering F-theory on these compactification manifolds. Gauge groups and matter are

already present in six-dimensional F-theory models and we therefore focused on computing the six-dimensional effective action in the presence of Abelian gauge groups by extending the work of [54]. Finding the effective action of F-theory in a given dimension consists of several parts: First one reduces M-theory on the relevant Calabi-Yau manifold, then one computes a circle-compactification of a generic even-dimensional supergravity, and finally one integrates out massive modes to match the quantum-corrected circle theory to the M-theory compactification.

For the first time, we determined the low-energy effective theory of F-theory on Calabi-Yau manifolds with multiple and possibly non-holomorphic sections. We found that non-holomorphy of the zero section can lead to a shift in the Kaluza-Klein hierarchy such that the zero mode of the Kaluza-Klein tower of a charged field may no longer be the lightest mode. In the absence of such shifts, we proved that the gravitational and mixed anomalies of a general six-dimensional F-theory model are automatically canceled.

With the Abelian gauge groups under control, we then proceeded to study the effective action of F-theory on a genus-one fibered Calabi-Yau manifold without section. We found that the physical implication of such a model is the presence of an additional massive Abelian gauge field. In order to carry out the M-/F-theory duality, it is necessary to perform a fluxed circle reduction, where the Stückelberg axion of the massive gauge field has a non-trivial flux background. Furthermore, we showed that one can employ a conifold transition from the circle-reduced theory of F-theory with a massive $U(1)$ to a circle-reduction of another F-theory model with a massless gauge field. Geometrically, this process can easily be understood: Under the conifold transition, the two-section is disentangled and transformed into two separate independent global sections that give rise to a rank-one Mordell-Weil group.

Last of all, we explored another feature of F-theory models without section, namely the presence of discrete symmetries. Since the axion that gives a mass to the gauge field is doubly-charged in the models with a two-section¹, we expect a \mathbb{Z}_2 remnant of the formerly massless Abelian symmetry to survive. And in fact, a close analysis of the relevant geometry shows that the only realized Yukawa couplings are those with neutral charges under the discrete symmetry, leading to the conclusion that discrete symmetries in F-theory models can be implemented by models without sections. Notably, this is another example of physical intuition motivating a mathematical result, namely that certain matter curves should be distinguishable and therefore consist of multiple reducible components. This is a well-defined geometric property property that one would a priori not have associated with the presence of a multisection.

¹In the case of an n -section, the charge of the axion is adjusted correspondingly.

11.2 Future Areas of Research

There are various exciting ways in which the research presented in this work could be extended. In addition to the more global long-term research objectives mentioned at the end of this section, there exist several very specific, albeit somewhat technical projects that one could initiate immediately. The most obvious objective would be to understand the large number of complete intersection fibrations that have become accessible with the introduction of the algorithm to compute their Weierstrass forms. Repeatedly, we have had to revise our understanding of F-theory models upon encountering more general cases and there is good reason to expect the same to happen again for the much larger set of models that have now been unlocked.

In order to carry out the same manipulations for complete intersection fibers that we can already perform for hypersurface fibers, it might be helpful to first solve two technical problems: Classifying three-dimensional tops and speeding up star triangulations of polytopes. A classification of higher-dimensional tops similar to that of [161] would allow one to systematically and quickly construct all toric singularity resolutions inside a given fiber. In the two-dimensional case, the geometry of the tops is closely related to the intersection matrix of the exceptional divisors. Generalized to higher dimensions, the relation is not as obvious, but we would expect it to exist nevertheless. Easier and yet possibly of more practical importance is an efficient implementation of star triangulations in Sage. As suggested in [179], the type of triangulation relevant to our set-ups can be made considerably faster by exploiting that they are star triangulations with respect to the origin, since the full triangulation can then be reduced to triangulating the facets. In fact, one could go further and repeat this step recursively, which should ideally allow for a massive parallelization of the problem. Another feature ubiquitous in complete intersection fiber models is the presence of product gauge groups. It would be important to understand their geometry in detail and control the singularity enhancement along the overlap of different gauge singularities.

Compared to just over a year ago, multisections in F-theory are now much better understood. Nevertheless, only the simplest examples have been tackled yet and a systematic treatment of an arbitrary genus-one fibered Calabi-Yau manifold may still prove difficult. One of the simplest questions concerns the type of divisor basis one can choose for a general genus-one fibration: Can one possibly have multiple independent multisections but no section? Would it be possible to construct models with a two-section and a three-section that are independent in homology and that do not have a globally defined section? If so, what is the effective physics of such a set-up? Moreover, we have seen that multisections lead to discrete symmetry groups. So far, they have all been Abelian — can one also construct non-Abelian groups? Clearly, this may be less straightforward, as the Abelian symmetry groups appear to be related to the Mordell-Weil group of the mirror dual of the fiber, which must always be Abelian. However, it is conceivable that the Mordell-Weil group only captures the center of the discrete symmetry, similarly to how only the Cartan generators are present in

the M-theory reduction and the W-bosons are supplied by additional M2 brane states.

Another promising and ambitious direction of research is to improve our understanding of the entire landscape of F-theory models. It is already known that many F-theory compactifications can be connected to each other by Higgsings or transitions between different wedges in the Coulomb branch of the field theory. Given how enticing a *global* understanding of the set all of F-theory vacua would be, it seems promising to extend the network mapped out in [144] to complete intersections. A more difficult, but possibly very rewarding question to ask is whether complicated field theoretic dualities, for example in four and six dimensions, can be incorporated into such a network of F-theory vacua. A program of this kind was initiated in [232, 233] and it would be interesting to pursue this further. Insights into such dualities may also benefit from a better understanding of the duality between F-theory with Abelian gauge factors and the Heterotic String as well as a better control over the weak-coupling limit of F-theory. Both are interesting and complex topics on their own and merit detailed study.

Finally, there is a plethora of issues that we touched only briefly on in [section 2.6](#) and which need to be addressed if F-theory is ever to produce a realistic GUT model. Of all the problems mentioned here, this is very likely the most complex. And yet, it must eventually be answered if string theory studied through F-theory is some day to be taken seriously as a candidate for a theory of everything.

Part V

Appendices

Appendix A

A Brief Introduction to Toric Geometry

In this appendix, we would like to briefly introduce a few of the key concepts of toric geometry used in this work. All of the results mentioned here have long been known in the math literature and we would like to point out two of the standard works on toric geometry, namely [234, 235]. There also exists a number of introductions to toric geometry in the physics literature, such as [215, 236–238] and we draw from all of them here.

Toric varieties owe their name to a very special property that is the underlying reason for the ease with which many calculations can be reduced to combinatorial problems: A toric variety X of dimension d contains a d -dimensional algebraic torus $\mathbb{T}^d \cong (\mathbb{C}^*)^d$ together with an action of this torus on the variety itself:

$$\mathbb{T}^d \times X \rightarrow X \tag{A.0.1}$$

Every d -dimensional toric variety can be obtained from a quotient

$$X = \frac{\mathbb{C}^n \setminus Z}{(\mathbb{C}^*)^m \times \Gamma}, \tag{A.0.2}$$

where $d = n - m$ and Z is the union of a set of hyperplanes containing the origin. In particular, this means that $\mathbb{T}^d \subseteq \mathbb{C}^n \setminus Z$. Then the algebraic torus inside in X is contained in what survives after quotienting $\mathbb{C}^n \setminus Z$ by \mathbb{T}^m . In the next subsection, we will explain how to encode the explicit torus action and the data in [Equation A.0.2](#) using a set of combinatorial objects.

A.1 Toric Varieties from Fans

Before making a connection to toric varieties, let us introduce a few conventions and define the key objects.

Let $N \cong \mathbb{Z}^d = \mathbb{Z}^{n-m}$ be a lattice and denote its dual lattice by $M \cong \mathbb{Z}^d$. The tensor product with \mathbb{R} , $N_{\mathbb{R}} = N \otimes \mathbb{R}$, is the d -dimensional vector space obtained by allowing real coefficients for the generators of N . By a *rational polyhedral cone* σ in $N_{\mathbb{R}}$ we mean the set

$$\sigma = \langle v_1 \dots v_k \rangle \equiv \left\{ \sum_i a_i v_i, a_i \in \mathbb{R}_{\geq 0} \right\} \quad (\text{A.1.1})$$

generated by k vectors $\{v_i \in N\}$. We denote by $-\sigma$ the cone generated by $\{-v_i \in N\}$. If $\sigma \cap -\sigma = \{0\}$, then σ is called *strongly convex*. A cone σ' that is spanned by a subset of the generators of σ and is part of the boundary of σ is called a *face* of σ . If σ' is k -dimensional, then it is called a k -face of σ .

A collection of strictly convex rational polyhedral cones $\{\sigma_i\}$ is called a fan Σ if it satisfies the following two properties:

- Every face of a cone is also a cone of the fan.
- Given two cones σ_i and σ_j , their intersection $\sigma_i \cap \sigma_j$ is a face of both cones.

The one-dimensional cones, $\Sigma(1)$, are called *rays* and the $(\dim \Sigma - 1)$ -dimensional cones are the *facets* of Σ .

A fan Σ determines a toric variety X_{Σ} completely. Denote by v_1, \dots, v_n the rays of Σ and associate a homogeneous coordinate z_i to each of them. These z_i parametrize the space \mathbb{C}^n appearing in the numerator of Equation A.0.2. Next, to every subset of rays v_{i_1}, \dots, v_{i_k} that does not generate a cone of Σ , assign a hyperplane $z_{i_1} = \dots = z_{i_k} = 0$. The point set Z excluded from \mathbb{C}^n in Equation A.0.2 is the union of these hyperplanes. Furthermore, one can associate to each such subset of rays (or alternatively each such hyperplane) the monomial $\prod_{j=1}^k z_{i_j}$. The ideal in the coordinate ring $\mathbb{Q}[z_1, \dots, z_n]$ generated by these monomials is called the *Stanley-Reisner ideal* of X and we denote it by $\text{SRI}(X)$.

The torus action is also determined in terms of the rays. Consider the map

$$\phi : (\mathbb{C}^*)^n \rightarrow (\mathbb{C}^*)^{n-m}, (z_1, \dots, z_n) \mapsto \left(\prod_i z_i^{v_i^1}, \dots, \prod_i z_i^{v_i^{n-m}} \right). \quad (\text{A.1.2})$$

The preimage $I \equiv \phi^{-1}((1, \dots, 1)) \cong (\mathbb{C}^*)^m$ then determines the action that is divided out in Equation A.0.2. Let us understand how this works in detail: $(\mathbb{C}^*)^n$ has of course a natural action on \mathbb{C}^n simply by componentwise multiplication:

$$(\mathbb{C}^*)^n \times \mathbb{C}^n \rightarrow \mathbb{C}^n : ((\lambda_1, \dots, \lambda_n), (z_1, \dots, z_n)) \mapsto (\lambda_1 z_1, \dots, \lambda_n z_n) \quad (\text{A.1.3})$$

We can abbreviate this by writing $\lambda \cdot z$. Note that if $z \in (\mathbb{C}^*)^n$, then $\lambda \cdot z \in (\mathbb{C}^*)^n$, too. Now let $\lambda \in I$. Then $\phi(\lambda \cdot z) = \phi(z)$ for all $z \in (\mathbb{C}^*)^n$. One can hence divide out the group action generated by all elements of I and use the coordinates $\{\prod_i z_i^{v_i^j}, j = 1, \dots, n-m\}$ as affine

coordinates for the resulting space. It is easy to find an explicit expression for the group action generated by $I \cong (\mathbb{C}^*)^m$. By plugging a general ansatz into Equation A.1.2, one finds that I consists of elements

$$\left(\lambda^{Q_a^1}, \dots, \lambda^{Q_a^n}\right) \tag{A.1.4}$$

with charges Q_a^n satisfying

$$\sum_{i=1}^n v_i Q_a^i = 0. \tag{A.1.5}$$

Put differently, the m charge vectors Q_a are the linear relations that the rays v_i satisfy among each other.

The last missing ingredient in (A.0.2) is the discrete finite group Γ . Denote by N' the lattice generated by the rays of Σ . Then

$$\Gamma = \frac{N}{N'}. \tag{A.1.6}$$

If the rays do not generate all of N , there are thus additional orbifold singularities.

A.1.1 Examples and Connection to GLSM Description

Let us close this section by studying a few examples and by comparing this approach to the definition of a toric variety as the vacuum moduli space of a gauged linear sigma model.

To understand how this alternative description arises, consider n chiral superfields $Z_i \in \mathbb{C}$, $i = 1, \dots, n$ charged under the gauge group $U(1)^m$ and let the charge of the i^{th} field under the $U(1)$ factors be Q_a^i , $a = 1, \dots, m$. Furthermore, denote by z_i the scalar components of the superfields and by $\zeta_a \in \mathbb{R}$, $a = 1, \dots, m$ the m Kähler (or, in physics language, Fayet-Iliopoulos) parameters. Now consider the classical moduli space of vacua of this Abelian theory. As one learns in a lecture on supersymmetry, one obtains the moduli space by a two-step procedure. First, one has to solve the m real D-term constraints

$$\sum_{i=1}^n Q_a^i |z_i|^2 = \zeta_a \quad \forall \zeta_a, \quad a = 1, \dots, m \tag{A.1.7}$$

and secondly, one must fix the remaining $U(1)^m$ gauge freedom. If the choice of ζ_a is such that the resulting space is $(n - m)$ -complex-dimensional, then it is the toric variety corresponding to this GLSM.¹

We thus find the following dictionary between the description via a fan and the description in terms of a vacuum moduli space of a GLSM:

$$\begin{aligned} \text{scalar fields } z_i &\leftrightarrow \text{rays } v_i \\ \text{charge vectors } Q_a &\leftrightarrow \text{linear relations between rays } v_i \end{aligned} \tag{A.1.8}$$

¹For a general values of ζ_a and in particular $\zeta_a < 0$, there exist other non-geometric phases. A very nice discussion of such phases and the transitions between them is contained in [239].

The map between the two sides is not as obvious for the excluded set of points Z . In the fan picture Z can just be read off, while in the GLSM approach it generally depends on the choice of ζ_a . This difference might appear startling, as the ζ_a seem to be additional input. However, the same information is contained in the fan. While the Q_a depend solely on the rays of the fan, Z is determined also by higher-dimensional cones. In two dimensions there is a unique fan for a given set of rays. However, in higher dimensions this is no longer true and in general, there will be many different fans with the same set of rays.

To understand this, we start with the two-dimensional case. Given a set of rays $\{v_i\}$ $i = 1, \dots, n$, there is a unique way to order them, for instance by the angle between a ray and the positive part of the x -axis. Assuming that the rays obey this particular ordering, we can choose as two-dimensional cones

$$\sigma_i = \langle v_i v_{i+1} \rangle, \quad (\text{A.1.9})$$

where we set $v_{n+1} = v_1$ and together with the rays that gives us a fan Σ . For example, consider the four rays

$$\Sigma_{dP_1}(1) = \left\{ \begin{pmatrix} 1 \\ 0 \end{pmatrix}, \begin{pmatrix} 1 \\ 1 \end{pmatrix}, \begin{pmatrix} 0 \\ 1 \end{pmatrix}, \begin{pmatrix} -1 \\ -1 \end{pmatrix} \right\}. \quad (\text{A.1.10})$$

The unique fan with these rays is displayed in [figure A.1](#). To illustrate how to obtain a toric variety from a fan, let us follow the steps outlined above. Since there are $n = 4$ rays we start with four homogeneous coordinate parametrizing a \mathbb{C}^4 . Neither v_2 and v_4 , nor v_1 and v_3 are contained simultaneously in any of the cones, and therefore we must exclude the point set $Z = \{z_2 = z_4 = 0\} \cup \{z_1 = z_3 = 0\}$. The lattice is two-dimensional and thus there must be $m = n - 2 = 2$ independent relations between the four rays giving rise to two independent \mathbb{C}^* -actions. Two such relations are, for instance,

$$v_1 + v_3 + v_4 = 0, \quad v_2 + v_4 = 0. \quad (\text{A.1.11})$$

From their coefficients, we see that the two charge vectors are $Q_1 = (1 \ 0 \ 1 \ 1)^T$ and $Q_2 = (0 \ 1 \ 0 \ 1)^T$. Put differently, we quotient out the following two equivalence relations:

$$[z_1 : z_2 : z_3 : z_4] \sim [\lambda z_1 : z_2 : \lambda z_3 : \lambda z_4], \quad [z_1 : z_2 : z_3 : z_4] \sim [z_1 : \mu z_2 : z_3 : \mu z_4], \quad (\text{A.1.12})$$

where $\lambda, \mu \in \mathbb{C}^*$. Since the rays of [Equation A.1.10](#) generate \mathbb{Z}^2 , there is no additional discrete quotient.

In higher dimensions, there is no such unique ordering. As a simple illustration, consider the *conifold* whose fan has the following four rays:

$$\Sigma(1) = \left\{ \begin{pmatrix} 0 \\ 0 \\ 1 \end{pmatrix}, \begin{pmatrix} 1 \\ 0 \\ 1 \end{pmatrix}, \begin{pmatrix} 1 \\ 1 \\ 1 \end{pmatrix}, \begin{pmatrix} 0 \\ 1 \\ 1 \end{pmatrix} \right\} \quad (\text{A.1.13})$$

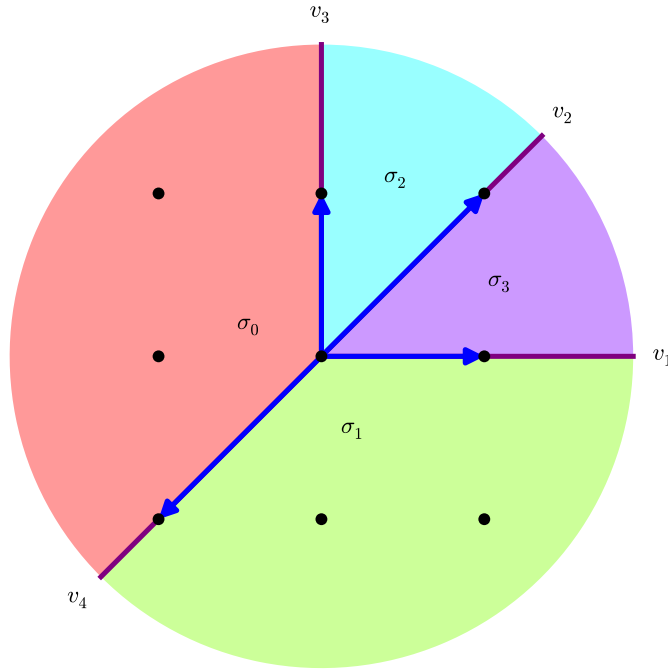


Figure A.1: Toric fan of dP_1 .

There are two inequivalent ways of splitting these four rays into two three-dimensional cones, namely either

$$\Sigma(3) = \{ \langle v_1 v_2 v_3 \rangle, \langle v_3 v_4 v_1 \rangle \} \tag{A.1.14}$$

or

$$\Sigma'(3) = \{ \langle v_1 v_2 v_4 \rangle, \langle v_2 v_3 v_4 \rangle \} . \tag{A.1.15}$$

Both of them generate perfectly valid fans, but they correspond to different resolutions of the space defined by

$$z_1 z_2 - z_3 z_4 = 0 \tag{A.1.16}$$

with $z_i \in \mathbb{C}$, which is singular at the origin $z_i = 0$. Neither Σ nor Σ' contain the singular point, but they exclude different point regions. We have

$$Z_\Sigma = \{ z_2 = z_4 = 0 \}, \quad Z_{\Sigma'} = \{ z_1 = z_3 = 0 \} . \tag{A.1.17}$$

Since the toric varieties X_Σ and $X_{\Sigma'}$ associated with the two fans have different excluded point sets, their intersection numbers will generally be different, too. Furthermore, also their Kähler and Mori cones disagree. In this sense the additional information contained in the ζ_a in the GLSM construction corresponds to choosing a fan given a fixed set of rays, as it is the Kähler and the Mori cones that depend directly on the ζ_a in the GLSM picture.

A.2 Compactness, Smoothness, and Orbit-Cone Correspondence

In this section we further explore the description of toric varieties using fans. We explain how to map subsets of the toric variety to associated cones of the fan and discuss how to read off complex properties of X_Σ such as smoothness and compactness from properties of the fan Σ .

A.2.1 Orbit-Cone Correspondence

The orbit-cone correspondence provides a neat visual interpretation of a toric fan Σ by associating the k -dimensional cones with k -codimensional subsets of X_Σ . To understand how the correspondence works, one must consider the orbits under the torus action.

First, recall that given a group G and an element $x \in X$ on which G acts the orbit $G.x$ is defined as

$$G.x = \{gx, \forall g \in G\} \tag{A.2.1}$$

and the set of all different orbits is the familiar quotient X/G . Consider now the orbits of \mathbb{C}^n under the multiplicative action of $(\mathbb{C}^*)^n$. There is a total of 2^n orbits, $\binom{n}{k}$ of which one obtains by setting k coordinates of \mathbb{C}^n to zero. To be explicit, let $n = 3$. Then the eight different orbits are given by

$$\begin{array}{ccc} \underbrace{(0, 0, 0)}_{\text{zero-dimensional}} & \underbrace{(\lambda_1, 0, 0), (0, \lambda_1, 0), (0, 0, \lambda_1)}_{\text{one-dimensional}} & \\ \underbrace{(\lambda_1, \lambda_2, 0), (\lambda_1, 0, \lambda_2), (0, \lambda_1, \lambda_2)}_{\text{two-dimensional}} & \underbrace{(\lambda_1, \lambda_2, \lambda_3)}_{\text{three-dimensional}} & \end{array} \tag{A.2.2}$$

with $\lambda_i \in \mathbb{C}^*$. Put differently, there is always one n -dimensional orbit defined by $z_i \neq 0 \forall i$, $\binom{n}{1} = n$ $(n-1)$ -dimensional orbits defined by allowing precisely one coordinate to be zero, and similarly $\binom{n}{k}$ k -dimensional orbits defined by demanding that *exactly* k coordinates vanish.

Next, consider the closure of these torus orbits. The closure of a k -dimensional orbit is obtained by requiring that *at least* k coordinates vanish, i.e. one has the same expression as in [Equation A.2.2](#), but with $\lambda_i \in \mathbb{C}$. These closures form a poset, a partially ordered set, with respect to inclusion \subseteq . For the above example, the poset structure is illustrated in [figure A.2](#).

After this lengthy introduction, let us make the connection with toric varieties and their fans. Given a toric variety with n homogeneous coordinates as defined in [Equation A.0.2](#), we can analyze its orbits under the action of $(\mathbb{C}^*)^n$. The analysis is essentially the same as for \mathbb{C}^n , with the slight modification that the orbits contained in the excluded set Z are absent. The orbit closures of \mathbb{P}^2 , for example, are the same as those in [figure A.2](#) apart from the point $(0, 0, 0)$ that does not belong to \mathbb{P}^2 . Next, to every k -dimensional cone $\sigma = \langle v_{i_1} \dots v_{i_k} \rangle$ associate the orbit closure of codimension k defined as $\{z_{i_1} = \dots = z_{i_k} = 0\}$ and denote it by $V(\sigma)$. Conveniently, this map is bijective: There are exactly as many cones in Σ as there are

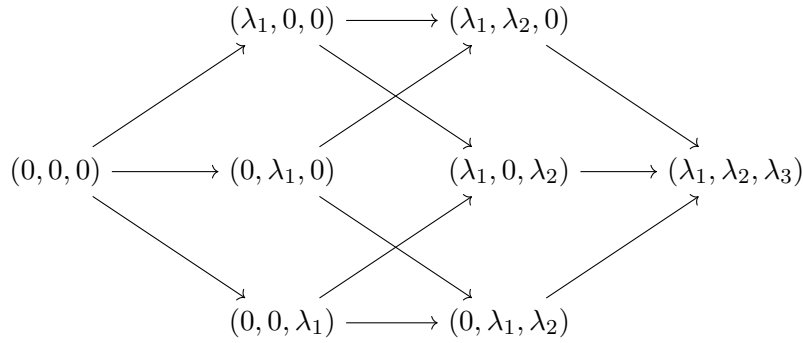


Figure A.2: Hasse diagram for the poset of the closures of the eight orbits of \mathbb{C}^3 under the action of $(\mathbb{C}^*)^3$. An arrow from A to B indicates that $A \subseteq B$. Here $\lambda_i \in \mathbb{C}$.

orbits in X_Σ with respect to the action of $(\mathbb{C}^*)^n$. Furthermore the cones of Σ form a poset with respect to inclusion as well and one has that $V(\sigma) \subseteq V(\sigma')$ if and only if $\sigma' \subseteq \sigma$.

Applied to one-dimensional cones, this means that one can associate the torus-invariant divisors defined by $z_i = 0$ for fixed i with the rays v_i of the fan.

A.2.2 Smoothness

Proving that a space is smooth is generally a difficult problem. However, in toric geometry the smoothness of a variety Σ can be translated into simple conditions on the fan Σ . Concretely, one can show that the following conditions hold:

- If all cones $\sigma \subseteq \Sigma$ are simplicial² and have unit volume³, then X_Σ is smooth.
- If all cones $\sigma \subseteq \Sigma$ are simplicial, then X_Σ has at most orbifold singularities.
- If there exists a cone $\sigma \subseteq \Sigma$ that is not simplicial, then X_Σ has non-orbifold singularities.

We will not prove these statements here, but instead present an example for each case. To begin with the most singular case, we recall the rays of the conifold given in [Equation A.1.13](#) and this time let the fan be generated by a single maximal-dimensional cone

$$\sigma = \langle v_1 v_2 v_3 v_4 \rangle. \tag{A.2.3}$$

²A k -cone is simplicial if it is generated by k rays.

³Here we measure the volume of a k -cone by computing the volume of the complex hull of the cone generators and the origin. If its volume is the same as the volume of the convex hull of k of the basis vectors of the lattice N and the origin, then we say that σ has unit volume.

Clearly, σ is not simplicial, since it is a three-dimensional cone that is generated by four rays. This toric variety is⁴ the hypersurface in \mathbb{C}^4 defined by

$$p = z_1 z_2 - z_3 z_4 = 0. \quad (\text{A.2.4})$$

Since $\partial_{z_i} p = p = 0$ at the origin, the variety has a singularity. Furthermore, it is not an orbifold singularity. In the previous section we saw how to remove the singularity by splitting the single three-cone into two three-cones. Each of these cones is simplicial and, as a quick computation shows, has unit volume and therefore both resolved toric varieties with fans generated by (A.1.14) and (A.1.15) are smooth spaces. As we have observed before, the singularity is removed by excluding the origin from the variety. In the unresolved case the excluded point set Z is empty, since all four rays are contained in the three-cone of Equation A.2.3. After subdividing this cone into two other cones, there no longer exists a cone containing all four rays and the origin is removed.

Next, consider the two-dimensional fan generated by the three rays

$$\Sigma_{\mathbb{P}^2/\mathbb{Z}_3}(1) = \left\{ \begin{pmatrix} -1 \\ 2 \end{pmatrix}, \begin{pmatrix} 2 \\ -1 \end{pmatrix}, \begin{pmatrix} -1 \\ -1 \end{pmatrix} \right\} \quad (\text{A.2.5})$$

and the two-cone $\sigma = \langle v_1 v_2 \rangle$. It is simplicial and its volume is

$$\frac{1}{2} \det \begin{pmatrix} 2 & -1 \\ -1 & 2 \end{pmatrix} = \frac{3}{2}, \quad (\text{A.2.6})$$

which is three times the volume of the unit cell generated by the two canonical basis vectors of \mathbb{Z}^2 . One finds the same for the other two cones. In fact, we can see directly from the definition of Equation A.0.2 that this variety has an orbifold singularity. There are $n = 3$ rays, the excluded point set is $Z = \{(0, 0, 0)\}$, and the \mathbb{C}^* -action by which we quotient is $z_i \sim \lambda z_i$ with $\lambda \in \mathbb{C}^*$. However, the lattice N' generated by the three rays of Equation A.2.5 is a proper sublattice of N of index three. Therefore the discrete subgroup Γ appearing in the definition of the toric variety is \mathbb{Z}_3 in this case and the resulting toric variety is $\mathbb{P}^2/\mathbb{Z}_3$.

Finally, the toric variety with the fan from figure A.1 is an example of a smooth toric variety. Obviously, all cones are simplicial and one easily computes that all cones have unit volume.

Let us remark that the results from toric geometry that we use in order to do cohomology and intersection theory computations still hold for compact varieties with orbifold singularities, but not for more general varieties such as the conifold. From now on we assume that the fans of our toric varieties are simplicial and complete.

⁴Unfortunately, we have not introduced the necessary framework in order to show this here. Roughly speaking, one can associate an affine patch to every cone of the fan, where the dimension of the patch equals the dimension of the cone. Since the fan of the unresolved conifold consists of only one maximal cone, the toric variety is defined by just a single affine patch (i.e. it is an *affine* toric variety) and one can show that this affine patch is given by Equation A.2.4.

A.3 Intersection Theory

A key quantity occurring again and again in F-theory calculations is the intersection form of the toric variety. Here we first introduce the general notion of divisors and line bundle in [subsection A.3.1](#) before giving a very loose definition of intersections between divisors in compact toric varieties in [subsection A.3.2](#).

A.3.1 Divisors and Line Bundles

There are different notions of *divisors*, but at our informal level we will consider a divisor to be a formal sum of holomorphic hypersurfaces⁵ with integer coefficients.

In a given affine patch U_α , every holomorphic hypersurface D_i is specified as the vanishing locus of a holomorphic polynomial $(p_i)_\alpha = 0$. Naturally, $(p_i)_\alpha$ is only determined up to functions that do not vanish on U_α . On the overlap between two patches U_α and U_β , $\frac{p_\alpha}{p_\beta}$ is holomorphic and non-zero, since the vanishing loci of $(p_i)_\alpha$ and $(p_i)_\beta$ inside $U_\alpha \cap U_\beta$ are identical. Given a divisor

$$D = \sum_i n_i D_i \quad \text{with } n_i \in \mathbb{Z} \quad (\text{A.3.1})$$

and an affine patch U_α one can assign to it a meromorphic function

$$p_\alpha = \prod_i (p_i)_\alpha^{n_i}. \quad (\text{A.3.2})$$

The zeros (poles) of p_α correspond to the positive (negative) components of D . On the overlaps $U_\alpha \cap U_\beta$, the functions $g_{\alpha\beta} = \frac{p_\alpha}{p_\beta}$ have neither poles nor zeros and one can interpret them as the transition functions of a holomorphic line bundle, which one denotes by $\mathcal{O}(D)$.

To reverse this procedure and obtain a divisor from a given line bundle $\mathcal{O}(D)$, consider global meromorphic sections s_a of $\mathcal{O}(D)$. By definition, these sections satisfy

$$\frac{(s_a)_\alpha}{(s_a)_\beta} = g_{\alpha\beta} \quad \text{for } s_a \in H^0(X, \mathcal{O}(D)) \quad (\text{A.3.3})$$

and therefore their zeros and poles (and their respective degrees) agree on the overlaps. Here X is the manifold whose divisors we are studying. Hence, we can assign a divisor $D^{(a)} = V(s_a)$ to each one of these sections. While the divisors $D^{(a)}$ are distinct, they lie in the same homology class and in particular, they are homologous to D :

$$[D] = [D^{(a)}] = [V(s_a)] \quad (\text{A.3.4})$$

⁵A hypersurface is a subvariety of codimension one. As an example, consider \mathbb{P}^2 with homogeneous coordinates $[z_0 : z_1 : z_2]$. Then the equation $z_0 = 0$ defines a holomorphic hypersurface and we denote the divisor consisting only of this hypersurface by $V(z_0)$.

Let us make a few more remarks. Firstly, a divisor is called *effective* if all the coefficients n_i in Equation A.3.1 are non-negative. Then the sections of the associated line bundle are *holomorphic*. Secondly, since you can add two divisors by adding the coefficients n_i , the set of divisors forms a natural group. Assigning a line bundle to a divisor is a homomorphism with respect to this group action and the addition is mapped to the tensor product on the line bundle side:

$$O(D_1 + D_2) = O(D_1) \otimes O(D_2) \quad (\text{A.3.5})$$

Finally, let us mention Poincaré duality. Assume that our manifold X is d -dimensional, compact and has no boundary. Then there exists an isomorphism

$$H_{n-k}(X) \cong H^k(X) \quad (\text{A.3.6})$$

mapping homology classes to their dual cohomology classes and vice versa. Denoting by ω_Y a form representing the cohomology class Poincaré-dual to the homology class $[Y]$ of a cycle $Y \subset X$, one has that

$$\int_Y \omega = \int_X \omega_Y \wedge \omega \quad (\text{A.3.7})$$

for closed forms ω . A common case we will encounter is the $(1, 1)$ -form dual to (the homology class of) a divisor D and according to the conventions above, we will denote it by ω_D .

A.3.2 Homology and Intersection Theory

The homology class $[D]$ of a divisor D inside a toric variety X is easy to determine. Assuming that X is not too singular⁶ the homology class depends only on the charges of the polynomials defining the divisor.

As we just explained, there is a one-to-one correspondence between homologically independent divisors and holomorphic line bundles. In particular, the most general polynomial defining a divisor of class $[D]$ is given by

$$p = \sum_a c_a s_a = 0, \quad \text{where } c_a \in \mathbb{C}, s_a \in H^0(X, \mathcal{O}(D)). \quad (\text{A.3.8})$$

Hence, two divisors are homologous if their defining polynomials are sections of the same line bundle. For toric varieties this is the case if and only if the two sections have the same charges under the $(\mathbb{C}^*)^m$ action. Note that this immediately implies that the group of holomorphic line bundles has rank m , as there are only m linearly independent charge vectors. From Poincaré duality it then follows that $h^{1,1} = \dim H^{1,1}(X) = m$.

⁶Whenever we do (co-)homology computations, we assume that our toric variety is compact and has at most orbifold singularities.

As an example, consider again \mathbb{P}^2 with homogeneous coordinates $[z_0 : z_1 : z_2]$. Since \mathbb{P}^2 is obtained by quotienting out a single \mathbb{C}^* action, we have that $H_2(\mathbb{P}^2, \mathbb{Z}) = H^{1,1}(\mathbb{P}^2, \mathbb{Z}) = \mathbb{Z}$. The generator of $H_2(\mathbb{P}^2, \mathbb{Z})$ is usually called $[H]$, the hyperplane class. All three fields z_i have charge one under the \mathbb{C}^* action and therefore they are all sections of $\mathcal{O}(H)$. Now consider a divisor of class $n[H]$. The sections of $\mathcal{O}(nH)$ are the monomials with charge n and there exist $\binom{n+2}{2} = \frac{(n+1)(n+2)}{2}$ of them. Then the most general polynomial defining a divisor of class $n[H]$ reads

$$p = \sum_{i+j+k=n} c_{ijk} z_0^i z_1^j z_2^k = 0. \quad (\text{A.3.9})$$

Next, let us briefly introduce the intersection product. Given a manifold X of complex dimension d and d divisors $D_i = 1, \dots, d$ we would like to consider the intersection product

$$[D_1] \cdot \dots \cdot [D_d] \equiv [D_1] \cap \dots \cap [D_d]. \quad (\text{A.3.10})$$

Inside a toric variety, this is easy to compute. In fact, using Poincaré-duality, it is simply

$$[D_1] \cdot \dots \cdot [D_d] = \int_X \omega_{D_1} \wedge \dots \wedge \omega_{D_d}, \quad (\text{A.3.11})$$

for which there exists a simple combinatorial formula, implemented for example in many computer algebra systems. In simple cases, the intersection products yields what one would intuitively expect: If X has no singularities and one can find representatives D_i of the classes $[D_i]$, such that the intersection of all these divisors is only a point set, then the result of Equation A.3.10 is just the number of these points counted with multiplicities.

In fact, returning to the familiar example of \mathbb{P}^n , we have that

$$\underbrace{H \cdot \dots \cdot H}_{n \text{ times}} = 1 \quad (\text{A.3.12})$$

since we can just pick $z_i = 0$ as a representative for the i^{th} factor. These n equations leave only z_0 undetermined and they thus have the single solution $[1 : 0 : \dots : 0]$.

A.4 The Chern Class and the Calabi-Yau Condition

According to Yau's proof [240, 241] of the Calabi conjecture, the vanishing of the first Chern class of a manifold implies that there it has a unique Ricci-flat Kähler metric and therefore we are interested in computing the Chern class of a given toric variety. In subsection A.4.1 we explain how to do that before noting in subsection A.4.2 that the first Chern class of a compact toric variety can never vanish.

A.4.1 Chern Classes

The total Chern class of a rank r holomorphic vector bundle V over X is the sum

$$c(V) = 1 + \sum_{i=1}^r c_i(V), \quad (\text{A.4.1})$$

where $c_r \in H^{2r}(X)$. Chern classes (and more generally, other characteristic classes) have many mathematical applications: For example, two smooth complex line bundles are the same if and only if their first Chern classes agree⁷. More importantly to us, Chern classes also appear in the effective actions obtained from compactifying on a Calabi-Yau.

For toric varieties X it is easy to compute the Chern class of their tangent bundle TX . Denoting by

$$D_i = V(z_i) \quad (\text{A.4.2})$$

the divisor obtained from setting the i^{th} homogeneous variable to zero, the total Chern class of TX is

$$c(TX) = \prod_i (1 + \omega_{D_i}), \quad (\text{A.4.3})$$

where the product is the wedge product of forms. In particular, this implies that the first Chern class is just the dual of the sum of all divisors D_i :

$$c_1(TX) = \sum_i \omega_{D_i}. \quad (\text{A.4.4})$$

Next, consider a hypersurface $Y \subset X$. In order to compute $c(TY)$, we split

$$TX = TY \oplus NY \quad (\text{A.4.5})$$

and use one of the key properties of the Chern class:

$$c(TX)|_Y = c(TY)c(NY) \quad (\text{A.4.6})$$

Furthermore, one has that $c(NY) = 1 + \omega_Y$ and therefore one finds that

$$c(TY) = \frac{c(TX)|_Y}{1 + \omega_Y} = \frac{\prod_i (1 + \omega_{D_i})}{1 + \omega_Y}. \quad (\text{A.4.7})$$

As a consequence,

$$c_1(TY) = c_1(TX)|_Y - \omega_Y. \quad (\text{A.4.8})$$

⁷Note that for holomorphic line bundles this need not be true.

In particular, a hypersurface $Y \subset X$ defines a Calabi-Yau manifold if its homology class is Poincaré-dual to the first Chern class of the ambient space.

As an example, let us consider once again \mathbb{P}^2 . Denote by ω_H the two-form dual to the hyperplane class generating H_2 as in [subsection A.3.2](#). Then we have that

$$c(T\mathbb{P}^2) = (1 + H)^3 = 1 + 3\omega_H + 3\omega_H \wedge \omega_H + \omega_H \wedge \omega_H \wedge \omega_H \tag{A.4.9}$$

and in particular $c_1(T\mathbb{P}^2) = 3\omega_H$. The bundle associated with the divisor dual to c_1 is the anticanonical bundle of B , i.e.

$$K_{\mathbb{P}^2}^{-1} = \mathcal{O}([c_1(T\mathbb{P}^2)]_{\text{PD}}). \tag{A.4.10}$$

Finally, let us note that in the physics literature one often speaks of the Chern class of X , where X is a complex manifold (and generally does not have the structure of a vector bundle), even though what is meant is usually the Chern class of the tangent bundle TX of X .

A.4.2 Compactness and the Calabi-Yau Condition

A toric variety is *compact* if and only if its fan Σ spans the whole lattice N . Such a fan Σ is called *complete*. For a proof of this statement see for example Chapter 2 of [\[234\]](#). Here we just give examples.

Since this thesis is concerned with F-theory compactifications, most of the examples given here are by design compact varieties, such as the ubiquitous \mathbb{P}^2 , the dP_1 whose fan is given by [figure A.1](#) or the $\mathbb{P}^2/\mathbb{Z}_3$ in [Equation A.2.5](#). Obviously, their fans cover all of \mathbb{Z}^2 . An example of a non-compact variety is the conifold of [Equation A.2.4](#). Since the z_i run over \mathbb{C}^4 without any additional equivalence relation, it is clearly non-compact and its fan does not cover all of \mathbb{Z}^3 .

Next, let us answer a seemingly unrelated question: When does a toric variety's first Chern class vanish? After all, we eventually wish to construct compact Calabi-Yau manifolds. In the previous subsection we found that the first Chern class is Poincaré-dual to the homology class

$$[D] = \sum_{i=1}^n [D_i], \tag{A.4.11}$$

where D_i is the torus-invariant divisor corresponding to the ray v_i . In coordinates it is defined by $z_i = 0$. Furthermore, we found that the homology class of D_i depends only on the charges of z_i under the $(\mathbb{C}^*)^m$ -action. In particular, the class of $[D]$ is trivial if and only if

$$\sum_{i=1}^n Q_a^i = 0 \quad \forall a. \tag{A.4.12}$$

However, that implies directly that all v_i lie in a plane.⁸ Since all rays end on a hyperplane, toric varieties with vanishing first Chern class can never be compact.

A.5 Reflexive Polytopes and Calabi-Yau Hypersurfaces

In the previous subsection we learned that Calabi-Yau manifolds constructed as toric varieties can never be compact. To nevertheless construct compact Calabi-Yau manifolds by using tools from toric geometry, we must look to hypersurfaces, or more generally complete intersections inside toric varieties.

In [subsection A.4.1](#) we described how to compute the Chern class of a hypersurface using the adjunction formula and found that

$$c_1(TY) = c_1(TX) - \omega_D \tag{A.5.1}$$

where Y is the hypersurface in X cut out by the divisor D . For $c_1(TY)$ to vanish, the divisor defining the hypersurface must be Poincaré-dual to the first Chern class of TX . In other words, the polynomials defining Y must be sections of K_X^{-1} , the anticanonical line bundle on X . One also says that Y must be an *anticanonical* hypersurface.

While it is easy to find the homology class of the divisor defining a Calabi-Yau hypersurface Y inside a toric variety X , ensuring that Y is smooth is much more involved. The conditions from [subsection A.2.2](#) allow us to check that X itself is smooth, but that still allows Y to be singular. Fortunately, there exists a convenient combinatorial construction ensuring that Y is smooth. Proving it is quite involved [\[242\]](#), but its application is not. Neglecting some mathematical details, the essence of the construction is as follows: There exists a class of toric varieties called smooth Gorenstein Fano varieties whose anticanonical divisor satisfies a set of regularity conditions, namely that it is Cartier and ample. The generic anticanonical hypersurface inside such a smooth Gorenstein Fano variety can be resolved to be smooth.⁹ These smooth Gorenstein Fano varieties are specified by *reflexive polytopes*, which we introduce next.

A *lattice polytope* in a lattice N is the convex hull of finitely many points in N , i.e.

$$P = \langle v_1, \dots, v_n \rangle_{\text{conv.}}, \quad v_i \in N. \tag{A.5.2}$$

If $\dim P = 2$, it is called a *lattice polygon*. We call set all elements of N lying inside P *integral points* of P . The minimal set of integral points spanning P are called its set of *vertices* and

⁸To see this, note that if $\sum_i v_i Q_a^i = 0$ and $\sum_i Q_a^i = 0$, then also $\sum_i (v_i - v_1) Q_a^i = 0$. Since the shifted vectors $v_i - v_1$ still satisfy the same number of relations as before, they span a plane together with the origin. After shifting back the origin becomes v_1 and therefore the v_i all lie in a hyperplane.

⁹More precisely, Batyrev's paper [\[242\]](#) states that the first singularities have at least codimension 4, which may become relevant in the construction of Calabi-Yau fourfolds.

Dimension	2	3	4	≥ 5
Reflexive polytopes	16	4, 319	473, 800, 776	?

Table A.1: The number of reflexive polytopes in different dimensions. Reflexive polytopes in three and four dimensions were classified in [243] and [244], respectively.

the integral points of P not lying on a boundary are called interior points. Given a lattice polytope P , its dual (or polar) polytope is defined as

$$P^\circ = \langle x \in M \mid \langle x, y \rangle \geq -1 \ \forall y \in P \rangle_{\text{conv.}} , \tag{A.5.3}$$

where M is the dual lattice to N . Since Equation A.5.3 maps every vertex y of P to an inequality that defines a facet of P° , there is a correspondence between vertices of a polytope and facets of the dual polytope. If P° is a lattice polytope, too, then P is called a *reflexive polytope*. Note that P and P° really are *dual* to each other in the sense that $(P^\circ)^\circ = P$ and hence P° is reflexive if and only if P is reflexive. Reflexive polytopes are very special. One can show that a reflexive polytope contains only the origin as an interior point and that up to $SL(\mathbb{Z})$ transformations, there are only finitely many reflexive polytopes in any given dimension d .

To obtain a smooth Gorenstein Fano variety X_Σ from such a polytope P , one must take all of its integral points and compute a fine, regular star triangulation¹⁰ with respect to the origin of this point set. The faces of this triangulation can then be used as generating cones of the toric fan Σ of X_Σ . Note that if we are just interested in a smooth hypersurface Y inside X_Σ and allow X_Σ to have singularities as long as Y misses them, then we do not need to use all points of P . Instead, we can restrict to those points that are not interior points of facets of P , since their rays in Σ correspond to divisors whose restriction to Y is trivial. The hypersurface equation $p = 0$ defining Y then reads

$$p = \sum_{y_j \in P^\circ} c_j \prod_{x_i \in P} z_i^{\langle y_j, x_i \rangle + 1} . \tag{A.5.4}$$

In summary, there exists a straightforward algorithm to construct compact Calabi-Yau manifolds that are smooth at least up to codimension four. Given a reflexive polytope P , one must find a regular fine star triangulation of the integral points of P that are not interior to facets. Then the fan constructed from this triangulation defines a toric variety whose generic anticanonical hypersurface is the Calabi-Yau manifold we are looking for. If $\dim P = 2$, then the resulting hypersurface is one-dimensional and has the topology of a genus-one curve, i.e. a torus. For $\dim P = 3$, the anticanonical hypersurface has two complex dimensions and is called a K3 surface. Finally, if $\dim P = n \geq 3$, then the embedded manifold is a Calabi-Yau n -fold.

¹⁰Computer packages such as TOPCOM or Sage provide the algorithms to compute triangulations.

A.6 Calabi-Yau Manifolds as Complete Intersections in Toric Varieties

Extending his work of [242], Batyrev described in [245] a combinatorial method of constructing complete intersection Calabi-Yau manifolds inside toric varieties. In order to generalize the construction of hypersurfaces to complete intersections, one must specify additional information. In the hypersurface case, the homology class of the divisor defined by the vanishing of Equation A.5.4 must be Poincaré-dual to the cohomology class of the first Chern class of the ambient space in order for the hypersurface to be Calabi-Yau. If instead the Calabi-Yau manifold is to be the intersection of several divisors, then their sum must still be dual to the first Chern class of the ambient space. However, the classes of the individual divisors are not fixed anymore.

One such way of additionally specifying the classes of the divisors defining the complete intersection proceeds by giving a *nef partition* of the reflexive polytope Δ° . A nef partition of Δ° into r parts is a set of lattices polytopes Δ_i and ∇_i with $i = 1, \dots, r$ satisfying

$$\begin{aligned} \Delta &= \Delta_1 + \dots + \Delta_r & \Delta^\circ &= \langle \nabla_1, \dots, \nabla_r \rangle_{\text{conv}} \\ \nabla^\circ &= \langle \Delta_1, \dots, \Delta_r \rangle_{\text{conv}} & \nabla &= \nabla_1 + \dots + \nabla_r \end{aligned} \tag{A.6.1}$$

with $\langle \cdot, \dots, \cdot \rangle_{\text{conv}}$ the convex hull, $+$ Minkowski addition, and

$$(\nabla_n, \Delta_m) \geq -\delta_{nm}, \tag{A.6.2}$$

where here we mean this to hold for every pair of points from ∇_n and Δ_m . Effectively, we have split the vertices of Δ° into r disjoint subsets spanning the polytopes ∇_i and made sure that they fulfill certain additional constraints. Given such a nef partition, we again define X_{n+r} to be the ambient variety obtained from Δ° as above. Furthermore, the nef partition specifies the following r equations defining the Calabi-Yau manifold Y_n :

$$p_m = \sum_{y_j \in \Delta_m} a_{m,j} \prod_{n=1}^r \prod_{x_i \in \nabla_n} z_i^{\langle y_j, x_i \rangle + \delta_{nm}}, \quad m = 1, \dots, r. \tag{A.6.3}$$

Note that one can also interpret a nef partition of Δ° as a nef partition of ∇° . In doing so, one exchanges Y_n by its mirror. Let us point out that the ambient space of a mirror manifold can differ for different nef partitions of the same polytope.

Finally, we remark that there are two special cases of nef partitions. The simplest one is a *direct product*. Given nef partitions of two reflexive polytopes $\Delta^{(1)\circ}$ and $\Delta^{(2)\circ}$, these define a nef partition of the polytope $\Delta^{(1)} \times \Delta^{(2)}$. The corresponding complete intersection manifold is then a direct product of complete intersections inside the direct product of the varieties corresponding to $\Delta^{(1)\circ}$ and $\Delta^{(2)\circ}$. The other special case corresponds to *projections*. If a nef partition has one component ∇_i that is spanned only by a single vertex v , then the complete intersection can be reduced to a complete intersection in a toric variety of one dimension less whose reflexive polytope is obtained by projecting Δ° along v .

A.6.1 Ids for Nef Partitions

Since reflexive polytopes of dimension smaller or equal to four have been classified, it is reasonable to assign a given nef partition a unique identifier within this classification. Reflexive polytopes already have a unique id as assigned by the PALP database. This id obeys

$$\#_{\text{points}}(P) < \#_{\text{points}}(P') \Rightarrow id(P) < id(P') \tag{A.6.4}$$

and

$$\#_{\text{points}}(P) = \#_{\text{points}}(P') \wedge \#_{\text{vertices}}(P) < \#_{\text{vertices}}(P') \Rightarrow id(P) < id(P'), \tag{A.6.5}$$

that is, the polytopes are ordered by the number of integral points and the number of vertices. Sage can be used to compute the PALP index of a given reflexive polytope. To furthermore identify the nef partitions uniquely, we run `nef.x` via the

$$\text{ReflexivePolytope.nef_partitions}() \tag{A.6.6}$$

method of Sage on a given reflexive polytope in PALP normal form. This output is uniquely ordered and allows us to assign ids to the different nef partitions. By a nef partition with id (i, j) we therefore mean the $(j + 1)$ th nef partition of the three-dimensional reflexive polytope with PALP id i as determined by the `nef_partitions()` method of Sage.

A.7 The Kähler and the Mori Cone

Consider a complex variety X and in particular the set of irreducible holomorphic curves $\{\mathcal{C}_i\}$ on it. Then the cone consisting of the formal expressions

$$M(X) = \left\{ \sum_i a_i [\mathcal{C}_i], a_i \in \mathbb{R}_{\geq 0} \right\} \tag{A.7.1}$$

where $[\mathcal{C}_i]$ is the homology class of \mathcal{C}_i is called the *Mori cone* of X . One can obtain the generators of $M(X)$ by taking the transversal intersection of all combinations of $\dim_{\mathbb{C}}(X) - 1$ divisors on X .

Given the Mori cone, one can also consider its dual cone, the *Kähler cone*. It is given by the following formal expression:

$$K(X) = \left\{ \sum_j a_j [D_j], a_j \in \mathbb{R}_{\geq 0}, D_j \cap \mathcal{C} \geq 0 \forall \mathcal{C} \in M(X) \right\} \tag{A.7.2}$$

Employing Poincaré-duality the Kähler cone can equivalently be considered to be generated by all $(1, 1)$ -forms satisfying

$$K(X) = \left\{ J \in H^{1,1}(X, \mathbb{R}), \int_{\mathcal{C}} J \geq 0 \forall \mathcal{C} \in M(X) \right\}. \tag{A.7.3}$$

Denoting the $(1,1)$ -form in Equation A.7.3 by J already suggests that we can identify it with the Kähler form of the complex variety. In fact, since the volume element can be constructed by taking powers of the Kähler form, the above condition can be translated to demanding that the volume of a holomorphic curve is non-zero inside away from the boundaries of the Kähler cone. Hence the coordinates a_i on $K(X)$ can be interpreted as the Kähler moduli of the complex manifold. As one approaches the boundary of the Kähler cone, the volume of one of the Mori cone generators becomes zero. Since the volume of this particular curve becomes negative after crossing the boundary, this can be interpreted as the curve *flopping* out of the Mori cone.¹¹

While the Kähler cone and the Mori cone are defined for more general spaces than toric varieties, there exist simple combinatorial formulas to compute them for a toric variety. These are implemented in various computer algebra systems such as [139].

Lastly, let us note that, as the name already suggests, the Kähler parameters ζ_a used in the GLSM picture described in subsection A.1.1 are related to the a_i used here. Since \mathbb{C}^n has a natural Kähler form, the toric variety obtained as a quotient of \mathbb{C}^n inherits this form. The inherited Kähler form will depend on the ζ_a and by identifying it with an element of $K(X)$ as in Equation A.7.3, one can find a map between the a_i and the ζ_a .

A.7.1 The Kähler and the Mori Cone of Complete Intersections

The Kähler cone $K(Y)$ of a hypersurface or more generally a complete intersection Y inside a variety X is not necessarily the same as the Kähler cone $K(X)$ of the ambient variety. If the curve that is flopped (i.e. whose volume become negative) as one approaches the boundary of the Kähler cone $K(X)$ does not lie on Y , then the neighboring Kähler cone $K'(X')$ bordering on $K(X)$ should still be considered part of the Kähler cone of Y . We therefore define $K(Y)$ to be the *union* of $K(X)$ with all Kähler cones $K'(X')$ whose X' are related to X via a flop transition that does not affect Y . Similarly, as $M(Y)$ is still the dual cone of $K(Y)$, $M(Y)$ is the *intersection* of all Mori cones $M(X')$ with $M(X)$ for the same set of X' .

Fortunately, it is easy to compute $K(Y)$ and $M(Y)$ for toric ambient spaces X . All one needs to do is to compute all fine regular triangulations of the rays of the fan of X with the origin as the star and construct the toric varieties corresponding to the fans these triangulations define. Next, one computes the intersection form restricted to the complete intersection Y . The ambient varieties whose intersection form is the same on Y are exactly the sets of ambient varieties that are related to each other by flop transitions leaving Y invariant.

A.8 Toric morphisms and Toric Fibrations

The Calabi-Yau manifolds Y relevant for F-theory compactifications are genus-one fibrations, which means that there is a map $\pi' : Y \rightarrow B$, whose generic fiber is a torus. B is a

¹¹See [189] for further discussions on this matter.

$(\dim_{\mathbb{C}} Y - 1)$ -complex-dimensional manifold called the base manifold. From now on we will write Y_n to indicate that $\dim_{\mathbb{C}} Y = n$. In order to construct such Y_n , one can consider toric ambient spaces X_{n+1} that are fibered themselves. Then we have the following maps:

$$\begin{array}{ccccc} F & \longrightarrow & X_{n+c} & \xrightarrow{\pi} & B_{n-1} \\ \uparrow & & \uparrow & \nearrow \pi' & \\ E & \longrightarrow & Y_n & & \end{array}$$

Here F is the fiber of the toric ambient space fibration π and E is the genus-one fiber of the fibration π' of the Calabi-Yau n -fold Y_n . Since X_{n+c} is a toric variety and hence easy to manipulate, a good strategy is to focus on X_{n+c} and the projection map π' . To this end, let us review some material on toric morphisms and toric fibrations. For proofs and more technical details we refer to the original work of [174].

A *fan morphism* φ is a map from a fan $\Sigma' \subset N'$ to another fan $\Sigma \subset N$ such that for every cone $\sigma' \in \Sigma'$ there exists a cone $\sigma \in \Sigma$ with $\varphi(\sigma') \subseteq \sigma$, i.e. φ maps cones of Σ' into cones of Σ . Then φ induces a morphism $\tilde{\varphi}$ from $X_{\Sigma'}$ to X_{Σ} with the following properties relevant to us:

- φ is equivariant with respect to the homomorphism $T_{N'} \rightarrow T_N$ induced by φ and maps the full-dimensional torus orbit of $X_{\Sigma'}$ into the full-dimensional torus orbit of X_{Σ} .
- The fiber of $\tilde{\varphi}$ over a point $p \in X_{\Sigma}$ depends only on the T_N orbit that p is an element of.
- Every fiber of $\tilde{\varphi}$ is a (possibly reducible) toric variety.
- The generic fiber (that is the fiber over the full-dimensional torus) is irreducible and its embedding is a toric morphism.

If all the fibers of $\tilde{\varphi}$ have the same dimension, then φ is called a *fibration*.¹² Note that this does not mean that all fibers have to be isomorphic to each other. In order to understand these properties, we present a couple of examples illustrating how toric morphisms work.

A.8.1 The Hirzebruch Surfaces

Consider the Hirzebruch surface \mathbb{F}_n , whose fan is generated by the rays

$$\Sigma_{\mathbb{F}_n}(1) = \left\{ \begin{pmatrix} 1 \\ n \end{pmatrix}, \begin{pmatrix} -1 \\ 0 \end{pmatrix}, \begin{pmatrix} 0 \\ 1 \end{pmatrix}, \begin{pmatrix} 0 \\ -1 \end{pmatrix} \right\}. \tag{A.8.1}$$

¹²Whether or not $\tilde{\varphi}$ is a fibration is already encoded in the fan morphism φ : φ must be surjective and for any cone $\sigma \in \Sigma$ and any primitive preimage cone $\sigma' \in \Sigma'$ mapped to σ the linear map of vector spaces $\varphi_{\mathbb{R}}$ must induce a bijection between σ and σ' .

Denoting the homogeneous variables by z_i , the $(\mathbb{C}^*)^2$ -action is

$$[z_1 : z_2 : z_3 : z_4] = [\lambda z_1 : \lambda z_2 : z_3 : \lambda^n z_4], \quad [z_1 : z_2 : z_3 : z_4] = [z_1 : z_2 : \mu z_3 : \mu z_4] \quad (\text{A.8.2})$$

and the excluded point set is $Z_{\mathbb{F}_n} = \{z_1 = z_2 = 0\} \cup \{z_3 = z_4 = 0\}$. Then a fan morphism is induced by the following lattice map $\mathbb{Z}^2 \rightarrow \mathbb{Z}$:

$$\varphi = \begin{pmatrix} 1 & 0 \end{pmatrix} \quad (\text{A.8.3})$$

The image $\varphi(\Sigma_{\mathbb{F}_n})$ is the fan of a \mathbb{P}^1 . To find the coordinate expression of the corresponding toric morphism $\tilde{\varphi}$, one must express the images $\varphi(v_i)$, $v_i \in \Sigma_{bF_n}(1)$ through linear combinations of rays of $\Sigma_{\mathbb{P}^1}$ with non-negative coefficients:

$$\varphi(v_i) = \sum_j \varphi_{ij} w_j, \quad w_j \in \Sigma_{\mathbb{P}^1} \quad (\text{A.8.4})$$

The toric morphism $\tilde{\varphi}$ can then be written in homogeneous coordinates as

$$\tilde{\varphi} : \mathbb{F}_n \rightarrow \mathbb{P}^1, \quad [z_1 : z_2 : z_3 : z_4] \mapsto \left[\prod_i z_i^{\varphi_{i1}}, \prod_i z_i^{\varphi_{i2}} \right] = [z_1 : z_2]. \quad (\text{A.8.5})$$

It is easy to study the fibers of $\tilde{\varphi}$ over the different torus orbits of the base manifold \mathbb{P}^1 . \mathbb{P}^1 has only three torus orbits: The two points $[1 : 0]$ and $[0 : 1]$ and the big orbit $[1 : \lambda]$ with $\lambda \in \mathbb{C}^*$. They correspond to the two rays (-1) and (1) and to the zero-cone, respectively. Evaluating the preimages of (A.8.5) one finds that

$$\begin{aligned} \tilde{\varphi}^{-1}([1 : 0]) &= [1 : 0 : z_3 : z_4] \cong \mathbb{P}^1 \\ \tilde{\varphi}^{-1}([0 : 1]) &= [0 : 1 : z_3 : z_4] \cong \mathbb{P}^1 \\ \tilde{\varphi}^{-1}([1 : \lambda]) &= [1 : \lambda : z_3 : z_4] \cong \mathbb{P}^1. \end{aligned} \quad (\text{A.8.6})$$

To see that z_3 and z_4 really parametrize a \mathbb{P}^1 , note that we have used the first \mathbb{C}^* action from Equation A.8.2 to pick a representative of the \mathbb{P}^1 locus. The remaining \mathbb{C}^* action is that of a \mathbb{P}^1 and since $z_3 = z_4 = 0$ is contained in the excluded point set, the fibers really are \mathbb{P}^1 s. Since all fibers are \mathbb{P}^1 s, we say that $\tilde{\varphi}$ is not only a \mathbb{P}^1 -fibration, but a \mathbb{P}^1 -bundle.

A.8.2 A Fibration with a Reducible Fiber

Next, we examine a toric variety with a fibration that is not a bundle. Its rays are given by

$$\Sigma(1) = \left\{ \begin{pmatrix} 0 \\ 1 \\ 0 \end{pmatrix}, \begin{pmatrix} 1 \\ 0 \\ 0 \end{pmatrix}, \begin{pmatrix} -3 \\ -2 \\ 0 \end{pmatrix}, \begin{pmatrix} -5 \\ -3 \\ 1 \end{pmatrix}, \begin{pmatrix} -1 \\ -1 \\ -1 \end{pmatrix}, \begin{pmatrix} 0 \\ 0 \\ -1 \end{pmatrix} \right\}, \quad (\text{A.8.7})$$

but since they are three-dimensional, we must also provide the three-dimensional cones in order to specify the fan:

$$\Sigma(3) = \{ \langle v_1 v_2 v_4 \rangle, \langle v_1 v_2 v_6 \rangle, \langle v_1 v_3 v_4 \rangle, \langle v_1 v_3 v_6 \rangle, \langle v_2 v_3 v_4 \rangle, \langle v_2 v_3 v_5 \rangle, \langle v_2 v_5 v_6 \rangle, \langle v_3 v_5 v_6 \rangle \} \quad (\text{A.8.8})$$

This time the $(\mathbb{C}^*)^3$ action is given by

$$\begin{aligned} [z_1 : z_2 : z_3 : z_4 : z_5 : z_6] &= [\lambda^2 z_1 : \lambda^3 z_2 : \lambda z_3 : z_4 : z_5 : z_6] \\ [z_1 : z_2 : z_3 : z_4 : z_5 : z_6] &= [\mu^4 z_1 : \mu^6 z_2 : z_3 : \mu z_4 : \mu z_5 : z_6] \\ [z_1 : z_2 : z_3 : z_4 : z_5 : z_6] &= [\rho^3 z_1 : \rho^5 z_2 : z_3 : \rho z_4 : z_5 : \rho z_6] \end{aligned} \quad (\text{A.8.9})$$

and the excluded point set Z_{X_Σ} is

$$\begin{aligned} Z_{X_\Sigma} &= \{z_1 = z_5 = 0\} \cup \{z_4 = z_5 = 0\} \cup \{z_4 = z_6 = 0\} \\ &\cup \{z_1 = z_2 = z_3 = 0\} \cup \{z_2 = z_3 = z_6 = 0\}. \end{aligned} \quad (\text{A.8.10})$$

Similarly to before, the projection onto the last coordinate is a fan morphism given by

$$\varphi : \mathbb{Z}^3 \rightarrow \mathbb{Z}, \quad \varphi = \begin{pmatrix} 1 & 0 & 0 \end{pmatrix}. \quad (\text{A.8.11})$$

One can check that φ is indeed a fan morphism by explicitly computing the images $\varphi(\sigma)$ for every cone $\sigma \in \Sigma$. It induces a toric morphism from X_Σ to \mathbb{P}^1 that has the coordinate expression

$$\tilde{\varphi} : X_\Sigma \rightarrow \mathbb{P}^1, \quad [z_1 : z_2 : z_3 : z_4 : z_5 : z_6] \mapsto [z_4, z_5 z_6]. \quad (\text{A.8.12})$$

Let us now repeat what we did with the previous example and examine the fibers of the three torus orbits of the base. The generic fiber is

$$\tilde{\varphi}^{-1}([1 : \lambda]) = [z_1 : z_2 : z_3 : 1 : \lambda : 1], \quad (\text{A.8.13})$$

where we have used the last two \mathbb{C}^* actions to set z_4 and z_6 to 1. Since the generic fiber is parametrized by three homogeneous coordinates z_1, z_2 and z_3 with a single \mathbb{C}^* action $[z_1 : z_2 : z_3] = [\lambda^2 z_1 : \lambda^3 z_2 : \lambda_1 z_3]$ and the origin $z_1 = z_2 = z_3 = 0$ excluded, it is the weighted projective space \mathbb{P}_{231} . $\tilde{\varphi}$ is therefore a \mathbb{P}_{231} -fibration, but as we will see, it is not a \mathbb{P}_{231} -bundle.

Over $[0 : 1]$ the fiber is

$$\tilde{\varphi}^{-1}([0 : 1]) = [z_1 : z_2 : z_3 : 0 : 1 : 1] \cong \mathbb{P}_{231} \quad (\text{A.8.14})$$

due to the same reasons as for the generic fiber. However, things change over the point $[1 : 0]$. Since the second \mathbb{P}^1 coordinate entry of [Equation A.8.12](#) is a product, we must differentiate between two cases:

- $z_5 = 0$: We have $\tilde{\varphi}^{-1}([1 : 0])|_{z_5=0} = [z_1 : z_2 : z_3 : 1 : 0 : z_6]$. However, since $z_1 = z_5 = 0 \subset Z_{X_\Sigma}$, z_1 must be non-zero and we can scale it to one. The remaining coordinates are z_2, z_3 and z_6 . The \mathbb{C}^* action leaving $z_1 = z_4 = 1$ invariant is

$$[z_2 : z_3 : z_6] = [\lambda z_2 : \lambda z_3 : \lambda^2 z_6] \quad (\text{A.8.15})$$

and together with the excluded point set $\{z_2 = z_3 = z_6 = 0\}$ this fiber component is a weighted projective space \mathbb{P}_{112} . It can be embedded into X_Σ via

$$\iota_1 : \mathbb{P}_{112} \hookrightarrow X_\Sigma, [u, v, w] \mapsto [1 : u : v : 1 : 0 : w]. \quad (\text{A.8.16})$$

Note that this morphism is not a *toric morphism*, since it does not map the big torus orbit of \mathbb{P}_{112} defined by $uvw \neq 0$ into the big torus orbit of X_Σ .

- $z_6 = 0$: We have $\tilde{\varphi}^{-1}([1 : 0])|_{z_6=0} = [z_1 : z_2 : z_3 : 1 : z_5 : 0]$. This time, we cannot scale any additional coordinates to one and therefore the fiber over the divisor $z_6 = 0$ is parametrized by four coordinates subject to the two equivalence relations

$$\begin{aligned} [z_1 : z_2 : z_3 : z_5] &= [\lambda^2 z_1 : \lambda^3 z_2 : \lambda z_3 : z_5] \\ [z_1 : z_2 : z_3 : z_5] &= [z_1 : \mu z_2 : \mu z_3 : \mu^{-2} z_5]. \end{aligned} \quad (\text{A.8.17})$$

The excluded point set is $\{z_1 = z_5 = 0\} \cup \{z_2 = z_3 = 0\}$. The resulting variety F can be represented by the fan spanned by the four rays

$$\left\{ \begin{pmatrix} 1 \\ 0 \end{pmatrix}, \begin{pmatrix} 0 \\ 1 \end{pmatrix}, \begin{pmatrix} -2 \\ -3 \end{pmatrix}, \begin{pmatrix} -1 \\ -1 \end{pmatrix} \right\} \quad (\text{A.8.18})$$

and the map embedding this fiber component into X_Σ is

$$\iota_2 : F \hookrightarrow X_\Sigma, [x : y : z : w] \mapsto [x : y : z : 1 : w : 0]. \quad (\text{A.8.19})$$

F is a blowup of P_{231} at the point $y = z = 0$,¹³ as one can see either from the \mathbb{C}^* -actions in Equation A.8.17 or from the rays directly: The first three rays of Equation A.8.18 define the weighted projective space \mathbb{P}_{231} . The fourth ray subdivides the cone spanned by the rays corresponding to y and z and therefore the resulting variety is the blowup along the closure of the torus orbit dual to this cone.

In summary, $\tilde{\varphi}$ is a \mathbb{P}_{231} fibration over the base \mathbb{P}^1 , which means that the fiber of $\tilde{\varphi}$ is a \mathbb{P}_{231} over a generic point in the base. However, over the point $[0 : 1]$ the fiber changes and becomes a reducible toric variety consisting of a \mathbb{P}_{112} and the blowup of \mathbb{P}_{231} . In fact, it is already visible from the toric data in Equation A.8.7 that the fiber splits into two parts over $[1 : 0]$: The number of fiber components over a base cone is equal to the number of primitive preimage cones¹⁴ of that cone. The point $[1 : 0]$ corresponds to the ray (-1) and there are two rays of Σ that are mapped onto (-1) .

If the fan is obtained from a reflexive polytope P , as it often is in practice, there exists a direct way of searching for a toric fibration. Since the fiber of the fan morphism φ must be

¹³Here we assume that \mathbb{P}_{231} is parametrized by homogeneous coordinates x, y and z .

¹⁴Let $\varphi : \Sigma \rightarrow \Sigma'$ be a fan morphism, let $\sigma \in \Sigma$, and let $\sigma' = \phi(\sigma)$. Then σ is a primitive cone corresponding to σ' if there is no proper face τ of σ such that $\varphi(\tau) = \sigma'$.

the fan of another reflexive polytope P' , P must have a reflexive subpolytope in order for a toric fibration to exist. In particular, the subpolytope must have the origin as its only interior point. Software packages such as Sage [139] provide methods for enumerating subpolytopes of different dimensions.

Finally, let us point out that one can also compute the toric fans of the fiber components directly. For more information on that construction, we refer to [174].

Appendix B

Non-toric Non-Abelian Gauge Groups

Here we give a summary of the non-toric non-Abelian gauge groups that the generic fibrations with genus-one fibers inside three-dimensional Gorenstein Fano toric varieties have. For more details on how these were obtained we refer to [section 3.6](#) and remind the reader that the database

<http://wwth.mpp.mpg.de/members/jkeitel/Weierstrass/> (B.0.1)

contains the precise locations of the singularities for each nef partition.

Generic non-toric Kodaira singularities	Occurrences
No singularity	88
IV^*	3
$IV^* \times I_2$	8
$IV^* \times I_2 \times I_3$	9
$IV^* \times I_2^2$	4
$IV^* \times I_2^2 \times I_3$	4
$IV^* \times I_2^3 \times I_3$	1
$IV^* \times I_3^3$	1
$IV^* \times I_3^4$	1
$III^* \times I_2$	2
$III^* \times I_2 \times I_3$	4
$III^* \times I_2^2$	1
$III^* \times I_2^2 \times I_4$	1
$III^* \times I_2^3 \times I_4$	1
$II^* \times I_2 \times I_3$	1

Table B.1: List of generic non-toric E - and F_4 -type Kodaira singularities of codimension-two genus-one fibers and the number of times they occur.

Generic non-toric Kodaira singularities	Occurrences
I_0^*	39
$I_0^* \times I_2$	47
$I_0^* \times I_2 \times I_3$	15
$I_0^* \times I_2 \times I_3^2$	4
$I_0^* \times I_2^2$	27
$I_0^* \times I_2^2 \times I_3$	17
$I_0^* \times I_2^2 \times I_4$	5
$I_0^* \times I_2^2 \times I_4^2$	4
$I_0^* \times I_2^3$	15
$I_0^* \times I_2^3 \times I_4$	4
$I_0^* \times I_2^4$	2
$I_0^* \times I_2^4 \times I_4$	3
$I_0^* \times I_2^5$	2
I_1^*	9
$I_1^* \times I_2$	20
$I_1^* \times I_2 \times I_3$	9
$I_1^* \times I_2^2$	13
$I_1^* \times I_2^2 \times I_3$	8
$I_1^* \times I_2^2 \times I_3^2$	2
$I_1^* \times I_2^3$	4
$I_1^* \times I_2^3 \times I_3$	2
$I_2^* \times I_2$	3
$I_2^* \times I_2 \times I_3$	7
$I_2^* \times I_2^2$	5
$I_2^* \times I_2^2 \times I_4$	2
$I_2^* \times I_2^3 \times I_4$	2
$I_2^* \times I_2^4$	1
$I_2^* \times I_2^5$	1
$I_3^* \times I_2 \times I_3$	2
$I_3^* \times I_2^2 \times I_3$	1
$I_4^* \times I_2^2 \times I_4$	1

Table B.2: List of generic non-toric G_2 and SO -type Kodaira singularities of codimension-two genus-one fibers and the number of times they occur.

Generic non-toric Kodaira singularities	Occurrences
I_2	263
$I_2 \times I_3$	141
$I_2 \times I_3 \times I_4$	41
$I_2 \times I_3 \times I_5$	12
$I_2 \times I_3 \times I_6$	32
$I_2 \times I_3 \times I_7$	6
$I_2 \times I_3^2$	41
$I_2 \times I_3^2 \times I_4$	15
$I_2 \times I_3^3$	13
$I_2 \times I_4$	136
$I_2 \times I_4^2$	4
$I_2 \times I_4^4$	1
$I_2 \times I_5$	26
$I_2 \times I_6$	6
I_2^2	326
$I_2^2 \times I_3$	170
$I_2^2 \times I_3 \times I_4$	69
$I_2^2 \times I_3 \times I_5$	14
$I_2^2 \times I_3 \times I_6$	12
$I_2^2 \times I_3 \times I_7$	4
$I_2^2 \times I_3 \times I_8$	2
$I_2^2 \times I_3^2$	54
$I_2^2 \times I_3^2 \times I_4$	15
$I_2^2 \times I_3^2 \times I_5$	6
$I_2^2 \times I_3^3$	3
$I_2^2 \times I_3^3 \times I_4$	2
$I_2^2 \times I_4$	134
$I_2^2 \times I_4 \times I_6$	6
$I_2^2 \times I_4 \times I_8$	8
$I_2^2 \times I_4^2$	27
$I_2^2 \times I_4^3$	12
$I_2^2 \times I_4^4$	1
$I_2^2 \times I_5$	28
$I_2^2 \times I_6$	22
$I_2^2 \times I_7$	2

Table B.3: List of generic non-toric Sp and SU -type Kodaira singularities of codimension-two genus-one fibers and the number of times they occur, part I.

Generic non-toric Kodaira singularities Occurrences

I_2^3	260
$I_2^3 \times I_3$	121
$I_2^3 \times I_3 \times I_4$	24
$I_2^3 \times I_3 \times I_5$	4
$I_2^3 \times I_3 \times I_6$	4
$I_2^3 \times I_3^2$	16
$I_2^3 \times I_4$	85
$I_2^3 \times I_4 \times I_6$	6
$I_2^3 \times I_4^2$	10
$I_2^3 \times I_5$	10
I_2^4	133
$I_2^4 \times I_3$	30
$I_2^4 \times I_3 \times I_4$	2
$I_2^4 \times I_3^2$	4
$I_2^4 \times I_4$	29
$I_2^4 \times I_4^2$	10
$I_2^4 \times I_5$	2
$I_2^4 \times I_6$	4
$I_2^4 \times I_8$	2
I_2^5	32
$I_2^5 \times I_4$	22
$I_2^5 \times I_6$	4
I_2^6	14
$I_2^6 \times I_4$	2
I_2^7	1
I_2^8	1
I_3	93
I_3^2	2
I_3^3	4
$I_3^3 \times I_6$	4
$I_3^3 \times I_9$	2
I_3^4	6
$I_3^4 \times I_6$	4
I_3^5	2
I_4	95
I_4^4	1
I_5	12
I_6	2

Table B.4: List of generic non-toric Sp and SU -type Kodaira singularities of codimension-two genus-one fibers and the number of times they occur, part II.

Appendix C

Details on the Calabi-Yau Geometries

In this appendix, we collect several geometric calculations and results that are too specific to our F-theory models to be included in the general introduction to toric geometry in [Appendix A](#).

We begin with a proof in [section C.1](#) of the identities for the second Chern class of an elliptically fibered Calabi-Yau manifold that we used in [section 6.2](#). Next, we describe in [section C.2](#) how to compute the sign of a matter curve with a given weight using the Mori cone of the Calabi-Yau manifold. In [section C.3](#) we examine the pairs of manifolds with and without section that we studied in [section 9.3](#) more rigorously. Finally, in [section C.4](#) we list the generating cones of the fans of some of the ambient spaces used as examples in this work.

C.1 Exact identities for the Second Chern Class

Let us show explicitly that an elliptically fibered Calabi-Yau threefold Y obeys

$$\int_Y \omega_\alpha \wedge c_2(Y) = -12K_\alpha, \quad (\text{C.1.1})$$

where $\omega_\alpha = \pi^*(\omega_\alpha^b)$ is obtained by pulling back the $(1,1)$ -form $\omega_\alpha^b \in H^{1,1}(B)$. To do so, we first note that the adjunction formula implies that

$$\begin{aligned} c_2(D_\alpha) &= c_2(Y)|_{D_\alpha} + \omega_\alpha \wedge \omega_\alpha - \omega_\alpha \wedge c_1(Y)|_{D_\alpha} \\ &= c_2(Y)|_{D_\alpha} + \omega_\alpha \wedge \omega_\alpha, \end{aligned} \quad (\text{C.1.2})$$

since Y is Calabi-Yau. Recalling that triple intersections of vertical divisors vanish, we can therefore rewrite the above integral as

$$\int_Y \omega_\alpha \wedge c_2(Y) = \int_Y \omega_\alpha \wedge c_2(D_\alpha) = \int_{D_\alpha} c_2(D_\alpha) = \chi(D_\alpha). \quad (\text{C.1.3})$$

We are left with calculating the Euler characteristic of the vertical divisor D_α . Fortunately, we can exploit that D_α is obtained by smoothly fibering the generic fiber manifold over D_α^b . In particular, D_α^b is a smooth manifold of complex dimension 1 and we have rid ourselves of the reducible fiber components that Y has. Hence, we can use Theorem 4.3 of [88] and reduce the integral over D_α to an integral over only the base of the fibration. In fact, for one-dimensional base manifolds one finds that

$$\chi(D_\alpha) = 12 \int_{D_\alpha^b} c_1(B)|_{D_\alpha^b} = -12K_\alpha, \quad (\text{C.1.4})$$

no matter whether the elliptic fiber is embedded in an E_6 , E_7 or E_8 model, which concludes our short proof.

For completeness, let us briefly show how to calculate c_0 assuming now that the zero section is *holomorphic*. Note that this merely reproduces the calculation in [54]. Using (C.1.2) for the zero section instead of D_α , one finds that

$$\begin{aligned} \int_Y \omega_{\hat{0}} \wedge c_2(Y) &= \int_Y \omega_{\hat{0}} \wedge (c_2(B) - \omega_{\hat{0}}) = \int_B c_2(B) - c_1(B) \wedge c_1(B) \\ &= -8 + 2h^{1,1}(B), \end{aligned} \quad (\text{C.1.5})$$

where we have used adjunction for a second time in order to obtain $\omega_{\hat{0}}^2 = -\omega_{\hat{0}} \wedge c_1(B)$. Inserting (6.1.4), one finds that $c_0 = c_0 - \frac{1}{2}K^\alpha K_\alpha$ and computes

$$K^\alpha K_\alpha = \int_B c_1(B) \wedge c_1(B) = 10 - h^{1,1}(B). \quad (\text{C.1.6})$$

Putting everything together, one finally ends up with

$$c_0 = 52 - 4h^{1,1}(B) \quad \text{if } s_0 \text{ is holomorphic.} \quad (\text{C.1.7})$$

C.2 Signs of Matter Curves from the Mori Cone

To compute the sign of a matter curve labeled by a weight w , one can use the Mori cone $M(Y)$ ¹ of the Calabi-Yau manifold Y defining the F-theory compactification. Given $M(Y)$, we construct the extended relative Mori cone $\widehat{M}(Y)$ as follows:

- Take the intersection of $M(Y)$ with the cone of all curves that have zero intersection with vertical divisors D_α .
- Strictly speaking, this is all we need in order to obtain the extended relative Mori cone of Y . However, it is useful to choose a different basis. Hence, for each element m of this newly obtained cone do:

¹We refer to [subsection A.7.1](#) for more information on how to compute the Mori cone of a complete intersection inside a toric ambient space.

- Find the unique weight \mathbf{w} of the weight space of $\mathfrak{g} = \text{Lie}(G_{\text{nA}})$ such that

$$-\langle \alpha_I, \mathbf{w} \rangle = D_I \cdot m \tag{C.2.1}$$

for all simple roots α_I . Here, the right hand side is the intersection product between the exceptional divisor associated to minus the simple root α_I and the curve m .

- Determine the $U(1)$ charges (q_{KK}, q_n) of m under the Kaluza-Klein vector A^0 and the Abelian gauge group factor $U(1)^{n_{U(1)}}$ by taking intersection products

$$q_{KK} = D_0 \cdot m \tag{C.2.2a}$$

$$q_n = D_n \cdot m \quad n = 1, \dots, n_{U(1)}. \tag{C.2.2b}$$

- The charges (q_{KK}, q_n) together with the weight \mathbf{w} determine an element

$$\tilde{m} = (\mathbf{w}, q_{KK}, q_n) \in V \otimes \mathbb{Z}^{n_{U(1)}+1}, \tag{C.2.3}$$

where V is the weight space of \mathfrak{g} .

- $\widehat{M}(Y)$ is the cone spanned by all elements \tilde{m} .

Note that there are

$$h^{1,1}(Y) - h^{1,1}(B) = \text{rank } \mathfrak{g} + n_{U(1)} + 1 \tag{C.2.4}$$

independent intersection numbers that an element m which does not intersect vertical divisors can have. It is therefore crucial to include the charge under the Kaluza-Klein vector field A^0 to obtain a one-to-one map between fields on the circle reduced side and the intersection number between the curve m and an arbitrary divisor of Y . In the early calculations of [52, 95, 113], all fibral curves were assumed to have vanishing intersection with the zero section and therefore to carry no KK-charge. However, this works only as long as the Kaluza-Klein modes do not contribute to the loop-induced Chern-Simons coefficients. Given a weight $w = (\mathbf{w}, q_n)$, one can easily define its sign using the extended relative Mori cone $\widehat{M}(Y)$:

$$\text{sign}(w, n_{KK}) \equiv \begin{cases} +1 & \text{if } (\mathbf{w}, n_{KK}, q_n) \in \widehat{M}(Y) \\ -1 & \text{otherwise} \end{cases} \tag{C.2.5}$$

Note that the above definition gives an actual sign function, that is one satisfying

$$\text{sign}(w, n_{KK}) = -\text{sign}(-w, -n_{KK}), \tag{C.2.6}$$

only if either the curve associated with the weight w or its conjugate, $-w$, is contained in the extended relative Mori cone. Since the Mori cone is convex, they can never both be contained in $\widehat{M}(Y)$. However, since physical states correspond to M2 branes wrapping either holomorphic or anti-holomorphic curves in the fiber [189], one has in fact that either w or $-w$ is an element of $\widehat{M}(Y)$ as long as these weights belong to representations that actually occur in the low-energy effective theory and hence the above definition makes sense.

C.3 Further Details on the No-Section Examples

In this section we include a few more details on the class of examples studied in [section 9.3](#). First we study in [subsection C.3.1](#) in more detail the loci of the resolved manifolds \mathbb{Y} along which the matter multiplets are located and then we prove carefully in [subsection C.3.2](#) that the deformed manifolds \mathcal{Y} do indeed not have a section.

C.3.1 Geometric Description of the Matter Multiplets in \mathbb{Y}

For the purposes of understanding the conifold transition, it was sufficient to understand the $\mathbf{1}_4$ states in [table 9.5](#). It is nevertheless interesting and somewhat illuminating to describe the geometric origin of the rest of the matter multiplets in the six-dimensional theory arising from F-theory on \mathbb{Y} .

We start with the $\mathbf{1}_2$ multiplets. In fact, the relevant curves have already been described in the $h^{1,1} = 3$ cases explicitly in [\[52\]](#) (under the names \mathcal{T}_n , $0 \leq n \leq 3$). We now review the discussion in that paper (using a slightly different approach). Let us assume $f \neq 0$. We want to understand under which conditions [Equation 9.3.11](#) factorizes into two \mathbb{P}^1 s. This happens whenever the Calabi-Yau equation factorizes as

$$\tilde{\phi} = (w + B)(ws + C) = 0 \tag{C.3.1}$$

for B, C to be determined. For simplicity we restrict ourselves to the case with $\deg(g) = 0$, and set $g = 1$. In this case, an easy argument shows that a holomorphic redefinition of w allows one to set $\alpha = \beta = 0$ in [Equation 9.3.3](#). In what follows we will implicitly perform such a redefinition.

Expanding [Equation C.3.1](#), and comparing with [Equation 9.3.11](#), we immediately conclude that

$$\begin{aligned} BC &= y_1 Q' \\ C + sB &= f y_2^2. \end{aligned} \tag{C.3.2}$$

By homogeneity and holomorphy, the most general form for B is given by

$$B = F y_1^2 s + G y_1 y_2 \tag{C.3.3}$$

with F, G polynomials in the x_i variables of the appropriate degree. (A term linear in w is also possible, but this can be reabsorbed in a redefinition of w .) Expanding the equations, and comparing order by order, we arrive at the equations

$$b = -F^2 \tag{C.3.4}$$

$$c = -2FG \tag{C.3.5}$$

$$d = Ff - G^2 \tag{C.3.6}$$

$$e = fG \tag{C.3.7}$$

which can be solved by

$$\begin{aligned} G &= \frac{e}{f} \\ F &= \frac{1}{f^3}(df^2 + e^2) \end{aligned} \tag{C.3.8}$$

as long as

$$\begin{aligned} b &= -\frac{1}{f^6}(d^2f^4 + 2df^2e^2 + e^4) \\ c &= -\frac{2}{f^4}(df^2e + e^3). \end{aligned} \tag{C.3.9}$$

The $\mathbf{1}_2$ multiplets live at the points in the base where this equation is satisfied. In order to count these points, we multiply the whole equation by appropriate powers of f (recall that $f \neq 0$ by assumption), obtaining the equations

$$\begin{aligned} P_1 &\equiv bf^6 + d^2f^4 + 2df^2e^2 + e^4 = 0 \\ P_2 &\equiv cf^4 + 2df^2e + 2e^3 = 0. \end{aligned} \tag{C.3.10}$$

This set of equations has $(3 \deg(e))(4 \deg(e)) = 12 \deg(e)^2$ solutions. Not all of these solutions correspond to $\mathbf{1}_2$ states, though, some solutions come from $f = e = 0$, which as discussed in [section 9.3](#) correspond to $\mathbf{1}_4$ multiplets instead. Each one of the solutions of $f = e = 0$ contributes $\deg_e(\text{Res}_f(P_1, P_2)) = 16$ spurious solutions to [\(C.3.10\)](#) (see [\[157\]](#)), so the final count for $\mathbf{1}_2$ multiplets is given by

$$H(\mathbf{1}_2) = 12 \deg(e)^2 - 16 \deg(f) \cdot \deg(e). \tag{C.3.11}$$

It is easy to check that this formula gives the right values for the entries with $\deg(g) = 0$ in [table 9.5](#).

Over the solutions of [\(C.3.10\)](#) with $f \neq 0$ in the base, the elliptic fiber factorizes into the curves

$$\begin{aligned} c_B &= \{w + Fy_1^2s + Gy_1y_2 = 0\} \\ c_C &= \{ws + fy_2^2 - F(sy_1)^2 - G(sy_1)y_2 = 0\}. \end{aligned} \tag{C.3.12}$$

The claim is that the hypermultiplets coming from wrapping M2 branes on these curves have charge two under [Equation 9.3.27](#). Notice first that, since we are assuming $f \neq 0$, both sections are holomorphic, and in particular $(c_B + c_C) \cdot \sigma_0 = (c_B + c_C) \cdot \sigma = 1$, since the two components of the fiber, taken together, span the class of the elliptic fiber. By the same token, the intersection is transversal, so necessarily one of the intersections vanishes, and the other is equal to one. More explicitly, an easy calculation gives

$$c_B \cdot \sigma_0 = c_C \cdot \sigma = 1, \tag{C.3.13}$$

$$c_B \cdot \sigma = c_C \cdot \sigma_0 = 0. \tag{C.3.14}$$

In addition, it is clear that $c_B \cdot [x_1] = c_C \cdot [x_1] = 0$, since the curves are localized over points in the base \mathbb{P}^2 , and for the $g \neq 0$ case that we are considering there is no intersection with the non-Abelian divisor. All in all, we obtain that $Q_{U(1)} = 2$.

We now consider $H(\mathbf{2}_3)$. We claim that these hypers come from the contracting spheres at $f = g = 0$. As discussed above, over this locus the T^2 fiber decomposes into three \mathbb{P}^1 components. We denote these components by \mathcal{C}_t , \mathcal{C}_{y_1} and \mathcal{C}_Ξ , and claim that the $\mathbf{2}_3$ hypers come from \mathcal{C}_{y_1} and \mathcal{C}_Ξ (the M2 states wrapping \mathcal{C}_t are rather associated with W bosons of $SU(2)$).

Consider first \mathcal{C}_Ξ . From the discussion above, we know that $\mathcal{C}_\Xi \cdot \sigma = 1$, $\mathcal{C}_\Xi \cdot \sigma_0 = 0$ (since σ_0 intersects the σ rational component), $\mathcal{C}_\Xi \cdot [x_1] = 0$ (by genericity) and $\mathcal{C}_\Xi \cdot [t] = 1$. Plugging into the charge formula, we conclude that $Q_{U(1)} = 3$. In addition, the $SU(2)$ Cartan is associated with $[t]$, so this is a charged state in the fundamental, with charge one under the Cartan.

Similarly, for \mathcal{C}_{y_1} we have that $\mathcal{C}_{y_1} \cdot \sigma_0 = 1$, $\mathcal{C}_{y_1} \cdot [x_1] = 0$ and $\mathcal{C}_{y_1} \cdot [t] = 1$. The intersection with σ is again somewhat subtle, since σ is non-holomorphic, wrapping the whole \mathcal{C}_{y_1} . By the moving fiber argument, $(\mathcal{C}_{y_1} + \mathcal{C}_\Xi + \mathcal{C}_t) \cdot \sigma = 1$, and from $(\mathcal{C}_\Xi + \mathcal{C}_t) \cdot \sigma = 2$ we conclude that $Q_{U(1)} = -1$. Plugging these values into the charge formula, we obtain $Q_{U(1)} = -3$. This state is also charged under the $SU(2)$ Cartan with charge one. Taking the conjugate state, we can complete the $\mathbf{2}_3$ multiplet, as advertised.

Let us now consider the $\mathbf{2}_1$ states. We consider factorizations of the form

$$\tilde{\phi} = t(b_0 y_1 s + b_1 y_2)(b_2 y_1^3 + b_3 y_1^2 y_2 s t + b_4 y_1 y_2^2 t + b_5 y_1 w s + b_6 y_2 w). \quad (\text{C.3.15})$$

Here the b_i are coefficients to be determined, and will depend on the coefficients b, c, \dots of the Calabi-Yau equation. Such a splitting exists whenever

$$g(x_i) = I_1(x_i) = 0, \quad (\text{C.3.16})$$

with $I_1(x_i) = b^2 f^3 + \dots$ a certain polynomial of the \mathbb{P}^2 coordinates x_i .² This will hold at

$$\begin{aligned} \deg(g) \cdot \deg(I_1) &= \deg(g) \cdot (2 \deg(b) + 3 \deg(f)) \\ &= -a^2 + 3ab - 2b^2 + 12a - 9b + 45 \end{aligned} \quad (\text{C.3.17})$$

points in the base. Comparing with [table 9.5](#) one easily sees that this expression reproduces the $H(\mathbf{2}_1)$ multiplicities, so we expect that these hypermultiplets come from M2 branes wrapping these degenerations. Let us check this claim explicitly.

Over a point satisfying [Equation C.3.16](#) we have that the fiber degenerates, and in addition, generically $b_1 \neq 0$ in [Equation C.3.15](#), since otherwise we would have three polynomials

²We computed [\(C.3.16\)](#) by computing the elimination ideal associated to solving for the b_i variables in [\(C.3.15\)](#) in terms of the Calabi-Yau coefficients, using SAGE [\[139\]](#).

intersecting over a point in \mathbb{P}^2 , which is non-generic. We can thus locally redefine y_2 in such a way that [Equation C.3.15](#) becomes

$$\tilde{\phi} = ty_2(b_2s^2y_1^3 + b_3y_1^2y_2st + b_4y_1y_2^2t + b_5y_1ws + b_6y_2w). \quad (\text{C.3.18})$$

(This redefinition of y_2 is not necessary, but it simplifies the presentation of the analysis.) Furthermore, comparing with the generic form [\(9.3.6\)](#) we can immediately identify $b_4 = e$, $b_6 = f$, and similarly for the other coefficients. We see that the fiber degenerates into three components: $\mathcal{C}_t = \{t = 0\}$, $\mathcal{C}_{y_2} = \{y_2 = 0\}$ and $\mathcal{C}_{\Xi'} = \{b_2y_1^3 + \dots\}$. Computing the intersections amongst the components, and between the components and the sections, is a completely straightforward exercise. The resulting non-vanishing intersections are

$$\mathcal{C}_t \cdot \mathcal{C}_{y_2} = \mathcal{C}_{y_2} \cdot \mathcal{C}_{\Xi'} = \mathcal{C}_{\Xi'} \cdot \mathcal{C}_t = 1 \quad (\text{C.3.19})$$

$$\mathcal{C}_{\Xi'} \cdot P = \mathcal{C}_t \cdot Q = 1. \quad (\text{C.3.20})$$

Plugging into the charge formula [\(9.3.30\)](#), we obtain that the M2 branes wrapped on \mathcal{C}_{y_2} , $\mathcal{C}_{\Xi'}$ form a doublet under $SU(2)$ (since they are charged under the Cartan) with $U(1)$ charge one, as expected from the counting above.

The last remaining set of states is $\mathbf{3}_0$. These have a somewhat different origin. Notice that they are adjoints of the $SU(2)$ group, this suggests that their origin comes from Wilson lines on the $SU(2)$ divisor, which we will call \mathbf{G} . Recall that this divisor is given by $\{g = 0\} \subset \mathbb{P}^2$, so its Euler character is, by adjunction:

$$\begin{aligned} \chi(\mathbf{G}) &= \int_{\mathbf{G}} c_1(T\mathbf{G}) = \int_{\mathbb{P}^2} [g] \wedge (3[x_1] - [g]) \\ &= \deg(g)(3 - \deg(g)) \end{aligned} \quad (\text{C.3.21})$$

or, equivalently, in terms of the genus $g_{\mathbf{G}}$ of \mathbf{G}

$$g_{\mathbf{G}} = 1 - \frac{\deg(g)}{2}(3 - \deg(g)). \quad (\text{C.3.22})$$

From the $SU(2)$ Wilson lines on the (two) one-cycles associated with each element of $g_{\mathbf{G}}$, together with scalars coming from reduction of C_3 on the same set of one-cycles (plus the contracting Cartan divisor), one obtains exactly $g_{\mathbf{G}}$ five-dimensional hypers in the adjoint representation, which lift to $g_{\mathbf{G}}$ six-dimensional hypers in F-theory. This reproduces precisely the count displayed in [table 9.5](#).

As an aside, let us highlight a small subtlety in checking six-dimensional anomaly cancellation. If one naively plugs the matter content in [table 9.5](#) into the six-dimensional anomaly cancellation conditions, one will see that the examples with $\mathbf{3}_0$ multiplets do not satisfy gravitational anomaly cancellation. The explanation is simple: deformations of \mathbf{G} can be described by complex structure moduli variation of the total Calabi-Yau, i.e. elements of $h^{2,1}(\mathcal{Y})$, but they are also encoded in the values of the Wilson lines over \mathbf{G} . In particular, since the gauge

group is $SU(2)$, there is a single Casimir invariant, and each Wilson line degree of freedom encodes one deformation modulus. We can see this a bit more precisely: as emphasized in [56], for instance, deformations of the \mathbf{G} locus are counted by sections the anticanonical bundle $K_{\mathbf{G}}$ of \mathbf{G} , and using Serre duality

$$\dim H^0(K_{\mathbf{G}}) = \dim H^1(\mathcal{O}_{\mathbf{G}}) = h^{0,1}(\mathbf{G}) \quad (\text{C.3.23})$$

which is precisely equal to $g_{\mathbf{G}}$ for a connected Riemann surface, such as \mathbf{G} . All in all, in order to avoid overcounting one should subtract $g_{\mathbf{G}}$ neutral hypers from the contribution of $h^{2,1}(\mathcal{Y})$ to the gravitational anomaly, or alternatively count the $\mathbf{3}_0$ multiplets with a multiplicity of two, instead of three.

C.3.2 Non-Existence of a Section for \mathcal{Y}

We would now like to show that the deformed spaces \mathcal{Y} considered in section 9.3 do not admit a section, but rather a bi-section. That is, there is no rational embedding of the base \mathbb{P}^2 into the total space such that the fiber is generically intersected at a single point. The best that we can do is to find divisors of the total space that project down to the base, but generically intersect the fiber twice, i.e. a two-section or a *bi-section*. The basic idea was described in [49, 212].

In order to prove this, we need to identify the fiber curve first. This is easy, it is simply given by $\mathcal{T} = [x_1]^2 \cap \mathcal{Y}$, which is intuitively easy to understand: the fiber is obtained by taking the preimage of a point (with class $[x_1]^2$) in the base \mathbb{P}^2 .

Now we need to prove that there is no section \mathbf{S} . In all of our examples, the Kähler cone of the Calabi-Yau \mathcal{Y} can be generated by the restrictions of the toric divisors $[x_1]$, $[y_1]$, and in the cases with $h^{1,1}(\mathcal{Y}) = 3$, also $[w]$. We thus parametrize

$$\mathbf{S} = a[x_1] + b[y_1] + c[w] \quad (\text{C.3.24})$$

with coefficients (a priori not necessarily integral) to be determined. The generic intersection between the T^2 fiber and the section is given by

$$\mathcal{T} \cdot \mathbf{S} = 2b + 4c. \quad (\text{C.3.25})$$

Showing that this can never be equal to one would follow if $b, c \in \mathbb{Z}$. This is indeed the case, as we now show. Consider first the case with $h^{1,1}(\mathcal{Y}) = 3$, since it is somewhat simpler. Over a locus in the base given by

$$g(x_i) = I_2(x_i) = 0 \quad (\text{C.3.26})$$

with³

$$\begin{aligned} I_2(x_i) = & f^4 b^2 - \beta f^3 b c + \alpha f^3 c^2 + \beta^2 f^2 b d - 2\alpha f^3 b d - \alpha \beta f^2 c d + \alpha^2 f^2 d^2 - \beta^3 f b e \\ & + 3\alpha \beta f^2 b e + \alpha \beta^2 f c e - 2\alpha^2 f^2 c e - \alpha^2 \beta f d e + \alpha^3 f e^2 + \beta^4 b a - 4\alpha \beta^2 f b a \\ & + 2\alpha^2 f^2 b a - \alpha \beta^3 c a + 3\alpha^2 \beta f c a + \alpha^2 \beta^2 d a - 2\alpha^3 f d a - \alpha^3 \beta e a + \alpha^4 a^2, \end{aligned} \quad (\text{C.3.27})$$

³As in subsection C.3.1 this is obtained using SAGE [139].

the Calabi-Yau equation (9.3.2) factorizes into three factors

$$\phi = t(b_0y_1 + b_1y_2)(b_2y_1^3 + b_3y_1^2y_2t + b_4y_1y_2^2t + b_5y_2^3t + b_6y_1w + b_7y_2w). \quad (\text{C.3.28})$$

The important part for our analysis is that this defines three holomorphic curves in the Calabi-Yau: $\mathcal{C}_t = \{t = 0\}$, $\mathcal{C}_y = \{b_0y_1 + b_1y_2 = 0\}$ and \mathcal{C}_Ξ for the other component. (The notation is intended to be reminiscent of that used in subsection C.3.1. Indeed, the matter we just found is precisely the $\mathbf{2}_1$ and $\mathbf{2}_3$ multiplets on the resolved side taken together, since after the Higgsing of the $U(1)$ they cannot be separated anymore.) Computing the intersection numbers with the generators of the Kähler cone chosen in (C.3.24) is an easy exercise, we get

$$\begin{aligned} \mathcal{C}_t \cdot [y_1] &= 1 \\ \mathcal{C}_y \cdot [w] &= 1 \end{aligned} \quad (\text{C.3.29})$$

with all other intersections vanishing. Since the intersection between a divisor and a curve in a smooth space has to be integral, by intersecting \mathbf{S} with these curves we conclude that $b, c \in \mathbb{Z}$, and thus $\mathcal{T} \cdot \mathbf{S} \in 2\mathbb{Z}$. In conclusion, there is no section, but rather a bi-section.

This argument fails for the cases with $h^{1,1}(\mathcal{Y}) = 2$, since $g = 0$ has no solutions. From the previous discussion it is nevertheless clear what to do, though: the $\mathbf{1}_2$ states on the resolved side \mathbb{Y} that we described in subsection C.3.1 will survive the conifold transition, and appear on the deformed side \mathcal{Y} as loci on the \mathbb{P}^2 base where the fiber degenerates as

$$\phi = (w + B)(w + D). \quad (\text{C.3.30})$$

Computing the intersection numbers one gets

$$\begin{aligned} \mathcal{C}_B \cdot [y_1] &= \mathcal{C}_D \cdot [y_1] = 1 \\ \mathcal{C}_B \cdot [x_1] &= \mathcal{C}_D \cdot [x_1] = 0 \end{aligned} \quad (\text{C.3.31})$$

and since a putative section $\mathbf{S} = a[x_1] + b[y_1]$ has intersection $\mathbf{S} \cdot \mathcal{T} = 2b$ with the fiber \mathcal{T} , this shows that indeed we have no section, but rather a bi-section.

C.4 Fans of various Ambient Spaces

Toric varieties whose dimension is larger than two are not uniquely specified by the rays of the fan, since there are usually many different ways of obtaining a regular fan with these rays. In this part of the appendix we therefore provide the generating cones of the fans for the toric ambient spaces of some of the Calabi-Yau geometries studied in the main text of this work.

C.4.1 Fan of the Threefold with Non-Toric Section

In table 5.4 we listed the rays of the fan defining a Calabi-Yau threefold with non-toric section. Different choices for the fan will result in different intersection numbers, but not in different

$U(1)$ charges. Nevertheless, we give the fan to be as concrete as possible. For the threefold hypersurface, we pick

$$\begin{aligned} \Sigma = \{ & \langle u_1 f_0 u_2 f_1 \rangle, \langle u_1 f_2 u_2 f_1 \rangle, \langle e_0 u_1 f_3 f_0 \rangle, \langle e_0 f_3 f_0 u_2 \rangle, \langle u_1 f_3 f_0 u_2 \rangle, \\ & \langle u_1 f_3 f_2 e_3 \rangle, \langle f_3 f_2 e_3 u_2 \rangle, \langle u_1 f_3 f_2 u_2 \rangle, \langle u_1 e_1 e_2 f_1 \rangle, \langle u_1 f_2 e_2 f_1 \rangle, \\ & \langle u_1 f_2 e_3 e_2 \rangle, \langle e_1 u_2 e_2 f_1 \rangle, \langle f_2 u_2 e_2 f_1 \rangle, \langle f_2 e_3 u_2 e_2 \rangle, \langle e_0 u_1 e_1 f_1 \rangle, \\ & \langle e_0 u_1 f_0 f_1 \rangle, \langle e_0 u_1 e_1 e_2 \rangle, \langle e_0 f_0 u_2 f_1 \rangle, \langle e_0 e_1 u_2 f_1 \rangle, \langle e_0 e_1 u_2 e_2 \rangle, \\ & \langle u_1 f_3 e_3 e_4 \rangle, \langle e_0 u_1 f_3 e_4 \rangle, \langle e_0 f_3 u_2 e_4 \rangle, \langle f_3 e_3 u_2 e_4 \rangle, \langle e_0 u_1 e_2 e_4 \rangle, \\ & \left. \langle u_1 e_3 e_2 e_4 \rangle, \langle e_3 u_2 e_2 e_4 \rangle, \langle e_0 u_2 e_2 e_4 \rangle \right\}. \end{aligned} \quad (\text{C.4.1})$$

C.4.2 Fans of the Threefolds with Abelian Gauge Groups

Here we display the fans of the three Calabi-Yau threefolds presented in [section 9.2](#). Note that two of the varieties had phases where the zero-section was either holomorphic or not. In those cases, we provide fans for both phases. We denote the generating cones by listing the homogeneous coordinates corresponding to the rays that span the cone.

$$\begin{aligned} \Sigma_{I, \text{hol.}} = \{ & \langle u_1 u_2 f_0 f_1 \rangle, \langle u_1 u_2 f_0 f_3 \rangle, \langle u_1 u_2 f_1 f_2 \rangle, \langle u_1 u_2 f_2 f_3 \rangle, \langle u_1 e_0 e_1 f_1 \rangle, \\ & \langle u_1 e_0 e_1 f_2 \rangle, \langle u_1 e_0 f_0 f_1 \rangle, \langle u_1 e_0 f_0 f_3 \rangle, \langle u_1 e_0 f_2 f_3 \rangle, \langle u_1 e_1 f_1 f_2 \rangle, \\ & \langle u_2 e_0 e_1 f_1 \rangle, \langle u_2 e_0 e_1 f_2 \rangle, \langle u_2 e_0 f_0 f_1 \rangle, \langle u_2 e_0 f_0 f_3 \rangle, \langle u_2 e_0 f_2 f_3 \rangle, \\ & \left. \langle u_2 e_1 f_1 f_2 \rangle \right\} \end{aligned} \quad (\text{C.4.2})$$

$$\begin{aligned} \Sigma_{I, \text{non-hol.}} = \{ & \langle u_1 u_2 f_0 f_1 \rangle, \langle u_1 u_2 f_0 f_3 \rangle, \langle u_1 u_2 f_1 f_2 \rangle, \langle u_1 u_2 f_2 f_3 \rangle, \langle u_1 e_0 e_1 f_0 \rangle, \\ & \langle u_1 e_0 e_1 f_2 \rangle, \langle u_1 e_0 f_0 f_3 \rangle, \langle u_1 e_0 f_2 f_3 \rangle, \langle u_1 e_1 f_0 f_1 \rangle, \langle u_1 e_1 f_1 f_2 \rangle, \\ & \langle u_2 e_0 e_1 f_0 \rangle, \langle u_2 e_0 e_1 f_2 \rangle, \langle u_2 e_0 f_0 f_3 \rangle, \langle u_2 e_0 f_2 f_3 \rangle, \langle u_2 e_1 f_0 f_1 \rangle, \\ & \left. \langle u_2 e_1 f_1 f_2 \rangle \right\} \end{aligned} \quad (\text{C.4.3})$$

$$\begin{aligned} \Sigma_{II} = \{ & \langle u_1 u_2 f_0 f_2 \rangle, \langle u_1 u_2 f_0 f_3 \rangle, \langle u_1 u_2 f_1 f_3 \rangle, \langle u_1 u_2 f_1 f_4 \rangle, \langle u_1 u_2 f_2 f_4 \rangle, \\ & \langle u_1 e_0 e_1 e_4 \rangle, \langle u_1 e_0 e_1 f_0 \rangle, \langle u_1 e_0 e_4 f_0 \rangle, \langle u_1 e_1 e_2 e_4 \rangle, \langle u_1 e_1 e_2 f_0 \rangle, \\ & \langle u_1 e_2 e_3 e_4 \rangle, \langle u_1 e_2 e_3 f_1 \rangle, \langle u_1 e_2 f_0 f_3 \rangle, \langle u_1 e_2 f_1 f_3 \rangle, \langle u_1 e_3 e_4 f_4 \rangle, \\ & \langle u_1 e_3 f_1 f_4 \rangle, \langle u_1 e_4 f_0 f_2 \rangle, \langle u_1 e_4 f_2 f_4 \rangle, \langle u_2 e_0 e_1 e_4 \rangle, \langle u_2 e_0 e_1 f_0 \rangle, \\ & \langle u_2 e_0 e_4 f_0 \rangle, \langle u_2 e_1 e_2 e_4 \rangle, \langle u_2 e_1 e_2 f_0 \rangle, \langle u_2 e_2 e_3 e_4 \rangle, \langle u_2 e_2 e_3 f_1 \rangle, \\ & \langle u_2 e_2 f_0 f_3 \rangle, \langle u_2 e_2 f_1 f_3 \rangle, \langle u_2 e_3 e_4 f_4 \rangle, \langle u_2 e_3 f_1 f_4 \rangle, \langle u_2 e_4 f_0 f_2 \rangle, \\ & \left. \langle u_2 e_4 f_2 f_4 \rangle \right\} \end{aligned} \quad (\text{C.4.4})$$

$$\begin{aligned}
\Sigma_{III, \text{hol.}} = & \left\{ \langle u_1 u_2 f_0 f_2 \rangle, \langle u_1 u_2 f_0 f_4 \rangle, \langle u_1 u_2 f_1 f_3 \rangle, \langle u_1 u_2 f_1 f_4 \rangle, \langle u_1 u_2 f_2 f_3 \rangle, \right. \\
& \langle u_1 e_0 e_1 e_4 \rangle, \langle u_1 e_0 e_1 f_2 \rangle, \langle u_1 e_0 e_4 f_0 \rangle, \langle u_1 e_0 f_0 f_2 \rangle, \langle u_1 e_1 e_2 e_3 \rangle, \\
& \langle u_1 e_1 e_2 f_2 \rangle, \langle u_1 e_1 e_3 e_4 \rangle, \langle u_1 e_2 e_3 f_1 \rangle, \langle u_1 e_2 f_1 f_3 \rangle, \langle u_1 e_2 f_2 f_3 \rangle, \\
& \langle u_1 e_3 e_4 f_4 \rangle, \langle u_1 e_3 f_1 f_4 \rangle, \langle u_1 e_4 f_0 f_4 \rangle, \langle u_2 e_0 e_1 e_4 \rangle, \langle u_2 e_0 e_1 f_2 \rangle, \\
& \langle u_2 e_0 e_4 f_0 \rangle, \langle u_2 e_0 f_0 f_2 \rangle, \langle u_2 e_1 e_2 e_3 \rangle, \langle u_2 e_1 e_2 f_2 \rangle, \langle u_2 e_1 e_3 e_4 \rangle, \\
& \langle u_2 e_2 e_3 f_1 \rangle, \langle u_2 e_2 f_1 f_3 \rangle, \langle u_2 e_2 f_2 f_3 \rangle, \langle u_2 e_3 e_4 f_4 \rangle, \langle u_2 e_3 f_1 f_4 \rangle, \\
& \left. \langle u_2 e_4 f_0 f_4 \rangle \right\} \tag{C.4.5}
\end{aligned}$$

$$\begin{aligned}
\Sigma_{III, \text{non-hol.}} = & \left\{ \langle u_1 u_2 f_0 f_2 \rangle, \langle u_1 u_2 f_0 f_4 \rangle, \langle u_1 u_2 f_1 f_3 \rangle, \langle u_1 u_2 f_1 f_4 \rangle, \langle u_1 u_2 f_2 f_3 \rangle, \right. \\
& \langle u_1 e_0 e_1 e_4 \rangle, \langle u_1 e_0 e_1 f_0 \rangle, \langle u_1 e_0 e_4 f_0 \rangle, \langle u_1 e_1 e_2 e_3 \rangle, \langle u_1 e_1 e_2 f_2 \rangle, \\
& \langle u_1 e_1 e_3 e_4 \rangle, \langle u_1 e_1 f_0 f_2 \rangle, \langle u_1 e_2 e_3 f_1 \rangle, \langle u_1 e_2 f_1 f_3 \rangle, \langle u_1 e_2 f_2 f_3 \rangle, \\
& \langle u_1 e_3 e_4 f_1 \rangle, \langle u_1 e_4 f_0 f_4 \rangle, \langle u_1 e_4 f_1 f_4 \rangle, \langle u_2 e_0 e_1 e_4 \rangle, \langle u_2 e_0 e_1 f_0 \rangle, \\
& \langle u_2 e_0 e_4 f_0 \rangle, \langle u_2 e_1 e_2 e_3 \rangle, \langle u_2 e_1 e_2 f_2 \rangle, \langle u_2 e_1 e_3 e_4 \rangle, \langle u_2 e_1 f_0 f_2 \rangle, \\
& \langle u_2 e_2 e_3 f_1 \rangle, \langle u_2 e_2 f_1 f_3 \rangle, \langle u_2 e_2 f_2 f_3 \rangle, \langle u_2 e_3 e_4 f_1 \rangle, \langle u_2 e_4 f_0 f_4 \rangle, \\
& \left. \langle u_2 e_4 f_1 f_4 \rangle \right\} \tag{C.4.6}
\end{aligned}$$

Appendix D

Representation Theory

In this appendix, we briefly state the group theory conventions used in this paper and then proceed to prove three identities used to match one-loop Chern-Simons terms from five-dimensional F-theory with intersection numbers on the M-theory side in [section 7.3](#). For the sake of brevity, we denote the roots of the non-Abelian group by α instead of α_{nA} . For an introduction to the theory of Lie algebras and their representations, we refer for example to [\[246\]](#).

Let us begin by defining the coroot intersection matrix as

$$\mathcal{C}_{IJ} = \frac{1}{\lambda(\mathfrak{g})} \langle \alpha_I^\vee, \alpha_J^\vee \rangle = \frac{1}{\lambda(\mathfrak{g})} \frac{2}{\langle \alpha_J, \alpha_J \rangle} C_{IJ}, \quad (\text{D.0.1})$$

where $\langle \alpha_I^\vee, \alpha_J^\vee \rangle$ denotes the inner product between two coroots of the Lie algebra \mathfrak{g} and α_I are the simple roots of \mathfrak{g} . We also define

$$\lambda(\mathfrak{g}) = \frac{2}{\langle \alpha_{\text{max}}, \alpha_{\text{max}} \rangle}, \quad (\text{D.0.2})$$

where α_{max} is the root of the Lie algebra \mathfrak{g} with maximal length. The Cartan matrix is referred to as C_{IJ} . Note that for the simply-laced groups of ADE-type, \mathcal{C}_{IJ} and the Cartan matrix C_{IJ} coincide. Throughout this work the conventions for the normalization of the Cartan generators T^M are chosen such that

$$\text{tr}(T^M T^N) = \delta^{MN}, \quad (\text{D.0.3})$$

where the trace is taken in the fundamental representation of \mathfrak{g} . Note that this also fixes the normalization of the roots and weights.

Having fixed all notation, we proceed by proving the second equality in [Equation 7.3.14b](#). To do so, we show that

$$A_{\text{adj}} \lambda(\mathfrak{g}) \mathcal{C}_{IJ} = \sum_{\text{roots}} \langle \alpha_I^\vee, \alpha \rangle \langle \alpha_J^\vee, \alpha \rangle \quad (\text{D.0.4})$$

$$A_{\mathbf{R}}\lambda(\mathfrak{g})\mathcal{C}_{IJ} = \sum_{w \in \mathbf{R}} \langle \alpha_I^\vee, w \rangle \langle \alpha_J^\vee, w \rangle , \quad (\text{D.0.5})$$

where the second equation is a generalization of the first. These hold for any simple Lie algebra \mathfrak{g} and for all non-trivial, finite-dimensional irreducible representations \mathbf{R} .

Following [246] we first define an inner product on the Lie algebra \mathfrak{g}

$$\begin{aligned} \kappa : \mathfrak{g} \times \mathfrak{g} &\rightarrow \mathbb{C} \\ x, y &\mapsto \text{tr}(\text{ad}_x \circ \text{ad}_y) , \end{aligned} \quad (\text{D.0.6})$$

where the trace is taken in the adjoint representation of the Lie algebra. The above product is called the Killing form and it is bilinear and symmetric. It was proven by Cartan that for finite-dimensional semi-simple Lie algebras the Killing form κ is non-degenerate and, hence, so is its restriction to any Cartan sub-algebra $\mathfrak{g}_\circ \subset \mathfrak{g}$. We can therefore use the Killing form to identify the Cartan sub-algebra \mathfrak{g}_\circ with the dual space \mathfrak{g}_\circ^* , the space spanned by the roots. In particular, we identify $\alpha \in \mathfrak{g}_\circ^*$ with $T^\alpha \in \mathfrak{g}_\circ$ such that

$$\alpha(T) = c_\alpha \kappa(T^\alpha, T) \quad \forall T \in \mathfrak{g}_\circ , \quad (\text{D.0.7})$$

where c_α is some normalization constant. If one then chooses a basis of the Cartan sub-algebra $\{T^M\}_{M=1, \dots, \dim(\mathfrak{g}_\circ)}$ generating the non-Abelian gauge group, one can expand every T^α as

$$T^\alpha = a_M^\alpha T^M , \quad (\text{D.0.8})$$

In accordance with Equation D.0.3 we have normalized the Cartan generators as

$$\kappa(T^M T^N) = A_{\text{adj}} \delta^{MN} . \quad (\text{D.0.9})$$

Identifying \mathfrak{g}_\circ and \mathfrak{g}_\circ^* enables us to define a non-degenerate product on \mathfrak{g}_\circ^* via the Killing form by setting

$$(\alpha, \beta) := c_\alpha c_\beta \kappa(T^\alpha T^\beta) = c_\beta \alpha(T^\beta) . \quad (\text{D.0.10})$$

for any two roots $\alpha, \beta \in \mathfrak{g}_\circ^*$. By bilinearity, this extends to all of \mathfrak{g}_\circ^* .

Let us now use the following identity from [246] for any $\lambda, \mu \in \mathfrak{g}_\circ^*$:

$$(\lambda, \mu) = \sum_{\text{roots}} (\alpha, \lambda)(\alpha, \mu) . \quad (\text{D.0.11})$$

The right hand side of this equation can be expanded as

$$\begin{aligned}
\sum_{\text{roots}} (\alpha, \lambda)(\alpha, \mu) &= \sum_{\text{roots}} c_\alpha c_\lambda \kappa(T^\alpha, T^\lambda) c_\alpha c_\mu \kappa(T^\alpha, T^\mu) \\
&= \sum_{\text{roots}} c_\alpha c_\lambda a_M^\alpha a_N^\lambda \kappa(T^M, T^N) c_\alpha c_\mu a_K^\alpha a_L^\mu \kappa(T^K, T^L) \\
&= \sum_{\text{roots}} c_\alpha c_\lambda \frac{1}{c_\alpha A_{\text{adj}}} \alpha(T^M) \frac{1}{c_\lambda A_{\text{adj}}} \lambda(T^N) A_{\text{adj}} \delta^{MN} \times \\
&\quad c_\alpha c_\mu \frac{1}{c_\alpha A_{\text{adj}}} \alpha(T^K) \frac{1}{c_\mu A_{\text{adj}}} \mu(T^L) A_{\text{adj}} \delta^{KL} \\
&= \sum_{\text{roots}} \frac{1}{A_{\text{adj}}^2} \alpha(T^M) \lambda(T^M) \alpha(T^K) \mu(T^K) \\
&= \sum_{\text{roots}} \frac{1}{A_{\text{adj}}^2} \langle \alpha, \lambda \rangle \langle \alpha, \mu \rangle .
\end{aligned} \tag{D.0.12}$$

Similarly, the left hand side can be rewritten as

$$\begin{aligned}
(\lambda, \mu) &= c_\lambda c_\mu \kappa(T^\lambda, T^\mu) = c_\lambda c_\mu a_M^\lambda a_N^\mu \kappa(T^M, T^N) = c_\lambda c_\mu \frac{1}{c_\lambda A_{\text{adj}}} \lambda(T^M) \frac{1}{c_\mu A_{\text{adj}}} \mu(T^N) A_{\text{adj}} \delta^{MN} \\
&= \frac{1}{A_{\text{adj}}} \lambda(T^M) \mu(T^M) = \frac{1}{A_{\text{adj}}} \langle \lambda, \mu \rangle .
\end{aligned} \tag{D.0.13}$$

Combining the two equations then yields

$$A_{\text{adj}} \langle \lambda, \mu \rangle = \sum_{\text{roots}} \langle \alpha, \lambda \rangle \langle \alpha, \mu \rangle . \tag{D.0.14}$$

Now note that

$$\langle \alpha_I^\vee, \alpha_J^\vee \rangle = \frac{4 \langle \alpha_I, \alpha_J \rangle}{\langle \alpha_I, \alpha_I \rangle \langle \alpha_J, \alpha_J \rangle} = \lambda(\mathfrak{g}) \mathcal{C}_{IJ} \tag{D.0.15}$$

and insert the coroots α_I^\vee and α_J^\vee for λ and μ to obtain

$$A_{\text{adj}} \lambda(\mathfrak{g}) \mathcal{C}_{IJ} = \sum_{\text{roots}} \langle \alpha, \alpha_I^\vee \rangle \langle \alpha, \alpha_J^\vee \rangle , \tag{D.0.16}$$

which is exactly [Equation D.0.4](#).

Let us now proceed and prove [Equation D.0.5](#). As shown in [246], for any simple Lie algebra \mathfrak{g} and any finite-dimensional, non-trivial irreducible representation \mathbf{R} , the trace over \mathbf{R} is proportional to the trace in the adjoint representation. Hence,

$$\kappa_{\mathbf{R}}(x, y) := \text{tr}(\mathbf{R}(x)\mathbf{R}(y)) = K_{\mathbf{R}} \kappa(x, y) \tag{D.0.17}$$

for all $x, y \in \mathfrak{g}$ with the proportionality factor $K_{\mathbf{R}}$ depending of course on the representation \mathbf{R} . Using the definition of the inner product in Equation D.0.10, we then have for $\lambda, \mu \in \mathfrak{g}^*$ that

$$\begin{aligned} (\lambda, \mu) &= c_\lambda c_\mu \kappa_{\text{adj}}(T^\lambda, T^\mu) = c_\lambda c_\mu a_M^\lambda a_N^\mu \frac{1}{K_{\mathbf{R}}} \kappa_{\mathbf{R}}(T^M, T^N) \\ &= c_\lambda c_\mu \frac{1}{c_\lambda A_{\text{adj}}} \lambda(T^M) \frac{1}{c_\mu A_{\text{adj}}} \mu(T^N) \frac{1}{K_{\mathbf{R}}} \sum_{\mathbf{w} \in \mathbf{R}} \mathbf{w}(T^M) \mathbf{w}(T^N) \\ &= \frac{1}{A_{\text{adj}}^2} \lambda(T^M) \mu(T^N) \frac{1}{K_{\mathbf{R}}} \sum_{\mathbf{w} \in \mathbf{R}} \mathbf{w}(T^M) \mathbf{w}(T^N) = \frac{1}{A_{\text{adj}}^2} \frac{1}{K_{\mathbf{R}}} \sum_{\mathbf{w} \in \mathbf{R}} \langle \lambda, \mathbf{w} \rangle \langle \mu, \mathbf{w} \rangle . \end{aligned} \quad (\text{D.0.18})$$

In the third equality we used that the weights can be chosen to form an orthonormal basis of the representation space. Inserting Equation D.0.13, one then finds

$$\begin{aligned} K_{\mathbf{R}} A_{\text{adj}} \langle \lambda, \mu \rangle &= \sum_{\mathbf{w} \in \mathbf{R}} \langle \lambda, \mathbf{w} \rangle \langle \mu, \mathbf{w} \rangle \\ \Rightarrow A_{\mathbf{R}} \langle \lambda, \mu \rangle &= \sum_{\mathbf{w} \in \mathbf{R}} \langle \lambda, \mathbf{w} \rangle \langle \mu, \mathbf{w} \rangle , \end{aligned} \quad (\text{D.0.19})$$

which, after plugging in the coroots, finally yields Equation D.0.5:

$$A_{\mathbf{R}} \lambda(\mathfrak{g}) \mathcal{C}_{IJ} = \sum_{\mathbf{w} \in \mathbf{R}} \langle \alpha_I^\vee, \mathbf{w} \rangle \langle \alpha_J^\vee, \mathbf{w} \rangle . \quad (\text{D.0.20})$$

Last of all, we prove the identity

$$\sum_{\mathbf{w} \in \mathbf{R}} \langle \alpha, \mathbf{w} \rangle = 0 \quad (\text{D.0.21})$$

for any root α and any highest weight representation \mathbf{R} .

Given a representation \mathbf{R} of a Lie algebra \mathfrak{g} and a simple root α , \mathfrak{g} always contains an $\mathfrak{sl}(2, \mathbb{C})$ subalgebra defined as

$$s_\alpha = \mathfrak{g}_\alpha \oplus \mathfrak{g}_{-\alpha} \oplus [\mathfrak{g}_\alpha, \mathfrak{g}_{-\alpha}] . \quad (\text{D.0.22})$$

Here, \mathfrak{g}_α is the linear subspace of \mathfrak{g} spanned by elements $\mathfrak{l} \in \mathfrak{g}$ such that $[T^M, \mathfrak{l}] = \alpha^M \mathfrak{l}$, where T^M form the basis of the Cartan subalgebra of \mathfrak{g} . Now, the idea is to decompose \mathbf{R} into chains of representations of s_α in order to reduce the problem to dealing with $\mathfrak{sl}(2, \mathbb{C})$ representations. And in fact, this can easily be accomplished as follows. Given any weight \mathbf{w} of \mathbf{R} , acting with $\mathfrak{g}_{\pm\alpha}$ either annihilates \mathbf{w} or gives another weight $\mathbf{w}' = \mathbf{w} \pm \alpha$ of \mathbf{R} , since s_α is a subalgebra of \mathfrak{g} . The different orbits under the action of s_α therefore form a partition of the weights $\mathbf{w} \in \mathbf{R}$. For each such orbit, we pick the highest weight \mathbf{v} with of the $\mathfrak{sl}(2, \mathbb{C})$ representation associated with s_α and denote its dimension by $d_{\mathbf{v}}$. Then \mathbf{R} decomposes as

$$\mathbf{R} = \bigoplus_{\mathbf{v}} (V_{\mathbf{v}} \oplus V_{\mathbf{v}-\alpha} \cdots \oplus V_{\mathbf{v}-(d_{\mathbf{v}}-1)\alpha}) , \quad (\text{D.0.23})$$

where \mathbf{v} ranges over highest weights of s_α orbits and $V_{\mathbf{w}}$ is the subspace of \mathbf{R} spanned by \mathbf{w} . One can now rearrange Equation D.0.21 into sums over $\mathfrak{sl}(2, \mathbb{C})$ representations and take advantage of the fact that the representation theory of highest weight representations of $\mathfrak{sl}(2, \mathbb{C})$ is very simple. Since the weights of a such a representation with dimension d are just integer numbers given by

$$d-1, d-3, \dots, -(d-1), -(d-3), \quad (\text{D.0.24})$$

one can evaluate

$$\sum_{\mathbf{w} \in \mathbf{R}} \langle \mathbf{w}, \alpha \rangle = \sum_{\mathbf{v}} \sum_{i=0}^{d_{\mathbf{v}}-1} \langle \mathbf{v} - i\alpha, \alpha \rangle = \sum_{\mathbf{v}} \sum_{i=0}^{d_{\mathbf{v}}-1} (d-1-2i) = 0. \quad (\text{D.0.25})$$

Appendix E

Circle Reduction of the Six-Dimensional Action

In this appendix we explicitly carry out in [section E.2](#) the circle reduction of six-dimensional $\mathcal{N} = (1,0)$ supergravity as sketched in [section 6.3](#) and provide in [section E.3](#) some of the necessary formulae for the loop calculations that one encounters when integrating out the massive states of the circle-reduced theory. First, however, we summarize our conventions.

E.1 Supergravity Conventions

For all spacetime dimensions d , let us adopt the mostly plus convention for the metric $g_{\mu\nu}$, and the $(+++)$ conventions of [\[247\]](#) for the Riemann tensor. Furthermore, we denote the Levi-Civita tensor by $\epsilon_{\mu_1 \dots \mu_d}$ and use the above metric to raise its indices. With this definition we have in any coordinate system $(x^0, x^1, \dots, x^{d-1})$ that

$$\epsilon_{01 \dots (d-1)} = +\sqrt{-\det g_{\mu\nu}} . \quad (\text{E.1.1})$$

Then the following identity is satisfied for arbitrary $k = 0, \dots, d$:

$$\epsilon_{\mu_1 \dots \mu_k \lambda_{k+1} \dots \lambda_d} \epsilon^{\nu_1 \dots \nu_k \lambda_{k+1} \dots \lambda_d} = -k!(d-k!) \delta_{[\mu_1}^{\nu_1} \dots \delta_{\mu_k]}^{\nu_k} . \quad (\text{E.1.2})$$

We expand differential p -forms as

$$\lambda = \frac{1}{p!} \lambda_{\mu_1 \dots \mu_p} dx^{\mu_1} \wedge \dots \wedge dx^{\mu_p} , \quad (\text{E.1.3})$$

such that the wedge product of a p - and a q -form satisfies

$$(\alpha \wedge \beta)_{\mu_1 \dots \mu_{p+q}} = \frac{(p+q)!}{p!q!} \alpha_{[\mu_1 \dots \mu_p} \beta_{\mu_{p+1} \dots \mu_{p+q}]} . \quad (\text{E.1.4})$$

Next of all, exterior differentiation of a p -form yields

$$(d\alpha)_{\mu_0 \dots \mu_p} = (p+1) \partial_{[\mu_0} \alpha_{\mu_1 \dots \mu_p]} . \quad (\text{E.1.5})$$

In real coordinates and arbitrary spacetime dimension d , we take the Hodge dual of a p -form to be defined by the following expression:

$$(*\alpha)_{\mu_1 \dots \mu_{d-p}} = \frac{1}{p!} \alpha^{\nu_1 \dots \nu_p} \epsilon_{\nu_1 \dots \nu_p \mu_1 \dots \mu_{d-p}} . \quad (\text{E.1.6})$$

As a consequence,

$$\alpha \wedge *\beta = \frac{1}{p!} \alpha_{\mu_1 \dots \mu_p} \beta^{\mu_1 \dots \mu_p} *1 \quad (\text{E.1.7})$$

is satisfied identically for arbitrary p -forms α, β .

E.2 The Circle Reduction

To perform the circle reduction, we closely follow [54]. Upon compactification on a circle of radius r the six-dimensional metric is reduced to

$$d\hat{s}^2 = \tilde{g}_{\mu\nu} dx^\mu dx^\nu + r^2 Dy^2 , \quad (\text{E.2.1})$$

where

$$Dy = dy - A^0 , \quad A^0 = A^0_\mu dx^\mu \quad F^0 = dA^0 . \quad (\text{E.2.2})$$

Here $\tilde{g}_{\mu\nu}$ is the five-dimensional metric and the tilde indicates that one still has to perform a Weyl rescaling to obtain the Einstein-Hilbert term in the canonical form. Recall that six-dimensional quantities and indices are denoted by a hat and that five-dimensional fields do not depend on the circle coordinate y . The Kaluza-Klein vector A^0 enjoys a $U(1)$ gauge symmetry from S^1 -diffeomorphisms and has the usual Abelian field strength F^0 . The reduction of the Vielbeine is found to be

$$\hat{e}^a = \tilde{e}^a_\mu dx^\mu , \quad \hat{e}^5 = r Dy . \quad (\text{E.2.3})$$

The spin connection reduces to

$$\hat{\omega}_{ab} = \tilde{\omega}_{ab} + \tilde{\mathbf{a}}_{ab}^{(0)} Dy , \quad \hat{\omega}_{a5} = \tilde{\mathbf{b}}_a^{(1)} + \tilde{\mathbf{c}}_a^{(0)} Dy , \quad (\text{E.2.4})$$

where we have introduced the functions $\tilde{\mathbf{a}}_{ab}^{(0)}$, $\tilde{\mathbf{c}}_a^{(0)}$ and the one-form $\tilde{\mathbf{b}}_a^{(1)}$ given by

$$\tilde{\mathbf{a}}_{ab}^{(0)} = \frac{1}{2} r^2 \tilde{e}^{\mu}_a \tilde{e}^{\nu}_b F_{\mu\nu}^0 , \quad \tilde{\mathbf{b}}_a^{(1)} = \frac{1}{2} r \tilde{e}^{\lambda}_a F_{\lambda\mu}^0 dx^\mu , \quad \tilde{\mathbf{c}}_a^{(0)} = -\tilde{e}^{\lambda}_a \tilde{\nabla}_\lambda r . \quad (\text{E.2.5})$$

At leading order, the reduction of the Ricci-scalar is

$$\hat{R} = \tilde{R} + \dots , \quad (\text{E.2.6})$$

where we neglect higher curvature contributions.¹ The vectors are reduced according to

$$\hat{A} = A + \zeta Dy , \quad \hat{A}^m = A^m + \zeta^m Dy , \quad (\text{E.2.7})$$

¹We stress that for the moment we approach only a two-derivative reduction and therefore higher curvature contributions are omitted in the following. This affects the Green-Schwarz term, the tensor kinetic terms and the Einstein-Hilbert term, see also [section 6.3](#).

where A , A^m are five-dimensional vectors and ζ , ζ^m are five-dimensional scalars. The reduction of the tensors reads

$$\hat{B}^\alpha = B^\alpha - [A^\alpha - \frac{1}{2}a^\alpha \text{tr}(\tilde{\mathbf{a}}^{(0)}\tilde{\omega}) - 2\frac{b^\alpha}{\lambda(\mathfrak{g})} \text{tr}(\zeta A) - 2b_{mn}^\alpha \zeta^m A^n] \wedge Dy \quad (\text{E.2.8})$$

with a five-dimensional tensor B^α and a five-dimensional vector A^α . While the Abelian vector A^α has the usual field strength $F^\alpha = dA^\alpha$, the gauge invariant field strength for B^α turns out to be

$$G^\alpha = dB^\alpha - A^\alpha \wedge F^0 + \frac{1}{2}a^\alpha \tilde{\omega}_{grav}^{CS} + 2\frac{b^\alpha}{\lambda(\mathfrak{g})} \omega^{CS} + 2b_{mn}^\alpha \omega^{CS,mn}. \quad (\text{E.2.9})$$

As already mentioned in [section 6.3](#), the six-dimensional scalars reduce trivially to five-dimensional scalars.

One can now insert these reductions into the six-dimensional action [\(6.3.17\)](#). We show the results for the different terms separately. The Einstein-Hilbert term is reduced to

$$\hat{S}_{EH}^{(6)} = \int_{M_6} \frac{1}{2} \hat{R} \hat{*} 1 = \int_{M_6} \frac{1}{2} r \tilde{R} \tilde{*} 1 \wedge Dy. \quad (\text{E.2.10})$$

To obtain the corresponding term in the five-dimensional effective action, one has to integrate over the circle direction, which is just a trivial integration of Dy . Now the reduction of the Green-Schwarz terms takes the form²

$$\begin{aligned} S_{GS}^{(6)} &= \int_{M_6} -\Omega_{\alpha\beta} \frac{b^\alpha}{\lambda(\mathfrak{g})} \hat{B}_\beta \wedge \text{tr} \hat{F} \wedge \hat{F} - \Omega_{\alpha\beta} b_{mn}^\alpha \hat{B}_\beta \wedge \text{tr} \hat{F}^m \wedge \hat{F}^n \quad (\text{E.2.11}) \\ &= \int_{M_6} -\frac{1}{2} \Omega_{\alpha\beta} G^\alpha \wedge (\mathcal{F}^\beta - F^\beta) \wedge Dy + \Omega_{\alpha\beta} \frac{b^\alpha}{\lambda(\mathfrak{g})} A^\beta \wedge \text{tr}(F \wedge F) \wedge Dy \\ &\quad + \Omega_{\alpha\beta} b_{mn}^\alpha A^\beta \wedge F^m \wedge F^n \wedge Dy - 2\Omega_{\alpha\beta} \frac{b^\alpha}{\lambda(\mathfrak{g})} \omega^{CS} \wedge [2\frac{b^\beta}{\lambda(\mathfrak{g})} \text{tr}(\zeta F) \\ &\quad - \frac{b^\beta}{\lambda(\mathfrak{g})} \text{tr}(\zeta\zeta) F^0 + 2b_{mn}^\beta \zeta^m F^n - b_{mn}^\beta \zeta^m \zeta^n F^0] \wedge Dy - 2\Omega_{\alpha\beta} b_{kl}^\alpha \omega^{CS,kl} \wedge \\ &\quad [2\frac{b^\beta}{\lambda(\mathfrak{g})} \text{tr}(\zeta F) - \frac{b^\beta}{\lambda(\mathfrak{g})} \text{tr}(\zeta\zeta) F^0 + 2b_{mn}^\beta \zeta^m F^n - b_{mn}^\beta \zeta^m \zeta^n F^0] \wedge Dy \\ &\quad - 2\Omega_{\alpha\beta} \frac{b^\alpha}{\lambda(\mathfrak{g})} \frac{b^\beta}{\lambda(\mathfrak{g})} \text{tr} \zeta A \wedge [\text{tr} F \wedge F + \text{tr} \zeta \zeta F^0 \wedge F^0 - 2 \text{tr} \zeta F \wedge F^0] \wedge Dy \\ &\quad - 2\Omega_{\alpha\beta} \frac{b^\alpha}{\lambda(\mathfrak{g})} b_{mn}^\beta \zeta^m A^n \wedge [\text{tr} F \wedge F + \text{tr} \zeta \zeta F^0 \wedge F^0 - 2 \text{tr} \zeta F \wedge F^0] \wedge Dy \\ &\quad - 2\Omega_{\alpha\beta} b_{mn}^\alpha \frac{b^\beta}{\lambda(\mathfrak{g})} \text{tr} \zeta A \wedge [F^m \wedge F^n + \zeta^m \zeta^n F^0 \wedge F^0 - 2\zeta^m F^n \wedge F^0] \wedge Dy \\ &\quad - 2\Omega_{\alpha\beta} b_{mn}^\alpha b_{kl}^\beta \zeta^k A^l \wedge [F^m \wedge F^n + \zeta^m \zeta^n F^0 \wedge F^0 - 2\zeta^m F^n \wedge F^0] \wedge Dy. \end{aligned}$$

²In the following we omit terms without a Dy -factor, since these forms are integrated to zero along the circle direction.

The kinetic terms for the Abelian vectors are reduced to

$$\begin{aligned} & \int_{M_6} -2\Omega_{\alpha\beta} j^{\alpha\beta} b_{mn}^{\beta} \hat{F}^m \wedge \hat{*}\hat{F}^n \\ &= \int_{M_6} -2r\Omega_{\alpha\beta} j^{\alpha\beta} b_{mn}^{\beta} (F^m - \zeta^m F^0) \wedge \tilde{*}(F^n - \zeta^n F^0) \wedge Dy \\ & \quad - 2r^{-1}\Omega_{\alpha\beta} j^{\alpha\beta} b_{mn}^{\beta} d\zeta^m \wedge \tilde{*}d\zeta^n \wedge Dy, \end{aligned} \quad (\text{E.2.12})$$

while the reduction for the non-Abelian vectors was found in [54] to be

$$\begin{aligned} & \int_{M_6} -2\Omega_{\alpha\beta} j^{\alpha\beta} b^{\beta} \text{tr} \hat{F} \wedge \hat{*}\hat{F} \\ &= \int_{M_6} -2r\Omega_{\alpha\beta} j^{\alpha\beta} b^{\beta} \text{tr}(F - \zeta F^0) \wedge \tilde{*}(F - \zeta F^0) \wedge Dy \\ & \quad - 2r^{-1}\Omega_{\alpha\beta} j^{\alpha\beta} b^{\beta} \text{tr} D\zeta \wedge \tilde{*}D\zeta \wedge Dy, \end{aligned} \quad (\text{E.2.13})$$

where we have introduced the covariant derivative for the adjoint scalars in the vector multiplets as

$$D\zeta = d\zeta + [A, \zeta]. \quad (\text{E.2.14})$$

The kinetic terms of the six-dimensional tensors are found to reduce to

$$\begin{aligned} & \int_{M_6} -\frac{1}{4}g_{\alpha\beta} \hat{G}^{\alpha} \wedge \hat{*}\hat{G}^{\beta} \\ &= \int_{M_6} -\frac{1}{4}r g_{\alpha\beta} G^{\alpha} \wedge \tilde{*}G^{\beta} \wedge Dy - \frac{1}{4}r^{-1}g_{\alpha\beta} \mathcal{F}^{\alpha} \wedge \tilde{*}\mathcal{F}^{\beta} \wedge Dy, \end{aligned} \quad (\text{E.2.15})$$

where \mathcal{F}^{α} was defined in (6.3.18). While terms involving neutral six-dimensional scalars reduce trivially to five dimensions, this is not true for terms with charged scalars. One computes

$$\begin{aligned} & \int_{M_6} -h_{UV} \hat{D}q^U \wedge \hat{*}\hat{D}q^V \\ &= \int_{M_6} -rh_{UV} Dq^U \wedge \tilde{*}Dq^V \wedge Dy \\ & \quad - r^{-1}h_{UV} (\zeta^{\mathbf{R}U} q^U + \zeta^m q_m^{(U)} q^U) (\zeta^{\mathbf{R}V} q^V + \zeta^m q_m^{(V)} q^V) \tilde{*}1 \wedge Dy. \end{aligned} \quad (\text{E.2.16})$$

The expression Dq^U encodes the five-dimensional covariant derivative

$$Dq^U = dq^U + A^{\mathbf{R}U} q^U - iq_m^{(U)} A^m q^U \quad (\text{E.2.17})$$

and the $\zeta^{\mathbf{R}U}$ denote the scalars from the five-dimensional vector multiplet in the representation \mathbf{R}_U of the Lie-algebra, where \mathbf{R}_U is the representation q^U transforms in. The last line in (E.2.16) only contributes to the five-dimensional scalar potential. It is completed by reducing the six-dimensional scalar potential, which we did not carry out. Finally, the combination

of all of these terms makes up the full circle reduced classical bosonic two-derivative pseudo-action.

As in six dimensions, there is still some redundancy in this five-dimensional pseudo-action. In contrast to the six-dimensional case, we are nevertheless able to write down a proper action without any additional duality constraints. This works by dualizing the action, in particular replacing all tensors G^α by the vectors F^α . The connection between the vectors and tensors can be seen by reducing the duality constraint (6.3.16) to

$$r g_{\alpha\beta} \tilde{*}G^\beta = -\Omega_{\alpha\beta} \mathcal{F}^\beta. \quad (\text{E.2.18})$$

We can safely modify the Lagrangian by adding a total derivative

$$\begin{aligned} \Delta S^{(5)F} &= \int_{M_5} -\frac{1}{2} \Omega_{\alpha\beta} dB^\alpha \wedge F^\beta \\ &= \int_{M_5} -\frac{1}{2} \Omega_{\alpha\beta} G^\alpha \wedge F^\beta + \frac{1}{2} \Omega_{\alpha\beta} (-A^\alpha \wedge F^0 + 2 \frac{b^\alpha}{\lambda(\mathfrak{g})} \omega^{CS} + 2b_{mn}^\alpha \omega^{CS,mn}) \wedge F^\beta. \end{aligned} \quad (\text{E.2.19})$$

Varying the new action with respect to G^α gives precisely the reduced duality constraint (E.2.18). The terms in the five-dimensional action that change in the dualization procedure are

$$\begin{aligned} &\int_{M_5} -\frac{1}{4} r g_{\alpha\beta} G^\alpha \wedge \tilde{*}G^\beta - \frac{1}{4} r^{-1} g_{\alpha\beta} \mathcal{F}^\alpha \wedge \tilde{*}\mathcal{F}^\beta \\ &\quad - \frac{1}{2} \Omega_{\alpha\beta} G^\alpha \wedge (\mathcal{F}^\beta - F^\beta) + \Omega_{\alpha\beta} \frac{b^\alpha}{\lambda(\mathfrak{g})} A^\beta \wedge \text{tr}(F \wedge F) \\ &\quad + \Omega_{\alpha\beta} b_{mn}^\alpha A^\beta \wedge F^m \wedge F^n - \frac{1}{2} \Omega_{\alpha\beta} G^\alpha \wedge F^\beta \\ &\quad - \frac{1}{2} \Omega_{\alpha\beta} A^\alpha \wedge F^0 \wedge F^\beta + \Omega_{\alpha\beta} \frac{b^\alpha}{\lambda(G)} \omega^{CS} \wedge F^\beta + \Omega_{\alpha\beta} b_{mn}^\alpha \omega^{CS,mn} \wedge F^\beta \\ &= \int_{M_5} -\frac{1}{2} r^{-1} g_{\alpha\beta} \mathcal{F}^\alpha \wedge \tilde{*}\mathcal{F}^\beta + 2\Omega_{\alpha\beta} \frac{b^\alpha}{\lambda(\mathfrak{g})} A^\beta \wedge \text{tr} F \wedge F \\ &\quad + 2\Omega_{\alpha\beta} b_{mn}^\alpha A^\beta \wedge F^m \wedge F^n - \frac{1}{2} \Omega_{\alpha\beta} A^0 \wedge F^\alpha \wedge F^\beta, \end{aligned} \quad (\text{E.2.20})$$

where we inserted the reduced duality constraint (E.2.18).

The Einstein-Hilbert term is not in its canonical form yet. Performing the Weyl rescaling $\tilde{g}_{\mu\nu} = r^{-2/3} g_{\mu\nu}$ turns out to give the right result

$$S_{EH}^{(5)F} = \int_{M_5} \frac{1}{2} R * 1. \quad (\text{E.2.21})$$

Note that the Hodge star operator scales as $\tilde{*}\alpha = r^{-5/3} (r^{2/3})^p * \alpha$, where α is a p -form.

The final step is to push the theory onto the Coulomb branch, which means that we give a VEV to the scalars in the five-dimensional vector multiplets. The W-bosons get massive

and break the gauge group to its maximal torus. Additionally, the charged hypermultiplets acquire a mass and do not appear in the effective action. Including only massless modes, one obtains the final form (6.3.23) for the classical five-dimensional action on the Coulomb branch.

$$\begin{aligned}
S^{(5)F} = \int_{M_5} & + \frac{1}{2}R * 1 - \frac{2}{3}r^{-2}dr \wedge *dr - \frac{1}{2}g_{\alpha\beta}dj^\alpha \wedge *dj^\beta - h_{uv}dq^u \wedge *dq^v & (E.2.22) \\
& - 2r^{-2}\Omega_{\alpha\beta j}^\alpha b_{\hat{i}\hat{j}}^\beta d\zeta^{\hat{I}} \wedge *d\zeta^{\hat{J}} - \frac{1}{4}r^{8/3}F^0 \wedge *F^0 - \frac{1}{2}r^{-4/3}g_{\alpha\beta}\mathcal{F}^\alpha \wedge *\mathcal{F}^\beta \\
& - 2r^{2/3}\Omega_{\alpha\beta j}^\alpha b_{\hat{i}\hat{j}}^\beta (F^{\hat{I}} - \zeta^{\hat{I}}F^0) \wedge *(F^{\hat{J}} - \zeta^{\hat{J}}F^0) \\
& - \frac{1}{2}\Omega_{\alpha\beta}A^0 \wedge F^\alpha \wedge F^\beta + 2\Omega_{\alpha\beta}b_{\hat{i}\hat{j}}^\alpha A^\beta \wedge F^{\hat{I}} \wedge F^{\hat{J}} \\
& - 2\Omega_{\alpha\beta}b_{\hat{i}\hat{j}}^\alpha b_{\hat{i}\hat{j}}^\beta \zeta^{\hat{K}}\zeta^{\hat{L}}\zeta^{\hat{I}}A^{\hat{J}} \wedge F^0 \wedge F^0 \\
& + 2\Omega_{\alpha\beta}(b_{\hat{i}\hat{j}}^\alpha b_{\hat{K}\hat{L}}^\beta + 2b_{\hat{i}\hat{K}}^\alpha b_{\hat{j}\hat{L}}^\beta)\zeta^{\hat{K}}\zeta^{\hat{L}}A^{\hat{I}} \wedge F^{\hat{J}} \wedge F^0 \\
& - 2\Omega_{\alpha\beta}(2b_{\hat{i}\hat{j}}^\alpha b_{\hat{K}\hat{L}}^\beta + b_{\hat{i}\hat{L}}^\alpha b_{\hat{j}\hat{K}}^\beta)\zeta^{\hat{L}}A^{\hat{I}} \wedge F^{\hat{J}} \wedge F^{\hat{K}} ,
\end{aligned}$$

where we have chosen the Cartan generators to be in the coroot basis and used the notation introduced around (6.3.22). In order to obtain the full quantum effective action one has to integrate out the massive modes. This is partly done in section 7.3 and induces new Chern-Simons couplings.

E.3 Zeta Regularization for the Loop Calculations

In this section we explicitly derive expressions for the infinite sums appearing in the loop calculations of section 7.3. Since the n^{th} Kaluza-Klein-mode carries charge n under the Kaluza-Klein vector A^0 , the infinite sums over the KK-towers take in principle one of the following four forms

$$\begin{aligned}
\sum_{n=-\infty}^{+\infty} \text{sign}(x+n) & \quad \sum_{n=-\infty}^{+\infty} n \text{sign}(x+n) \\
\sum_{n=-\infty}^{+\infty} n^2 \text{sign}(x+n) & \quad \sum_{n=-\infty}^{+\infty} n^3 \text{sign}(x+n).
\end{aligned} \tag{E.3.1}$$

Here, the parameter x is the ratio of Coulomb branch mass and Kaluza-Klein mass, that is

$$x = \begin{cases} r\alpha \cdot \zeta \\ rw \cdot \zeta. \end{cases} \tag{E.3.2}$$

Let us now define the *floored* ratio of Coulomb branch mass and Kaluza-Klein mass

$$l := \lfloor |x| \rfloor, \tag{E.3.3}$$

as much depends only on this quantity. Then the first equation in (E.3.1) reads

$$\begin{aligned} \sum_{n=-\infty}^{+\infty} \text{sign}(x+n) &= \sum_{n=-l}^{+l} \text{sign}(x+n) + \sum_{n=l+1}^{+\infty} \text{sign}(x+n) + \sum_{n=-\infty}^{-l-1} \text{sign}(x+n) \\ &= \sum_{n=-l}^{+l} \text{sign}(x) + \sum_{n=l+1}^{+\infty} \text{sign}(n) + \sum_{n=-\infty}^{-l-1} \text{sign}(n) = (2l+1) \text{sign}(x). \end{aligned} \quad (\text{E.3.4})$$

Next, we calculate

$$\begin{aligned} \sum_{n=-\infty}^{+\infty} n^2 \text{sign}(x+n) &= \sum_{n=-l}^{+l} n^2 \text{sign}(x) + \sum_{n=l+1}^{+\infty} n^2 \text{sign}(n) + \sum_{n=-\infty}^{-l-1} n^2 \text{sign}(n) \\ &= 2 \sum_{n=1}^l n^2 \text{sign}(x) = \frac{l(l+1)(2l+1)}{3} \text{sign}(x), \end{aligned} \quad (\text{E.3.5})$$

where we performed the sum in the last step. The remaining two sums require zeta function regularization. Using

$$\zeta(-1) = -\frac{1}{12} \quad \zeta(-3) = \frac{1}{120}, \quad (\text{E.3.6})$$

we compute that

$$\begin{aligned} \sum_{n=-\infty}^{+\infty} n \text{sign}(x+n) &= \sum_{n=-l}^{+l} n \text{sign}(x) + \sum_{n=l+1}^{+\infty} n \text{sign}(n) + \sum_{n=-\infty}^{-l-1} n \text{sign}(n) \\ &= \sum_{n=l+1}^{+\infty} n + \sum_{n=1}^l n - \sum_{n=1}^l n + \sum_{n=-\infty}^{-l-1} (-n) + \sum_{n=-l}^{-1} (-n) - \sum_{n=-l}^{-1} (-n) \\ &= 2\zeta(-1) - 2 \sum_{n=1}^l n = -\frac{1}{6} - (l+1)l \end{aligned} \quad (\text{E.3.7})$$

and

$$\begin{aligned} \sum_{n=-\infty}^{+\infty} n^3 \text{sign}(x+n) &= \sum_{n=-l}^{+l} n^3 \text{sign}(x) + \sum_{n=l+1}^{+\infty} n^3 \text{sign}(n) + \sum_{n=-\infty}^{-l-1} n^3 \text{sign}(n) \\ &= \sum_{n=l+1}^{+\infty} n^3 + \sum_{n=1}^l n^3 - \sum_{n=1}^l n^3 + \sum_{n=-\infty}^{-l-1} (-n^3) + \sum_{n=-l}^{-1} (-n^3) - \sum_{n=-l}^{-1} (-n^3) \\ &= 2\zeta(-3) - 2 \sum_{n=1}^l n^3 = \frac{1}{60} - \frac{l^2(l+1)^2}{2}. \end{aligned} \quad (\text{E.3.8})$$

Bibliography

- [1] **ATLAS Collaboration** Collaboration, G. Aad *et. al.*, *Observation of a new particle in the search for the Standard Model Higgs boson with the ATLAS detector at the LHC*, *Phys.Lett.* **B716** (2012) 1–29, [[arXiv:1207.7214](#)].
- [2] K. Wilson and J. B. Kogut, *The Renormalization group and the epsilon expansion*, *Phys.Rept.* **12** (1974) 75–200.
- [3] K. G. Wilson, *The Renormalization Group: Critical Phenomena and the Kondo Problem*, *Rev.Mod.Phys.* **47** (1975) 773.
- [4] S. Weinberg, *A Model of Leptons*, *Phys.Rev.Lett.* **19** (1967) 1264–1266.
- [5] E. D’Hoker and D. Phong, *Two loop superstrings. 1. Main formulas*, *Phys.Lett.* **B529** (2002) 241–255, [[hep-th/0110247](#)].
- [6] K. Aoki, E. D’Hoker, and D. Phong, *Unitarity of Closed Superstring Perturbation Theory*, *Nucl.Phys.* **B342** (1990) 149–230.
- [7] M. B. Green and J. H. Schwarz, *Anomaly Cancellation in Supersymmetric D=10 Gauge Theory and Superstring Theory*, *Phys.Lett.* **B149** (1984) 117–122.
- [8] C. Hull and P. Townsend, *Unity of superstring dualities*, *Nucl.Phys.* **B438** (1995) 109–137, [[hep-th/9410167](#)].
- [9] P. Horava and E. Witten, *Heterotic and type I string dynamics from eleven-dimensions*, *Nucl.Phys.* **B460** (1996) 506–524, [[hep-th/9510209](#)].
- [10] T. Kaluza, *On the Problem of Unity in Physics*, *Sitzungsber.Preuss.Akad.Wiss.Berlin (Math.Phys.)* **1921** (1921) 966–972.
- [11] O. Klein, *Quantum Theory and Five-Dimensional Theory of Relativity. (In German and English)*, *Z.Phys.* **37** (1926) 895–906.
- [12] S. P. Martin, *A Supersymmetry primer*, *Adv.Ser.Direct.High Energy Phys.* **21** (2010) 1–153, [[hep-ph/9709356](#)].
- [13] K. A. Intriligator and N. Seiberg, *Lectures on Supersymmetry Breaking*, *Class.Quant.Grav.* **24** (2007) S741–S772, [[hep-ph/0702069](#)].
- [14] L. Susskind, *The Anthropic landscape of string theory*, [[hep-th/0302219](#)].
- [15] B. S. Acharya and M. R. Douglas, *A Finite landscape?*, [[hep-th/0606212](#)].
- [16] F. Denef, M. R. Douglas, and B. Florea, *Building a better racetrack*, *JHEP* **0406** (2004) 034,

- [[hep-th/0404257](#)].
- [17] F. Denef, *Les Houches Lectures on Constructing String Vacua*, [arXiv:0803.1194](#).
- [18] D. Baumann, *TASI Lectures on Inflation*, [arXiv:0907.5424](#).
- [19] D. Baumann and L. McAllister, *Inflation and String Theory*, [arXiv:1404.2601](#).
- [20] M. B. Green, J. Schwarz, and E. Witten, *SUPERSTRING THEORY. VOL. 1: INTRODUCTION*, *Cambridge Monogr.Math.Phys.* (1987).
- [21] M. B. Green, J. Schwarz, and E. Witten, *SUPERSTRING THEORY. VOL. 2: LOOP AMPLITUDES, ANOMALIES AND PHENOMENOLOGY*, .
- [22] J. Polchinski, *String theory. Vol. 1: An introduction to the bosonic string*, .
- [23] J. Polchinski, *String theory. Vol. 2: Superstring theory and beyond*, .
- [24] K. Becker, M. Becker, and J. Schwarz, *String theory and M-theory: A modern introduction*, .
- [25] R. Blumenhagen, D. Lüst, and S. Theisen, *Basic concepts of string theory*, .
- [26] T. Weigand, *Lectures on F-theory compactifications and model building*, *Class.Quant.Grav.* **27** (2010) 214004, [[arXiv:1009.3497](#)].
- [27] J. J. Heckman, *Particle Physics Implications of F-theory*, *Ann.Rev.Nucl.Part.Sci.* **60** (2010) 237–265, [[arXiv:1001.0577](#)].
- [28] A. Maharana and E. Palti, *Models of Particle Physics from Type IIB String Theory and F-theory: A Review*, *Int.J.Mod.Phys.* **A28** (2013) 1330005, [[arXiv:1212.0555](#)].
- [29] F. Bonetti, *Effective actions for F-theory compactifications and tensor theories*, .
- [30] M. R. Gaberdiel and B. Zwiebach, *Exceptional groups from open strings*, *Nucl.Phys.* **B518** (1998) 151–172, [[hep-th/9709013](#)].
- [31] O. DeWolfe and B. Zwiebach, *String junctions for arbitrary Lie algebra representations*, *Nucl.Phys.* **B541** (1999) 509–565, [[hep-th/9804210](#)].
- [32] A. Sen and B. Zwiebach, *Stable nonBPS states in F theory*, *JHEP* **0003** (2000) 036, [[hep-th/9907164](#)].
- [33] B. R. Greene, A. D. Shapere, C. Vafa, and S.-T. Yau, *Stringy Cosmic Strings and Noncompact Calabi-Yau Manifolds*, *Nucl.Phys.* **B337** (1990) 1.
- [34] G. W. Gibbons, M. B. Green, and M. J. Perry, *Instantons and seven-branes in type IIB superstring theory*, *Phys.Lett.* **B370** (1996) 37–44, [[hep-th/9511080](#)].
- [35] E. A. Bergshoeff, J. Hartong, T. Ortin, and D. Roest, *Seven-branes and Supersymmetry*, *JHEP* **0702** (2007) 003, [[hep-th/0612072](#)].
- [36] T. Banks, W. Fischler, S. Shenker, and L. Susskind, *M theory as a matrix model: A Conjecture*, *Phys.Rev.* **D55** (1997) 5112–5128, [[hep-th/9610043](#)].
- [37] A. Giveon, M. Porrati, and E. Rabinovici, *Target space duality in string theory*, *Phys.Rept.* **244** (1994) 77–202, [[hep-th/9401139](#)].
- [38] H. Dorn and H. Otto, *On T duality for open strings in general Abelian and nonAbelian gauge field backgrounds*, *Phys.Lett.* **B381** (1996) 81–88, [[hep-th/9603186](#)].

- [39] E. Alvarez, L. Alvarez-Gaume, and Y. Lozano, *An Introduction to T duality in string theory*, *Nucl.Phys.Proc.Suppl.* **41** (1995) 1–20, [[hep-th/9410237](#)].
- [40] C. Vafa, *Evidence for F theory*, *Nucl.Phys.* **B469** (1996) 403–418, [[hep-th/9602022](#)].
- [41] T. W. Grimm and R. Savelli, *Gravitational Instantons and Fluxes from M/F-theory on Calabi-Yau fourfolds*, *Phys.Rev.* **D85** (2012) 026003, [[arXiv:1109.3191](#)].
- [42] A. Grassi, J. Halverson, and J. L. Shaneson, *Matter From Geometry Without Resolution*, *JHEP* **1310** (2013) 205, [[arXiv:1306.1832](#)].
- [43] A. Grassi, J. Halverson, and J. L. Shaneson, *Non-Abelian Gauge Symmetry and the Higgs Mechanism in F-theory*, [arXiv:1402.5962](#).
- [44] A. Collinucci and R. Savelli, *T-branes as branes within branes*, [arXiv:1410.4178](#).
- [45] A. Collinucci and R. Savelli, *F-theory on singular spaces*, [arXiv:1410.4867](#).
- [46] K. Kodaira, *On compact analytic surfaces: Ii*, *Annals of Mathematics* (1963) 563–626.
- [47] R. Blumenhagen, B. Kors, D. Lust, and S. Stieberger, *Four-dimensional String Compactifications with D-Branes, Orientifolds and Fluxes*, *Phys.Rept.* **445** (2007) 1–193, [[hep-th/0610327](#)].
- [48] L. E. Ibanez and A. M. Uranga, *String theory and particle physics: An introduction to string phenomenology*, .
- [49] D. R. Morrison and C. Vafa, *Compactifications of F theory on Calabi-Yau threefolds. 1*, *Nucl.Phys.* **B473** (1996) 74–92, [[hep-th/9602114](#)].
- [50] D. R. Morrison and C. Vafa, *Compactifications of F theory on Calabi-Yau threefolds. 2.*, *Nucl.Phys.* **B476** (1996) 437–469, [[hep-th/9603161](#)].
- [51] T. W. Grimm and T. Weigand, *On Abelian Gauge Symmetries and Proton Decay in Global F-theory GUTs*, *Phys.Rev.* **D82** (2010) 086009, [[arXiv:1006.0226](#)].
- [52] D. R. Morrison and D. S. Park, *F-Theory and the Mordell-Weil Group of Elliptically-Fibered Calabi-Yau Threefolds*, *JHEP* **1210** (2012) 128, [[arXiv:1208.2695](#)].
- [53] T. W. Grimm, *The N=1 effective action of F-theory compactifications*, *Nucl.Phys.* **B845** (2011) 48–92, [[arXiv:1008.4133](#)].
- [54] F. Bonetti and T. W. Grimm, *Six-dimensional (1,0) effective action of F-theory via M-theory on Calabi-Yau threefolds*, *JHEP* **1205** (2012) 019, [[arXiv:1112.1082](#)].
- [55] R. Donagi and M. Wijnholt, *Model Building with F-Theory*, *Adv.Theor.Math.Phys.* **15** (2011) 1237–1318, [[arXiv:0802.2969](#)].
- [56] C. Beasley, J. J. Heckman, and C. Vafa, *GUTs and Exceptional Branes in F-theory - I*, *JHEP* **0901** (2009) 058, [[arXiv:0802.3391](#)].
- [57] C. Beasley, J. J. Heckman, and C. Vafa, *GUTs and Exceptional Branes in F-theory - II: Experimental Predictions*, *JHEP* **0901** (2009) 059, [[arXiv:0806.0102](#)].
- [58] H. Georgi and S. Glashow, *Unity of All Elementary Particle Forces*, *Phys.Rev.Lett.* **32** (1974) 438–441.
- [59] L. B. Anderson, A. Constantin, S.-J. Lee, and A. Lukas, *Hypercharge Flux in Heterotic*

- Compactifications*, *Phys.Rev.* **D91** (2015), no. 4 046008, [[arXiv:1411.0034](#)].
- [60] E. Dudas and E. Palti, *On hypercharge flux and exotics in F-theory GUTs*, *JHEP* **1009** (2010) 013, [[arXiv:1007.1297](#)].
- [61] J. Marsano, *Hypercharge Flux, Exotics, and Anomaly Cancellation in F-theory GUTs*, *Phys.Rev.Lett.* **106** (2011) 081601, [[arXiv:1011.2212](#)].
- [62] T. W. Grimm, M. Kerstan, E. Palti, and T. Weigand, *Massive Abelian Gauge Symmetries and Fluxes in F-theory*, *JHEP* **1112** (2011) 004, [[arXiv:1107.3842](#)].
- [63] C. Mayrhofer, E. Palti, and T. Weigand, *Hypercharge Flux in IIB and F-theory: Anomalies and Gauge Coupling Unification*, *JHEP* **1309** (2013) 082, [[arXiv:1303.3589](#)].
- [64] E. Palti, *A Note on Hypercharge Flux, Anomalies, and U(1)s in F-theory GUTs*, *Phys.Rev.* **D87** (2013), no. 8 085036, [[arXiv:1209.4421](#)].
- [65] J. J. Heckman and C. Vafa, *Flavor Hierarchy From F-theory*, *Nucl.Phys.* **B837** (2010) 137–151, [[arXiv:0811.2417](#)].
- [66] H. Hayashi, T. Kawano, R. Tatar, and T. Watari, *Codimension-3 Singularities and Yukawa Couplings in F-theory*, *Nucl.Phys.* **B823** (2009) 47–115, [[arXiv:0901.4941](#)].
- [67] J. J. Heckman, A. Tavanfar, and C. Vafa, *The Point of E(8) in F-theory GUTs*, *JHEP* **1008** (2010) 040, [[arXiv:0906.0581](#)].
- [68] V. Bouchard, J. J. Heckman, J. Seo, and C. Vafa, *F-theory and Neutrinos: Kaluza-Klein Dilution of Flavor Hierarchy*, *JHEP* **1001** (2010) 061, [[arXiv:0904.1419](#)].
- [69] J. P. Conlon and E. Palti, *Aspects of Flavour and Supersymmetry in F-theory GUTs*, *JHEP* **1001** (2010) 029, [[arXiv:0910.2413](#)].
- [70] A. Font and L. Ibanez, *Matter wave functions and Yukawa couplings in F-theory Grand Unification*, *JHEP* **0909** (2009) 036, [[arXiv:0907.4895](#)].
- [71] B. Andreas and G. Curio, *From Local to Global in F-Theory Model Building*, *J.Geom.Phys.* **60** (2010) 1089–1102, [[arXiv:0902.4143](#)].
- [72] R. Blumenhagen, T. W. Grimm, B. Jurke, and T. Weigand, *F-theory uplifts and GUTs*, *JHEP* **0909** (2009) 053, [[arXiv:0906.0013](#)].
- [73] C. Cordova, *Decoupling Gravity in F-Theory*, *Adv.Theor.Math.Phys.* **15** (2011) 689–740, [[arXiv:0910.2955](#)].
- [74] T. W. Grimm, *Axion Inflation in F-theory*, *Phys.Lett.* **B739** (2014) 201–208, [[arXiv:1404.4268](#)].
- [75] I. García-Etxebarria, T. W. Grimm, and I. Valenzuela, *Special Points of Inflation in Flux Compactifications*, [[arXiv:1412.5537](#)].
- [76] R. Friedman, J. Morgan, and E. Witten, *Vector bundles and F theory*, *Commun.Math.Phys.* **187** (1997) 679–743, [[hep-th/9701162](#)].
- [77] R. Donagi and M. Wijnholt, *Higgs Bundles and UV Completion in F-Theory*, *Commun.Math.Phys.* **326** (2014) 287–327, [[arXiv:0904.1218](#)].
- [78] J. Marsano, N. Saulina, and S. Schafer-Nameki, *Monodromies, Fluxes, and Compact Three-Generation F-theory GUTs*, *JHEP* **0908** (2009) 046, [[arXiv:0906.4672](#)].

- [79] J. Marsano, N. Saulina, and S. Schafer-Nameki, *Compact F-theory GUTs with $U(1)$ (PQ)*, *JHEP* **1004** (2010) 095, [[arXiv:0912.0272](#)].
- [80] M. J. Dolan, J. Marsano, N. Saulina, and S. Schafer-Nameki, *F-theory GUTs with $U(1)$ Symmetries: Generalities and Survey*, *Phys.Rev.* **D84** (2011) 066008, [[arXiv:1102.0290](#)].
- [81] M. J. Dolan, J. Marsano, and S. Schafer-Nameki, *Unification and Phenomenology of F-Theory GUTs with $U(1)_{PQ}$* , *JHEP* **1112** (2011) 032, [[arXiv:1109.4958](#)].
- [82] J. J. Heckman, H. Lin, and S.-T. Yau, *Building Blocks for Generalized Heterotic/F-theory Duality*, *Adv.Theor.Math.Phys.* **18** (2014) 1463–1503, [[arXiv:1311.6477](#)].
- [83] L. B. Anderson, J. J. Heckman, and S. Katz, *T-Branes and Geometry*, *JHEP* **1405** (2014) 080, [[arXiv:1310.1931](#)].
- [84] L. B. Anderson and W. Taylor, *Geometric constraints in dual F-theory and heterotic string compactifications*, *JHEP* **1408** (2014) 025, [[arXiv:1405.2074](#)].
- [85] F. Baume, E. Palti, and S. Schwieger, *On E_8 and F-Theory GUTs*, [[arXiv:1502.0387](#)].
- [86] A. Sen, *F theory and orientifolds*, *Nucl.Phys.* **B475** (1996) 562–578, [[hep-th/9605150](#)].
- [87] A. Sen, *Orientifold limit of F theory vacua*, *Phys.Rev.* **D55** (1997) 7345–7349, [[hep-th/9702165](#)].
- [88] P. Aluffi and M. Esole, *New Orientifold Weak Coupling Limits in F-theory*, *JHEP* **1002** (2010) 020, [[arXiv:0908.1572](#)].
- [89] M. Esole, J. Fullwood, and S.-T. Yau, *D_5 elliptic fibrations: non-Kodaira fibers and new orientifold limits of F-theory*, [[arXiv:1110.6177](#)].
- [90] M. Esole and R. Savelli, *Tate Form and Weak Coupling Limits in F-theory*, *JHEP* **1306** (2013) 027, [[arXiv:1209.1633](#)].
- [91] R. Donagi, S. Katz, and M. Wijnholt, *Weak Coupling, Degeneration and Log Calabi-Yau Spaces*, [[arXiv:1212.0553](#)].
- [92] A. Clinger, R. Donagi, and M. Wijnholt, *The Sen Limit*, *Adv.Theor.Math.Phys.* **18** (2014) 613–658, [[arXiv:1212.4505](#)].
- [93] A. P. Braun, A. Collinucci, and R. Valandro, *The fate of $U(1)$'s at strong coupling in F-theory*, *JHEP* **1407** (2014) 028, [[arXiv:1402.4054](#)].
- [94] K. A. Intriligator, D. R. Morrison, and N. Seiberg, *Five-dimensional supersymmetric gauge theories and degenerations of Calabi-Yau spaces*, *Nucl.Phys.* **B497** (1997) 56–100, [[hep-th/9702198](#)].
- [95] T. W. Grimm and H. Hayashi, *F-theory fluxes, Chirality and Chern-Simons theories*, *JHEP* **1203** (2012) 027, [[arXiv:1111.1232](#)].
- [96] H. Hayashi, C. Lawrie, and S. Schafer-Nameki, *Phases, Flops and F-theory: $SU(5)$ Gauge Theories*, *JHEP* **1310** (2013) 046, [[arXiv:1304.1678](#)].
- [97] H. Hayashi, C. Lawrie, D. R. Morrison, and S. Schafer-Nameki, *Box Graphs and Singular Fibers*, *JHEP* **1405** (2014) 048, [[arXiv:1402.2653](#)].
- [98] A. P. Braun and S. Schafer-Nameki, *Box Graphs and Resolutions I*, [[arXiv:1407.3520](#)].

- [99] M. Esole, S.-H. Shao, and S.-T. Yau, *Singularities and Gauge Theory Phases*, [arXiv:1402.6331](#).
- [100] M. Esole, S.-H. Shao, and S.-T. Yau, *Singularities and Gauge Theory Phases II*, [arXiv:1407.1867](#).
- [101] M. Esole and S.-T. Yau, *Small resolutions of $SU(5)$ -models in F -theory*, *Adv.Theor.Math.Phys.* **17** (2013) 1195–1253, [[arXiv:1107.0733](#)].
- [102] C. Lawrie and S. Schäfer-Nameki, *The Tate Form on Steroids: Resolution and Higher Codimension Fibers*, *JHEP* **1304** (2013) 061, [[arXiv:1212.2949](#)].
- [103] M. Kuntzler and S. Schafer-Nameki, *Tate Trees for Elliptic Fibrations with Rank one Mordell-Weil group*, [arXiv:1406.5174](#).
- [104] M. Esole, M. J. Kang, and S.-T. Yau, *A New Model for Elliptic Fibrations with a Rank One Mordell-Weil Group: I. Singular Fibers and Semi-Stable Degenerations*, [arXiv:1410.0003](#).
- [105] F. Bonetti, T. W. Grimm, and S. Hohenegger, *Non-Abelian Tensor Towers and $(2,0)$ Superconformal Theories*, *JHEP* **1305** (2013) 129, [[arXiv:1209.3017](#)].
- [106] J. J. Heckman, D. R. Morrison, and C. Vafa, *On the Classification of 6D SCFTs and Generalized ADE Orbifolds*, *JHEP* **1405** (2014) 028, [[arXiv:1312.5746](#)].
- [107] M. Del Zotto, J. J. Heckman, A. Tomasiello, and C. Vafa, *6d Conformal Matter*, *JHEP* **1502** (2015) 054, [[arXiv:1407.6359](#)].
- [108] J. J. Heckman, *More on the Matter of 6D SCFTs*, [arXiv:1408.0006](#).
- [109] M. Del Zotto, J. J. Heckman, D. R. Morrison, and D. S. Park, *6D SCFTs and Gravity*, [arXiv:1412.6526](#).
- [110] B. Haghighat, A. Klemm, G. Lockhart, and C. Vafa, *Strings of Minimal 6d SCFTs*, [arXiv:1412.3152](#).
- [111] J. J. Heckman, D. R. Morrison, T. Rudelius, and C. Vafa, *Atomic Classification of 6D SCFTs*, [arXiv:1502.0540](#).
- [112] K. Ohmori, H. Shimizu, Y. Tachikawa, and K. Yonekura, *Anomaly polynomial of general 6d SCFTs*, *PTEP* **2014** (2014), no. 10 103B07, [[arXiv:1408.5572](#)].
- [113] M. Cvetič, T. W. Grimm, and D. Klevers, *Anomaly Cancellation And Abelian Gauge Symmetries In F -theory*, *JHEP* **1302** (2013) 101, [[arXiv:1210.6034](#)].
- [114] T. W. Grimm, A. Kapfer, and J. Keitel, *Effective action of 6D F -Theory with $U(1)$ factors: Rational sections make Chern-Simons terms jump*, *JHEP* **1307** (2013) 115, [[arXiv:1305.1929](#)].
- [115] T. W. Grimm and A. Kapfer, *Anomaly Cancellation in Field Theory and F -theory on a Circle*, [arXiv:1502.0539](#).
- [116] D. R. Morrison and W. Taylor, *Classifying bases for 6D F -theory models*, *Central Eur.J.Phys.* **10** (2012) 1072–1088, [[arXiv:1201.1943](#)].
- [117] D. R. Morrison and W. Taylor, *Toric bases for 6D F -theory models*, *Fortsch.Phys.* **60** (2012) 1187–1216, [[arXiv:1204.0283](#)].
- [118] W. Taylor, *On the Hodge structure of elliptically fibered Calabi-Yau threefolds*, *JHEP* **1208**

- (2012) 032, [[arXiv:1205.0952](#)].
- [119] G. Martini and W. Taylor, *6D F-theory models and elliptically fibered Calabi-Yau threefolds over semi-toric base surfaces*, [arXiv:1404.6300](#).
- [120] S. B. Johnson and W. Taylor, *Calabi-Yau threefolds with large $h^{2,1}$* , *JHEP* **1410** (2014) 23, [[arXiv:1406.0514](#)].
- [121] D. R. Morrison and W. Taylor, *Non-Higgsable clusters for 4D F-theory models*, [arXiv:1412.6112](#).
- [122] N. Seiberg and W. Taylor, *Charge Lattices and Consistency of 6D Supergravity*, *JHEP* **1106** (2011) 001, [[arXiv:1103.0019](#)].
- [123] V. Kumar, D. R. Morrison, and W. Taylor, *Global aspects of the space of 6D $N = 1$ supergravities*, *JHEP* **1011** (2010) 118, [[arXiv:1008.1062](#)].
- [124] V. Kumar, D. S. Park, and W. Taylor, *6D supergravity without tensor multiplets*, *JHEP* **1104** (2011) 080, [[arXiv:1011.0726](#)].
- [125] D. S. Park and W. Taylor, *Constraints on 6D Supergravity Theories with Abelian Gauge Symmetry*, *JHEP* **1201** (2012) 141, [[arXiv:1110.5916](#)].
- [126] T. W. Grimm and W. Taylor, *Structure in 6D and 4D $N=1$ supergravity theories from F-theory*, *JHEP* **1210** (2012) 105, [[arXiv:1204.3092](#)].
- [127] F. Bonetti, T. W. Grimm, and S. Hohenegger, *Exploring 6D origins of 5D supergravities with Chern-Simons terms*, *JHEP* **1305** (2013) 124, [[arXiv:1303.2661](#)].
- [128] T. W. Grimm, R. Savelli, and M. Weissenbacher, *On α' corrections in $N=1$ F-theory compactifications*, *Phys.Lett.* **B725** (2013) 431–436, [[arXiv:1303.3317](#)].
- [129] T. W. Grimm, J. Keitel, R. Savelli, and M. Weissenbacher, *From M-theory higher curvature terms to α' corrections in F-theory*, [arXiv:1312.1376](#).
- [130] T. W. Grimm, T. G. Pugh, and M. Weissenbacher, *On M-theory fourfold vacua with higher curvature terms*, [arXiv:1408.5136](#).
- [131] T. W. Grimm, T. G. Pugh, and M. Weissenbacher, *The effective action of warped M-theory reductions with higher derivative terms - Part I*, [arXiv:1412.5073](#).
- [132] N. C. Bizet, A. Klemm, and D. V. Lopes, *Landscaping with fluxes and the $E8$ Yukawa Point in F-theory*, [arXiv:1404.7645](#).
- [133] C. Lüdeling and F. Ruehle, *F-theory duals of singular heterotic $K3$ models*, *Phys.Rev.* **D91** (2015), no. 2 026010, [[arXiv:1405.2928](#)].
- [134] A. Grassi and D. R. Morrison, *Anomalies and the Euler characteristic of elliptic Calabi-Yau threefolds*, *Commun.Num.Theor.Phys.* **6** (2012) 51–127, [[arXiv:1109.0042](#)].
- [135] P. Deligne, *Courbes elliptiques: formulaire d'après j. tate*, in *Modular functions of one variable, IV (Proc. Internat. Summer School, Univ. Antwerp, Antwerp, 1972)*, vol. 476, pp. 53–73, 1975.
- [136] S. Y. An, S. Y. Kim, D. C. Marshall, S. H. Marshall, W. G. McCallum, and A. R. Perlis, *Jacobians of genus one curves*, *Journal of Number Theory* **90** (2001), no. 2 304–315.
- [137] V. Braun, *Toric Elliptic Fibrations and F-Theory Compactifications*, *JHEP* **1301** (2013) 016, [[arXiv:1110.4883](#)].

- [138] G. Salmon, *A Treatise on Conic Sections: Containing an Account of Some of the Most Important Modern Algebraic and Geometric Methods*. Chelsea Publishing Series. Chelsea Publishing Company, 1954.
- [139] W. Stein *et. al.*, *Sage Mathematics Software (Version 6.2)*. The Sage Development Team, 2014. <http://www.sagemath.org>.
- [140] P. Berglund and T. Hubsch, *On a residue representation of deformation, Koszul and chiral rings*, *Int.J.Mod.Phys.* **A10** (1995) 3381–3430, [[hep-th/9411131](#)].
- [141] V. Braun and J. Keitel, *Invariants of Two Ternary Quadratics*. The Sage Development Team, 2013. <http://trac.sagemath.org/17305>.
- [142] S. Y. An, S. Y. Kim, D. C. Marshall, S. H. Marshall, W. G. McCallum, and A. R. Perlis, *Jacobians of genus one curves*, *J. Number Theory* **90** (2001) 304–315.
- [143] V. Braun, T. W. Grimm, and J. Keitel, *Geometric Engineering in Toric F-Theory and GUTs with U(1) Gauge Factors*, *JHEP* **1312** (2013) 069, [[arXiv:1306.0577](#)].
- [144] D. Klevers, D. K. Mayorga Pena, P.-K. Oehlmann, H. Piragua, and J. Reuter, *F-Theory on all Toric Hypersurface Fibrations and its Higgs Branches*, *JHEP* **1501** (2015) 142, [[arXiv:1408.4808](#)].
- [145] V. Braun, T. W. Grimm, and J. Keitel, *New Global F-theory GUTs with U(1) symmetries*, *JHEP* **1309** (2013) 154, [[arXiv:1302.1854](#)].
- [146] R. Blumenhagen, B. Jurke, T. Rahn, and H. Roschy, *Cohomology of Line Bundles: Applications*, *J.Math.Phys.* **53** (2012) 012302, [[arXiv:1010.3717](#)].
- [147] M. Kreuzer and H. Skarke, *PALP: A Package for analyzing lattice polytopes with applications to toric geometry*, *Comput.Phys.Commun.* **157** (2004) 87–106, [[math/0204356](#)].
- [148] A. Novoseltsev, *Lattice polytope module for Sage*. The Sage Development Team, 2010. http://www.sagemath.org/doc/reference/geometry/sage/geometry/lattice_polytope.html.
- [149] V. Braun and A. Novoseltsev, *Toric geometry module for Sage*. The Sage Development Team, 2013. <http://www.sagemath.org/doc/reference/schemes/sage/schemes/toric/variety.html>.
- [150] W. Decker, G.-M. Greuel, G. Pfister, and H. Schönemann, “SINGULAR 3-1-6 — A computer algebra system for polynomial computations.” <http://www.singular.uni-kl.de>, 2012.
- [151] A. Grassi and V. Perduca, *Weierstrass models of elliptic toric K3 hypersurfaces and symplectic cuts*, *Adv.Theor.Math.Phys.* **17** (2013) 741–770, [[arXiv:1201.0930](#)].
- [152] C. Mayrhofer, E. Palti, O. Till, and T. Weigand, *Discrete Gauge Symmetries by Higgsing in four-dimensional F-Theory Compactifications*, *JHEP* **1412** (2014) 068, [[arXiv:1408.6831](#)].
- [153] L. B. Anderson, I. García-Etxebarria, T. W. Grimm, and J. Keitel, *Physics of F-theory compactifications without section*, *JHEP* **1412** (2014) 156, [[arXiv:1406.5180](#)].
- [154] I. García-Etxebarria, T. W. Grimm, and J. Keitel, *Yukawas and discrete symmetries in F-theory compactifications without section*, *JHEP* **1411** (2014) 125, [[arXiv:1408.6448](#)].
- [155] M. Cvetič, R. Donagi, D. Klevers, H. Piragua, and M. Poretschkin, *F-Theory Vacua with \mathbb{Z}_3 Gauge Symmetry*, [[arXiv:1502.0695](#)].

- [156] J. Borchmann, C. Mayrhofer, E. Palti, and T. Weigand, *Elliptic fibrations for $SU(5) \times U(1) \times U(1)$ F-theory vacua*, *Phys.Rev.* **D88** (2013), no. 4 046005, [[arXiv:1303.5054](#)].
- [157] M. Cvetič, D. Klevers, and H. Piragua, *F-Theory Compactifications with Multiple $U(1)$ -Factors: Constructing Elliptic Fibrations with Rational Sections*, *JHEP* **1306** (2013) 067, [[arXiv:1303.6970](#)].
- [158] M. Cvetič, D. Klevers, H. Piragua, and P. Song, *Elliptic fibrations with rank three Mordell-Weil group: F-theory with $U(1) \times U(1) \times U(1)$ gauge symmetry*, *JHEP* **1403** (2014) 021, [[arXiv:1310.0463](#)].
- [159] V. Braun, T. W. Grimm, and J. Keitel, *Complete Intersection Fibers in F-Theory*, *JHEP* **1503** (2015) 125, [[arXiv:1411.2615](#)].
- [160] C. Mayrhofer, D. R. Morrison, O. Till, and T. Weigand, *Mordell-Weil Torsion and the Global Structure of Gauge Groups in F-theory*, *JHEP* **1410** (2014) 16, [[arXiv:1405.3656](#)].
- [161] V. Bouchard and H. Skarke, *Affine Kac-Moody algebras, CHL strings and the classification of tops*, *Adv.Theor.Math.Phys.* **7** (2003) 205–232, [[hep-th/0303218](#)].
- [162] P. Candelas and A. Font, *Duality between the webs of heterotic and type II vacua*, *Nucl.Phys.* **B511** (1998) 295–325, [[hep-th/9603170](#)].
- [163] L. Lin and T. Weigand, *Towards the Standard Model in F-theory*, *Fortsch.Phys.* **63** (2015), no. 2 55–104, [[arXiv:1406.6071](#)].
- [164] J. Borchmann, C. Mayrhofer, E. Palti, and T. Weigand, *$SU(5)$ Tops with Multiple $U(1)$ s in F-theory*, *Nucl.Phys.* **B882** (2014) 1–69, [[arXiv:1307.2902](#)].
- [165] T. Shioda, *Mordell-Weil lattices and Galois representation, I*, *Proceedings of the Japan Academy, Series A, Mathematical Sciences* **65** (1989), no. 7 268–271.
- [166] T. Shioda, *On the Mordell-Weil lattices*, *Comment. Math. Univ. St. Paul* **39** (1990), no. 2 211–240.
- [167] M. Cvetič, A. Grassi, D. Klevers, and H. Piragua, *Chiral Four-Dimensional F-Theory Compactifications With $SU(5)$ and Multiple $U(1)$ -Factors*, *JHEP* **1404** (2014) 010, [[arXiv:1306.3987](#)].
- [168] R. Blumenhagen, T. W. Grimm, B. Jurke, and T. Weigand, *Global F-theory GUTs*, *Nucl.Phys.* **B829** (2010) 325–369, [[arXiv:0908.1784](#)].
- [169] T. W. Grimm, S. Krause, and T. Weigand, *F-Theory GUT Vacua on Compact Calabi-Yau Fourfolds*, *JHEP* **1007** (2010) 037, [[arXiv:0912.3524](#)].
- [170] R. Donagi and M. Wijnholt, *Breaking GUT Groups in F-Theory*, *Adv.Theor.Math.Phys.* **15** (2011) 1523–1604, [[arXiv:0808.2223](#)].
- [171] N. Seiberg and E. Witten, *Comments on string dynamics in six-dimensions*, *Nucl.Phys.* **B471** (1996) 121–134, [[hep-th/9603003](#)].
- [172] P. Candelas, D.-E. Diaconescu, B. Florea, D. R. Morrison, and G. Rajesh, *Codimension three bundle singularities in F theory*, *JHEP* **0206** (2002) 014, [[hep-th/0009228](#)].
- [173] R. Miranda, *Smooth models for elliptic threefolds*, in *The birational geometry of degenerations (Cambridge, Mass., 1981)*, vol. 29 of *Progr. Math.*, pp. 85–133. Birkhäuser Boston, Mass.,

- 1983.
- [174] Y. Hu, C.-H. Liu, and S.-T. Yau, *Toric morphisms and fibrations of toric Calabi-Yau hypersurfaces*, *Adv.Theor.Math.Phys.* **6** (2003) 457–505, [[math/0010082](#)].
 - [175] R. Wazir, *Arithmetic on Elliptic Threefolds*, *ArXiv Mathematics e-prints* (Dec., 2001) [[math/0112](#)].
 - [176] D. R. Morrison and W. Taylor, *Matter and singularities*, *JHEP* **1201** (2012) 022, [[arXiv:1106.3563](#)].
 - [177] V. Braun and D. R. Morrison, *F-theory on Genus-One Fibrations*, *JHEP* **1408** (2014) 132, [[arXiv:1401.7844](#)].
 - [178] D. R. Morrison and W. Taylor, *Sections, multisections, and $U(1)$ fields in F-theory*, [[arXiv:1404.1527](#)].
 - [179] C. Long, L. McAllister, and P. McGuirk, *Heavy Tails in Calabi-Yau Moduli Spaces*, *JHEP* **1410** (2014) 187, [[arXiv:1407.0709](#)].
 - [180] P. C. Argyres and M. R. Douglas, *New phenomena in $SU(3)$ supersymmetric gauge theory*, *Nucl.Phys.* **B448** (1995) 93–126, [[hep-th/9505062](#)].
 - [181] P. C. Argyres, M. R. Plesser, N. Seiberg, and E. Witten, *New $N=2$ superconformal field theories in four-dimensions*, *Nucl.Phys.* **B461** (1996) 71–84, [[hep-th/9511154](#)].
 - [182] P. C. Argyres and N. Seiberg, *S-duality in $N=2$ supersymmetric gauge theories*, *JHEP* **0712** (2007) 088, [[arXiv:0711.0054](#)].
 - [183] E. Witten, *Some comments on string dynamics*, [[hep-th/9507121](#)].
 - [184] E. Witten, *Five-branes and M theory on an orbifold*, *Nucl.Phys.* **B463** (1996) 383–397, [[hep-th/9512219](#)].
 - [185] H. Hayashi, R. Tatar, Y. Toda, T. Watari, and M. Yamazaki, *New Aspects of Heterotic-F Theory Duality*, *Nucl.Phys.* **B806** (2009) 224–299, [[arXiv:0805.1057](#)].
 - [186] F. Bonetti, T. W. Grimm, and S. Hohenegger, *A Kaluza-Klein inspired action for chiral p-forms and their anomalies*, *Phys.Lett.* **B720** (2013) 424–427, [[arXiv:1206.1600](#)].
 - [187] F. Bonetti, T. W. Grimm, and S. Hohenegger, *One-loop Chern-Simons terms in five dimensions*, *JHEP* **1307** (2013) 043, [[arXiv:1302.2918](#)].
 - [188] D. S. Park, *Anomaly Equations and Intersection Theory*, *JHEP* **1201** (2012) 093, [[arXiv:1111.2351](#)].
 - [189] E. Witten, *Phase transitions in M theory and F theory*, *Nucl.Phys.* **B471** (1996) 195–216, [[hep-th/9603150](#)].
 - [190] I. Antoniadis, S. Ferrara, R. Minasian, and K. Narain, *R^{**4} couplings in M and type II theories on Calabi-Yau spaces*, *Nucl.Phys.* **B507** (1997) 571–588, [[hep-th/9707013](#)].
 - [191] H. Nishino and E. Sezgin, *New couplings of six-dimensional supergravity*, *Nucl.Phys.* **B505** (1997) 497–516, [[hep-th/9703075](#)].
 - [192] S. Ferrara, F. Riccioni, and A. Sagnotti, *Tensor and vector multiplets in six-dimensional supergravity*, *Nucl.Phys.* **B519** (1998) 115–140, [[hep-th/9711059](#)].

- [193] F. Riccioni and A. Sagnotti, *Some properties of tensor multiplets in six-dimensional supergravity*, *Nucl.Phys.Proc.Suppl.* **67** (1998) 68–73, [[hep-th/9711077](#)].
- [194] F. Riccioni, *Abelian vector multiplets in six-dimensional supergravity*, *Phys.Lett.* **B474** (2000) 79–84, [[hep-th/9910246](#)].
- [195] A. Sagnotti, *A Note on the Green-Schwarz mechanism in open string theories*, *Phys.Lett.* **B294** (1992) 196–203, [[hep-th/9210127](#)].
- [196] V. Sadov, *Generalized Green-Schwarz mechanism in F theory*, *Phys.Lett.* **B388** (1996) 45–50, [[hep-th/9606008](#)].
- [197] R. Suzuki and Y. Tachikawa, *More anomaly-free models of six-dimensional gauged supergravity*, *J.Math.Phys.* **47** (2006) 062302, [[hep-th/0512019](#)].
- [198] E. Bergshoeff, F. Coomans, E. Sezgin, and A. Van Proeyen, *Higher Derivative Extension of 6D Chiral Gauged Supergravity*, *JHEP* **1207** (2012) 011, [[arXiv:1203.2975](#)].
- [199] T. W. Grimm and T. G. Pugh, *Gauged supergravities and their symmetry-breaking vacua in F-theory*, *JHEP* **1306** (2013) 012, [[arXiv:1302.3223](#)].
- [200] S. Ferrara, R. Minasian, and A. Sagnotti, *Low-energy analysis of M and F theories on Calabi-Yau threefolds*, *Nucl.Phys.* **B474** (1996) 323–342, [[hep-th/9604097](#)].
- [201] V. Kumar, D. R. Morrison, and W. Taylor, *Mapping 6D $N = 1$ supergravities to F-theory*, *JHEP* **1002** (2010) 099, [[arXiv:0911.3393](#)].
- [202] P. Townsend, K. Pilch, and P. van Nieuwenhuizen, *Selfduality in Odd Dimensions*, *Phys.Lett.* **B136** (1984) 38.
- [203] L. Alvarez-Gaume and E. Witten, *Gravitational Anomalies*, *Nucl.Phys.* **B234** (1984) 269.
- [204] C. Mayrhofer, E. Palti, O. Till, and T. Weigand, *On Discrete Symmetries and Torsion Homology in F-Theory*, [[arXiv:1410.7814](#)].
- [205] E. Witten, *Nonperturbative superpotentials in string theory*, *Nucl.Phys.* **B474** (1996) 343–360, [[hep-th/9604030](#)].
- [206] B. Smyth, *Differential Geometry of Complex Hypersurfaces.*, *Annals of Mathematics, Vol. 85* **2** (1967) 246–266.
- [207] K. Yano and S. Ishihara, *Normal circle bundles of complex hypersurfaces.*, *Kōdai Math. Semin. Rep.* **20** (1968) 29–53.
- [208] A. Strominger, S.-T. Yau, and E. Zaslow, *Mirror symmetry is T duality*, *Nucl.Phys.* **B479** (1996) 243–259, [[hep-th/9606040](#)].
- [209] I. Moss, *Dimensional Reductions*, *Newcastle Postgraduate Notebook Series*.
<http://research.ncl.ac.uk/cosmology/reviews/>.
- [210] S. Chioffi and S. Salamon, *The intrinsic torsion of $SU(3)$ and G_2 structures*, *ArXiv Mathematics e-prints* (Feb., 2002) [[math/0202282](#)].
- [211] H. Jockers and J. Louis, *The Effective action of D7-branes in $N = 1$ Calabi-Yau orientifolds*, *Nucl.Phys.* **B705** (2005) 167–211, [[hep-th/0409098](#)].
- [212] K. Oguiso, *On algebraic fiber space structures on a calabi-yau 3-fold*, *International Journal of Mathematics* **04** (1993), no. 03 439–465.

- [213] A. Strominger, *Massless black holes and conifolds in string theory*, *Nucl.Phys.* **B451** (1995) 96–108, [[hep-th/9504090](#)].
- [214] B. R. Greene, D. R. Morrison, and A. Strominger, *Black hole condensation and the unification of string vacua*, *Nucl.Phys.* **B451** (1995) 109–120, [[hep-th/9504145](#)].
- [215] B. R. Greene, *String theory on Calabi-Yau manifolds*, [hep-th/9702155](#).
- [216] T. Mohaupt and F. Saueressig, *Effective supergravity actions for conifold transitions*, *JHEP* **0503** (2005) 018, [[hep-th/0410272](#)].
- [217] S. Krause, C. Mayrhofer, and T. Weigand, *G_4 flux, chiral matter and singularity resolution in F-theory compactifications*, *Nucl.Phys.* **B858** (2012) 1–47, [[arXiv:1109.3454](#)].
- [218] M. Bies, C. Mayrhofer, C. Pehle, and T. Weigand, *Chow groups, Deligne cohomology and massless matter in F-theory*, [arXiv:1402.5144](#).
- [219] C. Mayrhofer, E. Palti, and T. Weigand, *$U(1)$ symmetries in F-theory GUTs with multiple sections*, *JHEP* **1303** (2013) 098, [[arXiv:1211.6742](#)].
- [220] M. Cvetič, D. Klevers, and H. Piragua, *F-Theory Compactifications with Multiple $U(1)$ -Factors: Addendum*, *JHEP* **1312** (2013) 056, [[arXiv:1307.6425](#)].
- [221] S. Cecotti, C. Cordova, J. J. Heckman, and C. Vafa, *T-Branes and Monodromy*, *JHEP* **1107** (2011) 030, [[arXiv:1010.5780](#)].
- [222] L. Aparicio, A. Font, L. E. Ibanez, and F. Marchesano, *Flux and Instanton Effects in Local F-theory Models and Hierarchical Fermion Masses*, *JHEP* **1108** (2011) 152, [[arXiv:1104.2609](#)].
- [223] J. Marsano and S. Schafer-Nameki, *Yukawas, G-flux, and Spectral Covers from Resolved Calabi-Yau's*, *JHEP* **1111** (2011) 098, [[arXiv:1108.1794](#)].
- [224] A. Font, L. E. Ibanez, F. Marchesano, and D. Regalado, *Non-perturbative effects and Yukawa hierarchies in F-theory $SU(5)$ Unification*, *JHEP* **1303** (2013) 140, [[arXiv:1211.6529](#)].
- [225] A. Font, F. Marchesano, D. Regalado, and G. Zoccarato, *Up-type quark masses in $SU(5)$ F-theory models*, *JHEP* **1311** (2013) 125, [[arXiv:1307.8089](#)].
- [226] M. Haack and J. Louis, *Duality in heterotic vacua with four supercharges*, *Nucl.Phys.* **B575** (2000) 107–133, [[hep-th/9912181](#)].
- [227] R. Blumenhagen, M. Cvetič, S. Kachru, and T. Weigand, *D-Brane Instantons in Type II Orientifolds*, *Ann.Rev.Nucl.Part.Sci.* **59** (2009) 269–296, [[arXiv:0902.3251](#)].
- [228] B. R. Greene, D. R. Morrison, and C. Vafa, *A Geometric realization of confinement*, *Nucl.Phys.* **B481** (1996) 513–538, [[hep-th/9608039](#)].
- [229] H. Ooguri and C. Vafa, *Summing up D instantons*, *Phys.Rev.Lett.* **77** (1996) 3296–3298, [[hep-th/9608079](#)].
- [230] K. Intriligator, H. Jockers, P. Mayr, D. R. Morrison, and M. R. Plesser, *Conifold Transitions in M-theory on Calabi-Yau Fourfolds with Background Fluxes*, *Adv.Theor.Math.Phys.* **17** (2013) 601–699, [[arXiv:1203.6662](#)].
- [231] T. W. Grimm, T.-W. Ha, A. Klemm, and D. Klevers, *Computing Brane and Flux Superpotentials in F-theory Compactifications*, *JHEP* **1004** (2010) 015, [[arXiv:0909.2025](#)].

- [232] I. García-Etxebarria, B. Heidenreich, and T. Wrase, *New $N=1$ dualities from orientifold transitions. Part I. Field Theory*, *JHEP* **1310** (2013) 007, [[arXiv:1210.7799](#)].
- [233] I. García-Etxebarria, B. Heidenreich, and T. Wrase, *New $N=1$ dualities from orientifold transitions - Part II: String Theory*, *JHEP* **1310** (2013) 006, [[arXiv:1307.1701](#)].
- [234] W. Fulton, *Introduction to toric varieties*. No. 131. Princeton University Press, 1993.
- [235] D. A. Cox, J. B. Little, and H. K. Schenck, *Toric varieties*. American Mathematical Soc., 2011.
- [236] M. Kreuzer, *Toric geometry and Calabi-Yau compactifications*, *Ukr.J.Phys.* **55** (2010) 613–625, [[hep-th/0612307](#)].
- [237] V. Bouchard, *Lectures on complex geometry, Calabi-Yau manifolds and toric geometry*, [[hep-th/0702063](#)].
- [238] C. Closset, *Toric geometry and local Calabi-Yau varieties: An Introduction to toric geometry (for physicists)*, [[arXiv:0901.3695](#)].
- [239] E. Witten, *Phases of $N=2$ theories in two-dimensions*, *Nucl.Phys.* **B403** (1993) 159–222, [[hep-th/9301042](#)].
- [240] S.-T. Yau, *Calabi's conjecture and some new results in algebraic geometry*, *Proceedings of the National Academy of Sciences* **74** (1977), no. 5 1798–1799.
- [241] S.-T. Yau, *On the ricci curvature of a compact kähler manifold and the complex monge-ampère equation, i*, *Communications on pure and applied mathematics* **31** (1978), no. 3 339–411.
- [242] V. V. Batyrev, *Dual polyhedra and mirror symmetry for Calabi-Yau hypersurfaces in toric varieties*, *J.Alg.Geom.* **3** (1994) 493–545, [[alg-geom/9310003](#)].
- [243] M. Kreuzer and H. Skarke, *Classification of reflexive polyhedra in three-dimensions*, *Adv.Theor.Math.Phys.* **2** (1998) 847–864, [[hep-th/9805190](#)].
- [244] M. Kreuzer and H. Skarke, *Complete classification of reflexive polyhedra in four-dimensions*, *Adv.Theor.Math.Phys.* **4** (2002) 1209–1230, [[hep-th/0002240](#)].
- [245] V. V. Batyrev and L. A. Borisov, *On Calabi-Yau complete intersections in toric varieties*, [[alg-geom/9412017](#)].
- [246] J. Fuchs and C. Schweigert, *Symmetries, Lie algebras and representations: A graduate course for physicists*, .
- [247] C. W. Misner, K. Thorne, and J. Wheeler, *Gravitation*, .